Scuola Internazionale Superiore di Studi Avanzati
Area of Physics
Theoretical Particle Physics Curriculum

Phenomenology of the Discrete Symmetry Approach to Neutrino Mixing and Leptonic CP Violation

Candidate: **Arsenii V. Titov**

Supervisor: **Professor Serguey T. Petcov**

A thesis submitted for the degree of Doctor of Philosophy

Trieste
August 2017

Abstract

The discovery of neutrino oscillations caused by non-zero neutrino masses and neutrino mixing opened new field of research in particle physics. The impressive experimental progress made in the last two decades allowed to measure neutrino oscillation parameters with a relatively high precision. However, in spite of the experimental progress, the mechanism of neutrino mass generation as well as the dynamics behind the peculiar pattern of neutrino mixing which emerged from the experimental data remain currently unknown. The present PhD thesis is devoted to the problem of understanding the origin of the observed pattern of neutrino mixing and, more generally, the origin of (lepton) flavour. Our particular focus is on predictions for leptonic CP violation, since the status of CP symmetry in the lepton sector is also unknown at the moment. Driven by the measured values of the neutrino mixing parameters, we adopt symmetry approach to neutrino mixing, based on the assumption of existence of a (lepton) flavour symmetry described by a non-Abelian finite (discrete) group. At low energies this symmetry is broken down to residual symmetries of the charged lepton and neutrino mass matrices. The residual symmetries correspond to Abelian subgroups of the original flavour symmetry group. The most distinct feature of the discrete symmetry approach is correlations between the neutrino mixing angles and the CP violation phases present in the neutrino mixing matrix. These correlations are referred to as neutrino mixing sum rules. We first consider all types of the residual symmetries for which such correlations are expected and derive the corresponding sum rules for the Dirac CP violation phase. Using the derived sum rules, we obtain predictions for the Dirac phase in the cases of several discrete flavour symmetries. Further, we concentrate on a scenario in which the main contribution to neutrino mixing comes from the neutrino sector and explore in a systematic way possible charged lepton corrections. These corrections are required to reconstitute compatibility of highly symmetric mixing patterns, such as, for instance, tri-bimaximal mixing, with the experimental data. Again, our main focus is on leptonic Dirac CP violation. In a number of phenomenologically interesting cases, we perform a statistical analysis of the predictions for the Dirac phase, using (i) the results of the global analysis of neutrino oscillation data and (ii) the prospective uncertainties on the neutrino mixing angles. Next, we derive sum rules for the Majorana phases, which are present in the neutrino mixing matrix if massive neutrinos are Majorana particles. We demonstrate how generalised CP invariance of the neutrino Majorana mass term constrains the Majorana phases and obtain predictions for the effective Majorana mass in neutrinoless double beta decay. Finally, we investigate the impact of renormalisation group corrections on the sum rule predictions for the Dirac phase in the cases of the neutrino Majorana mass term generated by the Weinberg (dimension 5) operator added to (i) the Standard Model and (ii) the Minimal Supersymmetric Standard Model.

List of publications

The present PhD thesis is based on the following publications listed in chronological order:

1. I. Girardi, S. T. Petcov and A. V. Titov, *Determining the Dirac CP Violation Phase in the Neutrino Mixing Matrix from Sum Rules*, *Nucl. Phys.* **B 894** (2015) 733–768 [arXiv:1410.8056] (in part);

2. I. Girardi, S. T. Petcov and A. V. Titov, *Predictions for the Leptonic Dirac CP Violation Phase: A Systematic Phenomenological Analysis*, *Eur. Phys. J.* **C 75** (2015) 345 [arXiv:1504.00658];

3. I. Girardi, S. T. Petcov, A. J. Stuart and A. V. Titov, *Leptonic Dirac CP Violation Predictions from Residual Discrete Symmetries*, *Nucl. Phys.* **B 902** (2016) 1–57 [arXiv:1509.02502];

4. I. Girardi, S. T. Petcov and A. V. Titov, *Predictions for the Majorana CP Violation Phases in the Neutrino Mixing Matrix and Neutrinoless Double Beta Decay*, *Nucl. Phys.* **B 911** (2016) 754–804 [arXiv:1605.04172];

5. J. Gehrlein, S. T. Petcov, M. Spinrath and A. V. Titov, *Renormalisation Group Corrections to Neutrino Mixing Sum Rules*, *JHEP* **11** (2016) 146 [arXiv:1608.08409].

The research performed by the author during his PhD studies has also led to the following articles:

6. I. Girardi, S. T. Petcov and A. V. Titov, *Predictions for the Dirac CP Violation Phase in the Neutrino Mixing Matrix*, *Int. J. Mod. Phys.* **A 30** (2015) 1530035 [arXiv:1504.02402];

7. J. T. Penedo, S. T. Petcov and A. V. Titov, *Neutrino Mixing and Leptonic CP Violation from S_4 Flavour and Generalised CP Symmetries*, arXiv:1705.00309.

The results of the performed research presented at international conferences and workshops are summarised in the following contributions to conference proceedings co-authored by the author:

1. I. Girardi, S. T. Petcov and A. V. Titov, *Predictions for the Dirac Phase in the Neutrino Mixing Matrix and Sum Rules*, *J. Phys. Conf. Ser.* **631** (2015) 012051;

2. I. Girardi, S. Petcov and A. Titov, *Predicting the Leptonic Dirac CP Violation Phase from Sum Rules*, *PoS* **EPS-HEP2015** (2015) 039;

3. I. Girardi, S. T. Petcov and A. V. Titov, *The Leptonic Dirac CP-Violating Phase from Sum Rules*, *J. Phys. Conf. Ser.* **718** (2016) 062060;

4. I. Girardi, S. Petcov and A. Titov, *CPV Predictions from Flavour Symmetries*, *PoS* **NOW2016** (2016) 027.

Contents

List of publications v

1 Introduction 1
- 1.1 Three neutrino mixing . . . 2
- 1.2 Discrete flavour symmetries . . . 6
- 1.3 Generalised CP symmetry . . . 13
- 1.4 Outline of the thesis . . . 17

2 Leptonic Dirac CP violation from residual discrete symmetries 19
- 2.1 Preliminary considerations . . . 19
- 2.2 Pattern A: $G_e = Z_2$ and $G_\nu = Z_n$, $n > 2$ or $Z_n \times Z_m$, $n, m \geq 2$ . . . 22
  - 2.2.1 Case A1: $U_{12}(\theta^e_{12}, \delta^e_{12})$ . . . 23
  - 2.2.2 Case A2: $U_{13}(\theta^e_{13}, \delta^e_{13})$ . . . 24
  - 2.2.3 Case A3: $U_{23}(\theta^e_{23}, \delta^e_{23})$ . . . 25
  - 2.2.4 Results for $G_f = A_4$ (T'), S_4 and A_5 . . . 26
- 2.3 Pattern B: $G_e = Z_n$, $n > 2$ or $Z_n \times Z_m$, $n, m \geq 2$ and $G_\nu = Z_2$ . . . 28
  - 2.3.1 Case B1: $U_{13}(\theta^\nu_{13}, \delta^\nu_{13})$ . . . 28
  - 2.3.2 Case B2: $U_{23}(\theta^\nu_{23}, \delta^\nu_{23})$ . . . 29
  - 2.3.3 Case B3: $U_{12}(\theta^\nu_{12}, \delta^\nu_{12})$ . . . 29
  - 2.3.4 Results for $G_f = A_4$ (T'), S_4 and A_5 . . . 30
- 2.4 Pattern C: $G_e = Z_2$ and $G_\nu = Z_2$ . . . 31
  - 2.4.1 Case C1: $U_{12}(\theta^e_{12}, \delta^e_{12})$ and $U_{13}(\theta^\nu_{13}, \delta^\nu_{13})$ . . . 31
  - 2.4.2 Case C2: $U_{13}(\theta^e_{13}, \delta^e_{13})$ and $U_{12}(\theta^\nu_{12}, \delta^\nu_{12})$ . . . 32
  - 2.4.3 Case C3: $U_{12}(\theta^e_{12}, \delta^e_{12})$ and $U_{23}(\theta^\nu_{23}, \delta^\nu_{23})$ . . . 33
  - 2.4.4 Case C4: $U_{13}(\theta^e_{13}, \delta^e_{13})$ and $U_{23}(\theta^\nu_{23}, \delta^\nu_{23})$ . . . 34
  - 2.4.5 Case C5: $U_{23}(\theta^e_{23}, \delta^e_{23})$ and $U_{13}(\theta^\nu_{13}, \delta^\nu_{13})$ . . . 35
  - 2.4.6 Case C6: $U_{23}(\theta^e_{23}, \delta^e_{23})$ and $U_{12}(\theta^\nu_{12}, \delta^\nu_{12})$ . . . 36
  - 2.4.7 Case C7: $U_{12}(\theta^e_{12}, \delta^e_{12})$ and $U_{12}(\theta^\nu_{12}, \delta^\nu_{12})$ . . . 37
  - 2.4.8 Case C8: $U_{13}(\theta^e_{13}, \delta^e_{13})$ and $U_{13}(\theta^\nu_{13}, \delta^\nu_{13})$ . . . 38
  - 2.4.9 Case C9: $U_{23}(\theta^e_{23}, \delta^e_{23})$ and $U_{23}(\theta^\nu_{23}, \delta^\nu_{23})$ . . . 39
  - 2.4.10 Results for $G_f = A_4$ (T'), S_4 and A_5 . . . 40
- 2.5 Summary of the results for patterns A, B and C . . . 42
- 2.6 Pattern D: fully broken G_e and $G_\nu = Z_n$, $n > 2$ or $Z_n \times Z_m$, $n, m \geq 2$ . . . 47
  - 2.6.1 Case D1: $U_{23}(\theta^e_{23}, \delta^e_{23})\, U_{12}(\theta^e_{12}, \delta^e_{12})$ . . . 47
  - 2.6.2 Case D2: $U_{13}(\theta^e_{13}, \delta^e_{13})\, U_{12}(\theta^e_{12}, \delta^e_{12})$ . . . 49
  - 2.6.3 Case D3: $U_{12}(\theta^e_{12}, \delta^e_{12})\, U_{23}(\theta^e_{23}, \delta^e_{23})$ . . . 49
  - 2.6.4 Case D4: $U_{13}(\theta^e_{13}, \delta^e_{13})\, U_{23}(\theta^e_{23}, \delta^e_{23})$ . . . 50
  - 2.6.5 Case D5: $U_{23}(\theta^e_{23}, \delta^e_{23})\, U_{13}(\theta^e_{13}, \delta^e_{13})$ . . . 50
  - 2.6.6 Case D6: $U_{12}(\theta^e_{12}, \delta^e_{12})\, U_{13}(\theta^e_{13}, \delta^e_{13})$ . . . 52
- 2.7 Pattern E: $G_e = Z_n$, $n > 2$ or $Z_n \times Z_m$, $n, m \geq 2$ and fully broken G_ν . . . 54
  - 2.7.1 Case E1: $U_{12}(\theta^\nu_{12}, \delta^\nu_{12})\, U_{13}(\theta^\nu_{13}, \delta^\nu_{13})$ . . . 54

2.7.2 Case E2: $U_{12}(\theta^\nu_{12}, \delta^\nu_{12})\, U_{23}(\theta^\nu_{23}, \delta^\nu_{23})$ . . . 55
2.7.3 Case E3: $U_{23}(\theta^\nu_{23}, \delta^\nu_{23})\, U_{12}(\theta^\nu_{12}, \delta^\nu_{12})$ . . . 56
2.7.4 Case E4: $U_{23}(\theta^\nu_{23}, \delta^\nu_{23})\, U_{13}(\theta^\nu_{13}, \delta^\nu_{13})$ . . . 57
2.7.5 Case E5: $U_{13}(\theta^\nu_{13}, \delta^\nu_{13})\, U_{12}(\theta^\nu_{12}, \delta^\nu_{12})$ . . . 57
2.7.6 Case E6: $U_{13}(\theta^\nu_{13}, \delta^\nu_{13})\, U_{23}(\theta^\nu_{23}, \delta^\nu_{23})$ . . . 58
2.8 Summary of the predictions for $G_f = A_4$ (T'), S_4 and A_5 . . . 60
2.9 Conclusions . . . 63

3 Phenomenology of sum rules for the Dirac phase 65
3.1 Framework . . . 65
3.2 Mixing schemes with $\tilde{U}_e^\dagger = R_{ij}(\theta^e_{ij})$ and $\tilde{U}_\nu = R_{23}(\theta^\nu_{23})\, R_{12}(\theta^\nu_{12})$ . . . 68
3.2.1 Case A1: θ^e_{12} . . . 68
3.2.2 Case A2: θ^e_{13} . . . 69
3.3 Mixing schemes with $\tilde{U}_e^\dagger = R_{ij}(\theta^e_{ij})\, R_{kl}(\theta^e_{kl})$ and $\tilde{U}_\nu = R_{23}(\theta^\nu_{23})\, R_{12}(\theta^\nu_{12})$ . . . 70
3.3.1 Case B1: θ^e_{12} and θ^e_{23} . . . 70
3.3.2 Case B2: θ^e_{13} and θ^e_{23} . . . 71
3.3.3 Case B3: θ^e_{12} and θ^e_{13} . . . 72
3.4 Mixing schemes with $\tilde{U}_e^\dagger = R_{ij}(\theta^e_{ij})$ and $\tilde{U}_\nu = R_{23}(\theta^\nu_{23})\, R_{13}(\theta^\nu_{13})\, R_{12}(\theta^\nu_{12})$ . . . 74
3.4.1 Case C1: θ^e_{12} . . . 75
3.4.2 Case C2: θ^e_{13} . . . 77
3.5 Summary of the sum rules . . . 78
3.6 Predictions for the Dirac phase δ and the rephasing invariant $J_{\rm CP}$ . . . 80
3.7 Statistical analysis . . . 83
3.7.1 Case B1 . . . 84
3.7.2 Case B2 . . . 87
3.7.3 Case C1 . . . 89
3.7.4 Case C2 . . . 92
3.8 Summary and conclusions . . . 92

4 The Majorana phases and neutrinoless double beta decay 97
4.1 Mixing schemes with $\tilde{U}_e^\dagger = R_{ij}(\theta^e_{ij})$ and $\tilde{U}_\nu = R_{23}(\theta^\nu_{23})\, R_{12}(\theta^\nu_{12})$ . . . 98
4.1.1 Case A1: θ^e_{12} . . . 98
4.1.2 Case A2: θ^e_{13} . . . 101
4.2 Mixing schemes with $\tilde{U}_e^\dagger = R_{ij}(\theta^e_{ij})\, R_{kl}(\theta^e_{kl})$ and $\tilde{U}_\nu = R_{23}(\theta^\nu_{23})\, R_{12}(\theta^\nu_{12})$ . . . 103
4.2.1 Case B1: θ^e_{12} and θ^e_{23} . . . 103
4.2.2 Case B2: θ^e_{13} and θ^e_{23} . . . 105
4.2.3 Case B3: θ^e_{12} and θ^e_{13} . . . 107
4.3 Mixing schemes with $\tilde{U}_e^\dagger = R_{ij}(\theta^e_{ij})$ and $\tilde{U}_\nu = R_{23}(\theta^\nu_{23})\, R_{13}(\theta^\nu_{13})\, R_{12}(\theta^\nu_{12})$ . . . 109
4.3.1 Case C1: θ^e_{12} . . . 110
4.3.2 Case C2: θ^e_{13} . . . 112
4.4 Summary of the sum rules for the Majorana phases . . . 114
4.5 Predictions . . . 115
4.5.1 Dirac phase . . . 115
4.5.2 Majorana phases . . . 116
4.5.3 Neutrinoless double beta decay . . . 120
4.6 Implications of a generalised CP symmetry . . . 126
4.7 Summary and conclusions . . . 130

5 Renormalisation group corrections to neutrino mixing sum rules 133
5.1 Introductory remarks . . . 133
5.2 Mixing sum rules . . . 134
5.3 Analytical estimates . . . 135
5.3.1 General effects of radiative corrections . . . 135
5.3.2 Allowed parameter regions with RG corrections . . . 136
5.3.3 Implications of $\alpha_2 - \alpha_1 = 0$ and π and small $\tan\beta$ . . . 139
5.3.4 Remarks on the case of zero θ_{23}^e . . . 145
5.4 Numerical results . . . 146
5.4.1 Numerical approach . . . 146
5.4.2 Results in the case of non-zero θ_{23}^e . . . 147
5.4.3 Results in the case of zero θ_{23}^e . . . 152
5.5 Summary and conclusions . . . 157

6 Conclusions and outlook 159

A Symmetry of a phenomenologically viable generalised CP transformation 161

B The groups A_4, T', S_4 and A_5 163

C Parametrisations of a 3×3 unitary matrix 165

D Parametrisations of the PMNS matrix for fully broken G_e or G_ν 167

E Results for $G_f = A_5$ and generalised CP symmetry 169

F Statistical details 171

G Results for the atmospheric angle 175

H Likelihood functions for $\cos\delta$ 177

Bibliography 187

Acknowledgements 201

Chapter 1

Introduction

In spite of the tremendous success of the Standard Model (SM) [1–3] of particle interactions in understanding fundamental physics at distances as tiny as 10^{-18} meters (or energies as high as hundreds of GeV), now we certainly know that the SM is incomplete. The most conspicuous reason of this incompleteness, and thus a clear indication of existence of physics beyond the SM (BSM), is the experimentally established fact that neutrinos have mass. In the SM neutrinos are massless. The phenomenon of neutrino oscillations, induced by non-zero neutrino mass and non-trivial neutrino mixing, was first theoretically predicted by Bruno Pontecorvo in 1957 [4, 5]. It took more than forty years before this phenomenon was firmly established experimentally. The discovery of neutrino oscillations by the Super-Kamiokande (Super-K) experiment in Japan in 1998 [6] and by the Sudbury Neutrino Observatory (SNO) in Canada in 2001 [7] led to the Nobel Prize in Physics awarded in 2015 to Takaaki Kajita and Arthur B. McDonald.

The impressive experimental progress made in the last two decades allowed to measure neutrino oscillation parameters with a relatively high precision (see, e.g., [8]). However, notwithstanding this progress, many long-standing fundamental questions in neutrino physics still remain unresolved. They include questions from the list given below.

- What is the nature of massive neutrinos, i.e., are they Dirac of Majorana particles?
- What is the absolute neutrino mass scale, i.e., what is the mass of the lightest out of three neutrinos, existence of which have been firmly established?
- What type of the mass spectrum do neutrinos obey, with so-called normal ordering, i.e., with $m_1 < m_2 < m_3$, or with inverted ordering, i.e., with $m_3 < m_1 < m_2$?
- What is the mechanism of neutrino mass generation?
- Is CP invariance violated in the lepton sector of particle interactions?
- What is the origin of the observed pattern of neutrino mixing? Is there any symmetry behind this pattern?
- Do sterile neutrinos, i.e., those that take no part in the standard weak interactions, exist?
- Are heavy sterile neutrinos, if any, responsible for generating the observed baryon asymmetry of the Universe (BAU)?

The present PhD thesis is devoted to the problem of understanding the origin of the observed pattern of neutrino mixing. This problem is an integral part of the more general fundamental problem in particle physics of understanding the origins of flavour in the

quark and lepton sectors, i.e., of the patterns of quark masses and mixing, and of the charged lepton and neutrino masses and of neutrino mixing.

Driven by the measured values of the neutrino mixing parameters, we decide to adopt symmetry approach to this problem, which is based on the assumption of existence at some energy scale of a (lepton) flavour symmetry. Moreover, this symmetry is assumed to correspond to a non-Abelian finite group. Before describing this approach in detail, let us first recall the reference 3-neutrino mixing scheme and the current knowledge of the neutrino oscillation parameters.

1.1 Three neutrino mixing

All compelling neutrino oscillation data are compatible with the existence of three flavour neutrinos: electron neutrino, ν_e, muon neutrino, ν_μ, and tauon neutrino, ν_τ [8]. These neutrinos take part in the charged current (CC) weak interactions, which are described by the following Lagrangian density:

$$-\mathcal{L}_{\rm CC} = \frac{g}{\sqrt{2}} \sum_{\ell=e,\mu,\tau} \overline{\ell_L}(x)\, \gamma_\alpha\, \nu_{\ell L}(x)\, W^{\alpha\dagger}(x) + \text{h.c.}, \tag{1.1}$$

with g being the weak gauge coupling constant, and ℓ_L and $\nu_{\ell L}$ being the left-handed (LH) charged lepton and flavour neutrino fields, respectively. The flavour neutrino fields are linear combinations of the LH components of the fields $\nu_j(x)$, $j = 1, 2, 3$, of neutrinos with definite masses:

$$\nu_{\ell L}(x) = \sum_{j=1}^{3} U_{\ell j}\, \nu_{jL}(x)\,, \tag{1.2}$$

where U is the 3×3 unitary Pontecorvo-Maki-Nakagawa-Sakata (PMNS) neutrino mixing matrix [4, 5, 9]. In the standard parametrisation[1] this matrix reads [8]

$$\begin{aligned} U &= \begin{pmatrix} 1 & 0 & 0 \\ 0 & c_{23} & s_{23} \\ 0 & -s_{23} & c_{23} \end{pmatrix} \begin{pmatrix} c_{13} & 0 & s_{13}e^{-i\delta} \\ 0 & 1 & 0 \\ -s_{13}e^{i\delta} & 0 & c_{13} \end{pmatrix} \begin{pmatrix} c_{12} & s_{12} & 0 \\ -s_{12} & c_{12} & 0 \\ 0 & 0 & 1 \end{pmatrix} \begin{pmatrix} 1 & 0 & 0 \\ 0 & e^{i\frac{\alpha_{21}}{2}} & 0 \\ 0 & 0 & e^{i\frac{\alpha_{31}}{2}} \end{pmatrix} \\ &= \begin{pmatrix} c_{12}c_{13} & s_{12}c_{13} & s_{13}e^{-i\delta} \\ -s_{12}c_{23} - c_{12}s_{23}s_{13}e^{i\delta} & c_{12}c_{23} - s_{12}s_{23}s_{13}e^{i\delta} & s_{23}c_{13} \\ s_{12}s_{23} - c_{12}c_{23}s_{13}e^{i\delta} & -c_{12}s_{23} - s_{12}c_{23}s_{13}e^{i\delta} & c_{23}c_{13} \end{pmatrix} \begin{pmatrix} 1 & 0 & 0 \\ 0 & e^{i\frac{\alpha_{21}}{2}} & 0 \\ 0 & 0 & e^{i\frac{\alpha_{31}}{2}} \end{pmatrix}, \end{aligned} \tag{1.3}$$

where θ_{12}, θ_{13}, θ_{23} are the three neutrino mixing angles, $\theta_{ij} \in [0, \pi/2]$, ($c_{ij} \equiv \cos\theta_{ij}$ and $s_{ij} \equiv \sin\theta_{ij}$), δ is the Dirac CP violation (CPV) phase, $\delta \in [0, 2\pi)$, and α_{21}, α_{31} are the two Majorana CPV phases [13], $\alpha_{ij} \in [0, 2\pi)$. The Majorana phases are present in the neutrino mixing matrix only if massive neutrinos are Majorana particles.

Together with three masses of ν_j, m_1, m_2, m_3, we obtain 7 parameters in the case of Dirac neutrinos (3 angles and 1 Dirac phase) and 9 parameters in the case of Majorana neutrinos (3 angles, 1 Dirac phase and 2 Majorana phases), which should be added to the list of 19 parameters of the SM to account for massive neutrinos. We recall that the 19 parameters of the SM are 3 charged lepton masses, 6 quark masses, 3 mixing angles and 1

[1] For the Cabibbo-Kobayashi-Maskawa (CKM) quark mixing matrix [10, 11] the parametrisation in eq. (1.3) (obviously, without the diagonal phase matrix on the right) has been first proposed in [12].

CPV phase of the CKM matrix, 3 gauge coupling constants, corresponding to each factor of the $SU(3) \times SU(2) \times U(1)$ gauge group of the SM, mass of the Higgs boson and its vacuum expectation value (VEV), and the QCD vacuum angle.

The neutrino oscillation probabilities depend on the neutrino masses via the neutrino mass squared differences $\Delta m^2_{ij} \equiv m^2_i - m^2_j$, $i \neq j$. In the case of 3-neutrino mixing there are two independent neutrino mass squared differences, which can be chosen as Δm^2_{21} and Δm^2_{31}. The standard choice has become $0 < \Delta m^2_{21} < |\Delta m^2_{31}|$ [8]. The smaller mass squared difference is responsible for the solar ν_e oscillations, while the larger one drives the atmospheric and accelerator ν_μ and $\overline{\nu}_\mu$ oscillations. For this reason, Δm^2_{21} and Δm^2_{31} are sometimes referred to as the *solar* and *atmospheric* neutrino mass squared differences.

At present, the sign of Δm^2_{31} is unknown. This gives rise to two possible types of the neutrino mass spectrum:

- spectrum with *normal ordering (NO)*, for which

$$m_1 < m_2 < m_3\,, \quad m_2 = \sqrt{m_1^2 + \Delta m^2_{21}}\,, \quad m_3 = \sqrt{m_1 + \Delta m^2_{31}}\,; \tag{1.4}$$

- spectrum with *inverted ordering (IO)*, for which

$$m_3 < m_1 < m_2\,, \quad m_1 = \sqrt{m_3^2 + \Delta m^2_{23} - \Delta m^2_{21}}\,, \quad m_2 = \sqrt{m_3^2 + \Delta m^2_{23}}\,. \tag{1.5}$$

Note that we have expressed the neutrino masses in terms of the (unknown at the moment) lightest neutrino mass, m_1 for NO and m_3 for IO, the solar neutrino mass squared difference Δm^2_{21} and the largest positive mass squared difference in each case, i.e., Δm^2_{31} for NO and Δm^2_{23} for IO.

All the neutrino oscillation parameters except for the Dirac CPV phase δ, i.e., $\sin^2\theta_{12}$, $\sin^2\theta_{13}$, $\sin^2\theta_{23}$, Δm^2_{21} and Δm^2_{31} (Δm^2_{23}) in the case of NO (IO) neutrino mass spectrum, have been determined with a relatively high precision in the latest global analyses of the neutrino oscillation data [14, 15] (see also [16]). In Table 1.1 we present the best fit values, 1σ, 2σ and 3σ allowed ranges of the neutrino oscillation parameters found in [14]. The best fit values of $\sin^2\theta_{ij}$ given in the table translate to $\theta_{12} \approx 33.02^\circ$, $\theta_{13} \approx 8.43^\circ$ (8.45°), $\theta_{23} \approx 40.7^\circ$ (50.1°) for the NO (IO) neutrino mass spectrum. Thus, the observed pattern of neutrino mixing is very different from that of quark mixing, for which the corresponding mixing angles read: $\theta^q_{12} \approx 13.00^\circ$, $\theta^q_{13} \approx 0.211^\circ$ and $\theta^q_{23} \approx 2.42^\circ$ [17].

It follows from the results presented in Table 1.1 that the 1σ relative uncertainties in the determination of the oscillation parameters, defined as $(x_{\rm up} - x_{\rm low})/[3\,(x_{\rm up} + x_{\rm low})]$, where $x_{\rm up}$ ($x_{\rm low}$) is the upper (lower) 3σ bound on a parameter x, read: 5.7% ($\sin^2\theta_{12}$), 4% ($\sin^2\theta_{13}$), 8% ($\sin^2\theta_{23}$), 2.3% (Δm^2_{21}) and 1.6% (Δm^2_{31}, Δm^2_{23}).

What concerns the Dirac CPV phase δ, the latest global analysis [14] disfavours values of δ in the range 0.17π–0.76π (0.15π–0.69π) in the case of NO (IO) spectrum at more than 3σ confidence level (C.L.), thus strengthening the hint found in the earlier global fits [16, 18, 19] that δ lies around $3\pi/2$. If δ is neither 0 nor π, CP invariance in the lepton sector does not hold. In this case, taking into account the measured values of the neutrino mixing angles, δ generates CP-violating effects in neutrino oscillations, i.e., a difference between the probabilities $P(\nu_\ell \to \nu_{\ell'})$ and $P(\overline{\nu}_\ell \to \overline{\nu}_{\ell'})$, $\ell \neq \ell' = e$, μ, τ, of $\nu_\ell \to \nu_{\ell'}$ and $\overline{\nu}_\ell \to \overline{\nu}_{\ell'}$ oscillations in vacuum [13, 20, 21].

The magnitude of CP-violating effects in neutrino oscillations is controlled by the rephasing invariant $J_{\rm CP}$ [22]:

$$J_{\rm CP} = {\rm Im}\left(U^*_{e1}\,U^*_{\mu 3}\,U_{e3}\,U_{\mu 1}\right)\,, \tag{1.6}$$

Table 1.1. The best fit values, 1σ, 2σ and 3σ ranges of the neutrino oscillation parameters obtained in the global analysis of the neutrino oscillation data performed in [14].

Parameter	Best fit	1σ range	2σ range	3σ range
$\sin^2\theta_{12}/10^{-1}$	2.97	2.81–3.14	2.65–3.34	2.50–3.54
$\sin^2\theta_{13}/10^{-2}$ (NO)	2.15	2.08–2.22	1.99–2.31	1.90–2.40
$\sin^2\theta_{13}/10^{-2}$ (IO)	2.16	2.07–2.24	1.98–2.33	1.90–2.42
$\sin^2\theta_{23}/10^{-1}$ (NO)	4.25	4.10–4.46	3.95–4.70	3.81–6.15
$\sin^2\theta_{23}/10^{-1}$ (IO)	5.89	4.17–4.48 $\oplus$ 5.67–6.05	3.99–4.83 $\oplus$ 5.33–6.21	3.84–6.36
δ/π (NO)	1.38	1.18–1.61	1.00–1.90	0–0.17 $\oplus$ 0.76–2
δ/π (IO)	1.31	1.12–1.62	0.92–1.88	0–0.15 $\oplus$ 0.69–2
$\Delta m^2_{21}/10^{-5}$ eV^2	7.37	7.21–7.54	7.07–7.73	6.93–7.96
$\Delta m^2_{31}/10^{-3}$ eV^2 (NO)	2.56	2.53–2.60	2.49–2.64	2.45–2.69
$\Delta m^2_{23}/10^{-3}$ eV^2 (IO)	2.54	2.51–2.58	2.47–2.62	2.42–2.66

which is analogous to the Jarlskog invariant of the CKM matrix [23, 24]. In the standard parametrisation of the PMNS matrix, the rephasing invariant reads

$$J_{\rm CP} = \frac{1}{8}\sin 2\theta_{12}\sin 2\theta_{23}\sin 2\theta_{13}\cos\theta_{13}\sin\delta\,. \tag{1.7}$$

Thus, taking into account a relatively good precision in the determination of the neutrino mixing angles, the size of CP-violating effects in neutrino oscillations depends on the value of δ, which has yet to be determined with higher confidence. Using the best fit values of $\sin^2\theta_{ij}$ and δ from Table 1.1, we find $J_{\rm CP} \approx -0.0301$ (-0.0267) for the NO (IO) neutrino mass spectrum. If the current best fit value of δ does not change significantly in the future, CP-violating effects in neutrino oscillations will be relatively large.

Establishing the status of Dirac CP violation is among the highest priority goals of the research programmes of the current and future planned accelerator long-baseline (LBL) neutrino oscillation experiments. The Tokai to Kamioka (T2K) [25–28] and NuMI[2] Off-Axis ν_e Appearance (NOνA) [29–31] experiments in Japan and the USA, respectively, are currently taking data. The T2HK experiment [32], in which the future Hyper-Kamiokande (Hyper-K) detector is planned to be used as a far detector instead of the Super-K detector used in T2K, and the Deep Underground Neutrino Experiment (DUNE) [33–36] in the USA are presently being developed. If δ is indeed around $3\pi/2$, T2HK and DUNE will be able to establish CP violation at more than 5σ C.L.

Unlike the Dirac phase, the Majorana phases α_{21} and α_{31} do not affect the flavour neutrino oscillation probabilities $P(\nu_\ell \to \nu_{\ell'})$ and $P(\overline{\nu}_\ell \to \overline{\nu}_{\ell'})$ [13, 37]. However, they are very important for processes characteristic for massive *Majorana* neutrinos, in which the total lepton charge L changes by two units, $\Delta L = 2$ (see, e.g., [38, 39] for reviews). One widely discussed and experimentally relevant example is *neutrinoless double beta decay* ($(\beta\beta)_{0\nu}$-decay),

$$(A, Z) \;\to\; (A, Z+2) + e^- + e^-\,, \tag{1.8}$$

(see, e.g., [40–42] and also [43, 44] for the latest reviews), which we will discuss in Chapter 4. The predictions for the rates of the lepton flavour violating processes, $\mu \to e + \gamma$ and

[2] NuMI stands for Neutrinos at the Main Injector.

$\mu \to 3\,e$ decays, $\mu - e$ conversion in nuclei, etc., in theories of neutrino mass generation with massive Majorana neutrinos also depend on the Majorana phases (see, e.g., [45–47]).

In addition, there exists the intriguing possibility that the Dirac phase and/or the Majorana phases in the PMNS matrix can provide the CP violation necessary for the generation of the observed matter-antimatter asymmetry of the Universe [48, 49]. This possibility can be realised within the leptogenesis scenario of the baryon asymmetry generation [50, 51], which is based on the type I seesaw mechanism of neutrino mass generation [52–55].

Depending on the *absolute neutrino mass scale*, i.e., the value of the lightest neutrino mass, which is at present unknown, the neutrino mass spectrum can be

- *normal hierarchical (NH)*, if $m_1 \ll m_2 < m_3$ and thus

$$m_2 \approx \sqrt{\Delta m^2_{21}} \approx 0.0086 \text{ eV} \quad \text{and} \quad m_3 \approx \sqrt{\Delta m^2_{31}} \approx 0.0506 \text{ eV}\,;$$

- *inverted hierarchical (IH)*, if $m_3 \ll m_1 < m_2$ and thus, neglecting also $\Delta m^2_{21}/\Delta m^2_{23} \approx 0.03$,

$$m_1 \approx m_2 \approx \sqrt{\Delta m^2_{23}} \approx 0.0504 \text{ eV}\,;$$

- *quasi-degenerate (QD)*, if $m_1 \approx m_2 \approx m_3$, and thus

$$m^2_j \gg \Delta m^2_{31}\ (\Delta m^2_{23})\,, \quad m_j \gtrsim 0.1 \text{ eV}\,, \quad j = 1, 2, 3\,.$$

Here we have used the best fit values of the neutrino mass squared differences from Table 1.1.

All the three possibilities above are compatible with the existing limits on the absolute neutrino mass scale. The most sensitive model-independent and direct method of determining the neutrino mass is the investigation of the endpoint region of a β-decay,

$$(A, Z) \to (A, Z+1) + e^- + \overline{\nu}_e\,, \tag{1.9}$$

spectrum [56, 57]. Usually the "average electron (anti)neutrino mass" $m_{\overline{\nu}_e}$ is determined:

$$m^2_{\overline{\nu}_e} = \sum_{j=1}^{3} m^2_j\,|U^2_{ej}|\,. \tag{1.10}$$

This sum averages over all the three neutrino mass eigenstates ν_j contributing to the (anti)electron neutrino and no phases of the PMNS matrix U enter, i.e., the decay modes into the different ν_j states add incoherently (see, e.g., [58]). The most stringent upper bounds on $m_{\overline{\nu}_e}$ have been obtained in experiments measuring the endpoint of the electron spectrum in the β-decay of tritium,

$$^3\text{H} \to {}^3\text{He}^+ + e^- + \overline{\nu}_e\,. \tag{1.11}$$

Namely, the Troitsk and Mainz neutrino mass experiments set, respectively, the following limits:

$$m_{\overline{\nu}_e} < 2.05 \text{ eV} \ \ [59] \qquad \text{and} \qquad m_{\overline{\nu}_e} < 2.3 \text{ eV} \ \ [60]\,, \tag{1.12}$$

both limits are at 95% C.L. The Karlsruhe Tritium Neutrino (KATRIN) experiment plans to improve this limit by one order of magnitude down to 0.2 eV (90% C.L.) or discover

the actual mass at 5σ, if it turns out to be larger than 0.35 eV [61]. Thus, this experiment will probe the region of the QD neutrino mass spectrum. For a review on direct neutrino mass experiments see, e.g., [62].

Cosmology also provides information on the absolute neutrino mass scale. The relevant cosmological observable is the sum of neutrino masses $\sum_j m_j$. Assuming a modified by three *degenerate* massive neutrinos version of the Λ Cold Dark Matter (ΛCDM) model, the Planck collaboration has obtained the following limit [63]:

$$\sum_j m_j < 0.23 \text{ eV} \quad (95\% \text{ C.L.}) \,. \tag{1.13}$$

This bound has been obtained taking into account the cosmic microwave background (CMB) temperature power spectrum data, low multipole, $\ell < 30$, polarisation data, results on gravitational lensing, and in addition, baryon acoustic oscillation (BAO) measurements and supernovae data. The sensitivity to $\sum_j m_j$ is planned to be improved by the future Euclid mission [64]. Note, however, that the cosmological bounds are to some extent model and analysis dependent.

Thus, the data show that neutrino masses are much smaller than the masses of all the other fermions present in the SM. This fact points towards the existence of a new fundamental scale in particle physics, i.e., to new physics beyond that predicted by the SM.

1.2 Discrete flavour symmetries

The masses of quarks, charged leptons and neutrinos, and the forms of the quark and neutrino mixing matrices result from the corresponding mass matrices formulated in the flavour basis. Let us briefly consider how this happens in the lepton sector. After electroweak (EW) symmetry breaking the charged lepton mass term reads

$$\overline{\ell_L}\, M_e\, \ell_R + \text{h.c.}, \tag{1.14}$$

where $\ell_L = (e_L, \mu_L, \tau_L)^T$, $\ell_R = (e_R, \mu_R, \tau_R)^T$, and M_e is the charged lepton mass matrix. What concerns neutrinos, the existing data imply that the flavour neutrinos ν_ℓ (antineutrinos $\overline{\nu}_\ell$) produced in weak interaction processes are predominantly LH (right-handed (RH)) [8]. Using only the LH fields $\nu_{\ell L}$, one can construct the so-called *Majorana mass term*:

$$\overline{(\nu_L)^c}\, M_\nu\, \nu_L + \text{h.c.}, \tag{1.15}$$

where $\nu_L = (\nu_{eL}, \nu_{\mu L}, \nu_{\tau L})^T$, $(\nu_{\ell L})^c = C\, \overline{\nu_{\ell L}}^T$, C being the charge-conjugation matrix, and M_ν is the neutrino Majorana mass matrix. If the RH neutrino fields N_{iR}, $i = 1, ..., n$, exist, then one can build also the *Dirac mass term*:

$$\overline{N_R}\, M_\nu^{\text{D}}\, \nu_L + \text{h.c.}, \tag{1.16}$$

with $N_R = (N_{1R}, ..., N_{nR})$, and M_ν^{D} being the neutrino Dirac mass matrix.

Diagonalising the charged lepton and neutrino mass matrices, we can go to the mass basis in which the charged lepton and neutrino fields possess definite masses. Namely, since M_e is a complex matrix, it can be diagonalised as

$$U_e^\dagger\, M_e\, V_e = \text{diag}(m_e, m_\mu, m_\tau) \,, \tag{1.17}$$

with U_e and V_e being 3×3 unitary matrices. The neutrino Majorana mass matrix M_ν is a complex symmetric matrix. Thus, it can be diagonalised by a unitary matrix U_ν as follows (see, e.g., [38]):

$$U_\nu^T \, M_\nu \, U_\nu = \mathrm{diag}(m_1, m_2, m_3) \, . \tag{1.18}$$

In the case of Dirac neutrinos, diagonalisation of M_ν^{D} is analogous to that of M_e in eq. (1.17), namely,

$$V_\nu^\dagger \, M_\nu^{\mathrm{D}} \, U_\nu = \mathrm{diag}(m_1, m_2, m_3) \, , \tag{1.19}$$

where V_ν and U_ν are unitary matrices. Expressing the LH charged lepton and neutrino flavour fields, which take part in the CC weak interactions, eq. (1.1), in terms of the fields with definite masses, we find that the PMNS matrix is given by

$$U = U_e^\dagger \, U_\nu \tag{1.20}$$

for both Majorana and Dirac neutrinos. Thus, we see that the structure of the neutrino mixing matrix U originates from the forms of the charged lepton and neutrino mass matrices.

The fundamental question one would like to answer is whether there exists any organising principle which dictates the flavour structures of the mass matrices M_e and M_ν, and thus explains the observed neutrino mixing pattern. We share the viewpoint of the author of [65], who writes: *"We believe, and we are not alone in holding this view, that with the observed pattern of neutrino mixing Nature is "sending" us a message. The message is encoded in the values of the neutrino mixing angles, leptonic CP violation phases and neutrino masses."* In the present thesis, we try to decipher the Nature's message relying on symmetry principles, which proved to be so powerful in particle physics. Namely, we take the view that the forms of the mass matrices, and hence the observed neutrino mixing pattern, are dictated by a *flavour symmetry*.

This is one of the possible approaches to the flavour problem, which, however, can be motivated by the data on neutrino mixing summarised in Section 1.1. Indeed, inspecting Table 1.1, we see that the best fit values of θ_{12} and θ_{23} deviate from the possible symmetry value of $\pi/4$ (the case of maximal mixing) by approximately 0.2 and 0.08, respectively, while the best fit value of θ_{13} deviates from 0 (no mixing) by approximately 0.15. Note that these corrections are of order of or smaller than the Cabibbo angle $\theta_{12}^q \approx 0.225$, which might hint on a possible connection between the quark and lepton sectors. This connection can be realised, e.g., within grand unified theories (GUTs) [66, 67].

A flavour or *family* symmetry is sometimes referred to as a *horizontal* symmetry, as opposed to a GUT symmetry which unifies quarks and leptons within a family. A flavour symmetry can be either Abelian or non-Abelian. The idea of an Abelian flavour symmetry goes back to 1978, when Colin Froggatt and Holger Nielsen proposed to explain the hierarchies of the quark masses and mixing angles in terms of an underlying $U(1)_{\mathrm{FN}}$ symmetry [68]. Namely, in their set-up, the three generations of quark fields are assumed to have different charges under $U(1)_{\mathrm{FN}}$. Hence, the Yukawa interaction terms of the form

$$\overline{Q_{iL}} \, H \, q_{jR} \, , \tag{1.21}$$

where Q_{iL} and q_{jR}, $i, j = 1, 2, 3$, are the quark weak doublets and singlets, respectively, and H is the Higgs doublet, have positive integer charges n_{ij}. These charges get compensated by introducing a scalar field ϕ with a $U(1)_{\mathrm{FN}}$ charge of -1 and multiplying eq. (1.21) by

$$c_{ij} \left(\frac{\phi}{\Lambda} \right)^{n_{ij}} \, ,$$

with c_{ij} being order one coefficients and Λ being a high-energy scale. The field ϕ is called *flavon*. After ϕ acquires a VEV, $\langle\phi\rangle$, which breaks the $U(1)_{\rm FN}$ symmetry, the matrix of Yukawa couplings $\mathcal{Y}_{ij}$ reads

$$\mathcal{Y}_{ij} = c_{ij}\,\epsilon^{n_{ij}}\,, \quad \text{where} \quad \epsilon = \frac{\langle\phi\rangle}{\Lambda}\,.$$

Providing appropriate assignment of the $U(1)_{\rm FN}$ charges, the matrix $\mathcal{Y}_{ij}$ has hierarchical structure. Thus, this approach is mainly useful to explain hierarchies between the Yukawa couplings and not their absolute values, since the coefficients c_{ij} are undetermined.

A description of non-hierarchical flavour structures such as the observed pattern of neutrino mixing requires a non-Abelian flavour symmetry. In this case, the three generations of leptons (and quarks) can be unified into multiplets which transform under certain irreducible representations of the flavour symmetry group G_f. If one aims at unification of all three families at high energies, G_f must contain a 3-dimensional irreducible representation. Requiring this representation to exist restricts G_f to be $U(3)$ or a subgroup thereof.

The flavour symmetry group can be either continuous or *discrete*.[3] The latter allows for rotations in the flavour space by fixed (large) angles, which is particularly attractive in view of the fact that two of the three neutrino mixing angles are large. Before the discovery of a non-zero value of the *reactor* mixing angle θ_{13} by the Double Chooz [69], Daya Bay [70] and RENO [71] experiments in 2012, neutrino oscillation data were highly compatible with the tri-bimaximal (TBM) mixing pattern [72–75] (see also [76]) characterised by $\sin^2\theta_{12} = 1/3$, $\sin^2\theta_{23} = 1/2$ and $\sin^2\theta_{13} = 0$. This highly symmetric mixing pattern can be derived from small non-Abelian discrete groups such as A_4 [77–79]. A_4 is the group of even permutations of four objects, which is isomorphic to the group of rotational symmetries of a regular tetrahedron. In light of the present neutrino oscillation data implying the non-zero value of the reactor angle and pointing to a deviation of the atmospheric angle from $\pi/4$ and a non-trivial value of the Dirac CPV phase δ (see Table 1.1), TBM mixing is ruled out. However, it can still be viewed as a leading order approximation which requires certain corrections. In the next chapters we will study possible corrections to this and other symmetric mixing patterns in great detail. Now let us briefly review the basic concepts of the approach to neutrino mixing based on a discrete flavour symmetry (see [80–82] for reviews).

The approach of interest is based on the assumption of the existence at some high-energy scale of a (lepton) flavour symmetry corresponding to a non-Abelian discrete group G_f. Different fields contained in a theory transform under irreducible representations of the flavour symmetry group. Namely, a field $\varphi(x)$ in a generic irreducible representation $\mathbf{r}$ of G_f transforms under the action of G_f as

$$\varphi(x) \xrightarrow{G_f} \rho_{\mathbf{r}}(g)\,\varphi(x)\,, \quad g \in G_f\,, \tag{1.22}$$

where $\rho_{\mathbf{r}}(g)$ is the unitary representation matrix for the element g in the irreducible representation $\mathbf{r}$. The theory at high energies is invariant under these transformations. Usually, the representation under which the LH lepton fields are transformed is assumed to be 3-dimensional, because one aims at unification of the three lepton families at high energies.

[3] Throughout this thesis under *discrete* groups we will mean those with finite number of elements. They are also called *finite* groups. Note that there are also discrete groups with infinite number of elements as, e.g., the braid groups.

At low energies the flavour symmetry has necessarily to be broken such that the three flavours can be distinguished. In specific models G_f gets broken spontaneously after flavon fields ϕ_i, which are neutral under the SM gauge group, but transform in certain irreducible representations of G_f, acquire VEVs. After flavour symmetry breaking some subgroups of G_f may remain unbroken in the charged lepton and neutrino sectors. We will denote these subgroups as G_e and G_ν, respectively, and refer to them as *residual symmetries* of the charged lepton and neutrino mass matrices.[4] These symmetries must be Abelian for the reason explained below.

The largest possible exact symmetry of the neutrino Majorana mass matrix M_ν, eq. (1.15), having three non-zero and non-degenerate eigenvalues, is a $Z_2 \times Z_2 \times Z_2$ symmetry. The largest possible exact symmetry of the charged lepton Dirac mass matrix M_e, eq. (1.14), is $U(1) \times U(1) \times U(1)$. Restricting ourselves to the case in which G_f is a subgroup of $SU(3)$ instead of $U(3)$, the indicated largest possible exact symmetries reduce respectively to $Z_2 \times Z_2$ and $U(1) \times U(1)$ because of the special determinant condition imposed from $SU(3)$. The residual symmetries G_e and G_ν, being subgroups of G_f, should also be contained in $U(1) \times U(1)$ and $Z_2 \times Z_2$ ($U(1) \times U(1)$) for massive Majorana (Dirac) neutrinos, respectively. Thus, G_e and G_ν must be Abelian.

The residual symmetries constrain the forms of the 3×3 unitary matrices U_e and U_ν, and thus, the form of the PMNS matrix U (see eq. (1.20)). The matrix U_e diagonalises the product $M_e M_e^\dagger$ as

$$U_e^\dagger \, M_e M_e^\dagger \, U_e = \mathrm{diag}(m_e^2, m_\mu^2, m_\tau^2) \, . \tag{1.23}$$

The invariance of the charged lepton mass term under G_e, i.e., under transformations

$$\ell_L(x) \xrightarrow{G_e} \rho_{\mathbf{3}}(g_e) \, \ell_L(x) \, , \quad g_e \in G_e \, , \tag{1.24}$$

where the three generations of the LH lepton fields are assumed to transform in a 3-dimensional irreducible representation **3** of G_f, implies

$$\rho_{\mathbf{3}}(g_e)^\dagger \, M_e M_e^\dagger \, \rho_{\mathbf{3}}(g_e) = M_e M_e^\dagger \, , \quad g_e \in G_e \, . \tag{1.25}$$

As can be seen from this equation, the matrices $\rho_{\mathbf{3}}(g_e)$ and $M_e M_e^\dagger$ commute, implying that they are diagonalised by the same matrix U_e, namely,

$$U_e^\dagger \, \rho_{\mathbf{3}}(g_e) \, U_e = \rho_{\mathbf{3}}(g_e)^{\mathrm{diag}} \, , \quad g_e \in G_e \, . \tag{1.26}$$

Thus, knowing the matrices $\rho_{\mathbf{3}}(g_e)$, one can derive the form of the matrix U_e.

Analogously, the invariance of the neutrino Majorana mass term in eq. (1.15) under G_ν, which acts on $\nu_L(x)$ as

$$\nu_L(x) \xrightarrow{G_\nu} \rho_{\mathbf{3}}(g_\nu) \, \nu_L(x) \, , \quad g_\nu \in G_\nu \, , \tag{1.27}$$

implies

$$\rho_{\mathbf{3}}(g_\nu)^T \, M_\nu \, \rho_{\mathbf{3}}(g_\nu) = M_\nu \, , \quad g_\nu \in G_\nu \, . \tag{1.28}$$

It is not difficult to show that also in this case the matrices $\rho_{\mathbf{3}}(g_\nu)$ and $M_\nu^\dagger M_\nu$ [5] commute, and therefore they can be diagonalised simultaneously by the same matrix U_ν, i.e.,

$$U_\nu^\dagger \, \rho_{\mathbf{3}}(g_\nu) \, U_\nu = \rho_{\mathbf{3}}(g_\nu)^{\mathrm{diag}} \, , \quad g_\nu \in G_\nu \, . \tag{1.29}$$

[4] Note that the residual symmetries can be bigger than subgroups of G_f, if accidental symmetries are present.

[5] We assume the right-left convention for the neutrino mass term, i.e., that used in eq. (1.15).

Again, once the matrices $\rho_{\mathbf{3}}(g_\nu)$ are specified, the form of U_ν is known up to diagonal phase matrix on the right containing two phases which contribute to the Majorana phases $\alpha_{21,31}$ and permutations of columns. In the case of Dirac neutrinos with the mass term given in eq. (1.16), the condition in eq. (1.28) is modified as follows:

$$\rho_{\mathbf{3}}(g_\nu)^\dagger \, M_\nu^{\mathrm{D}\dagger} M_\nu^{\mathrm{D}} \, \rho_{\mathbf{3}}(g_\nu) = M_\nu^{\mathrm{D}\dagger} M_\nu^{\mathrm{D}} \,, \quad g_\nu \in G_\nu \,. \tag{1.30}$$

The types of residual symmetry allowed in this case and discussed in detail in Chapter 2 are the same as those of the charged lepton mass term.

In the case of Majorana neutrinos, there are two possible types of the residual symmetry G_ν. It can be either a $Z_2 \times Z_2$ symmetry (which sometimes is identified in the literature with the Klein four group) or a Z_2 symmetry. These two types characterise two approaches in model building: *direct* approach when $G_\nu = Z_2 \times Z_2$, and *semi-direct* approach when $G_\nu = Z_2$ [82]. Since the neutrino Majorana mass matrix M_ν is always symmetric under a certain $Z_2 \times Z_2$ symmetry (see, e.g., [82] for a proof), the second Z_2 factor in semi-direct models arises accidentally. To be more specific, below we present a concrete example of how TBM mixing arises in the direct and semi-direct approaches.

First, let us consider S_4 as a flavour symmetry group. S_4 is the symmetric group of permutations of four objects. This group is isomorphic to the group of rotational symmetries of a cube. It has 24 elements in total. S_4 can be defined in terms of three *generators* S, T and U, satisfying [83]

$$S^2 = T^3 = U^2 = (ST)^3 = (SU)^2 = (TU)^2 = (STU)^4 = 1 \,, \tag{1.31}$$

with 1 being the identity element of the group. In the basis for S_4 from [84] the matrices for the generators S, T and U in the representation **3** read[6]

$$S = \frac{1}{3}\begin{pmatrix} -1 & 2 & 2 \\ 2 & -1 & 2 \\ 2 & 2 & -1 \end{pmatrix} , \quad T = \begin{pmatrix} 1 & 0 & 0 \\ 0 & \omega^2 & 0 \\ 0 & 0 & \omega \end{pmatrix} \quad \text{and} \quad U = -\begin{pmatrix} 1 & 0 & 0 \\ 0 & 0 & 1 \\ 0 & 1 & 0 \end{pmatrix} , \tag{1.32}$$

where $\omega = e^{2\pi i/3}$. It is worth noting that this basis for S_4 has been worked out in [84] in order to connect S_4 downwards to A_4 generated by S and T. Indeed, S and T in eq. (1.32) represent the widely known Altarelli-Feruglio basis for A_4 [85]. S and U are order two elements (because their square is 1) and each of them generates a Z_2 subgroup of S_4, namely, $Z_2^S = \{1, S\}$ and $Z_2^U = \{1, U\}$. Moreover, since they commute, they form the $Z_2^S \times Z_2^U = \{1, S, U, SU\}$ subgroup of S_4. We notice further that both S and U are diagonalised by the TBM mixing matrix U_{TBM}, which reads

$$U_{\mathrm{TBM}} = \begin{pmatrix} \sqrt{\frac{2}{3}} & \sqrt{\frac{1}{3}} & 0 \\ -\sqrt{\frac{1}{6}} & \sqrt{\frac{1}{3}} & -\sqrt{\frac{1}{2}} \\ -\sqrt{\frac{1}{6}} & \sqrt{\frac{1}{3}} & \sqrt{\frac{1}{2}} \end{pmatrix} . \tag{1.33}$$

T is an element of order three, and thus, it generates the $Z_3^T = \{1, T, T^2\}$ subgroup of S_4. If $G_e = Z_3^T$ and $G_\nu = Z_2^S \times Z_2^U$, we have $U_e = \mathrm{diag}(1, 1, 1)$ and $U_\nu = U_{\mathrm{TBM}}$. Thus, the PMNS matrix $U = U_{\mathrm{TBM}}$. This is an example of the direct approach.

[6] For simplicity we use the same notation (S, T and U) for the generators and their 3-dimensional representation matrices.

Now let us consider $G_f = A_4$. As we have mentioned earlier, A_4 is the group of even permutations of four objects, and it is isomorphic to the group of rotational symmetries of a regular tetrahedron. A_4 is a subgroup of S_4 consisting of 12 elements. It can be obtained from S_4 by simply dropping U generator, which leads to the following presentation rules:

$$S^2 = T^3 = (ST)^3 = 1\,. \tag{1.34}$$

Now G_f can be broken down to Z_2^S in the neutrino sector. In order to gain TBM mixing the U symmetry must arise accidentally. An example of such a semi-direct model is provided by the famous Altarelli-Feruglio A_4 model of TBM mixing [79, 85].

In principle, the flavour symmetry G_f can be fully broken in the neutrino sector, such that no Z_2 factor of the low-energy $Z_2 \times Z_2$ symmetry forms a subgroup of G_f. This is so-called *indirect* model building approach. Finally, we note that the classification in the direct, semi-direct and indirect approaches is entirely based on the origin of the $Z_2 \times Z_2$ symmetry of the neutrino Majorana mass matrix, formulated in a basis of (approximately) *diagonal* charged leptons (see [82] for further details).

Except for A_4 and S_4, many discrete groups have been extensively studied in the literature, including S_3, T', A_5, $\Delta(27)$, $\Delta(96)$ and D_n (we refer the reader to ref. [81] and to Table 2 in [82] for the original references), as well as series $\Delta(6n^2)$ [86] and $\Sigma(n\phi)$ [87].[7] The choice of these groups is related to the fact that they lead to values of the neutrino mixing angles, which can differ from the measured values at most by subleading corrections.

For instance, the groups A_4, S_4 and T' are commonly utilised to generate TBM mixing, as we have already seen. The group S_4 can also be used to generate bimaximal (BM) mixing [88–90].[8] This symmetric mixing pattern is characterised by maximal *solar* and *atmospheric* mixings, i.e., $\sin^2\theta_{12} = \sin^2\theta_{23} = 1/2$, and by $\theta_{13} = 0$. The BM mixing matrix $U_{\rm BM}$ reads

$$U_{\rm BM} = \begin{pmatrix} \frac{1}{\sqrt{2}} & \frac{1}{\sqrt{2}} & 0 \\ -\frac{1}{2} & \frac{1}{2} & -\frac{1}{\sqrt{2}} \\ -\frac{1}{2} & \frac{1}{2} & \frac{1}{\sqrt{2}} \end{pmatrix}\,. \tag{1.35}$$

The group A_5, which is the group of even permutations of five objects, and which is isomorphic to the rotational symmetry group of an icosahedron, can be utilised to generate golden ratio type A (GRA) mixing [92–94]:

$$U_{\rm GRA} = \begin{pmatrix} \sqrt{\frac{r}{\sqrt{5}}} & \sqrt{\frac{1}{\sqrt{5}\,r}} & 0 \\ -\frac{1}{\sqrt{2}}\sqrt{\frac{1}{\sqrt{5}\,r}} & \frac{1}{\sqrt{2}}\sqrt{\frac{r}{\sqrt{5}}} & -\frac{1}{\sqrt{2}} \\ -\frac{1}{\sqrt{2}}\sqrt{\frac{1}{\sqrt{5}\,r}} & \frac{1}{\sqrt{2}}\sqrt{\frac{r}{\sqrt{5}}} & \frac{1}{\sqrt{2}} \end{pmatrix}\,, \tag{1.36}$$

where $r = (1+\sqrt{5})/2$ is the golden ratio (a solution of $x^2 - x - 1 = 0$). Thus, this mixing pattern is characterised by $\sin^2\theta_{12} = 1/(\sqrt{5}\,r) \approx 0.276$, $\sin^2\theta_{23} = 1/2$ and $\sin^2\theta_{13} = 0$.

The dihedral groups D_{10} and D_{12}, which are the symmetries (rotations and reflections) of a regular decagon and a regular dodecagon, can lead to golden ratio type B (GRB)

[7] We would like to note that the D_n groups, and, in particular, $S_3 \cong D_3$, do not admit 3-dimensional irreducible representations.

[8] Bimaximal mixing can also be a consequence of the conservation of the lepton charge $L' = L_e - L_\mu - L_\tau$ (LC) [91], supplemented by a $\mu - \tau$ symmetry.

mixing [95, 96] and hexagonal (HG) mixing [97, 98], respectively. D_{10} leads to $\theta_{12} = \pi/5$, which is the external angle of a regular decagon, and the GRB mixing matrix $U_{\rm GRB}$ reads

$$U_{\rm GRB} = \begin{pmatrix} \frac{r}{2} & \frac{1}{2}\sqrt{\frac{\sqrt{5}}{r}} & 0 \\ -\frac{1}{2\sqrt{2}}\sqrt{\frac{\sqrt{5}}{r}} & \frac{r}{2\sqrt{2}} & -\frac{1}{\sqrt{2}} \\ -\frac{1}{2\sqrt{2}}\sqrt{\frac{\sqrt{5}}{r}} & \frac{r}{2\sqrt{2}} & \frac{1}{\sqrt{2}} \end{pmatrix}, \tag{1.37}$$

which corresponds to $\sin^2\theta_{12} = \sqrt{5}/(4\,r) \approx 0.345$, $\sin^2\theta_{23} = 1/2$ and $\sin^2\theta_{13} = 0$. Analogously, D_{12} leads to $\theta_{12} = \pi/6$, which is the external angle of a regular dodecagon. The HG mixing matrix yields

$$U_{\rm HG} = \begin{pmatrix} \frac{\sqrt{3}}{2} & \frac{1}{2} & 0 \\ -\frac{1}{2\sqrt{2}} & \frac{\sqrt{3}}{2\sqrt{2}} & -\frac{1}{\sqrt{2}} \\ -\frac{1}{2\sqrt{2}} & \frac{\sqrt{3}}{2\sqrt{2}} & \frac{1}{\sqrt{2}} \end{pmatrix}. \tag{1.38}$$

Thus, in this case we have $\sin^2\theta_{12} = 1/4$, $\sin^2\theta_{23} = 1/2$ and $\sin^2\theta_{13} = 0$.

All these highly symmetric mixing patterns *per se* are nowadays ruled out. However, they still can be viewed as a leading order approximation which requires certain corrections. These corrections should be able to generate a non-zero value of θ_{13} as well as a possible deviation of θ_{23} from $\pi/4$. One obvious source of such corrections is the charged lepton sector. Namely, if a model is formulated in a basis of *non-diagonal* charged leptons, but the neutrino mass matrix is still invariant under certain residual symmetry, there will be a contribution to the PMNS matrix from the matrix U_e which diagonalises $M_e M_e^\dagger$ (cf. eq. (1.20)). This contribution can provide the requisite corrections to the symmetric mixing patterns discussed above. These *charged lepton corrections* will play central role in the neutrino mixing schemes constructed and discussed in the next chapters.

The current value of θ_{13} opens up a possibility to observe CP violation in neutrino oscillations, and thus, to establish the value of the Dirac CPV phase δ. In theories with discrete flavour symmetries the values of (some of) the mixing angles in the reference 3-neutrino mixing scheme we are going to consider in what follows, if not fixed, are often correlated between themselves. Moreover, there exists a correlation between the value of the Dirac CPV phase δ and the values of the three neutrino mixing angles θ_{12}, θ_{13} and θ_{23}, which includes also symmetry dependent fixed parameter(s) (see [99–107] and references quoted therein). These correlations are usually referred to as *neutrino mixing sum rules*. As we have already indicated, the sum rules for the Dirac phase δ, in particular, depend on the underlying symmetry form of the PMNS matrix [99–103] (see also, e.g., [104, 105, 107]), which in turn is determined by the assumed lepton favour symmetry that typically has to be broken, and by the residual unbroken symmetries in the charged lepton and neutrino sectors (see, e.g., [80, 81, 101, 103, 108]). They can be tested experimentally (see, e.g., [100, 104, 106, 109–111]). These tests can provide unique information about the possible existence of a new fundamental symmetry in the lepton sector, which determines the pattern of neutrino mixing [99]. Sufficiently precise experimental data on the neutrino mixing angles and on the Dirac CPV phase can also be used to distinguish between different possible underlying flavour symmetries leading to viable patterns of neutrino mixing.

The neutrino mixing sum rules constitute the main subject of the present thesis. In particular, in Chapter 2, we will systematically derive such sum rules for all types of the

residual symmetries G_e and G_ν of the charged lepton and neutrino mass terms, for which correlations between the mixing parameters are expected. Further, in Chapter 3, we will perform a comprehensive phenomenological analysis of predictions for the Dirac CPV phase δ in a number of phenomenologically interesting cases.

Before concluding this brief introduction to the discrete symmetry approach to neutrino mixing, we would like to point out that alternative approaches, such as *anarchy* [112–115], have been studied in the literature. In the anarchy paradigm the neutrino mixing angles are treated as environmental quantities. The main consequence of this approach is the absence of whatever correlations between the neutrino oscillation parameters. On the contrary, the most distinctive feature of the symmetry (*order*) approach is the correlations we have mentioned above. Recently, there was a new interesting proposal [116] generalising the current discrete symmetry approach. The author has considered a class of supersymmetric (SUSY) and *modular-invariant* models, in the simplest version of which Yukawa couplings are modular forms and the only flavon whose VEV breaks a flavour symmetry is the modulus, a complex field transforming in a certain way under the action of the modular group. In the particular case of modular forms being constant functions, the new construction reproduces a class of SUSY models with discrete flavour symmetries which has been extensively studied in the literature so far.

1.3 Generalised CP symmetry

Discrete flavour symmetries can also be combined with CP invariance in a non-trivial way [117, 118]. This, in particular, allows one to obtain predictions for the Majorana phases in the PMNS matrix, which otherwise remain typically unconstrained. Indeed, eq. (1.29), which represents the residual flavour symmetry constraint on the matrix U_ν, is invariant under re-phasing of columns of U_ν. This implies that U_ν, and thus, the PMNS matrix U, are defined up to re-phasing of columns, i.e., a flavour symmetry alone does not constrain the Majorana phases.

Let us first recall how CP transformations are defined in a consistent way without imposing any flavour symmetry. Taking into account the mass terms in eqs. (1.14) and (1.15) and the CC weak interactions described by eq. (1.1), we obtain the following Lagrangian (valid at energies below the EW symmetry breaking scale):

$$-\mathcal{L} = \overline{\ell_L}\, M_e\, \ell_R + \overline{(\nu_L)^c}\, M_\nu\, \nu_L + \frac{g}{\sqrt{2}}\, \overline{\ell_L}\, \gamma_\alpha\, \nu_L\, W^{\alpha\dagger} + \text{h.c.} \tag{1.39}$$

The so-called *generalised CP transformations* are defined as follows [119]:

$$\ell_L(x) \xrightarrow{CP} i X_L \gamma^0 C\, \overline{\ell_L}^T(x')\,, \tag{1.40}$$

$$\ell_R(x) \xrightarrow{CP} i X_R \gamma^0 C\, \overline{\ell_R}^T(x')\,, \tag{1.41}$$

$$\nu_L(x) \xrightarrow{CP} i X_L \gamma^0 C\, \overline{\nu_L}^T(x')\,, \tag{1.42}$$

where X_L and X_R are unitary matrices acting on flavour space and $x' = (t, -\mathbf{x})$. Note that the transformations of ℓ_L and ν_L should involve the same matrix X_L in order to preserve CP invariance of the CC weak interaction Lagrangian in the flavour basis. Then, the Lagrangian in eq. (1.39) conserves CP if and only if the charged lepton and neutrino mass matrices satisfy the following relations:

$$X_L^\dagger\, M_e\, X_R = M_e^*\,, \tag{1.43}$$

$$X_L^T\, M_\nu\, X_L = M_\nu^* \,. \tag{1.44}$$

We would like to notice that the "canonical" (traditional) CP transformations can be obtained from those given in eqs. (1.40)–(1.42) by setting both X_L and X_R to the identity matrix.

Now we turn to a theory that respects both a flavour symmetry and a *generalised CP symmetry*. Such a theory in addition to be invariant under the transformations from eq. (1.22), will remain unchanged under the generalised CP transformation given by

$$\varphi(x) \xrightarrow{CP} X_{\mathbf{r}}\, \varphi^*(x') \,, \tag{1.45}$$

where $X_{\mathbf{r}}$ is a unitary matrix, and the action of CP on the spinor indices given in eqs. (1.40)–(1.42) has been omitted for the case of φ being a spinor.

The form of $X_{\mathbf{r}}$ is constrained considerably due to the presence of a flavour symmetry [117,118]. Namely, if we first perform a generalised CP transformation, followed by a flavour symmetry transformation, and subsequently an inverse generalised CP transformation, we find

$$\varphi(x) \xrightarrow{CP} X_{\mathbf{r}}\, \varphi^*(x') \xrightarrow{G_f} X_{\mathbf{r}}\, \rho_{\mathbf{r}}(g)^*\, \varphi^*(x') \xrightarrow{CP^{-1}} X_{\mathbf{r}}\, \rho_{\mathbf{r}}(g)^*\, X_{\mathbf{r}}^{-1}\, \varphi(x) \,. \tag{1.46}$$

The theory should be invariant under this sequence of transformations, and thus, the resulting transformation must correspond to a flavour symmetry transformation (cf. eq. (1.22)) $\rho_{\mathbf{r}}(g')$, with g' being some element of G_f, i.e., we have

$$X_{\mathbf{r}}\, \rho_{\mathbf{r}}(g)^*\, X_{\mathbf{r}}^{-1} = \rho_{\mathbf{r}}(g') \,, \qquad g \,,\, g' \in G_f \,. \tag{1.47}$$

This equation defines the *consistency condition*, which has to be respected for consistent implementation of a generalised CP symmetry along with a flavour symmetry [117, 118].

Several comments on this consistency condition are in order.

- Equation (1.47) has to be satisfied for *all* irreducible representations $\mathbf{r}$ simultaneously, i.e., the elements g and g' must be the same for all $\mathbf{r}$.

- The generalised CP transformation $X_{\mathbf{r}}$ maps the group element g onto g'. Furthermore, it preserves the flavour symmetry group structure, i.e.,

  $$X_{\mathbf{r}}\, \rho_{\mathbf{r}}(g_1 g_2)^*\, X_{\mathbf{r}}^{-1} = X_{\mathbf{r}}\, \rho_{\mathbf{r}}(g_1)^*\, X_{\mathbf{r}}^{-1}\, X_{\mathbf{r}}\, \rho_{\mathbf{r}}(g_2)^*\, X_{\mathbf{r}}^{-1} = \rho_{\mathbf{r}}(g_1' g_2') \qquad \forall\, g_{1,2} \in G_f \,,$$

  $$X_{\mathbf{r}}\, \rho_{\mathbf{r}}(1)^*\, X_{\mathbf{r}}^{-1} = \rho_{\mathbf{r}}(1) \,,$$

  where 1 is the identity element of G_f, and therefore $X_{\mathbf{r}}$ realises a *homomorphism* of the flavour symmetry group G_f.

- For *faithful* representations $\mathbf{r}$, i.e., those for which $\rho_{\mathbf{r}}$ maps each element of G_f to a distinct matrix, eq. (1.47) defines a unique mapping of G_f to itself. In this case, $X_{\mathbf{r}}$ realises an *automorphism* of G_f.

- If $X_{\mathbf{r}}$ is a solution to eq. (1.47), then $e^{i\alpha} X_{\mathbf{r}}$, where α is an arbitrary phase, is also a solution. Moreover, if $X_{\mathbf{r}}$ is a solution to eq. (1.47), then $\rho_{\mathbf{r}}(h)\, X_{\mathbf{r}}$, where h is an element of G_f, is also a solution. Indeed, for $\rho_{\mathbf{r}}(h)\, X_{\mathbf{r}}$ we have

  $$\rho_{\mathbf{r}}(h)\, X_{\mathbf{r}}\, \rho_{\mathbf{r}}(g)^*\, X_{\mathbf{r}}^{-1}\, \rho_{\mathbf{r}}^{-1}(h) = \rho_{\mathbf{r}}(h)\, \rho_{\mathbf{r}}(g')\, \rho_{\mathbf{r}}(h^{-1}) = \rho_{\mathbf{r}}(h g' h^{-1}) \qquad \forall\, h \in G_f \,.$$

  Therefore the generalised CP transformation $\rho_{\mathbf{r}}(h)\, X_{\mathbf{r}}$ maps the group element g to $hg'h^{-1}$, i.e., to an element from the *conjugacy class* of g'. Thus, for a given irreducible representation $\mathbf{r}$, the consistency condition defines $X_{\mathbf{r}}$ up to an overall phase and a G_f transformation.

- It follows from eq. (1.47) that the elements g and g' must be of the same order.
- For a discrete flavour symmetry group G_f, it is sufficient to impose eq. (1.47) to the group's generators.

In ref. [117] the unitary matrix $X_{\mathbf{r}}$ has been chosen to be symmetric. In this way, one has

$$\varphi(x) \xrightarrow{CP} X_{\mathbf{r}}\, \varphi^*(x') \xrightarrow{CP} X_{\mathbf{r}}\, X_{\mathbf{r}}^*\, \varphi(x) = \varphi(x)\,, \tag{1.48}$$

i.e., the generalised CP transformation $X_{\mathbf{r}}$ applied twice to a field gives the field itself.[9] With this choice, it has been shown (see Appendix B in [117]) that combining the flavour symmetry group G_f with the group $H_{\rm CP}$ generated by the generalised CP transformation leads to a semi-direct product of these two groups, i.e., the full symmetry group $G_{\rm CP} = G_f \rtimes H_{\rm CP}$.

Analogously to flavour symmetry breaking, the full symmetry group $G_{\rm CP}$ can be broken in such a way, that $M_e\, M_e^\dagger$ and M_ν remain invariant under its subgroups $G^e_{\rm CP} = G_e \rtimes H^e_{\rm CP}$ and $G^\nu_{\rm CP} = G_\nu \rtimes H^\nu_{\rm CP}$, respectively. As in the previous section, we assume that the three generations of the LH lepton fields transform in a 3-dimensional irreducible representation $\mathbf{3}$ of G_f. Invariance of $M_e\, M_e^\dagger$ and M_ν under the residual symmetries $G^e_{\rm CP}$ and $G^\nu_{\rm CP}$ imply that in addition to eqs. (1.25) and (1.28), the following equations hold:

$$X^\dagger_{\mathbf{3}e}\, M_e M_e^\dagger\, X_{\mathbf{3}e} = \left(M_e M_e^\dagger\right)^*\,, \quad X_{\mathbf{3}e} \in H^e_{\rm CP}\,, \tag{1.49}$$

$$X^T_{\mathbf{3}\nu}\, M_\nu\, X_{\mathbf{3}\nu} = M_\nu^*\,, \quad X_{\mathbf{3}\nu} \in H^\nu_{\rm CP}\,. \tag{1.50}$$

Moreover, the consistency condition as that in eq. (1.47) has to be satisfied in each sector, i.e.,

$$X_{\mathbf{3}e}\, \rho_{\mathbf{3}}(g_e)^*\, X^{-1}_{\mathbf{3}e} = \rho_{\mathbf{3}e}(g'_e)\,, \qquad g_e\,,\, g'_e \in G_e\,, \tag{1.51}$$

$$X_{\mathbf{3}\nu}\, \rho_{\mathbf{3}}(g_\nu)^*\, X^{-1}_{\mathbf{3}\nu} = \rho_{\mathbf{3}\nu}(g'_\nu)\,, \qquad g_\nu\,,\, g'_\nu \in G_\nu\,. \tag{1.52}$$

The conditions in eqs. (1.49) and (1.50) restrict further the charged lepton and neutrino mass matrices, and thus, the form of the PMNS matrix.

It can be shown that the matrix $X_{\mathbf{3}\nu}$ has to be symmetric in order for all the three neutrino masses to be different [117, 120], as is required by experimental data. In Appendix A, we provide an explicit proof of this statement. In this case, eq. (1.50) leads to

$$U_\nu^\dagger\, X_{\mathbf{3}\nu}\, U_\nu^* = {\rm diag}(\pm 1, \pm 1, \pm 1)\,, \tag{1.53}$$

where the matrix U_ν diagonalises M_ν as in eq. (1.18) with real eigenvalues m_j, $j = 1, 2, 3$. Equation (1.53) is clearly not invariant under re-phasing of columns of U_ν. Thus, in the set-up with a residual generalised CP symmetry in the neutrino sector, also the Majorana phases in the PMNS matrix can be predicted.[10]

In the recent years, the approach involving both a discrete flavour symmetry and a generalised CP symmetry was extensively explored in the literature. The list of the considered flavour symmetry groups includes A_4 [118, 121], T' [122], S_4 [117, 120, 123–127],

[9] However, the authors of [117] comment that it is possible to generalise the requirement of $X_{\mathbf{r}}\, X_{\mathbf{r}}^* = 1_{\mathbf{r}\times\mathbf{r}}$ to $X_{\mathbf{r}}\, X_{\mathbf{r}}^*$ being a flavour symmetry transformation, as we can appreciate from eq. (1.48).

[10] As long as there are no unconstrained contributions to them from the charged lepton sector (see Chapter 4 for such examples).

A_5 [128–131], $\Delta(27)$ [132], $\Delta(48)$ [133, 134] and $\Delta(96)$ [135], as well as series $\Delta(3n^2)$ [136, 137] and $\Delta(6n^2)$ [137–139].

In many of the studies listed above the full symmetry group $G_{\rm CP}$ is broken down in the charged lepton sector to a residual symmetry $G^e_{\rm CP}$ such that it fixes completely the matrix U_e, e.g., $G^e_{\rm CP} = Z_3$, while the residual symmetry of the neutrino sector $G^\nu_{\rm CP}$ is chosen to be $Z_2 \times H^\nu_{\rm CP}$, which determines U_ν up to right multiplication by a rotation matrix on a free angle θ^ν (see, e.g., [117]). In this case, all the six mixing parameters (three angles and three phases) only depend on this single parameter. For example, in the set-up considered in [117] (see also [120]) and based on $G_{\rm CP} = S_4 \rtimes H_{\rm CP}$, in the case of $G_{\rm CP}$ broken to $G_e = Z_3^T$ and $G_\nu = Z_2^S \times H^\nu_{\rm CP}$, with $H^\nu_{\rm CP}$ being generated by $X_{\mathbf{3}\nu} = \rho_{\mathbf{3}}(U)$,[11] the authors find:

$$\sin^2\theta_{13} = \frac{2}{3}\sin^2\theta^\nu\,, \quad \sin^2\theta_{12} = \frac{1}{2+\cos 2\theta^\nu} = \frac{1}{3\left(1-\sin^2\theta_{13}\right)}\,, \quad \sin^2\theta_{23} = \frac{1}{2}\,, \tag{1.54}$$

$$|\sin\delta| = 1\,, \quad \sin\alpha_{21} = \sin\alpha_{31} = 0\,. \tag{1.55}$$

There are several important features, which this example demonstrates. Firstly, as we can see, the free parameter θ^ν generates a non-zero value of the reactor angle. Secondly, the exact values of the leptonic CPV phases such as 0 or π, or else $\pi/2$ or $3\pi/2$, are quite typical for the considered one-parameter set-up. Thirdly, the values of some of the mixing angles are strongly correlated between themselves. This should be expected, since we have only one free parameter. Fixing $\sin^2\theta_{13}$ to its best fit value from Table 1.1, we find from eq. (1.54) $\sin^2\theta_{12} = 0.341$. Therefore, in this example, both $\sin^2\theta_{12}$ and $\sin^2\theta_{23}$ are outside their presently allowed 2σ ranges (see Table 1.1). Moreover, this example cannot account for possible non-maximal Dirac CP violation. Thus, on the one hand the considered set-up is very attractive because of its high predictivity, while on the other hand it is difficult to expect a very good agreement with the data.

Scenarios in which the neutrino mixing angles and the leptonic CPV phases are functions of two or three parameters have also been considered in the literature (see, e.g., [122, 126, 127, 131, 140]). In these scenarios, the residual symmetry $G^e_{\rm CP}$ of the charged lepton mass term is typically assumed to be a Z_2 ($Z_2 \times H^e_{\rm CP}$) symmetry or to be fully broken. In spite of the larger number of parameters in terms of which the mixing angles and the CPV phases are expressed, the values of the CPV phases are predicted to be correlated with the values of the three neutrino mixing angles.

A set-up with $G^e_{\rm CP} = Z_2 \times H^e_{\rm CP}$ and $G^\nu_{\rm CP} = Z_2 \times H^\nu_{\rm CP}$ has been recently considered in [126]. The resulting PMNS matrix in such a scheme depends on two free real parameters — two angles θ^ν and θ^e. The authors have obtained several phenomenologically viable neutrino mixing patterns from $G_{\rm CP} = S_4 \rtimes H_{\rm CP}$, broken to all possible residual symmetries of the type indicated above. Breaking patterns allowing for three free parameters have been investigated in [122, 127, 131, 140]. In [131] and [127], respectively, $G_{\rm CP} = A_5 \rtimes H_{\rm CP}$ and $G_{\rm CP} = S_4 \rtimes H_{\rm CP}$ broken to $G^e_{\rm CP} = Z_2$ and $G^\nu_{\rm CP} = Z_2 \times H^\nu_{\rm CP}$ have been considered. In this case, the matrix U_e depends on an angle θ^e and a phase δ^e, while the matrix U_ν depends on an angle θ^ν.

In Chapter 4, we will investigate in detail another breaking pattern, characterised by $G_{\rm CP}$ completely broken in the charged lepton sector and broken down to $G^\nu_{\rm CP} = Z_2 \times Z_2 \rtimes H^\nu_{\rm CP}$, which also involves three free parameters (two angles and a phase), but

[11] S, T and U are the generators of S_4 in the basis for its 3-dimensional representation **3** given in eq. (1.32).

all of them coming from the charged lepton sector. In particular, in Chapter 4 we will concentrate on obtaining predictions for the Majorana phases in such a scenario.

The specific correlations between the values of the three neutrino mixing angles, which characterise the one-parameter set-ups, do not hold in the two- and three-parameter scenarios. In addition, the Dirac CPV phase in the two- and three-parameter scenarios is predicted to have non-trivial values which are correlated with the values of the three neutrino mixing angles and differ from 0, π, $\pi/2$ and $3\pi/2$. The indicated differences between the predictions of the different scenarios, in principle, make it possible to distinguish between them experimentally by improving the precision on each of the three measured neutrino mixing angles, and by performing a sufficiently precise measurement of the Dirac CPV phase.

1.4 Outline of the thesis

The remainder of the present PhD thesis consists of five chapters. Four of them address certain aspects of the discrete symmetry approach to neutrino mixing and leptonic CP violation introduced in the preceding sections, while the last chapter contains conclusions and an outlook. Below we briefly summarise the content of each chapter.

In Chapter 2, assuming that the observed pattern of 3-neutrino mixing is related to the existence of a lepton flavour symmetry, corresponding to a non-Abelian discrete group G_f, and that G_f is broken to specific *residual symmetries* G_e and G_ν of the charged lepton and neutrino mass terms, we derive *sum rules* for the cosine of the Dirac phase δ of the PMNS matrix U. We systematically consider all types of the residual symmetries for which correlations between the mixing angles and δ are expected, namely,

(A) $G_e = Z_2$ and $G_\nu = Z_n$, $n > 2$ or $Z_n \times Z_m$, $n, m \geq 2$;

(B) $G_e = Z_n$, $n > 2$ or $Z_n \times Z_m$, $n, m \geq 2$ and $G_\nu = Z_2$;

(C) $G_e = Z_2$ and $G_\nu = Z_2$;

(D) G_e is fully broken and $G_\nu = Z_n$, $n > 2$ or $Z_n \times Z_m$, $n, m \geq 2$;

(E) $G_e = Z_n$, $n > 2$ or $Z_n \times Z_m$, $n, m \geq 2$ and G_ν is fully broken.

For given G_e and G_ν, the sum rules for $\cos\delta$ thus derived are exact, within the approach employed, and are valid, in particular, for any G_f containing G_e and G_ν as subgroups. We identify the cases when the value of $\cos\delta$ cannot be determined, or cannot be uniquely determined, without making additional assumptions on unconstrained parameters. In a large class of cases considered the value of $\cos\delta$ can be unambiguously predicted once the flavour symmetry G_f and the corresponding residual symmetries are specified. We present predictions for $\cos\delta$ in these cases for the flavour symmetry groups S_4, A_4, T' and A_5, requiring that the measured values of the 3-neutrino mixing parameters $\sin^2\theta_{12}$, $\sin^2\theta_{13}$ and $\sin^2\theta_{23}$, taking into account their respective 3σ uncertainties, are successfully reproduced. This chapter is based on ref. [101].

In Chapter 3, driven by the idea that the main contribution to neutrino mixing comes from the neutrino sector, i.e., from the matrix U_ν diagonalising the neutrino mass matrix, we take a closer look at pattern D in the list above, i.e., the one characterised by G_e being fully broken and $G_\nu = Z_n$, $n > 2$ or $Z_n \times Z_m$, $n, m \geq 2$. In this case, the residual symmetry G_ν determines completely the form of the matrix U_ν (up to re-phasing of columns and

their permutations), while the matrix U_e remains, in general, unconstrained. Assuming U_ν to have one of the symmetry forms introduced in Section 1.2, i.e., BM, TBM, GRA, GRB or HG, we explore in a systematic way possible *charged lepton corrections*, i.e., various forms of the matrix U_e diagonalising $M_e M_e^\dagger$, which can reconstitute compatibility of the symmetry forms in question with the experimental data. We consider only those forms of U_e which allow one to express δ as a function of the three neutrino mixing angles present in the PMNS matrix U and the fixed angles contained in U_ν. In a number of phenomenologically interesting cases, we perform a statistical analysis of the predictions for the Dirac CPV phase by constructing the likelihood function for $\cos\delta$, using (i) the results of the global analysis of neutrino oscillation data, and (ii) the prospective uncertainties on the neutrino mixing angles. Our results show that the measurement of the Dirac phase in the neutrino mixing matrix, together with an improvement of the precision on the mixing angles, can provide unique information as regards the possible existence of a new fundamental symmetry in the lepton sector. This chapter is based on ref. [100] and, in part, on ref. [109].

Chapter 4 extends the discussion of the neutrino mixing patterns considered in Chapter 3, but there our main focus is on predictions for the *Majorana phases* in the PMNS matrix U. We show that for most of the mixing schemes explored in Chapter 3 the Majorana phases α_{21} and α_{31} can be expressed in terms of the three neutrino mixing angles of the standard parametrisation of U and the angles and the two Majorana-like phases ξ_{21} and ξ_{31} present, in general, in U_ν. The angles in U_ν are fixed by a residual flavour symmetry G_ν. First, we derive predictions for phase differences $(\alpha_{21} - \xi_{21})$ and $(\alpha_{31} - \xi_{31})$, which in many cases are completely determined by the values of the mixing angles. Second, we demonstrate that the requirement of generalised CP invariance of the neutrino Majorana mass term discussed in Section 1.3 implies $\xi_{21} = 0$ or π and $\xi_{31} = 0$ or π, and therefore the Majorana phases themselves are predicted in terms of the mixing angles only. For these values of ξ_{21} and ξ_{31} and the best fit values of θ_{12}, θ_{23} and θ_{13}, we present predictions for the effective Majorana mass in $(\beta\beta)_{0\nu}$-decay that depends on the values of the Majorana phases. This chapter is based on ref. [140].

In Chapter 5, we will be concerned with *renormalisation group (RG) corrections* to the sum rule predictions for the Dirac CPV phase δ. In Chapters 2–4 as well as often in the literature, it is assumed that neutrino mixing sum rules are exactly realised at low energies, where experiments take place. However, as every quantity in quantum field theory, the mixing parameters get affected by RG running. In Chapter 5, we consider as an example two particular sum rules from Chapter 3 and assume that they hold at a certain high-energy scale, which we choose to be the seesaw scale $M_S \approx 10^{13}$ GeV. The main question we want to address is how stable the predictions for δ are under the RG corrections. We investigate the impact of these corrections on the sum rule predictions for δ in the cases of neutrino Majorana mass term generated by the Weinberg (dimension 5) operator [141] added to (i) the SM, and (ii) the minimal SUSY extension of the SM (MSSM). Our results show that in the first scenario the RG effects on the sum rule predictions for the Dirac CPV phase are negligible, while in the second scenario they increase with increasing absolute neutrino mass scale, $\min(m_j)$, $j = 1, 2, 3$, and $\tan\beta$, and for $\min(m_j) \gtrsim 0.01$ eV and $\tan\beta \gtrsim 30$ have to be taken into account to realistically probe the sum rule predictions. This chapter is based on ref. [142].

Finally, in Chapter 6, we draw conclusions and present an outlook.

Chapter 2

Leptonic Dirac CP violation from residual discrete symmetries

In the present chapter, we assume that the observed pattern of 3-neutrino mixing is related to the existence of a flavour symmetry, which is described by a non-Abelian discrete group G_f. At certain energy scale this symmetry gets broken down to *residual symmetries* of the charged lepton and neutrino mass terms. These residual symmetries correspond to Abelian subgroups G_e and G_ν of the group G_f. We consider different breaking patterns for which correlations between (i) the values of (some of) the three neutrino mixing angles, θ_{12}, θ_{13} and θ_{23}, and (ii) the mixing angles and the Dirac CPV phase δ are expected. Namely, we systematically investigate the following types of residual symmetries:

(A) $G_e = Z_2$ and $G_\nu = Z_n$, $n > 2$ or $Z_n \times Z_m$, $n, m \geq 2$;

(B) $G_e = Z_n$, $n > 2$ or $Z_n \times Z_m$, $n, m \geq 2$ and $G_\nu = Z_2$;

(C) $G_e = Z_2$ and $G_\nu = Z_2$;

(D) G_e is fully broken and $G_\nu = Z_n$, $n > 2$ or $Z_n \times Z_m$, $n, m \geq 2$;

(E) $G_e = Z_n$, $n > 2$ or $Z_n \times Z_m$, $n, m \geq 2$ and G_ν is fully broken.

This chapter is organised as follows. In Section 2.1, we describe the parametrisations of the PMNS matrix depending on the residual symmetries G_e and G_ν given above. In Sections 2.2, 2.3 and 2.4, we consider breaking patterns A, B, C and derive *mixing sum rules*, in particular, for $\cos\delta$. At the end of each of these sections we present numerical predictions for $\cos\delta$ in the cases of the flavour symmetry groups $G_f = A_4$, T', S_4 and A_5 described in Appendix B. We choose these groups since they are among the smallest non-Abelian groups (in terms of the number of elements) possessing 3-dimensional irreducible representations. In Section 2.5, we provide a summary of the sum rules derived in Sections 2.2–2.4. Further, in Sections 2.6 and 2.7, we derive mixing sum rules in cases D and E, respectively. In these cases, as we will see, the value of $\cos\delta$ cannot be fixed without additional assumptions on the unconstrained matrix U_e or U_ν. In Section 2.8, we present a summary of the numerical results. Finally, Section 2.9 contains the conclusions of this chapter.

2.1 Preliminary considerations

As we have shown in Section 1.2, the residual symmetries of the charged lepton and neutrino mass matrices constrain the forms of the diagonalising unitary matrices U_e and U_ν (see eqs. (1.23)–(1.29)), and thus, the form of the PMNS matrix U. Below we demonstrate how it applies to the different types of residual symmetries.

If $G_e = Z_n$, $n > 2$ or $Z_n \times Z_m$, $n, m \geq 2$, the matrix U_e is fixed by the matrix $\rho_{\mathbf{3}}(g_e)$ (up to multiplication by diagonal phase matrices on the right and permutations of columns, as can be seen from eq. (1.26)), $U_e = U_e^\circ$. In the case of a smaller symmetry, i.e., $G_e = Z_2$, U_e is defined up to a $U(2)$ transformation in the degenerate subspace, because in this case $\rho_{\mathbf{3}}(g_e)$ has a degenerate eigenvalue. Therefore,

$$U_e = U_e^\circ \, U_{ij}(\theta_{ij}^e, \delta_{ij}^e) \, \Psi_k \, \Psi_l \,, \tag{2.1}$$

where U_{ij} is a complex rotation in the i-j plane and Ψ_k, Ψ_l are diagonal phase matrices,

$$\Psi_1 = \text{diag}\left(e^{i\psi_1}, 1, 1\right) \,, \quad \Psi_2 = \text{diag}\left(1, e^{i\psi_2}, 1\right) \,, \quad \Psi_3 = \text{diag}\left(1, 1, e^{i\psi_3}\right) \,. \tag{2.2}$$

The angle θ_{ij}^e and the phases δ_{ij}^e, ψ_1, ψ_2 and ψ_3 are free parameters. As an example of the explicit form of $U_{ij}(\theta_{ij}^a, \delta_{ij}^a)$, we give the expression of the matrix $U_{12}(\theta_{12}^a, \delta_{12}^a)$:

$$U_{12}(\theta_{12}^a, \delta_{12}^a) = \begin{pmatrix} \cos\theta_{12}^a & \sin\theta_{12}^a e^{-i\delta_{12}^a} & 0 \\ -\sin\theta_{12}^a e^{i\delta_{12}^a} & \cos\theta_{12}^a & 0 \\ 0 & 0 & 1 \end{pmatrix} \,, \tag{2.3}$$

where $a = e, \nu, \circ$. The indices e, ν indicate the free parameters, while "$\circ$" indicates the angles and phases which are fixed. The complex rotation matrices $U_{23}(\theta_{23}^a, \delta_{23}^a)$ and $U_{13}(\theta_{13}^a, \delta_{13}^a)$ are defined in an analogous way. The real rotation matrices $R_{ij}(\theta_{ij}^a)$ can be obtained from $U_{ij}(\theta_{ij}^a, \delta_{ij}^a)$ setting δ_{ij}^a to zero, i.e., $R_{ij}(\theta_{ij}^a) = U_{ij}(\theta_{ij}^a, 0)$. In the absence of a residual symmetry no constraints are present for the unitary mixing matrix U_e, which can be in general expressed in terms of nine real parameters, e.g., three rotation angles and six phases.

Similar considerations apply to the neutrino sector. If $G_\nu = Z_n$, $n > 2$ or $Z_n \times Z_m$, $n, m \geq 2$ for Dirac neutrinos, or $G_\nu = Z_2 \times Z_2$ for Majorana neutrinos, the matrix U_ν is fixed up to permutations of columns and right multiplication by diagonal phase matrices by the residual symmetry (see eq. (1.29)), i.e., $U_\nu = U_\nu^\circ$. If the symmetry is smaller, $G_\nu = Z_2$, then

$$U_\nu = U_\nu^\circ \, U_{ij}(\theta_{ij}^\nu, \delta_{ij}^\nu) \, \Psi_k \, \Psi_l \,. \tag{2.4}$$

Obviously, in the absence of a residual symmetry, U_ν is unconstrained.

In all the cases considered above where G_e and G_ν are non-trivial, the matrices $\rho_{\mathbf{3}}(g_e)$ and $\rho_{\mathbf{3}}(g_\nu)$ are diagonalised by U_e° and U_ν°:

$$(U_e^\circ)^\dagger \, \rho_{\mathbf{3}}(g_e) \, U_e^\circ = \rho_{\mathbf{3}}(g_e)^{\text{diag}} \quad \text{and} \quad (U_\nu^\circ)^\dagger \, \rho_{\mathbf{3}}(g_\nu) \, U_\nu^\circ = \rho_{\mathbf{3}}(g_\nu)^{\text{diag}} \,.$$

In what follows we define U° as the matrix fixed by the residual symmetries, which, in general, gets contributions from both the charged lepton and neutrino sectors, $U^\circ = (U_e^\circ)^\dagger U_\nu^\circ$. Since U° is a unitary 3×3 matrix, we will parametrise it in terms of three angles and six phases. These, however, as we are going to explain, reduce effectively to three angles and one phase, since the other five phases contribute to the Majorana phases of the PMNS mixing matrix, unphysical charged lepton phases and/or to a redefinition of the free parameters contained in U_e and U_ν. Furthermore, we will use the notation θ_{ij}^e, θ_{ij}^ν, δ_{ij}^e, δ_{ij}^ν for the free angles and phases contained in U, while the parameters marked with a circle contained in U°, e.g., θ_{ij}°, δ_{ij}°, are fixed by the residual symmetries.

In the case when $G_e = Z_2$ and $G_\nu = Z_n$, $n > 2$ or $Z_n \times Z_m$, $n, m \geq 2$ for massive Dirac neutrinos, or $G_\nu = Z_2 \times Z_2$ for Majorana neutrinos, we have:

$$U = U_{ij}(\theta_{ij}^e, \delta_{ij}^e) \, \Psi_j^\circ \, U^\circ(\theta_{12}^\circ, \theta_{13}^\circ, \theta_{23}^\circ, \{\delta_{kl}^\circ\}) \, Q_0$$

$$= \Psi_j^\circ \, U_{ij}(\theta_{ij}^e, \delta_{ij}^e - \psi_j^\circ) \, U^\circ(\theta_{12}^\circ, \theta_{13}^\circ, \theta_{23}^\circ, \{\delta_{kl}^\circ\}) \, Q_0 \,, \tag{2.5}$$

where $(ij) = (12), (13), (23)$ and $\{\delta_{kl}^\circ\} = \{\delta_{12}^\circ, \delta_{13}^\circ, \delta_{23}^\circ\}$. The unitary matrix U° contains three angles and three phases, since the additional three phases can be absorbed by redefining the charged lepton fields and the free parameter δ_{ij}^e (see below). Here Ψ_j° is a diagonal matrix containing a fixed phase in the j-th position. Namely,

$$\Psi_1^\circ = \text{diag}\left(e^{i\psi_1^\circ}, 1, 1\right) \,, \quad \Psi_2^\circ = \text{diag}\left(1, e^{i\psi_2^\circ}, 1\right) \,, \quad \Psi_3^\circ = \text{diag}\left(1, 1, e^{i\psi_3^\circ}\right) \,. \tag{2.6}$$

The matrix Q_0, defined as

$$Q_0 = \text{diag}\left(1, e^{i\frac{\xi_{21}}{2}}, e^{i\frac{\xi_{31}}{2}}\right) \,, \tag{2.7}$$

is a diagonal matrix containing two free parameters contributing to the Majorana phases. Since the presence of the phase ψ_j° amounts to a redefinition of the free parameter δ_{ij}^e, we denote $(\delta_{ij}^e - \psi_j^\circ)$ as δ_{ij}^e. This allows us to employ the following parametrisation for U:

$$U = U_{ij}(\theta_{ij}^e, \delta_{ij}^e) \, U^\circ(\theta_{12}^\circ, \theta_{13}^\circ, \theta_{23}^\circ, \delta_{kl}^\circ) \, Q_0 \,, \tag{2.8}$$

where the unphysical phase matrix Ψ_j° on the left has been removed by charged lepton re-phasing and the set of three phases $\{\delta_{kl}^\circ\}$ reduces to only one phase, δ_{kl}°, since the other two contribute to redefinitions of Q_0, δ_{ij}^e and to unphysical phases. The possible forms of the matrix U°, which we are going to employ, are given in Appendix C.

For the breaking patterns $G_e = Z_n$, $n > 2$ or $Z_n \times Z_m$, $n, m \geq 2$ and $G_\nu = Z_2$, valid for both Majorana and Dirac neutrinos, we have:

$$\begin{aligned} U &= U^\circ(\theta_{12}^\circ, \theta_{13}^\circ, \theta_{23}^\circ, \delta_{kl}^\circ) \, \Psi_i^\circ \, \Psi_j^\circ \, U_{ij}(\theta_{ij}^\nu, \delta_{ij}^\nu) \, Q_0 \\ &= U^\circ(\theta_{12}^\circ, \theta_{13}^\circ, \theta_{23}^\circ, \delta_{kl}^\circ) \, U_{ij}(\theta_{ij}^\nu, \delta_{ij}^\nu - \psi_i^\circ + \psi_j^\circ) \, \Psi_i^\circ \, \Psi_j^\circ \, Q_0 \,, \end{aligned} \tag{2.9}$$

where $(ij) = (12), (13), (23)$, and the two free phases, which contribute to the Majorana phases of the PMNS matrix if the massive neutrinos are Majorana particles, have been included in the diagonal phase matrix Q_0. Notice that if neutrinos are assumed to be Dirac instead of Majorana, then the matrix Q_0 can be removed through re-phasing of the Dirac neutrino fields. Without loss of generality we can redefine the combination $\delta_{ij}^\nu - \psi_i^\circ + \psi_j^\circ$ as δ_{ij}^ν and the combination $\Psi_i^\circ \, \Psi_j^\circ \, Q_0$ as Q_0, so that the following parametrisation of U is obtained:

$$U = U^\circ(\theta_{12}^\circ, \theta_{13}^\circ, \theta_{23}^\circ, \delta_{kl}^\circ) \, U_{ij}(\theta_{ij}^\nu, \delta_{ij}^\nu) \, Q_0 \,. \tag{2.10}$$

In the case of $G_e = Z_2$ and $G_\nu = Z_2$ for both Dirac and Majorana neutrinos, we can write

$$\begin{aligned} U &= U_{ij}(\theta_{ij}^e, \delta_{ij}^e) \, \Psi_j^\circ \, U^\circ(\theta_{12}^\circ, \theta_{13}^\circ, \theta_{23}^\circ, \delta_{kl}^\circ) \, \Psi_r^\circ \, \Psi_s^\circ \, U_{rs}(\theta_{rs}^\nu, \delta_{rs}^\nu) \, Q_0 \\ &= \Psi_j^\circ \, U_{ij}(\theta_{ij}^e, \delta_{ij}^e - \psi_j^\circ) \, U^\circ(\theta_{12}^\circ, \theta_{13}^\circ, \theta_{23}^\circ, \delta_{kl}^\circ) \, U_{rs}(\theta_{rs}^\nu, \delta_{rs}^\nu - \psi_r^\circ + \psi_s^\circ) \, \Psi_r^\circ \, \Psi_s^\circ \, Q_0 \,, \end{aligned} \tag{2.11}$$

with $(ij) = (12), (13), (23)$, $(rs) = (12), (13), (23)$. The phase matrices Ψ_i° are defined as in eq. (2.6). Similarly to the previous cases, we can redefine the parameters in such a way that U can be cast in the following form:

$$U = U_{ij}(\theta_{ij}^e, \delta_{ij}^e) \, U^\circ(\theta_{12}^\circ, \theta_{13}^\circ, \theta_{23}^\circ, \delta_{kl}^\circ) \, U_{rs}(\theta_{rs}^\nu, \delta_{rs}^\nu) \, Q_0 \,, \tag{2.12}$$

where Q_0 can be phased away if neutrinos are assumed to be Dirac particles.[12]

If G_e is fully broken and $G_\nu = Z_n$, $n > 2$ or $Z_n \times Z_m$, $n, m \geq 2$ for Dirac neutrinos or $G_\nu = Z_2 \times Z_2$ for Majorana neutrinos, the form of U reads

$$U = U(\theta^e_{12}, \theta^e_{13}, \theta^e_{23}, \delta^e_{rs})\, \Psi_2\, \Psi_3\, U^\circ(\theta^\circ_{12}, \theta^\circ_{13}, \theta^\circ_{23}, \{\delta^\circ_{kl}\})\, Q_0\,, \tag{2.13}$$

where the phase matrices Ψ_2 and Ψ_3 are defined as in eq. (2.2). Notice that in general we can effectively parametrise U° in terms of three angles and one phase since of the set of three phases $\{\delta^\circ_{kl}\}$, two contribute to a redefinition of the matrices Q_0, Ψ_2 and Ψ_3. Furthermore, under the additional assumptions on the form of $U(\theta^e_{12}, \theta^e_{13}, \theta^e_{23}, \delta^e_{rs})$ and also taking $\{\delta^\circ_{kl}\} = 0$, the form of U given in eq. (2.13) leads to the sum rules derived in [99,100] and studied in detail in Chapter 3. In the numerical analyses performed in [99,100,109], the angles θ°_{ij} have been set, in particular, to the values corresponding to the TBM, BM, GRA, GRB and HG symmetry forms.

Finally, for the breaking patterns $G_e = Z_n$, $n > 2$ or $Z_n \times Z_m$, $n, m \geq 2$ and G_ν fully broken when considering both Dirac and Majorana neutrino possibilities, the form of U can be derived from eq. (2.13) by interchanging the fixed and the free parameters. Namely,

$$U = U^\circ(\theta^\circ_{12}, \theta^\circ_{13}, \theta^\circ_{23}, \delta^\circ_{kl})\, \Psi_2\, \Psi_3\, U(\theta^\nu_{12}, \theta^\nu_{13}, \theta^\nu_{23}, \delta^\nu_{rs})\, Q_0\,. \tag{2.14}$$

The cases found in eqs. (2.8), (2.10), (2.12), (2.13) and (2.14) are summarised in Table 2.1. The reduction of the number of free parameters indicated with arrows corresponds to a redefinition of the charged lepton fields.

In this chapter, we will use the best fit values and the 3σ allowed ranges of the parameters $\sin^2\theta_{12}$, $\sin^2\theta_{23}$ and $\sin^2\theta_{13}$ found in ref. [18]. They read:

$$(\sin^2\theta_{12})_{\rm BF} = 0.308\,, \quad 0.259 \leq \sin^2\theta_{12} \leq 0.359\,, \tag{2.15}$$

$$(\sin^2\theta_{23})_{\rm BF} = 0.437\ (0.455)\,, \quad 0.374\ (0.380) \leq \sin^2\theta_{23} \leq 0.626\ (0.641)\,, \tag{2.16}$$

$$(\sin^2\theta_{13})_{\rm BF} = 0.0234\ (0.0240)\,, \quad 0.0176\ (0.0178) \leq \sin^2\theta_{13} \leq 0.0295\ (0.0298)\,. \tag{2.17}$$

Here the values (values in brackets) correspond to the NO (IO) neutrino mass spectrum.

We note finally that the titles of the following sections refer to the residual symmetries of the charged lepton and neutrino mass matrices, while the titles of the subsections reflect the free complex rotations contained in the corresponding parametrisation of U, eqs. (2.8), (2.10), (2.12), (2.13) and (2.14).

2.2 Pattern A: $G_e = Z_2$ and $G_\nu = Z_n$, $n > 2$ or $Z_n \times Z_m$, $n, m \geq 2$

In this section, we derive sum rules for $\cos\delta$ for the cases given in eq. (2.8). Recall that the matrix U_e is fixed up to a complex rotation in one plane by the residual $G_e = Z_2$ symmetry, while U_ν is completely determined (up to multiplication by diagonal phase matrices on the right and permutations of columns) by the $G_\nu = Z_2 \times Z_2$ residual symmetry in the case of neutrino Majorana mass term, or by $G_\nu = Z_n$, $n > 2$ or $Z_n \times Z_m$, $n, m \geq 2$, residual symmetries if the massive neutrinos are Dirac particles. At the end of this section we

[12] We will not repeat this statement further, but it should be always understood that if the massive neutrinos are Dirac fermions, then two phases in the matrix Q_0 are unphysical and can be removed from U by a re-phasing of the Dirac neutrino fields.

Table 2.1. Number of effective free parameters, degrees of freedom (d.o.f.), contained in U relevant for the PMNS angles and the Dirac phase (and the Majorana phases) in the cases of the different breaking patterns of G_f to G_e and G_ν. Arrows indicate the reduction of the number of parameters, which can be absorbed with a redefinition of the charged lepton fields.

$G_e \subset G_f$	$G_\nu \subset G_f$	U_e d.o.f.	U_ν d.o.f.	U d.o.f.
fully broken	fully broken	$9 \to 6$	$9 \to 8$	$12 \to 4$ $(+2)$
Z_2	fully broken	$4 \to 2$	$9 \to 8$	$10 \to 4$ $(+2)$
$\begin{cases} Z_n,\ n > 2 \\ Z_n \times Z_m,\ n, m \geq 2 \end{cases}$	fully broken	0	$9 \to 8$	$8 \to 4$ $(+2)$
fully broken	Z_2	$9 \to 6$	4	$10 \to 4$ $(+2)$
fully broken	$\begin{cases} Z_n,\ n > 2 \\ Z_n \times Z_m,\ n, m \geq 2 \end{cases}$	$9 \to 6$	2	$8 \to 4$ $(+2)$
Z_2	Z_2	$4 \to 2$	4	4 $(+2)$
$\begin{cases} Z_n,\ n > 2 \\ Z_n \times Z_m,\ n, m \geq 2 \end{cases}$	Z_2	0	4	2 $(+2)$
Z_2	$\begin{cases} Z_n,\ n > 2 \\ Z_n \times Z_m,\ n, m \geq 2 \end{cases}$	$4 \to 2$	2	2 $(+2)$
$\begin{cases} Z_n,\ n > 2 \\ Z_n \times Z_m,\ n, m \geq 2 \end{cases}$	$\begin{cases} Z_n,\ n > 2 \\ Z_n \times Z_m,\ n, m \geq 2 \end{cases}$	0	2	0 $(+2)$

will present results of a study of the possibility of reproducing the observed values of the lepton mixing parameters $\sin^2\theta_{12}$, $\sin^2\theta_{13}$ and $\sin^2\theta_{23}$ and of obtaining physically viable predictions for $\cos\delta$ in the cases when the residual symmetries $G_e = Z_2$ and $G_\nu = Z_n$, $n > 2$ or $Z_n \times Z_m$, $n, m \geq 2$, originate from the breaking of the lepton flavour symmetries A_4, T', S_4 and A_5.

2.2.1 Case A1: $U_{12}(\theta^e_{12}, \delta^e_{12})$

Employing the parametrisation of the PMNS matrix U given in eq. (2.8) with $(ij) = (12)$ and the parametrisation of U° given as

$$U^\circ(\theta^\circ_{12}, \theta^\circ_{13}, \theta^\circ_{23}, \delta^\circ_{12}) = U_{12}(\theta^\circ_{12}, \delta^\circ_{12})\, R_{23}(\theta^\circ_{23})\, R_{13}(\theta^\circ_{13})\,, \tag{2.18}$$

we get for U (see Appendix C for details):

$$U = U_{12}(\theta^e_{12}, \delta^e_{12})\, U_{12}(\theta^\circ_{12}, \delta^\circ_{12})\, R_{23}(\theta^\circ_{23})\, R_{13}(\theta^\circ_{13})\, Q_0\,. \tag{2.19}$$

The results derived in Appendix C and given in eq. (C.6) allow us to cast eq. (2.19) in the form

$$U = R_{12}(\hat\theta_{12})\, P_1(\hat\delta_{12})\, R_{23}(\theta^\circ_{23})\, R_{13}(\theta^\circ_{13})\, Q_0\,, \quad P_1(\hat\delta_{12}) = \mathrm{diag}(e^{i\hat\delta_{12}}, 1, 1)\,, \tag{2.20}$$

with $\hat{\delta}_{12} = \alpha - \beta$, where $\sin\hat{\theta}_{12}$, α and β are defined as in eqs. (C.7) and (C.8) after setting $i = 1$, $j = 2$, $\theta^a_{12} = \theta^e_{12}$, $\delta^a_{12} = \delta^e_{12}$, $\theta^b_{12} = \theta^\circ_{12}$ and $\delta^b_{12} = \delta^\circ_{12}$. Using eq. (2.20) and the standard parametrisation of the PMNS matrix U given in eq. (1.3), we find:

$$\sin^2\theta_{13} = |U_{e3}|^2 = \cos^2\hat{\theta}_{12}\sin^2\theta^\circ_{13} + \cos^2\theta^\circ_{13}\sin^2\hat{\theta}_{12}\sin^2\theta^\circ_{23} + \frac{1}{2}\sin 2\hat{\theta}_{12}\sin 2\theta^\circ_{13}\sin\theta^\circ_{23}\cos\hat{\delta}_{12}\,, \tag{2.21}$$

$$\sin^2\theta_{23} = \frac{|U_{\mu 3}|^2}{1-|U_{e3}|^2} = \frac{1}{\cos^2\theta_{13}}\left[\sin^2\theta^\circ_{13} - \sin^2\theta_{13} + \cos^2\theta^\circ_{13}\sin^2\theta^\circ_{23}\right], \tag{2.22}$$

$$\sin^2\theta_{12} = \frac{|U_{e2}|^2}{1-|U_{e3}|^2} = \frac{\cos^2\theta^\circ_{23}\sin^2\hat{\theta}_{12}}{\cos^2\theta_{13}}\,. \tag{2.23}$$

From eqs. (2.21) and (2.22) we get the following correlation between the values of $\sin^2\theta_{13}$ and $\sin^2\theta_{23}$:

$$\sin^2\theta_{13} + \cos^2\theta_{13}\sin^2\theta_{23} = \sin^2\theta^\circ_{13} + \cos^2\theta^\circ_{13}\sin^2\theta^\circ_{23}\,. \tag{2.24}$$

Notice that eq. (2.23) implies that

$$\sin^2\hat{\theta}_{12} = \frac{\cos^2\theta_{13}\sin^2\theta_{12}}{\cos^2\theta^\circ_{23}}\,. \tag{2.25}$$

In order to obtain a sum rule for $\cos\delta$, we compare the expressions for the absolute value of the element $U_{\tau 2}$ of the PMNS matrix in the standard parametrisation and in the parametrisation defined in eq. (2.20),

$$|U_{\tau 2}| = |\cos\theta_{12}\sin\theta_{23} + \sin\theta_{13}\cos\theta_{23}\sin\theta_{12}e^{i\delta}| = |\sin\theta^\circ_{23}|\,. \tag{2.26}$$

From the above equation we get for $\cos\delta$:

$$\cos\delta = \frac{\cos^2\theta_{13}(\sin^2\theta^\circ_{23} - \cos^2\theta_{12}) + \cos^2\theta^\circ_{13}\cos^2\theta^\circ_{23}(\cos^2\theta_{12} - \sin^2\theta_{12}\sin^2\theta_{13})}{\sin 2\theta_{12}\sin\theta_{13}|\cos\theta^\circ_{13}\cos\theta^\circ_{23}|(\cos^2\theta_{13} - \cos^2\theta^\circ_{13}\cos^2\theta^\circ_{23})^{\frac{1}{2}}}\,. \tag{2.27}$$

For the considered specific residual symmetries G_e and G_ν, the predicted value of $\cos\delta$ in case A1 discussed in this subsection depends on the chosen discrete flavour symmetry G_f via the values of the angles θ°_{13} and θ°_{23}.

The method of derivation of the sum rule for $\cos\delta$ of interest employed in the present subsection and consisting, in particular, of choosing adequate parametrisations of the PMNS matrix U (in terms of the complex rotations of U_e and of U_ν) and of the matrix U° (determined by the symmetries G_e, G_ν and G_f), which allows to express the PMNS matrix U in terms of minimal numbers of angle and phase parameters, will be used also in all subsequent sections of this chapter. The technical details related to the method are given in Appendices C and D.

We note finally that in the case of $\delta^\circ_{12} = 0$, the symmetry forms TBM, BM, GRA, GRB and HG, defined in eqs. (1.33), (1.35), (1.36), (1.37) and (1.38), respectively, can be obtained from $U^\circ = R_{12}(\theta^\circ_{12})R_{23}(\theta^\circ_{23})R_{13}(\theta^\circ_{13})$ for specific values of the angles given in Table 2.2.

2.2.2 Case A2: $U_{13}(\theta^e_{13}, \delta^e_{13})$

Using the parametrisation of the PMNS matrix U given in eq. (2.8) with $(ij) = (13)$ and the following parametrisation of U°,

$$U^\circ(\theta^\circ_{12}, \theta^\circ_{13}, \theta^\circ_{23}, \delta^\circ_{13}) = U_{13}(\theta^\circ_{13}, \delta^\circ_{13})\, R_{23}(\theta^\circ_{23})\, R_{12}(\theta^\circ_{12})\,, \tag{2.28}$$

Table 2.2. The TBM, BM, GRA, GRB and HG symmetry forms obtained in terms of the three rotations $R_{12}(\theta^\circ_{12})\, R_{23}(\theta^\circ_{23})\, R_{13}(\theta^\circ_{13})$.

Mixing	θ°_{12}	θ°_{23}	θ°_{13}
TBM	$\pi/4$	$-\sin^{-1}(1/\sqrt{3})$	$\pi/6$
BM	$\sin^{-1}\sqrt{2/3}$	$-\pi/6$	$\sin^{-1}(1/\sqrt{3})$
GRA	$\sin^{-1}\sqrt{(7-\sqrt{5})/11}$	$-\sin^{-1}\sqrt{(5+\sqrt{5})/20}$	$\sin^{-1}\sqrt{(7-\sqrt{5})/22}$
GRB	$\sin^{-1}\sqrt{2(15-2\sqrt{5})/41}$	$-\sin^{-1}\sqrt{(3+\sqrt{5})/16}$	$\sin^{-1}\sqrt{(15-2\sqrt{5})/41}$
HG	$\sin^{-1}\sqrt{2/5}$	$-\sin^{-1}\sqrt{3/8}$	$\sin^{-1}\sqrt{1/5}$

we get for U (for details see Appendix C):

$$U = U_{13}(\theta^e_{13}, \delta^e_{13})\, U_{13}(\theta^\circ_{13}, \delta^\circ_{13})\, R_{23}(\theta^\circ_{23})\, R_{12}(\theta^\circ_{12})\, Q_0\,. \tag{2.29}$$

The results derived in Appendix C and presented in eq. (C.6) allow us to recast eq. (2.29) in the following form:

$$U = R_{13}(\hat\theta_{13})\, P_1(\hat\delta_{13})\, R_{23}(\theta^\circ_{23})\, R_{12}(\theta^\circ_{12})\, Q_0\,, \quad P_1(\hat\delta_{13}) = \mathrm{diag}(e^{i\hat\delta_{13}}, 1, 1)\,. \tag{2.30}$$

Here $\hat\delta_{13} = \alpha - \beta$, where $\sin\hat\theta_{13}$, α and β are defined as in eqs. (C.7) and (C.8) after setting $i = 1$, $j = 3$, $\theta^a_{13} = \theta^e_{13}$, $\delta^a_{13} = \delta^e_{13}$, $\theta^b_{13} = \theta^\circ_{13}$ and $\delta^b_{13} = \delta^\circ_{13}$. Using eq. (2.30) and the standard parametrisation of the PMNS matrix U, we find:

$$\sin^2\theta_{13} = |U_{e3}|^2 = \sin^2\hat\theta_{13}\cos^2\theta^\circ_{23}\,, \tag{2.31}$$

$$\sin^2\theta_{23} = \frac{|U_{\mu3}|^2}{1-|U_{e3}|^2} = \frac{\sin^2\theta^\circ_{23}}{1-\sin^2\theta_{13}}\,, \tag{2.32}$$

$$\sin^2\theta_{12} = \frac{|U_{e2}|^2}{1-|U_{e3}|^2} = \frac{1}{1-\sin^2\theta_{13}}\Big[\cos^2\hat\theta_{13}\sin^2\theta^\circ_{12} + \cos^2\theta^\circ_{12}\sin^2\hat\theta_{13}\sin^2\theta^\circ_{23} - \frac{1}{2}\sin 2\hat\theta_{13}\sin 2\theta^\circ_{12}\sin\theta^\circ_{23}\cos\hat\delta_{13}\Big]\,. \tag{2.33}$$

Thus, in this scheme, as it follows from eq. (2.32), the value of $\sin^2\theta_{23}$ is predicted once the symmetry group G_f is fixed. This prediction, when confronted with the measured value of $\sin^2\theta_{23}$, constitutes an important test of the scheme considered for any given discrete (lepton flavour) symmetry group G_f, which contains the residual symmetry groups $G_e = Z_2$ and $G_\nu = Z_n$, $n > 2$ and/or $Z_n \times Z_m$, $n, m \geq 2$ as subgroups.

The sum rule for $\cos\delta$ reads

$$\cos\delta = -\frac{\cos^2\theta_{13}(\cos^2\theta^\circ_{12}\cos^2\theta^\circ_{23} - \cos^2\theta_{12}) + \sin^2\theta^\circ_{23}(\cos^2\theta_{12} - \sin^2\theta_{12}\sin^2\theta_{13})}{\sin 2\theta_{12}\sin\theta_{13}|\sin\theta^\circ_{23}|(\cos^2\theta_{13} - \sin^2\theta^\circ_{23})^{\frac{1}{2}}}\,. \tag{2.34}$$

The dependence of $\cos\delta$ on G_f in this case is via the values of the angles θ°_{12} and θ°_{23}.

2.2.3 Case A3: $U_{23}(\theta^e_{23}, \delta^e_{23})$

In the case with $(ij) = (23)$, as can be shown, $\cos\delta$ does not satisfy a sum rule, i.e., it cannot be expressed in terms of the three neutrino mixing angles θ_{12}, θ_{13} and θ_{23} and the

other fixed angle parameters of the scheme. Indeed, employing the parametrisation of U° as $U^\circ(\theta^\circ_{12},\theta^\circ_{13},\theta^\circ_{23},\delta^\circ_{23}) = U_{23}(\theta^\circ_{23},\delta^\circ_{23})\,R_{13}(\theta^\circ_{13})\,R_{12}(\theta^\circ_{12})$, we can write the PMNS matrix in the following form:

$$U = U_{23}(\theta^e_{23},\delta^e_{23})\,U_{23}(\theta^\circ_{23},\delta^\circ_{23})\,R_{13}(\theta^\circ_{13})\,R_{12}(\theta^\circ_{12})\,Q_0\,. \tag{2.35}$$

Using the results derived in Appendix C and shown in eq. (C.6), we can recast eq. (2.35) as

$$U = R_{23}(\hat\theta_{23})\,P_2(\hat\delta_{23})\,R_{13}(\theta^\circ_{13})\,R_{12}(\theta^\circ_{12})\,Q_0\,,\quad P_2(\hat\delta_{23}) = \mathrm{diag}(1,e^{i\hat\delta_{23}},1)\,, \tag{2.36}$$

with $\hat\delta_{23} = \alpha - \beta$, where $\sin\hat\theta_{23}$, α and β are defined as in eqs. (C.7) and (C.8) after setting $i=2$, $j=3$, $\theta^a_{23}=\theta^e_{23}$, $\delta^a_{23}=\delta^e_{23}$, $\theta^b_{23}=\theta^\circ_{23}$ and $\delta^b_{23}=\delta^\circ_{23}$. Comparing eq. (2.36) and the standard parametrisation of the PMNS matrix, we find that $\sin^2\theta_{13}=\sin^2\theta^\circ_{13}$, $\sin^2\theta_{23}=\sin^2\hat\theta_{23}$, $\sin^2\theta_{12}=\sin^2\theta^\circ_{12}$ and $\cos\delta = \pm\cos\hat\delta_{23}$.

It follows from the preceding equations, in particular, that since, for any given G_f compatible with the considered residual symmetries, θ°_{13} and θ°_{12} have fixed values, the values of both $\sin^2\theta_{13}$ and $\sin^2\theta_{12}$ are predicted. The predictions depend on the chosen symmetry G_f. Due to these predictions the scheme under discussion can be tested for any given discrete symmetry candidate G_f, compatible, in particular, with the considered residual symmetries.

We have also seen that δ is related only to an unconstrained phase parameter of the scheme. In the case of a flavour symmetry G_f which, in particular, allows to reproduce correctly the observed values of $\sin^2\theta_{12}$ and $\sin^2\theta_{13}$, it might be possible to obtain physically viable prediction for $\cos\delta$ by employing a generalised CP invariance constraint. An example of the effect that generalised CP invariance has on restricting CPV phases is given in Appendix E. Investigating the implications of the generalised CP invariance constraint in the charged lepton or the neutrino sector in all the cases considered by us is, however, beyond the scope of the present thesis.

2.2.4 Results for $G_f = A_4$ (T'), S_4 and A_5

The cases detailed in subsections 2.2.1–2.2.3 can all be obtained from the groups A_4 (T'),[13] S_4 and A_5, when breaking them to $G_e = Z_2$ and $G_\nu = Z_n$ ($n \geq 3$) in the case of Dirac neutrinos, or $G_\nu = Z_2 \times Z_2$ in the case of both Dirac and Majorana neutrinos.[14] We now give an explicit example of how these cases can occur in A_4.

In the case of the group A_4 (see, e.g., [85]), the structure of the breaking patterns discussed, e.g., in subsection 2.2.1 can be realised when (i) the S generator of A_4 is preserved in the neutrino sector, and when, due to an accidental symmetry, the mixing matrix is fixed to be tri-bimaximal, $U^\circ_\nu = U_{\rm TBM}$, up to permutations of the columns, and (ii) a $Z_2^{T^2ST}$ or $Z_2^{TST^2}$ is preserved in the charged lepton sector. The group element generating the Z_2 symmetry is diagonalised by the matrix U°_e. Therefore the angles θ°_{12}, θ°_{13} and θ°_{23} are obtained from the product $U^\circ = (U^\circ_e)^\dagger U^\circ_\nu$. The same structure (the structure discussed in subsection 2.2.2) can be obtained in a similar manner from the flavour groups S_4 and A_5 (A_4, S_4 and A_5).

[13] In what follows we take T' in parentheses, because we restrict ourselves to the triplet representation for the LH charged lepton and neutrino fields, and when working with 3-dimensional and 1-dimensional representations of T', there is no way to distinguish T' from A_4 [143].

[14] We only consider $Z_2 \times Z_2$ when it is an actual subgroup of G_f.

We have investigated the possibility of reproducing the observed values of the lepton mixing parameters $\sin^2\theta_{12}$, $\sin^2\theta_{13}$ and $\sin^2\theta_{23}$ as well as obtaining physically viable predictions for $\cos\delta$ in the cases of residual symmetries $G_e = Z_2$ and $G_\nu = Z_n$, $n > 2$ or $Z_n \times Z_m$, $n, m \geq 2$ [15] (Dirac neutrinos), or $G_\nu = Z_2 \times Z_2$ (Majorana neutrinos), discussed in subsections 2.2.1, 2.2.2 and 2.2.3, assuming that these residual symmetries originate from the breaking of the flavour symmetries A_4 (T'), S_4 and A_5. The analysis was performed using the best fit values of the three lepton mixing parameters $\sin^2\theta_{12}$, $\sin^2\theta_{23}$ and $\sin^2\theta_{13}$ from eqs. (2.15)–(2.17). The results we have obtained for the symmetries A_4 (T'), S_4 and A_5 are summarised below.

We have found that in the cases under discussion, i.e., in cases A1, A2 and A3, and flavour symmetries $G_f = A_4$ (T'), S_4 and A_5, with the exceptions to be discussed below, it is impossible either to reproduce at least one of the measured values of $\sin^2\theta_{12}$, $\sin^2\theta_{13}$ and $\sin^2\theta_{23}$ even taking into account its respective 3σ uncertainty, or to get physically viable values of $\cos\delta$ satisfying $|\cos\delta| \leq 1$. In cases A1 and A2 and the flavour groups A_4 and S_4, for instance, the values of $\cos\delta$ are unphysical. Using the group $G_f = A_5$ leads either to unphysical values of $\cos\delta$, or to values of $\sin^2\theta_{23}$ which lie outside the corresponding 3σ allowed interval. In case A3, the symmetry A_4, e.g., leads to $(\sin^2\theta_{12}, \sin^2\theta_{13}) = (0, 0)$ or (1,0).

As mentioned earlier, there are three exceptions in which we can still get phenomenologically viable results. In the A1 case (A2 case) and the S_4 flavour symmetry, one obtains bimaximal mixing corrected by a complex rotation in the 1-2 plane[16] (1-3 plane). The PMNS angle θ_{23} is predicted to have a value corresponding to $\sin^2\theta_{23} = 0.488$ ($\sin^2\theta_{23} = 0.512$). For the best fit values of $\sin^2\theta_{12}$ and $\sin^2\theta_{13}$ we find that $\cos\delta = -1.29$ ($\cos\delta = +1.29$). However, using the value of $\sin^2\theta_{12} = 0.348$, which lies in the 3σ allowed interval, one gets the same value of $\sin^2\theta_{23}$ and $\cos\delta = -0.993$ ($\cos\delta = 0.993$), while in the part of the 3σ allowed interval of $\sin^2\theta_{12}$, $0.348 \leq \sin^2\theta_{12} \leq 0.359$, we have $-0.993 \leq \cos\delta \leq -0.915$ ($0.993 \geq \cos\delta \geq 0.915$).

Also in the A1 case (A2 case) but with the A_5 flavour symmetry and residual symmetry $G_\nu = Z_3$, which is only possible if the massive neutrinos are Dirac particles, we get the predictions $\sin^2\theta_{23} = 0.553$ ($\sin^2\theta_{23} = 0.447$) and $\cos\delta = 0.716$ ($\cos\delta = -0.716$). In the A1 case (A2 case) with the A_5 flavour symmetry and residual symmetry $G_\nu = Z_5$, which can be realised for neutrino Dirac mass term only, for the best fit values of $\sin^2\theta_{12}$ and $\sin^2\theta_{13}$ we get the predictions $\sin^2\theta_{23} = 0.630$ ($\sin^2\theta_{23} = 0.370$), which is slightly outside the 3σ range) and $\cos\delta = -1.12$ ($\cos\delta = 1.12$). However, using the value of $\sin^2\theta_{12} = 0.321$, which lies in the 1σ allowed interval of $\sin^2\theta_{12}$, one gets the same value of $\sin^2\theta_{23}$ and $\cos\delta = -0.992$ ($\cos\delta = 0.992$). In the part of the 3σ allowed interval of $\sin^2\theta_{12}$, $0.321 \leq \sin^2\theta_{12} \leq 0.359$, one has $-0.992 \leq \cos\delta \leq -0.633$ ($0.992 \geq \cos\delta \geq 0.633$).

[15] Note that there are no subgroups of the type $Z_n \times Z_m$ bigger than $Z_2 \times Z_2$ in the cases of A_4, S_4 and A_5.

[16] For case A1 it can been shown that

$$\mathrm{diag}(-1,1,1)\, U(\theta_{12}^\circ, \delta_{12}^\circ)\, R(\theta_{23}^\circ)\, R(\theta_{13}^\circ)\, \mathrm{diag}(1,-1,1) = U_{\rm BM}\,, \tag{2.37}$$

if $\theta_{23}^\circ = \sin^{-1}(1/2)$, $\theta_{13}^\circ = \sin^{-1}(\sqrt{1/3})$, $\theta_{12}^\circ = \tan^{-1}(\sqrt{3/2} + \sqrt{1/2})$ and $\delta_{12}^\circ = 0$. Therefore, one has BM mixing corrected from the left by a $U(2)$ transformation in the degenerate subspace in the 1-2 plane. Note that our results are in agreement with those obtained in [125].

2.3 Pattern B: $G_e = Z_n$, $n > 2$ or $Z_n \times Z_m$, $n, m \geq 2$ and $G_\nu = Z_2$

In this section, we derive sum rules for $\cos\delta$ in the case given in eq. (2.10). We recall that for $G_e = Z_n$, $n > 2$ or $Z_n \times Z_m$, $n, m \geq 2$ and $G_\nu = Z_2$ of interest, the matrix U_e is unambiguously determined (up to multiplication by diagonal phase matrices on the right and permutations of columns), while the matrix U_ν is determined up to a complex rotation in one plane.

2.3.1 Case B1: $U_{13}(\theta^\nu_{13}, \delta^\nu_{13})$

Combining the parametrisation of the PMNS matrix U given in eq. (2.10) with $(ij) = (13)$ and the parametrisation of U° as

$$U^\circ(\theta^\circ_{12}, \theta^\circ_{13}, \theta^\circ_{23}, \delta^\circ_{13}) = R_{23}(\theta^\circ_{23})\, R_{12}(\theta^\circ_{12})\, U_{13}(\theta^\circ_{13}, \delta^\circ_{13})\,, \tag{2.38}$$

we get for U (the details are given again in Appendix C):

$$U = R_{23}(\theta^\circ_{23})\, R_{12}(\theta^\circ_{12})\, U_{13}(\theta^\circ_{13}, \delta^\circ_{13})\, U_{13}(\theta^\nu_{13}, \delta^\nu_{13})\, Q_0\,. \tag{2.39}$$

The results derived in Appendix C and reported in eq. (C.6) allow us to recast eq. (2.39) in the form

$$U = R_{23}(\theta^\circ_{23})\, R_{12}(\theta^\circ_{12})\, P_3(\hat\delta_{13})\, R_{13}(\hat\theta_{13})\, Q_0\,, \quad P_3(\hat\delta_{13}) = \mathrm{diag}(1, 1, e^{i\hat\delta_{13}})\,. \tag{2.40}$$

Here $\hat\delta_{13} = -\alpha - \beta$ and we have redefined $P_{13}(\alpha, \beta)\, Q_0$ as Q_0, where $P_{13}(\alpha, \beta) = \mathrm{diag}(e^{i\alpha}, 1, e^{i\beta})$ and the expressions for $\sin^2\hat\theta_{13}$, α and β can be obtained from eqs. (C.7) and (C.8), by setting $i = 1$, $j = 3$, $\theta^a_{13} = \theta^\circ_{13}$, $\delta^a_{13} = \delta^\circ_{13}$, $\theta^b_{13} = \theta^\nu_{13}$ and $\delta^b_{13} = \delta^\nu_{13}$. Using eq. (2.40) and the standard parametrisation of the PMNS matrix U, we find:

$$\sin^2\theta_{13} = |U_{e3}|^2 = \cos^2\theta^\circ_{12}\sin^2\hat\theta_{13}\,, \tag{2.41}$$

$$\begin{aligned}\sin^2\theta_{23} = \frac{|U_{\mu3}|^2}{1-|U_{e3}|^2} = \frac{1}{\cos^2\theta_{13}}\Big[&\cos^2\theta^\circ_{23}\sin^2\hat\theta_{13}\sin^2\theta^\circ_{12} + \cos^2\hat\theta_{13}\sin^2\theta^\circ_{23} \\ &- \frac{1}{2}\sin 2\hat\theta_{13}\sin 2\theta^\circ_{23}\sin\theta^\circ_{12}\cos\hat\delta_{13}\Big]\,,\end{aligned} \tag{2.42}$$

$$\sin^2\theta_{12} = \frac{|U_{e2}|^2}{1-|U_{e3}|^2} = \frac{\sin^2\theta^\circ_{12}}{\cos^2\theta_{13}}\,. \tag{2.43}$$

It follows from eq. (2.43) that in the case under discussion the values of $\sin^2\theta_{12}$ and $\sin^2\theta_{13}$ are correlated.

A sum rule for $\cos\delta$ can be derived by comparing the expressions for the absolute value of the element $U_{\tau2}$ of the PMNS matrix in the standard parametrisation and in the one obtained using eq. (2.40):

$$|U_{\tau2}| = |\cos\theta_{12}\sin\theta_{23} + \sin\theta_{13}\cos\theta_{23}\sin\theta_{12}e^{i\delta}| = |\cos\theta^\circ_{12}\sin\theta^\circ_{23}|\,. \tag{2.44}$$

From this equation we get

$$\cos\delta = -\frac{\cos^2\theta_{13}(\cos^2\theta^\circ_{12}\cos^2\theta^\circ_{23} - \cos^2\theta_{23}) + \sin^2\theta^\circ_{12}(\cos^2\theta_{23} - \sin^2\theta_{13}\sin^2\theta_{23})}{\sin 2\theta_{23}\sin\theta_{13}|\sin\theta^\circ_{12}|(\cos^2\theta_{13} - \sin^2\theta^\circ_{12})^{\frac{1}{2}}}\,. \tag{2.45}$$

The dependence of the predictions for $\cos\delta$ on G_f is in this case via the values of θ°_{12} and θ°_{23}.

2.3.2 Case B2: $U_{23}(\theta^\nu_{23}, \delta^\nu_{23})$

Utilising the parametrisation of the PMNS matrix U given in eq. (2.10) with $(ij) = (23)$ and the following parametrisation of U°,

$$U^\circ(\theta^\circ_{12}, \theta^\circ_{13}, \theta^\circ_{23}, \delta^\circ_{23}) = R_{13}(\theta^\circ_{13})\, R_{12}(\theta^\circ_{12})\, U_{23}(\theta^\circ_{23}, \delta^\circ_{23})\,, \tag{2.46}$$

we obtain for U (Appendix C contains the relevant details):

$$U = R_{13}(\theta^\circ_{13})\, R_{12}(\theta^\circ_{12})\, U_{23}(\theta^\circ_{23}, \delta^\circ_{23})\, U_{23}(\theta^\nu_{23}, \delta^\nu_{23})\, Q_0\,. \tag{2.47}$$

The results given in eq. (C.6) in Appendix C make it possible to bring eq. (2.47) to the form

$$U = R_{13}(\theta^\circ_{13})\, R_{12}(\theta^\circ_{12})\, P_3(\hat{\delta}_{23})\, R_{23}(\hat{\theta}_{23})\, Q_0\,, \quad P_3(\hat{\delta}_{23}) = \mathrm{diag}(1, 1, e^{i\hat{\delta}_{23}})\,. \tag{2.48}$$

Here $\hat{\delta}_{23} = -\alpha - \beta$ and we have redefined $P_{23}(\alpha, \beta)\, Q_0$ as Q_0, where $P_{23}(\alpha, \beta) = \mathrm{diag}(1, e^{i\alpha}, e^{i\beta})$. Using eq. (2.48) and the standard parametrisation of the PMNS matrix U, we find:

$$\begin{aligned}\sin^2\theta_{13} = |U_{e3}|^2 &= \cos^2\theta^\circ_{13}\sin^2\theta^\circ_{12}\sin^2\hat{\theta}_{23} + \sin^2\theta^\circ_{13}\cos^2\hat{\theta}_{23} \\ &\quad + \frac{1}{2}\sin 2\hat{\theta}_{23}\sin 2\theta^\circ_{13}\sin\theta^\circ_{12}\cos\hat{\delta}_{23}\,,\end{aligned} \tag{2.49}$$

$$\sin^2\theta_{23} = \frac{|U_{\mu 3}|^2}{1 - |U_{e3}|^2} = \frac{\cos^2\theta^\circ_{12}\sin^2\hat{\theta}_{23}}{\cos^2\theta_{13}}\,, \tag{2.50}$$

$$\sin^2\theta_{12} = \frac{|U_{e2}|^2}{1 - |U_{e3}|^2} = \frac{\cos^2\theta_{13} - \cos^2\theta^\circ_{12}\cos^2\theta^\circ_{13}}{\cos^2\theta_{13}}\,. \tag{2.51}$$

Equation (2.51) implies that, as in the case investigated in the preceding subsection, the values of $\sin^2\theta_{12}$ and $\sin^2\theta_{13}$ are correlated.

The sum rule for $\cos\delta$ of interest can be obtained by comparing the expressions for the absolute value of the element $U_{\tau 1}$ of the PMNS matrix in the standard parametrisation and in the one obtained using eq. (2.48):

$$|U_{\tau 1}| = |\sin\theta_{12}\sin\theta_{23} - \sin\theta_{13}\cos\theta_{12}\cos\theta_{23}e^{i\delta}| = |\cos\theta^\circ_{12}\sin\theta^\circ_{13}|\,. \tag{2.52}$$

From the above equation we get for $\cos\delta$:

$$\cos\delta = \frac{\cos^2\theta_{13}(\sin^2\theta^\circ_{12} - \cos^2\theta_{23}) + \cos^2\theta^\circ_{12}\cos^2\theta^\circ_{13}(\cos^2\theta_{23} - \sin^2\theta_{13}\sin^2\theta_{23})}{\sin 2\theta_{23}\sin\theta_{13}|\cos\theta^\circ_{12}\cos\theta^\circ_{13}|(\cos^2\theta_{13} - \cos^2\theta^\circ_{12}\cos^2\theta^\circ_{13})^{\frac{1}{2}}}\,. \tag{2.53}$$

The dependence of $\cos\delta$ on G_f is realised in this case through the values of θ°_{12} and θ°_{13}.

2.3.3 Case B3: $U_{12}(\theta^\nu_{12}, \delta^\nu_{12})$

In this case, as we show below, $\cos\delta$ does not satisfy a sum rule, and thus is, in general, a free parameter. Indeed, using the parametrisation of U° as $U^\circ(\theta^\circ_{12}, \theta^\circ_{13}, \theta^\circ_{23}, \delta^\circ_{12}) = R_{23}(\theta^\circ_{23})\, R_{13}(\theta^\circ_{13})\, U_{12}(\theta^\circ_{12}, \delta^\circ_{12})$ we get the following expression for U:

$$U = R_{23}(\theta^\circ_{23})\, R_{13}(\theta^\circ_{13})\, U_{12}(\theta^\circ_{12}, \delta^\circ_{12})\, U_{12}(\theta^\nu_{12}, \delta^\nu_{12})\, Q_0\,. \tag{2.54}$$

After recasting eq. (2.54) in the form

$$U = R_{23}(\theta_{23}^{\circ})\, R_{13}(\theta_{13}^{\circ})\, P_2(\hat{\delta}_{12})\, R_{12}(\hat{\theta}_{12})\, Q_0\,, \quad P_2(\hat{\delta}_{12}) = \mathrm{diag}(1, e^{i\hat{\delta}_{12}}, 1)\,, \tag{2.55}$$

where $\hat{\delta}_{12} = -\alpha - \beta$, we find that $\sin^2\theta_{13} = \sin^2\theta_{13}^{\circ}$, $\sin^2\theta_{23} = \sin^2\theta_{23}^{\circ}$, $\sin^2\theta_{12} = \sin^2\hat{\theta}_{12}$ and $\cos\delta = \pm\cos\hat{\delta}_{12}$.

It follows from the expressions for the neutrino mixing parameters thus derived that, given a discrete symmetry G_f which can lead to the considered breaking patterns, the values of $\sin^2\theta_{13}$ and $\sin^2\theta_{23}$ are predicted. This, in turn, allows to test the phenomenological viability of the scheme under discussion for any appropriately chosen discrete lepton flavour symmetry G_f.

In what concerns the phase δ, it is expressed in terms of an unconstrained phase parameter present in the scheme we are considering. The comment made at the end of subsection 2.2.3 is valid also in this case. Namely, given a non-Abelian discrete flavour symmetry G_f which allows one to reproduce correctly the observed values of $\sin^2\theta_{13}$ and $\sin^2\theta_{23}$, it might be possible to obtain physically viable prediction for $\cos\delta$ by employing a generalised CP invariance constraint in the charged lepton or the neutrino sector.

2.3.4 Results for $G_f = A_4$ (T'), S_4 and A_5

The schemes discussed in subsections 2.3.1–2.3.3 are realised when breaking $G_f = A_4$ (T'), S_4 and A_5, to $G_e = Z_n$ ($n \geq 3$) or $Z_2 \times Z_2$ and $G_\nu = Z_2$, for both Dirac and Majorana neutrinos. As a reminder to the reader, we investigate the case of $Z_2 \times Z_2$ when it is an actual subgroup of G_f. As an explicit example of how this breaking can occur, we will consider the case of $G_f = A_4$ (T'). The other cases when $G_f = S_4$ or A_5 can be obtained from the breaking of S_4 and A_5 to the relevant subgroups as given in [125] and [144], respectively.

In the case of the group A_4 (see, e.g., [85]), the structure of the breaking patterns discussed, e.g., in subsection 2.3.1 can be obtained by breaking A_4 (i) in the charged lepton sector to any of the four Z_3 subgroups, namely, Z_3^T, Z_3^{ST}, Z_3^{TS}, Z_3^{STS}, and (ii) to any of the three Z_2 subgroups, namely, Z_2^S, $Z_2^{T^2ST}$, $Z_2^{TST^2}$, in the neutrino sector. In this case, the matrix $U^{\circ} = U_{\rm TBM}$ gets corrected by a complex rotation matrix in the 1-3 plane coming from the neutrino sector.

The results of the study performed by us of the phenomenological viability of the schemes with residual symmetries $G_e = Z_n$, $n > 2$ or $Z_n \times Z_m$, $n, m \geq 2$ and $G_\nu = Z_2$, discussed in subsections 2.3.1, 2.3.2 and 2.3.3, when the residual symmetries result from the breaking of the flavour symmetries A_4 (T'), S_4 and A_5, are described below. We present results only in the cases in which we obtain values of $\sin^2\theta_{12}$, $\sin^2\theta_{13}$ and $\sin^2\theta_{23}$ compatible with their respective measured values (including the corresponding 3σ uncertainties) and physically acceptable values of $\cos\delta$.

For $G_f = A_4$, we find that only case B1 with $G_e = Z_3$ is phenomenologically viable. In this case, we have $(\sin^2\theta_{12}^{\circ}, \sin^2\theta_{23}^{\circ}) = (1/3, 1/2)$, which leads to the predictions $\sin^2\theta_{12} = 0.341$ and $\cos\delta = 0.570$. We find precisely the same results in case B1 if $G_f = S_4$ and $G_e = Z_3$. Phenomenologically viable results are obtained for $G_f = S_4$ and $G_e = Z_3$ in case B2 as well. In this case, $(\sin^2\theta_{12}^{\circ}, \sin^2\theta_{13}^{\circ}) = (1/6, 1/5)$, implying the predictions $\sin^2\theta_{12} = 0.317$ and $\cos\delta = -0.269$. If $G_e = Z_4$ or $Z_2 \times Z_2$ results from $G_f = S_4$, we get in case B1 $(\sin^2\theta_{12}^{\circ}, \sin^2\theta_{23}^{\circ}) = (1/4, 1/3)$ and correspondingly $\sin^2\theta_{12} = 0.256$ (which lies slightly outside the 3σ allowed range of $\sin^2\theta_{12}$) and the unphysical value of $\cos\delta = -1.19$. These two values are obtained for the best fit values of $\sin^2\theta_{23}$ and $\sin^2\theta_{13}$. However, for

$\sin^2\theta_{23} = 0.419$ we find the physical value $\cos\delta = -0.990$, while in the part of the 3σ allowed interval of $\sin^2\theta_{23}$, $0.374 \leq \sin^2\theta_{23} \leq 0.419$, we have $-0.495 \geq \cos\delta \geq -0.990$.

If $G_f = A_5$, we find phenomenologically viable results (i) for $G_e = Z_3$, in case B1, (ii) for $G_e = Z_5$, in cases B1 and B2, and (iii) for $G_e = Z_2 \times Z_2$, in case B2. More specifically, if $G_e = Z_3$, we obtain in case B1 $(\sin^2\theta^\circ_{12}, \sin^2\theta^\circ_{23}) = (1/3, 1/2)$ leading to the predictions $\sin^2\theta_{12} = 0.341$ and $\cos\delta = 0.570$. For $G_e = Z_5$ in case B1 (case B2) we find $(\sin^2\theta^\circ_{12}, \sin^2\theta^\circ_{23}) = (0.276, 1/2)$ ($(\sin^2\theta^\circ_{12}, \sin^2\theta^\circ_{13}) = (0.138, 0.160)$), which leads to the predictions $\sin^2\theta_{12} = 0.283$ and $\cos\delta = 0.655$ ($\sin^2\theta_{12} = 0.259$ and $\cos\delta = -0.229$). Finally, for $G_e = Z_2 \times Z_2$ in case B2 we have two sets of values for $(\sin^2\theta^\circ_{12}, \sin^2\theta^\circ_{13})$. The first one, $(\sin^2\theta^\circ_{12}, \sin^2\theta^\circ_{13}) = (0.096, 0.276)$, together with the best fit values of $\sin^2\theta_{13}$ and $\sin^2\theta_{23}$, leads to $\sin^2\theta_{12} = 0.330$ and $\cos\delta = -1.36$. However, $\cos\delta$ takes the physical value of $\cos\delta = -0.996$ for $\sin^2\theta_{23} = 0.518$. In the part of the 3σ allowed interval of values of $\sin^2\theta_{23}$, $0.518 \leq \sin^2\theta_{23} \leq 0.641$, we have $-0.996 \leq \cos\delta \leq -0.478$. For the second set of values, $(\sin^2\theta^\circ_{12}, \sin^2\theta^\circ_{13}) = (1/4, 0.127)$, we get the predictions $\sin^2\theta_{12} = 0.330$ and $\cos\delta = 0.805$.

2.4 Pattern C: $G_e = Z_2$ and $G_\nu = Z_2$

In this section, we derive sum rules for $\cos\delta$ in the case given in eq. (2.12). We recall that when the residual symmetries are $G_e = Z_2$ and $G_\nu = Z_2$, each of the matrices U_e and U_ν is determined up to a complex rotation in one plane.

2.4.1 Case C1: $U_{12}(\theta^e_{12}, \delta^e_{12})$ and $U_{13}(\theta^\nu_{13}, \delta^\nu_{13})$

Similar to the already considered cases we combine the parametrisation of the PMNS matrix U given in eq. (2.12) with $(ij) = (12)$ and $(rs) = (13)$, with the parametrisation of U° given as

$$U^\circ(\theta^\circ_{12}, \theta^\circ_{13}, \theta^\circ_{23}, \delta^\circ_{12}, \delta^\circ_{13}) = U_{12}(\theta^\circ_{12}, \delta^\circ_{12})\, R_{23}(\theta^\circ_{23})\, U_{13}(\theta^\circ_{13}, \delta^\circ_{13})\,, \tag{2.56}$$

and get the following expression for U (as usual, we refer to Appendix C for details):

$$U = U_{12}(\theta^e_{12}, \delta^e_{12})\, U_{12}(\theta^\circ_{12}, \delta^\circ_{12})\, R_{23}(\theta^\circ_{23})\, U_{13}(\theta^\circ_{13}, \delta^\circ_{13})\, U_{13}(\theta^\nu_{13}, \delta^\nu_{13})\, Q_0\,. \tag{2.57}$$

Utilising the results derived in Appendix C and reported in eq. (C.6), we can recast eq. (2.57) in the form

$$U = R_{12}(\hat\theta^e_{12})\, P_1(\hat\delta)\, R_{23}(\theta^\circ_{23})\, R_{13}(\hat\theta^\nu_{13})\, Q_0\,, \quad P_1(\hat\delta) = \mathrm{diag}(e^{i\hat\delta}, 1, 1)\,. \tag{2.58}$$

Here $\hat\delta = \alpha^e - \beta^e + \alpha^\nu + \beta^\nu$ and we have redefined the matrix Q_0 by absorbing the diagonal phase matrix $P_{13}(-\beta^\nu, -\alpha^\nu) = \mathrm{diag}(e^{-i\beta^\nu}, 1, e^{-i\alpha^\nu})$ in it. Using eq. (2.58) and the standard parametrisation of the PMNS matrix U, we find:

$$\begin{aligned}\sin^2\theta_{13} &= |U_{e3}|^2 = \cos^2\hat\theta^e_{12}\sin^2\hat\theta^\nu_{13} + \cos^2\hat\theta^\nu_{13}\sin^2\hat\theta^e_{12}\sin^2\theta^\circ_{23} \\ &\quad + \frac{1}{2}\sin 2\hat\theta^e_{12}\sin 2\hat\theta^\nu_{13}\sin\theta^\circ_{23}\cos\hat\delta\,,\end{aligned} \tag{2.59}$$

$$\sin^2\theta_{23} = \frac{|U_{\mu3}|^2}{1-|U_{e3}|^2} = \frac{\sin^2\hat\theta^\nu_{13} - \sin^2\theta_{13} + \cos^2\hat\theta^\nu_{13}\sin^2\theta^\circ_{23}}{1-\sin^2\theta_{13}}\,, \tag{2.60}$$

$$\sin^2\theta_{12} = \frac{|U_{e2}|^2}{1-|U_{e3}|^2} = \frac{\sin^2\hat\theta^e_{12}\cos^2\theta^\circ_{23}}{1-\sin^2\theta_{13}}\,. \tag{2.61}$$

The sum rule for $\cos\delta$ of interest can be derived by comparing the expressions for the absolute value of the element $U_{\tau 2}$ of the PMNS matrix in the standard parametrisation and in the one obtained using eq. (2.58):

$$|U_{\tau 2}| = |\cos\theta_{12}\sin\theta_{23} + \sin\theta_{13}\cos\theta_{23}\sin\theta_{12}e^{i\delta}| = |\sin\theta^{\circ}_{23}|\,. \tag{2.62}$$

From the above equation we get for $\cos\delta$:

$$\cos\delta = \frac{\sin^2\theta^{\circ}_{23} - \cos^2\theta_{12}\sin^2\theta_{23} - \cos^2\theta_{23}\sin^2\theta_{12}\sin^2\theta_{13}}{\sin\theta_{13}\sin 2\theta_{23}\sin\theta_{12}\cos\theta_{12}}\,. \tag{2.63}$$

Given the assumed breaking pattern, $\cos\delta$ depends on the flavour symmetry G_f via the value of θ°_{23}. Using the best fit values of the standard mixing angles for the NO neutrino mass spectrum and the requirement $|\cos\delta| \leq 1$, we find that $\sin^2\theta^{\circ}_{23}$ should lie in the following interval: $0.236 \leq \sin^2\theta^{\circ}_{23} \leq 0.377$. Fixing two of the three angles to their best fit values and varying the third one in its 3σ experimentally allowed range and considering all the three possible combinations, we get that $|\cos\delta| \leq 1$ if $0.195 \leq \sin^2\theta^{\circ}_{23} \leq 0.504$.

2.4.2 Case C2: $U_{13}(\theta^{e}_{13}, \delta^{e}_{13})$ and $U_{12}(\theta^{\nu}_{12}, \delta^{\nu}_{12})$

As in the preceding case, we use the parametrisation of the PMNS matrix U given in eq. (2.12) but this time with $(ij) = (13)$ and $(rs) = (12)$, and the parametrisation of U° as

$$U^{\circ}(\theta^{\circ}_{12}, \theta^{\circ}_{13}, \theta^{\circ}_{23}, \delta^{\circ}_{12}, \delta^{\circ}_{13}) = U_{13}(\theta^{\circ}_{13}, \delta^{\circ}_{13})\, R_{23}(\theta^{\circ}_{23})\, U_{12}(\theta^{\circ}_{12}, \delta^{\circ}_{12})\,, \tag{2.64}$$

to get for U (again the details can be found in Appendix C):

$$U = U_{13}(\theta^{e}_{13}, \delta^{e}_{13})\, U_{13}(\theta^{\circ}_{13}, \delta^{\circ}_{13})\, R_{23}(\theta^{\circ}_{23})\, U_{12}(\theta^{\circ}_{12}, \delta^{\circ}_{12})\, U_{12}(\theta^{\nu}_{12}, \delta^{\nu}_{12})\, Q_0\,. \tag{2.65}$$

The results derived in Appendix C and reported in eq. (C.6) allow us to rewrite the expression for U in eq. (2.65) as follows:

$$U = R_{13}(\hat{\theta}^{e}_{13})\, P_1(\hat{\delta})\, R_{23}(\theta^{\circ}_{23})\, R_{12}(\hat{\theta}^{\nu}_{12})\, Q_0\,, \quad P_1(\hat{\delta}) = \mathrm{diag}(e^{i\hat{\delta}}, 1, 1)\,, \tag{2.66}$$

where $\hat{\delta} = \alpha^{e} - \beta^{e} + \alpha^{\nu} + \beta^{\nu}$, and also in this case we have redefined the matrix Q_0 by absorbing the phase matrix $P_{12}(-\beta^{\nu}, -\alpha^{\nu}) = \mathrm{diag}(e^{-i\beta^{\nu}}, e^{-i\alpha^{\nu}}, 1)$ in it. From eq. (2.66) and the standard parametrisation of the PMNS matrix U we get:

$$\sin^2\theta_{13} = |U_{e3}|^2 = \cos^2\theta^{\circ}_{23}\sin^2\hat{\theta}^{e}_{13}\,, \tag{2.67}$$

$$\sin^2\theta_{23} = \frac{|U_{\mu 3}|^2}{1 - |U_{e3}|^2} = \frac{\sin^2\theta^{\circ}_{23}}{\cos^2\theta_{13}}\,, \tag{2.68}$$

$$\begin{aligned}\sin^2\theta_{12} = \frac{|U_{e2}|^2}{1 - |U_{e3}|^2} = \frac{1}{1 - \sin^2\theta_{13}}\Big[&\cos^2\hat{\theta}^{e}_{13}\sin^2\hat{\theta}^{\nu}_{12} + \cos^2\hat{\theta}^{\nu}_{12}\sin^2\hat{\theta}^{e}_{13}\sin^2\theta^{\circ}_{23} \\ &- \frac{1}{2}\sin 2\hat{\theta}^{e}_{13}\sin 2\hat{\theta}^{\nu}_{12}\sin\theta^{\circ}_{23}\cos\hat{\delta}\Big]\,.\end{aligned} \tag{2.69}$$

Given the value of $\sin^2\theta^{\circ}_{23}$, eq. (2.68) implies the existence of a correlation between the values of $\sin^2\theta_{23}$ and $\sin^2\theta_{13}$.

Comparing the expressions for the absolute value of the element $U_{\mu 1}$ of the PMNS matrix in the standard parametrisation and in the one obtained using eq. (2.66), we have

$$|U_{\mu 1}| = |\sin\theta_{12}\cos\theta_{23} + \sin\theta_{13}\sin\theta_{23}\cos\theta_{12}e^{i\delta}| = |\sin\hat{\theta}^{\nu}_{12}\cos\theta^{\circ}_{23}|\,. \tag{2.70}$$

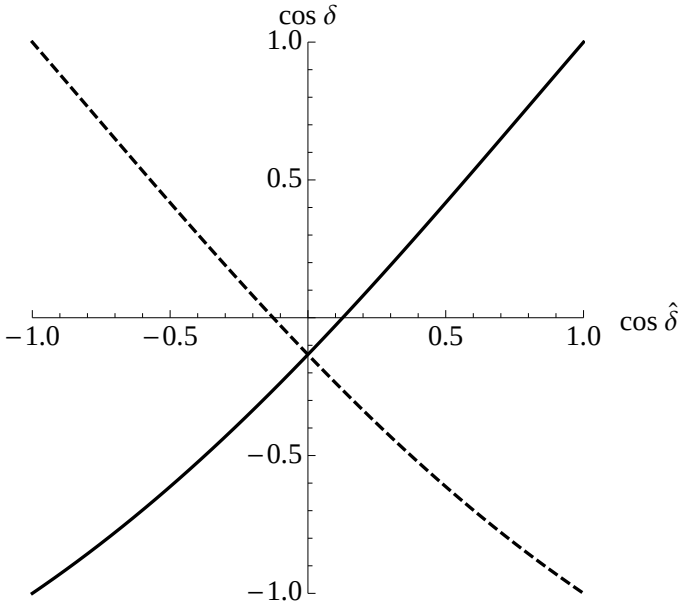

Figure 2.1. Dependence of $\cos\delta$ on $\cos\hat{\delta}$ in the case of $G_f = S_4$ with $\sin^2\theta^\circ_{23} = 1/2$. The mixing parameters $\sin^2\theta_{12}$ and $\sin^2\theta_{13}$ have been fixed to their best fit values for the NO neutrino mass spectrum quoted in eqs. (2.15) and (2.17). The solid (dashed) line is for the case when $\sin 2\hat{\theta}^e_{13}\sin 2\hat{\theta}^\nu_{12}$ is positive (negative).

From the above equations we get for $\cos\delta$:

$$\cos\delta = \frac{\cos^2\theta_{13}(\cos^2\theta^\circ_{23}\sin^2\hat{\theta}^\nu_{12} - \sin^2\theta_{12}) + \sin^2\theta^\circ_{23}(\sin^2\theta_{12} - \cos^2\theta_{12}\sin^2\theta_{13})}{\sin 2\theta_{12}\sin\theta_{13}|\sin\theta^\circ_{23}|(\cos^2\theta_{13} - \sin^2\theta^\circ_{23})^{\frac{1}{2}}}\,. \quad (2.71)$$

In this case, $\cos\delta$ is a function of the known neutrino mixing angles θ_{12} and θ_{13}, of the angle θ°_{23} fixed by G_f and the assumed symmetry breaking pattern, as well as of the phase parameter $\hat{\delta}$ of the scheme. Predictions for $\cos\delta$ can only be obtained when $\hat{\delta}$ is fixed by additional considerations of, e.g., generalised CP invariance, symmetries, etc. In view of this we show in Fig. 2.1 $\cos\delta$ as a function of $\cos\hat{\delta}$ for the best fit values of $\sin^2\theta_{12}$ and $\sin^2\theta_{13}$, and for the value $\sin^2\theta^\circ_{23} = 1/2$ corresponding to $G_f = S_4$. We do not find phenomenologically viable cases for A_4 (T') and A_5. Therefore we do not present such a plot for these groups.

2.4.3 Case C3: $U_{12}(\theta^e_{12}, \delta^e_{12})$ and $U_{23}(\theta^\nu_{23}, \delta^\nu_{23})$

We get for the PMNS matrix U,

$$U = U_{12}(\theta^e_{12}, \delta^e_{12})\, U_{12}(\theta^\circ_{12}, \delta^\circ_{12})\, R_{13}(\theta^\circ_{13})\, U_{23}(\theta^\circ_{23}, \delta^\circ_{23})\, U_{23}(\theta^\nu_{23}, \delta^\nu_{23})\, Q_0\,, \quad (2.72)$$

utilising the parametrisations of U shown in eq. (2.12) with $(ij) = (12)$ and $(rs) = (23)$ and that of U° given below (further details can be found in Appendix C),

$$U^\circ(\theta^\circ_{12}, \theta^\circ_{13}, \theta^\circ_{23}, \delta^\circ_{12}, \delta^\circ_{23}) = U_{12}(\theta^\circ_{12}, \delta^\circ_{12})\, R_{13}(\theta^\circ_{13})\, U_{23}(\theta^\circ_{23}, \delta^\circ_{23})\,. \quad (2.73)$$

With the help of the results derived in Appendix C and especially of eq. (C.6), the expression in eq. (2.72) for the PMNS matrix U can be brought to the form

$$U = R_{12}(\hat{\theta}^e_{12})\, P_2(\hat{\delta})\, R_{13}(\theta^\circ_{13})\, R_{23}(\hat{\theta}^\nu_{23})\, Q_0\,, \quad P_2(\hat{\delta}) = \mathrm{diag}(1, e^{i\hat{\delta}}, 1)\,, \quad (2.74)$$

where $\hat{\delta} = \beta^e - \alpha^e + \alpha^\nu + \beta^\nu$ and, as in the preceding cases, we have redefined the phase matrix Q_0 by absorbing the phase matrix $P_{23}(-\beta^\nu, -\alpha^\nu) = \text{diag}(1, e^{-i\beta^\nu}, e^{-i\alpha^\nu})$ in it. Using eq. (2.74) and the standard parametrisation of the PMNS matrix U, we find:

$$\sin^2\theta_{13} = |U_{e3}|^2 = \sin^2\hat{\theta}^e_{12}\sin^2\hat{\theta}^\nu_{23} + \cos^2\hat{\theta}^e_{12}\cos^2\hat{\theta}^\nu_{23}\sin^2\theta^\circ_{13} + \frac{1}{2}\sin 2\hat{\theta}^e_{12}\sin 2\hat{\theta}^\nu_{23}\sin\theta^\circ_{13}\cos\hat{\delta}\,, \tag{2.75}$$

$$\sin^2\theta_{23} = \frac{|U_{\mu 3}|^2}{1-|U_{e3}|^2} = \frac{\sin^2\hat{\theta}^\nu_{23} - \sin^2\theta_{13} + \cos^2\hat{\theta}^\nu_{23}\sin^2\theta^\circ_{13}}{1-\sin^2\theta_{13}}\,, \tag{2.76}$$

$$\sin^2\theta_{12} = \frac{|U_{e2}|^2}{1-|U_{e3}|^2} = \frac{\sin^2\hat{\theta}^e_{12} - \sin^2\theta_{13} + \cos^2\hat{\theta}^e_{12}\sin^2\theta^\circ_{13}}{1-\sin^2\theta_{13}}\,. \tag{2.77}$$

The sum rule for $\cos\delta$ of interest can be derived, e.g., by comparing the expressions for the absolute value of the element $U_{\tau 1}$ of the PMNS matrix in the standard parametrisation and in the one obtained using eq. (2.74):

$$|U_{\tau 1}| = |\sin\theta_{12}\sin\theta_{23} - \sin\theta_{13}\cos\theta_{12}\cos\theta_{23}e^{i\delta}| = |\sin\theta^\circ_{13}|\,. \tag{2.78}$$

For $\cos\delta$ we get:

$$\cos\delta = \frac{\sin^2\theta_{12}\sin^2\theta_{23} - \sin^2\theta^\circ_{13} + \cos^2\theta_{12}\cos^2\theta_{23}\sin^2\theta_{13}}{\sin\theta_{13}\sin 2\theta_{23}\sin\theta_{12}\cos\theta_{12}}\,. \tag{2.79}$$

In this case, in contrast to that considered in the preceding subsection, $\cos\delta$ is predicted once the angle θ°_{13}, i.e., the flavour symmetry G_f, is fixed. Using the best fit values of $\sin^2\theta_{12}$, $\sin^2\theta_{13}$ and $\sin^2\theta_{23}$ for the NO neutrino mass spectrum, we find that physical values of $\cos\delta$ satisfying $|\cos\delta| \leq 1$ can be obtained only if $\sin^2\theta^\circ_{13}$ lies in the following interval: $0.074 \leq \sin^2\theta^\circ_{13} \leq 0.214$. Fixing two of the three neutrino mixing parameters $\sin^2\theta_{12}$, $\sin^2\theta_{13}$ and $\sin^2\theta_{23}$ to their best fit values and varying the third one in its 3σ experimentally allowed range and taking into account all the three possible combinations, we get that $|\cos\delta| \leq 1$ provided $0.056 \leq \sin^2\theta^\circ_{13} \leq 0.267$.

2.4.4 Case C4: $U_{13}(\theta^e_{13}, \delta^e_{13})$ and $U_{23}(\theta^\nu_{23}, \delta^\nu_{23})$

The parametrisation of the PMNS matrix U, to be used further,

$$U = U_{13}(\theta^e_{13}, \delta^e_{13})\, U_{13}(\theta^\circ_{13}, \delta^\circ_{13})\, R_{12}(\theta^\circ_{12})\, U_{23}(\theta^\circ_{23}, \delta^\circ_{23})\, U_{23}(\theta^\nu_{23}, \delta^\nu_{23})\, Q_0\,, \tag{2.80}$$

is found in this case from the parametrisations of the matrix U given in eq. (2.12) with $(ij) = (13)$ and $(rs) = (23)$ and that of U° shown below (see Appendix C for details),

$$U^\circ(\theta^\circ_{12}, \theta^\circ_{13}, \theta^\circ_{23}, \delta^\circ_{13}, \delta^\circ_{23}) = U_{13}(\theta^\circ_{13}, \delta^\circ_{13})\, R_{12}(\theta^\circ_{12})\, U_{23}(\theta^\circ_{23}, \delta^\circ_{23})\,. \tag{2.81}$$

The results presented in eq. (C.6) of Appendix C allow us to recast eq. (2.80) in the form

$$U = R_{13}(\hat{\theta}^e_{13})\, P_3(\hat{\delta})\, R_{12}(\theta^\circ_{12})\, R_{23}(\hat{\theta}^\nu_{23})\, Q_0\,, \quad P_3(\hat{\delta}) = \text{diag}(1, 1, e^{i\hat{\delta}})\,. \tag{2.82}$$

Here $\hat{\delta} = \beta^e - \alpha^e - \alpha^\nu - \beta^\nu$ and we have absorbed the phase matrix $P_{23}(\alpha^\nu, \beta^\nu) = \text{diag}(1, e^{i\alpha^\nu}, e^{i\beta^\nu})$ in the matrix Q_0. Using eq. (2.82) and the standard parametrisation of the PMNS matrix U, we find:

$$\sin^2\theta_{13} = |U_{e3}|^2 = \cos^2\hat{\theta}^\nu_{23}\sin^2\hat{\theta}^e_{13} + \cos^2\hat{\theta}^e_{13}\sin^2\hat{\theta}^\nu_{23}\sin^2\theta^\circ_{12}$$

$$+ \frac{1}{2} \sin 2\hat{\theta}^e_{13} \sin 2\hat{\theta}^\nu_{23} \sin\theta^\circ_{12} \cos\hat{\delta}\,, \tag{2.83}$$

$$\sin^2\theta_{23} = \frac{|U_{\mu 3}|^2}{1-|U_{e3}|^2} = \frac{\cos^2\theta^\circ_{12}\sin^2\hat{\theta}^\nu_{23}}{1-\sin^2\theta_{13}}\,, \tag{2.84}$$

$$\sin^2\theta_{12} = \frac{|U_{e2}|^2}{1-|U_{e3}|^2} = \frac{\sin^2\hat{\theta}^e_{13} - \sin^2\theta_{13} + \cos^2\hat{\theta}^e_{13}\sin^2\theta^\circ_{12}}{1-\sin^2\theta_{13}}\,. \tag{2.85}$$

Comparing the expressions for the absolute value of the element $U_{\mu 1}$ of the PMNS matrix in the standard parametrisation and in the one obtained using eq. (2.82), we find

$$|U_{\mu 1}| = |\sin\theta_{12}\cos\theta_{23} + \sin\theta_{13}\sin\theta_{23}\cos\theta_{12}e^{i\delta}| = |\sin\theta^\circ_{12}|\,. \tag{2.86}$$

From the above equation we get for $\cos\delta$:

$$\cos\delta = \frac{\sin^2\theta^\circ_{12} - \cos^2\theta_{23}\sin^2\theta_{12} - \cos^2\theta_{12}\sin^2\theta_{13}\sin^2\theta_{23}}{\sin\theta_{13}\sin 2\theta_{23}\sin\theta_{12}\cos\theta_{12}}\,. \tag{2.87}$$

The predicted value of $\cos\delta$ depends on the discrete symmetry G_f through the value of the angle θ°_{12}. Using the best fit values of the standard mixing angles for the NO neutrino mass spectrum and the requirement $|\cos\delta| \leq 1$, we find that $\sin^2\theta^\circ_{12}$ should lie in the following interval: $0.110 \leq \sin^2\theta^\circ_{12} \leq 0.251$. Fixing two of the three neutrino mixing angles to their best fit values and varying the third one in its 3σ experimentally allowed range and accounting for all the three possible combinations, we get that $|\cos\delta| \leq 1$ if $0.057 \leq \sin^2\theta^\circ_{12} \leq 0.281$.

2.4.5 Case C5: $U_{23}(\theta^e_{23}, \delta^e_{23})$ and $U_{13}(\theta^\nu_{13}, \delta^\nu_{13})$

The parametrisation of the PMNS matrix U, which is convenient for our further analysis,

$$U = U_{23}(\theta^e_{23}, \delta^e_{23})\, U_{23}(\theta^\circ_{23}, \delta^\circ_{23})\, R_{12}(\theta^\circ_{12})\, U_{13}(\theta^\circ_{13}, \delta^\circ_{13})\, U_{13}(\theta^\nu_{13}, \delta^\nu_{13})\, Q_0\,, \tag{2.88}$$

can be obtained in this case utilising the parametrisations of the matrix U given in eq. (2.12) with $(ij) = (23)$ and $(rs) = (13)$ and that of the matrix U° given below (for details see Appendix C),

$$U^\circ(\theta^\circ_{12}, \theta^\circ_{13}, \theta^\circ_{23}, \delta^\circ_{13}, \delta^\circ_{23}) = U_{23}(\theta^\circ_{23}, \delta^\circ_{23})\, R_{12}(\theta^\circ_{12})\, U_{13}(\theta^\circ_{13}, \delta^\circ_{13})\,. \tag{2.89}$$

The expression in eq. (2.88) for U can further be cast in a "minimal" form with the help of eq. (C.6) in Appendix C:

$$U = R_{23}(\hat{\theta}^e_{23})\, P_3(\hat{\delta})\, R_{12}(\theta^\circ_{12})\, R_{13}(\hat{\theta}^\nu_{13})\, Q_0\,, \quad P_3(\hat{\delta}) = \mathrm{diag}(1, 1, e^{i\hat{\delta}})\,, \tag{2.90}$$

where $\hat{\delta} = \beta^e - \alpha^e - \alpha^\nu - \beta^\nu$ and we have absorbed the matrix $P_{13}(\alpha^\nu, \beta^\nu) = \mathrm{diag}(e^{i\alpha^\nu}, 1, e^{i\beta^\nu})$ in the phase matrix Q_0. Using eq. (2.90) and the standard parametrisation of the PMNS matrix U, we find:

$$\sin^2\theta_{13} = |U_{e3}|^2 = \cos^2\theta^\circ_{12}\sin^2\hat{\theta}^\nu_{13}\,, \tag{2.91}$$

$$\sin^2\theta_{23} = \frac{|U_{\mu 3}|^2}{1-|U_{e3}|^2} = \frac{1}{1-\sin^2\theta_{13}}\Big[\cos^2\hat{\theta}^\nu_{13}\sin^2\hat{\theta}^e_{23} + \cos^2\hat{\theta}^e_{23}\sin^2\hat{\theta}^\nu_{13}\sin^2\theta^\circ_{12} - \frac{1}{2}\sin 2\hat{\theta}^e_{23}\sin 2\hat{\theta}^\nu_{13}\sin\theta^\circ_{12}\cos\hat{\delta}\Big]\,, \tag{2.92}$$

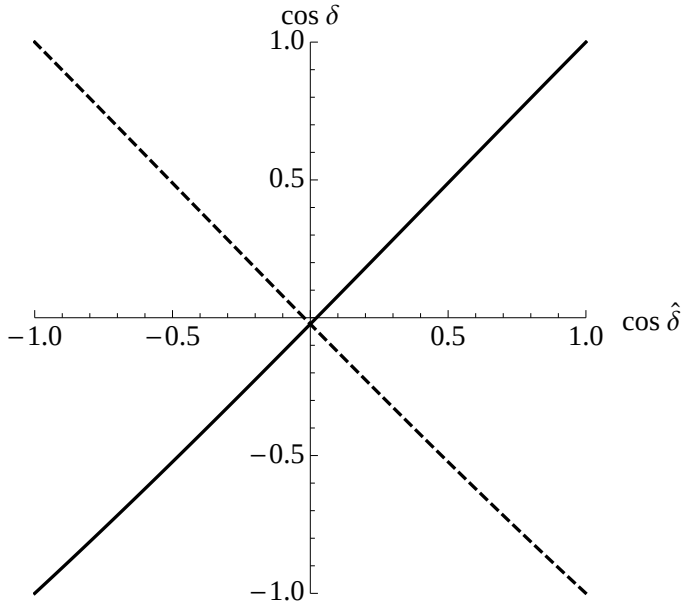

Figure 2.2. Dependence of $\cos\delta$ on $\cos\hat{\delta}$ in the case of $G_f = S_4$ or A_5 with $\sin^2\theta_{12}^\circ = 1/4$. The mixing parameters $\sin^2\theta_{23}$ and $\sin^2\theta_{13}$ have been fixed to their best fit values for the NO neutrino mass spectrum quoted in eqs. (2.16) and (2.17). The solid (dashed) line is for the case when $\sin 2\hat{\theta}_{23}^e \sin 2\hat{\theta}_{13}^\nu$ is positive (negative).

$$\sin^2\theta_{12} = \frac{|U_{e2}|^2}{1-|U_{e3}|^2} = \frac{\sin^2\theta_{12}^\circ}{1-\sin^2\theta_{13}}\,. \tag{2.93}$$

We note that, given G_f, the values of $\sin^2\theta_{12}$ and $\sin^2\theta_{13}$ are correlated. This allows one to perform a critical test of the scheme under study once the discrete symmetry group G_f has been specified.

The sum rule for $\cos\delta$ of interest can be derived, e.g., by comparing the expressions for the absolute value of the element $U_{\tau 2}$ of the PMNS matrix in the standard parametrisation and in the one obtained using eq. (2.90):

$$|U_{\tau 2}| = |\cos\theta_{12}\sin\theta_{23} + \sin\theta_{13}\cos\theta_{23}\sin\theta_{12}e^{i\delta}| = |\cos\theta_{12}^\circ \sin\hat{\theta}_{23}^e|\,. \tag{2.94}$$

This leads to

$$\cos\delta = \frac{\cos^2\theta_{13}(\cos^2\theta_{12}^\circ\sin^2\hat{\theta}_{23}^e - \sin^2\theta_{23}) + \sin^2\theta_{12}^\circ(\sin^2\theta_{23} - \cos^2\theta_{23}\sin^2\theta_{13})}{\sin 2\theta_{23}\sin\theta_{13}|\sin\theta_{12}^\circ|(\cos^2\theta_{13} - \sin^2\theta_{12}^\circ)^{\frac{1}{2}}}\,. \tag{2.95}$$

Similar to case C2 analysed in subsection 2.4.2, $\cos\delta$ is a function of the known neutrino mixing angles θ_{13} and θ_{23}, of the angle θ_{12}° fixed by G_f and the assumed symmetry breaking pattern, as well as of the phase parameter $\hat{\delta}$ of the scheme. Predictions for $\cos\delta$ can be obtained if $\hat{\delta}$ is fixed by additional considerations of, e.g., generalised CP invariance, symmetries, etc. In view of this we show in Fig. 2.2 $\cos\delta$ as a function of $\cos\hat{\delta}$ for the best fit values of $\sin^2\theta_{13}$ and $\sin^2\theta_{23}$, and for the value $\sin^2\theta_{12}^\circ = 1/4$ corresponding to $G_f = S_4$ and A_5. We do not find phenomenologically viable cases for A_4 (T'). Therefore we do not present such a plot for these groups.

2.4.6 Case C6: $U_{23}(\theta_{23}^e, \delta_{23}^e)$ and $U_{12}(\theta_{12}^\nu, \delta_{12}^\nu)$

We show below that in this case $\cos\delta$ coincides (up to a sign) with the cosine of an unconstrained CPV phase parameter of the scheme and therefore cannot be determined

from the values of the neutrino mixing angles and of the angles determined by the residual symmetries. Indeed, using the parametrisation of the matrix U given in eq. (2.12) with $(ij) = (23)$ and $(rs) = (12)$ and the parametrisation of U° as follows (see Appendix C for details),

$$U^\circ(\theta^\circ_{12}, \theta^\circ_{13}, \theta^\circ_{23}, \delta^\circ_{12}, \delta^\circ_{23}) = U_{23}(\theta^\circ_{23}, \delta^\circ_{23})\, R_{13}(\theta^\circ_{13})\, U_{12}(\theta^\circ_{12}, \delta^\circ_{12})\,, \tag{2.96}$$

we get for U:

$$U = U_{23}(\theta^e_{23}, \delta^e_{23})\, U_{23}(\theta^\circ_{23}, \delta^\circ_{23})\, R_{13}(\theta^\circ_{13})\, U_{12}(\theta^\circ_{12}, \delta^\circ_{12})\, U_{12}(\theta^\nu_{12}, \delta^\nu_{12})\, Q_0\,. \tag{2.97}$$

The results derived in Appendix C in eq. (C.6) make it possible to recast eq. (2.97) in the form

$$U = R_{23}(\hat\theta^e_{23})\, P_2(\hat\delta)\, R_{13}(\theta^\circ_{13})\, R_{12}(\hat\theta^\nu_{12})\, Q_0\,, \quad P_2(\hat\delta) = \mathrm{diag}(1, e^{i\hat\delta}, 1)\,. \tag{2.98}$$

Here $\hat\delta = \alpha^e - \beta^e - \alpha^\nu - \beta^\nu$ and, as in the preceding cases, we have redefined the phase matrix Q_0 by absorbing the phase matrix $P_{12}(\alpha^\nu, \beta^\nu) = \mathrm{diag}(e^{i\alpha^\nu}, e^{i\beta^\nu}, 1)$ in it. Using eq. (2.98) and the standard parametrisation of the PMNS matrix U, we find that $\sin^2\theta_{13} = \sin^2\theta^\circ_{13}$, $\sin^2\theta_{23} = \sin^2\hat\theta^e_{23}$ and $\sin^2\theta_{12} = \sin^2\hat\theta^\nu_{12}$. Comparing the absolute value of the element $U_{\tau 1}$ allows us to find that $\cos\delta = \pm\cos\hat\delta$. Thus, for a given flavour symmetry G_f, the value of $\sin^2\theta_{13}$ is predicted. This allows to test the phenomenological viability of the case under discussion, since the value of $\sin^2\theta_{13}$ is known experimentally with a relatively high precision.

A comment, analogous to those made in similar cases considered in subsections 2.2.3 and 2.3.3, is in order. Namely, for a non-Abelian flavour symmetry G_f which allows to reproduce correctly the observed values of $\sin^2\theta_{12}$, $\sin^2\theta_{13}$ and $\sin^2\theta_{23}$, it might be possible to obtain physically viable prediction for $\cos\delta$ by employing generalised CP invariance in the charged lepton or the neutrino sector.

2.4.7 Case C7: $U_{12}(\theta^e_{12}, \delta^e_{12})$ and $U_{12}(\theta^\nu_{12}, \delta^\nu_{12})$

Using the following parametrisation of U°,

$$U^\circ(\theta^\circ_{12}, \tilde\theta^\circ_{12}, \theta^\circ_{23}, \delta^\circ_{12}, \tilde\delta^\circ_{12}) = U_{12}(\theta^\circ_{12}, \delta^\circ_{12})\, R_{23}(\theta^\circ_{23})\, U_{12}(\tilde\theta^\circ_{12}, \tilde\delta^\circ_{12})\,, \tag{2.99}$$

we have for U:

$$U = U_{12}(\theta^e_{12}, \delta^e_{12})\, U_{12}(\theta^\circ_{12}, \delta^\circ_{12})\, R_{23}(\theta^\circ_{23})\, U_{12}(\tilde\theta^\circ_{12}, \tilde\delta^\circ_{12})\, U_{12}(\theta^\nu_{12}, \delta^\nu_{12})\, Q_0\,. \tag{2.100}$$

Utilising the results derived in Appendix C and reported in eq. (C.6), we can recast eq. (2.100) in the form

$$U = R_{12}(\hat\theta^e_{12})\, P_1(\hat\delta)\, R_{23}(\theta^\circ_{23})\, R_{12}(\hat\theta^\nu_{12})\, Q_0\,, \quad P_1(\hat\delta) = \mathrm{diag}(e^{i\hat\delta}, 1, 1)\,. \tag{2.101}$$

Here $\hat\delta = \alpha^e - \beta^e + \alpha^\nu + \beta^\nu$ and we have redefined the matrix Q_0 by absorbing the diagonal phase matrix $P_{12}(-\beta^\nu, -\alpha^\nu) = \mathrm{diag}(e^{-i\beta^\nu}, e^{-i\alpha^\nu}, 1)$ in it. Using eq. (2.101) and the standard parametrisation of the PMNS matrix U, we find:

$$\sin^2\theta_{13} = |U_{e3}|^2 = \sin^2\theta^\circ_{23}\sin^2\hat\theta^e_{12}\,, \tag{2.102}$$

$$\sin^2\theta_{23} = \frac{|U_{\mu 3}|^2}{1-|U_{e3}|^2} = \frac{\sin^2\theta^\circ_{23}\cos^2\hat\theta^e_{12}}{1-\sin^2\theta_{13}}\,, \tag{2.103}$$

$$\sin^2\theta_{12} = \frac{|U_{e2}|^2}{1-|U_{e3}|^2} = \frac{1}{1-\sin^2\theta_{13}}\big[\cos^2\theta^\circ_{23}\cos^2\hat\theta^\nu_{12}\sin^2\hat\theta^e_{12} + \cos^2\hat\theta^e_{12}\sin^2\hat\theta^\nu_{12}$$

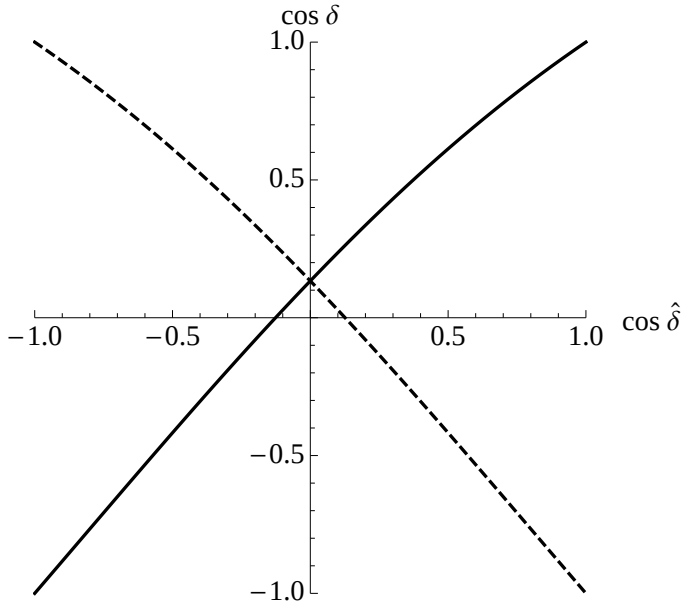

Figure 2.3. Dependence of $\cos\delta$ on $\cos\hat{\delta}$ in the case of $G_f = S_4$ with $\sin^2\theta^\circ_{23} = 1/2$. The mixing parameters $\sin^2\theta_{12}$ and $\sin^2\theta_{13}$ have been fixed to their best fit values for the NO neutrino mass spectrum quoted in eqs. (2.15) and (2.17). The solid (dashed) line is for the case when $\sin 2\hat{\theta}^e_{12}\sin 2\hat{\theta}^\nu_{12}$ is positive (negative).

$$+\frac{1}{2}\sin 2\hat{\theta}^e_{12}\sin 2\hat{\theta}^\nu_{12}\cos\theta^\circ_{23}\cos\hat{\delta}\Big]\,. \tag{2.104}$$

From eqs. (2.102) and (2.103) we see that the angles θ_{13} and θ_{23} are correlated:

$$\sin^2\theta_{23} = \frac{\sin^2\theta^\circ_{23} - \sin^2\theta_{13}}{1-\sin^2\theta_{13}}\,. \tag{2.105}$$

Comparing the expressions for the absolute value of the element $U_{\tau 1}$ of the PMNS matrix in the standard parametrisation and in the one obtained using eq. (2.101), we have

$$|U_{\tau 1}| = |\sin\theta_{12}\sin\theta_{23} - \sin\theta_{13}\cos\theta_{23}\cos\theta_{12}e^{i\delta}| = |\sin\hat{\theta}^\nu_{12}\sin\theta^\circ_{23}|\,. \tag{2.106}$$

From the above equations we get for $\cos\delta$:

$$\cos\delta = \frac{\sin^2\theta_{13}(\cos^2\theta_{12}\cos^2\theta^\circ_{23} - \sin^2\theta_{12}) + \sin^2\theta^\circ_{23}(\sin^2\theta_{12} - \cos^2\theta_{13}\sin^2\hat{\theta}^\nu_{12})}{\sin 2\theta_{12}\sin\theta_{13}|\cos\theta^\circ_{23}|(\sin^2\theta^\circ_{23} - \sin^2\theta_{13})^{\frac{1}{2}}}\,. \tag{2.107}$$

In this case, $\cos\delta$ is a function of the known neutrino mixing angles θ_{12} and θ_{13}, of the angle θ°_{23} fixed by G_f and the assumed symmetry breaking pattern, as well as of the phase parameter $\hat{\delta}$ of the scheme. Predictions for $\cos\delta$ can only be obtained when $\hat{\delta}$ is fixed by additional considerations of, e.g., generalised CP invariance, symmetries, etc. In view of this we show in Fig. 2.3 $\cos\delta$ as a function of $\cos\hat{\delta}$ for the best fit values of $\sin^2\theta_{12}$ and $\sin^2\theta_{13}$, and for the value $\sin^2\theta^\circ_{23} = 1/2$ corresponding to $G_f = S_4$. We do not find phenomenologically viable cases for $G_f = A_4$ (T') and A_5.

2.4.8 Case C8: $U_{13}(\theta^e_{13}, \delta^e_{13})$ and $U_{13}(\theta^\nu_{13}, \delta^\nu_{13})$

Using the following parametrisation of U°,

$$U^\circ(\theta^\circ_{13}, \tilde{\theta}^\circ_{13}, \theta^\circ_{23}, \delta^\circ_{13}, \tilde{\delta}^\circ_{13}) = U_{13}(\theta^\circ_{13}, \delta^\circ_{13})\, R_{23}(\theta^\circ_{23})\, U_{13}(\tilde{\theta}^\circ_{13}, \tilde{\delta}^\circ_{13})\,, \tag{2.108}$$

we have for U:

$$U = U_{13}(\theta^e_{13}, \delta^e_{13})\, U_{13}(\theta^\circ_{13}, \delta^\circ_{13})\, R_{23}(\theta^\circ_{23})\, U_{13}(\tilde{\theta}^\circ_{13}, \tilde{\delta}^\circ_{13})\, U_{13}(\theta^\nu_{13}, \delta^\nu_{13})\, Q_0\,. \tag{2.109}$$

Utilising the results derived in Appendix C and reported in eq. (C.6), we can recast eq. (2.109) in the form

$$U = R_{13}(\hat{\theta}^e_{13})\, P_1(\hat{\delta})\, R_{23}(\theta^\circ_{23})\, R_{13}(\hat{\theta}^\nu_{13})\, Q_0\,, \quad P_1(\hat{\delta}) = \mathrm{diag}(e^{i\hat{\delta}}, 1, 1)\,. \tag{2.110}$$

Here $\hat{\delta} = \alpha^e - \beta^e + \alpha^\nu + \beta^\nu$ and we have redefined the matrix Q_0 by absorbing the diagonal phase matrix $P_{13}(-\beta^\nu, -\alpha^\nu) = \mathrm{diag}(e^{-i\beta^\nu}, 1, e^{-i\alpha^\nu})$ in it. Using eq. (2.110) and the standard parametrisation of the PMNS matrix U, we find:

$$\begin{aligned}\sin^2\theta_{13} = |U_{e3}|^2 &= \cos^2\theta^\circ_{23}\cos^2\hat{\theta}^\nu_{13}\sin^2\hat{\theta}^e_{13} + \cos^2\hat{\theta}^e_{13}\sin^2\hat{\theta}^\nu_{13} \\ &\quad + \frac{1}{2}\sin 2\hat{\theta}^e_{13}\sin 2\hat{\theta}^\nu_{13}\cos\theta^\circ_{23}\cos\hat{\delta}\,,\end{aligned} \tag{2.111}$$

$$\sin^2\theta_{23} = \frac{|U_{\mu 3}|^2}{1-|U_{e3}|^2} = \frac{\sin^2\theta^\circ_{23}\cos^2\hat{\theta}^\nu_{13}}{1-\sin^2\theta_{13}}\,, \tag{2.112}$$

$$\sin^2\theta_{12} = \frac{|U_{e2}|^2}{1-|U_{e3}|^2} = \frac{\sin^2\theta^\circ_{23}\sin^2\hat{\theta}^e_{13}}{1-\sin^2\theta_{13}}\,. \tag{2.113}$$

The sum rule for $\cos\delta$ of interest can be derived by comparing the expressions for the absolute value of the element $U_{\mu 2}$ of the PMNS matrix in the standard parametrisation and in the one obtained using eq. (2.110):

$$|U_{\mu 2}| = |\cos\theta_{12}\cos\theta_{23} - \sin\theta_{13}\sin\theta_{23}\sin\theta_{12}e^{i\delta}| = |\cos\theta^\circ_{23}|\,. \tag{2.114}$$

From the above equation we get for $\cos\delta$:

$$\cos\delta = \frac{\cos^2\theta_{12}\cos^2\theta_{23} - \cos^2\theta^\circ_{23} + \sin^2\theta_{12}\sin^2\theta_{23}\sin^2\theta_{13}}{\sin\theta_{13}\sin 2\theta_{23}\sin\theta_{12}\cos\theta_{12}}\,. \tag{2.115}$$

Given the assumed breaking pattern, $\cos\delta$ depends on the flavour symmetry G_f via the value of θ°_{23}. Using the best fit values of the standard mixing angles for the NO neutrino mass spectrum and the requirement $|\cos\delta| \leq 1$, we find that $\sin^2\theta^\circ_{23}$ should lie in the following interval: $0.537 \leq \sin^2\theta^\circ_{23} \leq 0.677$. Fixing two of the three angles to their best fit values and varying the third one in its 3σ experimentally allowed range and considering all the three possible combinations, we get that $|\cos\delta| \leq 1$ if $0.496 \leq \sin^2\theta^\circ_{23} \leq 0.805$.

2.4.9 Case C9: $U_{23}(\theta^e_{23}, \delta^e_{23})$ and $U_{23}(\theta^\nu_{23}, \delta^\nu_{23})$

Using the following parametrisation of U°,

$$U^\circ(\theta^\circ_{23}, \tilde{\theta}^\circ_{23}, \theta^\circ_{12}, \delta^\circ_{23}, \tilde{\delta}^\circ_{23}) = U_{23}(\theta^\circ_{23}, \delta^\circ_{23})\, R_{12}(\theta^\circ_{12})\, U_{23}(\tilde{\theta}^\circ_{23}, \tilde{\delta}^\circ_{23})\,, \tag{2.116}$$

we have for U:

$$U = U_{23}(\theta^e_{23}, \delta^e_{23})\, U_{23}(\theta^\circ_{23}, \delta^\circ_{23})\, R_{12}(\theta^\circ_{12})\, U_{23}(\tilde{\theta}^\circ_{23}, \tilde{\delta}^\circ_{23})\, U_{23}(\theta^\nu_{23}, \delta^\nu_{23})\, Q_0\,. \tag{2.117}$$

Utilising the results derived in Appendix C and reported in eq. (C.6), we can recast eq. (2.117) in the form

$$U = R_{23}(\hat{\theta}^e_{23})\, P_2(\hat{\delta})\, R_{12}(\theta^\circ_{12})\, R_{23}(\hat{\theta}^\nu_{23})\, Q_0\,, \quad P_2(\hat{\delta}) = \mathrm{diag}(1, e^{i\hat{\delta}}, 1)\,. \tag{2.118}$$

Here $\hat{\delta} = \alpha^e - \beta^e + \alpha^\nu + \beta^\nu$ and we have redefined the matrix Q_0 by absorbing the diagonal phase matrix $P_{23}(\alpha^\nu, \beta^\nu) = \text{diag}(1, e^{i\alpha^\nu}, e^{i\beta^\nu})$ in it. Using eq. (2.118) and the standard parametrisation of the PMNS matrix U, we find:

$$\sin^2\theta_{13} = |U_{e3}|^2 = \sin^2\theta^\circ_{12}\sin^2\hat{\theta}^\nu_{23}\,, \tag{2.119}$$

$$\sin^2\theta_{23} = \frac{|U_{\mu 3}|^2}{1-|U_{e3}|^2} = \frac{1}{1-\sin^2\theta_{13}}\Big[\cos^2\theta^\circ_{12}\cos^2\hat{\theta}^e_{23}\sin^2\hat{\theta}^\nu_{23} + \cos^2\hat{\theta}^\nu_{23}\sin^2\hat{\theta}^e_{23} + \frac{1}{2}\sin 2\hat{\theta}^e_{23}\sin 2\hat{\theta}^\nu_{23}\cos\theta^\circ_{12}\cos\hat{\delta}\Big]\,, \tag{2.120}$$

$$\sin^2\theta_{12} = \frac{|U_{e2}|^2}{1-|U_{e3}|^2} = \frac{\sin^2\theta^\circ_{12}\cos^2\hat{\theta}^\nu_{23}}{1-\sin^2\theta_{13}}\,. \tag{2.121}$$

From eqs. (2.119) and (2.121) we find that the angles θ_{13} and θ_{12} are correlated:

$$\sin^2\theta_{12} = \frac{\sin^2\theta^\circ_{12} - \sin^2\theta_{13}}{1-\sin^2\theta_{13}}\,. \tag{2.122}$$

Comparing the expressions for the absolute value of the element $U_{\tau 1}$ of the PMNS matrix in the standard parametrisation and in the one obtained using eq. (2.118), we have

$$|U_{\tau 1}| = |\sin\theta_{12}\sin\theta_{23} - \sin\theta_{13}\cos\theta_{23}\cos\theta_{12}e^{i\delta}| = |\sin\hat{\theta}^e_{23}\sin\theta^\circ_{12}|\,. \tag{2.123}$$

From the above equations we get for $\cos\delta$:

$$\cos\delta = \frac{\sin^2\theta_{13}(\cos^2\theta_{23}\cos^2\theta^\circ_{12} - \sin^2\theta_{23}) + \sin^2\theta^\circ_{12}(\sin^2\theta_{23} - \cos^2\theta_{13}\sin^2\hat{\theta}^e_{23})}{\sin 2\theta_{23}\sin\theta_{13}|\cos\theta^\circ_{12}|(\sin^2\theta^\circ_{12} - \sin^2\theta_{13})^{\frac{1}{2}}}\,. \tag{2.124}$$

In this case, $\cos\delta$ is a function of the known neutrino mixing angles θ_{23} and θ_{13}, of the angle θ°_{12} fixed by G_f and the assumed symmetry breaking pattern, as well as of the phase parameter $\hat{\delta}$ of the scheme. Predictions for $\cos\delta$ can only be obtained when $\hat{\delta}$ is fixed by additional considerations of, e.g., generalised CP invariance, symmetries, etc. In view of this we show in Fig. 2.4 $\cos\delta$ as a function of $\cos\hat{\delta}$ for the best fit values of $\sin^2\theta_{23}$ and $\sin^2\theta_{13}$, and for the value $\sin^2\theta^\circ_{12} = (r+2)/(4r+4) \approx 0.345$, $r = (1+\sqrt{5})/2$ being the golden ratio, corresponding to $G_f = A_5$. We do not find phenomenologically viable cases for $G_f = A_4$ (T') and S_4.

2.4.10 Results for $G_f = A_4$ (T'), S_4 and A_5

The schemes considered in Sections 2.4.1–2.4.9 can be applied when considering the breaking G_f to $G_e = Z_2$ and $G_\nu = Z_2$, for both Majorana and Dirac neutrinos. As explicit examples of this, we now consider $G_f = A_4$ (T'), S_4 and A_5 broken to $G_e = Z_2$ and $G_\nu = Z_2$. As such, we have considered all possible combinations of residual Z_2 symmetries for a given flavour symmetry group, namely, $G_e = Z_2$ and $G_\nu = Z_2$ for $G_f = A_4$ (T'), S_4, A_5. For instance, in the cases of the schemes described in subsections 2.4.1–2.4.5, and $G_f = S_4$ broken to $G_e = Z^a_2$ and $G_\nu = Z^b_2$ with $(a,b) = (T^2U, U)$, (T^2U, SU), (T^2U, TU), $(T^2U, STSU)$, etc. (a total of 24 combinations of order two elements), the value of the relevant parameter contained in the fixed matrix U° yields $\sin^2\theta^\circ_{23} = 1/4$, $\sin^2\theta^\circ_{23} = 1/2$, $\sin^2\theta^\circ_{13} = 1/4$, $\sin^2\theta^\circ_{12} = 1/4$, and $\sin^2\theta^\circ_{12} = 1/4$, respectively. In A_5 for cases C1, C3, C4 and C5 we find the sine square of the corresponding fixed angle in the matrix U° to be 1/4,

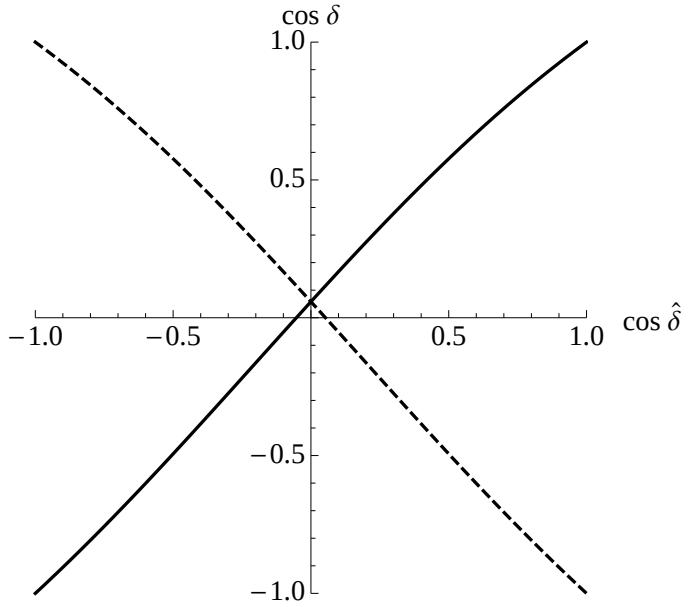

Figure 2.4. Dependence of $\cos\delta$ on $\cos\hat{\delta}$ in the case of $G_f = A_5$ with $\sin^2\theta_{12}^\circ = (r+2)/(4r+4) \approx 0.345$. The mixing parameters $\sin^2\theta_{23}$ and $\sin^2\theta_{13}$ have been fixed to their best fit values for the NO neutrino mass spectrum quoted in eqs. (2.16) and (2.17). The solid (dashed) line is for the case when $\sin 2\hat{\theta}_{23}^e \sin 2\hat{\theta}_{23}^\nu$ is positive (negative).

e.g., for $G_e = Z_2^a$ and $G_\nu = Z_2^b$ with $(a,b) = (S, ST^2ST^3S)$, (S, ST^3ST^2S), (S, T^2ST^3), (S, T^3ST^2), etc. (in total, for 60 combinations of order two elements).

For the symmetry group A_4, we find that none of the combinations of the residual symmetries $G_e = Z_2$ and $G_\nu = Z_2$ provide physical values of $\cos\delta$ and phenomenologically viable results for the neutrino mixing angles simultaneously.

For $G_f = S_4$, using the best fit values of the mixing angles θ_{12}, θ_{13} and θ_{23}, we get $\cos\delta = -0.806$, -1.52 and 0.992 in cases C1, C3 and C4, respectively. Physically acceptable value of $\cos\delta$ in case C3 can be obtained for $\sin^2\theta_{23} = 0.562$ allowed at 3σ, for which $\cos\delta = -0.996$. In the part of the 3σ allowed range of $\sin^2\theta_{23}$, $0.562 \leq \sin^2\theta_{23} \leq 0.641$, we have $-0.996 \leq \cos\delta \leq -0.690$. Further, in case C2, in which the relevant parameter $\sin^2\theta_{23}^\circ = 1/2$, the value of $\cos\delta$ is not fixed, while the atmospheric angle is predicted to have a value corresponding to $\sin^2\theta_{23} = 0.512$. Similarly, in case C5 the value of $\cos\delta$ is not fixed, while $\sin^2\theta_{12} = 0.256$ (which is slightly outside the corresponding 3σ interval). In case C7 we find that $\cos\delta$ is not fixed and $\sin^2\theta_{23} = 0.488$. Finally, for C8 with $\sin^2\theta_{23}^\circ = 1/2$ and $3/4$, using the best fit values of the neutrino mixing angles for the NO spectrum, we have $\cos\delta = -1.53$ and 2.04, respectively. The physical values of $\cos\delta$ can be obtained, using, e.g., the values of $\sin^2\theta_{23} = 0.380$ and 0.543, for which $\cos\delta = -0.995$ and 0.997, respectively. In the parts of the 3σ allowed range of $\sin^2\theta_{23}$, $0.374 \leq \sin^2\theta_{23} \leq 0.380$ and $0.543 \leq \sin^2\theta_{23} \leq 0.641$, we have $-0.938 \geq \cos\delta \geq -0.995$ and $0.997 \geq \cos\delta \geq 0.045$, respectively.

For the A_5 symmetry group, cases C1 with $\sin^2\theta_{23}^\circ = 1/4$, C3 with $\sin^2\theta_{13}^\circ = 1/4$ and C4 with $\sin^2\theta_{12}^\circ = 1/4$ lead to the same predictions obtained with $G_f = S_4$, namely, $\cos\delta = -0.806$, -1.52 and 0.992, respectively. Moreover, in case C3 (case C4) the value of $\sin^2\theta_{13}^\circ = 0.096$ ($\sin^2\theta_{12}^\circ = 0.096$) is found, which along with the best fit values of the mixing angles gives $\cos\delta = 0.688$ ($\cos\delta = -1.21$). Using the value of $\sin^2\theta_{23} = 0.487$ allowed at 2σ, one gets in case C4 $\cos\delta = -0.997$, while in the part of the 3σ allowed range of $\sin^2\theta_{23}$, $0.487 \leq \sin^2\theta_{23} \leq 0.641$, we have $-0.997 \leq \cos\delta \leq -0.376$. Note also, if $\sin^2\theta_{23}$

is fixed to its best fit value, one can obtain the physical value of $\cos\delta = -0.999$ using $\sin^2\theta_{12} = 0.277$. For the part of the 3σ allowed range of $\sin^2\theta_{12}$, $0.259 \leq \sin^2\theta_{12} \leq 0.277$, one gets $-0.871 \geq \cos\delta \geq -0.999$. Cases C5 and C8 are the same as for the S_4 symmetry group. Finally, in case C9, the value of $\cos\delta$ is not fixed, while using the best fit value of the reactor angle, we get $\sin^2\theta_{12} = 0.330$.

2.5 Summary of the results for patterns A, B and C

The sum rules for $\cos\delta$ derived in Sections 2.2, 2.3 and 2.4 are summarised in Tables 2.3 and 2.4. The sum rules for $\sin^2\theta_{12}$, $\sin^2\theta_{13}$ and $\sin^2\theta_{23}$, which lead to predictions for the indicated neutrino mixing parameters once the discrete flavour symmetry G_f is fixed, are given in Tables 2.5 and 2.6. In the cases in Tables 2.5 and 2.6 in which $\cos\delta$ is unconstrained, a relatively precise measurement of $\sin^2\theta_{12}$, $\sin^2\theta_{13}$ or $\sin^2\theta_{23}$ can provide a critical test of the corresponding schemes due to constraints satisfied by the indicated neutrino mixing parameters.

A general comment on the results derived in Sections 2.2, 2.3 and 2.4 is in order. Since we do not have any information on the mass matrices, we have the freedom to permute the columns of the matrices U_e and U_ν, or equivalently, the columns and the rows of the PMNS matrix U. The results in Tables 2.3 and 2.4 cover all the possibilities because, as we demonstrate below, the permutations bring one of the considered cases into another considered case. For example, consider the case of $U = U_{13}(\theta^e_{13}, \delta^e_{13})\, U^\circ\, U_{23}(\theta^\nu_{23}, \delta^\nu_{23})\, Q_0$. The permutation of the second and third rows of U is given by

$$\pi_{23}\, U = \pi_{23}\, U_{13}(\theta^e_{13}, \delta^e_{13})\, \pi^T_{23}\, \pi_{23}\, U^\circ\, U_{23}(\theta^\nu_{23}, \delta^\nu_{23})\, Q_0\,,$$

where we have defined

$$\pi_{23} = \begin{pmatrix} 1 & 0 & 0 \\ 0 & 0 & 1 \\ 0 & 1 & 0 \end{pmatrix}\,. \tag{2.125}$$

Since the combination $\pi_{23}\, U_{13}(\theta^e_{13}, \delta^e_{13})\, \pi^T_{23}$ gives a unitary matrix $U_{12}(\theta^e_{13}, \delta^e_{13})$, the resulting PMNS matrix U' after the redefinition $\theta^e_{13} \to \theta^e_{12}$, $\delta^e_{13} \to \delta^e_{12}$ and $\pi_{23}\, U^\circ \to U^\circ$ yields

$$U' = U_{12}(\theta^e_{12}, \delta^e_{12})\, U^\circ\, U_{23}(\theta^\nu_{23}, \delta^\nu_{23})\, Q_0\,,$$

which represents another case present in Table 2.4. It is worth noting that the freedom in redefining the matrix U° follows from the fact that U° is a general 3×3 unitary matrix and hence can be parametrised as described in Section 2.1 and in Appendix C. All the other permutations should be treated in the same way and lead to similar results.

Table 2.3. Summary of the sum rules for $\cos\delta$. Cases A1, A2 and A3 correspond to $G_e = Z_2$ and $G_\nu = Z_n$, $n > 2$ or $Z_n \times Z_m$, $n, m \geq 2$, while cases B1, B2 and B3 correspond to $G_e = Z_n$, $n > 2$ or $Z_n \times Z_m$, $n, m \geq 2$ and $G_\nu = Z_2$. See text for further details.

Case	Parametrisation of the PMNS matrix U	Sum rule for $\cos\delta$
A1	$U_{12}(\theta^e_{12}, \delta^e_{12})\, U_{12}(\theta^\circ_{12}, \delta^\circ_{12})\, R_{23}(\theta^\circ_{23})\, R_{13}(\theta^\circ_{13})\, Q_0$	$\dfrac{\cos^2\theta_{13}(\sin^2\theta^\circ_{23} - \cos^2\theta_{12}) + \cos^2\theta^\circ_{13}\cos^2\theta^\circ_{23}(\cos^2\theta_{12} - \sin^2\theta_{12}\sin^2\theta_{13})}{\sin 2\theta_{12}\sin\theta_{13}\lvert\cos\theta^\circ_{13}\cos\theta^\circ_{23}\rvert(\cos^2\theta_{13} - \cos^2\theta^\circ_{13}\cos^2\theta^\circ_{23})^{\frac{1}{2}}}$
A2	$U_{13}(\theta^e_{13}, \delta^e_{13})\, U_{13}(\theta^\circ_{13}, \delta^\circ_{13})\, R_{23}(\theta^\circ_{23})\, R_{12}(\theta^\circ_{12})\, Q_0$	$-\dfrac{\cos^2\theta_{13}(\cos^2\theta^\circ_{12}\cos^2\theta^\circ_{23} - \cos^2\theta_{12}) + \sin^2\theta^\circ_{23}(\cos^2\theta_{12} - \sin^2\theta_{12}\sin^2\theta_{13})}{\sin 2\theta_{12}\sin\theta_{13}\lvert\sin\theta^\circ_{23}\rvert(\cos^2\theta_{13} - \sin^2\theta^\circ_{23})^{\frac{1}{2}}}$
A3	$U_{23}(\theta^e_{23}, \delta^e_{23})\, U_{23}(\theta^\circ_{23}, \delta^\circ_{23})\, R_{13}(\theta^\circ_{13})\, R_{12}(\theta^\circ_{12})\, Q_0$	$\pm\cos\hat{\delta}_{23}$
B1	$R_{23}(\theta^\circ_{23})\, R_{12}(\theta^\circ_{12})\, U_{13}(\theta^\circ_{13}, \delta^\circ_{13})\, U_{13}(\theta^\nu_{13}, \delta^\nu_{13})\, Q_0$	$-\dfrac{\cos^2\theta_{13}(\cos^2\theta^\circ_{12}\cos^2\theta^\circ_{23} - \cos^2\theta_{23}) + \sin^2\theta^\circ_{12}(\cos^2\theta_{23} - \sin^2\theta_{13}\sin^2\theta_{23})}{\sin 2\theta_{23}\sin\theta_{13}\lvert\sin\theta^\circ_{12}\rvert(\cos^2\theta_{13} - \sin^2\theta^\circ_{12})^{\frac{1}{2}}}$
B2	$R_{13}(\theta^\circ_{13})\, R_{12}(\theta^\circ_{12})\, U_{23}(\theta^\circ_{23}, \delta^\circ_{23})\, U_{23}(\theta^\nu_{23}, \delta^\nu_{23})\, Q_0$	$\dfrac{\cos^2\theta_{13}(\sin^2\theta^\circ_{12} - \cos^2\theta_{23}) + \cos^2\theta^\circ_{12}\cos^2\theta^\circ_{13}(\cos^2\theta_{23} - \sin^2\theta_{13}\sin^2\theta_{23})}{\sin 2\theta_{23}\sin\theta_{13}\lvert\cos\theta^\circ_{12}\cos\theta^\circ_{13}\rvert(\cos^2\theta_{13} - \cos^2\theta^\circ_{12}\cos^2\theta^\circ_{13})^{\frac{1}{2}}}$
B3	$R_{23}(\theta^\circ_{23})\, R_{13}(\theta^\circ_{13})\, U_{12}(\theta^\circ_{12}, \delta^\circ_{12})\, U_{12}(\theta^\nu_{12}, \delta^\nu_{12})\, Q_0$	$\pm\cos\hat{\delta}_{12}$

Table 2.4. Summary of the sum rules for $\cos\delta$. Cases C1–C9 correspond to $G_e = Z_2$ and $G_\nu = Z_2$. See text for further details.

Case	Parametrisation of the PMNS matrix U	Sum rule for $\cos\delta$
C1	$U_{12}(\theta^e_{12},\delta^e_{12})\,U_{12}(\theta^\circ_{12},\delta^\circ_{12})\,R_{23}(\theta^\circ_{23})\,U_{13}(\theta^\circ_{13},\delta^\circ_{13})\,U_{13}(\theta^\nu_{13},\delta^\nu_{13})\,Q_0$	$\dfrac{\sin^2\theta^\circ_{23}-\cos^2\theta_{12}\sin^2\theta_{23}-\cos^2\theta_{23}\sin^2\theta_{12}\sin^2\theta_{13}}{\sin\theta_{13}\sin 2\theta_{23}\sin\theta_{12}\cos\theta_{12}}$
C2	$U_{13}(\theta^e_{13},\delta^e_{13})\,U_{13}(\theta^\circ_{13},\delta^\circ_{13})\,R_{23}(\theta^\circ_{23})\,U_{12}(\theta^\circ_{12},\delta^\circ_{12})\,U_{12}(\theta^\nu_{12},\delta^\nu_{12})\,Q_0$	$\dfrac{\cos^2\theta_{13}(\cos^2\theta^\circ_{23}\sin^2\hat\theta^\nu_{12}-\sin^2\theta_{12})+\sin^2\theta^\circ_{23}(\sin^2\theta_{12}-\cos^2\theta_{12}\sin^2\theta_{13})}{\sin 2\theta_{12}\sin\theta_{13}\lvert\sin\theta^\circ_{23}\rvert(\cos^2\theta_{13}-\sin^2\theta^\circ_{23})^{\frac{1}{2}}}$
C3	$U_{12}(\theta^e_{12},\delta^e_{12})\,U_{12}(\theta^\circ_{12},\delta^\circ_{12})\,R_{13}(\theta^\circ_{13})\,U_{23}(\theta^\circ_{23},\delta^\circ_{23})\,U_{23}(\theta^\nu_{23},\delta^\nu_{23})\,Q_0$	$\dfrac{\sin^2\theta_{12}\sin^2\theta_{23}-\sin^2\theta^\circ_{13}+\cos^2\theta_{12}\cos^2\theta_{23}\sin^2\theta_{13}}{\sin\theta_{13}\sin 2\theta_{23}\sin\theta_{12}\cos\theta_{12}}$
C4	$U_{13}(\theta^e_{13},\delta^e_{13})\,U_{13}(\theta^\circ_{13},\delta^\circ_{13})\,R_{12}(\theta^\circ_{12})\,U_{23}(\theta^\circ_{23},\delta^\circ_{23})\,U_{23}(\theta^\nu_{23},\delta^\nu_{23})\,Q_0$	$\dfrac{\sin^2\theta^\circ_{12}-\cos^2\theta_{23}\sin^2\theta_{12}-\cos^2\theta_{12}\sin^2\theta_{13}\sin^2\theta_{23}}{\sin\theta_{13}\sin 2\theta_{23}\sin\theta_{12}\cos\theta_{12}}$
C5	$U_{23}(\theta^e_{23},\delta^e_{23})\,U_{23}(\theta^\circ_{23},\delta^\circ_{23})\,R_{12}(\theta^\circ_{12})\,U_{13}(\theta^\circ_{13},\delta^\circ_{13})\,U_{13}(\theta^\nu_{13},\delta^\nu_{13})\,Q_0$	$\dfrac{\cos^2\theta_{13}(\cos^2\theta^\circ_{12}\sin^2\hat\theta^e_{23}-\sin^2\theta_{23})+\sin^2\theta^\circ_{12}(\sin^2\theta_{23}-\cos^2\theta_{23}\sin^2\theta_{13})}{\sin 2\theta_{23}\sin\theta_{13}\lvert\sin\theta^\circ_{12}\rvert(\cos^2\theta_{13}-\sin^2\theta^\circ_{12})^{\frac{1}{2}}}$
C6	$U_{23}(\theta^e_{23},\delta^e_{23})\,U_{23}(\theta^\circ_{23},\delta^\circ_{23})\,R_{13}(\theta^\circ_{13})\,U_{12}(\theta^\circ_{12},\delta^\circ_{12})\,U_{12}(\theta^\nu_{12},\delta^\nu_{12})\,Q_0$	$\pm\cos\hat\delta$
C7	$U_{12}(\theta^e_{12},\delta^e_{12})\,U_{12}(\theta^\circ_{12},\delta^\circ_{12})\,R_{23}(\theta^\circ_{23})\,U_{12}(\tilde\theta^\circ_{12},\tilde\delta^\circ_{12})\,U_{12}(\theta^\nu_{12},\delta^\nu_{12})\,Q_0$	$\dfrac{\sin^2\theta_{13}(\cos^2\theta_{12}\cos^2\theta^\circ_{23}-\sin^2\theta_{12})+\sin^2\theta^\circ_{23}(\sin^2\theta_{12}-\cos^2\theta_{13}\sin^2\hat\theta^\nu_{12})}{\sin 2\theta_{12}\sin\theta_{13}\lvert\cos\theta^\circ_{23}\rvert(\sin^2\theta^\circ_{23}-\sin^2\theta_{13})^{\frac{1}{2}}}$
C8	$U_{13}(\theta^e_{13},\delta^e_{13})\,U_{13}(\theta^\circ_{13},\delta^\circ_{13})\,R_{23}(\theta^\circ_{23})\,U_{13}(\tilde\theta^\circ_{13},\tilde\delta^\circ_{13})\,U_{13}(\theta^\nu_{13},\delta^\nu_{13})\,Q_0$	$\dfrac{\cos^2\theta_{12}\cos^2\theta_{23}-\cos^2\theta^\circ_{23}+\sin^2\theta_{12}\sin^2\theta_{23}\sin^2\theta_{13}}{\sin\theta_{13}\sin 2\theta_{23}\sin\theta_{12}\cos\theta_{12}}$
C9	$U_{23}(\theta^e_{23},\delta^e_{23})\,U_{23}(\theta^\circ_{23},\delta^\circ_{23})\,R_{12}(\theta^\circ_{12})\,U_{23}(\tilde\theta^\circ_{23},\tilde\delta^\circ_{23})\,U_{23}(\theta^\nu_{23},\delta^\nu_{23})\,Q_0$	$\dfrac{\sin^2\theta_{13}(\cos^2\theta_{23}\cos^2\theta^\circ_{12}-\sin^2\theta_{23})+\sin^2\theta^\circ_{12}(\sin^2\theta_{23}-\cos^2\theta_{13}\sin^2\hat\theta^e_{23})}{\sin 2\theta_{23}\sin\theta_{13}\lvert\cos\theta^\circ_{12}\rvert(\sin^2\theta^\circ_{12}-\sin^2\theta_{13})^{\frac{1}{2}}}$

Table 2.5. Summary of the sum rules for $\sin^2\theta_{12}$, $\sin^2\theta_{13}$ and $\sin^2\theta_{23}$. Cases A1, A2 and A3 correspond to $G_e = Z_2$ and $G_\nu = Z_n$, $n > 2$ or $Z_n \times Z_m$, $n, m \geq 2$, while cases B1, B2 and B3 correspond to $G_e = Z_n$, $n > 2$ or $Z_n \times Z_m$, $n, m \geq 2$ and $G_\nu = Z_2$. See text for further details.

Case	Parametrisation of the PMNS matrix U	Sum rule for $\sin^2\theta_{12}$ and/or $\sin^2\theta_{13}$ and/or $\sin^2\theta_{23}$
A1	$U_{12}(\theta^e_{12}, \delta^e_{12})\, U_{12}(\theta^\circ_{12}, \delta^\circ_{12})\, R_{23}(\theta^\circ_{23})\, R_{13}(\theta^\circ_{13})\, Q_0$	$\sin^2\theta_{23} = \dfrac{\sin^2\theta^\circ_{13} - \sin^2\theta_{13} + \cos^2\theta^\circ_{13}\sin^2\theta^\circ_{23}}{1 - \sin^2\theta_{13}}$
A2	$U_{13}(\theta^e_{13}, \delta^e_{13})\, U_{13}(\theta^\circ_{13}, \delta^\circ_{13})\, R_{23}(\theta^\circ_{23})\, R_{12}(\theta^\circ_{12})\, Q_0$	$\sin^2\theta_{23} = \dfrac{\sin^2\theta^\circ_{23}}{1 - \sin^2\theta_{13}}$
A3	$U_{23}(\theta^e_{23}, \delta^e_{23})\, U_{23}(\theta^\circ_{23}, \delta^\circ_{23})\, R_{13}(\theta^\circ_{13})\, R_{12}(\theta^\circ_{12})\, Q_0$	$\sin^2\theta_{13} = \sin^2\theta^\circ_{13}\,, \quad \sin^2\theta_{12} = \sin^2\theta^\circ_{12}$
B1	$R_{23}(\theta^\circ_{23})\, R_{12}(\theta^\circ_{12})\, U_{13}(\theta^\circ_{13}, \delta^\circ_{13})\, U_{13}(\theta^\nu_{13}, \delta^\nu_{13})\, Q_0$	$\sin^2\theta_{12} = \dfrac{\sin^2\theta^\circ_{12}}{1 - \sin^2\theta_{13}}$
B2	$R_{13}(\theta^\circ_{13})\, R_{12}(\theta^\circ_{12})\, U_{23}(\theta^\circ_{23}, \delta^\circ_{23})\, U_{23}(\theta^\nu_{23}, \delta^\nu_{23})\, Q_0$	$\sin^2\theta_{12} = \dfrac{\cos^2\theta_{13} - \cos^2\theta^\circ_{12}\cos^2\theta^\circ_{13}}{1 - \sin^2\theta_{13}}$
B3	$R_{23}(\theta^\circ_{23})\, R_{13}(\theta^\circ_{13})\, U_{12}(\theta^\circ_{12}, \delta^\circ_{12})\, U_{12}(\theta^\nu_{12}, \delta^\nu_{12})\, Q_0$	$\sin^2\theta_{13} = \sin^2\theta^\circ_{13}\,, \quad \sin^2\theta_{23} = \sin^2\theta^\circ_{23}$

Table 2.6. Summary of the sum rules for $\sin^2\theta_{12}$, $\sin^2\theta_{13}$ and $\sin^2\theta_{23}$. Cases C1–C9 correspond to $G_e = Z_2$ and $G_\nu = Z_2$. See text for further details.

Case	Parametrisation of the PMNS matrix U	Sum rule for $\sin^2\theta_{12}$ and/or $\sin^2\theta_{13}$ and/or $\sin^2\theta_{23}$
C1	$U_{12}(\theta^e_{12},\delta^e_{12})\,U_{12}(\theta^\circ_{12},\delta^\circ_{12})\,R_{23}(\theta^\circ_{23})\,U_{13}(\theta^\circ_{13},\delta^\circ_{13})\,U_{13}(\theta^\nu_{13},\delta^\nu_{13})\,Q_0$	not fixed
C2	$U_{13}(\theta^e_{13},\delta^e_{13})\,U_{13}(\theta^\circ_{13},\delta^\circ_{13})\,R_{23}(\theta^\circ_{23})\,U_{12}(\theta^\circ_{12},\delta^\circ_{12})\,U_{12}(\theta^\nu_{12},\delta^\nu_{12})\,Q_0$	$\sin^2\theta_{23} = \dfrac{\sin^2\theta^\circ_{23}}{1-\sin^2\theta_{13}}$
C3	$U_{12}(\theta^e_{12},\delta^e_{12})\,U_{12}(\theta^\circ_{12},\delta^\circ_{12})\,R_{13}(\theta^\circ_{13})\,U_{23}(\theta^\circ_{23},\delta^\circ_{23})\,U_{23}(\theta^\nu_{23},\delta^\nu_{23})\,Q_0$	not fixed
C4	$U_{13}(\theta^e_{13},\delta^e_{13})\,U_{13}(\theta^\circ_{13},\delta^\circ_{13})\,R_{12}(\theta^\circ_{12})\,U_{23}(\theta^\circ_{23},\delta^\circ_{23})\,U_{23}(\theta^\nu_{23},\delta^\nu_{23})\,Q_0$	not fixed
C5	$U_{23}(\theta^e_{23},\delta^e_{23})\,U_{23}(\theta^\circ_{23},\delta^\circ_{23})\,R_{12}(\theta^\circ_{12})\,U_{13}(\theta^\circ_{13},\delta^\circ_{13})\,U_{13}(\theta^\nu_{13},\delta^\nu_{13})\,Q_0$	$\sin^2\theta_{12} = \dfrac{\sin^2\theta^\circ_{12}}{1-\sin^2\theta_{13}}$
C6	$U_{23}(\theta^e_{23},\delta^e_{23})\,U_{23}(\theta^\circ_{23},\delta^\circ_{23})\,R_{13}(\theta^\circ_{13})\,U_{12}(\theta^\circ_{12},\delta^\circ_{12})\,U_{12}(\theta^\nu_{12},\delta^\nu_{12})\,Q_0$	$\sin^2\theta_{13} = \sin^2\theta^\circ_{13}$
C7	$U_{12}(\theta^e_{12},\delta^e_{12})\,U_{12}(\theta^\circ_{12},\delta^\circ_{12})\,R_{23}(\theta^\circ_{23})\,U_{12}(\tilde\theta^\circ_{12},\tilde\delta^\circ_{12})\,U_{12}(\theta^\nu_{12},\delta^\nu_{12})\,Q_0$	$\sin^2\theta_{23} = \dfrac{\sin^2\theta^\circ_{23}-\sin^2\theta_{13}}{1-\sin^2\theta_{13}}$
C8	$U_{13}(\theta^e_{13},\delta^e_{13})\,U_{13}(\theta^\circ_{13},\delta^\circ_{13})\,R_{23}(\theta^\circ_{23})\,U_{13}(\tilde\theta^\circ_{13},\tilde\delta^\circ_{13})\,U_{13}(\theta^\nu_{13},\delta^\nu_{13})\,Q_0$	not fixed
C9	$U_{23}(\theta^e_{23},\delta^e_{23})\,U_{23}(\theta^\circ_{23},\delta^\circ_{23})\,R_{12}(\theta^\circ_{12})\,U_{23}(\tilde\theta^\circ_{23},\tilde\delta^\circ_{23})\,U_{23}(\theta^\nu_{23},\delta^\nu_{23})\,Q_0$	$\sin^2\theta_{12} = \dfrac{\sin^2\theta^\circ_{12}-\sin^2\theta_{13}}{1-\sin^2\theta_{13}}$

2.6 Pattern D: fully broken G_e and $G_\nu = Z_n$, $n > 2$ or $Z_n \times Z_m$, $n, m \geq 2$

If the discrete flavour symmetry G_f is fully broken in the charged lepton sector the matrix U_e is unconstrained and includes, in general, three rotation angle and three CPV phase parameters. It is impossible to derive predictions for the mixing angles and CPV phases in the PMNS matrix in this case. Therefore, we will consider in this section forms of U_e corresponding to one of the rotation angle parameters being equal to zero. Some of these forms of U_e correspond to a class of models of neutrino mass generation (see, e.g., [122, 145–149]) and lead, in particular, to sum rules for $\cos\delta$.

We give in Appendix D the most general parametrisations of U under the assumption that in the case of fully broken G_e one rotation angle in the matrix U_e vanishes. Cases D3 and D4 in Table D.1 with $\theta^\circ_{13} = 0$ have been analysed in [99, 100, 109], while case D6 has been investigated in [100]. We will consider them in detail in the next chapter.

2.6.1 Case D1: $U_{23}(\theta^e_{23}, \delta^e_{23})\, U_{12}(\theta^e_{12}, \delta^e_{12})$

We consider the following parametrisation of the PMNS matrix (see Appendix D):

$$U = U_{23}(\theta^e_{23}, \delta^e_{23})\, R_{12}(\hat{\theta}_{12})\, P_1(\hat{\delta})\, R_{23}(\theta^\circ_{23})\, R_{13}(\theta^\circ_{13})\, Q_0\,, \quad P_1(\hat{\delta}) = \mathrm{diag}(e^{i\hat{\delta}}, 1, 1). \tag{2.126}$$

We find that:

$$\sin^2\theta_{13} = |U_{e3}|^2 = \sin^2\theta_{13}(\hat{\theta}_{12}, \hat{\delta}, \theta^\circ_{13}, \theta^\circ_{23})\,, \tag{2.127}$$

$$\sin^2\theta_{23} = \frac{|U_{\mu 3}|^2}{1 - |U_{e3}|^2} = \sin^2\theta_{23}(\hat{\theta}_{12}, \hat{\delta}, \theta^e_{23}, \delta^e_{23}, \theta^\circ_{13}, \theta^\circ_{23})\,, \tag{2.128}$$

$$\sin^2\theta_{12} = \frac{|U_{e2}|^2}{1 - |U_{e3}|^2} = \frac{\cos^2\theta^\circ_{23}\sin^2\hat{\theta}_{12}}{\cos^2\theta_{13}}\,. \tag{2.129}$$

As it can be seen from the previous equations and the absolute value of the element $U_{\mu 2}$,

$$|U_{\mu 2}| = |\cos\theta^e_{23}\cos\hat{\theta}_{12}\cos\theta^\circ_{23} - e^{-i\delta^e_{23}}\sin\theta^e_{23}\sin\theta^\circ_{23}|\,, \tag{2.130}$$

a sum rule for $\cos\delta$ might be derived in the case of fixed δ^e_{23}. In the general case of free δ^e_{23} we find that $\cos\delta$ is a function of δ^e_{23}. Since in this case the analytical expression of $\cos\delta$ in terms of δ^e_{23} is rather complicated, we do not present this result here. Note that imposing either $\theta^\circ_{23} = 0$ or $\theta^\circ_{13} = 0$ is not enough to fix the value of $\cos\delta$. As eqs. (2.127) and (2.128) suggest, in the case of fixed δ^e_{23} there exist multiple solutions for the value of $\cos\delta$ for any given value of δ^e_{23}. This is demonstrated in Fig. 2.5, in which we plot $\cos\delta$ versus δ^e_{23}, assuming that the angles θ°_{13} and θ°_{23} have the values corresponding to the TBM, GRA, GRB and HG symmetry forms given in Table 2.2. The figure is obtained for $\hat{\theta}_{12}$ belonging to the first quadrant. The solid lines correspond to $\hat{\delta} = \cos^{-1}(\cos\hat{\delta})$, where $\cos\hat{\delta}$ is the solution of eq. (2.127), while the dashed lines correspond to $\hat{\delta} = 2\pi - \cos^{-1}(\cos\hat{\delta})$. Multiple lines reflect the fact that eq. (2.128) for θ^e_{23} has several solutions. We note that Fig. 2.5 remains the same for $\hat{\theta}_{12}$ belonging to the third quadrant, while for $\hat{\theta}_{12}$ lying in the second or fourth quadrant the solid and dashed lines interchange. For the BM symmetry form $\cos\hat{\delta}$ has an unphysical value, which indicates that the considered scheme with the BM form of the matrix diagonalising the neutrino mass matrix does not provide a good

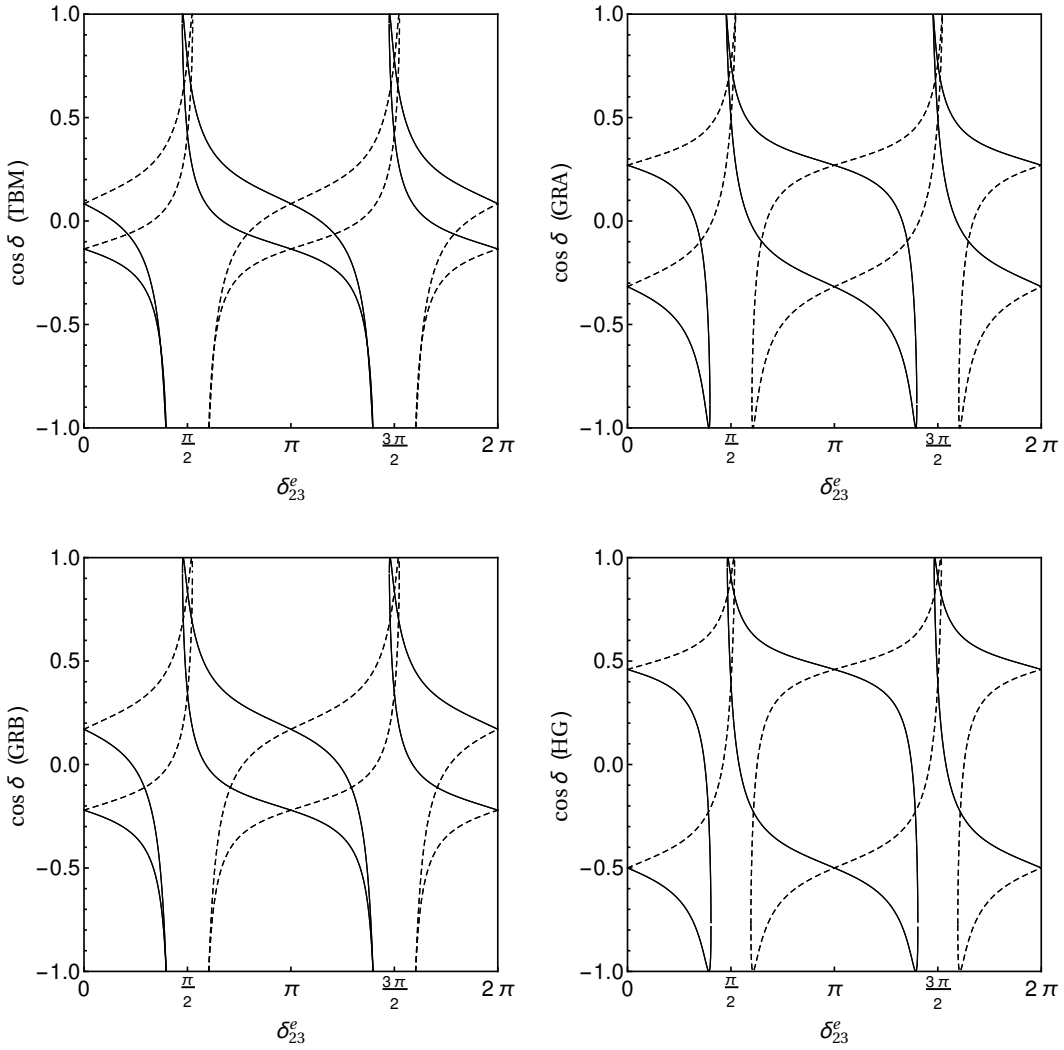

Figure 2.5. Dependence of $\cos\delta$ on δ^e_{23} in the cases of the TBM, GRA, GRB and HG symmetry forms. The mixing parameters $\sin^2\theta_{12}$, $\sin^2\theta_{23}$ and $\sin^2\theta_{13}$ have been fixed to their best fit values for the NO neutrino mass spectrum quoted in eqs. (2.15)–(2.17). The angle $\hat{\theta}_{12}$ is assumed to belong to the first quadrant. The solid lines correspond to $\hat{\delta} = \cos^{-1}(\cos\hat{\delta})$, where $\cos\hat{\delta}$ is the solution of eq. (2.127), while the dashed lines correspond to $\hat{\delta} = 2\pi - \cos^{-1}(\cos\hat{\delta})$. See text for further details.

description of the current data on the neutrino mixing angles [102].[17] Thus, we do not present such a plot in this case. If δ^e_{23} turns out to be fixed (by generalised CP invariance, symmetries, etc.), then, as can be seen from Fig. 2.5, $\cos\delta$ is predicted to take a value from a discrete set. For instance, when $\delta^e_{23} = 0$ or π, we have

$$\begin{aligned}
\cos\delta &= \{-0.135, 0.083\} \text{ for TBM;}\\
\cos\delta &= \{-0.317, 0.269\} \text{ for GRA;}\\
\cos\delta &= \{-0.221, 0.170\} \text{ for GRB;}\\
\cos\delta &= \{-0.500, 0.459\} \text{ for HG.}
\end{aligned}$$

[17] Note that the scheme under discussion corresponds to "inverse" ordering of the charged lepton corrections, i.e., $U_e^\dagger = U_{23}(\theta^e_{23}, \delta^e_{23})\, U_{12}(\theta^e_{12}, \delta^e_{12})$ (see [102]).

In the case of $\delta^e_{23} = \pi/2$ or $3\pi/2$, we find

$$\begin{aligned}
\cos\delta &= \{0.418, 0.779\} \text{ for TBM;} \\
\cos\delta &= \{0.498, 0.761\} \text{ for GRA;} \\
\cos\delta &= \{0.346, 0.837\} \text{ for GRB;} \\
\cos\delta &= \{0.394, 0.906\} \text{ for HG.}
\end{aligned}$$

2.6.2 Case D2: $U_{13}(\theta^e_{13}, \delta^e_{13})\, U_{12}(\theta^e_{12}, \delta^e_{12})$

We consider the following parametrisation of the PMNS matrix (see Appendix D):

$$U = U_{13}(\theta^e_{13}, \delta^e_{13})\, R_{12}(\hat{\theta}_{12})\, P_1(\hat{\delta})\, R_{23}(\theta^\circ_{23})\, R_{13}(\theta^\circ_{13})\, Q_0\,, \quad P_1(\hat{\delta}) = \mathrm{diag}(e^{i\hat{\delta}}, 1, 1)\,. \tag{2.131}$$

A sum rule for $\cos\delta$ is obtained in the cases of either $\theta^\circ_{23} = k\pi$, $k = 0, 1, 2$, or $\theta^\circ_{13} = q\pi/2$, $q = 0, 1, 2, 3, 4$. For the general form of U we find for the absolute value of the element $U_{\mu 2}$:

$$|U_{\mu 2}| = |\cos\hat{\theta}_{12} \cos\theta^\circ_{23}|\,, \tag{2.132}$$

which in each of the two limits indicated above is fixed because $|\cos\hat{\theta}_{12}|$ can be expressed in terms of the PMNS neutrino mixing angles. This can be seen from the following relation, which is obtained using the expressions for $|U_{\mu 3}|^2$ in the standard parametrisation of the PMNS matrix U and in the parametrisation given in eq. (2.131):

$$\cos^2\theta_{13} \sin^2\theta_{23} = |-e^{i\hat{\delta}} \sin\hat{\theta}_{12} \sin\theta^\circ_{13} + \cos\hat{\theta}_{12} \cos\theta^\circ_{13} \sin\theta^\circ_{23}|^2\,. \tag{2.133}$$

Equating the expression for $|U_{\mu 2}|$ given in eq. (2.132) with the one in the standard parametrisation, we find

$$\cos\delta = \frac{\cos^2\theta_{23}\cos^2\theta_{12} + \sin^2\theta_{12}\sin^2\theta_{13}\sin^2\theta_{23} - \cos^2\hat{\theta}_{12}\cos^2\theta^\circ_{23}}{\sin 2\theta_{23} \sin\theta_{12}\cos\theta_{12}\sin\theta_{13}}\,. \tag{2.134}$$

2.6.3 Case D3: $U_{12}(\theta^e_{12}, \delta^e_{12})\, U_{23}(\theta^e_{23}, \delta^e_{23})$

We consider the following parametrisation of the PMNS matrix (see Appendix D):

$$U = U_{12}(\theta^e_{12}, \delta^e_{12})\, R_{23}(\hat{\theta}_{23})\, P_2(\hat{\delta})\, R_{13}(\theta^\circ_{13})\, R_{12}(\theta^\circ_{12})\, Q_0\,, \quad P_2(\hat{\delta}) = \mathrm{diag}(1, e^{i\hat{\delta}}, 1)\,. \tag{2.135}$$

A sum rule for $\cos\delta$ can be derived in the cases of either $\theta^\circ_{13} = k\pi$, $k = 0, 1, 2$, or $\theta^\circ_{12} = q\pi/2$, $q = 0, 1, 2, 3, 4$. Indeed, the relation $\cos^2\theta_{13}\cos^2\theta_{23} = \cos^2\hat{\theta}_{23}\cos^2\theta^\circ_{13}$ (which can be obtained from the expressions for the element $U_{\tau 3}$ of the PMNS matrix U in the standard parametrisation and in the one given in eq. (2.135)) allows us to express $\cos^2\hat{\theta}_{23}$ in terms of the known product $\cos^2\theta_{13}\cos^2\theta_{23}$ and the parameter $\cos^2\theta^\circ_{13}$ which, in principle, is fixed by the symmetries G_f and G_ν. We have also

$$|U_{\tau 2}| = |e^{i\hat{\delta}} \cos\theta^\circ_{12} \sin\hat{\theta}_{23} + \cos\hat{\theta}_{23} \sin\theta^\circ_{12} \sin\theta^\circ_{13}|\,. \tag{2.136}$$

In the limits of either $\theta^\circ_{13} = k\pi$, $k = 0, 1, 2$, or $\theta^\circ_{12} = q\pi/2$, $q = 0, 1, 2, 3, 4$, $|U_{\tau 2}|$ does not depend on $\hat{\delta}$ and is also fixed. This makes it possible to derive a sum rule for $\cos\delta$. In the general case, $\cos\delta$ is a function of $\hat{\delta}$:

$$\cos\delta = \frac{2}{\sin 2\theta_{12} \sin 2\theta_{23} \sin\theta_{13} \cos^2\theta^\circ_{13}} \Big[\cos^2\theta^\circ_{12} \left(\cos^2\theta^\circ_{13} - \cos^2\theta_{13}\cos^2\theta_{23}\right)$$

$$- \cos^2\theta_{12}\sin^2\theta_{23}\cos^2\theta^\circ_{13} + \cos^2\theta_{23}\left(\cos^2\theta_{13}\sin^2\theta^\circ_{12}\sin^2\theta^\circ_{13} - \sin^2\theta_{12}\sin^2\theta_{13}\cos^2\theta^\circ_{13}\right)$$
$$+ \kappa\cos\hat{\delta}\cos\theta_{13}\cos\theta_{23}\sin 2\theta^\circ_{12}\sin\theta^\circ_{13}\left(\cos^2\theta^\circ_{13} - \cos^2\theta_{13}\cos^2\theta_{23}\right)^{\frac{1}{2}}\Big]\,, \tag{2.137}$$

where $\kappa = 1$ if $\hat{\theta}_{23}$ belongs to the first or third quadrant, and $\kappa = -1$ otherwise. For $\theta^\circ_{13} = 0$ the sum rule reduces to the one derived in [99] and discussed in detail in the next chapter.

2.6.4 Case D4: $U_{13}(\theta^e_{13}, \delta^e_{13})\, U_{23}(\theta^e_{23}, \delta^e_{23})$

We consider the following parametrisation of the PMNS matrix (see Appendix D):

$$U = U_{13}(\theta^e_{13}, \delta^e_{13})\, R_{23}(\hat{\theta}_{23})\, P_2(\hat{\delta})\, R_{13}(\theta^\circ_{13})\, R_{12}(\theta^\circ_{12})\, Q_0\,, \quad P_2(\hat{\delta}) = \mathrm{diag}(1, e^{i\hat{\delta}}, 1)\,. \tag{2.138}$$

In this case a sum rule for $\cos\delta$ exists provided either $\theta^\circ_{13} = k\pi$, $k = 0, 1, 2$, or $\theta^\circ_{12} = q\pi/2$, $q = 0, 1, 2, 3, 4$. This follows from the relation $|U_{\mu 3}|^2 = \cos^2\theta_{13}\sin^2\theta_{23} = \cos^2\theta^\circ_{13}\sin^2\hat{\theta}_{23}$ and the expression for $|U_{\mu 2}|$:

$$|U_{\mu 2}| = |e^{i\hat{\delta}}\cos\theta^\circ_{12}\cos\hat{\theta}_{23} - \sin\hat{\theta}_{23}\sin\theta^\circ_{12}\sin\theta^\circ_{13}|\,. \tag{2.139}$$

The sum rule of interest for $\cos\delta$ reads

$$\cos\delta = -\frac{2}{\sin 2\theta_{12}\sin 2\theta_{23}\sin\theta_{13}\cos^2\theta^\circ_{13}}\Big[\cos^2\theta^\circ_{12}\left(\cos^2\theta^\circ_{13} - \cos^2\theta_{13}\sin^2\theta_{23}\right)$$
$$- \cos^2\theta_{12}\cos^2\theta_{23}\cos^2\theta^\circ_{13} + \sin^2\theta_{23}\left(\cos^2\theta_{13}\sin^2\theta^\circ_{12}\sin^2\theta^\circ_{13} - \sin^2\theta_{12}\sin^2\theta_{13}\cos^2\theta^\circ_{13}\right)$$
$$- \kappa\cos\hat{\delta}\cos\theta_{13}\sin\theta_{23}\sin 2\theta^\circ_{12}\sin\theta^\circ_{13}\left(\cos^2\theta^\circ_{13} - \cos^2\theta_{13}\sin^2\theta_{23}\right)^{\frac{1}{2}}\Big]\,, \tag{2.140}$$

where $\kappa = 1$ if $\hat{\theta}_{23}$ belongs to the first or third quadrant, and $\kappa = -1$ otherwise. As in the previous case, $\cos\delta$ is a function of $\hat{\delta}$. For $\theta^\circ_{13} = 0$ the sum rule in eq. (2.140) reduces to the one derived in [100] and considered in the next chapter.

2.6.5 Case D5: $U_{23}(\theta^e_{23}, \delta^e_{23})\, U_{13}(\theta^e_{13}, \delta^e_{13})$

In this case, we consider the following parametrisation of the PMNS matrix (see Appendix D):

$$U = U_{23}(\theta^e_{23}, \delta^e_{23})\, R_{13}(\hat{\theta}_{13})\, P_1(\hat{\delta})\, R_{23}(\theta^\circ_{23})\, R_{12}(\theta^\circ_{12})\, Q_0\,, \quad P_1(\hat{\delta}) = \mathrm{diag}(e^{i\hat{\delta}}, 1, 1)\,. \tag{2.141}$$

We find that:

$$\sin^2\theta_{13} = |U_{e3}|^2 = \cos^2\theta^\circ_{23}\sin^2\hat{\theta}_{13}\,, \tag{2.142}$$
$$\sin^2\theta_{23} = \frac{|U_{\mu 3}|^2}{1 - |U_{e3}|^2} = \sin^2\theta_{23}(\hat{\theta}_{13}, \theta^e_{23}, \delta^e_{23}, \theta^\circ_{23})\,, \tag{2.143}$$
$$\sin^2\theta_{12} = \frac{|U_{e2}|^2}{1 - |U_{e3}|^2} = \sin^2\theta_{12}(\hat{\theta}_{13}, \hat{\delta}, \theta^\circ_{12}, \theta^\circ_{23})\,. \tag{2.144}$$

Since, as can be shown, $|U_{\mu 2}|$ is a function of the parameters θ^e_{23}, δ^e_{23}, $\hat{\delta}$, $\hat{\theta}_{13}$, θ°_{12} and θ°_{23}, and $\hat{\theta}_{13}$, and $\cos\hat{\delta}$ can be extracted from eqs. (2.142) and (2.144), respectively, it might

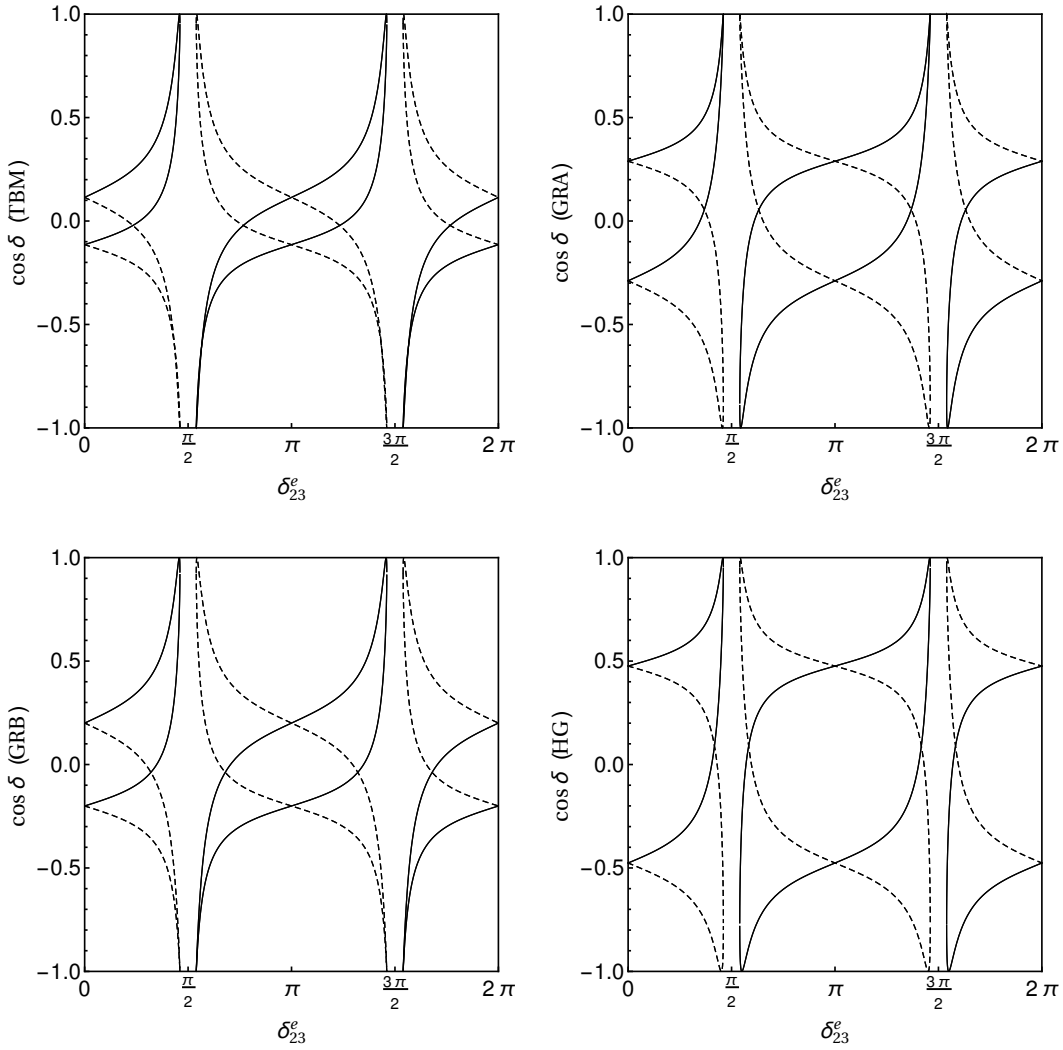

Figure 2.6. Dependence of $\cos\delta$ on δ^e_{23} in the cases of the TBM, GRA, GRB and HG symmetry forms. The mixing parameters $\sin^2\theta_{12}$, $\sin^2\theta_{23}$ and $\sin^2\theta_{13}$ have been fixed to their best fit values for the NO neutrino mass spectrum quoted in eqs. (2.15)–(2.17). The angle $\hat{\theta}_{13}$ is assumed to belong to the first quadrant. The solid lines correspond to $\hat{\delta} = \cos^{-1}(\cos\hat{\delta})$, where $\cos\hat{\delta}$ is the solution of eq. (2.144), while the dashed lines correspond to $\hat{\delta} = 2\pi - \cos^{-1}(\cos\hat{\delta})$. See text for further details.

be possible to find a sum rule for $\cos\delta$ in the case of fixed δ^e_{23}. Since in this case the analytical expression of $\cos\delta$ in terms of δ^e_{23} is rather complicated, we do not present it here. Note that imposing either $\theta^\circ_{12} = 0$ or $\theta^\circ_{23} = 0$ is not enough to fix the value of $\cos\delta$. Even in the case of fixed δ^e_{23} it follows from eqs. (2.143) and (2.144) that for any given value of δ^e_{23}, $\cos\delta$ can take several values. This can be understood, e.g., from eq. (2.144) which allows to fix $\cos\hat{\delta}$, but not $\sin\hat{\delta}$. This ambiguity, in particular, leads to multiple solutions for $\cos\delta$. In Fig. 2.6 we show these solutions in the cases of the TBM, GRA, GRB and HG symmetry forms. We remind that for these forms $\theta^\circ_{23} = -\pi/4$ and $\theta^\circ_{12} = \sin^{-1}(1/\sqrt{3})$ (TBM), $\theta^\circ_{12} = \sin^{-1}(1/\sqrt{2+r})$ (GRA), $r = (1+\sqrt{5})/2$ being the golden ratio, $\theta^\circ_{12} = \pi/5$ (GRB), and $\theta^\circ_{12} = \pi/6$ (HG). We assume $\hat{\theta}_{13}$ to lie in the first quadrant. The solid lines correspond to $\hat{\delta} = \cos^{-1}(\cos\hat{\delta})$, where $\cos\hat{\delta}$ is the solution of eq. (2.144), while the dashed lines correspond to $\hat{\delta} = 2\pi - \cos^{-1}(\cos\hat{\delta})$. Multiple lines reflect the fact that eq. (2.143) for θ^e_{23} has several solutions. We note that Fig. 2.6 does not

change in the case of $\hat{\theta}_{13}$ belonging to the third quadrant, while for $\hat{\theta}_{13}$ lying in the second or fourth quadrant the solid and dashed lines interchange. For $\delta^e_{23} = 0$ or π, we find

$$\begin{aligned}
\cos\delta &= \{-0.114, 0.114\} \text{ for TBM;} \\
\cos\delta &= \{-0.289, 0.289\} \text{ for GRA;} \\
\cos\delta &= \{-0.200, 0.200\} \text{ for GRB;} \\
\cos\delta &= \{-0.476, 0.476\} \text{ for HG.}
\end{aligned}$$

It is worth noting that in the scheme under consideration the values of δ^e_{23} in a vicinity of $\pi/2$ ($3\pi/2$) do not provide physical values of $\cos\delta$ (see Fig. 2.6).

2.6.6 Case D6: $U_{12}(\theta^e_{12}, \delta^e_{12})\, U_{13}(\theta^e_{13}, \delta^e_{13})$

It is convenient to consider the following parametrisation of the PMNS matrix U (see Appendix D):

$$U = U_{12}(\theta^e_{12}, \delta^e_{12})\, R_{13}(\hat{\theta}_{13})\, P_1(\hat{\delta})\, R_{23}(\theta^\circ_{23})\, R_{12}(\theta^\circ_{12})\, Q_0\,, \quad P_1(\hat{\delta}) = \mathrm{diag}(e^{i\hat{\delta}}, 1, 1)\,. \tag{2.145}$$

We find that a sum rule for $\cos\delta$ can be derived if either $\theta^\circ_{12} = q\pi/2$, $q = 0, 1, 2, 3, 4$, or $\theta^\circ_{23} = k\pi$, $k = 0, 1, 2$. Indeed, the relation $|U_{\tau 3}|^2 = \cos^2\theta_{13}\cos^2\theta_{23} = \cos^2\hat{\theta}_{13}\cos^2\theta^\circ_{23}$ allows us to determine $\cos^2\hat{\theta}_{13}$ in terms of the known quantity $\cos^2\theta_{13}\cos^2\theta_{23}$ and the parameter $\cos^2\theta^\circ_{23}$, which is fixed once G_f and G_ν are fixed. Further, we have

$$|U_{\tau 2}| = |e^{i\hat{\delta}}\sin\theta^\circ_{12}\sin\hat{\theta}_{13} + \cos\hat{\theta}_{13}\cos\theta^\circ_{12}\sin\theta^\circ_{23}|\,, \tag{2.146}$$

where the only unconstrained parameter is the phase $\hat{\delta}$. In the cases indicated above with either $\theta^\circ_{12} = q\pi/2$, $q = 0, 1, 2, 3, 4$, or $\theta^\circ_{23} = k\pi$, $k = 0, 1, 2$, the absolute value of the element $U_{\tau 2}$ does not depend on $\hat{\delta}$, which in turn allows a sum rule for $\cos\delta$ to be derived. In general, $\cos\delta$ is a function of $\hat{\delta}$:

$$\begin{aligned}
\cos\delta = \frac{2}{\sin 2\theta_{12}\sin 2\theta_{23}\sin\theta_{13}\cos^2\theta^\circ_{23}} \Big[& \sin^2\theta^\circ_{12}\left(\cos^2\theta^\circ_{23} - \cos^2\theta_{13}\cos^2\theta_{23}\right) \\
& - \cos^2\theta_{12}\sin^2\theta_{23}\cos^2\theta^\circ_{23} + \cos^2\theta_{23}\left(\cos^2\theta_{13}\cos^2\theta^\circ_{12}\sin^2\theta^\circ_{23} - \sin^2\theta_{12}\sin^2\theta_{13}\cos^2\theta^\circ_{23}\right) \\
& + \kappa\cos\hat{\delta}\cos\theta_{13}\cos\theta_{23}\sin 2\theta^\circ_{12}\sin\theta^\circ_{23}\left(\cos^2\theta^\circ_{23} - \cos^2\theta_{13}\cos^2\theta_{23}\right)^{\frac{1}{2}} \Big]\,,
\end{aligned} \tag{2.147}$$

where $\kappa = 1$ if $\hat{\theta}_{13}$ belongs to the first or third quadrant, and $\kappa = -1$ otherwise. In this case, the sum rule for $\cos\delta$ has been derived first in [100] assuming $\theta^\circ_{13} = 0$, but as we can see this result holds also for any fixed value of θ°_{13}, since the parametrisation given in eq. (2.145) and the corresponding one in [100] are the same after a redefinition of the parameters.

The sum rules derived in this section for pattern D are summarised in Table 2.7.

Table 2.7. Summary of the sum rules for $\cos\delta$ in the case of fully broken G_e and $G_\nu = Z_n$, $n > 2$ or $Z_n \times Z_m$, $n, m \geq 2$, under the assumption that the matrix U_e consists of two complex rotation matrices. The parameter $\kappa = 1$ if the corresponding hat angle belongs to the first or third quadrant, and $\kappa = -1$ otherwise. See text for further details.

Case	Parametrisation of the PMNS matrix U	Sum rule for $\cos\delta$
D2	$U_{13}(\theta^e_{13}, \delta^e_{13})\, R_{12}(\hat{\theta}_{12})\, P_1(\hat{\delta})\, R_{23}(\theta^\circ_{23})\, R_{13}(\theta^\circ_{13})\, Q_0$	$\dfrac{\cos^2\theta_{23}\cos^2\theta_{12} + \sin^2\theta_{12}\sin^2\theta_{13}\sin^2\theta_{23} - \cos^2\hat{\theta}_{12}\cos^2\theta^\circ_{23}}{\sin 2\theta_{23}\sin\theta_{12}\cos\theta_{12}\sin\theta_{13}}$
D3	$U_{12}(\theta^e_{12}, \delta^e_{12})\, R_{23}(\hat{\theta}_{23})\, P_2(\hat{\delta})\, R_{13}(\theta^\circ_{13})\, R_{12}(\theta^\circ_{12})\, Q_0$	$\dfrac{2}{\sin 2\theta_{12}\sin 2\theta_{23}\sin\theta_{13}\cos^2\theta^\circ_{13}}\Big[\cos^2\theta^\circ_{12}\left(\cos^2\theta^\circ_{13} - \cos^2\theta_{13}\cos^2\theta_{23}\right)$ $-\cos^2\theta_{12}\sin^2\theta_{23}\cos^2\theta^\circ_{13} + \cos^2\theta_{23}\left(\cos^2\theta_{13}\sin^2\theta^\circ_{12}\sin^2\theta^\circ_{13} - \sin^2\theta_{12}\sin^2\theta_{13}\cos^2\theta^\circ_{13}\right)$ $+\kappa\cos\hat{\delta}\cos\theta_{13}\cos\theta_{23}\sin 2\theta^\circ_{12}\sin\theta^\circ_{13}\left(\cos^2\theta^\circ_{13} - \cos^2\theta_{13}\cos^2\theta_{23}\right)^{\frac{1}{2}}\Big]$
D4	$U_{13}(\theta^e_{13}, \delta^e_{13})\, R_{23}(\hat{\theta}_{23})\, P_2(\hat{\delta})\, R_{13}(\theta^\circ_{13})\, R_{12}(\theta^\circ_{12})\, Q_0$	$-\dfrac{2}{\sin 2\theta_{12}\sin 2\theta_{23}\sin\theta_{13}\cos^2\theta^\circ_{13}}\Big[\cos^2\theta^\circ_{12}\left(\cos^2\theta^\circ_{13} - \cos^2\theta_{13}\sin^2\theta_{23}\right)$ $-\cos^2\theta_{12}\cos^2\theta_{23}\cos^2\theta^\circ_{13} + \sin^2\theta_{23}\left(\cos^2\theta_{13}\sin^2\theta^\circ_{12}\sin^2\theta^\circ_{13} - \sin^2\theta_{12}\sin^2\theta_{13}\cos^2\theta^\circ_{13}\right)$ $-\kappa\cos\hat{\delta}\cos\theta_{13}\sin\theta_{23}\sin 2\theta^\circ_{12}\sin\theta^\circ_{13}\left(\cos^2\theta^\circ_{13} - \cos^2\theta_{13}\sin^2\theta_{23}\right)^{\frac{1}{2}}\Big]$
D6	$U_{12}(\theta^e_{12}, \delta^e_{12})\, R_{13}(\hat{\theta}_{13})\, P_1(\hat{\delta})\, R_{23}(\theta^\circ_{23})\, R_{12}(\theta^\circ_{12})\, Q_0$	$\dfrac{2}{\sin 2\theta_{12}\sin 2\theta_{23}\sin\theta_{13}\cos^2\theta^\circ_{23}}\Big[\sin^2\theta^\circ_{12}\left(\cos^2\theta^\circ_{23} - \cos^2\theta_{13}\cos^2\theta_{23}\right)$ $-\cos^2\theta_{12}\sin^2\theta_{23}\cos^2\theta^\circ_{23} + \cos^2\theta_{23}\left(\cos^2\theta_{13}\cos^2\theta^\circ_{12}\sin^2\theta^\circ_{23} - \sin^2\theta_{12}\sin^2\theta_{13}\cos^2\theta^\circ_{23}\right)$ $+\kappa\cos\hat{\delta}\cos\theta_{13}\cos\theta_{23}\sin 2\theta^\circ_{12}\sin\theta^\circ_{23}\left(\cos^2\theta^\circ_{23} - \cos^2\theta_{13}\cos^2\theta_{23}\right)^{\frac{1}{2}}\Big]$

2.7 Pattern E: $G_e = Z_n$, $n > 2$ or $Z_n \times Z_m$, $n, m \geq 2$ and fully broken G_ν

When the discrete flavour symmetry G_f is fully broken in the neutrino sector, the matrix U_ν is unconstrained and includes, in general, three complex rotations and three phases, i.e., three angle and six CPV phase parameters. It is impossible to derive predictions for the mixing angles and CPV phases in the PMNS matrix in this case. Therefore we will consider in this section forms of U_ν corresponding to one of the rotation angle parameters being equal to zero. Some of these forms of U_ν correspond to a class of models of neutrino mass generation or phenomenological studies (see, e.g., [150]) and lead, in particular, to sum rules for $\cos\delta$. Since in this case G_f is fully broken in the neutrino sector, the $Z_2 \times Z_2$ symmetry of the Majorana mass term does arise accidentally. Therefore the matrix U_ν is not constrained by the symmetry group G_f. We give in Table D.1 in Appendix D the most general parametrisations of U under the assumption that for fully broken G_ν one rotation angle vanishes in the matrix U_ν.

2.7.1 Case E1: $U_{12}(\theta^\nu_{12}, \delta^\nu_{12})\, U_{13}(\theta^\nu_{13}, \delta^\nu_{13})$

It proves convenient to consider the following parametrisation of the PMNS matrix U in this case (see Appendix D):

$$U = R_{23}(\theta^\circ_{23})\, R_{13}(\theta^\circ_{13})\, P_1(\hat{\delta})\, R_{12}(\hat{\theta}_{12})\, U_{13}(\theta^\nu_{13}, \delta^\nu_{13})\, Q_0\,, \quad P_1(\hat{\delta}) = \mathrm{diag}(e^{i\hat{\delta}}, 1, 1)\,. \tag{2.148}$$

Consider first the case of $\theta^\circ_{13} = 0$. In this case the phase $\hat{\delta}$ is unphysical. Comparing this parametrisation of U with the standard parametrisation, we find:

$$\sin^2\theta_{13} = |U_{e3}|^2 = \sin^2\theta^\nu_{13}\cos^2\hat{\theta}_{12}\,, \tag{2.149}$$

$$\begin{aligned}\sin^2\theta_{23} = \frac{|U_{\mu 3}|^2}{1-|U_{e3}|^2} = \frac{1}{\cos^2\theta_{13}}\big[&\sin^2\theta^\circ_{23}\cos^2\theta^\nu_{13} + \cos^2\theta^\circ_{23}\sin^2\theta^\nu_{13}\sin^2\hat{\theta}_{12} \\ &- \frac{1}{2}\sin 2\theta^\circ_{23}\sin 2\theta^\nu_{13}\sin\hat{\theta}_{12}\cos\delta^\nu_{13}\big]\,,\end{aligned} \tag{2.150}$$

$$\sin^2\theta_{12} = \frac{|U_{e2}|^2}{1-|U_{e3}|^2} = \frac{\sin^2\hat{\theta}_{12}}{\cos^2\theta_{13}}\,. \tag{2.151}$$

From the ratio

$$\left|\frac{U_{\tau 2}}{U_{\mu 2}}\right|^2 = \tan^2\theta^\circ_{23}\,, \tag{2.152}$$

we get the following sum rule for $\cos\delta$:

$$\cos\delta = -\frac{\tan\theta_{12}}{\sin 2\theta_{23}\sin\theta_{13}}\left[\cos 2\theta^\circ_{23}\sin^2\theta_{13} + \left(\sin^2\theta_{23} - \sin^2\theta^\circ_{23}\right)\left(\cot^2\theta_{12} - \sin^2\theta_{13}\right)\right]\,. \tag{2.153}$$

Substituting the best fit values of the neutrino mixing angles for the NO neutrino mass spectrum and the value of $\theta^\circ_{23} = -\pi/4$, which corresponds to the TBM, BM, GRA, GRB and HG symmetry forms, we obtain $\cos\delta = 0.616$. We note that in the considered scheme the predictions for $\cos\delta$ are all the same for the symmetry forms mentioned above, since these forms are characterised by different values of the angle θ°_{12}, which has been absorbed by the free parameter $\hat{\theta}_{12}$. This "degeneracy" can be lifted in specific models in which the

value of θ_{12}^ν is fixed. Using the best fit values and the requirement $|\cos\delta| \leq 1$, we find that the allowed values of $\sin^2\theta_{23}^\circ$ belong to the following interval: $0.338 \leq \sin^2\theta_{23}^\circ \leq 0.538$.

In order to give the general result for $\cos\delta$ in the case of $\theta_{13}^\circ \neq 0$, we use the expression for $\sin^2\theta_{12}$ for non-zero θ_{13}°:

$$\sin^2\theta_{12} = \frac{|U_{e2}|^2}{1-|U_{e3}|^2} = \frac{\cos^2\theta_{13}^\circ \sin^2\hat{\theta}_{12}}{\cos^2\theta_{13}}\,. \tag{2.154}$$

Employing this relation in the expression for $|U_{\tau 2}|^2$, we get

$$\begin{aligned}\cos\delta = -\frac{2}{\sin 2\theta_{12}\sin 2\theta_{23}\sin\theta_{13}\cos^2\theta_{13}^\circ}\Big[&\cos^2\theta_{23}^\circ\left(\cos^2\theta_{13}^\circ - \sin^2\theta_{12}\cos^2\theta_{13}\right)\\ &- \cos^2\theta_{12}\cos^2\theta_{23}\cos^2\theta_{13}^\circ + \sin^2\theta_{12}\left(\cos^2\theta_{13}\sin^2\theta_{13}^\circ\sin^2\theta_{23}^\circ - \sin^2\theta_{13}\sin^2\theta_{23}\cos^2\theta_{13}^\circ\right)\\ &- \kappa\cos\hat{\delta}\sin\theta_{12}\cos\theta_{13}\sin\theta_{13}^\circ\sin 2\theta_{23}^\circ\left(\cos^2\theta_{13}^\circ - \sin^2\theta_{12}\cos^2\theta_{13}\right)^{\frac{1}{2}}\Big]\,,\end{aligned} \tag{2.155}$$

where $\kappa = 1$ if $\hat{\theta}_{12}$ belongs to the first or third quadrant, and $\kappa = -1$ otherwise.

Similar to cases C2, C5, C7 and C9 analysed in subsections 2.4.2, 2.4.5, 2.4.7 and 2.4.9, $\cos\delta$ is a function of the known neutrino mixing angles θ_{12}, θ_{13} and θ_{23}, of the angles θ_{13}° and θ_{23}° fixed by G_f and the assumed symmetry breaking pattern, as well as of the phase parameter $\hat{\delta}$ of the scheme. Predictions for $\cos\delta$ can be obtained if $\hat{\delta}$ is fixed by additional considerations of, e.g., generalised CP invariance, symmetries, etc.

For $\theta_{13}^\circ = k\pi$, $k = 0, 1, 2$, and/or $\theta_{23}^\circ = q\pi/2$, $q = 0, 1, 2, 3, 4$, $\cos\delta$ does not depend on $\hat{\delta}$ and κ. In the first case the expression in eq. (2.155) reduces to the sum rule given in eq. (2.153).

2.7.2 Case E2: $U_{12}(\theta_{12}^\nu, \delta_{12}^\nu)\, U_{23}(\theta_{23}^\nu, \delta_{23}^\nu)$

In this case, it is convenient to use another possible parametrisation of the PMNS matrix given in Appendix D. Namely,

$$U = R_{23}(\theta_{23}^\circ)\, R_{13}(\theta_{13}^\circ)\, P_1(\hat{\delta})\, R_{12}(\hat{\theta}_{12})\, U_{23}(\theta_{23}^\nu, \delta_{23}^\nu)\, Q_0\,, \quad P_1(\hat{\delta}) = \mathrm{diag}(e^{i\hat{\delta}}, 1, 1)\,. \tag{2.156}$$

Consider first the possibility of $\theta_{13}^\circ = 0$. Under this assumption we find:

$$\sin^2\theta_{13} = |U_{e3}|^2 = \sin^2\theta_{23}^\nu \sin^2\hat{\theta}_{12}\,, \tag{2.157}$$

$$\begin{aligned}\sin^2\theta_{23} = \frac{|U_{\mu 3}|^2}{1-|U_{e3}|^2} = \frac{1}{\cos^2\theta_{13}}\Big[&\sin^2\theta_{23}^\circ\cos^2\theta_{23}^\nu + \cos^2\theta_{23}^\circ\sin^2\theta_{23}^\nu\cos^2\hat{\theta}_{12}\\ &+ \frac{1}{2}\sin 2\theta_{23}^\circ\sin 2\theta_{23}^\nu\cos\hat{\theta}_{12}\cos\delta_{23}^\nu\Big]\,,\end{aligned} \tag{2.158}$$

$$\sin^2\theta_{12} = \frac{|U_{e2}|^2}{1-|U_{e3}|^2} = \frac{\cos^2\theta_{23}^\nu\sin^2\hat{\theta}_{12}}{\cos^2\theta_{13}}\,. \tag{2.159}$$

The sum rule of interest for $\cos\delta$ can be derived in this case using the ratio

$$\left|\frac{U_{\tau 1}}{U_{\mu 1}}\right|^2 = \tan^2\theta_{23}^\circ\,. \tag{2.160}$$

We get

$$\cos\delta = \frac{\cot\theta_{12}}{\sin 2\theta_{23}\sin\theta_{13}}\left[\cos 2\theta_{23}^{\circ}\sin^2\theta_{13} + \left(\sin^2\theta_{23} - \sin^2\theta_{23}^{\circ}\right)\left(\tan^2\theta_{12} - \sin^2\theta_{13}\right)\right] . \tag{2.161}$$

This sum rule can be formally obtained from the r.h.s. of eq. (2.153) by interchanging $\tan\theta_{12}$ and $\cot\theta_{12}$ and by multiplying it by -1. Substituting the best fit values of the neutrino mixing angles for the NO neutrino mass spectrum and the value of $\theta_{23}^{\circ} = -\pi/4$, we get $\cos\delta = -0.262$. Using the best fit values and the requirement $|\cos\delta| \leq 1$, we find that the allowed values of $\sin^2\theta_{23}^{\circ}$ belong to the following interval: $0.227 \leq \sin^2\theta_{23}^{\circ} \leq 0.659$.

In order to find a general result for $\cos\delta$ for arbitrary fixed $\theta_{13}^{\circ} \neq 0$, we use the following relation:

$$\cos^2\theta_{12}\cos^2\theta_{13} = \cos^2\hat{\theta}_{12}\cos^2\theta_{13}^{\circ} , \tag{2.162}$$

which follows from the expressions for $|U_{e1}|^2$ in the standard parametrisation and in the parametrisation given in eq. (2.156). With the help of this relation, using $|U_{\mu 1}|$, we get

$$\begin{aligned}\cos\delta = \frac{2}{\sin 2\theta_{12}\sin 2\theta_{23}\sin\theta_{13}\cos^2\theta_{13}^{\circ}}\Bigg[&\cos^2\theta_{23}^{\circ}\left(\cos^2\theta_{13}^{\circ} - \cos^2\theta_{12}\cos^2\theta_{13}\right) \\ &- \sin^2\theta_{12}\cos^2\theta_{23}\cos^2\theta_{13}^{\circ} + \cos^2\theta_{12}\left(\cos^2\theta_{13}\sin^2\theta_{13}^{\circ}\sin^2\theta_{23}^{\circ} - \sin^2\theta_{13}\sin^2\theta_{23}\cos^2\theta_{13}^{\circ}\right) \\ &+ \kappa\cos\hat{\delta}\cos\theta_{12}\cos\theta_{13}\sin\theta_{13}^{\circ}\sin 2\theta_{23}^{\circ}\left(\cos^2\theta_{13}^{\circ} - \cos^2\theta_{12}\cos^2\theta_{13}\right)^{\frac{1}{2}}\Bigg] ,\end{aligned} \tag{2.163}$$

where $\kappa = 1$ if $\hat{\theta}_{12}$ belongs to the first or third quadrant, and $\kappa = -1$ otherwise. Also in this case $\cos\delta$ is a function of the unconstrained phase parameter $\hat{\delta}$ of the scheme. Predictions for $\cos\delta$ can be obtained if $\hat{\delta}$ is fixed by additional considerations (e.g., generalised CP invariance, symmetries, etc.).

As like in case E1, for $\theta_{13}^{\circ} = k\pi$, $k = 0, 1, 2$, and/or $\theta_{23}^{\circ} = q\pi/2$, $q = 0, 1, 2, 3, 4$, $\cos\delta$ does not depend on $\hat{\delta}$ and κ. For $\theta_{13}^{\circ} = 0, \pi, 2\pi$, the sum rule in eq. (2.163) coincides with the sum rule given in eq. (2.161).

2.7.3 Case E3: $U_{23}(\theta_{23}^{\nu}, \delta_{23}^{\nu})\, U_{12}(\theta_{12}^{\nu}, \delta_{12}^{\nu})$

The convenient parametrisation for U to use in this case is given in Appendix D:

$$U = R_{13}(\theta_{13}^{\circ})\, R_{12}(\theta_{12}^{\circ})\, P_2(\hat{\delta})\, R_{23}(\hat{\theta}_{23})\, U_{12}(\theta_{12}^{\nu}, \delta_{12}^{\nu})\, Q_0 , \quad P_2(\hat{\delta}) = \mathrm{diag}(1, e^{i\hat{\delta}}, 1) .$$

We find that:

$$\sin^2\theta_{13} = |U_{e3}|^2 = \sin^2\theta_{13}(\hat{\theta}_{23}, \hat{\delta}, \theta_{12}^{\circ}, \theta_{13}^{\circ}) , \tag{2.164}$$

$$\sin^2\theta_{23} = \frac{|U_{\mu 3}|^2}{1 - |U_{e3}|^2} = \frac{\cos^2\theta_{12}^{\circ}\sin^2\hat{\theta}_{23}}{\cos^2\theta_{13}} , \tag{2.165}$$

$$\sin^2\theta_{12} = \frac{|U_{e2}|^2}{1 - |U_{e3}|^2} = \sin^2\theta_{12}(\hat{\theta}_{23}, \hat{\delta}, \theta_{12}^{\nu}, \delta_{12}^{\nu}, \theta_{12}^{\circ}, \theta_{13}^{\circ}) . \tag{2.166}$$

However, a sum rule for $\cos\delta$ cannot be obtained because $\cos\delta$ turns out to depend, in particular, on δ_{12}^{ν} which is an unconstrained phase parameter of the scheme considered, which can be seen from the expression for $|U_{\mu 1}|$:

$$|U_{\mu 1}| = |\cos\theta_{12}^{\nu}\sin\theta_{12}^{\circ} + e^{i(\hat{\delta}+\delta_{12}^{\nu})}\cos\hat{\theta}_{23}\cos\theta_{12}^{\circ}\sin\theta_{12}^{\nu}| . \tag{2.167}$$

The situation here is analogous to the cases analysed in subsections 2.6.1 and 2.6.5. Namely, considering a certain residual symmetry group G_e, from eq. (2.165) we find that $\sin^2\hat{\theta}_{23}$ is fixed. Then, $\cos\hat{\delta}$ is fixed (up to a sign) by eq. (2.164). Hence, θ^ν_{12} can be expressed in terms of δ^ν_{12} by virtue of eq. (2.166). Thus, numerical predictions for $\cos\delta$ can be obtained if δ^ν_{12} is fixed.

2.7.4 Case E4: $U_{23}(\theta^\nu_{23}, \delta^\nu_{23})\, U_{13}(\theta^\nu_{13}, \delta^\nu_{13})$

Employing the parametrisation for U given in Appendix D,

$$U = R_{13}(\theta^\circ_{13})\, R_{12}(\theta^\circ_{12})\, P_2(\hat{\delta})\, R_{23}(\hat{\theta}_{23})\, U_{13}(\theta^\nu_{13}, \delta^\nu_{13})\, Q_0\,, \quad P_2(\hat{\delta}) = \mathrm{diag}(1, e^{i\hat{\delta}}, 1)\,,$$

we find that $\cos\delta$ is a function of $\hat{\theta}_{23}$, θ°_{12} and the PMNS mixing angles. Therefore, $\cos\delta$ can be determined only in those cases when $\hat{\theta}_{23}$ is fixed. Using the result

$$\sin^2\theta_{12} = \frac{|U_{e2}|^2}{1-|U_{e3}|^2} = \frac{1}{\cos^2\theta_{13}}\Big[\cos^2\hat{\theta}_{23}\cos^2\theta^\circ_{13}\sin^2\theta^\circ_{12} + \sin^2\hat{\theta}_{23}\sin^2\theta^\circ_{13} - \frac{1}{2}\cos\hat{\delta}\sin 2\hat{\theta}_{23}\sin 2\theta^\circ_{13}\sin\theta^\circ_{12}\Big]\,, \tag{2.168}$$

we find these cases to be, for example: (i) $\theta^\circ_{12} = 0, \pi$, leading to the relation $\sin^2\theta_{12}\cos^2\theta_{13} = \sin^2\hat{\theta}_{23}\sin^2\theta^\circ_{13}$, (ii) $\theta^\circ_{13} = 0, \pi$, implying $\sin^2\theta_{12}\cos^2\theta_{13} = \cos^2\hat{\theta}_{23}\sin^2\theta^\circ_{12}$, (iii) $\theta^\circ_{13} = \pi/2, 3\pi/2$, giving $\sin^2\theta_{12}\cos^2\theta_{13} = \sin^2\hat{\theta}_{23}$. For this reason we give $\cos\delta$ as a function of the angle $\hat{\theta}_{23}$. Namely, the sum rule of interest, which is obtained using $|U_{\mu 2}| = |\cos\hat{\theta}_{23}\cos\theta^\circ_{12}|$, reads

$$\cos\delta = \frac{\cos^2\theta_{12}\cos^2\theta_{23} + \sin^2\theta_{12}\sin^2\theta_{13}\sin^2\theta_{23} - \cos^2\hat{\theta}_{23}\cos^2\theta^\circ_{12}}{\sin 2\theta_{23}\sin\theta_{12}\cos\theta_{12}\sin\theta_{13}}\,. \tag{2.169}$$

The dependence of $\cos\delta$ on G_f is realised via the values of the angles θ°_{12} and θ°_{13}.

2.7.5 Case E5: $U_{13}(\theta^\nu_{13}, \delta^\nu_{13})\, U_{12}(\theta^\nu_{12}, \delta^\nu_{12})$

The parametrisation for the PMNS matrix U employed by us in this subsection is given in Appendix D:

$$U = R_{23}(\theta^\circ_{23})\, R_{12}(\theta^\circ_{12})\, P_1(\hat{\delta})\, R_{13}(\hat{\theta}_{13})\, U_{12}(\theta^\nu_{12}, \delta^\nu_{12})\, Q_0\,, \quad P_1(\hat{\delta}) = \mathrm{diag}(e^{i\hat{\delta}}, 1, 1)\,.$$

We find that:

$$\sin^2\theta_{13} = |U_{e3}|^2 = \cos^2\theta^\circ_{12}\sin^2\hat{\theta}_{13}\,, \tag{2.170}$$

$$\sin^2\theta_{23} = \frac{|U_{\mu 3}|^2}{1-|U_{e3}|^2} = \sin^2\theta_{23}(\hat{\theta}_{13}, \hat{\delta}, \theta^\circ_{12}, \theta^\circ_{23})\,, \tag{2.171}$$

$$\sin^2\theta_{12} = \frac{|U_{e2}|^2}{1-|U_{e3}|^2} = \sin^2\theta_{12}(\hat{\theta}_{13}, \hat{\delta}, \theta^\nu_{12}, \delta^\nu_{12}, \theta^\circ_{12})\,. \tag{2.172}$$

However, a sum rule for $\cos\delta$ cannot be obtained because $\cos\delta$ turns out to depend, in particular, on δ^ν_{12} which is an unconstrained phase parameter of the scheme considered. This can be seen, e.g., from the expression for $|U_{\mu 1}|$:

$$|U_{\mu 1}| = |\cos\theta^\nu_{12}(e^{i\hat{\delta}}\sin\theta^\circ_{12}\cos\theta^\circ_{23}\cos\hat{\theta}_{13} + \sin\hat{\theta}_{13}\sin\theta^\circ_{23}) + e^{i\delta^\nu_{12}}\cos\theta^\circ_{12}\cos\theta^\circ_{23}\sin\theta^\nu_{12}|. \tag{2.173}$$

Similarly to the case analysed in subsection 2.7.3, for a certain residual symmetry group G_e, from eq. (2.170) we find that $\sin^2\hat{\theta}_{13}$ is fixed. Then, $\cos\hat{\delta}$ is fixed (up to a sign) by eq. (2.171), and so the angle θ^{ν}_{12} can be expressed in terms of δ^{ν}_{12} by virtue of eq. (2.172). Therefore, numerical predictions for $\cos\delta$ can be obtained if δ^{ν}_{12} is fixed.

2.7.6 Case E6: $U_{13}(\theta^{\nu}_{13}, \delta^{\nu}_{13})\, U_{23}(\theta^{\nu}_{23}, \delta^{\nu}_{23})$

The parametrisation of the PMNS matrix U utilised by us in the present subsection is given in Appendix D:

$$U = R_{23}(\theta^{\circ}_{23})\, R_{12}(\theta^{\circ}_{12})\, P_1(\hat{\delta})\, R_{13}(\hat{\theta}_{13})\, U_{23}(\theta^{\nu}_{23}, \delta^{\nu}_{23})\, Q_0\,, \quad P_1(\hat{\delta}) = \mathrm{diag}(e^{i\hat{\delta}}, 1, 1)\,.$$

A sum rule and predictions for $\cos\delta$ can be derived in the cases of either $\theta^{\circ}_{23} = q\pi/2$, $q = 0, 1, 2, 3, 4$, or $\theta^{\circ}_{12} = k\pi$, $k = 0, 1, 2$. Indeed, using the relation

$$|U_{e1}|^2 = \cos^2\theta_{12}\cos^2\theta_{13} = \cos^2\hat{\theta}_{13}\cos^2\theta^{\circ}_{12}\,, \tag{2.174}$$

we can express $\cos^2\hat{\theta}_{13}$ in terms of the product of PMNS neutrino mixing parameters $\cos^2\theta_{12}\cos^2\theta_{13}$ and, the fixed by G_f parameter, $\cos^2\theta^{\circ}_{12}$. The sum rule of interest for $\cos\delta$ can be derived, e.g., from the expression for the absolute value of the element $U_{\mu 1}$:

$$|U_{\mu 1}| = |e^{-i\hat{\delta}}\cos\hat{\theta}_{13}\cos\theta^{\circ}_{23}\sin\theta^{\circ}_{12} + \sin\hat{\theta}_{13}\sin\theta^{\circ}_{23}|\,, \tag{2.175}$$

since in any of the two limits indicated above, $\theta^{\circ}_{23} = q\pi/2$, $q = 0, 1, 2, 3, 4$, or $\theta^{\circ}_{12} = k\pi$, $k = 0, 1, 2$, $|U_{\mu 1}|$ does not depend on $\hat{\delta}$. In fact, it is given only in terms of the known PMNS neutrino mixing parameters and an angle (either θ°_{23} or θ°_{12}) which is fixed by the symmetry G_f. In the general case, $\cos\delta$ is a function of $\hat{\delta}$. Using eqs. (2.174) and (2.175), we get

$$\begin{aligned}\cos\delta = \frac{2}{\sin 2\theta_{12}\sin 2\theta_{23}\sin\theta_{13}\cos^2\theta^{\circ}_{12}}\Big[&\sin^2\theta^{\circ}_{23}\left(\cos^2\theta^{\circ}_{12} - \cos^2\theta_{12}\cos^2\theta_{13}\right)\\ &- \sin^2\theta_{12}\cos^2\theta_{23}\cos^2\theta^{\circ}_{12} + \cos^2\theta_{12}\left(\cos^2\theta_{13}\sin^2\theta^{\circ}_{12}\cos^2\theta^{\circ}_{23} - \sin^2\theta_{13}\sin^2\theta_{23}\cos^2\theta^{\circ}_{12}\right)\\ &+ \kappa\cos\hat{\delta}\cos\theta_{12}\cos\theta_{13}\sin\theta^{\circ}_{12}\sin 2\theta^{\circ}_{23}\left(\cos^2\theta^{\circ}_{12} - \cos^2\theta_{12}\cos^2\theta_{13}\right)^{\frac{1}{2}}\Big]\,,\end{aligned} \tag{2.176}$$

where $\kappa = 1$ if $\hat{\theta}_{13}$ lies in the first or third quadrant, and $\kappa = -1$ otherwise. For $\theta^{\circ}_{12} = k\pi$, $k = 0, 1, 2$, and/or $\theta^{\circ}_{23} = q\pi/2$, $q = 0, 1, 2, 3, 4$, $\cos\delta$ does not depend on $\hat{\delta}$ and κ.

The sum rules derived in this section for pattern E are summarised in Table 2.8.

Table 2.8. Summary of the sum rules for $\cos\delta$ in the case of $G_e = Z_n$, $n > 2$ or $Z_n \times Z_m$, $n, m \geq 2$ and fully broken G_ν, under the assumption that the matrix U_ν consists of two complex rotation matrices. The parameter $\kappa = 1$ if the corresponding hat angle belongs to the first or third quadrant, and $\kappa = -1$ otherwise. See text for further details.

Case	Parametrisation of the PMNS matrix U	Sum rule for $\cos\delta$
E1	$R_{23}(\theta^\circ_{23})\, R_{13}(\theta^\circ_{13})\, P_1(\hat{\delta})\, R_{12}(\hat{\theta}_{12})\, U_{13}(\theta^\nu_{13}, \delta^\nu_{13})\, Q_0$	$-\dfrac{2}{\sin 2\theta_{12} \sin 2\theta_{23} \sin\theta_{13} \cos^2\theta^\circ_{13}} \Big[\cos^2\theta^\circ_{23} \left(\cos^2\theta^\circ_{13} - \sin^2\theta_{12}\cos^2\theta_{13}\right)$ $- \cos^2\theta_{12}\cos^2\theta_{23}\cos^2\theta^\circ_{13} + \sin^2\theta_{12}\left(\cos^2\theta_{13}\sin^2\theta^\circ_{13}\sin^2\theta^\circ_{23} - \sin^2\theta_{13}\sin^2\theta_{23}\cos^2\theta^\circ_{13}\right)$ $-\kappa\cos\hat{\delta}\sin\theta_{12}\cos\theta_{13}\sin\theta^\circ_{13}\sin 2\theta^\circ_{23}\left(\cos^2\theta^\circ_{13} - \sin^2\theta_{12}\cos^2\theta_{13}\right)^{\frac{1}{2}} \Big]$
E2	$R_{23}(\theta^\circ_{23})\, R_{13}(\theta^\circ_{13})\, P_1(\hat{\delta})\, R_{12}(\hat{\theta}_{12})\, U_{23}(\theta^\nu_{23}, \delta^\nu_{23})\, Q_0$	$\dfrac{2}{\sin 2\theta_{12} \sin 2\theta_{23} \sin\theta_{13} \cos^2\theta^\circ_{13}} \Big[\cos^2\theta^\circ_{23} \left(\cos^2\theta^\circ_{13} - \cos^2\theta_{12}\cos^2\theta_{13}\right)$ $- \sin^2\theta_{12}\cos^2\theta_{23}\cos^2\theta^\circ_{13} + \cos^2\theta_{12}\left(\cos^2\theta_{13}\sin^2\theta^\circ_{13}\sin^2\theta^\circ_{23} - \sin^2\theta_{13}\sin^2\theta_{23}\cos^2\theta^\circ_{13}\right)$ $+\kappa\cos\hat{\delta}\cos\theta_{12}\cos\theta_{13}\sin\theta^\circ_{13}\sin 2\theta^\circ_{23}\left(\cos^2\theta^\circ_{13} - \cos^2\theta_{12}\cos^2\theta_{13}\right)^{\frac{1}{2}} \Big]$
E4	$R_{13}(\theta^\circ_{13})\, R_{12}(\theta^\circ_{12})\, P_2(\hat{\delta})\, R_{23}(\hat{\theta}_{23})\, U_{13}(\theta^\nu_{13}, \delta^\nu_{13})\, Q_0$	$\dfrac{\cos^2\theta_{12}\cos^2\theta_{23} + \sin^2\theta_{12}\sin^2\theta_{13}\sin^2\theta_{23} - \cos^2\hat{\theta}_{23}\cos^2\theta^\circ_{12}}{\sin 2\theta_{23}\sin\theta_{12}\cos\theta_{12}\sin\theta_{13}}$
E6	$R_{23}(\theta^\circ_{23})\, R_{12}(\theta^\circ_{12})\, P_1(\hat{\delta})\, R_{13}(\hat{\theta}_{13})\, U_{23}(\theta^\nu_{23}, \delta^\nu_{23})\, Q_0$	$\dfrac{2}{\sin 2\theta_{12} \sin 2\theta_{23} \sin\theta_{13} \cos^2\theta^\circ_{12}} \Big[\sin^2\theta^\circ_{23} \left(\cos^2\theta^\circ_{12} - \cos^2\theta_{12}\cos^2\theta_{13}\right)$ $- \sin^2\theta_{12}\cos^2\theta_{23}\cos^2\theta^\circ_{12} + \cos^2\theta_{12}\left(\cos^2\theta_{13}\sin^2\theta^\circ_{12}\cos^2\theta^\circ_{23} - \sin^2\theta_{13}\sin^2\theta_{23}\cos^2\theta^\circ_{12}\right)$ $+\kappa\cos\hat{\delta}\cos\theta_{12}\cos\theta_{13}\sin\theta^\circ_{12}\sin 2\theta^\circ_{23}\left(\cos^2\theta^\circ_{12} - \cos^2\theta_{12}\cos^2\theta_{13}\right)^{\frac{1}{2}} \Big]$

Table 2.9. The phenomenologically viable case for the symmetry group A_4. The values of $\cos\delta$ and $\sin^2\theta_{12}$ predicted in case B1 have been obtained using the best fit values of $\sin^2\theta_{23}$ and $\sin^2\theta_{13}$ for the NO spectrum quoted in eqs. (2.16) and (2.17).

(G_e, G_ν)	Case	$\sin^2\theta^\circ_{ij}$	$\cos\delta$	$\sin^2\theta_{ij}$
(Z_3, Z_2)	B1	$(\sin^2\theta^\circ_{12}, \sin^2\theta^\circ_{23}) = (1/3, 1/2)$	0.570	$\sin^2\theta_{12} = 0.341$

2.8 Summary of the predictions for $G_f = A_4$ (T'), S_4 and A_5

In this section, we summarise the numerical results obtained in the cases of the discrete flavour symmetry groups A_4 (T'), S_4 and A_5, which have been already discussed in subsections 2.2.4, 2.3.4 and 2.4.10. In Tables 2.9–2.11 we give the values of the fixed parameters $\sin^2\theta^\circ_{ij}$, obtained from the diagonalisation of the corresponding group elements which lead to physical values of $\cos\delta$ and phenomenologically viable results for the "standard" mixing angles θ_{12}, θ_{13} and θ_{23}. In the cases when the standard mixing angles are not fixed by the schemes in Tables 2.9–2.11, we use their best fit values for the NO spectrum quoted in eqs. (2.15)–(2.17). For the cases in the tables marked with an asterisk, physical values of $\cos\delta$, i.e., $|\cos\delta| \leq 1$, cannot be obtained employing the best fit values of the neutrino mixing angles θ_{12}, θ_{13} and θ_{23}, but they can be achieved for values of the relevant mixing parameters allowed at 3σ. Note that unphysical values of $\cos\delta$, $|\cos\delta| > 1$, occur when the relations between the parameters of the scheme and the standard parametrisation mixing angles cannot be fulfilled for given values of $\sin^2\theta_{12}$, $\sin^2\theta_{13}$ and $\sin^2\theta_{23}$. Indeed the parameter space of $\sin^2\theta_{12}$, $\sin^2\theta_{13}$ and $\sin^2\theta_{23}$ is reduced by these constraints coming from the schemes.

For the symmetry group A_4, we find that the residual symmetries

- $(G_e, G_\nu) = (Z_2, Z_2)$ in cases C1–C9;
- $(G_e, G_\nu) = (Z_3, Z_2)$ in cases B2 and B3;
- $(G_e, G_\nu) = (Z_2 \times Z_2, Z_2)$ in cases B1, B2 and B3;
- $(G_e, G_\nu) = (Z_2, Z_3)$ or $(Z_2, Z_2 \times Z_2)$ in cases A1, A2 and A3

do not provide phenomenologically viable results for $\cos\delta$ and/or the standard mixing angles. It is worth noticing that the predicted value of $\sin^2\theta_{12} = 0.341$ in Table 2.9 is within the 2σ allowed range [18]. Varying $\sin^2\theta_{13}$, which enters into the expression for $\sin^2\theta_{12}$, within its respective 3σ allowed range for the NO neutrino mass spectrum, we find $0.339 \leq \sin^2\theta_{12} \leq 0.343$.

For the symmetry group S_4, we find that the residual symmetries

- $(G_e, G_\nu) = (Z_2, Z_2)$ in cases C6 and C9;
- $(G_e, G_\nu) = (Z_3, Z_2)$ in case B3;
- $(G_e, G_\nu) = (Z_4, Z_2)$ or $(Z_2 \times Z_2, Z_2)$ in cases B2 and B3;
- $(G_e, G_\nu) = (Z_2, Z_3)$ in cases A1, A2 and A3;
- $(G_e, G_\nu) = (Z_2, Z_4)$ or $(Z_2, Z_2 \times Z_2)$ in case A3

Table 2.10. The phenomenologically viable cases for the symmetry group S_4. The predicted values of $\cos\delta$ and $\sin^2\theta_{12}$ or $\sin^2\theta_{23}$ have been obtained using the best fit values for the NO spectrum of the other two (not fixed) neutrino mixing parameters ($\sin^2\theta_{13}$ and $\sin^2\theta_{23}$, or $\sin^2\theta_{12}$ and $\sin^2\theta_{13}$) quoted in eqs. (2.15)–(2.17). In the cases marked with an asterisk, physical values of $\cos\delta$ cannot be obtained employing the best fit values of the mixing angles, but are possible for values of the relevant neutrino mixing parameters lying in their respective 3σ allowed intervals. See text for further details.

(G_e, G_ν)	Case	$\sin^2\theta^\circ_{ij}$	$\cos\delta$	$\sin^2\theta_{ij}$
(Z_2, Z_2)	C1	$\sin^2\theta^\circ_{23} = 1/4$	-0.806	not fixed
	C2	$\sin^2\theta^\circ_{23} = 1/2$	not fixed	$\sin^2\theta_{23} = 0.512$
	C3	$\sin^2\theta^\circ_{13} = 1/4$	-1^*	not fixed
	C4	$\sin^2\theta^\circ_{12} = 1/4$	0.992	not fixed
	C5	$\sin^2\theta^\circ_{12} = 1/4$	not fixed	$\sin^2\theta_{12} = 0.256$
	C7	$\sin^2\theta^\circ_{23} = 1/2$	not fixed	$\sin^2\theta_{23} = 0.488$
	C8	$\sin^2\theta^\circ_{23} = 1/2,\ 3/4$	$-1^*,\ 1^*$	not fixed
(Z_3, Z_2)	B1	$(\sin^2\theta^\circ_{12}, \sin^2\theta^\circ_{23}) = (1/3, 1/2)$	0.570	$\sin^2\theta_{12} = 0.341$
	B2	$(\sin^2\theta^\circ_{12}, \sin^2\theta^\circ_{13}) = (1/6, 1/5)$	-0.269	$\sin^2\theta_{12} = 0.317$
$(Z_4, Z_2),\ (Z_2 \times Z_2, Z_2)$	B1	$(\sin^2\theta^\circ_{12}, \sin^2\theta^\circ_{23}) = (1/4, 1/3)$	-1^*	$\sin^2\theta_{12} = 0.256$
$(Z_2, Z_4),\ (Z_2, Z_2 \times Z_2)$	A1	$(\sin^2\theta^\circ_{13}, \sin^2\theta^\circ_{23}) = (1/3, 1/4)$	-1^*	$\sin^2\theta_{23} = 0.488$
	A2	$(\sin^2\theta^\circ_{12}, \sin^2\theta^\circ_{23}) = (1/2, 1/2)$	1^*	$\sin^2\theta_{23} = 0.512$

do not provide phenomenologically viable results for $\cos\delta$ and/or for the standard mixing angles.

The cases in Table 2.10 marked with an asterisk are discussed below. Firstly, using the best fit values of $\sin^2\theta_{12}$ and $\sin^2\theta_{13}$, we get a physical value of $\cos\delta$ in case C3 for the minimal value of $\sin^2\theta_{23} = 0.562$, for which $\cos\delta = -0.996$. For C8 with $\sin^2\theta^\circ_{23} = 1/2$ and 3/4, using the best fit values of the neutrino mixing angles for the NO spectrum, we have $\cos\delta = -1.53$ and 2.04, respectively. The physical values of $\cos\delta$ can be obtained, using, e.g., the values of $\sin^2\theta_{23} = 0.380$ and 0.543, for which $\cos\delta = -0.995$ and 0.997, respectively. In the parts of the 3σ allowed range of $\sin^2\theta_{23}$, $0.374 \leq \sin^2\theta_{23} \leq 0.380$ and $0.543 \leq \sin^2\theta_{23} \leq 0.641$, we have $-0.938 \geq \cos\delta \geq -0.995$ and $0.997 \geq \cos\delta \geq 0.045$, respectively. Secondly, in case B1 we obtain $\cos\delta = -0.990$ employing the best fit value of $\sin^2\theta_{13}$ and the maximal value of $\sin^2\theta_{23} = 0.419$. Finally, utilising the best fit value of $\sin^2\theta_{13}$, we get physical values of $\cos\delta$ in cases A1 and A2 for the minimal value of $\sin^2\theta_{12} = 0.348$, for which $\cos\delta = -0.993$ and 0.993, respectively. Note that for the cases in which $\sin^2\theta_{23}$ is fixed, the predicted values are within the corresponding 2σ range, while in the cases in which $\sin^2\theta_{12}$ is fixed, the values of $\sin^2\theta_{12} = 0.341$ and 0.317 are within 2σ and 1σ, respectively. The value of $\sin^2\theta_{12} = 0.256$ lies slightly outside the 3σ allowed range quoted in eq. (2.15).

For the symmetry group A_5, we find that the residual symmetries

- $(G_e, G_\nu) = (Z_2, Z_2)$ in cases C2, C6 and C7;
- $(G_e, G_\nu) = (Z_3, Z_2)$ in cases B2 and B3;

Table 2.11. The phenomenologically viable cases for the symmetry group A_5. The predicted values of $\cos\delta$ and $\sin^2\theta_{12}$ or $\sin^2\theta_{23}$ have been obtained using the best fit values of the other standard mixing angles for the NO spectrum quoted in eqs. (2.15)–(2.17). In the cases marked with an asterisk, physical values of $\cos\delta$ cannot be obtained employing the best fit values of the mixing angles, but are possible for values of the relevant neutrino mixing parameters lying in their respective 3σ allowed intervals. See text for further details.

(G_e, G_ν)	Case	$\sin^2\theta_{ij}^\circ$	$\cos\delta$	$\sin^2\theta_{ij}$
(Z_2, Z_2)	C1	$\sin^2\theta_{23}^\circ = 1/4$	-0.806	not fixed
	C3	$\sin^2\theta_{13}^\circ = 0.0955,\ 1/4$	$0.688,\ -1^*$	not fixed
	C4	$\sin^2\theta_{12}^\circ = 0.0955,\ 1/4$	$-1^*,\ 0.992$	not fixed
	C5	$\sin^2\theta_{12}^\circ = 1/4$	not fixed	$\sin^2\theta_{12} = 0.256$
	C8	$\sin^2\theta_{23}^\circ = 3/4$	1^*	not fixed
	C9	$\sin^2\theta_{12}^\circ = 0.3455$	not fixed	$\sin^2\theta_{12} = 0.330$
(Z_3, Z_2)	B1	$(\sin^2\theta_{12}^\circ, \sin^2\theta_{23}^\circ) = (1/3, 1/2)$	0.570	$\sin^2\theta_{12} = 0.341$
(Z_5, Z_2)	B1	$(\sin^2\theta_{12}^\circ, \sin^2\theta_{23}^\circ) = (0.2764, 1/2)$	0.655	$\sin^2\theta_{12} = 0.283$
	B2	$(\sin^2\theta_{12}^\circ, \sin^2\theta_{13}^\circ) = (0.1382, 0.1604)$	-0.229	$\sin^2\theta_{12} = 0.259$
$(Z_2 \times Z_2, Z_2)$	B2	$(\sin^2\theta_{12}^\circ, \sin^2\theta_{13}^\circ) = \begin{cases} (0.0955, 0.2764) \\ (1/4, 0.1273) \end{cases}$	$\begin{matrix} -1^* \\ 0.805 \end{matrix}$	$\sin^2\theta_{12} = 0.330$
(Z_2, Z_3)	A1	$(\sin^2\theta_{13}^\circ, \sin^2\theta_{23}^\circ) = (0.2259, 0.4363)$	0.716	$\sin^2\theta_{23} = 0.553$
	A2	$(\sin^2\theta_{12}^\circ, \sin^2\theta_{23}^\circ) = (0.2259, 0.4363)$	-0.716	$\sin^2\theta_{23} = 0.447$
(Z_2, Z_5)	A1	$(\sin^2\theta_{13}^\circ, \sin^2\theta_{23}^\circ) = (0.4331, 0.3618)$	-1^*	$\sin^2\theta_{23} = 0.630$
	A2	$(\sin^2\theta_{12}^\circ, \sin^2\theta_{23}^\circ) = (0.4331, 0.3618)$	1^*	$\sin^2\theta_{23} = 0.370$

- $(G_e, G_\nu) = (Z_5, Z_2)$ in case B3;
- $(G_e, G_\nu) = (Z_2 \times Z_2, Z_2)$ in cases B1 and B3;
- $(G_e, G_\nu) = (Z_2, Z_3)$ or (Z_2, Z_5) in case A3;
- $(G_e, G_\nu) = (Z_2, Z_2 \times Z_2)$ in cases A1, A2 and A3

do not provide phenomenologically viable results for $\cos\delta$ and/or for the standard mixing angles θ_{12}, θ_{13} and θ_{23}.

We will describe next the cases in Table 2.11 marked with an asterisk, apart from those which have also been found for $G_f = S_4$ and discussed earlier. Using the best fit values of $\sin^2\theta_{12}$ and $\sin^2\theta_{13}$, we get a physical value of $\cos\delta$ in case C4 for the minimal value of $\sin^2\theta_{23} = 0.487$, for which $\cos\delta = -0.997$. Instead using the best fit values of $\sin^2\theta_{13}$ and $\sin^2\theta_{23}$ one gets the physical values of $\cos\delta = -1$ for the maximal value of $\sin^2\theta_{12} = 0.277$. Employing the best fit value of $\sin^2\theta_{13}$, we find a physical value of $\cos\delta$ in case B2 with residual symmetries $(G_e, G_\nu) = (Z_2 \times Z_2, Z_2)$ for the minimal value of $\sin^2\theta_{23} = 0.518$, for which $\cos\delta = -0.996$. Similarly for cases A1 and A2 with residual symmetries $(G_e, G_\nu) = (Z_2, Z_5)$, the values of $\cos\delta = -0.992$ and 0.992 are obtained using the minimal value of $\sin^2\theta_{12} = 0.321$.

The values of $\sin^2\theta_{ij}^\circ$ in Table 2.11 used to compute $\cos\delta$ and $\sin^2\theta_{ij}$ are the following ones: $1/(4r^2) \approx 0.0955$, $(3-r)/4 \approx 0.3455$, $1/(2+r) \approx 0.2764$, $1/(4+2r) \approx 0.1382$,

$1/(3+2r) \approx 0.1604$, $1/(3+3r) \approx 0.1273$, $2/(4r^2-r) \approx 0.2259$, $r/(6r-6) \approx 0.4363$, $(6r-4)/(10r-3) \approx 0.4331$, $(1-r)/(8-6r) \approx 0.3618$.

2.9 Conclusions

In this chapter, we have employed the discrete symmetry approach to understanding the observed pattern of 3-neutrino mixing and, within this approach, have derived sum rules and predictions for the Dirac phase δ present in the PMNS neutrino mixing matrix U. The approach is based on the assumption of the existence at some energy scale of a (lepton) flavour symmetry corresponding to a non-Abelian discrete group G_f. The flavour symmetry group G_f can be broken, in general, to different residual symmetry subgroups G_e and G_ν of the charged lepton and neutrino mass terms, respectively. Given G_f, typically there are more than one (but still a finite number of) possible residual symmetries G_e and G_ν. The residual symmetries can constrain the forms of the 3×3 unitary matrices U_e and U_ν, which diagonalise the charged lepton and neutrino mass matrices, and the product of which represents the PMNS neutrino mixing matrix U, $U = U_e^\dagger U_\nu$. Thus, by constraining the form of the matrices U_e and U_ν, the residual symmetries constrain also the form of the PMNS matrix U. This can lead, in particular, to a correlation between the values of the PMNS neutrino mixing angles θ_{12}, θ_{13} and θ_{23}, which have been determined experimentally with a rather good precision, and the value of the cosine of the Dirac CPV phase δ present in U, i.e., to a sum rule for $\cos\delta$. The sum rule for $\cos\delta$ thus obtained depends on residual symmetries G_e and G_ν and in some cases can involve, in addition to θ_{12}, θ_{13} and θ_{23}, parameters which cannot be constrained even when G_f is fixed. For a given fixed G_f, unambiguous predictions for the value of $\cos\delta$ can be derived in the cases when, apart from the parameters determined by G_f (and G_e and G_ν), only θ_{12}, θ_{13} and θ_{23} enter into the expression for the respective sum rule.

We have derived sum rules for $\cos\delta$ considering the following discrete residual symmetries:

(A) $G_e = Z_2$ and $G_\nu = Z_n$, $n > 2$ or $Z_n \times Z_m$, $n, m \geq 2$ (Section 2.2);

(B) $G_e = Z_n$, $n > 2$ or $Z_n \times Z_m$, $n, m \geq 2$ and $G_\nu = Z_2$ (Section 2.3);

(C) $G_e = Z_2$ and $G_\nu = Z_2$ (Section 2.4);

(D) G_e is fully broken and $G_\nu = Z_n$, $n > 2$ or $Z_n \times Z_m$, $n, m \geq 2$ (Section 2.6);

(E) $G_e = Z_n$, $n > 2$ or $Z_n \times Z_m$, $n, m \geq 2$ and G_ν is fully broken (Section 2.7).

The sum rules are summarised in Tables 2.3, 2.4, 2.7 and 2.8. For given G_e and G_ν, the sum rules for $\cos\delta$ we have derived are exact, within the approach employed, and are valid, in particular, for any G_f containing G_e and G_ν as subgroups. We have identified the cases when the value of $\cos\delta$ cannot be determined, or cannot be uniquely determined, from the sum rule without making additional assumptions on unconstrained parameters (cases A3 in Section 2.2 and B3 in Section 2.3 (see also Table 2.3); cases C2, C5, C6, C7 and C9 in Section 2.4 (see also Table 2.4); the cases discussed in Sections 2.6 and 2.7). In the majority of the phenomenologically viable cases we have considered, the value of $\cos\delta$ can be unambiguously predicted once the flavour symmetry G_f is fixed. In certain cases of fixed G_f, G_e and G_ν, correlations between the values of some of the measured neutrino mixing parameters $\sin^2\theta_{12}$, $\sin^2\theta_{13}$ and $\sin^2\theta_{23}$, are predicted, and/or the values of some

of these parameters, typically of $\sin^2\theta_{12}$ or $\sin^2\theta_{23}$, are fixed. These correlations and predictions are summarised in Tables 2.5 and 2.6. We have found that a relatively large number of these cases are not phenomenologically viable, i.e., they lead to results which are not compatible with the existing data on neutrino mixing. We have derived predictions for $\cos\delta$ for the flavour symmetry groups $G_f = A_4$, T', S_4 and A_5 using the best fit values of $\sin^2\theta_{12}$, $\sin^2\theta_{13}$ and $\sin^2\theta_{23}$, when $\cos\delta$ is unambiguously determined by the corresponding sum rule. We have presented the predictions for $\cos\delta$ only in the phenomenologically viable cases, i.e., when the measured values of the 3-neutrino mixing parameters $\sin^2\theta_{12}$, $\sin^2\theta_{13}$ and $\sin^2\theta_{23}$, taking into account their respective 3σ uncertainties, are successfully reproduced. These predictions, together with the predictions for the value of one of the mixing parameters $\sin^2\theta_{12}$ and $\sin^2\theta_{23}$, in the cases when it is fixed by the symmetries, are summarised in Tables 2.9–2.11.

The results derived in this chapter show, in particular, that with the accumulation of more precise data on the PMNS neutrino mixing parameters $\sin^2\theta_{12}$, $\sin^2\theta_{13}$ and $\sin^2\theta_{23}$, and with the measurement of the Dirac phase δ present in the neutrino mixing matrix U, it will be possible to critically test the predictions of the current phenomenologically viable theories, models and schemes of neutrino mixing based on different non-Abelian discrete (lepton) flavour symmetries G_f and sets of their non-trivial subgroups of residual symmetries G_e and G_ν, operative respectively in the charged lepton and neutrino sectors, and thus, critically test the discrete symmetry approach to understanding the observed pattern of neutrino mixing.

Chapter 3

Phenomenology of sum rules for the Dirac phase

In this chapter, we will be driven by the idea that the main contribution to the PMNS matrix U comes from the neutrino sector, i.e., from the matrix U_ν diagonalising the neutrino mass matrix. In terms of the breaking patterns explored in Chapter 2, we take a closer look at pattern D, which is characterised by fully broken flavour symmetry in the charged lepton sector and a residual symmetry $G_\nu = Z_n$, $n > 2$ or $Z_n \times Z_m$, $n, m \geq 2$ preserved in the neutrino sector. In this case, as we have seen in the preceding chapter, the residual symmetry G_ν determines completely the form of the matrix U_ν (up to re-phasing of columns and their permutations), while the matrix U_e remains, in general, unconstrained. Assuming U_ν to have one of the symmetry forms introduced in Section 1.2, i.e., BM, TBM, GRA, GRB or HG, we explore in a systematic way possible *charged lepton corrections*, i.e., various forms of the matrix U_e diagonalising $M_e M_e^\dagger$, which can reconstitute compatibility of the symmetry forms in question with the experimental data. We consider only those forms of U_e which allow one to express δ as a function of the three neutrino mixing angles present in the PMNS matrix U and the fixed angles contained in U_ν.

3.1 Framework

In what follows we will exploit the fact that in the general case the PMNS mixing matrix U has the following form [151] (see also Appendix C):

$$U = U_e^\dagger \, U_\nu = \tilde{U}_e^\dagger \, \Psi \, \tilde{U}_\nu \, Q_0 \,, \tag{3.1}$$

where $\tilde{U}_e$ and $\tilde{U}_\nu$ are CKM-like 3×3 unitary matrices, and Ψ and Q_0 are diagonal phase matrices each containing in general two phases:

$$\Psi = \text{diag}\left(1, e^{-i\psi}, e^{-i\omega}\right) \,, \quad Q_0 = \text{diag}\left(1, e^{i\frac{\xi_{21}}{2}}, e^{i\frac{\xi_{31}}{2}}\right) \,. \tag{3.2}$$

Note that the matrix Q_0 is exactly the same defined in eq. (2.7), and the phases ξ_{21} and ξ_{31} contribute to the Majorana phases in the PMNS matrix. We will further assume that, up to subleading perturbative corrections (and phase matrices), the PMNS matrix U has a specific known form $\tilde{U}_\nu$ that is dictated by continuous and/or discrete symmetries, or by arguments related to symmetries. As we have already pointed out in Section 1.2, this assumption seems very natural in view of the observation that the measured values of the three neutrino mixing angles differ from certain possible symmetry values by subdominant corrections.

In particular, we will consider the widely discussed TBM, BM, GRA, GRB and HG forms of $\tilde{U}_\nu$, defined in eqs. (1.33), (1.35), (1.36), (1.37) and (1.38), respectively. For all

these forms the matrix $\tilde{U}_\nu$ represents a product of two orthogonal matrices describing rotations in the 1-2 and 2-3 planes on fixed angles θ^ν_{12} and θ^ν_{23}:

$$\tilde{U}_\nu = R_{23}(\theta^\nu_{23})\, R_{12}(\theta^\nu_{12})\,, \tag{3.3}$$

where

$$R_{12}\,(\theta^\nu_{12}) = \begin{pmatrix} \cos\theta^\nu_{12} & \sin\theta^\nu_{12} & 0 \\ -\sin\theta^\nu_{12} & \cos\theta^\nu_{12} & 0 \\ 0 & 0 & 1 \end{pmatrix}\,, \quad R_{23}\,(\theta^\nu_{23}) = \begin{pmatrix} 1 & 0 & 0 \\ 0 & \cos\theta^\nu_{23} & \sin\theta^\nu_{23} \\ 0 & -\sin\theta^\nu_{23} & \cos\theta^\nu_{23} \end{pmatrix}\,. \tag{3.4}$$

Thus, in such a parametrisation, $\tilde{U}_\nu$ does not include a rotation in the 1-3 plane, i.e., $\theta^\nu_{13} = 0$. Moreover, for all the symmetry forms quoted above one has also $\theta^\nu_{23} = -\pi/4$. As we have already seen in subsection 2.6.5, the forms differ by the value of the angle θ^ν_{12}, and, correspondingly, of $\sin^2\theta^\nu_{12}$. Namely, $\sin^2\theta^\nu_{12} = 1/3$ (TBM), $\sin^2\theta^\nu_{12} = 1/2$ (BM), $\sin^2\theta^\nu_{12} = (2+r)^{-1} \approx 0.276$ (GRA), r being the golden ratio, $r = (1+\sqrt{5})/2$, $\sin^2\theta^\nu_{12} = (3-r)/4 \approx 0.345$ (GRB), and $\sin^2\theta^\nu_{12} = 1/4$ (HG).

As is clear from the preceding discussion, the values of the angles in the matrix $\tilde{U}_\nu$, which are fixed by symmetry arguments, typically differ from the values determined experimentally by relatively small perturbative corrections. In the approach we are following, the requisite corrections are provided by the angles in the matrix $\tilde{U}_e$. The matrix $\tilde{U}_e$ in the general case depends on three angles and one phase [151]. However, in a class of theories of (lepton) flavour and neutrino mass generation, based on a GUT and/or a discrete symmetry (see, e.g., [122, 145–149]), $\tilde{U}_e$ is an orthogonal matrix which describes one rotation in the 1-2 plane,

$$\tilde{U}_e = R^{-1}_{12}(\theta^e_{12})\,, \tag{3.5}$$

or two rotations in the planes 1-2 and 2-3,

$$\tilde{U}_e = R^{-1}_{23}(\theta^e_{23})\, R^{-1}_{12}(\theta^e_{12})\,, \tag{3.6}$$

θ^e_{12} and θ^e_{23} being the corresponding rotation angles. Other possibilities include $\tilde{U}_e$ being an orthogonal matrix which describes (i) one rotation in the 1-3 plane,[18]

$$\tilde{U}_e = R^{-1}_{13}(\theta^e_{13})\,, \tag{3.7}$$

or (ii) two rotations in any other two of the three planes, e.g.,[19]

$$\tilde{U}_e = R^{-1}_{23}(\theta^e_{23})\, R^{-1}_{13}(\theta^e_{13})\,, \quad \text{or} \tag{3.8}$$

$$\tilde{U}_e = R^{-1}_{13}(\theta^e_{13})\, R^{-1}_{12}(\theta^e_{12})\,. \tag{3.9}$$

The use of the inverse matrices in eqs. (3.5)–(3.9) is a matter of convenience — this allows us to lighten the notations in expressions which will appear further in the text.

It was shown in [99] (see also [102]) that for $\tilde{U}_\nu$ and $\tilde{U}_e$ given in eqs. (3.3) and (3.6), the Dirac phase δ present in the PMNS matrix satisfies a sum rule by which it is expressed in

[18] The case of $\tilde{U}_e$ representing a rotation in the 2-3 plane is ruled out for the five symmetry forms of $\tilde{U}_\nu$ listed above, since in this case a realistic value of $\theta_{13} \neq 0$ cannot be generated.

[19] We consider only "standard" ordering of the two rotations in $\tilde{U}_e$ (see [102]).

terms of the three neutrino mixing angles measured in the neutrino oscillation experiments and the angle θ_{12}^{ν}. This sum rule reads [99]

$$\cos\delta = \frac{\tan\theta_{23}}{\sin 2\theta_{12}\sin\theta_{13}}\left[\cos 2\theta_{12}^{\nu} + \left(\sin^2\theta_{12} - \cos^2\theta_{12}^{\nu}\right)\left(1 - \cot^2\theta_{23}\,\sin^2\theta_{13}\right)\right]. \quad (3.10)$$

For the specific values of $\theta_{12}^{\nu} = \pi/4$ and $\theta_{12}^{\nu} = \sin^{-1}(1/\sqrt{3})$, i.e., for the BM (LC) and TBM forms of $\tilde{U}_{\nu}$, eq. (3.10) reduces to the expressions for $\cos\delta$ derived first in [102]. As we have pointed out in subsection 2.6.3, this sum rule is a particular case of the one in eq. (2.137). Within the approach employed, the expression for $\cos\delta$ given in eq. (3.10) is exact. In [99] the correction to the sum rule in eq. (3.10) due to a non-zero angle $\theta_{13}^{e} \ll 1$ in $\tilde{U}_{e}$, corresponding to

$$\tilde{U}_{e} = R_{23}^{-1}(\theta_{23}^{e})\,R_{13}^{-1}(\theta_{13}^{e})\,R_{12}^{-1}(\theta_{12}^{e}) \quad (3.11)$$

with $|\sin\theta_{13}^{e}| \ll 1$, was also derived.

In the present chapter, we derive new sum rules for $\cos\delta$ using the general approach employed, in particular, in [99]. We perform a systematic study of the forms of the matrices $\tilde{U}_{e}$ and $\tilde{U}_{\nu}$, for which it is possible to derive sum rules for $\cos\delta$ of the type of eq. (3.10), but for which the sum rules of interest do not exist in the literature. More specifically, we consider the following forms of $\tilde{U}_{e}$ and $\tilde{U}_{\nu}$:

- $\tilde{U}_{\nu} = R_{23}(\theta_{23}^{\nu})R_{12}(\theta_{12}^{\nu})$ with fixed θ_{23}^{ν} and θ_{12}^{ν}, and[20]
  (A1) $\tilde{U}_{e} = R_{12}^{-1}(\theta_{12}^{e})$,
  (A2) $\tilde{U}_{e} = R_{13}^{-1}(\theta_{13}^{e})$,
  (B2) $\tilde{U}_{e} = R_{23}^{-1}(\theta_{23}^{e})\,R_{13}^{-1}(\theta_{13}^{e})$,
  (B3) $\tilde{U}_{e} = R_{13}^{-1}(\theta_{13}^{e})\,R_{12}^{-1}(\theta_{12}^{e})$;
- $\tilde{U}_{\nu} = R_{23}(\theta_{23}^{\nu})\,R_{13}(\theta_{13}^{\nu})\,R_{12}(\theta_{12}^{\nu})$ with fixed θ_{23}^{ν}, θ_{13}^{ν} and θ_{12}^{ν}, and
  (C1) $\tilde{U}_{e} = R_{12}^{-1}(\theta_{12}^{e})$,
  (C2) $\tilde{U}_{e} = R_{13}^{-1}(\theta_{13}^{e})$.

In each of these cases, we obtain the respective sum rule for $\cos\delta$ for arbitrary fixed values of all angles contained in the matrix $\tilde{U}_{\nu}$. Next we derive predictions for $\cos\delta$ and the rephasing invariant $J_{\rm CP}$ defined in eq. (1.6), performing a statistical analysis using the current (the prospective) uncertainties in the determination of the neutrino mixing parameters $\sin^2\theta_{12}$, $\sin^2\theta_{13}$, $\sin^2\theta_{23}$ and δ ($\sin^2\theta_{12}$, $\sin^2\theta_{13}$ and $\sin^2\theta_{23}$).

The remainder of the present chapter is organised as follows. In Section 3.2, we consider cases A1 and A2. In these cases, the PMNS matrix contains one rotation from the charged lepton sector and two rotations from the neutrino sector and reads

$$U = R_{ij}(\theta_{ij}^{e})\,\Psi\,R_{23}(\theta_{23}^{\nu})\,R_{12}(\theta_{12}^{\nu})\,Q_{0}\,, \quad (3.12)$$

with $(ij) = (12)$, (13). In Section 3.3, we analyse cases B2 and B3 in which the PMNS matrix contains two rotations from the charged lepton sector and two rotations from the neutrino sector, i.e.,

$$U = R_{ij}(\theta_{ij}^{e})\,R_{kl}(\theta_{kl}^{e})\,\Psi\,R_{23}(\theta_{23}^{\nu})\,R_{12}(\theta_{12}^{\nu})\,Q_{0}\,, \quad (3.13)$$

[20] Case B1, i.e., that with $\tilde{U}_{e} = R_{23}^{-1}(\theta_{23}^{e})\,R_{12}^{-1}(\theta_{12}^{e})$, has been studied in detail in refs. [99, 102].

with $(ij) - (kl) = (13) - (23), (12) - (13)$. Further, in Section 3.4, we generalise the schemes considered in Section 3.2 by allowing also a third rotation matrix to be present in $\tilde{U}_\nu$:

$$U = R_{ij}(\theta^e_{ij})\, \Psi\, R_{23}(\theta^\nu_{23})\, R_{13}(\theta^\nu_{13})\, R_{12}(\theta^\nu_{12})\, Q_0\,, \tag{3.14}$$

with $(ij) = (12)$ in case C1, and $(ij) = (13)$ in case C2. In Section 3.5, we provide a summary of the sum rules derived in Sections 3.2–3.4. Using the sum rules for $\cos\delta$, in Section 3.6, we obtain numerical predictions for $\cos\delta$, δ and $J_{\rm CP}$ in each case for certain values of the angles θ^ν_{ij} fixed by (arguments associated with) flavour symmetries. In Section 3.7, we perform a statistical analysis of these predictions. Section 3.8 contains summary of the results obtained in the present chapter and conclusions.

3.2 Mixing schemes with $\tilde{U}^\dagger_e = R_{ij}(\theta^e_{ij})$ and $\tilde{U}_\nu = R_{23}(\theta^\nu_{23})\, R_{12}(\theta^\nu_{12})$

In this section, we derive the sum rules for $\cos\delta$ of interest in the case when the matrix $\tilde{U}_\nu = R_{23}(\theta^\nu_{23})\, R_{12}(\theta^\nu_{12})$ with fixed (e.g., symmetry) values of the angles θ^ν_{23} and θ^ν_{12}, gets correction only due to one rotation from the charged lepton sector. The neutrino mixing matrix U has the form given in eq. (3.12). We do not consider the cases of eq. (3.12) (i) with $(ij) = (23)$, because the reactor angle θ_{13} does not get corrected and remains zero, and (ii) with $(ij) = (12)$ and $\theta^\nu_{23} = -\pi/4$, which has been already analysed in detail in [99].

3.2.1 Case A1: θ^e_{12}

For $\theta^\nu_{23} = -\pi/4$ the sum rule for $\cos\delta$ in this case was derived in ref. [99] and is given in eq. (50) therein. Here we consider the case of an arbitrary fixed value of the angle θ^ν_{23}. Using eq. (3.12) with $(ij) = (12)$, one finds the following expressions for the mixing angles θ_{13} and θ_{23} of the standard parametrisation of the PMNS matrix:

$$\sin^2\theta_{13} = |U_{e3}|^2 = \sin^2\theta^e_{12}\sin^2\theta^\nu_{23}\,, \tag{3.15}$$

$$\sin^2\theta_{23} = \frac{|U_{\mu 3}|^2}{1-|U_{e3}|^2} = \frac{\sin^2\theta^\nu_{23} - \sin^2\theta_{13}}{1-\sin^2\theta_{13}}\,. \tag{3.16}$$

Although eq. (3.10) was derived in [99] for $\theta^\nu_{23} = -\pi/4$ and $\tilde{U}_e = R^{-1}_{23}(\theta^e_{23})R^{-1}_{12}(\theta^e_{12})$, it is not difficult to convince oneself that it holds also in the case under discussion for an arbitrary fixed value of θ^ν_{23}. The sum rule for $\cos\delta$ of interest, expressed in terms of the angles θ_{12}, θ_{13}, θ^ν_{12} and θ^ν_{23}, can be obtained from eq. (3.10) by using the expression for $\sin^2\theta_{23}$ given in eq. (3.16). The result reads

$$\begin{aligned}\cos\delta = \frac{(\cos 2\theta_{13} - \cos 2\theta^\nu_{23})^{\frac{1}{2}}}{\sqrt{2}\sin 2\theta_{12}\sin\theta_{13}|\cos\theta^\nu_{23}|}\Bigg[&\cos 2\theta^\nu_{12} \\ &+ \left(\sin^2\theta_{12} - \cos^2\theta^\nu_{12}\right)\frac{2\sin^2\theta^\nu_{23} - (3+\cos 2\theta^\nu_{23})\sin^2\theta_{13}}{\cos 2\theta_{13} - \cos 2\theta^\nu_{23}}\Bigg]\,.\end{aligned} \tag{3.17}$$

Setting $\theta^\nu_{23} = -\pi/4$ in eq. (3.17), one reproduces the sum rule given in eq. (50) in ref. [99].

3.2.2 Case A2: θ_{13}^e

In the present subsection, we consider the parametrisation of the neutrino mixing matrix given in eq. (3.12) with $(ij) = (13)$. In this set-up, the phase ψ in the matrix Ψ is unphysical (it can be absorbed in the μ field) and therefore, effectively, $\Psi = \mathrm{diag}\,(1, 1, e^{-i\omega})$. Using eq. (3.12) with $(ij) = (13)$ and $\theta_{23}^\nu = -\pi/4$ first and the standard parametrisation of U, we get:

$$\sin^2\theta_{13} = |U_{e3}|^2 = \frac{1}{2}\sin^2\theta_{13}^e\,, \tag{3.18}$$

$$\sin^2\theta_{23} = \frac{|U_{\mu 3}|^2}{1-|U_{e3}|^2} = \frac{1}{2\,(1-\sin^2\theta_{13})}\,, \tag{3.19}$$

$$\sin^2\theta_{12} = \frac{|U_{e2}|^2}{1-|U_{e3}|^2} = \frac{1}{1-\sin^2\theta_{13}}\left[\frac{1}{2}\sin^2\theta_{13}^e\cos^2\theta_{12}^\nu + \cos^2\theta_{13}^e\sin^2\theta_{12}^\nu + \frac{1}{\sqrt{2}}\sin 2\theta_{13}^e\cos\omega\sin\theta_{12}^\nu\cos\theta_{12}^\nu\right]. \tag{3.20}$$

From eqs. (3.18) and (3.20) we obtain an expression for $\cos\omega$ in terms of the measured mixing angles θ_{12}, θ_{13} and the known θ_{12}^ν:[21]

$$\cos\omega = \frac{1-\sin^2\theta_{13}}{\sin 2\theta_{12}^\nu\sin\theta_{13}(1-2\sin^2\theta_{13})^{\frac{1}{2}}}\left[\sin^2\theta_{12} - \sin^2\theta_{12}^\nu - \cos 2\theta_{12}^\nu\frac{\sin^2\theta_{13}}{1-\sin^2\theta_{13}}\right]. \tag{3.21}$$

Further, one can find a relation between $\sin\delta$ ($\cos\delta$) and $\sin\omega$ ($\cos\omega$) by comparing the imaginary (real) part of the combination $U_{e1}^* U_{\mu 3}^* U_{e3} U_{\mu 1}$, written by using eq. (3.12) with $(ij) = (13)$ and in the standard parametrisation of U. For the relation between $\sin\delta$ and $\sin\omega$ we get

$$\sin\delta = -\frac{\sin 2\theta_{12}^\nu}{\sin 2\theta_{12}}\sin\omega\,. \tag{3.22}$$

The sum rule for $\cos\delta$ of interest can be derived by substituting $\cos\omega$ from eq. (3.21) in the relation between $\cos\delta$ and $\cos\omega$ (which is not difficult to derive and we do not present it here).[22] We obtain

$$\cos\delta = -\frac{(1-2\sin^2\theta_{13})^{\frac{1}{2}}}{\sin 2\theta_{12}\sin\theta_{13}}\left[\cos 2\theta_{12}^\nu + (\sin^2\theta_{12} - \cos^2\theta_{12}^\nu)\frac{1-3\sin^2\theta_{13}}{1-2\sin^2\theta_{13}}\right]. \tag{3.23}$$

We note that the expression for $\cos\delta$ thus found differs only by an overall minus sign from the analogous expression for $\cos\delta$ derived in [99] in case A1 (see eq. (50) in [99]).

In eq. (1.7) we have given the expression for the rephasing invariant $J_{\rm CP}$ in the standard parametrisation of the PMNS matrix. Below and in the next sections we give for completeness also the expressions of the $J_{\rm CP}$ factor in terms of the independent parameters of the set-up considered. In terms of the parameters ω, θ_{13}^e and θ_{12}^ν of the set-up discussed in the present subsection, $J_{\rm CP}$ is given by

$$J_{\rm CP} = -\frac{1}{8\sqrt{2}}\sin\omega\sin 2\theta_{13}^e\sin 2\theta_{12}^\nu\,. \tag{3.24}$$

[21] We note that the expression for $\cos\omega$ we have obtained coincides with that for $\cos\phi$ in case A1 found in [99] (cf. eq. (46) therein).

[22] We would like to notice that this method of deriving sum rules for $\cos\delta$ is alternative to the method employed by us in Chapter 2. The method we use in this subsection has been successfully applied in ref. [99].

In the case of an arbitrary fixed value of the angle θ_{23}^{ν} the expressions for the mixing angles θ_{13} and θ_{23} take the following form:

$$\sin^2\theta_{13} = |U_{e3}|^2 = \sin^2\theta_{13}^{e}\cos^2\theta_{23}^{\nu}\,, \tag{3.25}$$

$$\sin^2\theta_{23} = \frac{|U_{\mu 3}|^2}{1-|U_{e3}|^2} = \frac{\sin^2\theta_{23}^{\nu}}{1-\sin^2\theta_{13}}\,. \tag{3.26}$$

The sum rule for $\cos\delta$ in this case can be obtained with a simpler procedure we made use of in Chapter 2, namely, by equating the expressions for the absolute value of the element $U_{\mu 1}$ of the PMNS matrix in the two parametrisations employed in the present subsection:

$$|U_{\mu 1}| = |\cos\theta_{23}\sin\theta_{12} + e^{i\delta}\cos\theta_{12}\sin\theta_{13}\sin\theta_{23}| = |\cos\theta_{23}^{\nu}\sin\theta_{12}^{\nu}|\,, \tag{3.27}$$

From eq. (3.27) we get

$$\begin{aligned}\cos\delta = -\frac{(\cos 2\theta_{13}+\cos 2\theta_{23}^{\nu})^{\frac{1}{2}}}{\sqrt{2}\sin 2\theta_{12}\sin\theta_{13}|\sin\theta_{23}^{\nu}|}\Bigg[\cos 2\theta_{12}^{\nu} \\ + \left(\sin^2\theta_{12}-\cos^2\theta_{12}^{\nu}\right)\frac{2\cos^2\theta_{23}^{\nu}-(3-\cos 2\theta_{23}^{\nu})\sin^2\theta_{13}}{\cos 2\theta_{13}+\cos 2\theta_{23}^{\nu}}\Bigg]\,.\end{aligned} \tag{3.28}$$

We will use the sum rules for $\cos\delta$ derived in the present and the next two sections to obtain predictions for $\cos\delta$, δ and for the $J_{\rm CP}$ factor in Section 3.6.

3.3 Mixing schemes with $\tilde{U}_e^{\dagger} = R_{ij}(\theta_{ij}^{e})\,R_{kl}(\theta_{kl}^{e})$ and $\tilde{U}_{\nu} = R_{23}(\theta_{23}^{\nu})\,R_{12}(\theta_{12}^{\nu})$

As we have seen in the preceding Section, in the case of one rotation from the charged lepton sector and for $\theta_{23}^{\nu} = -\pi/4$, the mixing angle θ_{23} cannot deviate significantly from $\pi/4$ due to the smallness of the angle θ_{13}. If the matrix $\tilde{U}_{\nu}$ has one of the symmetry forms considered in this chapter, the matrix $\tilde{U}_e$ has to contain at least two rotations in order to be possible to reproduce the current best fit values of the neutrino mixing parameters, quoted in eqs. (2.15)–(2.17). This conclusion will remain valid if higher precision measurements of $\sin^2\theta_{23}$ confirm that θ_{23} deviates significantly from $\pi/4$. In what follows we investigate different combinations of two rotations from the charged lepton sector and derive a sum rule for $\cos\delta$ in each set-up. First, we briefly remind the results obtained in case B1 which has been thoroughly analysed in refs. [99, 102].

3.3.1 Case B1: θ_{12}^{e} and θ_{23}^{e}

As we have already noted in subsection 3.2.1, the resulting sum rule for $\cos\delta$ in this case, which is given in eq. (3.10), has been derived first in [99] for $\theta_{23}^{\nu} = -\pi/4$. However, it holds for an arbitrary fixed value of θ_{23}^{ν}.

The $J_{\rm CP}$ factor in the parametrisation of the PMNS matrix corresponding to the case under consideration has the following form [102]:

$$J_{\rm CP} = -\frac{1}{8}\sin 2\theta_{12}^{e}\sin 2\theta_{12}^{\nu}\sin 2\hat{\theta}_{23}\sin\hat{\theta}_{23}\sin\phi\,, \tag{3.29}$$

where the angle $\hat{\theta}_{23}$ and the phase ϕ are defined in the next subsection in eqs. (3.32) and (3.35), respectively.

3.3.2 Case B2: θ^e_{13} and θ^e_{23}

Following the method used in ref. [102], the PMNS matrix U from eq. (3.13) with $(ij) - (kl) = (13) - (23)$, can be cast in the form

$$U = R_{13}(\theta^e_{13})\, P_1\, R_{23}(\hat{\theta}_{23})\, R_{12}(\theta^\nu_{12})\, \hat{Q}\,, \tag{3.30}$$

where the angle $\hat{\theta}_{23}$ is determined (i) for $\theta^\nu_{23} = -\pi/4$ by

$$\sin^2\hat{\theta}_{23} = \frac{1}{2}\left(1 - \sin 2\theta^e_{23}\cos(\omega - \psi)\right)\,, \tag{3.31}$$

and (ii) for an arbitrary fixed value of θ^ν_{23} by

$$\sin^2\hat{\theta}_{23} = \sin^2\theta^e_{23}\cos^2\theta^\nu_{23} + \cos^2\theta^e_{23}\sin^2\theta^\nu_{23} + \frac{1}{2}\sin 2\theta^e_{23}\sin 2\theta^\nu_{23}\cos(\omega - \psi)\,. \tag{3.32}$$

The phase matrices P_1 and $\hat{Q}$ have the following form:

$$P_1 = \mathrm{diag}(1, 1, e^{-i\alpha}), \quad \text{and} \quad \hat{Q} = Q_1\, Q_0\,, \quad \text{with} \quad Q_1 = \mathrm{diag}(1, 1, e^{i\beta})\,, \tag{3.33}$$

where the phases α and β are given by

$$\alpha = \gamma + \psi + \omega\,, \quad \text{with} \quad \gamma = \arg\left(e^{-i\psi}\cos\theta^e_{23}\sin\theta^\nu_{23} + e^{-i\omega}\sin\theta^e_{23}\cos\theta^\nu_{23}\right)\,, \tag{3.34}$$

$$\beta = \gamma - \phi\,, \quad \text{where} \quad \phi = \arg\left(e^{-i\psi}\cos\theta^e_{23}\cos\theta^\nu_{23} - e^{-i\omega}\sin\theta^e_{23}\sin\theta^\nu_{23}\right)\,. \tag{3.35}$$

Using eq. (3.30) and the standard parametrisation of U, we find:

$$\sin^2\theta_{13} = |U_{e3}|^2 = \sin^2\theta^e_{13}\cos^2\hat{\theta}_{23}\,, \tag{3.36}$$

$$\sin^2\theta_{23} = \frac{|U_{\mu 3}|^2}{1 - |U_{e3}|^2} = \frac{\sin^2\hat{\theta}_{23}}{1 - \sin^2\theta_{13}}\,, \tag{3.37}$$

$$\sin^2\theta_{12} = \frac{|U_{e2}|^2}{1 - |U_{e3}|^2} = \frac{1}{1 - \sin^2\theta_{13}}\Bigg[\cos^2\theta^e_{13}\sin^2\theta^\nu_{12} - \frac{1}{2}\sin\hat{\theta}_{23}\sin 2\theta^e_{13}\sin 2\theta^\nu_{12}\cos\alpha + \cos^2\theta^\nu_{12}\sin^2\theta^e_{13}\sin^2\hat{\theta}_{23}\Bigg]\,. \tag{3.38}$$

The first two equations allow one to express θ^e_{13} and $\hat{\theta}_{23}$ in terms of θ_{13} and θ_{23}. Equation (3.38) allows us to find $\cos\alpha$ as a function of the PMNS mixing angles θ_{12}, θ_{13}, θ_{23} and the angle θ^ν_{12}:

$$\cos\alpha = 2\,\frac{\sin^2\theta^\nu_{12}\cos^2\theta_{23} + \cos^2\theta^\nu_{12}\sin^2\theta_{23}\sin^2\theta_{13} - \sin^2\theta_{12}\left(1 - \sin^2\theta_{23}\cos^2\theta_{13}\right)}{\sin 2\theta^\nu_{12}\sin 2\theta_{23}\sin\theta_{13}}\,. \tag{3.39}$$

The relation[23] between $\sin\delta$ ($\cos\delta$) and $\sin\alpha$ ($\cos\alpha$) can be found by comparing the imaginary (real) part of the quantity $U^*_{e1}U^*_{\mu 3}U_{e3}U_{\mu 1}$, written using eq. (3.30) and using the standard parametrisation of U:

$$\sin\delta = \frac{\sin 2\theta^\nu_{12}}{\sin 2\theta_{12}}\sin\alpha\,, \tag{3.40}$$

[23] We note that the expression in eq. (3.39) for $\cos\alpha$ can be obtained formally from the r.h.s. of eq. (22) for $\cos\phi$ in [99] by substituting $\sin\theta_{23}$ with $\cos\theta_{23}$ and vice versa and by changing its overall sign.

$$\cos\delta = \frac{\sin 2\theta_{12}^{\nu}}{\sin 2\theta_{12}}\cos\alpha - \frac{\sin\theta_{13}}{\sin 2\theta_{12}}\tan\theta_{23}\left(\cos 2\theta_{12} + \cos 2\theta_{12}^{\nu}\right) . \tag{3.41}$$

The sum rule expression for $\cos\delta$ as a function of the mixing angles θ_{12}, θ_{13}, θ_{23} and θ_{12}^{ν}, with θ_{12}^{ν} having an arbitrary fixed value, reads

$$\cos\delta = -\frac{\cot\theta_{23}}{\sin 2\theta_{12}\sin\theta_{13}}\left[\cos 2\theta_{12}^{\nu} + \left(\sin^2\theta_{12} - \cos^2\theta_{12}^{\nu}\right)\left(1 - \tan^2\theta_{23}\,\sin^2\theta_{13}\right)\right] . \tag{3.42}$$

This sum rule for $\cos\delta$ can be obtained formally from the r.h.s. of eq. (3.10) by interchanging $\tan\theta_{23}$ and $\cot\theta_{23}$ and by multiplying it by -1. Thus, in the case of $\theta_{23} = \pi/4$, the predictions for $\cos\delta$ in the case under consideration will differ from those obtained using eq. (3.10) only by a sign. We would like to emphasise that, as the sum rule in eq. (3.10), the sum rule in eq. (3.42) is valid for any fixed value of θ_{23}^{ν}. Finally, we note that the sum rule in eq. (3.42) is a particular case of that in eq. (2.140) derived in subsection 2.6.4.

The $J_{\rm CP}$ factor has the following form in the parametrisation of the PMNS matrix employed in the present subsection:

$$J_{\rm CP} = \frac{1}{8}\sin 2\theta_{13}^{e}\sin 2\theta_{12}^{\nu}\sin 2\hat{\theta}_{23}\cos\hat{\theta}_{23}\sin\alpha\,. \tag{3.43}$$

3.3.3 Case B3: θ_{12}^{e} and θ_{13}^{e}

In this subsection, we consider the parametrisation of the matrix U defined in eq. (3.13) with $(ij)-(kl) = (12)-(13)$ under the assumption of vanishing ω, i.e., $\Psi = \mathrm{diag}(1, e^{-i\psi}, 1)$. In the case of non-fixed ω it is impossible to express $\cos\delta$ *only* in terms of the independent angles of the scheme. We will comment more on this case later.

Using the parametrisation given in eq. (3.13) with $\theta_{23}^{\nu} = -\pi/4$ and $\omega = 0$ and the standard one, we find:

$$\sin^2\theta_{13} = |U_{e3}|^2 = \frac{1}{2}\sin^2\theta_{12}^{e} + \frac{1}{2}\cos^2\theta_{12}^{e}\sin^2\theta_{13}^{e} - X_{\psi}\,, \tag{3.44}$$

$$\sin^2\theta_{23} = \frac{|U_{\mu 3}|^2}{1-|U_{e3}|^2} = \frac{1}{\cos^2\theta_{13}}\left[\frac{1}{2}\cos^2\theta_{12}^{e} + \frac{1}{2}\sin^2\theta_{12}^{e}\sin^2\theta_{13}^{e} + X_{\psi}\right] , \tag{3.45}$$

$$\sin^2\theta_{12} = \frac{|U_{e2}|^2}{1-|U_{e3}|^2} = \frac{\zeta\sin^2\theta_{12}^{e} + \xi}{1-\sin^2\theta_{13}}\,, \tag{3.46}$$

where

$$X_{\psi} = \frac{1}{2}\sin 2\theta_{12}^{e}\sin\theta_{13}^{e}\cos\psi\,, \tag{3.47}$$

$$\zeta = \cos^2\theta_{13}^{e}\cos 2\theta_{12}^{\nu} + \frac{1}{4\sqrt{2}}\sin 2\theta_{12}^{\nu}\cot\theta_{13}^{e}(3\cos 2\theta_{13}^{e} - 1)\,, \tag{3.48}$$

$$\xi = \cos^2\theta_{13}^{e}\sin^2\theta_{12}^{\nu} + \frac{1}{2}(\cos 2\theta_{13} - \cos 2\theta_{13}^{e})\cos^2\theta_{12}^{\nu} + \frac{1}{2\sqrt{2}}\sin 2\theta_{12}^{\nu}(3\cos\theta_{13}^{e}\sin\theta_{13}^{e} - 2\cot\theta_{13}^{e}\sin^2\theta_{13})\,. \tag{3.49}$$

The dependence on $\cos\psi$ in eq. (3.46) has been eliminated by solving eq. (3.44) for X_{ψ}. It follows from eqs. (3.44) and (3.45) that $\sin^2\theta_{13}^{e}$ is a function of the known mixing angles θ_{13} and θ_{23}:

$$\sin^2\theta_{13}^{e} = 1 - 2\cos^2\theta_{13}\cos^2\theta_{23}\,. \tag{3.50}$$

Inverting the formula for $\sin^2\theta_{12}$ allows us to find $\sin^2\theta_{12}^e$, which is given by

$$\sin^2\theta_{12}^e = \Big[4\left[\cos 2\theta_{12}^\nu(\cos 2\theta_{13}^e + \sin^2\theta_{13}) - \cos 2\theta_{12}\cos^2\theta_{13}\right]\tan\theta_{13}^e + \sqrt{2}\sin 2\theta_{12}^\nu \times (3\cos 2\theta_{13}^e - 2\cos 2\theta_{13} - 1)\Big]\Big[4\cos 2\theta_{12}^\nu \sin 2\theta_{13}^e + \sqrt{2}(3\cos 2\theta_{13}^e - 1)\sin 2\theta_{12}^\nu\Big]^{-1}. \tag{3.51}$$

Using eqs. (3.44) and (3.51), we can write $\cos\psi$ in terms of the standard parametrisation mixing angles and the known θ_{13}^e and θ_{12}^ν:

$$\cos\psi = \frac{\sin^2\theta_{12}^e + \cos^2\theta_{12}^e\sin^2\theta_{13}^e - 2\sin^2\theta_{13}}{\sin 2\theta_{12}^e \sin\theta_{13}^e}\,. \tag{3.52}$$

We find the relation between $\sin\delta$ and $\sin\psi$ by employing again the standard procedure of comparing the expressions of the $J_{\rm CP}$ factor in the two parametrisations — the standard one and that defined in eq. (3.13) (with $\theta_{23}^\nu = -\pi/4$ and $\omega = 0$):

$$\sin\delta = \frac{\sin 2\theta_{12}^e \sin\psi}{4\sin 2\theta_{12}\sin 2\theta_{13}\sin\theta_{23}}\left[2\sqrt{2}\sin 2\theta_{13}^e\cos 2\theta_{12}^\nu + (3\cos 2\theta_{13}^e - 1)\sin 2\theta_{12}^\nu\right], \tag{3.53}$$

where $\sin 2\theta_{12}^e$ ($\sin 2\theta_{13}^e$ and $\cos 2\theta_{13}^e$) can be expressed in terms of θ_{12}, θ_{13}, θ_{23} and θ_{12}^ν (θ_{13} and θ_{23}) using eq. (3.51) (eq. (3.50)).

We use a much simpler procedure to find $\cos\delta$. Namely, we compare the expressions for the absolute value of the element $U_{\tau 1}$ of the PMNS matrix in the standard parametrisation and in the symmetry related one, eq. (3.13) with $\theta_{23}^\nu = -\pi/4$ and $\omega = 0$, considered in the present subsection:

$$|U_{\tau 1}| = |\sin\theta_{23}\sin\theta_{12} - \sin\theta_{13}\cos\theta_{23}\cos\theta_{12}e^{i\delta}| = |\sin\theta_{13}^e\cos\theta_{12}^\nu + \frac{1}{\sqrt{2}}\cos\theta_{13}^e\sin\theta_{12}^\nu|\,. \tag{3.54}$$

From the above equation we get for $\cos\delta$:

$$\cos\delta = -\frac{2}{\sin 2\theta_{12}\sin 2\theta_{23}\sin\theta_{13}}\Big[\cos^2\theta_{23}\sin^2\theta_{12}\sin^2\theta_{13} + \cos^2\theta_{12}\sin^2\theta_{23} - \left(\sqrt{\cos^2\theta_{13}\cos^2\theta_{23}}\cos\theta_{12}^\nu - \kappa\sqrt{1 - 2\cos^2\theta_{13}\cos^2\theta_{23}}\sin\theta_{12}^\nu\right)^2\Big], \tag{3.55}$$

where $\kappa = 1$ if θ_{13}^e belongs to the first or third quadrant, and $\kappa = -1$ if θ_{13}^e is in the second or the fourth one. In the parametrisation under discussion, eq. (3.13) with $(ij) - (kl) = (12) - (13)$, $\theta_{23}^\nu = -\pi/4$ and $\omega = 0$, we have

$$J_{\rm CP} = \frac{\sqrt{2}}{32}\cos\theta_{13}^e\sin 2\theta_{12}^e\left(2\sqrt{2}\cos 2\theta_{12}^\nu\sin 2\theta_{13}^e + (3\cos 2\theta_{13}^e - 1)\sin 2\theta_{12}^\nu\right)\sin\psi\,. \tag{3.56}$$

In the case of non-vanishing ω, using the same method and eq. (3.50), which also holds for $\omega \neq 0$, allows us to show that $\cos\delta$ is a function of $\cos\omega$ as well:

$$\cos\delta = -\frac{2\cos^2\theta_{23}}{\sin 2\theta_{12}\sin 2\theta_{23}\sin\theta_{13}}\Big[(1 - 2\cos^2\theta_{13}\cos^2\theta_{23})\frac{\cos^2\theta_{12}^\nu}{\cos^2\theta_{23}} - \sin^2\theta_{12}\tan^2\theta_{23}$$

$$+ (\cos^2\theta_{13}\sin^2\theta^\nu_{12} - \cos^2\theta_{12}\sin^2\theta_{13}) + \kappa\frac{\cos\theta_{13}}{\cos\theta_{23}}\sqrt{1-2\cos^2\theta_{13}\cos^2\theta_{23}}\cos\omega\sin 2\theta^\nu_{12}\Big]\,. \tag{3.57}$$

Finally, we generalise eq. (3.57) to the case of an arbitrary fixed value of θ^ν_{23}. In this case

$$\sin^2\theta^e_{13} = \frac{1-\cos^2\theta_{13}\cos^2\theta_{23}-\sin^2\theta^\nu_{23}}{\cos^2\theta^\nu_{23}}\,, \tag{3.58}$$

and eqs. (3.54) and (3.57) read:

$$\begin{aligned}|U_{\tau 1}| &= \left|\sin\theta_{23}\sin\theta_{12} - \sin\theta_{13}\cos\theta_{23}\cos\theta_{12}e^{i\delta}\right| \\ &= \left|\cos\theta^\nu_{12}\sin\theta^e_{13} - e^{-i\omega}\cos\theta^e_{13}\sin\theta^\nu_{12}\sin\theta^\nu_{23}\right|\,,\end{aligned} \tag{3.59}$$

$$\begin{aligned}\cos\delta = {}& \frac{1}{\sin 2\theta_{12}\sin 2\theta_{23}\sin\theta_{13}}\Bigg[\frac{2\kappa\cos\omega\sin 2\theta^\nu_{12}\sin\theta^\nu_{23}\cos\theta_{13}\cos\theta_{23}}{\cos^2\theta^\nu_{23}} \\ & \times(\cos^2\theta^\nu_{23} - \cos^2\theta_{13}\cos^2\theta_{23})^{\frac{1}{2}} \\ & - \cos 2\theta^\nu_{12}\Big(1 - \frac{\cos^2\theta_{13}\cos^2\theta_{23}}{\cos^2\theta^\nu_{23}}(\sin^2\theta^\nu_{23}+1)\Big) + \cos 2\theta_{12}\big(\cos^2\theta_{23}\sin^2\theta_{13} - \sin^2\theta_{23}\big)\Bigg]\,.\end{aligned} \tag{3.60}$$

This expression for $\cos\delta$ corresponds to the sum rule in eq. (2.147). See the discussion at the end of subsection 2.6.6.

It follows from the results for $\cos\delta$ obtained for $\cos\omega \neq 0$, eqs. (3.57) and (3.60), that in the case analysed in the present subsection, one can obtain predictions for $\cos\delta$ only in theoretical models in which the value of the phase ω is fixed.

3.4 Mixing schemes with $\tilde{U}^\dagger_e = R_{ij}(\theta^e_{ij})$ and $\tilde{U}_\nu = R_{23}(\theta^\nu_{23})\,R_{13}(\theta^\nu_{13})\,R_{12}(\theta^\nu_{12})$

We consider next a generalisation of the cases analysed in Section 3.2 with the presence of a third rotation matrix in $\tilde{U}_\nu$ arising from the neutrino sector, i.e., we employ the parametrisation of U given in eq. (3.14). Non-zero values of θ^ν_{13} are inspired by certain types of flavour symmetries (see, e.g., [152–155]). In the case of $\theta^\nu_{12} = \theta^\nu_{23} = -\pi/4$ and $\theta^\nu_{13} = \sin^{-1}(1/3)$, for instance, we have the so-called tri-permuting (TP) pattern, which was proposed and studied in [153]. To obtain numerical predictions for $\cos\delta$, δ and the $J_{\rm CP}$ factor in Section 3.6, we will consider three representative values of θ^ν_{13} discussed in the literature: $\theta^\nu_{13} = \pi/20,\ \pi/10$ and $\sin^{-1}(1/3)$.

For the parametrisation of the matrix U given in eq. (3.14) with $(ij) = (23)$, no constraints on the phase δ can be obtained. Indeed, after we recast U in the form

$$U = R_{23}(\hat{\theta}_{23})\,Q_1\,R_{13}(\theta^\nu_{13})\,R_{12}(\theta^\nu_{12})\,Q_0\,, \tag{3.61}$$

where $\sin^2\hat{\theta}_{23}$ and Q_1 are given in eqs. (3.32) and (3.33), respectively, we find employing a similar procedure used in the previous sections:

$$\sin^2\theta_{13} = \sin^2\theta^\nu_{13}\,,\quad \sin^2\theta_{23} = \sin^2\hat{\theta}_{23}\,,\quad \sin^2\theta_{12} = \sin^2\theta^\nu_{12}\,,\quad \sin\delta = \sin\beta\,. \tag{3.62}$$

Thus, there is no correlation between the Dirac CPV phase δ and the mixing angles in this set-up.

3.4.1 Case C1: θ_{12}^e

In the parametrisation of the matrix U given in eq. (3.14) with $(ij) = (12)$, the phase ω in the matrix Ψ is unphysical (it "commutes" with $R_{12}(\theta_{12}^e)$ and can be absorbed by the μ field). Hence, the matrix Ψ contains only one physical phase ϕ, $\Psi = \mathrm{diag}\,(1, e^{i\phi}, 1)$, and $\phi \equiv -\psi$. Taking this into account and using eq. (3.14) with $(ij) = (12)$ and $\theta_{23}^\nu = -\pi/4$, we get the following expressions for $\sin^2\theta_{13}$, $\sin^2\theta_{23}$ and $\sin^2\theta_{12}$:

$$\sin^2\theta_{13} = |U_{e3}|^2 = \frac{1}{2}\sin^2\theta_{12}^e\cos^2\theta_{13}^\nu + \cos^2\theta_{12}^e\sin^2\theta_{13}^\nu - X_{12}\sin\theta_{13}^\nu\,, \tag{3.63}$$

$$\sin^2\theta_{23} = \frac{|U_{\mu 3}|^2}{1-|U_{e3}|^2} = 1 - \frac{\cos^2\theta_{13}^\nu}{2\,(1-\sin^2\theta_{13})}\,, \tag{3.64}$$

$$\begin{aligned}\sin^2\theta_{12} = \frac{|U_{e2}|^2}{1-|U_{e3}|^2} = \frac{1}{1-\sin^2\theta_{13}}\Big[&\frac{1}{2}\sin^2\theta_{12}^e\,(\cos\theta_{12}^\nu + \sin\theta_{12}^\nu\sin\theta_{13}^\nu)^2 \\ &+ \cos^2\theta_{12}^e\cos^2\theta_{13}^\nu\sin^2\theta_{12}^\nu + X_{12}\sin\theta_{12}^\nu\,(\cos\theta_{12}^\nu + \sin\theta_{12}^\nu\sin\theta_{13}^\nu)\Big]\,,\end{aligned} \tag{3.65}$$

where

$$X_{12} = \frac{1}{\sqrt{2}}\sin 2\theta_{12}^e\cos\theta_{13}^\nu\cos\phi\,. \tag{3.66}$$

Solving eq. (3.63) for X_{12} and inserting the solution in eq. (3.65), we find $\sin^2\theta_{12}$ as a function of θ_{13}, θ_{12}^ν, θ_{13}^ν and θ_{12}^e:

$$\sin^2\theta_{12} = \frac{\alpha\sin^2\theta_{12}^e + \beta}{1-\sin^2\theta_{13}}\,. \tag{3.67}$$

Here the parameters α and β are given by:

$$\alpha = \frac{1}{4}\left[2\cos 2\theta_{12}^\nu + \sin 2\theta_{12}^\nu\frac{\cos^2\theta_{13}^\nu}{\sin\theta_{13}^\nu}\right]\,, \tag{3.68}$$

$$\beta = \sin\theta_{12}^\nu\left[\cos^2\theta_{13}\sin\theta_{12}^\nu + \cos\theta_{12}^\nu\left(\sin\theta_{13}^\nu - \frac{\sin^2\theta_{13}}{\sin\theta_{13}^\nu}\right)\right]\,. \tag{3.69}$$

Inverting the formula for $\sin^2\theta_{12}$ allows us to express $\sin^2\theta_{12}^e$ in terms of θ_{12}, θ_{13}, θ_{12}^ν, θ_{13}^ν:

$$\sin^2\theta_{12}^e = \frac{2\cos^2\theta_{13}\sin\theta_{13}^\nu(\sin^2\theta_{12} - \sin^2\theta_{12}^\nu) + \sin 2\theta_{12}^\nu\sin^2\theta_{13} - \sin 2\theta_{12}^\nu\sin^2\theta_{13}^\nu}{\cos 2\theta_{12}^\nu\sin\theta_{13}^\nu + \cos\theta_{12}^\nu\sin\theta_{12}^\nu\cos^2\theta_{13}^\nu}. \tag{3.70}$$

In the limit of vanishing θ_{13}^ν we have $\sin^2\theta_{12}^e = 2\sin^2\theta_{13}$, which corresponds to the case of negligible θ_{23}^e considered in [99].

Using eq. (3.65), one can express $\cos\phi$ in terms of the "standard" mixing angles θ_{12}, θ_{13} and the angles θ_{12}^e, θ_{12}^ν and θ_{13}^ν which are assumed to have known values:

$$\begin{aligned}\cos\phi = &\left[2\cos^2\theta_{13}(\sin\theta_{12}^e)^{-2}(\sin\theta_{12}^\nu)^{-2}\sin^2\theta_{12} - 2\cos^2\theta_{13}^\nu\cot^2\theta_{12}^e - (\cot\theta_{12}^\nu + \sin\theta_{13}^\nu)^2\right] \\ &\times(\cos\theta_{13}^\nu)^{-1}\tan\theta_{12}^e\left[2\sqrt{2}(\cot\theta_{12}^\nu + \sin\theta_{13}^\nu)\right]^{-1}\,.\end{aligned} \tag{3.71}$$

We note that from the requirements $(0 < \sin^2\theta_{12}^e < 1)\wedge(-1 < \cos\phi < 1)$ one can obtain for a given θ_{13}^ν, each of the symmetry values of θ_{12}^ν considered and $\theta_{23}^\nu = -\pi/4$, lower and upper

bounds on the value of $\sin^2\theta_{12}$. These bounds will be discussed in Section 3.6. Comparing the expressions for $J_{\rm CP}$ obtained using eq. (3.14) with $(ij) = (12)$ and $\theta^\nu_{23} = -\pi/4$, and in the standard parametrisation of U, one gets the relation between $\sin\phi$ and $\sin\delta$:

$$\sin\delta = -\frac{\sin 2\theta^e_{12}}{2\sin 2\theta_{12}\sin 2\theta_{13}\sin\theta_{23}}\left[\cos^2\theta^\nu_{13}\sin 2\theta^\nu_{12} + 2\cos 2\theta^\nu_{12}\sin\theta^\nu_{13}\right]\sin\phi\,. \tag{3.72}$$

Similarly to the method employed in the previous section, we use the equality of the expressions for $|U_{\tau 1}|$ in the two parametrisations in order to derive the sum rule for $\cos\delta$ of interest:

$$|U_{\tau 1}| = |\sin\theta_{23}\sin\theta_{12} - \sin\theta_{13}\cos\theta_{23}\cos\theta_{12}e^{i\delta}| = \frac{1}{\sqrt{2}}|\sin\theta^\nu_{12} + \cos\theta^\nu_{12}\sin\theta^\nu_{13}|\,. \tag{3.73}$$

From the above equation we find the following sum rule for $\cos\delta$:

$$\cos\delta = \frac{1}{\sin 2\theta_{12}\sin\theta_{13}|\cos\theta^\nu_{13}|(1-2\sin^2\theta_{13}+\sin^2\theta^\nu_{13})^{\frac{1}{2}}}\Big[\left(1-2\sin^2\theta_{13}+\sin^2\theta^\nu_{13}\right)\sin^2\theta_{12}$$
$$+\cos^2\theta_{12}\sin^2\theta_{13}\cos^2\theta^\nu_{13} - \cos^2\theta_{13}\left(\sin\theta^\nu_{12}+\cos\theta^\nu_{12}\sin\theta^\nu_{13}\right)^2\Big]\,. \tag{3.74}$$

For $\theta^\nu_{13} = 0$ this sum rule reduces to the sum rule for $\cos\delta$ given in eq. (50) in [99].

In the parametrisation of the PMNS matrix considered in this subsection, the rephasing invariant $J_{\rm CP}$ has the form:

$$J_{\rm CP} = -\frac{1}{8\sqrt{2}}\sin\phi\cos\theta^\nu_{13}\sin 2\theta^e_{12}\left[\cos^2\theta^\nu_{13}\sin 2\theta^\nu_{12} + 2\sin\theta^\nu_{13}\cos 2\theta^\nu_{12}\right]\,. \tag{3.75}$$

In the case when θ^ν_{23} has a fixed value which differs from $-\pi/4$, the expression for $\sin^2\theta_{23}$, eq. (3.64), changes as follows:

$$\sin^2\theta_{23} = \frac{|U_{\mu 3}|^2}{1-|U_{e3}|^2} = 1 - \frac{\cos^2\theta^\nu_{23}\cos^2\theta^\nu_{13}}{1-\sin^2\theta_{13}}\,. \tag{3.76}$$

Equations (3.73) and (3.74) are also modified:

$$|U_{\tau 1}| = \left|\sin\theta_{23}\sin\theta_{12} - \sin\theta_{13}\cos\theta_{23}\cos\theta_{12}e^{i\delta}\right| = |\sin\theta^\nu_{12}\sin\theta^\nu_{23} - \cos\theta^\nu_{23}\cos\theta^\nu_{12}\sin\theta^\nu_{13}|\,, \tag{3.77}$$

and

$$\cos\delta = \frac{1}{\sin 2\theta_{12}\sin\theta_{13}|\cos\theta^\nu_{13}\cos\theta^\nu_{23}|(\cos^2\theta_{13}-\cos^2\theta^\nu_{13}\cos^2\theta^\nu_{23})^{\frac{1}{2}}}$$
$$\times\Big[(\cos^2\theta_{13}-\cos^2\theta^\nu_{13}\cos^2\theta^\nu_{23})\sin^2\theta_{12} + \cos^2\theta_{12}\sin^2\theta_{13}\cos^2\theta^\nu_{13}\cos^2\theta^\nu_{23}$$
$$-\cos^2\theta_{13}(\cos\theta^\nu_{12}\sin\theta^\nu_{13}\cos\theta^\nu_{23} - \sin\theta^\nu_{12}\sin\theta^\nu_{23})^2\Big]\,. \tag{3.78}$$

In the case of bi-trimaximal mixing [152], i.e., for $\theta^\nu_{12} = \theta^\nu_{23} = \tan^{-1}(\sqrt{3}-1)$ and $\theta^\nu_{13} = \sin^{-1}((3-\sqrt{3})/6)$, the sum rule we have derived reduces to the sum rule obtained in [111]. However, this case is statistically disfavoured by the current global neutrino oscillation data.

3.4.2 Case C2: θ_{13}^e

Here we switch to the parametrisation of the matrix U given in eq. (3.14) with $(ij) = (13)$. Now the phase ψ in the matrix Ψ is unphysical, and $\Psi = \mathrm{diag}(1, 1, e^{-i\omega})$. Fixing $\theta_{23}^\nu = -\pi/4$ and using also the standard parametrisation of U, we find:

$$\sin^2\theta_{13} = |U_{e3}|^2 = \frac{1}{2}\sin^2\theta_{13}^e\cos^2\theta_{13}^\nu + \cos^2\theta_{13}^e\sin^2\theta_{13}^\nu + X_{13}\sin\theta_{13}^\nu\,, \tag{3.79}$$

$$\sin^2\theta_{23} = \frac{|U_{\mu3}|^2}{1-|U_{e3}|^2} = \frac{\cos^2\theta_{13}^\nu}{2\,(1-\sin^2\theta_{13})}\,, \tag{3.80}$$

$$\begin{aligned}\sin^2\theta_{12} = \frac{|U_{e2}|^2}{1-|U_{e3}|^2} = \frac{1}{1-\sin^2\theta_{13}}\Big[&\frac{1}{2}\sin^2\theta_{13}^e\,(\cos\theta_{12}^\nu - \sin\theta_{12}^\nu\sin\theta_{13}^\nu)^2 \\ &+ \cos^2\theta_{13}^e\cos^2\theta_{13}^\nu\sin^2\theta_{12}^\nu + X_{13}\sin\theta_{12}^\nu\,(\cos\theta_{12}^\nu - \sin\theta_{12}^\nu\sin\theta_{13}^\nu)\Big]\,.\end{aligned} \tag{3.81}$$

Here

$$X_{13} = \frac{1}{\sqrt{2}}\sin 2\theta_{13}^e\cos\theta_{13}^\nu\cos\omega\,. \tag{3.82}$$

Solving eq. (3.79) for X_{13} and inserting the solution in eq. (3.81), it is not difficult to find $\sin^2\theta_{12}$ as a function of θ_{13}, θ_{12}^ν, θ_{13}^ν and θ_{13}^e:

$$\sin^2\theta_{12} = \frac{\rho\sin^2\theta_{13}^e + \eta}{1-\sin^2\theta_{13}}\,, \tag{3.83}$$

where ρ and η are given by

$$\rho = \frac{1}{4}\left[2\cos 2\theta_{12}^\nu - \sin 2\theta_{12}^\nu\frac{\cos^2\theta_{13}^\nu}{\sin\theta_{13}^\nu}\right]\,, \tag{3.84}$$

$$\eta = \sin\theta_{12}^\nu\left[\cos^2\theta_{13}\sin\theta_{12}^\nu - \cos\theta_{12}^\nu\left(\sin\theta_{13}^\nu - \frac{\sin^2\theta_{13}}{\sin\theta_{13}^\nu}\right)\right]\,. \tag{3.85}$$

Using eq. (3.83) for $\sin^2\theta_{12}$ with ρ and η as given above, one can express $\sin^2\theta_{13}^e$ in terms of θ_{12}, θ_{13}, θ_{12}^ν, θ_{13}^ν:

$$\sin^2\theta_{13}^e = \frac{2\cos^2\theta_{13}\sin\theta_{13}^\nu(\sin^2\theta_{12} - \sin^2\theta_{12}^\nu) - \sin 2\theta_{12}^\nu\sin^2\theta_{13} + \sin 2\theta_{12}^\nu\sin^2\theta_{13}^\nu}{\cos 2\theta_{12}^\nu\sin\theta_{13}^\nu - \cos\theta_{12}^\nu\sin\theta_{12}^\nu\cos^2\theta_{13}^\nu}\,. \tag{3.86}$$

In the limit of vanishing θ_{13}^ν we find $\sin^2\theta_{13}^e = 2\sin^2\theta_{13}$, as obtained in subsection 3.2.2.

Further, using eq. (3.81), we can write $\cos\omega$ in terms of the standard parametrisation mixing angles and the known θ_{13}^e, θ_{12}^ν and θ_{13}^ν:

$$\begin{aligned}\cos\omega = &\Big[2\cos^2\theta_{13}(\sin\theta_{13}^e)^{-2}(\sin\theta_{12}^\nu)^{-2}\sin^2\theta_{12} - 2\cos^2\theta_{13}^\nu\cot^2\theta_{13}^e - (\cot\theta_{12}^\nu - \sin\theta_{13}^\nu)^2\Big] \\ &\times(\cos\theta_{13}^\nu)^{-1}\tan\theta_{13}^e\Big[2\sqrt{2}(\cot\theta_{12}^\nu - \sin\theta_{13}^\nu)\Big]^{-1}\,.\end{aligned} \tag{3.87}$$

Analogously to the case considered in the preceding subsection, from the requirements $(0 < \sin^2\theta_{13}^e < 1) \wedge (-1 < \cos\omega < 1)$ one can obtain for a given θ_{13}^ν, each of the symmetry values of θ_{12}^ν considered and $\theta_{23}^\nu = -\pi/4$ lower and upper bounds on the value of $\sin^2\theta_{12}$. These bounds will be discussed in Section 3.6.

Comparing again the imaginary parts of $U^*_{e1}U^*_{\mu 3}U_{e3}U_{\mu 1}$, obtained using eq. (3.14) with $(ij) = (13)$ and $\theta^\nu_{23} = -\pi/4$, and in the standard parametrisation of U, one gets the following relation between $\sin\omega$ and $\sin\delta$ for arbitrarily fixed θ^ν_{12} and θ^ν_{13}:

$$\sin\delta = -\frac{\sin 2\theta^e_{13}}{2\sin 2\theta_{12}\sin 2\theta_{13}\cos\theta_{23}}\left[\cos^2\theta^\nu_{13}\sin 2\theta^\nu_{12} - 2\cos 2\theta^\nu_{12}\sin\theta^\nu_{13}\right]\sin\omega\,. \tag{3.88}$$

Exploiting the equality of the expressions for $|U_{\mu 1}|$ written in the two parametrisations,

$$|U_{\mu 1}| = \left|\cos\theta_{23}\sin\theta_{12} + e^{i\delta}\cos\theta_{12}\sin\theta_{13}\sin\theta_{23}\right| = \frac{1}{\sqrt{2}}\left|\cos\theta^\nu_{12}\sin\theta^\nu_{13} - \sin\theta^\nu_{12}\right|\,, \tag{3.89}$$

we get the following sum rule for $\cos\delta$:

$$\begin{aligned}\cos\delta = -\frac{1}{\sin 2\theta_{12}\sin\theta_{13}|\cos\theta^\nu_{13}|(1-2\sin^2\theta_{13}+\sin^2\theta^\nu_{13})^{\frac{1}{2}}}\Big[&\left(1-2\sin^2\theta_{13}+\sin^2\theta^\nu_{13}\right)\sin^2\theta_{12}\\ &+\cos^2\theta_{12}\sin^2\theta_{13}\cos^2\theta^\nu_{13} - \cos^2\theta_{13}\left(\sin\theta^\nu_{12}-\cos\theta^\nu_{12}\sin\theta^\nu_{13}\right)^2\Big]\,.\end{aligned} \tag{3.90}$$

For $\theta^\nu_{13} = 0$ this sum rule reduces to the sum rule for $\cos\delta$ given in eq. (3.23).

In the parametrisation of the PMNS matrix considered in this subsection, the $J_{\rm CP}$ factor reads:

$$J_{\rm CP} = -\frac{1}{8\sqrt{2}}\sin\omega\cos\theta^\nu_{13}\sin 2\theta^e_{13}\left[\cos^2\theta^\nu_{13}\sin 2\theta^\nu_{12} - 2\sin\theta^\nu_{13}\cos 2\theta^\nu_{12}\right]\,. \tag{3.91}$$

In the case of an arbitrary fixed value of θ^ν_{23}, as it is not difficult to show, we have:

$$\sin^2\theta_{23} = \frac{|U_{\mu 3}|^2}{1-|U_{e3}|^2} = \frac{\sin^2\theta^\nu_{23}\cos^2\theta^\nu_{13}}{1-\sin^2\theta_{13}}\,, \tag{3.92}$$

and

$$|U_{\mu 1}| = \left|\cos\theta_{23}\sin\theta_{12} + e^{i\delta}\cos\theta_{12}\sin\theta_{13}\sin\theta_{23}\right| = \left|\cos\theta^\nu_{12}\sin\theta^\nu_{13}\sin\theta^\nu_{23} + \sin\theta^\nu_{12}\cos\theta^\nu_{23}\right|\,. \tag{3.93}$$

Using eqs. (3.92) and (3.93), we obtain in this case

$$\begin{aligned}\cos\delta = &-\frac{1}{\sin 2\theta_{12}\sin\theta_{13}|\cos\theta^\nu_{13}\sin\theta^\nu_{23}|(\cos^2\theta_{13}-\cos^2\theta^\nu_{13}\sin^2\theta^\nu_{23})^{\frac{1}{2}}}\\ &\times\Big[(\cos^2\theta_{13}-\cos^2\theta^\nu_{13}\sin^2\theta^\nu_{23})\sin^2\theta_{12}+\cos^2\theta_{12}\sin^2\theta_{13}\cos^2\theta^\nu_{13}\sin^2\theta^\nu_{23}\\ &-\cos^2\theta_{13}(\cos\theta^\nu_{12}\sin\theta^\nu_{13}\sin\theta^\nu_{23}+\sin\theta^\nu_{12}\cos\theta^\nu_{23})^2\Big]\,.\end{aligned} \tag{3.94}$$

3.5 Summary of the sum rules

The sum rules derived in Sections 3.2–3.4 and corresponding to arbitrary fixed values of the angles contained in the matrix $\tilde{U}_\nu$, eqs. (3.10), (3.17), (3.28), (3.42), (3.60), (3.78) and (3.94), are summarised in Table 3.1. In Table 3.2 we give the corresponding formulae for $\sin^2\theta_{23}$.

Table 3.1. Summary of the sum rules for $\cos\delta$. The parameter $\kappa = 1$ if θ_{13}^{e} belongs to the first or third quadrant, and $\kappa = -1$ otherwise.

Case	Parametrisation of the PMNS matrix U	$\cos\delta$
A1	$R_{12}(\theta_{12}^{e})\,\Psi\,R_{23}(\theta_{23}^{\nu})\,R_{12}(\theta_{12}^{\nu})\,Q_0$	$\dfrac{(\cos 2\theta_{13}-\cos 2\theta_{23}^{\nu})^{\frac{1}{2}}}{\sqrt{2}\sin 2\theta_{12}\sin\theta_{13}\lvert\cos\theta_{23}^{\nu}\rvert}\left[\cos 2\theta_{12}^{\nu}+\left(\sin^2\theta_{12}-\cos^2\theta_{12}^{\nu}\right)\dfrac{2\sin^2\theta_{23}^{\nu}-(3+\cos 2\theta_{23}^{\nu})\sin^2\theta_{13}}{\cos 2\theta_{13}-\cos 2\theta_{23}^{\nu}}\right]$
A2	$R_{13}(\theta_{13}^{e})\,\Psi\,R_{23}(\theta_{23}^{\nu})\,R_{12}(\theta_{12}^{\nu})\,Q_0$	$-\dfrac{(\cos 2\theta_{13}+\cos 2\theta_{23}^{\nu})^{\frac{1}{2}}}{\sqrt{2}\sin 2\theta_{12}\sin\theta_{13}\lvert\sin\theta_{23}^{\nu}\rvert}\left[\cos 2\theta_{12}^{\nu}+\left(\sin^2\theta_{12}-\cos^2\theta_{12}^{\nu}\right)\dfrac{2\cos^2\theta_{23}^{\nu}-(3-\cos 2\theta_{23}^{\nu})\sin^2\theta_{13}}{\cos 2\theta_{13}+\cos 2\theta_{23}^{\nu}}\right]$
B1	$R_{12}(\theta_{12}^{e})\,R_{23}(\theta_{23}^{e})\,\Psi\,R_{23}(\theta_{23}^{\nu})\,R_{12}(\theta_{12}^{\nu})\,Q_0$	$\dfrac{\tan\theta_{23}}{\sin 2\theta_{12}\sin\theta_{13}}\left[\cos 2\theta_{12}^{\nu}+\left(\sin^2\theta_{12}-\cos^2\theta_{12}^{\nu}\right)\left(1-\cot^2\theta_{23}\,\sin^2\theta_{13}\right)\right]$
B2	$R_{13}(\theta_{13}^{e})\,R_{23}(\theta_{23}^{e})\,\Psi\,R_{23}(\theta_{23}^{\nu})\,R_{12}(\theta_{12}^{\nu})\,Q_0$	$-\dfrac{\cot\theta_{23}}{\sin 2\theta_{12}\sin\theta_{13}}\left[\cos 2\theta_{12}^{\nu}+\left(\sin^2\theta_{12}-\cos^2\theta_{12}^{\nu}\right)\left(1-\tan^2\theta_{23}\,\sin^2\theta_{13}\right)\right]$
B3	$R_{12}(\theta_{12}^{e})\,R_{13}(\theta_{13}^{e})\,\Psi\,R_{23}(\theta_{23}^{\nu})\,R_{12}(\theta_{12}^{\nu})\,Q_0$	$\dfrac{1}{\sin 2\theta_{12}\sin 2\theta_{23}\sin\theta_{13}}\Bigg[\dfrac{2\kappa\cos\omega\sin 2\theta_{12}^{\nu}\sin\theta_{23}^{\nu}\cos\theta_{13}\cos\theta_{23}}{\cos^2\theta_{23}^{\nu}}(\cos^2\theta_{23}^{\nu}-\cos^2\theta_{13}\cos^2\theta_{23})^{\frac{1}{2}}$ $-\cos 2\theta_{12}^{\nu}\Big(1-\dfrac{\cos^2\theta_{13}\cos^2\theta_{23}}{\cos^2\theta_{23}^{\nu}}(\sin^2\theta_{23}^{\nu}+1)\Big)+\cos 2\theta_{12}\big(\cos^2\theta_{23}\sin^2\theta_{13}-\sin^2\theta_{23}\big)\Bigg]$
C1	$R_{12}(\theta_{12}^{e})\,\Psi\,R_{23}(\theta_{23}^{\nu})\,R_{13}(\theta_{13}^{\nu})\,R_{12}(\theta_{12}^{\nu})\,Q_0$	$\dfrac{1}{\sin 2\theta_{12}\sin\theta_{13}\lvert\cos\theta_{13}^{\nu}\cos\theta_{23}^{\nu}\rvert(\cos^2\theta_{13}-\cos^2\theta_{13}^{\nu}\cos^2\theta_{23}^{\nu})^{\frac{1}{2}}}\Bigg[(\cos^2\theta_{13}-\cos^2\theta_{13}^{\nu}\cos^2\theta_{23}^{\nu})\sin^2\theta_{12}$ $+\cos^2\theta_{12}\sin^2\theta_{13}\cos^2\theta_{13}^{\nu}\cos^2\theta_{23}^{\nu}-\cos^2\theta_{13}(\cos\theta_{12}^{\nu}\sin\theta_{13}^{\nu}\cos\theta_{23}^{\nu}-\sin\theta_{12}^{\nu}\sin\theta_{23}^{\nu})^2\Bigg]$
C2	$R_{13}(\theta_{13}^{e})\,\Psi\,R_{23}(\theta_{23}^{\nu})\,R_{13}(\theta_{13}^{\nu})\,R_{12}(\theta_{12}^{\nu})\,Q_0$	$-\dfrac{1}{\sin 2\theta_{12}\sin\theta_{13}\lvert\cos\theta_{13}^{\nu}\sin\theta_{23}^{\nu}\rvert(\cos^2\theta_{13}-\cos^2\theta_{13}^{\nu}\sin^2\theta_{23}^{\nu})^{\frac{1}{2}}}\Bigg[(\cos^2\theta_{13}-\cos^2\theta_{13}^{\nu}\sin^2\theta_{23}^{\nu})\sin^2\theta_{12}$ $+\cos^2\theta_{12}\sin^2\theta_{13}\cos^2\theta_{13}^{\nu}\sin^2\theta_{23}^{\nu}-\cos^2\theta_{13}(\cos\theta_{12}^{\nu}\sin\theta_{13}^{\nu}\sin\theta_{23}^{\nu}+\sin\theta_{12}^{\nu}\cos\theta_{23}^{\nu})^2\Bigg]$

Table 3.2. Summary of the sum rules for $\sin^2\theta_{23}$. The formula for $\sin^2\hat{\theta}_{23}$ is given in eq. (3.32).

Case	Parametrisation of the PMNS matrix U	$\sin^2\theta_{23}$
A1	$R_{12}(\theta^e_{12})\,\Psi\,R_{23}(\theta^\nu_{23})\,R_{12}(\theta^\nu_{12})\,Q_0$	$\dfrac{\sin^2\theta^\nu_{23}-\sin^2\theta_{13}}{1-\sin^2\theta_{13}}$
A2	$R_{13}(\theta^e_{13})\,\Psi\,R_{23}(\theta^\nu_{23})\,R_{12}(\theta^\nu_{12})\,Q_0$	$\dfrac{\sin^2\theta^\nu_{23}}{1-\sin^2\theta_{13}}$
B1	$R_{12}(\theta^e_{12})\,R_{23}(\theta^e_{23})\,\Psi\,R_{23}(\theta^\nu_{23})\,R_{12}(\theta^\nu_{12})\,Q_0$	$\dfrac{\sin^2\hat{\theta}_{23}-\sin^2\theta_{13}}{1-\sin^2\theta_{13}}$
B2	$R_{13}(\theta^e_{13})\,R_{23}(\theta^e_{23})\,\Psi\,R_{23}(\theta^\nu_{23})\,R_{12}(\theta^\nu_{12})\,Q_0$	$\dfrac{\sin^2\hat{\theta}_{23}}{1-\sin^2\theta_{13}}$
B3	$R_{12}(\theta^e_{12})\,R_{13}(\theta^e_{13})\,\Psi\,R_{23}(\theta^\nu_{23})\,R_{12}(\theta^\nu_{12})\,Q_0$	$\dfrac{\sin^2\theta^\nu_{23}-\sin^2\theta_{13}+\sin^2\theta^e_{13}\cos^2\theta^\nu_{23}}{1-\sin^2\theta_{13}}$
C1	$R_{12}(\theta^e_{12})\,\Psi\,R_{23}(\theta^\nu_{23})\,R_{13}(\theta^\nu_{13})\,R_{12}(\theta^\nu_{12})\,Q_0$	$1-\dfrac{\cos^2\theta^\nu_{23}\cos^2\theta^\nu_{13}}{1-\sin^2\theta_{13}}$
C2	$R_{13}(\theta^e_{13})\,\Psi\,R_{23}(\theta^\nu_{23})\,R_{13}(\theta^\nu_{13})\,R_{12}(\theta^\nu_{12})\,Q_0$	$\dfrac{\sin^2\theta^\nu_{23}\cos^2\theta^\nu_{13}}{1-\sin^2\theta_{13}}$

3.6 Predictions for the Dirac phase δ and the rephasing invariant $J_{\rm CP}$

In this section, using the sum rules from Table 3.1 and the best fit values of the relevant neutrino mixing parameters quoted in eqs. (2.15)–(2.17), we obtain the predictions for $\cos\delta$, δ and the $J_{\rm CP}$ factor. In cases A1, A2 and B1–B3, we obtain such predictions for the TBM, BM, GRA, GRB and HG symmetry forms of the matrix $\tilde{U}_\nu$, while in cases C1 and C2 for specific pairs of the values of θ^ν_{13} and θ^ν_{12}, keeping θ^ν_{23} fixed to $-\pi/4$. We start with identifying these specific pairs.

In case C1, we find that only for particular values of θ^ν_{12} and θ^ν_{13}, among those considered by us, the allowed intervals of values of $\sin^2\theta_{12}$ satisfy the requirement that they contain in addition to the best fit value of $\sin^2\theta_{12}$ also the 1.5σ experimentally allowed range of $\sin^2\theta_{12}$. Indeed, combining the conditions $0<\sin^2\theta^e_{12}<1$ and $|\cos\phi|<1$, where $\sin^2\theta^e_{12}$ and $\cos\phi$ are given in eqs. (3.70) and (3.71), respectively, and allowing $\sin^2\theta_{13}$ to vary in the 3σ range for the NO spectrum, we get restrictions on the value of $\sin^2\theta_{12}$ presented in Table 3.3. We see from the table that only five out of 18 combinations of the angles θ^ν_{12} and θ^ν_{13} considered by us satisfy the requirement formulated above. In Table 3.3 these cases are marked with the subscripts I, II, III, IV, V, while the ones marked with an asterisk contain values of $\sin^2\theta_{12}$ allowed at 2σ [18].

Equation (3.64) implies that $\sin^2\theta_{23}$ is fixed by the value of θ^ν_{13}, and for the best fit value of $\sin^2\theta_{13}$ and the values of $\theta^\nu_{13}=0$, $\pi/20$, $\pi/10$, $\sin^{-1}(1/3)$, considered by us, we get, respectively: $\sin^2\theta_{23}=0.488$, 0.501, 0.537, 0.545. Therefore a measurement of $\sin^2\theta_{23}$ with a sufficiently high precision would rule out at least some of the cases with fixed values of θ^ν_{13} considered in the literature.

In case C2, a similar situation takes place. Namely, we find that only particular values

Table 3.3. Case C1: ranges of $\sin^2\theta_{12}$ obtained from the requirements $(0 < \sin^2\theta^e_{12} < 1) \wedge (-1 < \cos\phi < 1)$ allowing $\sin^2\theta_{13}$ to vary in the 3σ allowed range for the NO neutrino mass spectrum quoted in eq. (2.17). The cases for which the best fit value of $\sin^2\theta_{12} = 0.308$ is within the corresponding allowed ranges are marked with the subscripts I, II, III, IV, V. The cases marked with an asterisk contain values of $\sin^2\theta_{12}$ allowed at 2σ [18].

θ^ν_{13} / θ^ν_{12}	$\pi/20$	$\pi/10$	$\sin^{-1}(1/3)$
$\sin^{-1}(1/\sqrt{3})$	$(0.319, 0.654)^*$	$(0.471, 0.773)$	$(0.495, 0.789)$
$\pi/4$	$(0.484, 0.803)$	$(0.639, 0.897)$	$(0.662, 0.909)$
$-\pi/4$	$(0.197, 0.516)_{\rm III}$	$(0.103, 0.361)_{\rm I}$	$(0.091, 0.338)_{\rm IV}$
$\sin^{-1}(1/\sqrt{2+r})$	$(0.262, 0.594)_{\rm II}$	$(0.409, 0.719)$	$(0.434, 0.737)$
$\pi/5$	$(0.331, 0.666)^*$	$(0.484, 0.784)$	$(0.508, 0.800)$
$\pi/6$	$(0.236, 0.564)_{\rm V}$	$(0.380, 0.692)$	$(0.404, 0.710)$

Table 3.4. The same as in Table 3.3, but for case C2 and, correspondingly, the requirements $(0 < \sin^2\theta^e_{13} < 1) \wedge (-1 < \cos\omega < 1)$.

θ^ν_{13} / θ^ν_{12}	$\pi/20$	$\pi/10$	$\sin^{-1}(1/3)$
$\sin^{-1}(1/\sqrt{3})$	$(0.081, 0.348)_{\rm III}$	$(0.024, 0.209)$	$(0.019, 0.189)$
$\pi/4$	$(0.197, 0.516)_{\rm I}$	$(0.103, 0.361)_{\rm IV}$	$(0.091, 0.338)_{\rm II}$
$-\pi/4$	$(0.484, 0.803)$	$(0.639, 0.897)$	$(0.662, 0.909)$
$\sin^{-1}(1/\sqrt{2+r})$	$(0.051, 0.291)^*$	$(0.009, 0.161)$	$(0.006, 0.143)$
$\pi/5$	$(0.089, 0.361)_{\rm V}$	$(0.028, 0.220)$	$(0.022, 0.200)$
$\pi/6$	$(0.038, 0.264)$	$(0.004, 0.140)$	$(0.002, 0.123)$

of θ^ν_{12} and θ^ν_{13} allow one to obtain the best fit value of $\sin^2\theta_{12}$. Combining the requirements $0 < \sin^2\theta^e_{13} < 1$ and $|\cos\omega| < 1$, where $\sin^2\theta^e_{13}$ and $\cos\omega$ are given in eqs. (3.86) and (3.87), respectively, and allowing $\sin^2\theta_{13}$ to vary in its 3σ allowed range corresponding to the NO spectrum, we get restrictions on the value of $\sin^2\theta_{12}$ presented in Table 3.4. It follows from the results in Table 3.4 that only for five out of 18 combinations of the angles θ^ν_{12} and θ^ν_{13}, the best fit value of $\sin^2\theta_{12} = 0.308$ and the 1.5σ experimentally allowed interval of values of $\sin^2\theta_{12}$ are inside the allowed ranges. In Table 3.4 these cases are marked with the subscripts I, II, III, IV, V, while in the case marked with an asterisk, the allowed range contains values of $\sin^2\theta_{12}$ allowed at 2σ [18].

The values of $\sin^2\theta_{23}$ in case C2 depend on the reactor angle θ_{13} and θ^ν_{13} through eq. (3.80). Using the best fit value of $\sin^2\theta_{13}$ for the NO spectrum and eq. (3.80), we find $\sin^2\theta_{23} = 0.512, 0.499, 0.463, 0.455$ for $\theta^\nu_{13} = 0, \pi/20, \pi/10, \sin^{-1}(1/3)$, respectively. Thus, in the scheme under discussion $\sin^2\theta_{23}$ decreases with the increase of θ^ν_{13}, which is in contrast to the behaviour of $\sin^2\theta_{23}$ in case C1. As we have already remarked, a measurement of $\sin^2\theta_{23}$ with a sufficiently high precision, or at least the determination of the octant of θ_{23}, would allow one to exclude some of the values of θ^ν_{13} considered in the literature. In the further analysis of cases C1 and C2, we will consider the five pairs of values $[\theta^\nu_{13}, \theta^\nu_{12}]$ found in each of these cases.

Table 3.5. The predicted values of $\cos\delta$ using the best fit values of the mixing angles quoted in eqs. (2.15)–(2.17) and corresponding to neutrino mass spectrum with NO, except for case B3 with $\omega = 0$ and $\kappa = 1$, in which $\sin^2\theta_{23} = 0.48802$ is used. We have defined $a = \sin^{-1}(1/3)$, $b = \sin^{-1}(1/\sqrt{2+r})$ and $c = \sin^{-1}(1/\sqrt{3})$. See text for further details.

$\tilde{U}_\nu$	TBM	GRA	GRB	HG	BM (LC)
Case					
A1	-0.114	0.289	-0.200	0.476	
A2	0.114	-0.289	0.200	-0.476	
B1	-0.091	0.275	-0.169	0.445	
B2	0.151	-0.315	0.251	-0.531	
B3	-0.122	0.282	-0.208	0.469	
$[\theta^\nu_{13}, \theta^\nu_{12}]$	$[\pi/20, -\pi/4]$	$[\pi/10, -\pi/4]$	$[a, -\pi/4]$	$[\pi/20, b]$	$[\pi/20, \pi/6]$
C1	-0.222	0.760	0.911	-0.775	-0.562
$[\theta^\nu_{13}, \theta^\nu_{12}]$	$[\pi/20, c]$	$[\pi/20, \pi/4]$	$[\pi/10, \pi/4]$	$[a, \pi/4]$	$[\pi/20, \pi/5]$
C2	-0.866	0.222	-0.760	-0.911	-0.791

Table 3.6. The same as in Table 3.5, but for δ given in degrees. See text for further details.

$\tilde{U}_\nu$	TBM	GRA	GRB	HG	BM (LC)
Case					
A1	$97 \vee 263$	$73 \vee 287$	$102 \vee 258$	$62 \vee 298$	
A2	$83 \vee 277$	$107 \vee 253$	$78 \vee 282$	$118 \vee 242$	
B1	$95 \vee 265$	$74 \vee 286$	$100 \vee 260$	$64 \vee 296$	
B2	$81 \vee 279$	$108 \vee 252$	$75 \vee 285$	$122 \vee 238$	
B3	$97 \vee 263$	$74 \vee 286$	$102 \vee 258$	$62 \vee 298$	
$[\theta^\nu_{13}, \theta^\nu_{12}]$	$[\pi/20, -\pi/4]$	$[\pi/10, -\pi/4]$	$[a, -\pi/4]$	$[\pi/20, b]$	$[\pi/20, \pi/6]$
C1	$103 \vee 257$	$41 \vee 319$	$24 \vee 336$	$141 \vee 219$	$124 \vee 236$
$[\theta^\nu_{13}, \theta^\nu_{12}]$	$[\pi/20, c]$	$[\pi/20, \pi/4]$	$[\pi/10, \pi/4]$	$[a, \pi/4]$	$[\pi/20, \pi/5]$
C2	$150 \vee 210$	$77 \vee 283$	$139 \vee 221$	$156 \vee 204$	$142 \vee 218$

We show in Tables 3.5 and 3.6 the predictions for $\cos\delta$ and δ for all the cases considered in the present chapter using the best fit values of the neutrino mixing parameters $\sin^2\theta_{12}$, $\sin^2\theta_{23}$ and $\sin^2\theta_{13}$ quoted in eqs. (2.15)–(2.17), which enter into the sum rule expressions for $\cos\delta$, unless other values of the indicated mixing parameters are explicitly specified. We present results only for the NO neutrino mass spectrum, since the results for the IO spectrum differ insignificantly. Several comments are in order.

We do not present predictions for the BM (LC) symmetry form of $\tilde{U}_\nu$ in Tables 3.5 and 3.6, because for the best fit values of $\sin^2\theta_{12}$, $\sin^2\theta_{23}$, $\sin^2\theta_{13}$ the corresponding sum rules give unphysical values of $\cos\delta$ (see, however, refs. [99, 109]). Using the best fit value of $\sin^2\theta_{13}$, we get physical values of $\cos\delta$ for the BM symmetry form for the following

minimal values of $\sin^2\theta_{12}$:

$$\begin{aligned}
&\cos\delta = -0.993\ (\delta \approx \pi) \text{ for } \sin^2\theta_{12} = 0.348 \text{ in case A1},\\
&\cos\delta = +0.993\ (\delta \approx 0) \text{ for } \sin^2\theta_{12} = 0.348 \text{ in case A2},\\
&\cos\delta = -0.996\ (\delta \approx \pi) \text{ for } \sin^2\theta_{12} = 0.332 \text{ in case B1},\\
&\cos\delta = +0.997\ (\delta \approx 0) \text{ for } \sin^2\theta_{12} = 0.368 \text{ in case B2},\\
&\cos\delta = -0.994\ (\delta \approx \pi) \text{ for } \sin^2\theta_{12} = 0.349 \text{ in case B3},
\end{aligned}$$

where in case B3 we fixed $\sin^2\theta_{23} = 0.48802$ (we will comment later on this choice), while $\sin^2\theta_{23}$ was set to its best fit value in cases B1 and B2.

The predictions for $\cos\delta$ in cases A1 and A2 for each of the symmetry forms of $\tilde{U}_\nu$ considered differ only by sign. Case A1 and case B3 with $\omega = 0$ provide very similar predictions for $\cos\delta$.

In the schemes with three rotations in $\tilde{U}_\nu$ we consider, $\cos\delta$ has values which differ significantly (being larger in absolute value) from the values predicted by the schemes with two rotations in $\tilde{U}_\nu$ discussed by us, the only exceptions being (i) case C1 (C2) with $\theta^\nu_{13} = \pi/20$ and $\theta^\nu_{12} = -\pi/4$ ($\pi/4$), for which $|\cos\delta| = 0.222$, and (ii) case C1 with $[\theta^\nu_{13}, \theta^\nu_{12}] = [\pi/20, \pi/6]$ in which $\cos\delta = -0.562$.

The predictions for $\cos\delta$ in cases B1 and B2 differ for each of the symmetry forms of $\tilde{U}_\nu$ considered both by sign and magnitude. If the best fit value of θ_{23} were $\pi/4$, these predictions would differ only by sign.

In case B3 with $\omega = 0$, the predictions for $\cos\delta$ are very sensitive to the value of $\sin^2\theta_{23}$. Using the best fit values of $\sin^2\theta_{12}$ and $\sin^2\theta_{13}$ for the NO neutrino mass spectrum quoted in eqs. (2.15) and (2.17), we find from the constraints $(-1 < \cos\psi < 1)$ and $(0 < \sin^2\theta^e_{13} < 1) \wedge (0 < \sin^2\theta^e_{12} < 1)$, where $\sin^2\theta^e_{13}$, $\sin^2\theta^e_{12}$ and $\cos\psi$ are given in eqs. (3.50)–(3.52), that $\sin^2\theta_{23}$ should lie in the following intervals:

$$\begin{aligned}
&(0.488, 0.496) \cup (0.847, 0.909) \text{ for TBM};\\
&(0.488, 0.519) \cup (0.948, 0.971) \text{ for BM};\\
&(0.488, 0.497) \cup (0.807, 0.880) \text{ for GRA};\\
&(0.488, 0.498) \cup (0.856, 0.914) \text{ for GRB};\\
&(0.488, 0.500) \cup (0.787, 0.866) \text{ for HG}.
\end{aligned}$$

Obviously, the quoted intervals with $\sin^2\theta_{23} \geq 0.78$ are ruled out by the current data. We observe that a small increase of $\sin^2\theta_{23}$ from the value 0.48802 [24] produces a relatively large variation of $\cos\delta$. The strong dependence of $\cos\delta$ on $\sin^2\theta_{23}$ takes place for values of ω satisfying roughly $\cos\omega \gtrsim 0.01$. In contrast, for $\cos\omega = 0$, $\cos\delta$ exhibits a relatively weak dependence on $\sin^2\theta_{23}$. For the reasons related to the dependence of $\cos\delta$ on ω we are not going to present results of the statistical analysis, which we perform in the next section, in this case. This can be done in specific models of neutrino mixing, in which the value of the phase ω is fixed.

3.7 Statistical analysis

In the present section, we perform a statistical analysis of the predictions for $\cos\delta$ and the rephasing invariant $J_{\rm CP}$ in the cases of the mixing schemes considered in the present

[24] For $\sin^2\theta_{23} < 0.48802$, $\cos\delta$ has an unphysical (complex) value.

chapter. In each case, our goal is to derive the allowed ranges for $\cos\delta$ and $J_{\rm CP}$ for each of the symmetry forms of $\tilde{U}_\nu$ considered, predicted on the basis of (i) the current data on the neutrino mixing parameters [18] and (ii) the prospective uncertainties in the determination of the neutrino mixing angles. To this aim, we construct the χ^2 function as described in Appendix F.

We find that in case A1 the results for χ^2 as a function of δ or $J_{\rm CP}$ are rather similar to those obtained in the next subsection in case B1. The main difference between these two cases is the predictions for $\sin^2\theta_{23}$, which can deviate only by approximately $0.5\sin^2\theta_{13}$ from 0.5 in the first case and by a significantly larger amount in the second. As a consequence, the predictions in the first case are somewhat less favoured by the current data than in the second case, which is reflected in the higher value of χ^2 at the minimum, $\chi^2_{\rm min}$. Similar conclusions hold comparing the results in cases A2 and B2. Therefore, in what concerns these four cases, in what follows we will present results of the statistical analysis of the predictions for $\cos\delta$ and the $J_{\rm CP}$ factor only in cases B1 and B2.

3.7.1 Case B1

In Fig. 3.1 we show the likelihood function L, defined as

$$L(\cos\delta) = \exp\left(-\frac{\chi^2(\cos\delta)}{2}\right), \tag{3.95}$$

versus $\cos\delta$ for the NO neutrino mass spectrum. The results shown are obtained by marginalising over $\sin^2\theta_{13}$ and $\sin^2\theta_{23}$ for a fixed value of δ (see Appendix F for details). The dependence of the likelihood function on $\cos\delta$ in the case of IO neutrino mass spectrum differs little from that shown in Fig. 3.1. Given the global fit results, the likelihood function represents the most probable value of $\cos\delta$ for each of the considered symmetry forms of $\tilde{U}_\nu$. The $n\sigma$ C.L. region corresponds to the interval of values of $\cos\delta$ in which $L(\cos\delta) \geq L(\chi^2 = \chi^2_{\rm min}) \cdot L(\chi^2 = n^2)$.

As can be observed from Fig. 3.1, a rather precise measurement of $\cos\delta$ would allow one to distinguish between the different symmetry forms of $\tilde{U}_\nu$ considered by us. For the TBM and GRB forms there is a significant overlap of the corresponding likelihood functions. The same observation is valid for the GRA and HG forms. However, the overlap of the likelihood functions of these two groups of symmetry forms occurs only at 3σ level in a very small interval of values of $\cos\delta$. This implies that in order to distinguish between the TBM/GRB, GRA/HG and BM symmetry forms a not very demanding measurement (in terms of accuracy) of $\cos\delta$ might be sufficient. The value of the likelihood function at the maximum in Fig. 3.1 is equal to $\exp(-\chi^2_{\rm min}/2)$, which allows us to make conclusions about the compatibility of a given symmetry form of $\tilde{U}_\nu$ with the current global neutrino oscillation data.

In the left panel of Fig. 3.2 we present the likelihood function versus $\cos\delta$ within the Gaussian approximation (see Appendix F for details), using the best fit values of the mixing angles for the NO neutrino mass spectrum from eqs. (2.15)–(2.17) and the prospective relative 1σ uncertainties in the determination of $\sin^2\theta_{12}$ (0.7% from JUNO [156, 157]), $\sin^2\theta_{13}$ (almost 3% derived from an expected error on $\sin^2 2\theta_{13}$ of 3% from Daya Bay [158–160]) and $\sin^2\theta_{23}$ (5% [25] derived from the potential sensitivity of NOνA and T2K on $\sin^2 2\theta_{23}$ of 2% [158]). The BM case is very sensitive to the best fit values of $\sin^2\theta_{12}$ and $\sin^2\theta_{23}$ and is disfavoured at more than 2σ for the best fit values quoted

[25] This sensitivity can be achieved at future neutrino facilities [161].

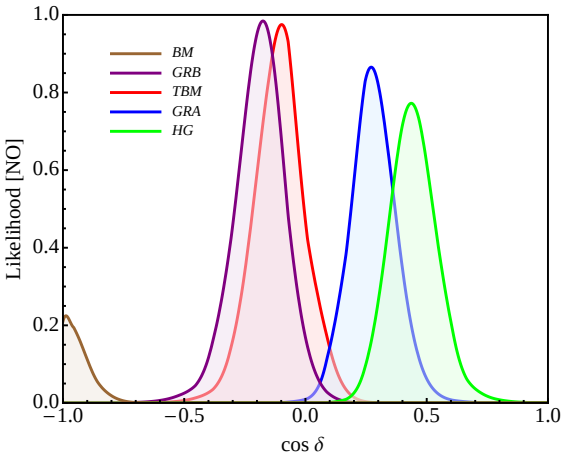

Figure 3.1. The likelihood function versus $\cos\delta$ for the NO neutrino mass spectrum after marginalising over $\sin^2\theta_{13}$ and $\sin^2\theta_{23}$ for the TBM, BM (LC), GRA, GRB and HG symmetry forms of the matrix $\tilde{U}_\nu$ in case B1. The results shown are obtained using eq. (3.10) and the results on the mixing parameters $\sin^2\theta_{12}$, $\sin^2\theta_{13}$, $\sin^2\theta_{23}$ and δ found in the global analysis of neutrino oscillation data [18].

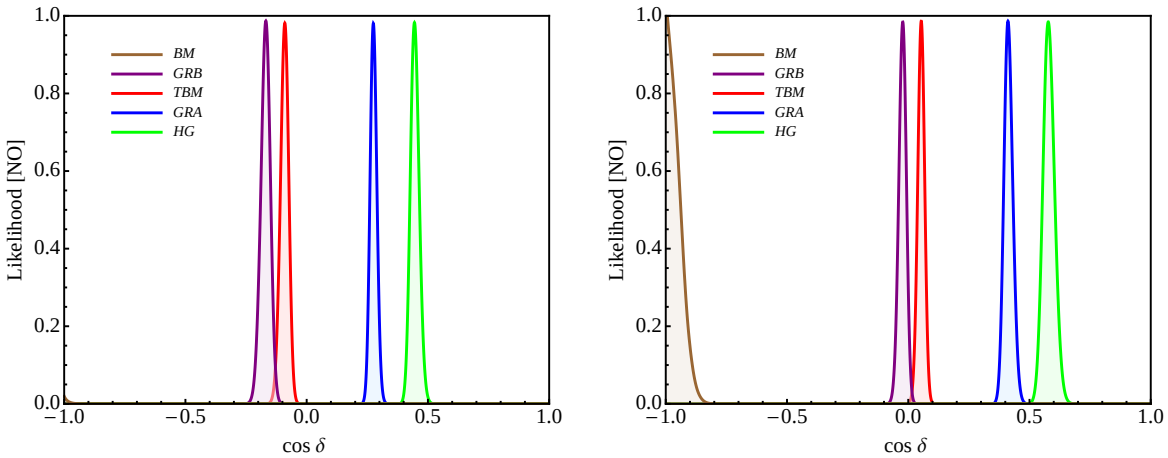

Figure 3.2. The same as in Fig. 3.1, but using the prospective 1σ uncertainties in the determination of the neutrino mixing angles within the Gaussian approximation (see Appendix F). In the left (right) panel, $(\sin^2\theta_{12})_{\rm BF} = 0.308$ (0.332), while $(\sin^2\theta_{13})_{\rm BF}$ and $(\sin^2\theta_{23})_{\rm BF}$ are fixed to their NO best fit values quoted in eqs. (2.17) and (2.16).

in eqs. (2.15)–(2.17). This case might turn out to be compatible with the data for larger (smaller) measured values of $\sin^2\theta_{12}$ ($\sin^2\theta_{23}$), as can be seen from the right panel of Fig. 3.2, which was obtained for $\sin^2\theta_{12} = 0.332$. With the increase of the value of $\sin^2\theta_{23}$ the BM form becomes increasingly disfavoured, while the TBM/GRB (GRA/HG) predictions for $\cos\delta$ are shifted somewhat — approximately by 0.1 — to the left (right) with respect to those shown in the left panel of Fig. 3.2. This shift is illustrated in Fig. 3.3, which is obtained for $\sin^2\theta_{23} = 0.579$, more precisely, for the best fit values found in [19] and corresponding to the IO neutrino mass spectrum. The measurement of $\sin^2\theta_{12}$, $\sin^2\theta_{13}$ and $\sin^2\theta_{23}$ with the quoted precision will open up the possibility to distinguish between the BM, TBM/GRB, GRA and HG forms of $\tilde{U}_\nu$. Distinguishing between the TBM and GRB forms would require relatively high precision measurement of $\cos\delta$.

We have performed also a statistical analysis in order to derive predictions for $J_{\rm CP}$. In Fig. 3.4 we present $N_\sigma \equiv \sqrt{\chi^2}$ as a function of $J_{\rm CP}$ for the NO and IO neutrino mass

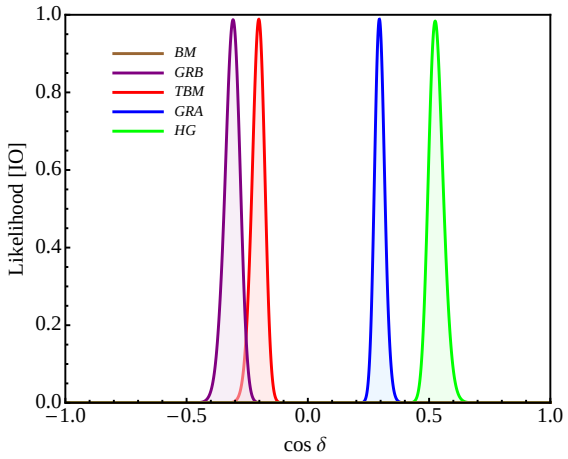

Figure 3.3. The same as in Fig. 3.2, but using the IO best fit values taken from [19].

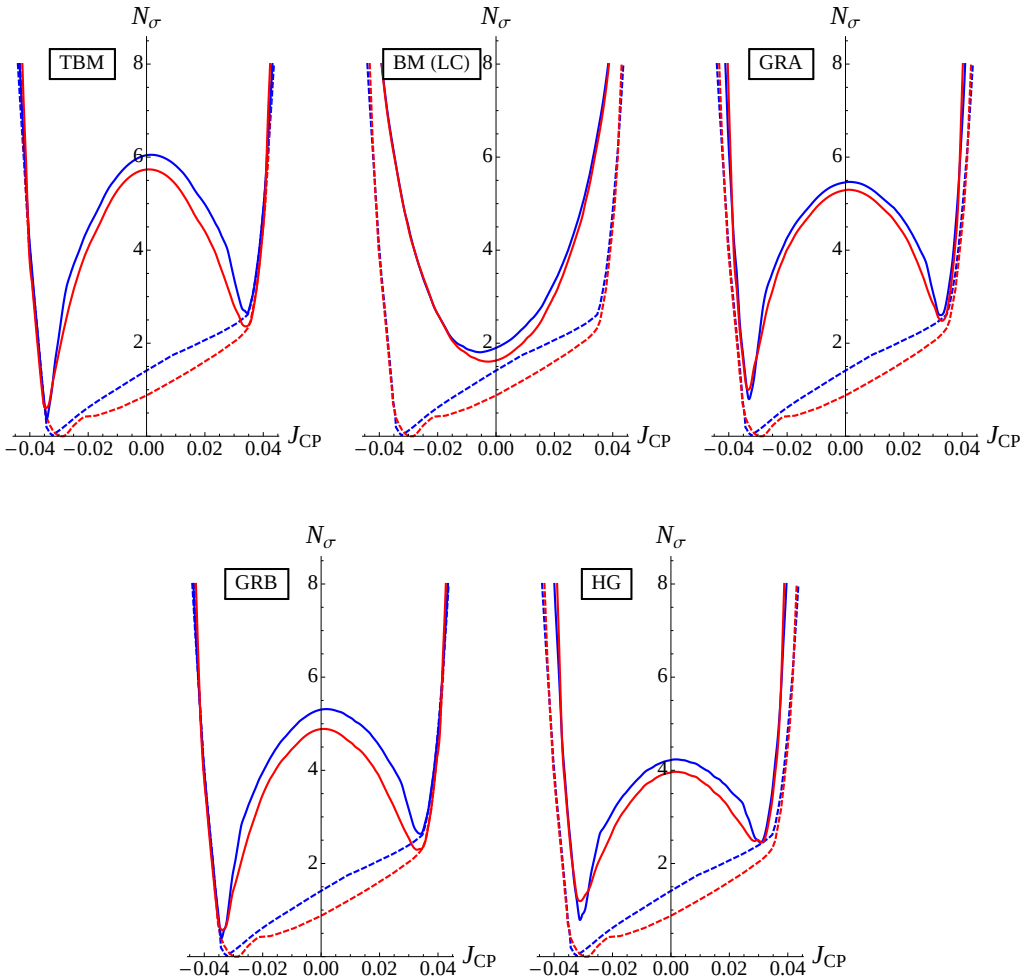

Figure 3.4. $N_\sigma \equiv \sqrt{\chi^2}$ as a function of $J_{\rm CP}$. The dashed lines represent the results of the global fit [18], while the solid lines represent the results we obtain for the TBM, BM (LC), GRA, GRB and HG symmetry forms of the matrix $\tilde{U}_\nu$ in case B1. The blue (red) lines are for the NO (IO) neutrino mass spectrum.

spectra. We minimise the value of χ^2 for a fixed value of $J_{\rm CP}$ by varying $\sin^2\theta_{13}$ and $\sin^2\theta_{23}$ (or, equivalently, $\sin^2\theta^e_{12}$ and $\sin^2\hat{\theta}_{23}$). The best fit values of $J_{\rm CP}$ and the corresponding 3σ ranges for the NO neutrino mass spectrum read:

$$J_{\rm CP} = -0.034\,, \quad -0.038 \leq J_{\rm CP} \leq -0.028, \;\; 0.031 \leq J_{\rm CP} \leq 0.036 \text{ for TBM;} \tag{3.96}$$

$$J_{\rm CP} = -0.005\,, \quad -0.026 \leq J_{\rm CP} \leq 0.021 \text{ for BM (LC);} \tag{3.97}$$

$$J_{\rm CP} = -0.033\,, \quad -0.037 \leq J_{\rm CP} \leq -0.027, \;\; 0.030 \leq J_{\rm CP} \leq 0.035 \text{ for GRA;} \tag{3.98}$$

$$J_{\rm CP} = -0.034\,, \quad -0.039 \leq J_{\rm CP} \leq -0.026, \;\; 0.031 \leq J_{\rm CP} \leq 0.036 \text{ for GRB;} \tag{3.99}$$

$$J_{\rm CP} = -0.031\,, \quad -0.035 \leq J_{\rm CP} \leq -0.020, \;\; 0.026 \leq J_{\rm CP} \leq 0.034 \text{ for HG.} \tag{3.100}$$

As Fig. 3.4 shows, the CP-conserving value of $J_{\rm CP} = 0$ is excluded in the cases of the TBM, GRA, GRB and HG neutrino mixing symmetry forms, respectively, at approximately 5σ, 4σ, 4σ and 3σ confidence levels with respect to the C.L. of the corresponding best fit values.[26] These results correspond to the confidence levels at which the CP-conserving values of $\delta = 0,\ \pi$ are excluded. In contrast, for the BM (LC) symmetry form, the CP-conserving value of δ, namely, $\delta \approx \pi$, is preferred and therefore the CP-violating effects in neutrino oscillations are predicted to be suppressed. The allowed range of the $J_{\rm CP}$ factor in the BM (LC) includes the CP-conserving value $J_{\rm CP} = 0$ at practically any C.L. As can be seen from eqs. (3.96)–(3.100), the 3σ allowed intervals of values of $J_{\rm CP}$ are rather narrow for all the symmetry forms considered, except for the BM (LC) form.

Finally, for completeness, we present in Appendix G also results of a statistical analysis of the predictions for the values of $\sin^2\theta_{23}$ in the cases of TBM, BM (LC), GRA, GRB and HG symmetry forms. We recall that of the three neutrino mixing parameters, $\sin^2\theta_{12}$, $\sin^2\theta_{13}$ and $\sin^2\theta_{23}$, $\sin^2\theta_{23}$ is determined in the global analyses of the neutrino oscillation data with the largest uncertainty.

3.7.2 Case B2

In the left panel of Fig. 3.5 we show the likelihood function defined in eq. (3.95) versus $\cos\delta$ for the NO neutrino mass spectrum in case B2.[27] The maxima of $L(\cos\delta)$, $L(\chi^2 = \chi^2_{\rm min})$, for the different symmetry forms of $\tilde{U}_\nu$ considered, correspond to the values of $\cos\delta$ given in Table 3.5. The results shown are obtained by marginalising over $\sin^2\theta_{13}$ and $\sin^2\theta_{23}$ for a fixed value of δ (for details of the statistical analysis see Appendix F).

As can be observed from the left panel of Fig. 3.5, for the TBM and GRB forms there is a substantial overlap of the corresponding likelihood functions. The same observation holds also for the GRA and HG forms. However, the likelihood functions of these two sets of symmetry forms overlap only at 3σ and in a small interval of values of $\cos\delta$. Thus, the TBM/GRB, GRA/HG and BM (LC) symmetry forms might be distinguished with a not very demanding (in terms of precision) measurement of $\cos\delta$. At the maximum, the likelihood function equals $\exp(-\chi^2_{\rm min}/2)$, and this value allows one to judge quantitatively about the compatibility of a given symmetry form with the global neutrino oscillation data, as we have pointed out in the preceding subsection.

In the right panel of Fig. 3.5 we present L versus $\cos\delta$ within the Gaussian approximation (see Appendix F), using the current best fit values of $\sin^2\theta_{12}$, $\sin^2\theta_{23}$, $\sin^2\theta_{13}$

[26] The confidence levels under discussion differ in the cases of NO and IO neutrino mass spectra, but as Fig. 3.4 indicates, in the cases considered these differences are rather small and we have not given them.

[27] The corresponding results for the IO neutrino mass spectrum differ little from those shown in the left panel of Fig. 3.5.

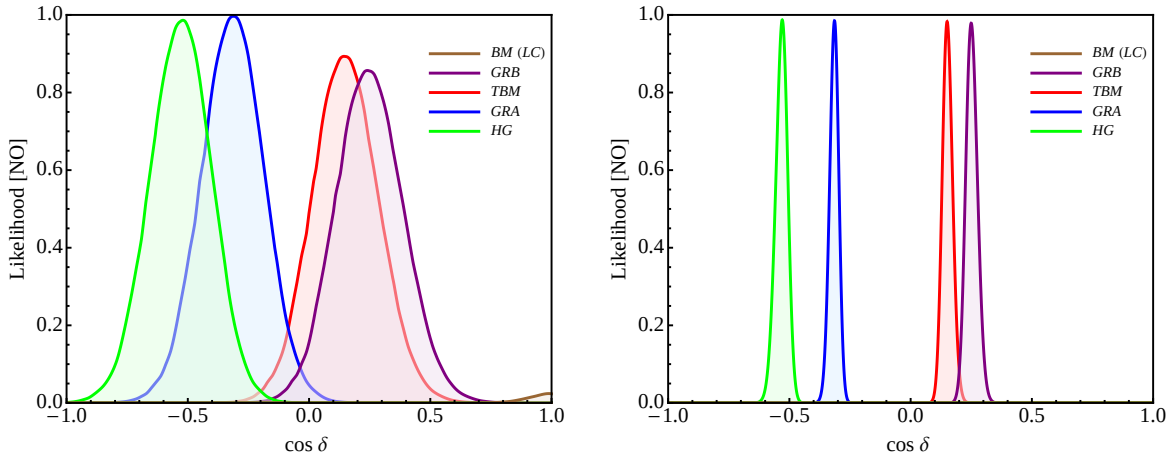

Figure 3.5. The likelihood function versus $\cos\delta$ for the NO neutrino mass spectrum after marginalising over $\sin^2\theta_{13}$ and $\sin^2\theta_{23}$ for the TBM, BM (LC), GRA, GRB and HG symmetry forms of the matrix $\tilde{U}_\nu$ in case B2. The results shown are obtained using eq. (3.42) and (i) the results on the mixing parameters $\sin^2\theta_{12}$, $\sin^2\theta_{13}$, $\sin^2\theta_{23}$ and δ found in the global analysis of neutrino oscillation data [18] (left panel), and (ii) the prospective 1σ uncertainties on $\sin^2\theta_{12}$, $\sin^2\theta_{13}$, $\sin^2\theta_{23}$ and the Gaussian approximation for the likelihood function (right panel). See text and Appendix F for further details.

for the NO spectrum, given in eqs. (2.15)–(2.17), and the prospective 1σ uncertainties in the measurement of these mixing parameters we have used in subsection 3.7.1. The BM (LC) case is quite sensitive to the values of $\sin^2\theta_{12}$ and $\sin^2\theta_{23}$ and for the best fit values is disfavoured at more than 2σ. The fact that the BM (LC) case is disfavoured by the current data can be understood, in particular, from the following observation. Using the best fit values of $\sin^2\theta_{13}$ and $\sin^2\theta_{12}$ as well as the constraint $-1 \leq \cos\alpha \leq 1$, where $\cos\alpha$ is defined in eq. (3.39), one finds that $\sin^2\theta_{23}$ should satisfy $\sin^2\theta_{23} \geq 0.63$, which practically coincides with the maximal value of $\sin^2\theta_{23}$ at 3σ (see eq. (2.16)).

It is interesting to compare the results in cases B1 and B2. The first thing to note is that for a given symmetry form, $\cos\delta$ is predicted to have opposite signs in these two cases. In case B2, one has $\cos\delta > 0$ for the TBM, GRB and BM (LC) symmetry forms of the matrix $\tilde{U}_\nu$, while $\cos\delta < 0$ for the GRA and HG forms. As in case B1, there are significant overlaps between the TBM/GRB and GRA/HG forms of $\tilde{U}_\nu$. The BM (LC) case is disfavoured at more than 2σ C.L. It is also important to note that due to the fact that the best fit value of $\sin^2\theta_{23} < 0.5$ (for the NO spectrum), the predictions for $\cos\delta$ for each symmetry form obtained in the two set-ups differ not only by sign but also in absolute value, as has been already pointed out in Section 3.3.2. Thus, a precise measurement of $\cos\delta$ would allow one to distinguish not only between the symmetry forms of $\tilde{U}_\nu$, but also could provide an indication about the structure of the matrix $\tilde{U}_e$.

For the rephasing invariant $J_{\rm CP}$, using the current global neutrino oscillation data for the NO neutrino mass spectrum, we find the following best fit values and the 3σ ranges:

$$J_{\rm CP} = -0.033\,, \quad -0.039 \leq J_{\rm CP} \leq -0.026, \;\; 0.030 \leq J_{\rm CP} \leq 0.036 \text{ for TBM;} \tag{3.101}$$

$$J_{\rm CP} = -0.004\,, \quad -0.026 \leq J_{\rm CP} \leq 0.023 \text{ for BM (LC) ;} \tag{3.102}$$

$$J_{\rm CP} = -0.032\,, \quad -0.037 \leq J_{\rm CP} \leq -0.024, \;\; 0.029 \leq J_{\rm CP} \leq 0.035 \text{ for GRA;} \tag{3.103}$$

$$J_{\rm CP} = -0.033\,, \quad -0.039 \leq J_{\rm CP} \leq -0.023, \;\; 0.028 \leq J_{\rm CP} \leq 0.036 \text{ for GRB;} \tag{3.104}$$

$$J_{\rm CP} = -0.028\,, \quad -0.035 \leq J_{\rm CP} \leq -0.014, \;\; 0.021 \leq J_{\rm CP} \leq 0.032 \text{ for HG.} \tag{3.105}$$

Thus, relatively large CP-violating effects in neutrino oscillations are predicted for all symmetry forms considered, the only exception being the case of the BM symmetry form.

Finally, we note that the predictions for $\sin^2\theta_{23}$ are rather similar in cases B1 and B2. We give, for completeness, $N_\sigma \equiv \sqrt{\chi^2}$ as a function of $\sin^2\theta_{23}$ in case B2 in Appendix G.

3.7.3 Case C1

In this subsection, we perform a statistical analysis of the predictions for $\cos\delta$ in cases I–V corresponding to specific forms of $\tilde{U}_\nu$ in case C1 (see Section 3.6). The analysis is similar to that performed for cases B1 and B2. The only difference is that when we consider the prospective sensitivities on the PMNS mixing angles, we will assume $\sin^2\theta_{23}$ to have the following potential best fit values: $\sin^2\theta_{23} = 0.488, 0.501, 0.537, 0.545$. Note that for the best fit value of $\sin^2\theta_{13}$, $\sin^2\theta_{23} = 0.488$ does not correspond to any of the values of θ^ν_{13} in the five cases of interest. Thus, $\sin^2\theta_{23} = 0.488$ is not the most probable value in any of these cases: depending on the case, the most probable value is one of the other three values of $\sin^2\theta_{23}$ listed above. We include results for $\sin^2\theta_{23} = 0.488$ to illustrate how the likelihood function changes if the experimentally determined best fit value of $\sin^2\theta_{23}$ differs from the value of $\sin^2\theta_{23}$ predicted in a given case.

In Fig. 3.6 we show the likelihood function versus $\cos\delta$ for all the cases marked with the subscripts in Table 3.3. The maxima of the likelihood function in the five cases considered take place at the corresponding values of $\cos\delta$ given in Table 3.5. As Fig. 3.6 clearly indicates, the cases differ not only in the predictions for $\sin^2\theta_{23}$, which in the considered set-up is a function of $\sin^2\theta^\nu_{13}$ and $\sin^2\theta_{13}$, but also in the predictions for $\cos\delta$. Given the values of θ_{12} and θ_{13}, the positions of the peaks are determined by the values of θ^ν_{12} and θ^ν_{13}.

Cases I and IV are disfavoured by the current data because the corresponding values of $\sin^2\theta_{23} = 0.537$ and 0.545 are disfavoured. Cases II, III and V are less favoured for the NO neutrino mass spectrum than for the IO spectrum since $\sin^2\theta_{23} = 0.501$ is less favoured for the first than for the second spectrum.

In Fig. 3.7 we show the predictions for $\cos\delta$ using the prospective precision in the measurement of $\sin^2\theta_{12}$, $\sin^2\theta_{13}$, $\sin^2\theta_{23}$, the best fit values for $\sin^2\theta_{12}$ and $\sin^2\theta_{13}$ as in eqs. (2.15) and (2.17) and the potential best fit values of $\sin^2\theta_{23} = 0.488, 0.501, 0.537, 0.545$. The values of $\sin^2\theta_{23}$ correspond in the scheme discussed to the best fit value of $\sin^2\theta_{13}$ in the cases which are compatible with the current 1.5σ range of allowed values of $\sin^2\theta_{12}$. The position of the peaks, obviously, does not depend explicitly on the assumed experimentally determined best fit value of $\sin^2\theta_{23}$. For the best fit value of $\sin^2\theta_{13}$ used, the corresponding sum rule for $\cos\delta$ depends on the given fixed value of θ^ν_{13}, and via it, on the predicted value of $\sin^2\theta_{23}$ (see eqs. (3.64) and (3.74)). Therefore, the compatibility of a given case with the considered hypothetical data on $\sin^2\theta_{23}$ clearly depends on the assumed best fit value of $\sin^2\theta_{23}$ determined from the data.

As the results shown in Fig. 3.7 indicate, distinguishing between cases I/IV and the other three cases would not require exceedingly high precision measurement of $\cos\delta$. Distinguishing between cases II, III and V would be more challenging in terms of the requisite precision on $\cos\delta$. In both cases the precision required will depend, in particular, on the experimentally determined best fit value of $\cos\delta$. As Fig. 3.7 also indicates, one of the discussed two groups of cases might be strongly disfavoured by the best fit value of $\sin^2\theta_{23}$ determined in the future high precision experiments.

We have performed also a statistical analysis of the predictions for the rephasing

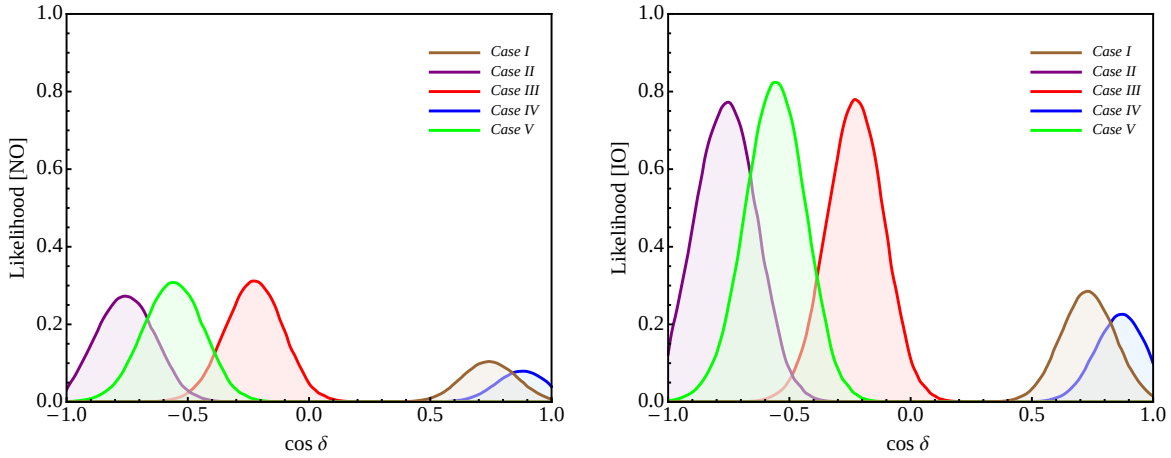

Figure 3.6. The likelihood function versus $\cos\delta$ for the NO (IO) neutrino mass spectrum in the left (right) panel after marginalising over $\sin^2\theta_{13}$ in case C1 with $[\theta^{\nu}_{13}, \theta^{\nu}_{12}]$ fixed as $[\pi/10, -\pi/4]$ (case I), $[\pi/20, b]$ (case II), $[\pi/20, -\pi/4]$ (case III), $[a, -\pi/4]$ (case IV), $[\pi/20, \pi/6]$ (case V), where $a = \sin^{-1}(1/3)$ and $b = \sin^{-1}(1/\sqrt{2+r})$, r being the golden ratio. The figure is obtained using the sum rule in eq. (3.74) and the results on $\sin^2\theta_{ij}$ and δ of the global fit [18].

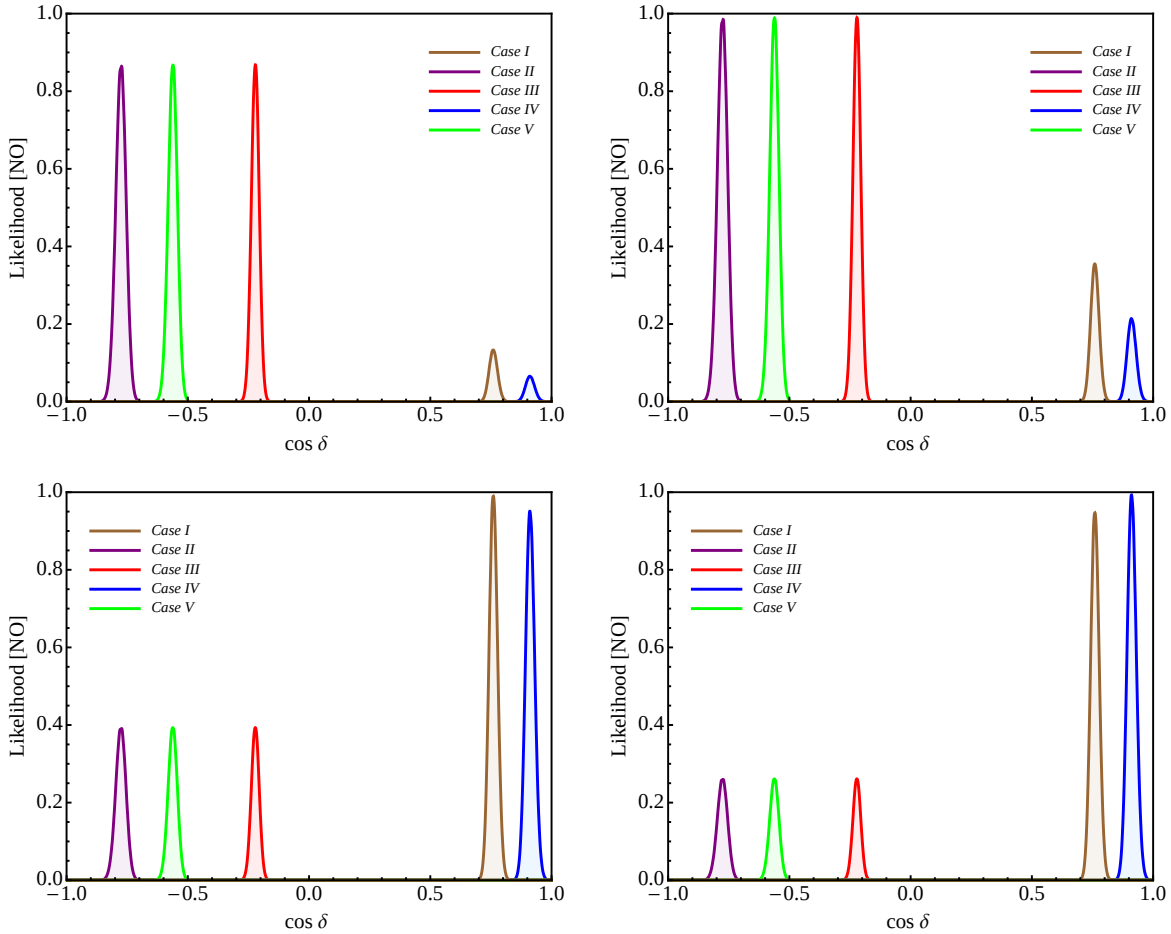

Figure 3.7. The same as in Fig. 3.6, but using the Gaussian approximation with the prospective uncertainties in the measurement of $\sin^2\theta_{ij}$, the best fit values of $\sin^2\theta_{12}$ and $\sin^2\theta_{13}$ as in eqs. (2.15) and (2.17) for the NO spectrum and the potential best fit values of $\sin^2\theta_{23}$. Upper left (right) panel: $(\sin^2\theta_{23})_{\rm BF} = 0.488$ (0.501); lower left (right) panel: $(\sin^2\theta_{23})_{\rm BF} = 0.537$ (0.545). See text and Appendix F for further details.

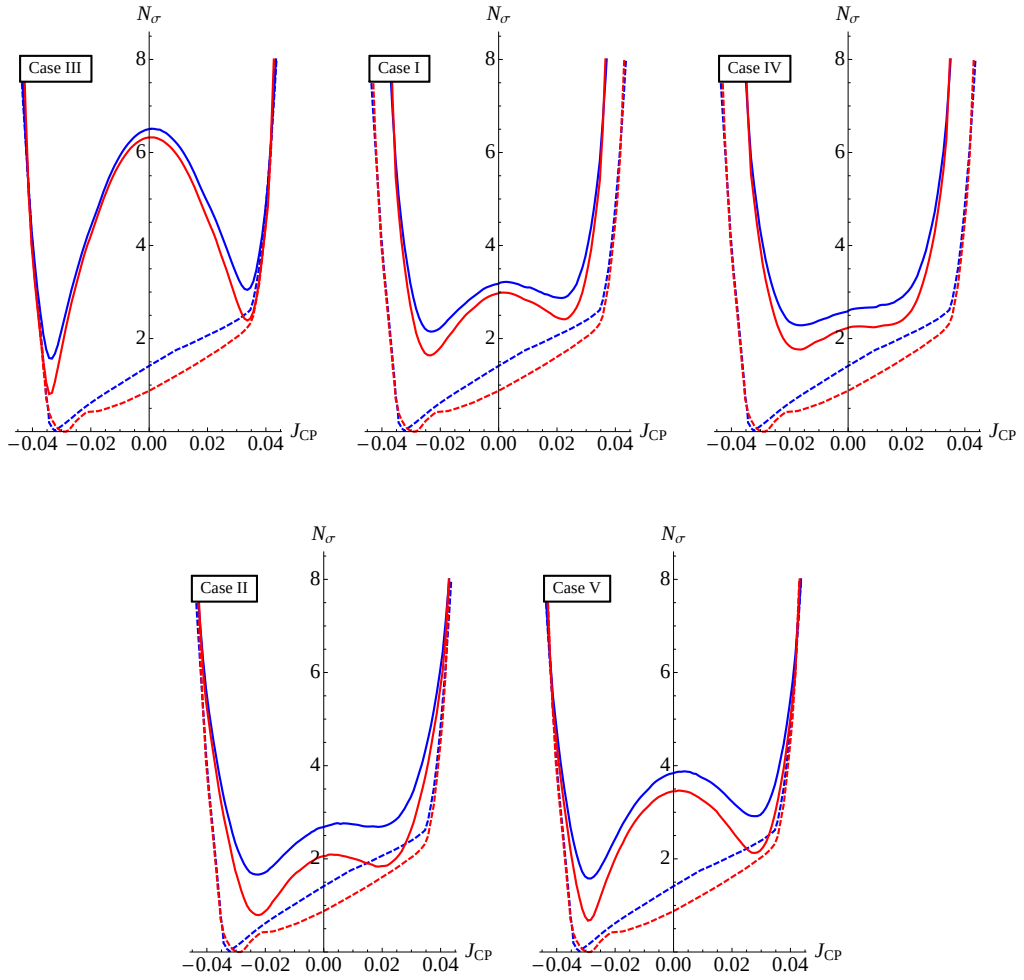

Figure 3.8. $N_\sigma \equiv \sqrt{\chi^2}$ as a function of $J_{\rm CP}$ in case C1 with $[\theta^\nu_{13}, \theta^\nu_{12}]$ fixed as $[\pi/10, -\pi/4]$ (case I), $[\pi/20, b]$ (case II), $[\pi/20, -\pi/4]$ (case III), $[a, -\pi/4]$ (case IV), $[\pi/20, \pi/6]$ (case V), where $a = \sin^{-1}(1/3)$ and $b = \sin^{-1}(1/\sqrt{2+r})$, r being the golden ratio. The dashed lines represent the results of the global fit [18], while the solid lines represent the results we obtain in our set-up. The blue (red) lines are for the NO (IO) neutrino mass spectrum.

invariant $J_{\rm CP}$, minimising χ^2 for fixed values of $J_{\rm CP}$. We give $N_\sigma \equiv \sqrt{\chi^2}$ as a function of $J_{\rm CP}$ in Fig. 3.8. The dashed lines represent the results of the global fit [18], while the solid lines represent the results we obtain for each of the considered cases, minimising the value of χ^2 in θ^e_{12} for a fixed value of $J_{\rm CP}$ using eq. (3.75). The blue lines correspond to the NO neutrino mass spectrum, while the red ones are for the IO spectrum. The value of χ^2 in the minimum, which corresponds to the best fit value of $J_{\rm CP}$ predicted in the model, allows one to conclude about compatibility of this model with the global neutrino oscillation data. As it can be observed from Fig. 3.8, the zero value of $J_{\rm CP}$ in cases III and V is excluded at more than 3σ with respect to the C.L. of the corresponding minimum. Although in the other three cases the best fit values of $J_{\rm CP}$ are relatively large, as their numerical values quoted below show, $J_{\rm CP} = 0$ is only weakly disfavoured statistically. The best fit values and the 3σ ranges of the rephasing invariant $J_{\rm CP}$, obtained using the global neutrino oscillation data for the NO neutrino mass spectrum, read:

$$J_{\rm CP} = -0.023\,, \quad -0.032 \leq J_{\rm CP} \leq 0.029 \text{ in case I;} \tag{3.106}$$

$$J_{\rm CP} = -0.022\,, \quad -0.035 \leq J_{\rm CP} \leq 0.031 \text{ in case II;} \tag{3.107}$$
$$J_{\rm CP} = -0.033\,, \quad -0.039 \leq J_{\rm CP} \leq -0.025,\ 0.030 \leq J_{\rm CP} \leq 0.036 \text{ in case III;} \tag{3.108}$$
$$J_{\rm CP} = -0.016\,, \quad -0.028 \leq J_{\rm CP} \leq 0.026 \text{ in case IV;} \tag{3.109}$$
$$J_{\rm CP} = -0.028\,, \quad -0.037 \leq J_{\rm CP} \leq -0.010,\ 0.018 \leq J_{\rm CP} \leq 0.034 \text{ in case V.} \tag{3.110}$$

3.7.4 Case C2

The statistical analyses of the predictions for $\cos\delta$ and $J_{\rm CP}$ performed in the present subsection are similar to those performed in the previous subsections. In particular, we show in Fig. 3.9 the dependence of the likelihood function on $\cos\delta$ using the current knowledge on the PMNS mixing angles and the Dirac CPV phase from the global fit results [18]. Due to the very narrow prediction for $\sin^2\theta_{23}$ in this set-up, the prospective sensitivity likelihood curve depends strongly on the assumed best fit value of $\sin^2\theta_{23}$. For this reason we present in Fig. 3.10 the predictions for $\cos\delta$ using the prospective sensitivities on the mixing angles, the best fit values for $\sin^2\theta_{12}$ and $\sin^2\theta_{13}$ as in eqs. (2.15) and (2.17) for the NO spectrum and the potential best fit values of $\sin^2\theta_{23} = 0.512,\ 0.499,\ 0.463,\ 0.455$. We use the value of $\sin^2\theta_{23} = 0.512$, corresponding to $\theta^{\nu}_{13} = 0$, for the same reason we used the value of $\sin^2\theta_{23} = 0.488$ in the analysis in the preceding subsection, where we gave also a detailed explanation.

As Fig. 3.10 clearly shows, the position of the peaks does not depend on the assumed best fit value of $\sin^2\theta_{23}$. However, the height of the peaks reflects to what degree the model is disfavoured due to the difference between the assumed best fit value of $\sin^2\theta_{23}$ and the value predicted in the corresponding model.

The results shown in Fig. 3.10 clearly indicate that (i) the measurement of $\cos\delta$ can allow one to distinguish between case I and the other four cases; (ii) distinguishing between cases II/III and cases IV/V might be possible, but is very challenging in terms of the precision on $\cos\delta$ required to achieve that; and (iii) distinguishing between cases II and III (cases IV and V) seems practically impossible. Some of, or even all, these cases would be strongly disfavoured if the best fit value of $\sin^2\theta_{23}$ determined with the assumed high precision in the future experiments were relatively large, say, $\sin^2\theta_{23} \gtrsim 0.54$.

The results on the predictions for the rephasing invariant $J_{\rm CP}$ are presented in Fig. 3.11, where we show the dependence of $N_\sigma \equiv \sqrt{\chi^2}$ on $J_{\rm CP}$. It follows from the results presented in Fig. 3.11, in particular, that $J_{\rm CP} = 0$ is excluded at more than 3σ with respect to the C.L. of the corresponding minimum only in case I. For the rephasing invariant $J_{\rm CP}$, using the global neutrino oscillation data, we find in the case of NO neutrino mass spectrum the following best fit values and 3σ ranges:

$$J_{\rm CP} = -0.033\,, \quad -0.039 \leq J_{\rm CP} \leq -0.025,\ 0.029 \leq J_{\rm CP} \leq 0.037 \text{ in case I;} \tag{3.111}$$
$$J_{\rm CP} = -0.016\,, \quad -0.028 \leq J_{\rm CP} \leq 0.025 \text{ in case II;} \tag{3.112}$$
$$J_{\rm CP} = -0.018\,, \quad -0.029 \leq J_{\rm CP} \leq 0.026 \text{ in case III;} \tag{3.113}$$
$$J_{\rm CP} = -0.023\,, \quad -0.031 \leq J_{\rm CP} \leq 0.029 \text{ in case IV;} \tag{3.114}$$
$$J_{\rm CP} = -0.022\,, \quad -0.030 \leq J_{\rm CP} \leq 0.028 \text{ in case V.} \tag{3.115}$$

3.8 Summary and conclusions

In the present chapter, we have derived predictions for the Dirac phase δ in the PMNS matrix $U = U_e^\dagger\, U_\nu = \tilde{U}_e^\dagger\, \Psi\, \tilde{U}_\nu\, Q_0$, where U_e ($\tilde{U}_e$) and U_ν ($\tilde{U}_\nu$) are 3×3 unitary (CKM-like)

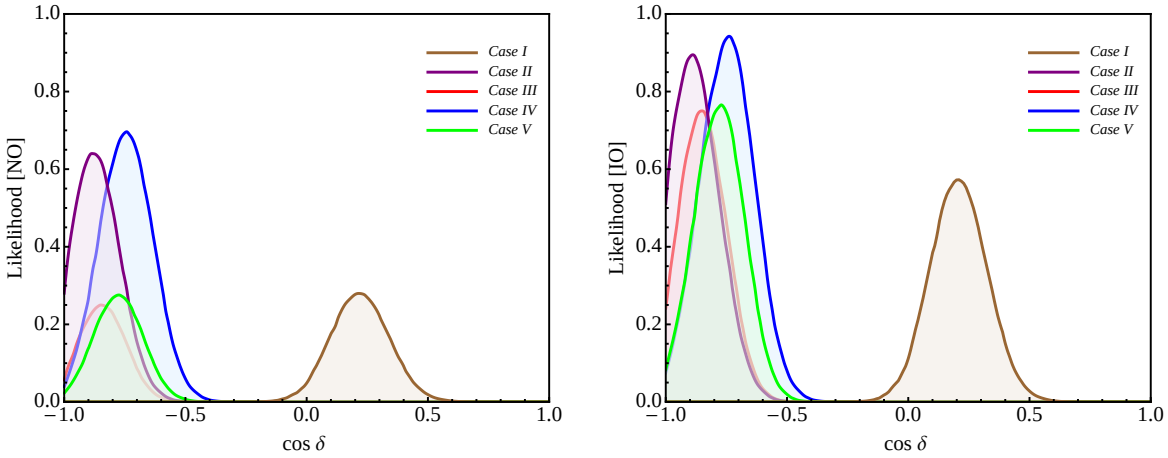

Figure 3.9. The likelihood function versus $\cos\delta$ for the NO (IO) neutrino mass spectrum in the left (right) panel after marginalising over $\sin^2\theta_{13}$ in case C2 with $[\theta^\nu_{13}, \theta^\nu_{12}]$ fixed as $[\pi/20, \pi/4]$ (case I), $[a, \pi/4]$ (case II), $[\pi/20, c]$ (case III), $[\pi/10, \pi/4]$ (case IV), $[\pi/20, \pi/5]$ (case V), where $a = \sin^{-1}(1/3)$ and $c = \sin^{-1}(1/\sqrt{3})$. The figure is obtained using the sum rule in eq. (3.90) and the results on $\sin^2\theta_{ij}$ and δ of the global fit [18].

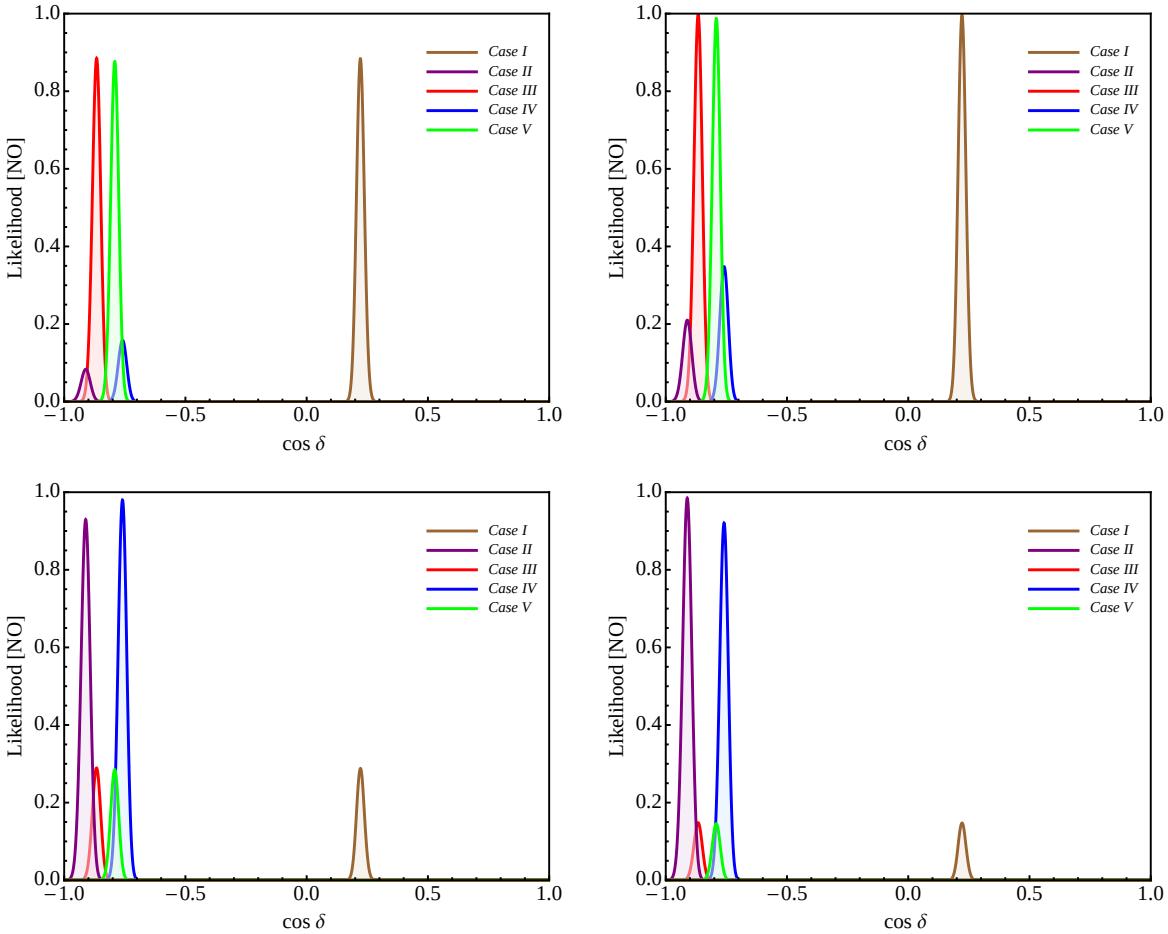

Figure 3.10. The same as in Fig. 3.9, but using the Gaussian approximation with the prospective uncertainties in the measurement of $\sin^2\theta_{ij}$, the best fit values of $\sin^2\theta_{12}$ and $\sin^2\theta_{13}$ as in eqs. (2.15) and (2.17) for the NO spectrum and the potential best fit values of $\sin^2\theta_{23}$. Upper left (right) panel: $(\sin^2\theta_{23})_{\rm BF} = 0.512$ (0.499); lower left (right) panel: $(\sin^2\theta_{23})_{\rm BF} = 0.463$ (0.455). See text and Appendix F for further details.

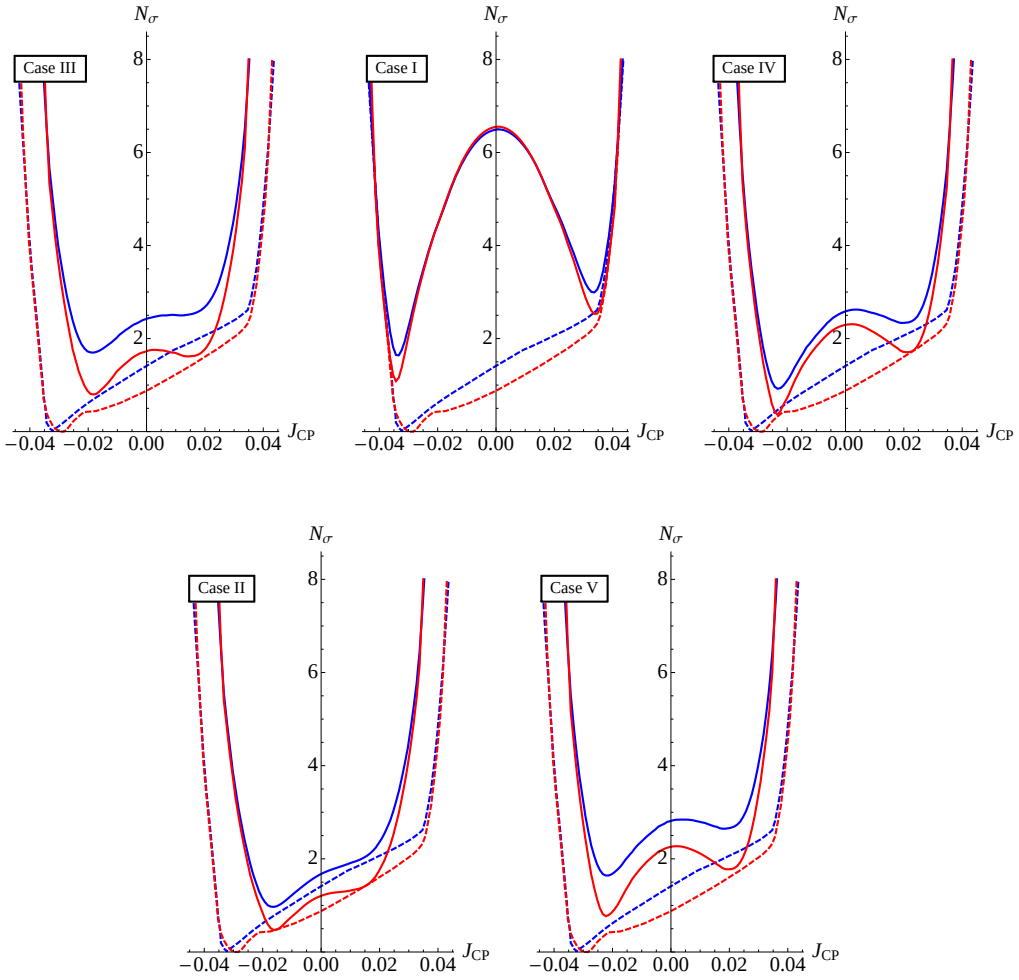

Figure 3.11. $N_\sigma \equiv \sqrt{\chi^2}$ as a function of $J_{\rm CP}$ in case C2 with $[\theta_{13}^\nu, \theta_{12}^\nu]$ fixed as $[\pi/20, \pi/4]$ (case I), $[a, \pi/4]$ (case II), $[\pi/20, c]$ (case III), $[\pi/10, \pi/4]$ (case IV), $[\pi/20, \pi/5]$ (case V), where $a = \sin^{-1}(1/3)$ and $c = \sin^{-1}(1/\sqrt{3})$. The dashed lines represent the results of the global fit [18], while the solid lines represent the results we obtain in our set-up. The blue (red) lines are for the NO (IO) neutrino mass spectrum.

matrices which arise from the diagonalisation, respectively, of the charged lepton and the neutrino mass matrices, and Ψ and Q_0 are diagonal phase matrices each containing in the general case two phases. After performing a systematic search, we have considered forms of $\tilde{U}_e$ and $\tilde{U}_\nu$ allowing us to express δ as a function of the PMNS mixing angles, θ_{12}, θ_{13} and θ_{23}, present in U, and the angles contained in $\tilde{U}_\nu$. We have derived such sum rules for $\cos\delta$ in the cases of forms for which the sum rules of interest do not exist in the literature. More specifically, we have derived new sum rules for $\cos\delta$ in the following cases:

(A1) $U = R_{12}(\theta_{12}^e)\, \Psi\, R_{23}(\theta_{23}^\nu)\, R_{12}(\theta_{12}^\nu)\, Q_0\,,$

(A2) $U = R_{13}(\theta_{13}^e)\, \Psi\, R_{23}(\theta_{23}^\nu)\, R_{12}(\theta_{12}^\nu)\, Q_0\,,$

(B2) $U = R_{13}(\theta_{13}^e)\, R_{23}(\theta_{23}^e)\, \Psi\, R_{23}(\theta_{23}^\nu)\, R_{12}(\theta_{12}^\nu)\, Q_0\,,$

(B3) $U = R_{12}(\theta_{12}^e)\, R_{13}(\theta_{13}^e)\, \Psi\, R_{23}(\theta_{23}^\nu)\, R_{12}(\theta_{12}^\nu)\, Q_0\,,$

(C1) $U = R_{12}(\theta^e_{12})\,\Psi\,R_{23}(\theta^\nu_{23})\,R_{13}(\theta^\nu_{13})\,R_{12}(\theta^\nu_{12})\,Q_0\,,$

(C2) $U = R_{13}(\theta^e_{13})\,\Psi\,R_{23}(\theta^\nu_{23})\,R_{13}(\theta^\nu_{13})\,R_{12}(\theta^\nu_{12})\,Q_0\,,$

where R_{ij} are real orthogonal matrices describing rotations in the i-j plane, and θ^e_{ij} and θ^ν_{ij} stand for the rotation angles contained in $\tilde{U}_e$ and $\tilde{U}_\nu$, respectively. Case B1 with

$$U = R_{12}(\theta^e_{12})\,R_{23}(\theta^e_{23})\,\Psi\,R_{23}(\theta^\nu_{23})\,R_{12}(\theta^\nu_{12})\,Q_0$$

has been extensively studied in [99, 102]. In the sum rules, $\cos\delta$ is expressed, in general, in terms of the three angles of the PMNS matrix, θ_{12}, θ_{13} and θ_{23}, measured, e.g., in the neutrino oscillation experiments, and the angles in $\tilde{U}_\nu$, which are assumed to have fixed known values. In case B3, $\cos\delta$ depends in addition on an a priori unknown phase ω, whose value can only be fixed in a self-consistent model of neutrino mass generation. A summary of the sum rules derived in the present chapter is given in Table 3.1.

To obtain predictions for $\cos\delta$, δ and the $J_{\rm CP}$ factor, which controls the magnitude of the CP-violating effects in neutrino oscillations, we have considered several forms of $\tilde{U}_\nu$ determined by, or associated with, symmetries, for which the angles in $\tilde{U}_\nu$ have specific values. More concretely, in cases A1, A2 and B1–B3, we have performed analyses for the TBM, BM (LC), GRA, GRB, and HG forms of $\tilde{U}_\nu$. For all these forms, we have $\theta^\nu_{23} = -\pi/4$ and $\theta^\nu_{13} = 0$. The forms differ by the value of the angle θ^ν_{12} given in Section 3.1. In cases C1 and C2 with non-zero fixed values of θ^ν_{13}, which are also inspired by certain types of flavour symmetries, we have considered three representative values of θ^ν_{13} discussed in the literature, $\theta^\nu_{13} = \pi/20,\ \pi/10$ and $\sin^{-1}(1/3)$, in combination with specific values of θ^ν_{12} — altogether five sets of different pairs of values of $[\theta^\nu_{13}, \theta^\nu_{12}]$ in each of the two cases. They are given in Table 3.5.

We first obtained predictions for $\cos\delta$ and δ using the best fit values of $\sin^2\theta_{12}$, $\sin^2\theta_{13}$ and $\sin^2\theta_{23}$ given in eqs. (2.15)–(2.17). They are summarised in Tables 3.5 and 3.6. The quoted values of $\cos\delta$ and δ in case B3 are for $\omega = 0$. We have not presented predictions for the BM (LC) symmetry form of $\tilde{U}_\nu$ in Tables 3.5 and 3.6, because for the best fit values of $\sin^2\theta_{12}$, $\sin^2\theta_{23}$ and $\sin^2\theta_{13}$, the corresponding sum rules were found to give unphysical values of $\cos\delta$.

We have performed next a statistical analysis of the predictions (i) for $\cos\delta$ and $J_{\rm CP}$ using the results of the global analysis of neutrino oscillation data, and (ii) for $\cos\delta$ using prospective sensitivities on the PMNS mixing angles. This was done by constructing the corresponding likelihood functions.

We have found that in case A1 the results for χ^2 as a function of δ or $J_{\rm CP}$ are rather similar to those obtained in case B1. The main difference between these two cases is the predictions for $\sin^2\theta_{23}$, which can deviate only by approximately $0.5\sin^2\theta_{13}$ from 0.5 in the first case, and by a significantly larger amount in the second. Similar conclusions hold comparing the results in cases A2 and B2. Therefore, in what concerns these four cases, we have presented results of the statistical analysis of the predictions for $\cos\delta$ and the $J_{\rm CP}$ factor only in cases B1 and B2. This was done for the TBM, BM (LC), GRA, GRB and HG forms of the matrix $\tilde{U}_\nu$. We have found, in particular, that for a given symmetry form, $\cos\delta$ is predicted to have opposite sign in cases B1 and B2. Namely, in case B2, one has $\cos\delta > 0$ for the TBM, GRB and BM (LC) forms, and $\cos\delta < 0$ for the GRA and HG forms, while in case B1 the situation is opposite. In both cases, there are significant overlaps between the predictions for $\cos\delta$ for the TBM and GRB forms, and for the GRA and HG forms. The BM (LC) case is disfavoured at more than 2σ C.L. Due to the fact that the best fit value of $\sin^2\theta_{23} < 0.5$ (for the NO spectrum), the predictions for $\cos\delta$

for each symmetry form, obtained in the discussed two set-ups, differ not only by sign but also in absolute value. We found also that in both cases relatively large CP-violating effects in neutrino oscillations are predicted for all symmetry forms considered, the only exception being the case of the BM symmetry form.

In cases C1 and C2, we have performed statistical analyses of the predictions for $\cos\delta$ and the $J_{\rm CP}$ factor for the five sets of values of the angles $[\theta_{13}^{\nu}, \theta_{12}^{\nu}]$ listed in Table 3.5. These sets differ for the two cases. For the values of $[\theta_{13}^{\nu}, \theta_{12}^{\nu}]$ given in Tables 3.5, the allowed intervals of values of $\sin^2\theta_{12}$ in cases C1 and C2, in particular, satisfy the requirement that they contain the best fit value and the 1.5σ experimentally allowed range of $\sin^2\theta_{12}$. In these two cases, the value of $\sin^2\theta_{23}$ is determined by the values of θ_{13}, θ_{13}^{ν} and θ_{23}^{ν} (see Table 3.2). In the statistical analyses we have performed θ_{23}^{ν} was set to $-\pi/4$. Setting $\sin^2\theta_{13}$ to its best fit value, in case C1 for $\theta_{13}^{\nu} = 0$, $\pi/20$, $\pi/10$ and $\sin^{-1}(1/3)$ we found, respectively, $\sin^2\theta_{23} = 0.488$, 0.501, 0.537 and 0.545. For the same values of $\sin^2\theta_{13}$ and θ_{13}^{ν}, we obtained in case C2, $\sin^2\theta_{23} = 0.512$, 0.499, 0.463 and 0.455.

Further, the statistical analyses we have performed showed that for each of the two set-ups, the five cases considered form two groups for which $\cos\delta$ differs in sign and in magnitude (Figs. 3.6 and 3.9). This suggests that distinguishing between the two groups for each of the two set-ups considered could be achieved with a not very demanding (in terms of precision) measurement of $\cos\delta$. In the analyses performed using the prospective sensitivities on $\sin^2\theta_{12}$, $\sin^2\theta_{13}$ and $\sin^2\theta_{23}$, assuming that the best fit values of $\sin^2\theta_{12}$, $\sin^2\theta_{13}$ will not change, we have chosen as potential best fit values of $\sin^2\theta_{23}$ those predicted by the two set-ups in the five cases considered (the values are listed in the preceding paragraph). These analyses have revealed, in particular, that for each of the two set-ups, distinguishing between the cases inside the two groups which provide opposite sign predictions for $\cos\delta$ would be more challenging in terms of the requisite precision on $\cos\delta$. For certain pairs of cases predicting $\cos\delta < -0.5$ in set-up C2, this seems impossible to achieve in practice. These conclusions are well illustrated by Figs. 3.7 and 3.10. However, we have found that, depending on the chosen potential best fit value of $\sin^2\theta_{23}$, some of the cases are strongly disfavoured. Thus, a high precision measurement of $\sin^2\theta_{23}$ would certainly rule out some of (if not all) the cases of the two set-ups we have considered.

The analysis performed of the predictions for the $J_{\rm CP}$ factor showed that in set-up C1, the CP-conserving value of $J_{\rm CP} = 0$ is excluded at more than 3σ with respect to the C.L. of the corresponding minimum, in two cases, namely, for $[\theta_{13}^{\nu}, \theta_{12}^{\nu}] = [\pi/20, -\pi/4]$ and $[\pi/20, \pi/6]$ (denoted in the text as cases III and V). In the other three cases in spite of the relatively large predicted best fit values of $J_{\rm CP}$, $J_{\rm CP} = 0$ is only weakly disfavoured (Fig. 3.8). In set-up C2, $J_{\rm CP} = 0$ is excluded at more than 3σ (with respect to the C.L. of the corresponding minimum), only in one case (denoted as case I in the text), namely, for $[\theta_{13}^{\nu}, \theta_{12}^{\nu}] = [\pi/20, \pi/4]$ (Fig. 3.11).

The results obtained in the present chapter show that the measurement of the Dirac phase in the PMNS mixing matrix, together with an improvement of the precision on the mixing angles θ_{12}, θ_{13} and θ_{23}, can provide unique information as regards the possible existence of symmetry in the lepton sector. These measurements could also provide an indication about the structure of the matrix $\tilde{U}_e$ originating from the charged lepton sector, and thus, about the charged lepton mass matrix.

Chapter 4

The Majorana phases and neutrinoless double beta decay

In the present chapter, we continue the discussion of the neutrino mixing schemes considered in Chapter 3 focusing on predictions for the *Majorana phases* in the PMNS matrix U. We show that for most of these mixing schemes the Majorana phases α_{21} and α_{31} can be expressed in terms of the three neutrino mixing angles θ_{12}, θ_{13} and θ_{23} and the angles and the two Majorana-like phases ξ_{21} and ξ_{31} present, in general, in U_ν (see eqs. (3.1) and (3.2)). The angles in U_ν are assumed to be fixed by a flavour symmetry. We demonstrate that the requirement of generalised CP invariance of the neutrino Majorana mass term discussed in Section 1.3 implies $\xi_{21} = 0$ or π and $\xi_{31} = 0$ or π, and therefore, in most of the cases, the Majorana phases themselves are predicted in terms of the mixing angles only.

Throughout this chapter, we will use the best fit values and 3σ allowed ranges of $\sin^2\theta_{12}$, $\sin^2\theta_{23}$ and $\sin^2\theta_{13}$ obtained in [162] and summarised below:

$$(\sin^2\theta_{12})_{\rm BF} = 0.297\,, \quad 0.250 \leq \sin^2\theta_{12} \leq 0.354\,, \tag{4.1}$$

$$(\sin^2\theta_{23})_{\rm BF} = 0.437\ (0.569)\,, \quad 0.379\ (0.383) \leq \sin^2\theta_{23} \leq 0.616\ (0.637)\,, \tag{4.2}$$

$$(\sin^2\theta_{13})_{\rm BF} = 0.0214\ (0.0218)\,, \quad 0.0185\ (0.0186) \leq \sin^2\theta_{13} \leq 0.0246\ (0.0248)\,. \tag{4.3}$$

The values (values in brackets) correspond to the NO (IO) neutrino mass spectrum.

Since the mixing schemes considered in the present chapter are the same as in the previous one, the structure of this chapter is analogous to that of Chapter 3. Namely, in Section 4.1, we obtain sum rules for $(\alpha_{21} - \xi_{21})$ and $(\alpha_{31} - \xi_{31})$ in cases A1 and A2 containing one rotation from the charged lepton sector, i.e., $\tilde{U}_e = R_{12}^{-1}(\theta_{12}^e)$ or $\tilde{U}_e = R_{13}^{-1}(\theta_{13}^e)$, and two rotations from the neutrino sector, $\tilde{U}_\nu = R_{23}(\theta_{23}^\nu)\, R_{12}(\theta_{12}^\nu)$. In these cases the PMNS matrix has the form given in eq. (3.12). We obtain results in the general case of arbitrary fixed values of θ_{23}^ν and θ_{12}^ν. In Section 4.2, we analyse cases B1, B2 and B3 with $\tilde{U}_e = R_{23}^{-1}(\theta_{23}^e)\, R_{12}^{-1}(\theta_{12}^e)$, $\tilde{U}_e = R_{23}^{-1}(\theta_{23}^e)\, R_{13}^{-1}(\theta_{13}^e)$ and $\tilde{U}_e = R_{13}^{-1}(\theta_{13}^e)\, R_{12}^{-1}(\theta_{12}^e)$, respectively, and the two rotations from the neutrino sector. The corresponding parametrisation of the PMNS matrix in these cases is given in eq. (3.13). Again we provide results for arbitrary fixed values of θ_{23}^ν and θ_{12}^ν. Further, in Section 4.3, we extend the analysis performed in Section 4.1 to cases C1 and C2, for which $\tilde{U}_\nu$ contains three rotations, $\tilde{U}_\nu = R_{23}(\theta_{23}^\nu)\, R_{13}(\theta_{13}^\nu)\, R_{12}(\theta_{12}^\nu)$, and the PMNS matrix is given by eq. (3.14). Section 4.4 contains a brief summary of the sum rules for the Majorana phases $\alpha_{21}/2$ and $\alpha_{31}/2$ derived in Sections 4.1–4.3. Using these sum rules, we present in Section 4.5 predictions for phase differences $(\alpha_{21}/2 - \xi_{21}/2)$, $(\alpha_{31}/2 - \xi_{31}/2)$, etc., which are determined only by the values of the three neutrino mixing angles θ_{12}, θ_{23} and θ_{13}, and of the fixed angles θ_{ij}^ν. In cases A1, A2 and B1–B3, we give results for values of θ_{23}^ν $(= -\pi/4)$ and θ_{12}^ν, corresponding to the TBM, BM (LC), GRA, GRB and HG symmetry forms of $\tilde{U}_\nu$. In each of cases C1 and

C2, the reported results are for $\theta^{\nu}_{23} = -\pi/4$ and five sets of values of θ^{ν}_{13} and θ^{ν}_{12} associated with symmetries, which have been identified in Section 3.6. We then set $(\xi_{21}, \xi_{31}) = (0,0)$, $(0,\pi)$, $(\pi,0)$ and (π,π) and use the resulting values of α_{21} and α_{31} to derive graphical predictions for the absolute value of the effective Majorana mass in $(\beta\beta)_{0\nu}$-decay, $|\langle m\rangle|$, as a function of the lightest neutrino mass in the schemes of mixing studied. We show in Section 4.6 that the requirement of generalised CP invariance of the neutrino Majorana mass term in the cases of A_4, T', S_4 and A_5 lepton flavour symmetries leads indeed to $\xi_{21} = 0$ or π, and $\xi_{31} = 0$ or π. Section 4.7 contains summary of the results of the present chapter and conclusions.

4.1 Mixing schemes with $\tilde{U}^{\dagger}_{e} = R_{ij}(\theta^{e}_{ij})$ and $\tilde{U}_{\nu} = R_{23}(\theta^{\nu}_{23})\, R_{12}(\theta^{\nu}_{12})$

In this section, we derive sum rules for α_{21} and α_{31} of interest in the case when the matrix $\tilde{U}_{\nu} = R_{23}(\theta^{\nu}_{23})\, R_{12}(\theta^{\nu}_{12})$ with fixed (e.g., symmetry) values of the angles θ^{ν}_{23} and θ^{ν}_{12}, gets correction only due to one rotation from the charged lepton sector. The neutrino mixing matrix U has the form given in eq. (3.12). We do not consider the case of eq. (3.12) with $(ij) = (23)$, because in this case the reactor angle $\theta_{13} = 0$, and thus, the measured value of $\theta_{13} \approx 0.15$ cannot be reproduced.

4.1.1 Case A1: θ^{e}_{12}

In the present subsection we consider the parametrisation of the neutrino mixing matrix given in eq. (3.12) with $(ij) = (12)$. In this parametrisation the PMNS matrix has the form

$$U = R_{12}(\theta^{e}_{12})\, \Psi\, R_{23}(\theta^{\nu}_{23})\, R_{12}(\theta^{\nu}_{12})\, Q_0\,. \tag{4.4}$$

The phase ω in the phase matrix Ψ is unphysical.

We are interested in deriving analytic expressions for the Majorana phases α_{21} and α_{31} (i) in terms of the parameters of the parametrisation in eq. (4.4), θ^{e}_{12}, ψ, θ^{ν}_{23}, θ^{ν}_{12}, ξ_{21} and ξ_{31}, and possibly (ii) in terms of the angles θ_{12}, θ_{13}, θ_{23} and the Dirac phase δ of the standard parametrisation of the PMNS matrix, the fixed angles θ^{ν}_{23} and θ^{ν}_{12}, and the phases ξ_{21} and ξ_{31}. The values of the phases α_{21} and α_{31} in the latter case, as we will see, indeed depend on the value of the Dirac phase δ.

The sum rules for α_{21} and α_{31} we are aiming to obtain in this subsection turn out to be a particular case of the sum rules derived in [99]. This becomes clear from a comparison of eq. (18) in [99], which fixes the parametrisation of U used in [99], and the expression for U in eq. (4.4). It shows that to get the sum rules for α_{21} and α_{31} of interest, one has formally to set $\hat{\theta}_{23} = \theta^{\nu}_{23}$, $\phi = -\psi$ and $\beta = 0$ in the sum rules for α_{21} and α_{31} derived in eq. (102) in [99] and to take into account the two possible signs of the product $c^{e}_{12}c^{\nu}_{23}s^{\nu}_{23} \equiv \cos\theta^{e}_{12}\cos\theta^{\nu}_{23}\sin\theta^{\nu}_{23}$:

$$\frac{\alpha_{21}}{2} = \beta_{e2} - \beta_{e1} + \frac{\xi_{21}}{2}\,, \tag{4.5}$$

$$\frac{\alpha_{31}}{2} = \beta_{e2} + \tilde{\varphi} + \frac{\xi_{31}}{2}\,, \quad e^{i\tilde{\varphi}} = \mathrm{sgn}(c^{e}_{12}c^{\nu}_{23}s^{\nu}_{23}) = +1 \text{ or } -1\,. \tag{4.6}$$

Thus, $\tilde{\varphi} = 0$ or π. The results in eqs. (4.5) and (4.6) can be obtained formally from eqs. (88), (89) and (95) in [99] by setting $\hat{\theta}_{23} = \theta_{23}^\nu$, $\phi = -\psi$, $Q_1 = \mathrm{diag}(1,1,1)$ and $Q_2 = \mathrm{diag}(1, e^{i(\beta_{e2}-\beta_{e1})}, \mathrm{sgn}(c_{12}^e c_{23}^\nu s_{23}^\nu)\, e^{i\beta_{e2}})$. We note that in the case considered of arbitrary fixed signs of c_{12}^e, $s_{12}^e \equiv \sin\theta_{12}^e$, c_{23}^ν and s_{23}^ν, the U_{e3} element of the PMNS matrix in eq. (95) in [99] must also be replaced by $U_{e3}\,\mathrm{sgn}(c_{12}^e s_{12}^e c_{23}^\nu)$. Correspondingly, in terms of the parametrisation in eq. (4.4) of the PMNS matrix, the phases β_{e2} and β_{e1} are given by eqs. (90) and (91) in [99]:

$$\beta_{e1} = \arg(U_{e1}) = \arg\left(c_{12}^e c_{12}^\nu - s_{12}^e c_{23}^\nu s_{12}^\nu e^{-i\psi}\right)\,, \tag{4.7}$$

$$\beta_{e2} = \arg(U_{e2}\, e^{-i\frac{\xi_{21}}{2}}) = \arg\left(c_{12}^e s_{12}^\nu + s_{12}^e c_{23}^\nu c_{12}^\nu e^{-i\psi}\right)\,, \tag{4.8}$$

where $c_{12}^\nu \equiv \cos\theta_{12}^\nu$ and $s_{12}^\nu \equiv \sin\theta_{12}^\nu$. For $\tilde{\varphi} = 0$, eq. (4.6) reduces to the expression for $\alpha_{31}/2$ in eq. (102) in [99].

As can be shown employing the formalism developed in [99] and taking into account the possibility of negative signs of $c_{12}^e s_{12}^\nu$ and $c_{12}^e c_{12}^\nu$, the expressions for the phases β_{e2} and β_{e1} in terms of the angles θ_{12}, θ_{13}, θ_{23} and the Dirac phase δ of the standard parametrisation of the PMNS matrix have the form:

$$\beta_{e2} = \arg\left(U_{\tau 1}\mathrm{sgn}(c_{12}^e s_{12}^\nu)\right) = \arg\left[\left(s_{12}s_{23} - c_{12}c_{23}s_{13}e^{i\delta}\right)\mathrm{sgn}(c_{12}^e s_{12}^\nu)\right]\,, \tag{4.9}$$

$$\beta_{e1} = \arg\left(U_{\tau 2}\, e^{i\pi}\mathrm{sgn}(c_{12}^e c_{12}^\nu)\, e^{-i\frac{\alpha_{21}}{2}}\right) = \arg\left[\left(c_{12}s_{23} + s_{12}c_{23}s_{13}e^{i\delta}\right)\mathrm{sgn}(c_{12}^e c_{12}^\nu)\right]\,. \tag{4.10}$$

For $\mathrm{sgn}(c_{12}^e s_{12}^\nu) = 1$ and $\mathrm{sgn}(c_{12}^e c_{12}^\nu) = 1$, eqs. (4.9) and (4.10) reduce respectively to eqs. (100) and (101) in ref. [99].

It follows from eqs. (4.9) and (4.10) that the phases β_{e1} and β_{e2} are determined by the values of the standard parametrisation mixing angles θ_{12}, θ_{13}, θ_{23} and of the Dirac phase δ. The phase δ is also determined (up to a sign ambiguity of $\sin\delta$) by the values of "standard" angles θ_{12}, θ_{13}, θ_{23} via the sum rule given in eq. (3.17). Since the relations in eqs. (4.5) and (4.6) between the Majorana phases α_{21} and α_{31} and the phases β_{e1} and β_{e2} involve the phases ξ_{21} and ξ_{31} originating from the diagonalisation of the neutrino Majorana mass term, α_{21} and α_{31} will be determined by the values of the "standard" neutrino mixing angles θ_{12}, θ_{13}, θ_{23} (up to the mentioned ambiguity related to the undetermined so far sign of $\sin\delta$), provided the values of ξ_{21} and ξ_{31} are known. Thus, predictions for the Majorana phases α_{21} and α_{31} can be obtained when the phases ξ_{21} and ξ_{31} are fixed by additional considerations of, e.g., generalised CP invariance, symmetries, etc. In theories with discrete lepton flavour symmetries the phases ξ_{21} and ξ_{31} are often determined by the employed symmetries of the theory (see, e.g., [122, 130, 131, 145, 149] and references quoted therein). We will show in Section 4.6 how the phases ξ_{21} and ξ_{31} are fixed by the requirement of generalised CP invariance of the neutrino Majorana mass term in the cases of the non-Abelian discrete flavour symmetries A_4, T', S_4 and A_5. In all these cases the generalised CP invariance constraint fixes the values of ξ_{21} and ξ_{31}, which allows us to obtain predictions for the Majorana phases α_{21} and α_{31}.

The phases β_{e1}, β_{e2}, ψ and δ can be shown to satisfy the relation:

$$\delta = \psi + \beta_{e1} + \beta_{e2} + \varphi\,, \quad e^{i\varphi} = \mathrm{sgn}(c_{12}^e s_{12}^e c_{23}^\nu) = +1 \text{ or } -1\,. \tag{4.11}$$

For $\varphi = 0$ ($\mathrm{sgn}(c_{12}^e s_{12}^e c_{23}^\nu) = +1$), this relation reduces to eq. (94) in ref. [99] by setting $\psi = -\phi$. From eqs. (4.5), (4.6) and (4.11) we get further

$$(\alpha_{31} - \xi_{31}) - \frac{1}{2}(\alpha_{21} - \xi_{21}) = \beta_{e1} + \beta_{e2} + 2\tilde{\varphi} = \delta - \psi - \varphi\,, \quad \varphi = 0 \text{ or } \pi\,, \tag{4.12}$$

where we took into account that $2\tilde{\varphi} = 0$ or 2π.

The Dirac phase δ and the phase ψ are related [99]. We will give below only the relation between $\sin\delta$ and $\sin\psi$. It can be obtained from eq. (28) in [99] by setting[28] $\phi = -\psi$ and by taking into account that in the case considered both signs of $\sin 2\theta^e_{12}\cos\theta^\nu_{23}$ are, in principle, allowed:[29]

$$\sin\delta = \mathrm{sgn}\left(\sin 2\theta^e_{12}\cos\theta^\nu_{23}\right)\frac{\sin 2\theta^\nu_{12}}{\sin 2\theta_{12}}\,\sin\psi\,. \tag{4.13}$$

We note that within the approach employed in our analysis, the results presented in eqs. (4.5)–(4.13) are exact and are valid for arbitrary fixed values of θ^ν_{12} and θ^ν_{23} and for arbitrary signs of $\sin\theta^e_{12}$ and $\cos\theta^e_{12}$ ($|\sin\theta^e_{12}|$ and $|\cos\theta^e_{12}|$ can be expressed in terms of θ_{13} and θ^ν_{23} as can be seen from eq. (3.15)).

Although the sum rules derived above allow to determine the values of the Majorana phases α_{21} and α_{31} (up to a two-fold ambiguity related to the ambiguity of $\mathrm{sgn}(\sin\delta)$ or of $\mathrm{sgn}(\sin\psi)$) if the phases ξ_{21} and ξ_{31} are known, we will present below an alternative method of determination of α_{21} and α_{31}, which can be used in the cases when the method developed in [99] cannot be applied. The alternative method makes use of the rephasing invariants associated with the two Majorana phases of the PMNS matrix.

In the case of 3-neutrino mixing under discussion there are, in principle, three independent CPV rephasing invariants. The first is the $J_{\rm CP}$ factor associated with the Dirac phase δ defined in eqs. (1.6) and (1.7). The other two, I_1 and I_2, are related to the two Majorana CPV phases in the PMNS matrix and can be chosen as [40, 163–165]:[30]

$$I_1 = \mathrm{Im}\left\{U^*_{e1}\,U_{e2}\right\}\,, \quad I_2 = \mathrm{Im}\left\{U^*_{e1}\,U_{e3}\right\}\,.$$

The rephasing invariants associated with the Majorana phases are not uniquely determined. Instead of I_1 defined above we could have chosen, e.g., $I'_1 = \mathrm{Im}\left\{U^*_{\tau1}\,U_{\tau2}\right\}$ or $I''_1 = \mathrm{Im}\left\{U_{\mu1}U^*_{\mu2}\right\}$, while instead of I_2 we could have used $I'_2 = \mathrm{Im}\left\{U^*_{\tau2}\,U_{\tau3}\right\}$, or $I''_2 = \mathrm{Im}\left\{U_{\mu2}\,U^*_{\mu3}\right\}$. However, the three invariants — $J_{\rm CP}$ and any two chosen Majorana phase invariants — form a complete set in the case of 3-neutrino mixing: any other two rephasing invariants associated with the Majorana phases can be expressed in terms of the two chosen Majorana phase invariants and the $J_{\rm CP}$ factor [163, 165]. We note also that CP violation due to the Majorana phase α_{21} requires that both $I_1 = \mathrm{Im}\left\{U^*_{e1}U_{e2}\right\} \neq 0$ and $\mathrm{Re}\left\{U^*_{e1}U_{e2}\right\} \neq 0$ [164]. Similarly, $I_2 = \mathrm{Im}\left\{U^*_{e1}U_{e3}\right\} \neq 0$ would imply violation of the CP symmetry only if in addition $\mathrm{Re}\left\{U^*_{e1}U_{e3}\right\} \neq 0$.

In the standard parametrisation of the PMNS matrix U, the rephasing invariants I_1 and I_2 are given by

$$I_1 = \cos\theta_{12}\sin\theta_{12}\cos^2\theta_{13}\sin(\alpha_{21}/2)\,, \tag{4.14}$$

$$I_2 = \cos\theta_{12}\sin\theta_{13}\cos\theta_{13}\sin(\alpha_{31}/2-\delta)\,. \tag{4.15}$$

Comparing these expressions with the expressions for I_1 and I_2 in the parametrisation of U defined in eq. (4.4), we can obtain sum rules for $\sin(\alpha_{21}/2)$ and $\sin(\alpha_{31}/2-\delta)$ in terms of θ^e_{12}, ψ, θ^ν_{12}, θ^ν_{23}, ξ_{21}, ξ_{31} and the standard parametrisation mixing angles θ_{12} and θ_{13}.

[28] The relation between $\cos\delta$ and $\cos\psi$ can be deduced from eq. (29) in [99].

[29] In [99] both $\sin 2\theta^e_{12}$ and $\cos\theta^\nu_{23}$ could be and were considered to be positive without loss of generality.

[30] The expressions for the invariants $I_{1,2}$ we give correspond to Majorana conditions satisfied by the fields of the light massive Majorana neutrinos, which do not contain phase factors, see, e.g., [40].

The resulting formulae are quite lengthy and we do not present them here. They can be found in ref. [140].

In terms of the standard parametrisation mixing angles θ_{12}, θ_{13}, θ_{23} and the Dirac phase δ, the angles θ_{12}^ν and θ_{23}^ν, and the phases ξ_{21} and ξ_{31}, the expressions for $\sin(\alpha_{21}/2)$ and $\sin(\alpha_{31}/2)$ read:

$$\sin(\alpha_{21}/2) = \frac{1}{\sin^2\theta_{23}^\nu \sin 2\theta_{12}^\nu}\Big[\sin 2\theta_{23}\sin\theta_{13}\big(\sin(\xi_{21}/2-\delta) - 2\cos^2\theta_{12}\cos\delta\sin(\xi_{21}/2)\big) + \sin(\xi_{21}/2)\sin 2\theta_{12}\big(\sin^2\theta_{23} - \cos^2\theta_{23}\sin^2\theta_{13}\big)\Big]\,, \tag{4.16}$$

$$\sin(\alpha_{31}/2) = \frac{\mathrm{sgn}(c_{23}^\nu)}{\sin\theta_{12}^\nu \sin\theta_{23}^\nu}\Big[\sin\theta_{12}\sin\theta_{23}\sin(\xi_{31}/2) - \cos\theta_{12}\cos\theta_{23}\sin\theta_{13}\sin(\xi_{31}/2+\delta)\Big]\,, \tag{4.17}$$

where, we recall, $\sin^2\theta_{23}^\nu = 1 - \cos^2\theta_{23}\cos^2\theta_{13}$.

The phases ξ_{21} and ξ_{31}, as we have already discussed, are supposed to be fixed by symmetry arguments. Thus, it proves convenient to have analytic expressions which allow to calculate the phase differences $(\alpha_{21}/2 - \xi_{21}/2)$ and $(\alpha_{31}/2 - \xi_{31}/2)$. We find for $\sin(\alpha_{21}/2 - \xi_{21}/2)$ and $\sin(\alpha_{31}/2 - \xi_{31}/2)$:

$$\sin(\alpha_{21}/2 - \xi_{21}/2) = -\frac{\sin 2\theta_{23}\sin\theta_{13}}{\sin^2\theta_{23}^\nu \sin 2\theta_{12}^\nu}\,\sin\delta\,, \tag{4.18}$$

$$\sin(\alpha_{31}/2 - \xi_{31}/2) = -\frac{\mathrm{sgn}(\cos\theta_{23}^\nu)}{\sin\theta_{12}^\nu\sin\theta_{23}^\nu}\,\sin\theta_{13}\cos\theta_{12}\cos\theta_{23}\sin\delta\,. \tag{4.19}$$

It follows from eqs. (4.18) and (4.19) that $|\sin(\alpha_{21(31)}/2 - \xi_{21(31)}/2)| \propto \sin\theta_{13}$. Using the results given in eqs. (4.5), (4.6), (4.9), (4.10), (3.17), and the best fit values of the neutrino oscillation parameters quoted in eqs. (4.1)–(4.3), we can obtain predictions for the values of the phases $(\alpha_{21}/2 - \xi_{21}/2)$ and $(\alpha_{31}/2 - \xi_{31}/2)$ for the symmetry forms of $\tilde{U}_\nu$ (TBM, BM (LC), GRA, etc.) considered. These predictions as well as predictions for the values of $(\alpha_{21}/2 - \xi_{21}/2)$ and $(\alpha_{31}/2 - \xi_{31}/2)$ in the cases investigated in the next subsection and in Sections 4.2 and 4.3 will be presented in Section 4.5.

4.1.2 Case A2: $\boldsymbol{\theta_{13}^e}$

In the present subsection, we consider the parametrisation of the neutrino mixing matrix given in eq. (3.12) with $(ij) = (13)$. In this parametrisation the PMNS matrix has the form

$$U = R_{13}(\theta_{13}^e)\,\Psi\, R_{23}(\theta_{23}^\nu)\, R_{12}(\theta_{12}^\nu)\, Q_0\,. \tag{4.20}$$

Now the phase ψ in the phase matrix Ψ is unphysical.

Equating the expressions for the rephasing invariant associated with the Dirac phase in the PMNS matrix, $J_{\rm CP}$, obtained in the standard parametrisation and in the parametrisation given in eq. (4.20) allows us to get a relation between $\sin\delta$ and $\sin\omega$:

$$\sin\delta = \mathrm{sgn}(\sin 2\theta_{13}^e \sin\theta_{23}^\nu)\frac{\sin 2\theta_{12}^\nu}{\sin 2\theta_{12}}\sin\omega\,. \tag{4.21}$$

As can be shown using the method developed in [99] and employed in the preceding subsection, the phases δ, $\alpha_{21}/2$ and $\alpha_{31}/2$ are related with the phase ω and the phases β_{e1} and β_{e2},

$$\beta_{e1} = \arg\left(U_{e1}\right) = \arg\left(c^e_{13}c^\nu_{12} + s^e_{13}s^\nu_{23}s^\nu_{12}e^{-i\omega}\right) , \tag{4.22}$$

$$\beta_{e2} = \arg(U_{e2}\, e^{-i\frac{\xi_{21}}{2}}) = \arg\left(c^e_{13}s^\nu_{12} - s^e_{13}s^\nu_{23}c^\nu_{12}e^{-i\omega}\right) , \tag{4.23}$$

in the following way:

$$\delta = \omega + \beta_{e1} + \beta_{e2} + \arg\left(s^e_{13}c^e_{13}s^\nu_{23}\right) , \tag{4.24}$$

$$\frac{\alpha_{21}}{2} = \beta_{e2} - \beta_{e1} + \frac{\xi_{21}}{2} , \tag{4.25}$$

$$\frac{\alpha_{31}}{2} = \beta_{e2} + \frac{\xi_{31}}{2} + \arg\left(c^e_{13}s^\nu_{23}c^\nu_{23}\right) . \tag{4.26}$$

From eqs. (4.24) – (4.26) we get a relation analogous to that in eq. (4.12) in the preceding subsection:

$$(\alpha_{31} - \xi_{31}) - \frac{1}{2}\left(\alpha_{21} - \xi_{21}\right) = \beta_{e1} + \beta_{e2} = \delta - \omega - \arg\left(s^e_{13}c^e_{13}s^\nu_{23}\right) , \tag{4.27}$$

where we took into account that $2\arg\left(c^e_{13}s^\nu_{23}c^\nu_{23}\right) = 0$ or 2π.

It is not difficult to derive expressions for β_{e1} and β_{e2} in terms of the angles θ_{12}, θ_{13}, θ_{23} and the phase δ of the standard parametrisation of the PMNS matrix. They read:

$$\beta_{e1} = \arg\left(U_{\mu 2}\,\mathrm{sgn}\left(c^e_{13}c^\nu_{12}\right)e^{-i\frac{\alpha_{21}}{2}}\right) = \arg\left[\left(c_{12}c_{23} - s_{12}s_{23}s_{13}e^{i\delta}\right)\mathrm{sgn}\left(c^e_{13}c^\nu_{12}\right)\right] , \tag{4.28}$$

$$\beta_{e2} = \arg\left(U_{\mu 1}\, e^{i\pi}\mathrm{sgn}\left(c^e_{13}s^\nu_{12}\right)\right) = \arg\left[\left(s_{12}c_{23} + c_{12}s_{23}s_{13}e^{i\delta}\right)\mathrm{sgn}\left(c^e_{13}s^\nu_{12}\right)\right] . \tag{4.29}$$

It proves convenient for the calculation of the Majorana phases to use expressions of $\sin(\alpha_{21}/2)$ and $\sin(\alpha_{31}/2)$ in terms of the standard parametrisation mixing angles θ_{12}, θ_{13}, θ_{23}, the Dirac phase δ, and the angles θ^ν_{12} and θ^ν_{23} fixed by symmetries. The expressions of interest are not difficult to derive and they read:

$$\begin{aligned}\sin(\alpha_{21}/2) = \frac{1}{\sin 2\theta^\nu_{12}\cos^2\theta^\nu_{23}}\Big[&- \sin 2\theta_{23}\sin\theta_{13}\left(\sin(\xi_{21}/2-\delta) - 2\cos^2\theta_{12}\cos\delta\sin(\xi_{21}/2)\right) \\ &+ \sin 2\theta_{12}\left(\cos^2\theta_{23} - \sin^2\theta_{23}\sin^2\theta_{13}\right)\sin(\xi_{21}/2)\Big] ,\end{aligned} \tag{4.30}$$

$$\sin(\alpha_{31}/2) = \frac{\mathrm{sgn}(s^\nu_{23})}{\sin\theta^\nu_{12}\cos\theta^\nu_{23}}\Big[\sin\theta_{12}\cos\theta_{23}\sin(\xi_{31}/2) + \cos\theta_{12}\sin\theta_{23}\sin\theta_{13}\sin(\xi_{31}/2+\delta)\Big] . \tag{4.31}$$

We recall that $\sin^2\theta^\nu_{23} = \cos^2\theta_{13}\sin^2\theta_{23}$ in this case (see eq. (3.26)).

The expressions for $\sin(\alpha_{21}/2 - \xi_{21})$ and $\sin(\alpha_{31}/2 - \xi_{31})$ take the simple forms:

$$\sin(\alpha_{21}/2 - \xi_{21}/2) = \frac{\sin 2\theta_{23}\sin\theta_{13}}{\sin 2\theta^\nu_{12}\cos^2\theta^\nu_{23}}\sin\delta\,, \tag{4.32}$$

$$\sin(\alpha_{31}/2 - \xi_{31}/2) = \frac{\mathrm{sgn}(s^\nu_{23})}{\sin\theta^\nu_{12}\cos\theta^\nu_{23}}\cos\theta_{12}\sin\theta_{23}\sin\theta_{13}\sin\delta\,. \tag{4.33}$$

Equations (4.32) and (4.33) do not allow one to obtain unique predictions for $\sin(\alpha_{21}/2 - \xi_{21}/2)$ and $\sin(\alpha_{31}/2 - \xi_{31}/2)$ because of the ambiguity in determining the sign of $\sin\delta$. As in the case discussed in the preceding subsection, we have $|\sin(\alpha_{21}/2 - \xi_{21}/2)| \propto \sin\theta_{13}$ and $|\sin(\alpha_{31}/2 - \xi_{31}/2)| \propto \sin\theta_{13}$.

4.2 Mixing schemes with $\tilde{U}_e^\dagger = R_{ij}(\theta_{ij}^e)\, R_{kl}(\theta_{kl}^e)$ and $\tilde{U}_\nu = R_{23}(\theta_{23}^\nu)\, R_{12}(\theta_{12}^\nu)$

As it follows from eqs. (3.16) and (3.26), in the cases when the matrix $\tilde{U}_e$ originating from the charged lepton sector contains one rotation angle (θ_{12}^e or θ_{13}^e) and $\theta_{23}^\nu = -\pi/4$, the mixing angle θ_{23} cannot deviate significantly from $\pi/4$ due to the smallness of the angle θ_{13}. If the matrix $\tilde{U}_\nu$ has one of the symmetry forms considered by us, the matrix $\tilde{U}_e$ has to contain at least two rotation angles in order to be possible to reproduce the current best fit values of the neutrino mixing parameters quoted in eqs. (4.1)–(4.3), or more generally, in order to be possible to account for deviations of $\sin^2\theta_{23}$ from 0.5 which are bigger than $\sin^2\theta_{13}$, i.e., for $\sin^2\theta_{23} \neq 0.5(1 \mp \sin^2\theta_{13})$. In this section, we consider the determination of the Majorana phases α_{21} and α_{31} in the cases when the matrix $\tilde{U}_e$ contains two rotation angles.

4.2.1 Case B1: θ_{12}^e and θ_{23}^e

The PMNS matrix in this scheme has the form

$$U = R_{12}(\theta_{12}^e)\, R_{23}(\theta_{23}^e)\, \Psi\, R_{23}(\theta_{23}^\nu)\, R_{12}(\theta_{12}^\nu)\, Q_0\,. \tag{4.34}$$

The scheme has been analysed in detail in [99], where a sum rule for $\cos\delta$ and analytic expressions for α_{21} and α_{31} were derived for $\theta_{23}^\nu = -\pi/4$. As we have pointed out in subsection 3.2.1, the sum rule for $\cos\delta$ found in [99] holds for an arbitrary fixed value of θ_{23}^ν. The sum rule under discussion is given in eq. (3.10). However, in contrast to the case considered in subsection 4.1.1, the PMNS mixing angle θ_{23} in the scheme under discussion can differ significantly from θ_{23}^ν and from $\pi/4$.

The PMNS matrix in eq. (4.34) can be recast in the following way [99]:

$$U = R_{12}(\theta_{12}^e)\, \Phi(\phi)\, R_{23}(\hat{\theta}_{23})\, R_{12}(\theta_{12}^\nu)\, \hat{Q}\,, \tag{4.35}$$

where $\Phi = \mathrm{diag}(1, e^{i\phi}, 1)$ and the angle $\hat{\theta}_{23}$, the matrix $\hat{Q}$ and the phases ϕ and β are defined in eqs. (3.32), (3.33), (3.34) and (3.35).

The analytic results on the Majorana phases α_{21} and α_{31}, on the relation between the Dirac phase δ and the phase ϕ, etc., derived in [99], do not depend explicitly on the value of the angle θ_{23}^ν and are valid in the case under consideration. Thus, generalising eqs. (88)–(91), (94) and (102) in [99] for arbitrary sings of s_{12}^e, c_{12}^e, s_{12}^ν and c_{12}^ν, we have:

$$\frac{\alpha_{21}}{2} = \beta_{e2} - \beta_{e1} + \frac{\xi_{21}}{2}\,, \quad \frac{\alpha_{31}}{2} = \beta_{e2} + \beta_{\mu 3} - \phi + \beta + \frac{\xi_{31}}{2}\,, \tag{4.36}$$

$$\delta = \beta_{e1} + \beta_{e2} + \beta_{\mu 3} - \beta_{e3} - \phi\,, \tag{4.37}$$

where

$$\beta_{e1} = \arg\left(U_{e1}\right) = \arg\left(c_{12}^e c_{12}^\nu - s_{12}^e \hat{c}_{23} s_{12}^\nu e^{i\phi}\right)\,, \tag{4.38}$$

$$\beta_{e2} = \arg\left(U_{e2}\, e^{-i\frac{\xi_{21}}{2}}\right) = \arg\left(c_{12}^e s_{12}^\nu + s_{12}^e \hat{c}_{23} c_{12}^\nu e^{i\phi}\right)\,, \tag{4.39}$$

$$\beta_{e3} = \arg\left(U_{e3} e^{-i\left(\beta + \frac{\xi_{31}}{2}\right)}\right) = \arg\left(s_{12}^e\right) + \phi\,, \tag{4.40}$$

$$\beta_{\mu 3} = \arg\left(U_{\mu 3} e^{-i\left(\beta + \frac{\xi_{31}}{2}\right)}\right) = \arg\left(c^e_{12}\right) + \phi\,, \tag{4.41}$$

with $\hat{c}_{23} \equiv \cos\hat{\theta}_{23}$. The preceding results can be obtained by casting U in eq. (4.35) in the standard parametrisation form. This leads, in particular, to additional contribution to the matrix $\hat{Q}$ of the Majorana phases, which takes the form $\hat{Q} = Q_2\, Q_1\, Q_0$, where the generalisation of the corresponding expression for Q_2 in [99] reads: $Q_2 = \mathrm{diag}\left(1, e^{i(\beta_{e2}-\beta_{e1})}, e^{i(\beta_{e2}+\beta_{\mu 3}-\phi)}\right)$. Note that we got rid of the common unphysical phase factor $e^{-i(\beta_{e2}+\beta_{\mu 3}-\phi)}$ in the matrix Q_2.

The expressions for the phases $(\beta_{e2} + \beta_{\mu 3} - \phi)$ and $(\beta_{e1} + \beta_{\mu 3} - \phi)$ in terms of the angles θ_{12}, θ_{13}, θ_{23} and the Dirac phases δ of the standard parametrisation of the PMNS matrix have the form (cf. eqs. (100) and (101) in ref. [99]):

$$\beta_{e2} + \beta_{\mu 3} - \phi = \arg\left(U_{\tau 1}\right) - \beta_{\tau 1} = \arg\left(s_{12}s_{23} - c_{12}c_{23}s_{13}e^{i\delta}\right) - \beta_{\tau 1}\,, \tag{4.42}$$

$$\beta_{e1} + \beta_{\mu 3} - \phi = \arg\left(U_{\tau 2} e^{-i\frac{\alpha_{21}}{2}}\right) - \beta_{\tau 2} = \arg\left(-c_{12}s_{23} - s_{12}c_{23}s_{13}e^{i\delta}\right) - \beta_{\tau 2}\,, \tag{4.43}$$

where

$$\beta_{\tau 1} = \arg(s^\nu_{12})\,, \quad \beta_{\tau 2} = \arg(-c^\nu_{12})\,. \tag{4.44}$$

We also have

$$\sin\delta = -\,\mathrm{sgn}\left(\sin 2\theta^e_{12}\right)\frac{\sin 2\theta^\nu_{12}}{\sin 2\theta_{12}}\,\sin\phi\,. \tag{4.45}$$

A few comments are in order. As like the cosine of the Dirac phase δ, $\cos\phi$ satisfies a sum rule by which it is expressed in terms of the three measured neutrino mixing angles θ_{12}, θ_{13} and θ_{23}, and is uniquely determined by the values of θ_{12}, θ_{13} and θ_{23} [99]. The values of $\sin\delta$ and $\sin\phi$, however, are fixed up to a sign. Through eq. (4.45) the signs $\sin\delta$ and $\sin\phi$ are correlated. Thus, δ and ϕ are predicted with an ambiguity related to the ambiguity of the sign of $\sin\delta$ (or of $\sin\phi$). Together with eqs. (4.42) and (4.43) this implies that also the phases β_{e1} and β_{e2} are determined by the values of θ_{12}, θ_{13}, θ_{23} and δ with a two-fold ambiguity. The knowledge of the difference $(\beta_{e2} - \beta_{e1})$ allows to determine the Majorana phase α_{21} (up to the discussed two-fold ambiguity) if the value of the phase ξ_{21} is known. In contrast, the knowledge of β_{e2} and ξ_{31} is not enough to predict the value of the Majorana phase α_{31} since it receives a contribution also from the phase β that cannot be fixed on general phenomenological grounds. It is possible to determine the phase β in certain specific cases (see [99] for a detailed discussion of the cases when β can be fixed). It should be noted, however, that the term involving the phase α_{31} in the $(\beta\beta)_{0\nu}$-decay effective Majorana mass $\langle m\rangle$ gives practically a negligible contribution in $|\langle m\rangle|$ in the cases of neutrino mass spectrum with IO or of QD type [40, 99]. In these cases we have [166, 167] $|\langle m\rangle| \gtrsim 0.014$ eV (see also, e.g., [8, 39]). Values of $|\langle m\rangle| \gtrsim 0.014$ eV are in the range of planned sensitivity of the future large scale $(\beta\beta)_{0\nu}$-decay experiments (see, e.g., [43]).

In terms of the "standard" angles θ_{12}, θ_{13}, θ_{23} and the phase δ, $\sin(\alpha_{21}/2)$ and $\sin(\alpha_{31}/2)$ are given by

$$\begin{aligned}\sin(\alpha_{21}/2) = \frac{\cos(\beta_{\tau 2} - \beta_{\tau 1})}{2|U_{\tau 1}U_{\tau 2}|}\Big[&\sin 2\theta_{23}\sin\theta_{13}\left(\sin(\delta + \xi_{21}/2) - 2\sin^2\theta_{12}\cos\delta\sin(\xi_{21}/2)\right)\\ &- \sin 2\theta_{12}\left(\sin^2\theta_{23} - \cos^2\theta_{23}\sin^2\theta_{13}\right)\sin(\xi_{21}/2)\Big]\,,\end{aligned} \tag{4.46}$$

$$\sin(\alpha_{31}/2) = \frac{\cos\beta_{\tau 1}}{|U_{\tau 1}|}\Big[\sin\theta_{12}\sin\theta_{23}\sin(\xi_{31}/2+\beta) - \cos\theta_{12}\cos\theta_{23}\sin\theta_{13}\sin(\delta+\beta+\xi_{31}/2)\Big]\,. \tag{4.47}$$

The sign factors $\cos(\beta_{\tau 2}-\beta_{\tau 1})$ and $\cos\beta_{\tau 1}$ are known once the angle θ_{12}^ν is fixed:

$$\cos(\beta_{\tau 2}-\beta_{\tau 1}) = -\,\mathrm{sgn}\,(s_{12}^\nu c_{12}^\nu)\;, \quad \cos\beta_{\tau 1} = \mathrm{sgn}\,(s_{12}^\nu)\;. \tag{4.48}$$

The expressions for $\sin(\alpha_{21}/2-\xi_{21}/2)$ and $\sin(\alpha_{31}/2-\xi_{31}/2-\beta)$ have the following simple forms:

$$\sin(\alpha_{21}/2-\xi_{21}/2) = \frac{\cos(\beta_{\tau 2}-\beta_{\tau 1})}{2|U_{\tau 1}U_{\tau 2}|}\sin 2\theta_{23}\sin\theta_{13}\sin\delta\,, \tag{4.49}$$

$$\sin(\alpha_{31}/2-\xi_{31}/2-\beta) = -\frac{\cos\beta_{\tau 1}}{|U_{\tau 1}|}\cos\theta_{12}\cos\theta_{23}\sin\theta_{13}\sin\delta\,. \tag{4.50}$$

It follows from eqs. (4.49) and (4.50) that since $\sin\delta$ can be expressed in terms of the "standard" neutrino mixing angles θ_{12}, θ_{23} and θ_{13}, $\sin(\alpha_{21}/2-\xi_{21}/2)$ and $\sin(\alpha_{31}/2-\xi_{31}/2-\beta)$ are determined (up to an ambiguity related to the sign of $\sin\delta$) by the values of θ_{12}, θ_{23} and θ_{13}. Equations (4.49) and (4.50) imply that also in the discussed case $|\sin(\alpha_{21}/2-\xi_{21}/2)| \propto \sin\theta_{13}$ and $|\sin(\alpha_{31}/2-\xi_{31}/2-\beta)| \propto \sin\theta_{13}$.

4.2.2 Case B2: θ_{13}^e and θ_{23}^e

In this subsection, we consider the parametrisation of the PMNS matrix as in eq. (3.13) with $(ij)-(kl) = (13)-(23)$. Analogously to the previous subsection, this parametrisation can be recast in the form of eq. (3.30). In explicit form this equation reads

$$U = \begin{pmatrix} c_{13}^e c_{12}^\nu + s_{13}^e \hat{s}_{23} s_{12}^\nu e^{-i\alpha} & c_{13}^e s_{12}^\nu - s_{13}^e \hat{s}_{23} c_{12}^\nu e^{-i\alpha} & s_{13}^e \hat{c}_{23} e^{-i\alpha} \\ -\hat{c}_{23} s_{12}^\nu & \hat{c}_{23} c_{12}^\nu & \hat{s}_{23} \\ -s_{13}^e c_{12}^\nu + c_{13}^e \hat{s}_{23} s_{12}^\nu e^{-i\alpha} & -s_{13}^e s_{12}^\nu - c_{13}^e \hat{s}_{23} c_{12}^\nu e^{-i\alpha} & c_{13}^e \hat{c}_{23} e^{-i\alpha} \end{pmatrix} \hat{Q}\,. \tag{4.51}$$

To bring this matrix to the standard parametrisation form, we first rewrite it as follows:

$$U = \begin{pmatrix} |U_{e1}| e^{i\beta_{e1}} & |U_{e2}| e^{i\beta_{e2}} & |U_{e3}| e^{i\beta_{e3}} \\ |U_{\mu 1}| e^{i\beta_{\mu 1}} & |U_{\mu 2}| e^{i\beta_{\mu 2}} & |U_{\mu 3}| \\ |U_{\tau 1}| e^{i\beta_{\tau 1}} & |U_{\tau 2}| e^{i\beta_{\tau 2}} & |U_{\tau 3}| e^{i\beta_{\tau 3}} \end{pmatrix} \hat{Q}\,, \tag{4.52}$$

where

$$\beta_{e1} = \arg\left(c_{13}^e c_{12}^\nu + s_{13}^e \hat{s}_{23} s_{12}^\nu e^{-i\alpha}\right)\,, \tag{4.53}$$

$$\beta_{e2} = \arg\left(c_{13}^e s_{12}^\nu - s_{13}^e \hat{s}_{23} c_{12}^\nu e^{-i\alpha}\right)\,, \tag{4.54}$$

$$\beta_{e3} = \arg\left(s_{13}^e\right) - \alpha\,, \tag{4.55}$$

$$\beta_{\mu 1} = \arg\left(-s_{12}^\nu\right)\,, \tag{4.56}$$

$$\beta_{\mu 2} = \arg\left(c_{12}^\nu\right)\,, \tag{4.57}$$

$$\beta_{\tau 1} = \arg\left(-s^e_{13}c^\nu_{12} + c^e_{13}\hat{s}_{23}s^\nu_{12}e^{-i\alpha}\right)\,, \tag{4.58}$$

$$\beta_{\tau 2} = \arg\left(-s^e_{13}s^\nu_{12} - c^e_{13}\hat{s}_{23}c^\nu_{12}e^{-i\alpha}\right)\,, \tag{4.59}$$

$$\beta_{\tau 3} = \arg\left(c^e_{13}\right) - \alpha\,. \tag{4.60}$$

We recall that the angle $\hat{\theta}_{23}$ belongs to the first quadrant by construction.

Further, comparing the expressions for the $J_{\rm CP}$ invariant in the standard parametrisation and in the parametrisation given in eq. (3.30), we have[31]

$$\sin\delta = \mathrm{sgn}\left(\sin 2\theta^e_{13}\right)\frac{\sin 2\theta^\nu_{12}}{\sin 2\theta_{12}}\sin\alpha\,. \tag{4.61}$$

It is not difficult to check that this relation holds if

$$\delta = \beta_{e1} + \beta_{e2} + \beta_{\tau 3} - \beta_{e3} + \alpha\,, \quad \beta_{\tau 3} - \beta_{e3} = 0 \text{ or } \pi\,, \tag{4.62}$$

which, in turn, suggests what rearrangement of the phases in the PMNS matrix in eq. (4.52) one has to do to bring it to the standard parametrisation form. Namely, the required rearrangement should be made in the following way:

$$U = P_2 \begin{pmatrix} |U_{e1}| & |U_{e2}| & |U_{e3}|e^{-i\delta} \\ |U_{\mu 1}|e^{i(\beta_{\mu 1}+\beta_{e2}+\beta_{\tau 3}+\alpha)} & |U_{\mu 2}|e^{i(\beta_{\mu 2}+\beta_{e1}+\beta_{\tau 3}+\alpha)} & |U_{\mu 3}| \\ |U_{\tau 1}|e^{i(\beta_{\tau 1}+\beta_{e2}+\alpha)} & |U_{\tau 2}|e^{i(\beta_{\tau 2}+\beta_{e1}+\alpha)} & |U_{\tau 3}| \end{pmatrix} Q_2\,\hat{Q}\,, \tag{4.63}$$

where

$$P_2 = \mathrm{diag}\left(e^{i(\beta_{e1}+\beta_{e2}+\beta_{\tau 3}+\alpha)}, 1, e^{i\beta_{\tau 3}}\right)\,, \tag{4.64}$$

$$\begin{aligned} Q_2 &= \mathrm{diag}\left(e^{-i(\beta_{e2}+\beta_{\tau 3}+\alpha)}, e^{-i(\beta_{e1}+\beta_{\tau 3}+\alpha)}, 1\right) \\ &= e^{-i(\beta_{e2}+\beta_{\tau 3}+\alpha)}\,\mathrm{diag}\left(1, e^{i(\beta_{e2}-\beta_{e1})}, e^{i(\beta_{e2}+\beta_{\tau 3}+\alpha)}\right)\,. \end{aligned} \tag{4.65}$$

The phases in the matrix P_2 are unphysical. The phases $(\beta_{e2} - \beta_{e1})$ and $(\beta_{e2} + \beta_{\tau 3} + \alpha)$ in the matrix Q_2 contribute to the Majorana phases α_{21} and α_{31}, respectively, while the common phase $(-\beta_{e2} - \beta_{\tau 3} - \alpha)$ in this matrix is unphysical and we will not keep it further. Thus, the Majorana phases in the PMNS matrix are determined by the phases in the product $Q_2\,\hat{Q}$:

$$\frac{\alpha_{21}}{2} = \beta_{e2} - \beta_{e1} + \frac{\xi_{21}}{2}\,, \quad \frac{\alpha_{31}}{2} = \beta_{e2} + \beta_{\tau 3} + \alpha + \beta + \frac{\xi_{31}}{2}\,, \quad \beta_{\tau 3} + \alpha = 0 \text{ or } \pi\,. \tag{4.66}$$

In terms of the standard parametrisation mixing angles θ_{12}, θ_{23}, θ_{13} and the Dirac phase δ the phases $(\beta_{e1} + \beta_{\tau 3} + \alpha)$ and $(\beta_{e2} + \beta_{\tau 3} + \alpha)$ read:

$$\beta_{e1} + \beta_{\tau 3} + \alpha = \arg\left(U_{\mu 2}e^{-i\frac{\alpha_{21}}{2}}\right) - \beta_{\mu 2} = \arg\left(c_{12}c_{23} - s_{12}s_{23}s_{13}e^{i\delta}\right) - \beta_{\mu 2}\,, \tag{4.67}$$

$$\beta_{e2} + \beta_{\tau 3} + \alpha = \arg\left(U_{\mu 1}\right) - \beta_{\mu 1} = \arg\left(-s_{12}c_{23} - c_{12}s_{23}s_{13}e^{i\delta}\right) - \beta_{\mu 1}\,. \tag{4.68}$$

In terms of the neutrino mixing angles θ_{12}, θ_{13}, θ_{23} and the phase δ we have:

$$\sin(\alpha_{21}/2) = -\frac{\cos(\beta_{\mu 2} - \beta_{\mu 1})}{2|U_{\mu 1}U_{\mu 2}|}\Big[\sin 2\theta_{23}\sin\theta_{13}\left(\sin(\delta + \xi_{21}/2) - 2\sin^2\theta_{12}\cos\delta\sin(\xi_{21}/2)\right)$$

[31] This relation is the generalisation of eq. (3.40) in subsection 3.3.2, where we considered θ^e_{13} to be in the first quadrant.

$$+ \sin 2\theta_{12} \left(\cos^2\theta_{23} - \sin^2\theta_{23}\sin^2\theta_{13}\right) \sin(\xi_{21}/2)\Big] \,, \tag{4.69}$$

$$\sin(\alpha_{31}/2) = -\frac{\cos\beta_{\mu 1}}{|U_{\mu 1}|}\Big[\sin\theta_{12}\cos\theta_{23}\sin(\beta + \xi_{31}/2) + \cos\theta_{12}\sin\theta_{23}\sin\theta_{13}\sin(\delta + \beta + \xi_{31}/2)\Big] \,. \tag{4.70}$$

Given the angle θ_{12}^ν, the sign factors $\cos(\beta_{\mu 2} - \beta_{\mu 1})$ and $\cos\beta_{\mu 1}$ are fixed, since

$$\cos(\beta_{\mu 2} - \beta_{\mu 1}) = -\,\mathrm{sgn}\,(s_{12}^\nu c_{12}^\nu) \,, \quad \cos\beta_{\mu 1} = -\,\mathrm{sgn}\,(s_{12}^\nu) \,. \tag{4.71}$$

As in the previous subsections, the expressions for $\sin(\alpha_{21}/2 - \xi_{21}/2)$ and $\sin(\alpha_{31}/2 - \xi_{31}/2 - \beta)$ are somewhat simpler:

$$\sin(\alpha_{21}/2 - \xi_{21}/2) = -\frac{\cos(\beta_{\mu 2} - \beta_{\mu 1})}{2|U_{\mu 1}U_{\mu 2}|}\sin 2\theta_{23}\sin\theta_{13}\sin\delta \,, \tag{4.72}$$

$$\sin(\alpha_{31}/2 - \xi_{31}/2 - \beta) = -\frac{\cos\beta_{\mu 1}}{|U_{\mu 1}|}\cos\theta_{12}\sin\theta_{23}\sin\theta_{13}\sin\delta \,. \tag{4.73}$$

Also in this case we have $|\sin(\alpha_{21}/2 - \xi_{21}/2)| \propto \sin\theta_{13}$ and $|\sin(\alpha_{31}/2 - \xi_{31}/2 - \beta)| \propto \sin\theta_{13}$.

We would like to note finally that formulae in eqs. (4.69) and (4.70) and eqs. (4.72) and (4.73) can be obtained formally from the corresponding formulae in subsection 4.2.1, eqs. (4.46) and (4.47) and eqs. (4.49) and (4.50), by making the following substitutions:

$$\theta_{23} \to \theta_{23} - \frac{\pi}{2} \quad \text{and} \quad \tau \to \mu \,. \tag{4.74}$$

4.2.3 Case B3: θ_{12}^e and θ_{13}^e

In this subsection, we switch to the parametrisation of the PMNS matrix U given in eq. (3.13) with $(ij) - (kl) = (12) - (13)$, i.e.,

$$U = R_{12}(\theta_{12}^e)\, R_{13}(\theta_{13}^e)\, \Psi\, R_{23}(\theta_{23}^\nu)\, R_{12}(\theta_{12}^\nu)\, Q_0 \,. \tag{4.75}$$

In explicit form this matrix reads:

$$U = \begin{pmatrix} |U_{e1}|e^{i\beta_{e1}} & |U_{e2}|e^{i\beta_{e2}} & |U_{e3}|e^{i\beta_{e3}} \\ |U_{\mu 1}|e^{i\beta_{\mu 1}} & |U_{\mu 2}|e^{i\beta_{\mu 2}} & |U_{\mu 3}|e^{i\beta_{\mu 3}} \\ |U_{\tau 1}|e^{i\beta_{\tau 1}} & |U_{\tau 2}|e^{i\beta_{\tau 2}} & |U_{\tau 3}|e^{i\beta_{\tau 3}} \end{pmatrix} Q_0 \,, \tag{4.76}$$

where

$$|U_{e1}|e^{i\beta_{e1}} = c_{12}^e c_{13}^e c_{12}^\nu - s_{12}^\nu \left(s_{12}^e c_{23}^\nu e^{-i\psi} - c_{12}^e s_{13}^e s_{23}^\nu e^{-i\omega}\right) \,, \tag{4.77}$$

$$|U_{e2}|e^{i\beta_{e2}} = c_{12}^e c_{13}^e s_{12}^\nu + c_{12}^\nu \left(s_{12}^e c_{23}^\nu e^{-i\psi} - c_{12}^e s_{13}^e s_{23}^\nu e^{-i\omega}\right) \,, \tag{4.78}$$

$$|U_{e3}|e^{i\beta_{e3}} = s_{12}^e s_{23}^\nu e^{-i\psi} + c_{12}^e s_{13}^e c_{23}^\nu e^{-i\omega} \,, \tag{4.79}$$

$$|U_{\mu 1}|e^{i\beta_{\mu 1}} = -s_{12}^e c_{13}^e c_{12}^\nu - s_{12}^\nu \left(c_{12}^e c_{23}^\nu e^{-i\psi} + s_{12}^e s_{13}^e s_{23}^\nu e^{-i\omega}\right) \,, \tag{4.80}$$

$$|U_{\mu 2}|e^{i\beta_{\mu 2}} = -s_{12}^e c_{13}^e s_{12}^\nu + c_{12}^\nu \left(c_{12}^e c_{23}^\nu e^{-i\psi} + s_{12}^e s_{13}^e s_{23}^\nu e^{-i\omega}\right) \,, \tag{4.81}$$

$$|U_{\mu 3}|e^{i\beta_{\mu 3}} = c^e_{12}s^\nu_{23}e^{-i\psi} - s^e_{12}s^e_{13}c^\nu_{23}e^{-i\omega}\,, \tag{4.82}$$

$$|U_{\tau 1}|e^{i\beta_{\tau 1}} = -s^e_{13}c^\nu_{12} + c^e_{13}s^\nu_{12}s^\nu_{23}e^{-i\omega}\,, \tag{4.83}$$

$$|U_{\tau 2}|e^{i\beta_{\tau 2}} = -s^e_{13}s^\nu_{12} - c^e_{13}c^\nu_{12}s^\nu_{23}e^{-i\omega}\,, \tag{4.84}$$

$$|U_{\tau 3}|e^{i\beta_{\tau 3}} = c^e_{13}c^\nu_{23}e^{-i\omega}\,. \tag{4.85}$$

According to eq. (3.58), the angle θ^e_{13} is expressed in terms of the known angles and can be determined up to a quadrant. The phase ω is a free phase parameter, which enters, e.g., the sum rule for $\cos\delta$ (see eq. (3.60)), so its presence is expected as well in the sum rules for the Majorana phases we are going to derive.

We aim as before to find an appropriate phase rearrangement in order to bring U to the standard parametrisation form. For that reason we compare first the expressions for the $J_{\rm CP}$ invariant in the standard parametrisation and in the parametrisation given in eq. (4.75) and find

$$\sin\delta = \frac{8\,\mathcal{J}}{\sin 2\theta_{12}\sin 2\theta_{23}\sin 2\theta_{13}\cos\theta_{13}}\,, \tag{4.86}$$

where $\mathcal{J}$ is the expression for $J_{\rm CP}$ in the parametrisation of U given in eq. (4.75):

$$\begin{aligned}\mathcal{J} = \frac{1}{8}\cos\theta^e_{13}\Big[\sin 2\theta^e_{12}\Big\{2\sin 2\theta^\nu_{12}\cos\theta^\nu_{23}\left[\left(\cos^2\theta^e_{13} - \cos^2\theta^\nu_{23}\right)\sin\psi - \sin^2\theta^e_{13}\sin^2\theta^\nu_{23}\sin(\psi - 2\omega)\right] \\ - \sin 2\theta^e_{13}\cos 2\theta^\nu_{12}\sin 2\theta^\nu_{23}\sin(\psi-\omega)\Big\} + 2\cos 2\theta^e_{12}\sin\theta^e_{13}\sin 2\theta^\nu_{12}\sin 2\theta^\nu_{23}\cos\theta^\nu_{23}\sin\omega\Big]\,.\end{aligned} \tag{4.87}$$

This expression looks cumbersome, but one can verify that the relation in eq. (4.86) holds if δ is given by

$$\delta = \beta_{e1} + \beta_{e2} + \beta_{\mu 3} + \beta_{\tau 3} - \beta_{e3} + \psi + \omega\,. \tag{4.88}$$

Now we can cast U in the following form:

$$U = P_2 \begin{pmatrix} |U_{e1}| & |U_{e2}| & |U_{e3}|e^{-i\delta} \\ |U_{\mu 1}|e^{i(\beta_{\mu 1}+\beta_{e2}+\beta_{\tau 3}+\psi+\omega)} & |U_{\mu 2}|e^{i(\beta_{\mu 2}+\beta_{e1}+\beta_{\tau 3}+\psi+\omega)} & |U_{\mu 3}| \\ |U_{\tau 1}|e^{i(\beta_{\tau 1}+\beta_{e2}+\beta_{\mu 3}+\psi+\omega)} & |U_{\tau 2}|e^{i(\beta_{\tau 2}+\beta_{e1}+\beta_{\mu 3}+\psi+\omega)} & |U_{\tau 3}| \end{pmatrix} Q_2\, Q_0\,, \tag{4.89}$$

where

$$P_2 = \mathrm{diag}\left(e^{i(\beta_{e1}+\beta_{e2}+\beta_{\mu 3}+\beta_{\tau 3}+\psi+\omega)}, e^{i\beta_{\mu 3}}, e^{i\beta_{\tau 3}}\right)\,, \tag{4.90}$$

$$\begin{aligned} Q_2 &= \mathrm{diag}\left(e^{-i(\beta_{e2}+\beta_{\mu 3}+\beta_{\tau 3}+\psi+\omega)}, e^{-i(\beta_{e1}+\beta_{\mu 3}+\beta_{\tau 3}+\psi+\omega)}, 1\right) \\ &= e^{-i(\beta_{e2}+\beta_{\mu 3}+\beta_{\tau 3}+\psi+\omega)}\ \mathrm{diag}\left(1, e^{i(\beta_{e2}-\beta_{e1})}, e^{i(\beta_{e2}+\beta_{\mu 3}+\beta_{\tau 3}+\psi+\omega)}\right)\,. \end{aligned} \tag{4.91}$$

The phases in the matrix P_2 as well as the overall phase in the matrix Q_2 are unphysical. Thus, for the Majorana phases we get:

$$\frac{\alpha_{21}}{2} = \beta_{e2} - \beta_{e1} + \frac{\xi_{21}}{2}\,, \quad \frac{\alpha_{31}}{2} = \beta_{e2} + \beta_{\mu 3} + \beta_{\tau 3} + \psi + \omega + \frac{\xi_{31}}{2}\,. \tag{4.92}$$

In terms of the standard parametrisation mixing angles θ_{12}, θ_{23}, θ_{13} and the Dirac phase δ we have:

$$\beta_{e1} + \beta_{\mu 3} + \psi + \omega = \arg\left(U_{\tau 2}e^{-i\frac{\alpha_{21}}{2}}\right) - \beta_{\tau 2} = \arg\left(-c_{12}s_{23} - s_{12}c_{23}s_{13}e^{i\delta}\right) - \beta_{\tau 2}\,, \tag{4.93}$$

$$\beta_{e2} + \beta_{\mu 3} + \psi + \omega = \arg\left(U_{\tau 1}\right) - \beta_{\tau 1} = \arg\left(s_{12}s_{23} - c_{12}c_{23}s_{13}e^{i\delta}\right) - \beta_{\tau 1}\,, \tag{4.94}$$

where $\beta_{\tau 1}$ and $\beta_{\tau 2}$ are the arguments of the expressions given in eqs. (4.83) and (4.84), respectively. They are fixed once the angles θ_{12}^ν and θ_{23}^ν, the quadrant to which θ_{13}^e belongs and the phase ω are known. Finally, we find:

$$\frac{\alpha_{21}}{2} = \arg\left(U_{\tau 1}U_{\tau 2}^* e^{i\frac{\alpha_{21}}{2}}\right) + \beta_{\tau 2} - \beta_{\tau 1} + \frac{\xi_{21}}{2}\,, \tag{4.95}$$

$$\frac{\alpha_{31}}{2} = \arg\left(U_{\tau 1}\right) + \beta_{\tau 3} - \beta_{\tau 1} + \frac{\xi_{31}}{2}\,, \tag{4.96}$$

where $\beta_{\tau 3}$ is the argument of the expression in eq. (4.85), which is fixed under the conditions specified above for $\beta_{\tau 1}$ and $\beta_{\tau 2}$.

The phases $(\alpha_{21}/2 - \xi_{21}/2 - (\beta_{\tau 2} - \beta_{\tau 1}))$ and $(\alpha_{31}/2 - \xi_{31}/2 - (\beta_{\tau 3} - \beta_{\tau 1}))$, as it follows from eqs. (4.95) and (4.96), are completely determined by the values of the standard parametrisation angles θ_{12}, θ_{23} and θ_{13}, and of the Dirac phase δ. It should be noted, however, that in the considered scheme the phase δ also depends on the phase ω, and thus, the phases $(\alpha_{21}/2 - \xi_{21}/2 - (\beta_{\tau 2} - \beta_{\tau 1}))$ and $(\alpha_{31}/2 - \xi_{31}/2 - (\beta_{\tau 3} - \beta_{\tau 1}))$ depend on ω via δ. In Section 3.6, we have given predictions for δ for $\omega = 0$ and $\mathrm{sgn}(\sin 2\theta_{13}^e) = 1$. Correspondingly, in Section 4.5 we will derive predictions for the values of the phases $(\alpha_{21}/2 - \xi_{21}/2)$ and $(\alpha_{31}/2 - \xi_{31}/2)$ for the same values of ω and $\mathrm{sgn}(\sin 2\theta_{13}^e)$, for which the predicted value of δ lies in its 2σ allowed interval [162].

We note finally that $\sin^2\theta_{23}$ is constrained by the requirements that $\cos\psi$, $\sin^2\theta_{12}^e$ and $\sin^2\theta_{13}^e$ possess physically acceptable values, to lie for both the NO and IO spectra in the following narrow intervals (see the discussion at the end of Section 3.6):

$$\begin{aligned}
&(0.489, 0.498) \text{ for TBM},\\
&(0.489, 0.496) \text{ for GRA},\\
&(0.489, 0.499) \text{ for GRB},\\
&(0.489, 0.499) \text{ for HG},\\
&(0.489, 0.521) \text{ for BM}.
\end{aligned}$$

Thus, we will present results for the phases of interest for the NO (IO) spectrum for $\sin^2\theta_{23} = 0.48907$ ($\sin^2\theta_{23} = 0.48886$).[32]

4.3 Mixing schemes with $\tilde{U}_e^\dagger = R_{ij}(\theta_{ij}^e)$ and $\tilde{U}_\nu = R_{23}(\theta_{23}^\nu)\, R_{13}(\theta_{13}^\nu)\, R_{12}(\theta_{12}^\nu)$

We consider next a generalisation of the cases analysed in Section 4.1 with the presence of a third rotation matrix in $\tilde{U}_\nu$ arising from the neutrino sector, i.e., we employ the parametrisation of U given in eq. (3.14). Non-zero values of θ_{13}^ν are inspired by certain types of flavour symmetries [152–155]. In the numerical analysis of the predictions for α_{21}, α_{31} and $|\langle m\rangle|$ we will perform in Section 4.5, we will consider three representative values of θ_{13}^ν discussed in the literature: $\theta_{13}^\nu = \pi/20$, $\pi/10$ and $\sin^{-1}(1/3)$. We are not going to consider the case in which the U matrix is parametrised as in eq. (3.14) with $(ij) = (23)$ for the reasons explained in [100], i.e., the absence of a correlation between the Dirac CPV phase δ and the mixing angles. It should be noted that for this and other cases for which

[32] For $\sin^2\theta_{23} < 0.48907$ ($\sin^2\theta_{23} < 0.48886$), $\cos\delta$ acquires an unphysical (complex) value.

it is not possible to derive such a correlation, different symmetry forms of $\tilde{U}_\nu$ can still be tested with an improvement of the precision in the measurement of the neutrino mixing angles. For instance, in the case corresponding to eq. (3.14) with $(ij) = (23)$, one has, as was shown in [100], $\sin^2\theta_{13} = \sin^2\theta^\nu_{13}$ and $\sin^2\theta_{12} = \sin^2\theta^\nu_{12}$, i.e., the angles θ_{13} and θ_{12} are predicted to have particular values when the angles θ^ν_{13} and θ^ν_{23} are fixed by a symmetry.

4.3.1 Case C1: θ^e_{12}

In this subsection, we consider the parametrisation of the PMNS matrix U given in eq. (3.14) with $(ij) = (12)$, i.e.,

$$U = R_{12}(\theta^e_{12})\,\Psi\,R_{23}(\theta^\nu_{23})\,R_{13}(\theta^\nu_{13})\,R_{12}(\theta^\nu_{12})\,Q_0\,. \tag{4.97}$$

In this case, the the matrix Ψ contains only one physical phase ϕ, $\Psi = \mathrm{diag}\,(1, e^{i\phi}, 1)$ (we have denoted $\phi \equiv -\psi$), since the phase ω in Ψ is unphysical and we have dropped it. The explicit form of the matrix U reads

$$U = \begin{pmatrix} |U_{e1}|e^{i\beta_{e1}} & |U_{e2}|e^{i\beta_{e2}} & |U_{e3}|e^{i\beta_{e3}} \\ |U_{\mu1}|e^{i\beta_{\mu1}} & |U_{\mu2}|e^{i\beta_{\mu2}} & |U_{\mu3}|e^{i\beta_{\mu3}} \\ |U_{\tau1}|e^{i\beta_{\tau1}} & |U_{\tau2}|e^{i\beta_{\tau2}} & |U_{\tau3}|e^{i\beta_{\tau3}} \end{pmatrix} Q_0\,, \tag{4.98}$$

where

$$|U_{e1}|e^{i\beta_{e1}} = c^e_{12}c^\nu_{12}c^\nu_{13} - s^e_{12}\left(s^\nu_{12}c^\nu_{23} + c^\nu_{12}s^\nu_{23}s^\nu_{13}\right)e^{i\phi}\,, \tag{4.99}$$

$$|U_{e2}|e^{i\beta_{e2}} = c^e_{12}s^\nu_{12}c^\nu_{13} + s^e_{12}\left(c^\nu_{12}c^\nu_{23} - s^\nu_{12}s^\nu_{23}s^\nu_{13}\right)e^{i\phi}\,, \tag{4.100}$$

$$|U_{e3}|e^{i\beta_{e3}} = c^e_{12}s^\nu_{13} + s^e_{12}s^\nu_{23}c^\nu_{13}e^{i\phi}\,, \tag{4.101}$$

$$|U_{\mu1}|e^{i\beta_{\mu1}} = -s^e_{12}c^\nu_{12}c^\nu_{13} - c^e_{12}\left(s^\nu_{12}c^\nu_{23} + c^\nu_{12}s^\nu_{23}s^\nu_{13}\right)e^{i\phi}\,, \tag{4.102}$$

$$|U_{\mu2}|e^{i\beta_{\mu2}} = -s^e_{12}s^\nu_{12}c^\nu_{13} + c^e_{12}\left(c^\nu_{12}c^\nu_{23} - s^\nu_{12}s^\nu_{23}s^\nu_{13}\right)e^{i\phi}\,, \tag{4.103}$$

$$|U_{\mu3}|e^{i\beta_{\mu3}} = -s^e_{12}s^\nu_{13} + c^e_{12}s^\nu_{23}c^\nu_{13}e^{i\phi}\,, \tag{4.104}$$

$$|U_{\tau1}|e^{i\beta_{\tau1}} = s^\nu_{12}s^\nu_{23} - c^\nu_{12}c^\nu_{23}s^\nu_{13}\,, \tag{4.105}$$

$$|U_{\tau2}|e^{i\beta_{\tau2}} = -c^\nu_{12}s^\nu_{23} - s^\nu_{12}c^\nu_{23}s^\nu_{13}\,, \tag{4.106}$$

$$|U_{\tau3}|e^{i\beta_{\tau3}} = c^\nu_{23}c^\nu_{13}\,. \tag{4.107}$$

Comparing the expressions for the $J_{\rm CP}$ invariant in the standard parametrisation and in the parametrisation given in eq. (4.97), one finds the following relation between $\sin\delta$ and $\sin\phi$:[33]

$$\sin\delta = \frac{\sin 2\theta^e_{12}\left[2\cos 2\theta^\nu_{12}\sin 2\theta^\nu_{23}\sin\theta^\nu_{13} - \left(\cos^2\theta^\nu_{13} + \left(\cos^2\theta^\nu_{13} - 2\right)\cos 2\theta^\nu_{23}\right)\sin 2\theta^\nu_{12}\right]}{2\,\mathrm{sgn}(\cos\theta^\nu_{23}\cos\theta^\nu_{13})\sin 2\theta_{12}\sin 2\theta_{13}\sin\theta_{23}}\sin\phi\,, \tag{4.108}$$

where we have used that in this scheme $\cos^2\theta_{23}\cos^2\theta_{13} = \cos^2\theta^\nu_{23}\cos^2\theta^\nu_{13}$. The relation in eq. (4.108) suggests the required rearrangement of the phases one has to perform to bring

[33] For $\theta^\nu_{23} = -\pi/4$ this relation reduces to eq. (3.72).

U given in eq. (4.98) to the standard parametrisation form. Namely, it can be shown that eq. (4.108) holds if

$$\delta = \beta_{e1} + \beta_{e2} + \beta_{\mu 3} - \beta_{e3} - \phi + \beta_{\tau 3}\,, \quad \beta_{\tau 3} = 0 \text{ or } \pi\,, \tag{4.109}$$

where $\beta_{\tau 3} = \arg(c_{23}^\nu c_{13}^\nu)$. The phase $\beta_{\tau 3}$ provides the sign factor $\mathrm{sgn}(\cos\theta_{23}^\nu \cos\theta_{13}^\nu)$ in the relation between $\sin\delta$ and $\sin\phi$, when one calculates $\sin\delta$ from eq. (4.109). Now we can cast U in the following form:

$$U = P_2 \begin{pmatrix} |U_{e1}| & |U_{e2}| & |U_{e3}|e^{-i\delta} \\ |U_{\mu 1}|e^{i(\beta_{\mu 1}+\beta_{e2}-\phi+\beta_{\tau 3})} & |U_{\mu 2}|e^{i(\beta_{\mu 2}+\beta_{e1}-\phi+\beta_{\tau 3})} & |U_{\mu 3}| \\ |U_{\tau 1}|e^{i(\beta_{\tau 1}+\beta_{e2}+\beta_{\mu 3}-\phi)} & |U_{\tau 2}|e^{i(\beta_{\tau 2}+\beta_{e1}+\beta_{\mu 3}-\phi)} & |U_{\tau 3}| \end{pmatrix} Q_2\, Q_0\,, \tag{4.110}$$

where

$$P_2 = \mathrm{diag}\left(e^{i(\beta_{e1}+\beta_{e2}+\beta_{\mu 3}-\phi)}, e^{i(\beta_{\mu 3}-\beta_{\tau 3})}, 1\right)\,, \tag{4.111}$$

$$\begin{aligned} Q_2 &= \mathrm{diag}\left(e^{-i(\beta_{e2}+\beta_{\mu 3}-\phi)}, e^{-i(\beta_{e1}+\beta_{\mu 3}-\phi)}, e^{i\beta_{\tau 3}}\right) \\ &= e^{-i(\beta_{e2}+\beta_{\mu 3}-\phi)}\ \mathrm{diag}\left(1, e^{i(\beta_{e2}-\beta_{e1})}, e^{i(\beta_{e2}+\beta_{\mu 3}-\phi+\beta_{\tau 3})}\right)\,. \end{aligned} \tag{4.112}$$

The phases in the matrix P_2 are unphysical. The Majorana phases get contribution from the matrix $Q_2 Q_0$ and read:

$$\frac{\alpha_{21}}{2} = \beta_{e2} - \beta_{e1} + \frac{\xi_{21}}{2}\,, \quad \frac{\alpha_{31}}{2} = \beta_{e2} + \beta_{\mu 3} - \phi + \beta_{\tau 3} + \frac{\xi_{31}}{2}\,, \quad \beta_{\tau 3} = 0 \text{ or } \pi\,. \tag{4.113}$$

In terms of the standard parametrisation mixing angles θ_{12}, θ_{23}, θ_{13} and the Dirac phase δ we have:

$$\beta_{e1} + \beta_{\mu 3} - \phi = \arg\left(U_{\tau 2} e^{-i\frac{\alpha_{21}}{2}}\right) - \beta_{\tau 2} = \arg\left(-c_{12}s_{23} - s_{12}c_{23}s_{13}e^{i\delta}\right) - \beta_{\tau 2}\,, \tag{4.114}$$

$$\beta_{e2} + \beta_{\mu 3} - \phi = \arg\left(U_{\tau 1}\right) - \beta_{\tau 1} = \arg\left(s_{12}s_{23} - c_{12}c_{23}s_{13}e^{i\delta}\right) - \beta_{\tau 1}\,, \tag{4.115}$$

where $\beta_{\tau 1}$ and $\beta_{\tau 2}$ can be 0 or π and are known when the angles θ_{12}^ν, θ_{23}^ν and θ_{13}^ν are fixed (see eqs. (4.105) and (4.106)).

Using eqs. (4.114) and (4.115), we get in terms of the standard parametrisation mixing angles θ_{12}, θ_{13}, θ_{23} and the Dirac phase δ:

$$\begin{aligned} \sin(\alpha_{21}/2) = \frac{\cos(\beta_{\tau 2} - \beta_{\tau 1})}{2|U_{\tau 1}U_{\tau 2}|}\Big[&\sin 2\theta_{23} \sin\theta_{13}\big(\sin(\delta + \xi_{21}/2) - 2\sin^2\theta_{12}\cos\delta\sin(\xi_{21}/2)\big) \\ &- \sin 2\theta_{12}\big(\sin^2\theta_{23} - \cos^2\theta_{23}\sin^2\theta_{13}\big)\sin(\xi_{21}/2)\Big]\,, \end{aligned} \tag{4.116}$$

$$\begin{aligned} \sin(\alpha_{31}/2) = \frac{\cos(\beta_{\tau 3} - \beta_{\tau 1})}{|U_{\tau 1}|}\Big[&\sin\theta_{12}\sin\theta_{23}\sin(\xi_{31}/2) \\ &- \cos\theta_{12}\cos\theta_{23}\sin\theta_{13}\sin(\delta + \xi_{31}/2)\Big]\,, \end{aligned} \tag{4.117}$$

where, according to eq. (3.76), $\cos^2\theta_{23}\cos^2\theta_{13} = \cos^2\theta_{23}^\nu \cos^2\theta_{13}^\nu$. Note that, as it follows from eqs. (4.105)–(4.107), the sign factors $\cos(\beta_{\tau 2} - \beta_{\tau 1})$ and $\cos(\beta_{\tau 3} - \beta_{\tau 1})$ are known when the angles θ_{ij}^ν are fixed.

Finally, we give the expressions for $\sin(\alpha_{21}/2-\xi_{21}/2)$ and $\sin(\alpha_{31}/2-\xi_{31}/2)$, which have a simpler form:

$$\sin(\alpha_{21}/2-\xi_{21}/2) = \frac{\cos(\beta_{\tau 2}-\beta_{\tau 1})}{2|U_{\tau 1}U_{\tau 2}|}\sin 2\theta_{23}\sin\theta_{13}\sin\delta\,, \tag{4.118}$$

$$\sin(\alpha_{31}/2-\xi_{31}/2) = -\frac{\cos(\beta_{\tau 3}-\beta_{\tau 1})}{|U_{\tau 1}|}\cos\theta_{12}\cos\theta_{23}\sin\theta_{13}\sin\delta\,. \tag{4.119}$$

Equations (4.118) and (4.119) imply, in particular, that $|\sin(\alpha_{21(31)}/2-\xi_{21(31)}/2)| \propto \sin\theta_{13}$.

4.3.2 Case C2: θ_{13}^e

In this subsection, we derive the formulae for the Majorana phases in the case when the PMNS matrix U is parametrised as in eq. (3.14) with $(ij) = (13)$, i.e.,

$$U = R_{13}(\theta_{13}^e)\,\Psi\,R_{23}(\theta_{23}^\nu)\,R_{13}(\theta_{13}^\nu)\,R_{12}(\theta_{12}^\nu)\,Q_0\,. \tag{4.120}$$

In this case the phase ψ in the matrix Ψ is unphysical, and $\Psi = \mathrm{diag}\,(1,1,e^{-i\omega})$. We will proceed in analogy with the previous subsection. We start by writing the matrix U in explicit form:

$$U = \begin{pmatrix} |U_{e1}|e^{i\beta_{e1}} & |U_{e2}|e^{i\beta_{e2}} & |U_{e3}|e^{i\beta_{e3}} \\ |U_{\mu 1}|e^{i\beta_{\mu 1}} & |U_{\mu 2}|e^{i\beta_{\mu 2}} & |U_{\mu 3}|e^{i\beta_{\mu 3}} \\ |U_{\tau 1}|e^{i\beta_{\tau 1}} & |U_{\tau 2}|e^{i\beta_{\tau 2}} & |U_{\tau 3}|e^{i\beta_{\tau 3}} \end{pmatrix} Q_0\,, \tag{4.121}$$

where

$$|U_{e1}|e^{i\beta_{e1}} = c_{13}^e c_{12}^\nu c_{13}^\nu + s_{13}^e\,(s_{12}^\nu s_{23}^\nu - c_{12}^\nu c_{23}^\nu s_{13}^\nu)\,e^{-i\omega}\,, \tag{4.122}$$

$$|U_{e2}|e^{i\beta_{e2}} = c_{13}^e s_{12}^\nu c_{13}^\nu - s_{13}^e\,(c_{12}^\nu s_{23}^\nu + s_{12}^\nu c_{23}^\nu s_{13}^\nu)\,e^{-i\omega}\,, \tag{4.123}$$

$$|U_{e3}|e^{i\beta_{e3}} = c_{13}^e s_{13}^\nu + s_{13}^e c_{23}^\nu c_{13}^\nu e^{-i\omega}\,, \tag{4.124}$$

$$|U_{\mu 1}|e^{i\beta_{\mu 1}} = -s_{12}^\nu c_{23}^\nu - c_{12}^\nu s_{23}^\nu s_{13}^\nu\,, \tag{4.125}$$

$$|U_{\mu 2}|e^{i\beta_{\mu 2}} = c_{12}^\nu c_{23}^\nu - s_{12}^\nu s_{23}^\nu s_{13}^\nu\,, \tag{4.126}$$

$$|U_{\mu 3}|e^{i\beta_{\mu 3}} = s_{23}^\nu c_{13}^\nu\,, \tag{4.127}$$

$$|U_{\tau 1}|e^{i\beta_{\tau 1}} = -s_{13}^e c_{12}^\nu c_{13}^\nu + c_{13}^e\,(s_{12}^\nu s_{23}^\nu - c_{12}^\nu c_{23}^\nu s_{13}^\nu)\,e^{-i\omega}\,, \tag{4.128}$$

$$|U_{\tau 2}|e^{i\beta_{\tau 2}} = -s_{13}^e s_{12}^\nu c_{13}^\nu - c_{13}^e\,(c_{12}^\nu s_{23}^\nu + s_{12}^\nu c_{23}^\nu s_{13}^\nu)\,e^{-i\omega}\,, \tag{4.129}$$

$$|U_{\tau 3}|e^{i\beta_{\tau 3}} = -s_{13}^e s_{13}^\nu + c_{13}^e c_{23}^\nu c_{13}^\nu e^{-i\omega}\,. \tag{4.130}$$

From the comparison of the expressions for $J_{\rm CP}$ in the standard parametrisation and in the parametrisation given in eq. (4.120), it follows that[34]

$$\sin\delta = \frac{\sin 2\theta_{13}^e\,[(\cos^2\theta_{13}^\nu - (\cos^2\theta_{13}^\nu - 2)\cos 2\theta_{23}^\nu)\sin 2\theta_{12}^\nu + 2\cos 2\theta_{12}^\nu \sin 2\theta_{23}^\nu \sin\theta_{13}^\nu]}{2\,\mathrm{sgn}(\sin\theta_{23}^\nu\cos\theta_{13}^\nu)\sin 2\theta_{12}\sin 2\theta_{13}\cos\theta_{23}}\sin\omega\,, \tag{4.131}$$

[34] For $\theta_{23}^\nu = -\pi/4$ this relation reduces to eq. (3.88).

where we have used the equality $\sin^2\theta_{23}\cos^2\theta_{13} = \sin^2\theta_{23}^\nu\cos^2\theta_{13}^\nu$ valid in this scheme. As can be shown, the relation between $\sin\delta$ and $\sin\omega$ in eq. (4.131) takes place if

$$\delta = \beta_{e1} + \beta_{e2} + \beta_{\tau 3} - \beta_{e3} + \omega + \beta_{\mu 3}\,, \quad \beta_{\mu 3} = 0 \text{ or } \pi\,, \tag{4.132}$$

where $\beta_{\mu 3} = \arg(s_{23}^\nu c_{13}^\nu)$. Knowing the expression for δ allows us to rearrange the phases in eq. (4.121) in such a way as to render U in the standard parametrisation form:

$$U = P_2 \begin{pmatrix} |U_{e1}| & |U_{e2}| & |U_{e3}|e^{-i\delta} \\ |U_{\mu 1}|e^{i(\beta_{\mu 1}+\beta_{e2}+\beta_{\tau 3}+\omega)} & |U_{\mu 2}|e^{i(\beta_{\mu 2}+\beta_{e1}+\beta_{\tau 3}+\omega)} & |U_{\mu 3}| \\ |U_{\tau 1}|e^{i(\beta_{\tau 1}+\beta_{e2}+\omega+\beta_{\mu 3})} & |U_{\tau 2}|e^{i(\beta_{\tau 2}+\beta_{e1}+\omega+\beta_{\mu 3})} & |U_{\tau 3}| \end{pmatrix} Q_2\, Q_0\,, \tag{4.133}$$

with

$$P_2 = \text{diag}\left(e^{i(\beta_{e1}+\beta_{e2}+\beta_{\tau 3}+\omega)}, 1, e^{i(\beta_{\tau 3}-\beta_{\mu 3})}\right)\,, \tag{4.134}$$

$$\begin{aligned} Q_2 &= \text{diag}\left(e^{-i(\beta_{e2}+\beta_{\tau 3}+\omega)}, e^{-i(\beta_{e1}+\beta_{\tau 3}+\omega)}, e^{i\beta_{\mu 3}}\right) \\ &= e^{-i(\beta_{e2}+\beta_{\tau 3}+\omega)}\ \text{diag}\left(1, e^{i(\beta_{e2}-\beta_{e1})}, e^{i(\beta_{e2}+\beta_{\tau 3}+\omega+\beta_{\mu 3})}\right)\,. \end{aligned} \tag{4.135}$$

The matrix P_2 contains unphysical phases which can be removed. The Majorana phases are determined by the phases in the product $Q_2\, Q_0$:

$$\frac{\alpha_{21}}{2} = \beta_{e2} - \beta_{e1} + \frac{\xi_{21}}{2}\,, \quad \frac{\alpha_{31}}{2} = \beta_{e2} + \beta_{\tau 3} + \omega + \beta_{\mu 3} + \frac{\xi_{31}}{2}\,, \quad \beta_{\mu 3} = 0 \text{ or } \pi\,. \tag{4.136}$$

In terms of the "standard" mixing angles θ_{12}, θ_{23}, θ_{13} and the Dirac phase δ one has:

$$\beta_{e1} + \beta_{\tau 3} + \omega = \arg\left(U_{\mu 2}e^{-i\frac{\alpha_{21}}{2}}\right) - \beta_{\mu 2} = \arg\left(c_{12}c_{23} - s_{12}s_{23}s_{13}e^{i\delta}\right) - \beta_{\mu 2}\,, \tag{4.137}$$

$$\beta_{e2} + \beta_{\tau 3} + \omega = \arg\left(U_{\mu 1}\right) - \beta_{\mu 1} = \arg\left(-s_{12}c_{23} - c_{12}s_{23}s_{13}e^{i\delta}\right) - \beta_{\mu 1}\,, \tag{4.138}$$

where $\beta_{\mu 1} = \arg(-s_{12}^\nu c_{23}^\nu - c_{12}^\nu s_{23}^\nu s_{13}^\nu)$ and $\beta_{\mu 2} = \arg(c_{12}^\nu c_{23}^\nu - s_{12}^\nu s_{23}^\nu s_{13}^\nu)$ can take values of 0 or π and are known when the angles θ_{12}^ν, θ_{23}^ν and θ_{13}^ν are fixed.

Using relations in eqs. (4.137) and (4.138) we get in terms of the standard parametrisation mixing angles θ_{12}, θ_{13}, θ_{23} and the Dirac phase δ:

$$\begin{aligned} \sin(\alpha_{21}/2) = -\frac{\cos(\beta_{\mu 2}-\beta_{\mu 1})}{2|U_{\mu 1}U_{\mu 2}|}\Big[&\sin 2\theta_{23}\sin\theta_{13}\big(\sin(\delta+\xi_{21}/2) - 2\sin^2\theta_{12}\cos\delta\sin(\xi_{21}/2)\big) \\ &+ \sin 2\theta_{12}\big(\cos^2\theta_{23} - \sin^2\theta_{23}\sin^2\theta_{13}\big)\sin(\xi_{21}/2)\Big]\,, \end{aligned} \tag{4.139}$$

$$\begin{aligned} \sin(\alpha_{31}/2) = -\frac{\cos(\beta_{\mu 3}-\beta_{\mu 1})}{|U_{\mu 1}|}\Big[&\sin\theta_{12}\cos\theta_{23}\sin(\xi_{31}/2) \\ &+ \cos\theta_{12}\sin\theta_{23}\sin\theta_{13}\sin(\delta+\xi_{31}/2)\Big]\,, \end{aligned} \tag{4.140}$$

where, according to eq. (3.92), $\sin^2\theta_{23}\cos^2\theta_{13} = \sin^2\theta_{23}^\nu\cos^2\theta_{13}^\nu$. As it follows from eqs. (4.125)–(4.127), the sign factors $\cos(\beta_{\mu 2}-\beta_{\mu 1})$ and $\cos(\beta_{\mu 3}-\beta_{\mu 1})$ are known once the angles θ_{ij}^ν are fixed.

Finally, we provide the expressions for $\sin(\alpha_{21}/2 - \xi_{21}/2)$ and $\sin(\alpha_{31}/2 - \xi_{31}/2)$:

$$\sin(\alpha_{21}/2 - \xi_{21}/2) = -\frac{\cos(\beta_{\mu 2} - \beta_{\mu 1})}{2|U_{\mu 1} U_{\mu 2}|} \sin 2\theta_{23} \sin\theta_{13} \sin\delta\,, \tag{4.141}$$

$$\sin(\alpha_{31}/2 - \xi_{31}/2) = -\frac{\cos(\beta_{\mu 3} - \beta_{\mu 1})}{|U_{\mu 1}|} \cos\theta_{12} \sin\theta_{23} \sin\theta_{13} \sin\delta\,. \tag{4.142}$$

As in the cases analysed in the preceding subsections, we have $|\sin(\alpha_{21}/2 - \xi_{21}/2)| \propto \sin\theta_{13}$ and $|\sin(\alpha_{31}/2 - \xi_{31}/2)| \propto \sin\theta_{13}$.

4.4 Summary of the sum rules for the Majorana phases

In the present section, we summarise the sum rules for the Majorana phases obtained in the previous sections. Throughout this section the neutrino mixing matrix U is assumed to be in the standard parametrisation.

In schemes A1, B1, B3 and C1 the sum rules for $\alpha_{21}/2$ and $\alpha_{31}/2$ can be cast in the form:

$$\frac{\alpha_{21}}{2} = \arg\left(U_{\tau 1} U^*_{\tau 2} e^{i\frac{\alpha_{21}}{2}}\right) + \varkappa_{21} + \frac{\xi_{21}}{2}\,, \tag{4.143}$$

$$\frac{\alpha_{31}}{2} = \arg\left(U_{\tau 1}\right) + \varkappa_{31} + \frac{\xi_{31}}{2}\,, \tag{4.144}$$

where the expressions for the phases $\varkappa_{21}$ and $\varkappa_{31}$, which should be used in these sum rules in each particular case, are given in Table 4.1. In schemes A1 and C1 the phases $\varkappa_{21}$ and $\varkappa_{31}$ take values 0 or π and are known once the angles θ^{ν}_{ij} are fixed. In scheme B1 (B3), $\varkappa_{31}$ ($\varkappa_{21}$ and $\varkappa_{31}$) depends (depend) on the free phase parameter β (ω).

In schemes A2, B2 and C2 we similarly have:

$$\frac{\alpha_{21}}{2} = \arg\left(U_{\mu 1} U^*_{\mu 2} e^{i\frac{\alpha_{21}}{2}}\right) + \varkappa_{21} + \frac{\xi_{21}}{2}\,, \tag{4.145}$$

$$\frac{\alpha_{31}}{2} = \arg\left(U_{\mu 1}\right) + \varkappa_{31} + \frac{\xi_{31}}{2}\,, \tag{4.146}$$

where the corresponding expressions for $\varkappa_{21}$ and $\varkappa_{31}$ are given again in Table 4.1. In cases A2 and C2 the phases $\varkappa_{21}$ and $\varkappa_{31}$ can take values 0 or π. They are fixed when the angles θ^{ν}_{ij} are given. The phase β, which is a free parameter as long as it is not fixed by additional arguments, enters the sum rule for $\alpha_{31}/2$ in scheme B2.

In all schemes considered the phases $(\alpha_{21}/2 - \xi_{21}/2 - \varkappa_{21})$ and $(\alpha_{31}/2 - \xi_{31}/2 - \varkappa_{31})$ are determined by the values of the neutrino mixing angles θ_{12}, θ_{23} and θ_{13}, and of the Dirac phase δ. The Dirac phase is determined in each scheme by a corresponding sum rule. In schemes A1, A2, C1 and C2 there is a correlation between the values of $\sin^2\theta_{23}$ and $\sin^2\theta_{13}$. The sum rules for $\cos\delta$ and the relevant expressions for $\sin^2\theta_{23}$ in the cases of interest, which should be used in eqs. (4.143)–(4.146), are given in Tables 3.1 and 3.2. In the following section, we use the sum rules given in eqs. (4.143)–(4.146) to obtain the numerical predictions for the Majorana phases in the PMNS matrix.

Table 4.1. The phases $\varkappa_{21}$ and $\varkappa_{31}$ entering the sum rules for the Majorana phases given in eqs. (4.143)–(4.146) for all the cases considered.

Case	$\varkappa_{21}$	$\varkappa_{31}$
A1	$\arg\left(-s^{\nu}_{12}c^{\nu}_{12}\right)$	$\arg\left(s^{\nu}_{12}s^{\nu}_{23}c^{\nu}_{23}\right)$
A2	$\arg\left(-s^{\nu}_{12}c^{\nu}_{12}\right)$	$\arg\left(-s^{\nu}_{12}s^{\nu}_{23}c^{\nu}_{23}\right)$
B1	$\arg\left(-s^{\nu}_{12}c^{\nu}_{12}\right)$	$\arg\left(s^{\nu}_{12}\right)+\beta$
B2	$\arg\left(-s^{\nu}_{12}c^{\nu}_{12}\right)$	$\arg\left(-s^{\nu}_{12}\right)+\beta$
B3	$\arg\left[\left(s^{e}_{13}s^{\nu}_{12}+c^{e}_{13}c^{\nu}_{12}s^{\nu}_{23}e^{-i\omega}\right)\left(s^{e}_{13}c^{\nu}_{12}-c^{e}_{13}s^{\nu}_{12}s^{\nu}_{23}e^{i\omega}\right)\right]$	$\arg\left[c^{e}_{13}c^{\nu}_{23}\left(c^{e}_{13}s^{\nu}_{12}s^{\nu}_{23}-s^{e}_{13}c^{\nu}_{12}e^{-i\omega}\right)\right]$
C1	$\arg\left[-\left(c^{\nu}_{12}s^{\nu}_{23}+s^{\nu}_{12}c^{\nu}_{23}s^{\nu}_{13}\right)\left(s^{\nu}_{12}s^{\nu}_{23}-c^{\nu}_{12}c^{\nu}_{23}s^{\nu}_{13}\right)\right]$	$\arg\left[c^{\nu}_{23}c^{\nu}_{13}\left(s^{\nu}_{12}s^{\nu}_{23}-c^{\nu}_{12}c^{\nu}_{23}s^{\nu}_{13}\right)\right]$
C2	$\arg\left[-\left(c^{\nu}_{12}c^{\nu}_{23}-s^{\nu}_{12}s^{\nu}_{23}s^{\nu}_{13}\right)\left(s^{\nu}_{12}c^{\nu}_{23}+c^{\nu}_{12}s^{\nu}_{23}s^{\nu}_{13}\right)\right]$	$\arg\left[-s^{\nu}_{23}c^{\nu}_{13}\left(s^{\nu}_{12}c^{\nu}_{23}+c^{\nu}_{12}s^{\nu}_{23}s^{\nu}_{13}\right)\right]$

4.5 Predictions

4.5.1 Dirac phase

In Table 4.2 we show predictions for the Dirac phase δ, obtained from the sum rules, derived in Chapter 3 and summarised in Table 3.1. The numerical values are obtained using the best fit values of the neutrino mixing parameters given in eqs. (4.1)–(4.3) for both the NO and IO spectra.[35] As we have seen in Chapter 3, in the BM (LC) case, the sum rules for $\cos\delta$ lead to unphysical values of $|\cos\delta| > 1$ if one uses as input the best fit values of $\sin^2\theta_{12}$, $\sin^2\theta_{23}$ and $\sin^2\theta_{13}$. This is an indication of the fact that the current data disfavours the BM (LC) form of $\tilde{U}_{\nu}$. In the case of the B1 scheme and the NO spectrum, for example, the BM (LC) form is disfavoured at approximately 2σ confidence level. Physical values of $\cos\delta$ are found for larger (smaller) values of $\sin^2\theta_{12}$ ($\sin^2\theta_{23}$). For, e.g., $\sin^2\theta_{12} = 0.354$, which is the 3σ upper bound of $\sin^2\theta_{12}$, and the best fit values of $\sin^2\theta_{23}$ and $\sin^2\theta_{13}$, we get $|\cos\delta| \leq 1$ in most of the schemes considered in the present article, the exceptions being schemes B1 with the IO spectrum, B2 with the NO spectrum and B3. The values of the Dirac phase corresponding to the BM (LC) form quoted in Table 4.2 are obtained for $\sin^2\theta_{12} = 0.354$ and the best fit values of $\sin^2\theta_{23}$ and $\sin^2\theta_{13}$.

In each of cases C1 and C2, we report results for $\theta^{\nu}_{23} = -\pi/4$ and five sets of values of $[\theta^{\nu}_{13}, \theta^{\nu}_{12}]$, associated with, or inspired by, models of neutrino mixing (see Section 3.6). These sets include the three values of $\theta^{\nu}_{13} = \pi/20$, $\pi/10$ and $a \equiv \sin^{-1}(1/3)$ and selected values of θ^{ν}_{12} from the set: $\pm\pi/4$, $b \equiv \sin^{-1}(1/\sqrt{2+r})$, $c \equiv \sin^{-1}(1/\sqrt{3})$ and $\pi/5$. The values in square brackets in Table 4.2 are those of $[\theta^{\nu}_{13}, \theta^{\nu}_{12}]$ used. In scheme C1 we define cases I, II, III, IV and V as the cases with $[\theta^{\nu}_{13}, \theta^{\nu}_{12}]$ being equal to $[\pi/20, -\pi/4]$, $[\pi/10, -\pi/4]$, $[a, -\pi/4]$, $[\pi/20, b]$ and $[\pi/20, \pi/6]$, respectively. In scheme C2 cases I, II, III, IV and V correspond to the following pairs: $[\pi/20, c]$, $[\pi/20, \pi/4]$, $[\pi/10, \pi/4]$, $[a, \pi/4]$ and $[\pi/20, \pi/5]$, respectively.

As can be seen from Table 4.2, the values of δ for the IO spectrum differ insignificantly from the values obtained for the NO one in all the schemes considered, except for the B1 and B2 ones. The difference between the NO and IO values of δ in the B1 and B2 schemes is a consequence of the difference between the best fit values of $\sin^2\theta_{23}$ corresponding to

[35] Table 4.2 based on the best fit values of $\sin^2\theta_{ij}$ quoted in eqs. (4.1)–(4.3) is an updated version of Table 3.6.

Table 4.2. The Dirac phase δ in degrees calculated from the sum rules in Table 3.1 using the best fit values of the neutrino mixing angles quoted in eqs. (4.1)–(4.3), except for scheme B3 and the BM (LC) form of $\tilde{U}_\nu$. The results shown for scheme B3 are obtained for $\omega = 0$, $\mathrm{sgn}\,(\sin 2\theta^e_{13}) = 1$, and for $\sin^2\theta_{23} = 0.48907$ (0.48886) for the NO (IO) spectrum. The numbers quoted for the BM (LC) form of $\tilde{U}_\nu$ are for $\sin^2\theta_{12} = 0.354$, which is the 3σ upper bound. For each cell the first number corresponds to $\delta = \cos^{-1}(\cos\delta)$, while the second number corresponds to $\delta = 2\pi - \cos^{-1}(\cos\delta)$. In cases C1 and C2, $\theta^\nu_{23} = -\pi/4$ and the values in square brackets are those of $[\theta^\nu_{13}, \theta^\nu_{12}]$ used. The letters a, b and c stand for $\sin^{-1}(1/3)$, $\sin^{-1}(1/\sqrt{2+r})$ and $\sin^{-1}(1/\sqrt{3})$, respectively. See text for further details.

Case	$\tilde{U}_\nu$ O	TBM	GRA	GRB	HG	BM (LC)
A1	NO	$101.9 \vee 258.1$	$77.3 \vee 282.7$	$107.2 \vee 252.8$	$65.3 \vee 294.7$	$176.5 \vee 183.5$
	IO	$101.7 \vee 258.3$	$77.3 \vee 282.7$	$107.0 \vee 253.0$	$65.5 \vee 294.5$	$171.1 \vee 188.9$
A2	NO	$78.1 \vee 281.9$	$102.7 \vee 257.3$	$72.8 \vee 287.2$	$114.7 \vee 245.3$	$3.5 \vee 356.5$
	IO	$78.3 \vee 281.7$	$102.7 \vee 257.3$	$73.0 \vee 287.0$	$114.6 \vee 245.4$	$8.9 \vee 351.1$
B1	NO	$99.9 \vee 260.1$	$77.7 \vee 282.3$	$104.8 \vee 255.2$	$66.9 \vee 293.1$	$153.4 \vee 206.6$
	IO	$104.9 \vee 255.1$	$76.4 \vee 283.6$	$111.3 \vee 248.7$	$62.4 \vee 297.6$	
B2	NO	$75.1 \vee 284.9$	$103.6 \vee 256.4$	$68.8 \vee 291.2$	$117.6 \vee 242.4$	
	IO	$80.5 \vee 279.5$	$102.2 \vee 257.8$	$75.7 \vee 284.3$	$112.8 \vee 247.2$	$29.1 \vee 330.9$
B3	NO	$103.5 \vee 256.5$	$78.8 \vee 281.2$	$108.9 \vee 251.1$	$66.9 \vee 293.1$	
	IO	$103.1 \vee 256.9$	$78.6 \vee 281.4$	$108.4 \vee 251.6$	$66.8 \vee 293.2$	
	$[\theta^\nu_{13}, \theta^\nu_{12}]$	$[\pi/20, -\pi/4]$	$[\pi/10, -\pi/4]$	$[a, -\pi/4]$	$[\pi/20, b]$	$[\pi/20, \pi/6]$
C1	NO	$108.7 \vee 251.3$	$44.8 \vee 315.2$	$29.7 \vee 330.3$	$154.9 \vee 205.1$	$132.8 \vee 227.2$
	IO	$108.5 \vee 251.5$	$45.2 \vee 314.8$	$30.5 \vee 329.5$	$153.7 \vee 206.3$	$132.3 \vee 227.7$
	$[\theta^\nu_{13}, \theta^\nu_{12}]$	$[\pi/20, c]$	$[\pi/20, \pi/4]$	$[\pi/10, \pi/4]$	$[a, \pi/4]$	$[\pi/20, \pi/5]$
C2	NO	$146.0 \vee 214.0$	$71.3 \vee 288.7$	$135.2 \vee 224.8$	$150.3 \vee 209.7$	$138.5 \vee 221.5$
	IO	$145.3 \vee 214.7$	$71.5 \vee 288.5$	$134.8 \vee 225.2$	$149.5 \vee 210.5$	$138.1 \vee 221.9$

the NO and IO spectra.[36] We use the values of δ from Table 4.2 to obtain predictions for the Majorana phases in the next subsection.

4.5.2 Majorana phases

In this subsection, we present results of the numerical analysis of the predictions for the Majorana phases, performed using the best fit values of the neutrino mixing parameters given in eqs. (4.1)–(4.3). These predictions are obtained from the sum rules in eqs. (4.143)–(4.146), in which we have used the proper expressions for $\sin^2\theta_{23}$ and $\cos\delta$ from Tables 3.1 and 3.2. We summarise the predictions for all the cases considered in Tables 4.3 and 4.4, in which we give, respectively, the values of the phase differences $(\alpha_{21}/2 - \xi_{21}/2)$ and $(\alpha_{31}/2 - \xi_{31}/2)$ found in schemes A1, A2, B3, C1 and C2. In the cases of schemes B1 and B2 we present in Table 4.4 results for the difference $(\alpha_{31}/2 - \xi_{31}/2 - \beta)$, since the

[36] We recall that $\sin^2\theta_{23}$ is a free parameter in schemes B1 and B2.

Table 4.3. The phase difference $(\alpha_{21}/2 - \xi_{21}/2)$ in degrees calculated using the best fit values of the neutrino mixing angles quoted in eqs. (4.1)–(4.3), except for scheme B3 and the BM (LC) form of $\tilde{U}_\nu$. For scheme B3 the results shown are obtained for $\omega = 0$, $\mathrm{sgn}\,(\sin 2\theta^e_{13}) = 1$ and $\sin^2\theta_{23} = 0.48907$ (0.48886) in the case of the NO (IO) spectrum. The numbers quoted for the BM (LC) form of $\tilde{U}_\nu$ are for the 3σ upper bound of $\sin^2\theta_{12} = 0.354$. For each cell the first number corresponds to $\delta = \cos^{-1}(\cos\delta)$, while the second number is obtained for $\delta = 2\pi - \cos^{-1}(\cos\delta)$. In cases C1 and C2, $\theta^\nu_{23} = -\pi/4$ and the values in square brackets are those of $[\theta^\nu_{13}, \theta^\nu_{12}]$ used. The letters a, b and c stand for $\sin^{-1}(1/3)$, $\sin^{-1}(1/\sqrt{2+r})$ and $\sin^{-1}(1/\sqrt{3})$, respectively. See text for further details.

Case	$\tilde{U}_\nu$ / O	TBM	GRA	GRB	HG	BM (LC)
A1	NO	$342.3 \vee 17.7$	$341.4 \vee 18.6$	$342.9 \vee 17.1$	$342.1 \vee 17.9$	$359.0 \vee 1.0$
	IO	$342.1 \vee 17.9$	$341.2 \vee 18.8$	$342.7 \vee 17.3$	$341.9 \vee 18.1$	$357.4 \vee 2.6$
A2	NO	$17.7 \vee 342.3$	$18.6 \vee 341.4$	$17.1 \vee 342.9$	$17.9 \vee 342.1$	$1.0 \vee 359.0$
	IO	$17.9 \vee 342.1$	$18.8 \vee 341.2$	$17.3 \vee 342.7$	$18.1 \vee 341.9$	$2.6 \vee 357.4$
B1	NO	$340.3 \vee 19.7$	$339.3 \vee 20.7$	$340.8 \vee 19.2$	$339.9 \vee 20.1$	$351.7 \vee 8.3$
	IO	$345.0 \vee 15.0$	$344.1 \vee 15.9$	$345.7 \vee 14.3$	$345.0 \vee 15.0$	
B2	NO	$15.1 \vee 344.9$	$16.0 \vee 344.0$	$14.4 \vee 345.6$	$15.0 \vee 345.0$	
	IO	$20.2 \vee 339.8$	$21.1 \vee 338.9$	$19.6 \vee 340.4$	$20.6 \vee 339.4$	$9.2 \vee 350.8$
B3	NO	$342.5 \vee 17.5$	$341.4 \vee 18.6$	$343.1 \vee 16.9$	$342.0 \vee 18.0$	
	IO	$342.3 \vee 17.7$	$341.2 \vee 18.8$	$342.9 \vee 17.1$	$341.8 \vee 18.2$	
	$[\theta^\nu_{13}, \theta^\nu_{12}]$	$[\pi/20, -\pi/4]$	$[\pi/10, -\pi/4]$	$[a, -\pi/4]$	$[\pi/20, b]$	$[\pi/20, \pi/6]$
C1	NO	$163.5 \vee 196.5$	$166.9 \vee 193.1$	$170.7 \vee 189.3$	$353.0 \vee 7.0$	$347.6 \vee 12.4$
	IO	$163.3 \vee 196.7$	$166.6 \vee 193.4$	$170.3 \vee 189.7$	$352.6 \vee 7.4$	$347.4 \vee 12.6$
	$[\theta^\nu_{13}, \theta^\nu_{12}]$	$[\pi/20, c]$	$[\pi/20, \pi/4]$	$[\pi/10, \pi/4]$	$[a, \pi/4]$	$[\pi/20, \pi/5]$
C2	NO	$11.6 \vee 348.4$	$16.5 \vee 343.5$	$13.1 \vee 346.9$	$9.3 \vee 350.7$	$13.5 \vee 346.5$
	IO	$11.9 \vee 348.1$	$16.7 \vee 343.3$	$13.4 \vee 346.6$	$9.7 \vee 350.3$	$13.7 \vee 346.3$

phase β, in general, is not fixed, unless some additional arguments are used that fix it. In the case of the B3 scheme the results are obtained for $\omega = 0$, $\mathrm{sgn}\,(\sin 2\theta^e_{13}) = 1$, and for $\sin^2\theta_{23} = 0.48907$ (0.48886) for the NO (IO) spectrum (see subsection 4.2.3 for details).

All the quoted phases are determined with a two-fold ambiguity owing to the fact that the Dirac phase δ, which enters into the expressions for all the phases under discussion, is determined with a two-fold ambiguity from the sum rules it satisfies in the schemes of interest. The absolute values of the sines of the phases quoted in Tables 4.3 and 4.4 are all proportional to $\sin\theta_{13}$, and thus, are relatively small. The results in cases A1 and B2 for the TBM, BM (LC), GRA, GRB and HG symmetry forms of $\tilde{U}_\nu$ considered were first obtained in [99] using the best fit values of $\sin^2\theta_{12}$, $\sin^2\theta_{23}$ and $\sin^2\theta_{13}$ from (the first e-archive version of) ref. [18]. Here, in particular, we update the results derived in [99].

As we have already noticed, in the BM (LC) case, the sum rules for $\cos\delta$ lead to unphysical values of $|\cos\delta| > 1$ if one uses as input the current best fit values of $\sin^2\theta_{12}$, $\sin^2\theta_{23}$ and $\sin^2\theta_{13}$. Physical values of $\cos\delta$ are found for larger (smaller) values of $\sin^2\theta_{12}$

Table 4.4. The same as in Table 4.3, but for the phase difference $(\alpha_{31}/2 - \xi_{31}/2)$ given in degrees. In cases B1 and B2 the presented numbers correspond to $(\alpha_{31}/2 - \xi_{31}/2 - \beta)$, where β is a free phase parameter. See text for further details.

Case	$\tilde{U}_\nu$ / O	TBM	GRA	GRB	HG	BM (LC)
A1	NO	$167.9 \vee 192.1$	$166.7 \vee 193.3$	$168.4 \vee 191.6$	$167.0 \vee 193.0$	$179.4 \vee 180.6$
	IO	$167.7 \vee 192.3$	$166.6 \vee 193.4$	$168.3 \vee 191.7$	$166.8 \vee 193.2$	$178.5 \vee 181.5$
A2	NO	$192.1 \vee 167.9$	$193.3 \vee 166.7$	$191.6 \vee 168.4$	$193.0 \vee 167.0$	$180.6 \vee 179.4$
	IO	$192.3 \vee 167.7$	$193.4 \vee 166.6$	$191.7 \vee 168.3$	$193.2 \vee 166.8$	$181.5 \vee 178.5$
B1	NO	$346.4 \vee 13.6$	$345.2 \vee 14.8$	$346.9 \vee 13.1$	$345.4 \vee 14.6$	$355.2 \vee 4.8$
	IO	$349.7 \vee 10.3$	$348.6 \vee 11.4$	$350.2 \vee 9.8$	$349.1 \vee 10.9$	
B2	NO	$10.3 \vee 349.7$	$11.4 \vee 348.6$	$9.8 \vee 350.2$	$11.0 \vee 349.0$	
	IO	$13.9 \vee 346.1$	$15.1 \vee 344.9$	$13.4 \vee 346.6$	$15.0 \vee 345.0$	$5.3 \vee 354.7$
B3	NO	$168.0 \vee 192.0$	$166.7 \vee 193.3$	$168.6 \vee 191.4$	$166.9 \vee 193.1$	
	IO	$167.9 \vee 192.1$	$166.6 \vee 193.4$	$168.4 \vee 191.6$	$166.8 \vee 193.2$	
	$[\theta^\nu_{13}, \theta^\nu_{12}]$	$[\pi/20, -\pi/4]$	$[\pi/10, -\pi/4]$	$[a, -\pi/4]$	$[\pi/20, b]$	$[\pi/20, \pi/6]$
C1	NO	$348.8 \vee 11.2$	$350.2 \vee 9.8$	$352.9 \vee 7.1$	$175.5 \vee 184.5$	$171.9 \vee 188.1$
	IO	$348.7 \vee 11.3$	$350.0 \vee 10.0$	$352.7 \vee 7.3$	$175.2 \vee 184.8$	$171.7 \vee 188.3$
	$[\theta^\nu_{13}, \theta^\nu_{12}]$	$[\pi/20, c]$	$[\pi/20, \pi/4]$	$[\pi/10, \pi/4]$	$[a, \pi/4]$	$[\pi/20, \pi/5]$
C2	NO	$188.8 \vee 171.2$	$191.2 \vee 168.8$	$189.8 \vee 170.2$	$187.1 \vee 172.9$	$190.1 \vee 169.9$
	IO	$189.0 \vee 171.0$	$191.3 \vee 168.7$	$190.0 \vee 170.0$	$187.3 \vee 172.7$	$190.3 \vee 169.7$

$(\sin^2\theta_{23})$. The values of the phases given in Tables 4.3 and 4.4 and corresponding to the BM (LC) form are obtained for the 3σ upper bound of $\sin^2\theta_{12} = 0.354$ and the best fit values of $\sin^2\theta_{23}$ and $\sin^2\theta_{13}$. For these values of the three mixing parameters $|\cos\delta|$ has an unphysical value greater than one only for schemes B1 with the IO spectrum, B2 with the NO spectrum and B3.

A few comments on the results presented in Tables 4.3 and 4.4 are in order. These results show that for a given scheme and fixed form of the matrix $\tilde{U}_\nu$, the difference between the predictions of the phases $(\alpha_{21}/2 - \xi_{21}/2)$ and $(\alpha_{31}/2 - \xi_{31}/2)$ or $(\alpha_{31}/2 - \xi_{31}/2 - \beta)$ for the NO and IO neutrino mass spectra are relatively small. The largest difference is approximately of 5° between the NO and IO values of $(\alpha_{21}/2 - \xi_{21}/2)$ in the B1 and B2 schemes. The same observation is valid for the variation of the phases with the variation of the form of $\tilde{U}_\nu$ within a given scheme, the only exceptions being (i) the BM (LC) form, for which the phases differ from those for the TBM, GRA, GRB and HG forms of $\tilde{U}_\nu$ of schemes A1, A2, B1 (NO spectrum) and B2 (IO spectrum) by approximately 10° to 16°, and (ii) the C1 scheme, in which the values of the phases $(\alpha_{21}/2 - \xi_{21}/2)$ and $(\alpha_{31}/2 - \xi_{31}/2)$ differ relatively little within the group of the first three cases in Tables 4.3 and 4.4 and within the group of the last two ones, but change significantly — approximately by π — when switching from a case of one of the groups to a case in the second group.

For a given symmetry form of $\tilde{U}_\nu$ — TBM, GRA, GRB and HG — the phase difference $(\alpha_{21}/2 - \xi_{21}/2)$ has very similar values for the A1, B1 and B3 schemes, they differ

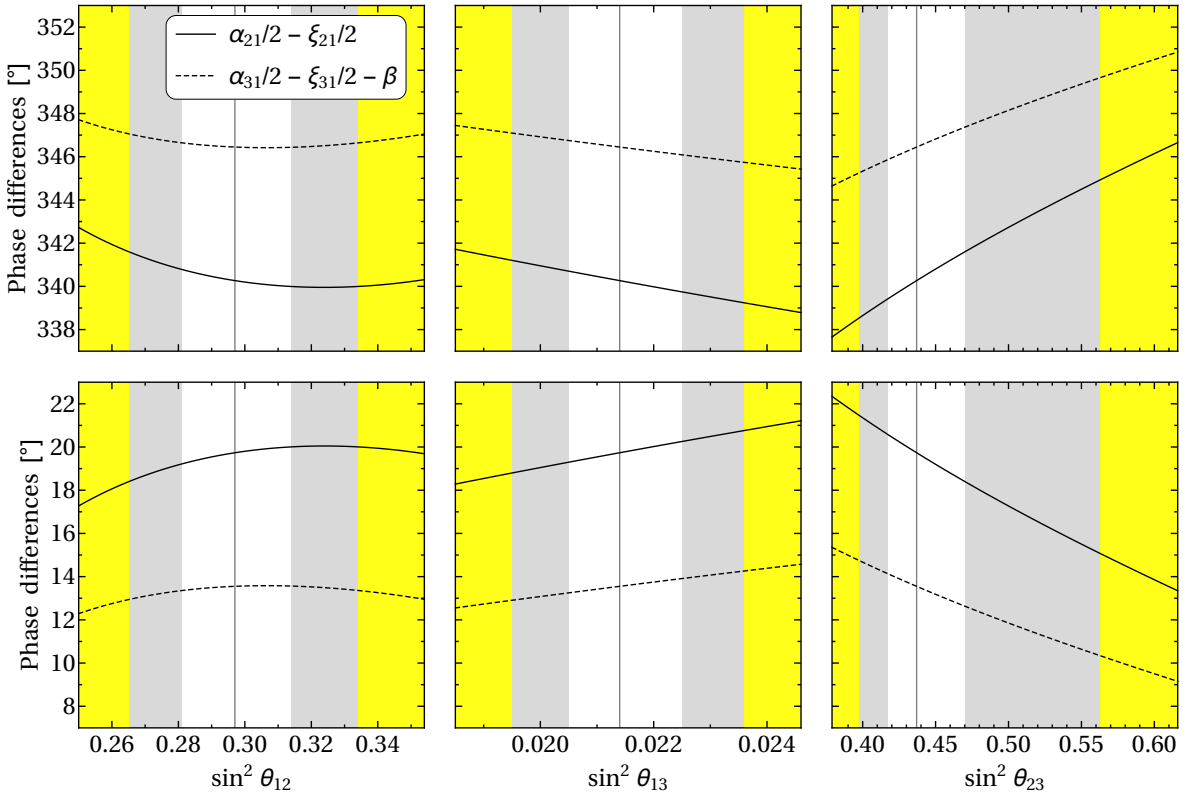

Figure 4.1. The phase differences $(\alpha_{21}/2 - \xi_{21}/2)$ (solid line) and $(\alpha_{31}/2 - \xi_{31}/2 - \beta)$ (dashed line) as functions of $\sin^2\theta_{ij}$ in case B1 and for the TBM symmetry form of the matrix $\tilde{U}_\nu$. The two other parameters, $\sin^2\theta_{kl}$ and $\sin^2\theta_{mn}$, $ij \neq kl \neq mn$, have been fixed to their best fit values for the NO spectrum. The upper panels correspond to $\delta = \cos^{-1}(\cos\delta)$, while the lower panels correspond to $\delta = 2\pi - \cos^{-1}(\cos\delta)$. The vertical line and the three coloured vertical bands indicate the best fit value and the 1σ, 2σ and 3σ allowed ranges of $\sin^2\theta_{ij}$.

approximately by at most 2°, and for the A2 and B2 schemes, for which the difference does not exceed 3°. However, the predictions for $(\alpha_{21}/2 - \xi_{21}/2)$ for schemes A1, B1, B3 and A2, B2 differ significantly — the sum of the values of $(\alpha_{21}/2 - \xi_{21}/2)$ for any of the A1, B1, B3 schemes and for any of the A2, B2 schemes being roughly equal to 2π. In contrast, for a given symmetry form of $\tilde{U}_\nu$ — TBM, GRA, GRB and HG — (i) the values of the phase difference $(\alpha_{31}/2 - \xi_{31}/2)$ $((\alpha_{31}/2 - \xi_{31}/2 - \beta))$ for schemes A1 and A2 (B1 and B2) differ significantly — by up to 26° (337°), and (ii) the values of $(\alpha_{31}/2 - \xi_{31}/2)$ and $(\alpha_{31}/2 - \xi_{31}/2 - \beta)$ are drastically different. At the same time, the values of $(\alpha_{31}/2 - \xi_{31}/2)$ for the A1 and B3 schemes practically coincide.

Further, we show how the predictions for the phase differences presented in Tables 4.3 and 4.4 change when the uncertainties in determination of the neutrino mixing parameters are taken into account. As an example, we consider cases B1 and B2 with the TBM form of the matrix $\tilde{U}_\nu$. We fix two of $\sin^2\theta_{ij}$ to their best fit values for the NO neutrino mass spectrum and vary the third one in its 3σ allowed range given in eqs. (4.1)–(4.3). We show the results for cases B1 and B2 in Figs. 4.1 and 4.2, respectively. As can be seen, the phase differences of interest depend weakly on $\sin^2\theta_{12}$ and $\sin^2\theta_{13}$. When these parameters are varied in their 3σ ranges, the variation of the phase differences is within a few degrees. The dependence on $\sin^2\theta_{23}$ is stronger: the maximal variations of $(\alpha_{21}/2 - \xi_{21}/2)$ and $(\alpha_{31}/2 - \xi_{31}/2 - \beta)$ are approximately of 9° and 6° in both cases.

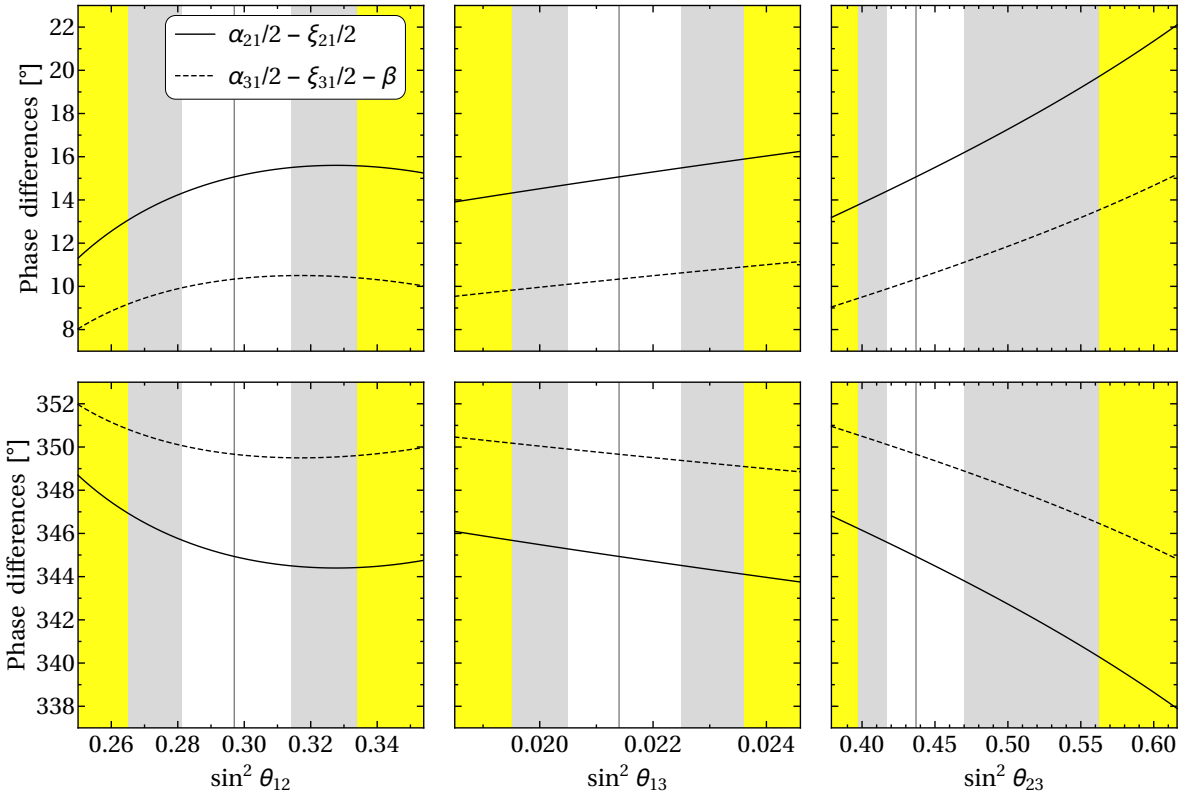

Figure 4.2. The same as in Fig. 4.1, but for case B2.

4.5.3 Neutrinoless double beta decay

If the light neutrinos with definite mass ν_j are Majorana fermions, their exchange can trigger processes in which the total lepton charge changes by two units, $|\Delta L| = 2$: $K^+ \to \pi^- + \mu^+ + \mu^+$, $e^- + (A, Z) \to e^+ + (A, Z-2)$, etc. The experimental searches for $(\beta\beta)_{0\nu}$-decay, $(A, Z) \to (A, Z+2) + e^- + e^-$, of even-even nuclei, such as ^{48}Ca, ^{76}Ge, ^{82}Se, ^{100}Mo, ^{116}Cd, ^{130}Te, ^{136}Xe, ^{150}Nd, etc., are unique in reaching the sensitivity that might allow to observe this process if it is triggered by the exchange of the light neutrinos ν_j (see, e.g., refs. [39, 41, 42]). In $(\beta\beta)_{0\nu}$-decay, two neutrons of the initial nucleus (A, Z) transform by exchanging virtual $\nu_{1,2,3}$ into two protons of the final state nucleus $(A, Z+2)$ and two free electrons. The corresponding $(\beta\beta)_{0\nu}$-decay amplitude has the form (see, e.g., refs. [38, 41, 42]):

$$\mathcal{A}\left((\beta\beta)_{0\nu}\right) = G_{\rm F}^2 \, \langle m \rangle \, M(A, Z) \,, \tag{4.147}$$

where $G_{\rm F}$ is the Fermi constant, $\langle m \rangle$ is the $(\beta\beta)_{0\nu}$-decay effective Majorana mass and $M(A, Z)$ is the nuclear matrix element of the process. The $(\beta\beta)_{0\nu}$-decay effective Majorana mass $\langle m \rangle$ contains all the dependence of $\mathcal{A}\left((\beta\beta)_{0\nu}\right)$ on the neutrino mixing parameters. The current experimental limits on $|\langle m \rangle|$ are in the range of $(0.1 - 0.7)$ eV. Most importantly, a large number of experiments of a new generation aim at sensitivity to $|\langle m \rangle| \sim (0.01 - 0.05)$ eV (for a detailed discussion of the current limits on $|\langle m \rangle|$ and of the currently running and future planned $(\beta\beta)_{0\nu}$-decay experiments and their prospective sensitivities see, e.g., the recent review article [43]).

The predictions for $|\langle m\rangle|$,[37]

$$|\langle m\rangle| = \left|\sum_{i=1}^{3} m_i U_{ei}^2\right| = \left|m_1 \cos^2\theta_{12}\cos^2\theta_{13} + m_2 \sin^2\theta_{12}\cos^2\theta_{13} e^{i\alpha_{21}} + m_3 \sin^2\theta_{13} e^{i(\alpha_{31}-2\delta)}\right| , \quad (4.148)$$

$m_{1,2,3}$ being the light Majorana neutrino masses, depend on the values of the Majorana phase α_{21} and on the Majorana-Dirac phase difference $(\alpha_{31} - 2\delta)$. In what follows we will derive predictions for $|\langle m\rangle|$ as a function of the lightest neutrino mass $m_{\rm min} \equiv \min(m_j)$, $j = 1, 2, 3$, for both the NO and IO neutrino mass spectra and for two values of each of the phases ξ_{21} and ξ_{31}: $\xi_{21} = 0$ or π, $\xi_{31} = 0$ or π. The choice of the two values of the phases ξ_{21} and ξ_{31} will be justified in the next section, where we show that the requirement of generalised CP invariance of the neutrino Majorana mass term in the cases of the A_4, T', S_4 and A_5 lepton flavour symmetries leads to the constraints $\xi_{21} = 0$ or π, $\xi_{31} = 0$ or π.

We recall that the two heavier neutrino masses are expressed in terms of the lightest neutrino mass and the two independent neutrino mass squared differences Δm^2_{21} and $\Delta m^2_{31(23)}$, in the case of NO (IO) spectrum, measured in neutrino oscillation experiments (see eqs. (1.4) and (1.5)). The best fit values and the 3σ allowed ranges of Δm^2_{21} and $\Delta m^2_{31(23)}$ obtained in the global analysis of the neutrino oscillation data performed in [162] we are going to use in our numerical study read:

$$(\Delta m^2_{21})_{\rm BF} = 7.37 \times 10^{-5}\ {\rm eV}^2\,, \quad 6.93 \times 10^{-5}\ {\rm eV}^2 \leq \Delta m^2_{21} \leq 7.97 \times 10^{-5}\ {\rm eV}^2\,, \quad (4.149)$$

$$(\Delta m^2_{31(23)})_{\rm BF} = 2.54\ (2.50) \times 10^{-3}\ {\rm eV}^2\,,$$

$$2.40\ (2.36) \times 10^{-3}\ {\rm eV}^2 \leq \Delta m^2_{31(23)} \leq 2.67\ (2.64) \times 10^{-3}\ {\rm eV}^2\,, \quad (4.150)$$

where the quoted values of Δm^2_{31} and Δm^2_{23} correspond to the NO and IO spectra, respectively.

As can be seen from Tables 4.2–4.4, the values of all three phases, δ, α_{21} and α_{31}, for scheme B3 with $\omega = 0$ and ${\rm sgn}\,(\sin 2\theta^e_{13}) = 1$ are very close to the values for scheme A1. Thus, the predictions for $|\langle m\rangle|$ in scheme B3 are practically the same as those for scheme A1 and we present predictions only for the latter.

In Fig. 4.3 we show the absolute value of the effective Majorana mass $|\langle m\rangle|$ versus the lightest neutrino mass $m_{\rm min}$ in the cases of schemes A1, A2, B1, B2, C1 and C2 for the NO (blue lines and bands) and IO (dark-red lines and bands) neutrino mass spectra using the best fit values of the mixing angles θ_{12} and θ_{13} quoted in eqs. (4.1) and (4.3), the best fit values of the two neutrino mass squared differences Δm^2_{21} and $\Delta m^2_{31(23)}$ given in eqs. (4.149) and (4.150), the values of the Dirac phase δ from Table 4.2 and the values of the Majorana phases α_{21} and α_{31} extracted from Tables 4.3 and 4.4 setting $(\xi_{21}, \xi_{31}) = (0, 0)$. In Figs. 4.4, 4.5 and 4.6 the values of (ξ_{21}, ξ_{31}) are fixed to $(0, \pi)$, $(\pi, 0)$ and (π, π), respectively.

In cases A1 and A2, the solid blue line corresponds to the TBM symmetry form of the matrix $\tilde{U}_\nu$, while the medium, small and tiny dashed blue lines are for the GRB, GRA and HG symmetry forms, respectively. In cases B1 and B2, the predicted values of $|\langle m\rangle|$ for all the symmetry forms considered are within the blue and dark-red bands obtained varying the phase β within the interval $[0, \pi]$. In case C1 (C2), the solid blue line stands for case I (II) characterised by $[\theta^\nu_{13}, \theta^\nu_{12}] = [\pi/20, -\pi/4]$ ($[\pi/20, \pi/4]$), while the large, medium, small

[37] For a discussion of the physics implications of a measurement of $|\langle m\rangle|$, i.e., of the physics potential of the $(\beta\beta)_{0\nu}$-decay experiments see, e.g., [41, 42, 168–171].

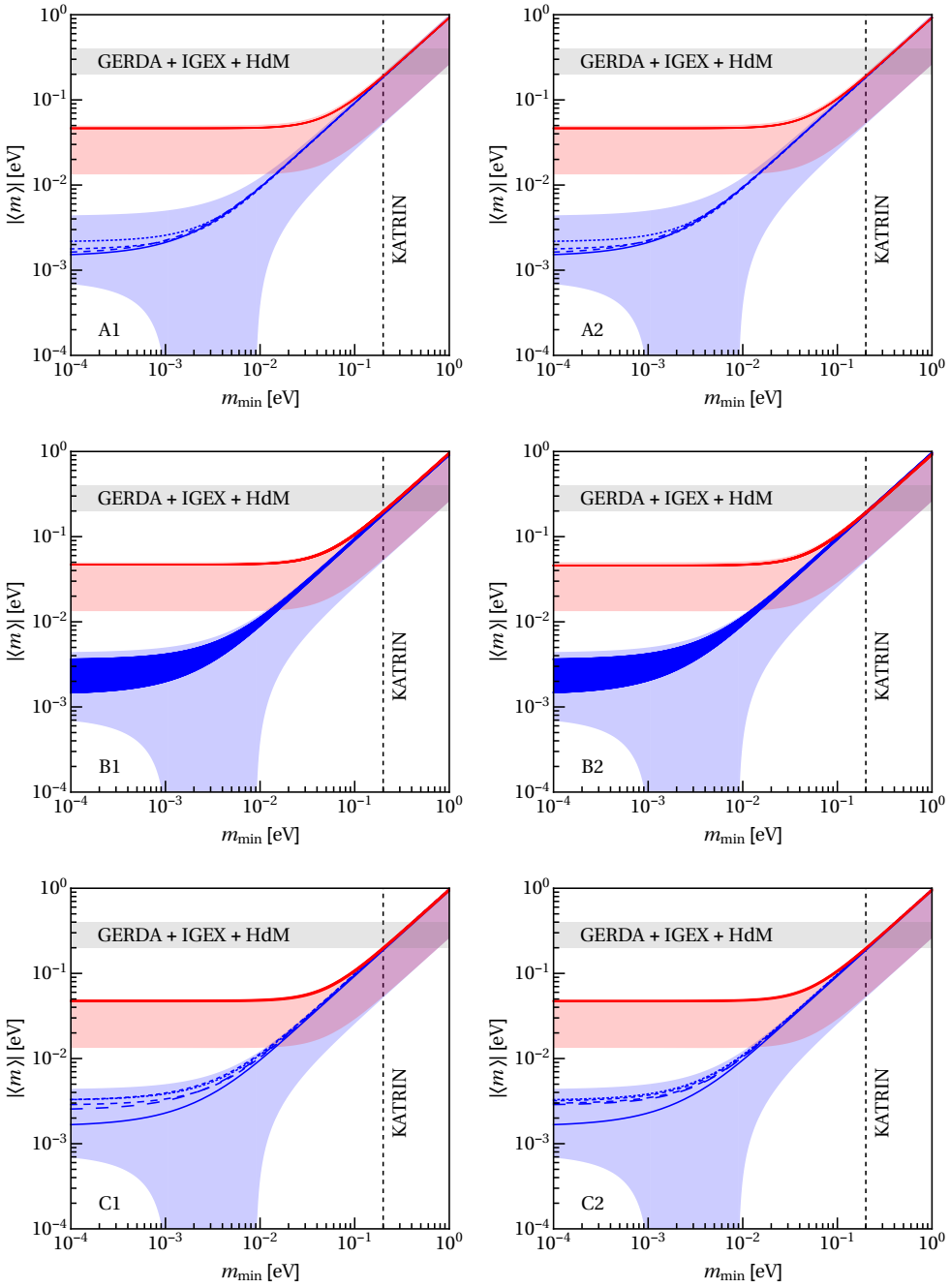

Figure 4.3. The absolute value of the effective Majorana mass $|\langle m \rangle|$ versus the lightest neutrino mass $m_{\rm min}$. The *blue (dark-red) lines* and *bands* correspond to $|\langle m \rangle|$ computed using the best fit values of θ_{12} and θ_{13} for the NO (IO) spectrum and the values of δ, α_{21} and α_{31} obtained using the corresponding sum rules and assuming $(\xi_{21}, \xi_{31}) = (0, 0)$. In cases A1 and A2, the *solid blue line* corresponds to the TBM symmetry form, while the *medium, small* and *tiny dashed blue lines* are for the GRB, GRA and HG symmetry forms, respectively. In cases B1 and B2, the predicted values of $|\langle m \rangle|$ for all the symmetry forms considered are within the blue and dark-red bands obtained varying the phase β in the interval $[0, \pi]$. In case C1 (C2), the *solid blue line* stands for case I (II), while the *large, medium, small* and *tiny dashed blue lines* are for cases V (III), II (V), IV (I) and III (IV), respectively. The *light-blue* and *light-red areas* are obtained varying the neutrino oscillation parameters θ_{12}, θ_{13}, Δm^2_{21} and $\Delta m^2_{31(23)}$ in their respective 3σ ranges quoted in eqs. (4.1), (4.3), (4.149) and (4.150) and the phases α_{21} and $(\alpha_{31} - 2\delta)$ in the interval $[0, 2\pi]$. The *horizontal grey band* indicates the upper bound on $|\langle m \rangle|$ of $(0.2 - 0.4)$ eV obtained in [172]. The *vertical dashed line* represents the prospective upper limit on $m_{\rm min}$ of 0.2 eV from the KATRIN experiment [61].

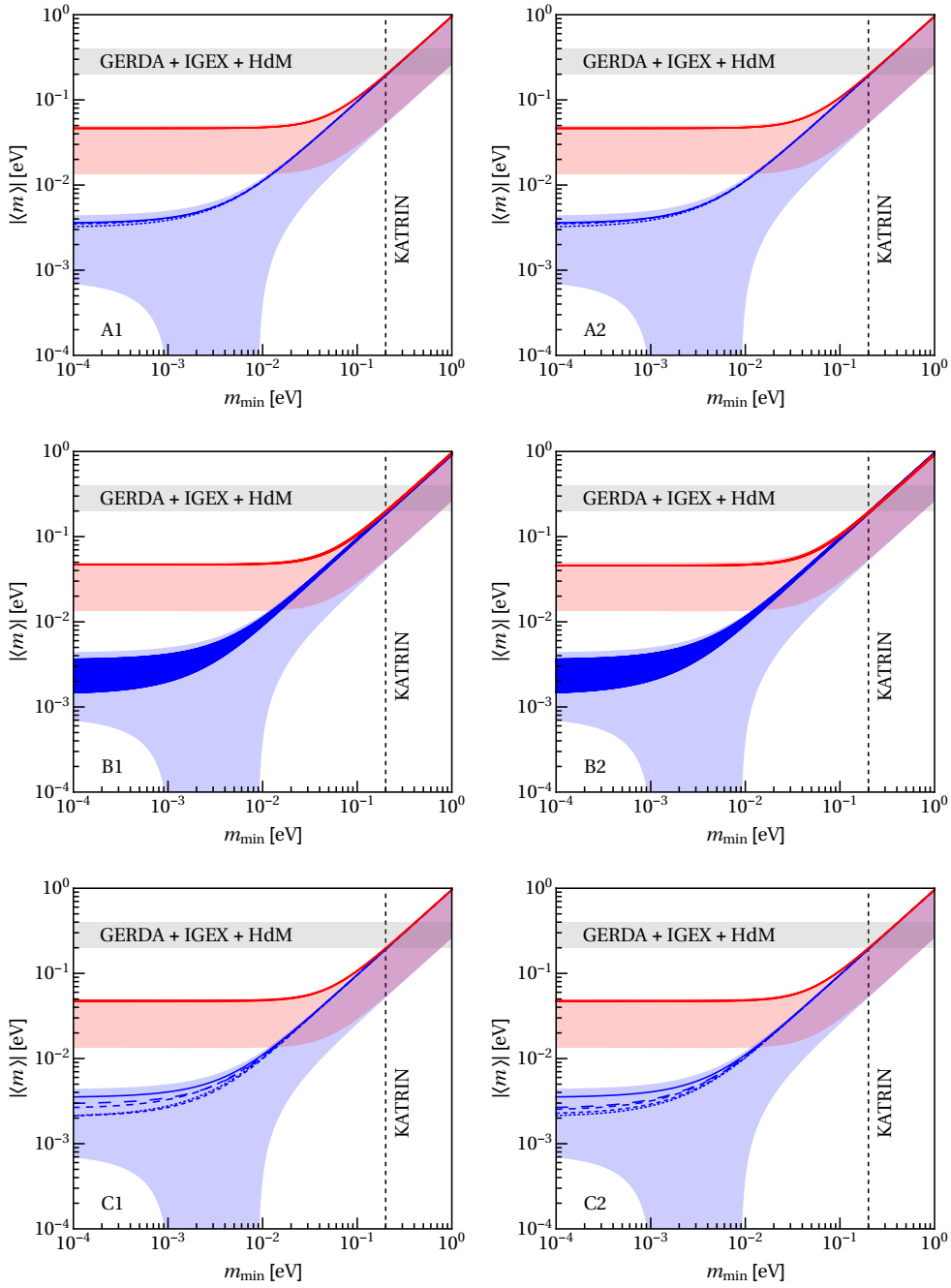

Figure 4.4. The same as in Fig. 4.3, but for $(\xi_{21}, \xi_{31}) = (0, \pi)$.

and tiny dashed blue lines are for cases V (III), II (V), IV (I) and III (IV), respectively, where the values of $[\theta_{13}^{\nu}, \theta_{12}^{\nu}]$ in each of these cases are given in subsection 4.5.1.

The light-blue and light-red areas are obtained varying the neutrino oscillation parameters θ_{12}, θ_{13}, Δm^2_{21} and $\Delta m^2_{31(23)}$ within their respective 3σ ranges quoted in eqs. (4.1), (4.3), (4.149) and (4.150), and the phases α_{21} and $(\alpha_{31} - 2\delta)$ within the interval $[0, 2\pi]$.[38]

[38]The absolute value of the effective Majorana mass as a function of α_{21} and $(\alpha_{31} - 2\delta)$, $|\langle m \rangle| = f(\alpha_{21}, \alpha_{31} - 2\delta)$, possesses the following symmetry:

$$f(\alpha_{21}, \alpha_{31} - 2\delta) = f(2\pi - \alpha_{21}, 2\pi - (\alpha_{31} - 2\delta))\,.$$

Thus, it is enough to vary one phase (e.g., α_{21}) in the interval $[0, \pi]$ and the second phase (e.g., $(\alpha_{31} - 2\delta)$) in the interval $[0, 2\pi]$.

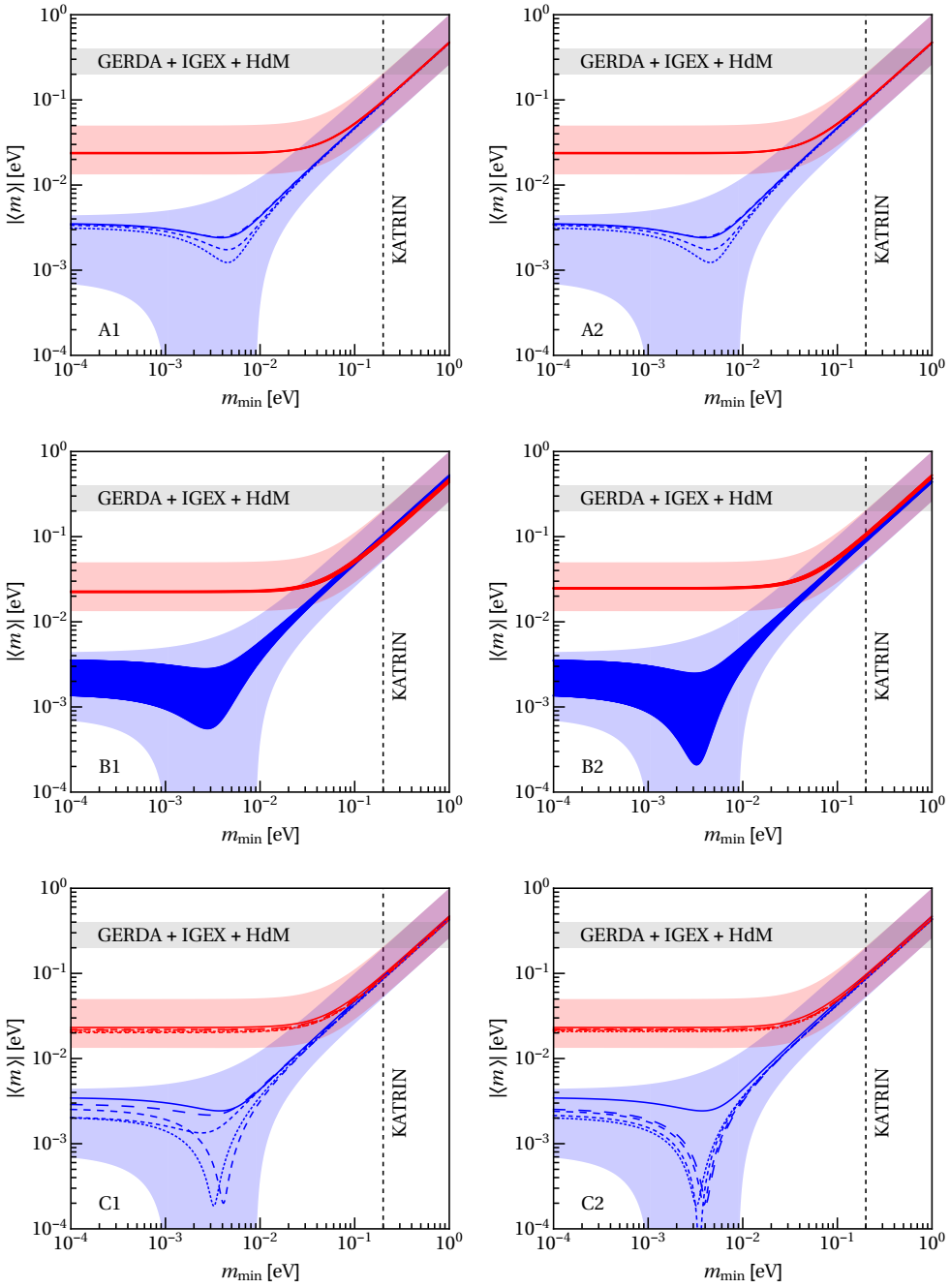

Figure 4.5. The same as in Fig. 4.3, but for $(\xi_{21}, \xi_{31}) = (\pi, 0)$.

The horizontal grey band indicates the upper bound on $|\langle m \rangle|$ of $(0.2 - 0.4)$ eV obtained in [172]. The vertical dashed line represents the prospective upper limit on $m_{\min}$ of 0.2 eV from the KATRIN experiment [61].

As Figs. 4.3 and 4.4 show, for $(\xi_{21}, \xi_{31}) = (0, 0)$ and $(0, \pi)$, the absolute value of the effective Majorana mass $|\langle m \rangle|$ for the IO spectrum has practically the maximal possible values for all schemes considered. In the case of the NO spectrum and $(\xi_{21}, \xi_{31}) = (0, 0)$, $|\langle m \rangle|$ is always bigger than $(1.5 - 2.0) \times 10^{-3}$ eV. For $(\xi_{21}, \xi_{31}) = (0, \pi)$, $|\langle m \rangle|$ has the maximal possible values in the A1 and A2 schemes as well in case I (II) of the C1 (C2) scheme; in the other cases of the C1 (C2) scheme, $|\langle m \rangle|$ is always bigger than 2.0×10^{-3} eV. In the B1 and B2 schemes and for the NO spectrum, $|\langle m \rangle|$ can have the maximal possible values for both sets of values of $(\xi_{21}, \xi_{31}) = (0, 0)$ and $(0, \pi)$.

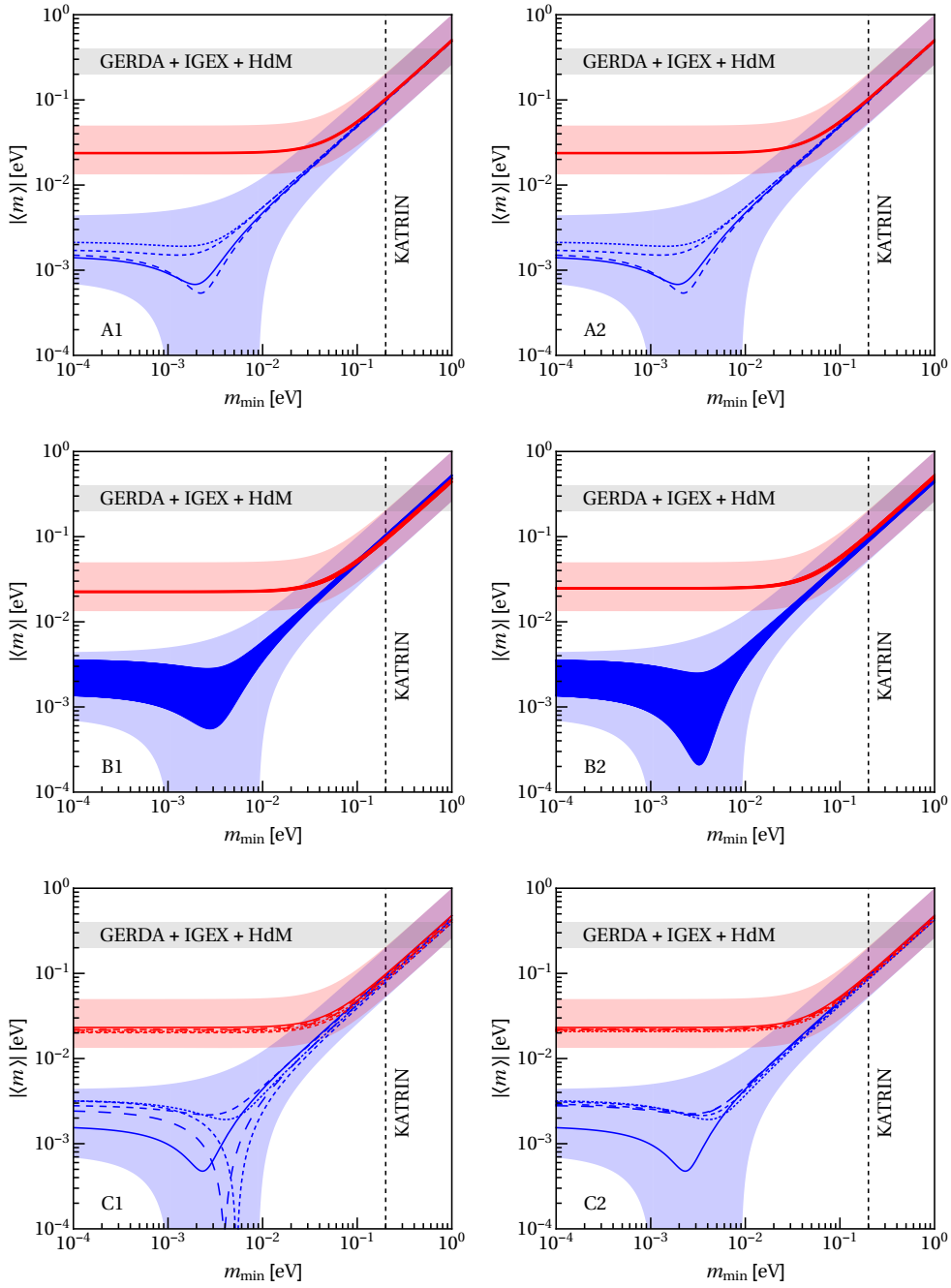

Figure 4.6. The same as in Fig. 4.3, but for $(\xi_{21}, \xi_{31}) = (\pi, \pi)$.

For $(\xi_{21}, \xi_{31}) = (\pi, 0)$ and (π, π) (Figs. 4.5 and 4.6) and the IO spectrum, a partial compensation between the three terms in $|\langle m \rangle|$ takes place for all schemes considered. However, $|\langle m \rangle| \gtrsim 2 \times 10^{-2}$ eV for all cases analysed by us. The mutual compensation between the different terms in $|\langle m \rangle|$ can be stronger in the case of the NO spectrum, when $|\langle m \rangle| \lesssim 10^{-3}$ eV in certain cases in specific intervals of values of m_1, typically between approximately 10^{-3} eV and 7×10^{-3} eV.

4.6 Implications of a generalised CP symmetry

In the present section, we derive constraints on the phases ξ_{21} and ξ_{31} in the matrix U_ν, which diagonalises the neutrino Majorana mass matrix M_ν, within the approach in which a lepton flavour symmetry G_f is combined with a generalised CP symmetry $H_{\rm CP}$, which has been discussed in Section 1.3. We examine successively the cases of $G_f = A_4$ (T'), S_4 and A_5 with the three LH charged leptons and three LH flavour neutrinos transforming in a 3-dimensional representation **3** of G_f. At low energies the flavour symmetry G_f has necessarily to be broken down to residual symmetries G_e and G_ν in the charged lepton and neutrino sectors, respectively. All the cases considered in the present study fall into the class of residual symmetries with trivial G_e (G_f being fully broken in the charged lepton sector) and $G_\nu = Z_2 \times Z_2$.[39]

The residual symmetry G_ν alone does not provide any information on the phases ξ_{21} and ξ_{31} of interest. Indeed, let $\bar{U}_\nu$ be a unitary matrix which diagonalises the complex symmetric neutrino Majorana mass matrix:

$$\bar{U}_\nu^T\, M_\nu\, \bar{U}_\nu = {\rm diag}\left(m_1 e^{-i\xi_1}, m_2 e^{-i\xi_2}, m_3 e^{-i\xi_3}\right)\,, \tag{4.151}$$

where m_i are non-negative non-degenerate masses[40] and ξ_i are phases contributing to the Majorana phases in the PMNS matrix. Let us introduce the matrices

$$\bar{Q}_0 = {\rm diag}\left(e^{i\frac{\xi_1}{2}}, e^{i\frac{\xi_2}{2}}, e^{i\frac{\xi_3}{2}}\right)\,, \tag{4.152}$$

and $U_\nu \equiv \bar{U}_\nu\, \bar{Q}_0$, such that

$$U_\nu^T\, M_\nu\, U_\nu = M_\nu^{\rm diag} \equiv {\rm diag}\left(m_1, m_2, m_3\right)\,. \tag{4.153}$$

Thus,

$$U_\nu = \bar{U}_\nu\, \bar{Q}_0 = e^{i\frac{\xi_1}{2}}\, \Psi_\nu\, \tilde{U}_\nu\, Q_0\,, \tag{4.154}$$

where Ψ_ν is a diagonal phase matrix containing, in general, two phases, $\xi_1/2$ is a common unphysical phase, and

$$Q_0 = {\rm diag}\left(1, e^{i\frac{\xi_2-\xi_1}{2}}, e^{i\frac{\xi_3-\xi_1}{2}}\right) = {\rm diag}\left(1, e^{i\frac{\xi_{21}}{2}}, e^{i\frac{\xi_{31}}{2}}\right)\,. \tag{4.155}$$

Clearly, the phases of interest are $\xi_{21} = \xi_2 - \xi_1$ and $\xi_{31} = \xi_3 - \xi_1$. It is clear from eq. (4.154) that the common phases of the columns of U_ν have been factorised in the matrix $\bar{Q}_0$.

The G_ν invariance of the neutrino mass matrix implies that eq. (1.28) holds. Further, using eq. (4.153), we find

$$\left(\rho_{\mathbf{3}}(g_\nu)^{\rm diag}\right)^T\, M_\nu^{\rm diag}\, \rho_{\mathbf{3}}(g_\nu)^{\rm diag} = M_\nu^{\rm diag}\,, \quad \text{with} \quad \rho_{\mathbf{3}}(g_\nu)^{\rm diag} = U_\nu^\dagger\, \rho_{\mathbf{3}}(g_\nu)\, U_\nu\,. \tag{4.156}$$

For $m_1 \neq m_2 \neq m_3$ and $\min(m_j) \neq 0$, $j = 1, 2, 3$, as it is not difficult to show, the matrix $\rho_{\mathbf{3}}(g_\nu)^{\rm diag}$ can have only the following form:

$$\rho_{\mathbf{3}}(g_\nu)^{\rm diag} = {\rm diag}\left(\pm 1, \pm 1, \pm 1\right)\,, \tag{4.157}$$

[39] As we have discussed in Section 1.2, there are two possibilities for $G_\nu = Z_2 \times Z_2$ to be realised. The first possibility is $G_\nu = Z_2 \times Z_2$ being an actual subgroup of G_f. Other possibility is that only one Z_2 subgroup of G_f is preserved, while the second Z_2 arises accidentally.

[40] It follows from the neutrino oscillation data that $m_1 \neq m_2 \neq m_3$, and that at least two of the three neutrino masses, $m_{2,3}$ ($m_{1,2}$) in the case of the NO (IO) spectrum, are non-zero. However, even if $m_1 = 0$ ($m_3 = 0$) at tree level and the zero value is not protected by a symmetry, m_1 (m_3) will get a non-zero contribution at least at two loop level [173, 174] and in the framework of a self-consistent (renormalisable) theory of neutrino mass generation this higher contribution will be finite.

where the signs of the three non-zero entries in $\rho_{\mathbf{3}}(g_\nu)^{\rm diag}$ are not correlated. Finally, from the preceding two equations we get

$$\rho_{\mathbf{3}}(g_\nu)^{\rm diag} = \bar{Q}_0\,\rho_{\mathbf{3}}(g_\nu)^{\rm diag}\,\bar{Q}_0^* = \bar{U}_\nu^\dagger\,\rho_{\mathbf{3}}(g_\nu)\,\bar{U}_\nu\,, \tag{4.158}$$

i.e., the phases ξ_i cancel out. Therefore, a lepton flavour symmetry alone does not lead to any constraints on the phases ξ_i, $i = 1, 2, 3$, and thus on the phases ξ_{21} and ξ_{31}.

Let us consider next the implications of a residual generalised CP symmetry $H^\nu_{\rm CP} \subset H_{\rm CP}$, which is preserved in the neutrino sector. In this case, the neutrino Majorana mass matrix in addition to eq. (1.28) satisfies eq. (1.50). Substituting M_ν from eq. (4.153), we find

$$\left(X^{\rm diag}_{\mathbf{3}\nu}\right)^T\, M_\nu^{\rm diag}\, X^{\rm diag}_{\mathbf{3}\nu} = M_\nu^{\rm diag}\,, \quad \text{with} \quad X^{\rm diag}_{\mathbf{3}\nu} = U_\nu^\dagger\, X_{\mathbf{3}\nu}\, U_\nu^*\,. \tag{4.159}$$

Again, since the three neutrino masses in $M_\nu^{\rm diag}$ have to be, as it follows from the data, non-degenerate, we have

$$X^{\rm diag}_{\mathbf{3}\nu} = {\rm diag}(\pm 1, \pm 1, \pm 1)\,. \tag{4.160}$$

Finally, using that $U_\nu \equiv \bar{U}_\nu\,\bar{Q}_0$, we obtain [175]

$${\rm diag}\left(\pm e^{i\xi_1}, \pm e^{i\xi_2}, \pm e^{i\xi_3}\right) = \bar{Q}_0\, X^{\rm diag}_{\mathbf{3}\nu}\,\bar{Q}_0 = \bar{U}_\nu^\dagger\, X_{\mathbf{3}\nu}\,\bar{U}_\nu^*\,. \tag{4.161}$$

Thus, we come to the conclusion that the phases ξ_i will be known once (i) the matrix $\bar{U}_\nu$ is fixed by the residual flavour symmetry G_ν, and (ii) the generalised CP transformations $X_{\mathbf{3}\nu} \in H^\nu_{\rm CP}$, which are consistent with G_ν (see eq. (1.52)), are identified.

Now we turn to concrete examples. For $G_f = A_4$, we choose to work in the Altarelli-Feruglio basis [85]. Preserving the S generator leads to $\bar{U}_\nu = U_{\rm TBM}$, provided there is an additional accidental $\mu-\tau$ symmetry [80]. Then, twelve generalised CP transformations consistent with the A_4 flavour symmetry for the triplet representation in the chosen basis have been found in [121], solving the consistency condition in eq. (1.47). These transformations can be summarised in a compact way as follows:

$$X_{\mathbf{3}} = \rho_{\mathbf{3}}(g)\,, \quad g \in A_4\,, \tag{4.162}$$

i.e., the generalised CP transformations consistent with the A_4 flavour symmetry are of the same form as the flavour symmetry group transformations [121]. They are given in Table 1 in [121] together with the elements $\hat{S}$ and $\hat{T}$ to which the generators S and T of A_4 are mapped by the consistency condition in eq. (1.47). Further, since in our case the residual flavour symmetry $G_\nu = Z_2 \times Z_2$, where one Z_2 factor corresponds to the preserved S generator, only those $X_{\mathbf{3}}$ are acceptable, for which $\hat{S} = S$. From Table 1 in [121] it follows that there are four such generalised CP transformations, namely, $\rho_{\mathbf{3}}(1)$, $\rho_{\mathbf{3}}(S)$, $\rho_{\mathbf{3}}(T^2ST)$ and $\rho_{\mathbf{3}}(TST^2)$, where 1 is the identity element of the group. The last two transformations are not symmetric in the chosen basis, and, as shown in [117, 121], lead to partially degenerate neutrino mass spectrum with two equal masses (see also Appendix A), which is ruled out by the neutrino oscillation data. Thus, we are left with two allowed generalised CP transformations, $\rho_{\mathbf{3}}(1)$ and $\rho_{\mathbf{3}}(S)$, for which we have:

$$U^\dagger_{\rm TBM}\,\rho_{\mathbf{3}}(1)\,U^*_{\rm TBM} = \rho_{\mathbf{3}}(1) = {\rm diag}(1, 1, 1)\,, \tag{4.163}$$

$$U^\dagger_{\rm TBM}\,\rho_{\mathbf{3}}(S)\,U^*_{\rm TBM} = {\rm diag}(-1, 1, -1)\,. \tag{4.164}$$

Finally, according to eq. (4.161), this implies that the phases ξ_i can be either 0 or π. The same conclusion holds for a T' flavour symmetry, because restricting ourselves to the

Table 4.5. The ten symmetric generalised CP transformations $X_{\mathbf{3}} = \rho_{\mathbf{3}}(g)$ consistent with the S_4 flavour symmetry for the triplet representation **3** in the chosen basis [176] determined by the consistency condition in eq. (1.47). The mapping $(T, S) \to (\hat{T}, \hat{S})$ is realised via the consistency condition applied to the group generators T and S, i.e., $X_{\mathbf{3}}\, \rho^*_{\mathbf{3}}(T)\, X^{-1}_{\mathbf{3}} = \rho_{\mathbf{3}}(\hat{T})$ and $X_{\mathbf{3}}\, \rho^*_{\mathbf{3}}(S)\, X^{-1}_{\mathbf{3}} = \rho_{\mathbf{3}}(\hat{S})$.

g, $X_{\mathbf{3}} = \rho_{\mathbf{3}}(g)$	$\hat{T}$	$\hat{S}$
$(ST^2)^2$	T	S
T^3	T^3	T^3ST
1	T^3	S
T	T^3	TST^3
T^2ST^2	STS	S
ST^2S	T	T^2ST^2
S	TST	S
T^2	T^3	T^2ST^2
STS	ST^2	ST^2ST
TST	T^2S	TST^2S

triplet representation for the LH charged lepton and neutrino fields, there is no way to distinguish T' from A_4 [143].

In the case of $G_f = S_4$, we choose to work in the basis given in [176]. The residual symmetry $G_\nu = Z_2 \times Z_2$, where one Z_2 factor corresponds to the preserved S generator in the chosen basis and the second one arises accidentally (a $\mu-\tau$ symmetry), leads to $\bar{U}_\nu = U_{\rm BM}$ [176]. As in the previous example, the generalised CP transformations consistent with the S_4 flavour symmetry are of the same form as the flavour symmetry group transformations [118]. Solving the consistency condition in eq. (1.47), we find ten symmetric generalised CP transformations consistent with the S_4 flavour symmetry for the triplet representation in the chosen basis. We summarise them in Table 4.5 together with elements $\hat{T}$ and $\hat{S}$ to which the consistency condition maps the group generators T and S.

From this table we see that there are four symmetric generalised CP transformations consistent with the preserved S generator, namely, $\rho_{\mathbf{3}}(1)$, $\rho_{\mathbf{3}}(S)$, $\rho_{\mathbf{3}}(T^2ST^2)$ and $\rho_{\mathbf{3}}(ST^2ST^2)$. Substituting them and $\bar{U}_\nu = U_{\rm BM}$ in eq. (4.161), we find:

$$U^\dagger_{\rm BM}\, \rho_{\mathbf{3}}(1)\, U^*_{\rm BM} = \rho_{\mathbf{3}}(1) = {\rm diag}(1,1,1)\,, \tag{4.165}$$

$$U^\dagger_{\rm BM}\, \rho_{\mathbf{3}}(S)\, U^*_{\rm BM} = {\rm diag}(1,-1,1)\,, \tag{4.166}$$

$$U^\dagger_{\rm BM}\, \rho_{\mathbf{3}}(T^2ST^2)\, U^*_{\rm BM} = {\rm diag}(-1,1,1)\,, \tag{4.167}$$

$$U^\dagger_{\rm BM}\, \rho_{\mathbf{3}}(ST^2ST^2)\, U^*_{\rm BM} = {\rm diag}(-1,-1,1)\,. \tag{4.168}$$

Therefore, also in this case the phases ξ_i are fixed by a residual generalised CP symmetry to be either 0 or π.

As a third example, we consider $G_f = A_5$. We employ the basis for the triplet representation of the generators S and T of this group given in [144]. The residual symmetry $G_\nu = Z_2 \times Z_2$ generated by S and $T^3ST^2ST^3$ leads to GRA mixing, i.e., $\bar{U}_\nu = U_{\rm GRA}$, as is shown in [144]. It is stated in [128] that the generalised CP transformations consistent with

Table 4.6. The 16 symmetric generalised CP transformations $X_{\mathbf{3}} = \rho_{\mathbf{3}}(g)$ consistent with the A_5 flavour symmetry for the triplet representation **3** in the chosen basis [144] determined by the consistency condition in eq. (1.47). The mapping $(T, S) \to (\hat{T}, \hat{S})$ is realised via the consistency condition applied to the group generators T and S, i.e., $X_{\mathbf{3}}\, \rho^*_{\mathbf{3}}(T)\, X^{-1}_{\mathbf{3}} = \rho_{\mathbf{3}}(\hat{T})$ and $X_{\mathbf{3}}\, \rho^*_{\mathbf{3}}(S)\, X^{-1}_{\mathbf{3}} = \rho_{\mathbf{3}}(\hat{S})$.

g, $X_{\mathbf{3}} = \rho_{\mathbf{3}}(g)$	$\hat{T}$	$\hat{S}$
$T^3ST^2ST^3$	STS	S
S	TST	S
$(ST^2)^2S$	ST^3	$(T^2S)^2T^4$
TST	T^2S	TST^2S
ST^3S	T^2ST	ST^3ST^2S
T^3ST^3	T^4ST^3	$T^2ST^2ST^3S$
$T^3ST^2ST^3S$	T	S
T	T^4	TST^4
T^2	T^4	T^2ST^3
1	T^4	S
T^3	T^4	T^3ST^2
T^4	T^4	T^4ST
ST^2S	TST^2	ST^2ST^3S
T^2ST^2	T^3ST^4	$T^4ST^2ST^3S$
STS	ST^2	ST^2ST
$(T^2S)^2T^2$	T^3S	$T^4(ST^2)^2$

A_5 are of the same form as the group transformations. Solving the consistency condition in eq. (1.47), we find 16 symmetric generalised CP transformations consistent with A_5 for the triplet representation in the working basis. We summarise them in Table 4.6, where we present also the elements $\hat{T}$ and $\hat{S}$.

It follows from this table that the generalised CP transformations consistent with $G_\nu = Z_2 \times Z_2$ of interest are of the same form of G_ν. Namely, they are $\rho_{\mathbf{3}}(1)$, $\rho_{\mathbf{3}}(S)$, $\rho_{\mathbf{3}}(T^3ST^2ST^3)$ and $\rho_{\mathbf{3}}(T^3ST^2ST^3S)$, and we have:

$$U^\dagger_{\rm GRA}\, \rho_{\mathbf{3}}(1)\, U^*_{\rm GRA} = \rho_{\mathbf{3}}(1) = {\rm diag}(1,1,1)\,, \tag{4.169}$$

$$U^\dagger_{\rm GRA}\, \rho_{\mathbf{3}}(S)\, U^*_{\rm GRA} = {\rm diag}(1,-1,-1)\,, \tag{4.170}$$

$$U^\dagger_{\rm GRA}\, \rho_{\mathbf{3}}(T^3ST^2ST^3)\, U^*_{\rm GRA} = {\rm diag}(-1,1,-1)\,, \tag{4.171}$$

$$U^\dagger_{\rm GRA}\, \rho_{\mathbf{3}}(T^3ST^2ST^3S)\, U^*_{\rm GRA} = {\rm diag}(-1,-1,1)\,. \tag{4.172}$$

Thus, as in the previous cases, the phases ξ_i are fixed by generalised CP symmetry to be either 0 or π.

It follows from the results derived in the present section that the two phases $\xi_{21} = \xi_2 - \xi_1$ and $\xi_{31} = \xi_3 - \xi_1$, present in the matrix Q_0 (see eq. (3.2)) and giving contributions to the Majorana phases α_{21} and α_{31} in the PMNS matrix, are constrained to be either 0 or π for all examples considered.

Finally, we note that although in the cases of the flavour symmetry groups considered — A_4, T', S_4 and A_5 — we choose to work in specific basis for the generators of each

symmetry group, the results on the phases $\xi_{1,2,3}$ we have obtained, as we show below, are basis-independent. Indeed, let B be a unitary matrix, which realises the change of basis. Then, the representation matrices of the group elements in the new basis, $\tilde{\rho}_{\mathbf{3}}(g)$, are given by

$$\tilde{\rho}_{\mathbf{3}}(g) = B\,\rho_{\mathbf{3}}(g)\,B^{\dagger}\,, \quad g \in G_f\,. \tag{4.173}$$

Expressing $\rho_{\mathbf{3}}(g)$ from this equation and substituting it in the consistency condition given in eq. (1.47) leads to

$$\tilde{X}_{\mathbf{3}}\,\tilde{\rho}^{*}_{\mathbf{3}}(g)\,\tilde{X}^{-1}_{\mathbf{3}} = \tilde{\rho}_{\mathbf{3}}(g')\,, \qquad g, g' \in G_f\,, \tag{4.174}$$

where

$$\tilde{X}_{\mathbf{3}} = B\,X_{\mathbf{3}}\,B^{T} \tag{4.175}$$

are the generalised CP transformations in the new basis. Now we substitute $X_{\mathbf{3}}$ from this equation in eq. (4.161) and obtain

$$\left(\tilde{\bar{U}}_{\nu}\right)^{\dagger}\,\tilde{X}_{\mathbf{3}\nu}\,\left(\tilde{\bar{U}}_{\nu}\right)^{*} = \bar{U}^{\dagger}_{\nu}\,X_{\mathbf{3}\nu}\,\bar{U}^{*}_{\nu} = \mathrm{diag}\left(\pm e^{i\xi_1}, \pm e^{i\xi_2}, \pm e^{i\xi_3}\right)\,, \tag{4.176}$$

where $\tilde{\bar{U}}_{\nu} = B\,\bar{U}_{\nu}$ is the matrix which diagonalises the neutrino Majorana mass matrix $\tilde{M}_{\nu}$, $\tilde{M}_{\nu} = B^{*} M_{\nu}\,B^{\dagger}$, in the new basis, i.e.,

$$\tilde{\bar{U}}^{T}_{\nu}\,\tilde{M}_{\nu}\,\tilde{\bar{U}}_{\nu} = \bar{U}^{T}_{\nu}\,M_{\nu}\,\bar{U}_{\nu} = \mathrm{diag}\left(m_1 e^{-i\xi_1}, m_2 e^{-i\xi_2}, m_3 e^{-i\xi_3}\right)\,. \tag{4.177}$$

What concerns the charged lepton sector, in all cases we consider in the present study a flavour symmetry G_f is completely broken in the charged lepton sector, i.e., the residual symmetry group G_e consists only of the identity element 1. The change of basis yields $\tilde{\rho}_{\mathbf{3}}(1) = B\,\rho_{\mathbf{3}}(1)\,B^{\dagger}$. As can be easily shown, the matrix $U'_e = B\,U_e$ diagonalises the hermitian matrix $\tilde{M}_e\,\tilde{M}^{\dagger}_e$, $\tilde{M}_e\,\tilde{M}^{\dagger}_e = B\,M_e\,M_e\,B^{\dagger}$, in the new basis, M_e being the charged lepton mass matrix in the initial basis. Namely,

$$U'^{\dagger}_e\,\tilde{M}_e\,\tilde{M}^{\dagger}_e\,U'_e = U^{\dagger}_e\,M_e\,M^{\dagger}_e\,U_e = \mathrm{diag}\left(m^2_e, m^2_{\mu}, m^2_{\tau}\right)\,. \tag{4.178}$$

Taking into account that $U'_{\nu} = B\,U_{\nu} = B\,\bar{U}_{\nu}\,\bar{Q}_0$, we obtain for the PMNS matrix U:

$$U = U'^{\dagger}_e\,U'_{\nu} = U^{\dagger}_e\,U_{\nu} = U^{\dagger}_e\,\bar{U}_{\nu}\,\bar{Q}_0\,. \tag{4.179}$$

Thus, as eqs. (4.176) and (4.179) demonstrate, the results for the phases ξ_i are basis-independent.

4.7 Summary and conclusions

In the present chapter, we have obtained predictions for the Majorana phases α_{21} and α_{31} of the PMNS matrix $U = U^{\dagger}_e\,U_{\nu} = \tilde{U}^{\dagger}_e\,\Psi\,\tilde{U}_{\nu}\,Q_0$, U_e ($\tilde{U}_e$) and U_{ν} ($\tilde{U}_{\nu}$) being 3×3 unitary (CKM-like) matrices arising from the diagonalisation, respectively, of the charged lepton and neutrino Majorana mass terms. Each of the diagonal phase matrices Ψ and Q_0 contains, in general, two phases. The phases in the matrix Q_0, ξ_{21} and ξ_{31}, contribute to the Majorana phases in the PMNS matrix. The study carried out in this chapter is a natural continuation of the analysis performed in Chapter 3 for the Dirac phase δ. We have considered forms of $\tilde{U}_e$ and $\tilde{U}_{\nu}$ permitting to express δ as a function of the mixing angles θ_{12}, θ_{13} and θ_{23} present in U, and the angles contained in $\tilde{U}_{\nu}$. As we have shown, for the same forms, the Majorana phases α_{21} and α_{31} are determined by the values of θ_{12}, θ_{13} and θ_{23}, the angles θ^{ν}_{ij} present in $\tilde{U}_{\nu}$ and the phases ξ_{21} and ξ_{31}. We have derived such sum rules for α_{21} and α_{31} in the following cases:

(A1) $U = R_{12}(\theta^e_{12})\,\Psi\,R_{23}(\theta^\nu_{23})\,R_{12}(\theta^\nu_{12})\,Q_0\,,$

(A2) $U = R_{13}(\theta^e_{13})\,\Psi\,R_{23}(\theta^\nu_{23})\,R_{12}(\theta^\nu_{12})\,Q_0\,,$

(B1) $U = R_{12}(\theta^e_{12})\,R_{23}(\theta^e_{23})\,\Psi\,R_{23}(\theta^\nu_{23})\,R_{12}(\theta^\nu_{12})\,Q_0\,,$

(B2) $U = R_{13}(\theta^e_{13})\,R_{23}(\theta^e_{23})\,\Psi\,R_{23}(\theta^\nu_{23})\,R_{12}(\theta^\nu_{12})\,Q_0\,,$

(B3) $U = R_{12}(\theta^e_{12})\,R_{13}(\theta^e_{13})\,\Psi\,R_{23}(\theta^\nu_{23})\,R_{12}(\theta^\nu_{12})\,Q_0\,,$

(C1) $U = R_{12}(\theta^e_{12})\,\Psi\,R_{23}(\theta^\nu_{23})\,R_{13}(\theta^\nu_{13})\,R_{12}(\theta^\nu_{12})\,Q_0\,,$

(C2) $U = R_{13}(\theta^e_{13})\,\Psi\,R_{23}(\theta^\nu_{23})\,R_{13}(\theta^\nu_{13})\,R_{12}(\theta^\nu_{12})\,Q_0\,,$

where R_{ij} are real matrices, $R^T = R^{-1}$, and θ^e_{ij} and θ^ν_{ij} denote the rotation angles in $\tilde{U}_e$ and $\tilde{U}_\nu$, respectively. The obtained sum rules are summarised in Section 4.4. In the sum rules, $\alpha_{21}/2$ and $\alpha_{31}/2$ are expressed, in general, in terms of the three measured angles of the PMNS matrix, θ_{12}, θ_{13} and θ_{23}, the phases $\xi_{21}/2$ and $\xi_{31}/2$ of the matrix Q_0, and the angles in $\tilde{U}_\nu$, which are supposed to have known values, determined by symmetries. In the cases of schemes B1 and B2 (scheme B3), $\alpha_{31}/2$ (δ, $\alpha_{21}/2$ and $\alpha_{31}/2$) depends (depend) on one additional, in general, unknown phase β (ω), whose value can only be fixed in a self-consistent theory of generation of neutrino masses and mixing.

In order to obtain predictions for the Majorana phases one has to specify, in particular, the values of the angles in the matrix $\tilde{U}_\nu$. In the present study, we have considered the TBM, BM, GRA, GRB and HG forms of $\tilde{U}_\nu$. All these forms are characterised by the same $\theta^\nu_{23} = -\pi/4$ and $\theta^\nu_{13} = 0$, but differ by the value of the angle θ^ν_{12}. For the forms cited above and used in the present study, the values of θ^ν_{12} are given in Section 3.1. In schemes C1 and C2, we have employed three representative fixed values of $\theta^\nu_{13} \neq 0$ considered in the literature and appearing in models with flavour symmetries, $\theta^\nu_{13} = \pi/20,\ \pi/10$ and $\sin^{-1}(1/3)$, together with certain fixed values of θ^ν_{12} — in total five different pairs of values of $[\theta^\nu_{13}, \theta^\nu_{12}]$ in each of the two schemes. These pairs are given in Table 4.2.

Thus, for the specific symmetry forms of $\tilde{U}_\nu$ listed above and used in our numerical analysis, the phase differences (i) $(\alpha_{21}/2 - \xi_{21}/2)$ and $(\alpha_{31}/2 - \xi_{31}/2)$ in schemes A1, A2, C1 and C2, (ii) $(\alpha_{21}/2 - \xi_{21}/2)$ and $(\alpha_{31}/2 - \xi_{31}/2 - \beta)$ in schemes B1 and B2, and (iii) $(\alpha_{21}/2 - \xi_{21}/2)$ and $(\alpha_{31}/2 - \xi_{31}/2)$ for a fixed ω in scheme B3, are determined completely by the values of the measured neutrino mixing angles θ_{12}, θ_{13} and θ_{23} and the angles in the matrix $\tilde{U}_\nu$. Using the best fit values of θ_{12}, θ_{13} and θ_{23}, we have obtained predictions for the phase differences listed above, which are summarised in Tables 4.3 and 4.4. In the case of scheme B3, we have set $\omega = 0$. For this value of ω the predicted value of the Dirac phase δ lies in the 2σ interval of allowed values [162]. The results reported in Tables 4.3 and 4.4 show that the phase differences of interest involving the Majorana phases are determined with a two-fold ambiguity by the values of θ_{12}, θ_{13} and θ_{23}. This is a consequence of the fact that, as long as the sign of $\sin\delta$ is not fixed by the data, the Dirac phase δ, on which the phase differences under discussion depend, is determined by the values of θ_{12}, θ_{13} and θ_{23} in the schemes studied by us with a two-fold ambiguity (see Chapter 3), as Table 4.2 also shows. The current data appear to favour negative values of $\sin\delta$. The predictions for the BM (LC) symmetry form of $\tilde{U}_\nu$ in Tables 4.3 and 4.4 correspond to the 3σ upper bound of allowed values of $\sin^2\theta_{12} = 0.354$ and the best fit values of $\sin^2\theta_{23}$ and $\sin^2\theta_{13}$, since using the best fit values of the three neutrino mixing angles one gets unphysical values of $|\cos\delta| > 1$ (see Chapter 3). Physical values of $\cos\delta$ are found for larger (smaller) values of $\sin^2\theta_{12}$ ($\sin^2\theta_{23}$). For $\sin^2\theta_{12} = 0.354$ and the best

fit values of $\sin^2\theta_{23}$ and $\sin^2\theta_{13}$, $|\cos\delta|$ has an unphysical value greater than one only for schemes B1 with the IO spectrum, B2 with the NO spectrum and B3, and for these cases we do not present results for the relevant phase differences.

We have investigated also how the predictions for the phase differences $(\alpha_{21}/2-\xi_{21}/2)$ and $(\alpha_{31}/2-\xi_{31}/2)$ $((\alpha_{31}/2-\xi_{31}/2-\beta))$ presented in Tables 4.3 and 4.4 change when the uncertainties in determination of the neutrino mixing parameters are taken into account (see Figs. 4.1 and 4.2 and the related discussion).

Extracting the values of the Majorana phases α_{21} and α_{31} from the results presented in Tables 4.3 and 4.4 for two fixed values of each of the phases ξ_{21} and ξ_{31}, $\xi_{21}=0$ and π, $\xi_{31}=0$ and π (altogether four cases), and using also the predicted values of the Dirac phase δ from Table 4.2 and the best fit values of $\sin^2\theta_{12}$, $\sin^2\theta_{23}$ and $\sin^2\theta_{13}$, we derived (in graphic form) predictions for the absolute value of the $(\beta\beta)_{0\nu}$-decay effective Majorana mass $|\langle m\rangle|$ as a function of the lightest neutrino mass $m_{\rm min}\equiv\min(m_j)$, $j=1,2,3$, for both the NO and IO neutrino mass spectra (Figs. 4.3–4.6). For schemes B1 and B2 the predictions are obtained by varying the phase β in the interval $[0,\pi]$. As a possible justification of the choice of the two values of the phases ξ_{21} and ξ_{31} used for the predictions of $|\langle m\rangle|$, we show that the requirement of generalised CP invariance of the neutrino Majorana mass term in the cases of the A_4, T', S_4 and A_5 lepton flavour symmetries leads to the constraints $\xi_{21}=0$ or π, $\xi_{31}=0$ or π.

The results derived in the present chapter for the Majorana CPV phases in the PMNS neutrino mixing matrix U complement the results obtained in Chapter 3 on the predictions for the Dirac phase δ in U in schemes in which the underlying form of U is determined by, or is associated with, discrete lepton flavour symmetries.

Chapter 5

Renormalisation group corrections to neutrino mixing sum rules

In this chapter, we will investigate the impact of *renormalisation group corrections* on the sum rule predictions for the Dirac CPV phase δ. It is often assumed that neutrino mixing sum rules are exactly realised at low energies, where experiments take place. However, as every quantity in quantum field theory, the mixing parameters get affected by RG running. We consider as an example two particular sum rules from Chapter 3 (cases A1 and B1) and assume that they hold at a certain high-energy scale, which we choose to be the seesaw scale $M_S \approx 10^{13}$ GeV. The main question we want to address is how stable the predictions for δ are under the RG corrections. We investigate the impact of these corrections on the sum rule predictions for δ in the cases of neutrino Majorana mass term generated by the Weinberg (dimension 5) operator [141] added to (i) the SM and (ii) the MSSM.

5.1 Introductory remarks

In the literature RG corrections to certain type of mixing sum rules have been studied before. The first attempt to study RG corrections to mixing angle sum rules, to our knowledge, has been made in [177] for the quark-lepton complementarity relations, $\theta_{12} + \theta_C \approx \pi/4$ and $\theta_{23} + \arcsin V_{cb} \approx \pi/4$, θ_C and V_{cb} being the Cabibbo angle and an element of the CKM quark mixing matrix. In [178] the RG corrections for the sum rule relating the element $U_{\tau 1}$ of the PMNS matrix to the element $(U_{\rm TBM})_{\tau 1} = -1/\sqrt{6}$ of the TBM mixing matrix (see eq. (1.33)), $|U_{\tau 1}| = 1/\sqrt{6}$, and for the leading order in θ_{13} versions of this sum rule, have been investigated. In refs. [177] and [178] the BM and TBM mixing schemes, respectively, were analysed. In [179] the study of RG perturbations has been done for an approximate (leading order) mixing sum rule and for normal hierarchical neutrino mass spectrum, $m_1 \ll m_2 < m_3$, neglecting terms of order $\mathcal{O}(m_1/m_2)$ and $\mathcal{O}(m_1/m_3)$. The authors of [179] extended their analysis to incorporate canonical normalisation effects besides RG corrections. Both type of corrections were assumed to be dominated by the third family effects. The authors of [111] estimated the size of RG corrections to the sum rules we will be considering in the present study by taking into account *only* the RG correction to θ_{12}.

In the present study, we go beyond these previous works (i) by considering the exact form of the general mixing sum rules derived in [99], (ii) by taking into account the RG corrections not only to the angle θ_{12}, but to all three neutrino mixing angles θ_{12}, θ_{23}, θ_{13} and the CPV phases, (iii) discussing not only the cases of BM or TBM mixing schemes, but also the cases of GRA, GRB and HG mixing schemes, and (iv) by considering both the cases of NO and IO neutrino mass spectra. We perform the analysis assuming that the neutrino Majorana mass matrix is generated by the Weinberg (dimension 5) operator [141].

The RG corrections to the sum rules of interest are calculated in the SM as well as in the MSSM.

Our study goes also beyond [180] where only the GRA, BM and TBM mixing schemes were analysed. We discuss different forms of the charged lepton mixing matrix and present a significantly larger number of results. In particular, we derive values of the neutrino mass scale and $\tan\beta \equiv v_u/v_d$, v_u and v_d being the VEVs of neutral components of the two Higgs doublets H_u and H_d of the MSSM, for which the various mixing schemes are still viable. We make a thorough numerical analysis from which we derive likelihood functions for the value of the Dirac CPV phase δ at low energies if the specified mixing sum rule holds at high energies.

The remainder of this chapter is organised as follows. After a short reminder of sum rules for the Dirac phase δ in Section 5.2, we present analytical estimates for the allowed parameter regions for δ taking RG corrections into account in Section 5.3. In Section 5.4, we present the numerical results for the different mixing schemes. Finally, we summarise and conclude in Section 5.5.

5.2 Mixing sum rules

In this section, we briefly review the mixing sum rules we will deal with in this chapter and fix notation and conventions. In the most general case the PMNS matrix U can be parametrised as in eq. (3.1). As it has been done in Chapter 3, we will consider the cases when $\tilde{U}_\nu$ has the BM, TBM, GRA, GRB and HG forms. For all these forms $\tilde{U}_\nu$ can be expressed as a product of 3×3 orthogonal matrices R_{23} and R_{12} describing rotations in the 2-3 and 1-2 planes, i.e.,

$$\tilde{U}_\nu = R_{23}(\theta^\nu_{23})\, R_{12}(\theta^\nu_{12})\,, \tag{5.1}$$

with $\theta^\nu_{23} = -\pi/4$ and different values of θ^ν_{12} given in Section 3.1. For the matrix $\tilde{U}_e$, following [99], we will consider two different forms both of which correspond to negligible θ^e_{13}. They are realised in a class of flavour models based on a GUT and/or a discrete symmetry (see, e.g., [122, 145–148, 181, 182]). The first form corresponding to case A1 of Chapter 3 is characterised also by zero θ^e_{23}, i.e.,

$$\tilde{U}_e = R^{-1}_{12}(\theta^e_{12})\,. \tag{5.2}$$

In this case, there is a correlation between the values of $\sin^2\theta_{23}$ and $\sin^2\theta_{13}$ given by eq. (3.16), which for all the symmetry forms of $\tilde{U}_\nu$ considered leads to

$$\sin^2\theta_{23} = \frac{1-2\sin^2\theta_{13}}{2\,(1-\sin^2\theta_{13})} = \frac{1}{2} - \frac{1}{2}\sin^2\theta_{13} + \mathcal{O}(\sin^4\theta_{13})\,. \tag{5.3}$$

This implies in turn that θ_{23} cannot deviate significantly from $\pi/4$ in case A1. The second form of $\tilde{U}_e$ corresponds to non-zero θ^e_{12} and θ^e_{23} (case B1), i.e.,

$$\tilde{U}_e = R^{-1}_{23}(\theta^e_{23})\, R^{-1}_{12}(\theta^e_{12})\,. \tag{5.4}$$

This matrix provides the corrections to $\tilde{U}_\nu$ necessary to reproduce the best fit values of all the three neutrino mixing angles θ_{12}, θ_{13} and θ_{23} in the PMNS matrix U without any further contributions like RG or other corrections.

It has been shown in [99] that for $\tilde{U}_\nu$ given in eq. (5.1) and $\tilde{U}_e$ determined in eqs. (5.2) or (5.4), the Dirac phase δ present in the PMNS matrix satisfies a sum rule in eq. (3.10), which we replicate here for convenience:

$$\cos\delta = \frac{\tan\theta_{23}}{\sin 2\theta_{12}\sin\theta_{13}}\left[\cos 2\theta_{12}^{\nu} + \left(\sin^2\theta_{12} - \cos^2\theta_{12}^{\nu}\right)\left(1 - \cot^2\theta_{23}\sin^2\theta_{13}\right)\right] . \tag{5.5}$$

Additionally, in the case of $\tilde{U}_e$ given in eq. (5.2), the correlation between θ_{23} and θ_{13}, eq. (5.3), has to be respected. The sum rule, eq. (5.5), in this case reduces to [99]

$$\cos\delta = \frac{(1-2\sin^2\theta_{13})^{\frac{1}{2}}}{\sin 2\theta_{12}\sin\theta_{13}}\left[\cos 2\theta_{12}^{\nu} + \left(\sin^2\theta_{12} - \cos^2\theta_{12}^{\nu}\right)\frac{1-3\sin^2\theta_{13}}{1-2\sin^2\theta_{13}}\right] . \tag{5.6}$$

In what follows we refer to the case with $\tilde{U}_e$ given in eq. (5.2) (eq. (5.4)) as to the case of zero (non-zero) θ_{23}^{e}. In this chapter, we study the impact of the RG corrections on the mixing sum rules in eqs. (5.5) and (5.6), and the angle sum rule in eq. (5.3), which are assumed to hold at some high-energy scale specified later.

In Chapter 3, other forms of the matrices $\tilde{U}_e$ and $\tilde{U}_\nu$ corresponding to different rotations and leading to the sum rules for $\cos\delta$ and $\sin^2\theta_{23}$ given in Tables 3.1 and 3.2, respectively, have been investigated. The RG corrections to their predictions, however, are expected to be similar to the corrections which take place for the sum rules described above. For this reason we will not consider them in the present chapter.

5.3 Analytical estimates

Before we present our numerical results in the next section, we give in this section analytical estimates of the effect of radiative corrections on the mixing sum rules. We discuss how we obtain constraints on the mass scale and on $\tan\beta$ (in the MSSM) from the requirement that the mixing sum rule has to be fulfilled at the high scale.

5.3.1 General effects of radiative corrections

The running of the mixing parameters is already known for quite some time, see, e.g., [183]. One might wonder if RG corrections have a large impact on the predicted value for δ from the sum rule in eq. (5.5). Indeed, we expect large RG corrections for a large Yukawa coupling (large $\tan\beta$) and a heavy neutrino mass scale. To be more precise, the β-functions of the mixing angles, in the leading order in θ_{13} and neglecting the electron and muon Yukawa couplings in comparison to the tau one, depend on the tau Yukawa coupling y_τ, the absolute neutrino mass scale (or $\min(m_j)$, $j = 1,2,3$), the mixing angles, the type of spectrum (NO or IO) the neutrino masses obey, the Majorana phases α_1 and α_2,[41] and in the MSSM, on $\tan\beta$. In the leading order in θ_{13} only the β-function for θ_{13} depends on δ. The β-functions read up to $\mathcal{O}(\theta_{13})$ [183]:

$$\frac{\mathrm{d}\,\theta_{12}}{\mathrm{d}\,\ln(\mu/\mu_0)} = -\frac{Cy_\tau^2}{32\pi^2}\sin 2\theta_{12}s_{23}^2\frac{\left|m_1 e^{i\alpha_1} + m_2 e^{i\alpha_2}\right|^2}{\Delta m_{21}^2} + \mathcal{O}(\theta_{13}) , \tag{5.7}$$

$$\frac{\mathrm{d}\,\theta_{13}}{\mathrm{d}\,\ln(\mu/\mu_0)} = \frac{Cy_\tau^2}{32\pi^2}\sin 2\theta_{12}\sin 2\theta_{23}\frac{m_3}{\Delta m_{32}^2(1+\zeta)}$$

[41] The Majorana phases α_1 and α_2 are related to those of the standard parametrisation of the PMNS matrix [8], α_{21} and α_{31}, as follows: $\alpha_{21} = \alpha_1 - \alpha_2$ and $\alpha_{31} = \alpha_1$.

$$\times \left[m_1 \cos(\alpha_1 - \delta) - (1+\zeta) m_2 \cos(\alpha_2 - \delta) - \zeta m_3 \cos\delta\right] + \mathcal{O}(\theta_{13}) \,, \tag{5.8}$$

$$\frac{\mathrm{d}\,\theta_{23}}{\mathrm{d}\,\ln(\mu/\mu_0)} = -\frac{C y_\tau^2}{32\pi^2} \sin 2\theta_{23} \frac{1}{\Delta m^2_{32}} \left[c_{12}^2 \left|m_2 \mathrm{e}^{i\alpha_2} + m_3\right|^2 + s_{12}^2 \frac{\left|m_1 \mathrm{e}^{i\alpha_1} + m_3\right|^2}{1+\zeta}\right] + \mathcal{O}(\theta_{13}) \,, \tag{5.9}$$

with μ being the renormalisation scale, $\zeta = \Delta m^2_{21}/\Delta m^2_{32}$ and $C y_\tau^2/(32\pi^2) \approx 0.3 \cdot 10^{-6}\,(1 + \tan^2\beta)$ in the MSSM and $C y_\tau^2/(32\pi^2) \approx -0.5 \cdot 10^{-6}$ in the SM. In the SM there is no $\tan\beta$ enhancement and hence the effects are usually relatively small.

We would like to note at this point that we consider here only minimal scenarios, namely, the SM and the MSSM augmented with Majorana neutrino masses. In standard seesaw scenarios it would be correct to integrate out the additional heavy states at their respective mass scale which would change the β-functions and the running. Nevertheless, we want to assume the heavy masses all to be roughly of the same order, so that it is a good approximation to impose the sum rule at the high scale and use the minimal β-functions for the running. For low scale seesaw mechanisms this would certainly be a bad approximation, but there the sum rule should be realised at the low scale as well and running effects can be more generally expected to be small.

To give an idea about the size of the effect of interest we show in Fig. 5.1 results for $\cos\delta$ as derived from the sum rule in eq. (5.5) for the GRA mixing scheme. We used the `REAP` package [184] to solve the renormalisation group equations (RGEs) for the mixing parameters between the low-energy scale M_Z and the high-energy scale which we have set equal to the seesaw scale $M_S \approx 10^{13}$ GeV. We only consider the case with $\theta_{12}^e \neq 0$, $\theta_{23}^e \neq 0$ and $\theta_{13}^e = 0$. We have set all mass squared differences and angles to their best fit values given in eqs. (4.1)–(4.3), (4.149) and (4.150), scanned over the lightest neutrino mass and chose random values for the low energy Majorana phases. For the SM case we see no effect, while for $\tan\beta = 30$ and 50, the RG effects are significant. Even for a moderate $\tan\beta$ in the MSSM and a relatively small mass scale $m_{\text{lightest}} \approx 0.04$ eV the effect is non-negligible. Since the running of the angles is stronger for the IO neutrino mass spectrum, the effect for the prediction of $\cos\delta$ is larger in this case. It is furthermore in particular remarkable that the corrections do not go to zero for m_3 going to zero in this case. This is due to the well-known fact, cf. [183], that the β-functions for δ and θ_{12} are in this limit enhanced by a factor of $\Delta m^2_{23}/\Delta m^2_{21}$. Together with the $\tan\beta$ enhancement this leads to quite sizeable effects for all relevant neutrino mass scales.

5.3.2 Allowed parameter regions with RG corrections

In this subsection, we derive constraints on $\tan\beta$ (in the case of the MSSM) and the mass of the lightest neutrino, m_{lightest}, by imposing the mixing sum rule at the high scale and by requiring that $\cos\delta \in [-1, 1]$ at the high scale. We have chosen the high scale to be equal to the seesaw scale $M_S \approx 10^{13}$ GeV. The BM mixing scheme is strongly disfavoured for the current best fit values of the neutrino mixing angles without taking the RG corrections into account. Thus, one of the questions we are interested in is whether the corrections can reconstitute the validity of the BM scheme even for the best fit values of the angles.

We give first analytical estimates of the RG effects on eq. (5.5). At the high scale we can write, for instance, for the mixing angles

$$\theta_{ij}(M_S) = \theta_{ij}(M_Z) + \delta\theta_{ij} \equiv \theta_{ij} + \delta\theta_{ij} \,, \tag{5.10}$$

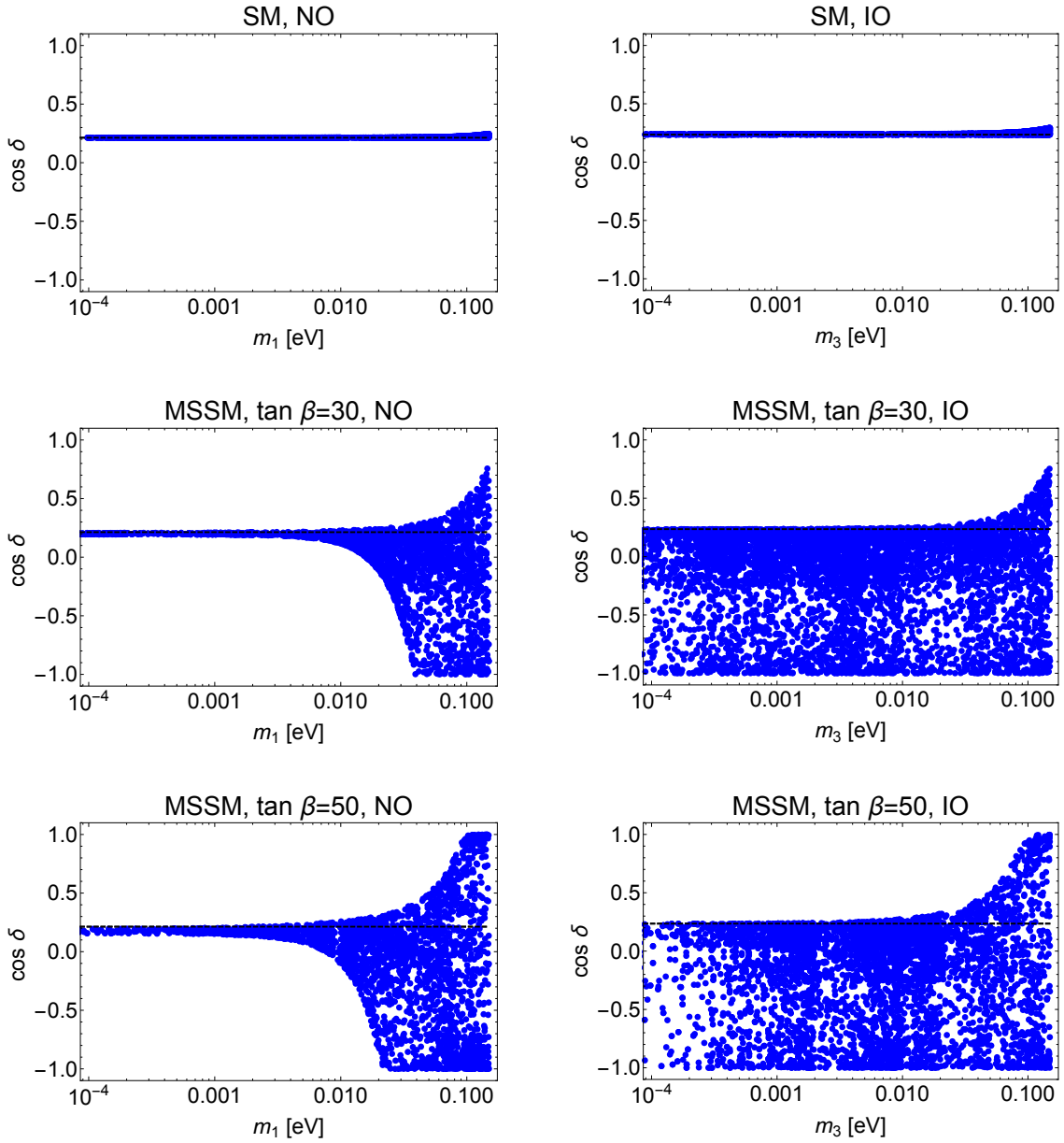

Figure 5.1. Results for the predicted value of $\cos\delta$ from the sum rule in eq. (5.5) for the GRA mixing scheme in the case of $\theta_{23}^{e} \neq 0$. The black dashed lines represent the tree level result. The blue points are our scan points. For the angles and the mass squared differences we took the best fit values quoted in eqs. (4.1)–(4.3), (4.149) and (4.150). We let the parameters run between the high scale $M_S \approx 10^{13}$ GeV and the low scale M_Z. The Majorana phases are chosen randomly between 0 and 2π. The plots on the left (right) side correspond to the NO (IO) neutrino mass spectrum.

where $\delta\theta_{ij}$ is the RG correction or the difference between the high-scale and low-scale values of the mixing angle θ_{ij}. Since the RG corrections are small we can expand the mixing sum rule at the high scale in the small quantities and find

$$\begin{aligned}\cos\delta(M_S) &\approx \cos\delta(M_Z) + \delta(\cos\delta) \\ &= \frac{\tan\theta_{23}}{\sin 2\theta_{12}\sin\theta_{13}}\left[\cos 2\theta_{12}^{\nu} + \left(\sin^2\theta_{12} - \cos^2\theta_{12}^{\nu}\right)\left(1 - \cot^2\theta_{23}\sin^2\theta_{13}\right)\right] \\ &+ f_{13}(\theta_{13},\theta_{12},\theta_{23},\theta_{12}^{\nu})\,\delta\theta_{13}\end{aligned}$$

$$+ f_{23}(\theta_{13}, \theta_{12}, \theta_{23}, \theta_{12}^{\nu})\, \delta\theta_{23} + f_{12}(\theta_{13}, \theta_{12}, \theta_{23}, \theta_{12}^{\nu})\, \delta\theta_{12}\,, \tag{5.11}$$

where the f_{ij} are prefactors from the expansion. For the angles and mass squared differences at the low scale we use the best fit values. Note that the Dirac phase δ appears in the β-functions for the mixing angles. Here we use the approximation $\delta(M_Z) \approx \delta(M_S)$ and evaluate the value from the sum rule neglecting RG corrections. This is formally correct since their inclusion would be a two-loop correction. The Majorana phases are free parameters.

For the best fit values of the angles the function f_{12} is always positive independent of the value of θ_{12}^{ν}. Since the sign of $\delta\theta_{12}$ is always negative to leading order in θ_{13}, the correction to $\cos\delta(M_Z)$ due to the running of θ_{12} has a fixed negative sign in this approximation. The sign of the correction due to the running of θ_{23} depends on θ_{12}^{ν} and the mass ordering: $\delta\theta_{23}$ is positive for inverted ordering and negative for normal ordering and f_{23} is negative for $\theta_{12}^{\nu} \gtrsim 33^{\circ}$. The sign of the correction due to the running of θ_{13} depends on the CPV phases and θ_{12}^{ν}.

For BM mixing the function f_{13} dominates in $\delta(\cos\delta)$, in contrast to the other mixing patterns for which f_{12} has the largest influence. This means that the contribution in TBM, GRA, GRB and HG mixings due to the running of θ_{12}, which is larger than the contributions due to the running of the other angles (except for the case of a parametric suppression of the β-function which will be discussed later), is additionally enhanced by the large prefactor f_{12} making the $\delta\theta_{12}$ even more important.

Since the running depends also on the unknown Majorana phases we will vary them and give in the rest of the subsection the results for minimal or maximal corrections. Note that minimal corrections can also correspond to negative values of $\delta(\cos\delta)$.

The allowed parameter regions in the m_{lightest}-$\tan\beta$ plane for the GRA and HG cases are shown in Fig. 5.2. For minimal corrections the parameter regions get severely constrained, $\tan\beta > 20$ is incompatible with $\cos\delta(M_S) \in [-1, 1]$ for the IO spectrum; for the NO spectrum it is incompatible with $\cos\delta(M_S) \in [-1, 1]$ for $m_1 \gtrsim 0.06$ eV. This can be understood since $\cos\delta(M_Z)$ is positive for GRA mixing and the dominant contribution to $\delta(\cos\delta)$ comes from the correction due to $\delta\theta_{12}$, which is negative. A similar argument holds also for HG mixing.

For TBM and GRB, $\cos\delta(M_Z)$ is negative and the corrections further decrease the value. The plots for the allowed parameter regions can be found in Fig. 5.3.

For BM mixing, $\cos\delta(M_Z) < -1$ for the best fit values of the angles, which is ruled out. As best approximation for the value of δ in the β-functions we use then $\delta(M_Z) = \pi$. The dominant contribution to the correction is due to $\delta\theta_{13}$, which is positive for the maximal correction. Since f_{13} is also positive in BM mixing, the value of $\cos\delta(M_S)$ increases. Hence, the RG corrections have shifted $\cos\delta(M_S)$ to allowed values, but for too large values of $\tan\beta$ the corrections overshoot $\cos\delta(M_S) = 1$ and the points are excluded. The allowed banana-shaped parameter regions are displayed in Fig. 5.4.

Note that in this example we have only employed the constraint on δ from eq. (5.5) at the high-energy scale. This corresponds to the scheme where $\theta_{23}^{e} \neq 0$. To fulfil the sum rule, θ_{12} is allowed to run weakly. In the case of the SM running, the RG effects are already small. In the case of the MSSM running, they are relatively small if the Majorana phases satisfy the relation $\alpha_2 \approx \alpha_1 + \pi$.

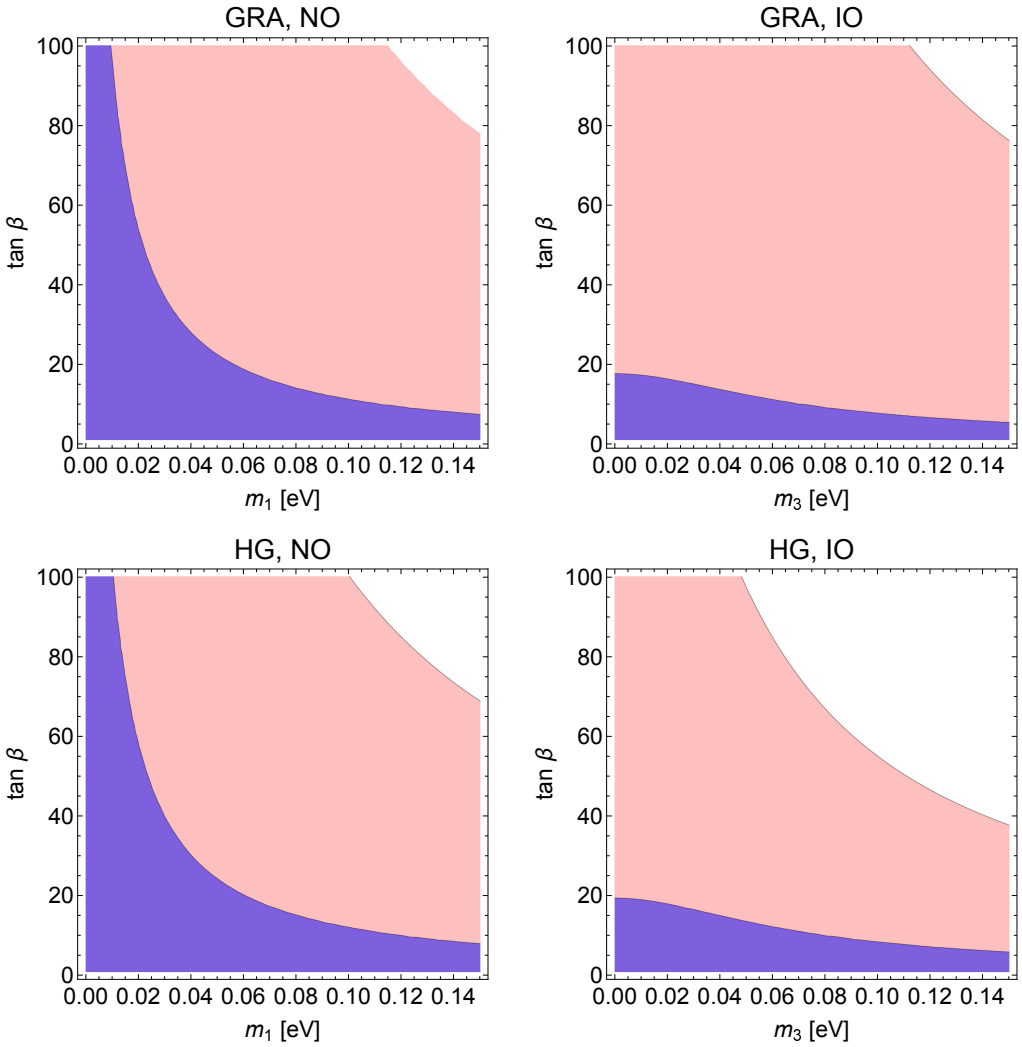

Figure 5.2. Allowed regions for $\tan\beta$ and m_{lightest} for the NO and IO spectra in the cases of minimal (blue) and maximal (pink) corrections for $\cos\delta$ in the GRA mixing scheme (upper plots) and the HG mixing scheme (lower plots). We used the best fit values for the mixing angles. The high-energy scale is set to 10^{13} GeV.

5.3.3 Implications of $\alpha_2 - \alpha_1 = 0$ and π and small $\tan\beta$

In this subsection, we show how the specific values of the difference of the Majorana phases, namely, $\alpha_2 - \alpha_1 = 0$ and π, contribute to the total likelihood profile obtained after the RG corrections are taken into account. These values might seem to be very special at a first glance but in fact many symmetric matrices belong at leading order to one of the two cases. The CP-violating effects of the requisite corrections from $\tilde{U}_e$ then might be controlled using, for instance, spontaneous CP violation with the discrete vacuum alignment method proposed in [185].

These two cases are also interesting because they correspond to extremal values of the neutrinoless double beta decay observable — the effective Majorana mass $|\langle m\rangle|$ (see eq. (4.148)) in the cases of neutrino mass spectrum with IO or of QD type (see, e.g., [8, 39, 40]). For $\alpha_2 - \alpha_1 = 0$, $|\langle m\rangle|$ is maximal in the two cases, while if $\alpha_2 - \alpha_1 = \pi$, $|\langle m\rangle|$ has a minimal value for both types of spectrum. In the case of IO spectrum and $m_3 \ll m_{1,2}$, for example, $|\langle m\rangle| \approx \sqrt{\Delta m^2_{23}}\cos^2\theta_{13} \approx 0.05$ eV if $\alpha_2 - \alpha_1 = 0$, while for $\alpha_2 - \alpha_1 = \pi$ we have $|\langle m\rangle| \approx \sqrt{\Delta m^2_{23}}\cos^2\theta_{13}\cos 2\theta_{12} \approx 0.014$ eV, where we have used the

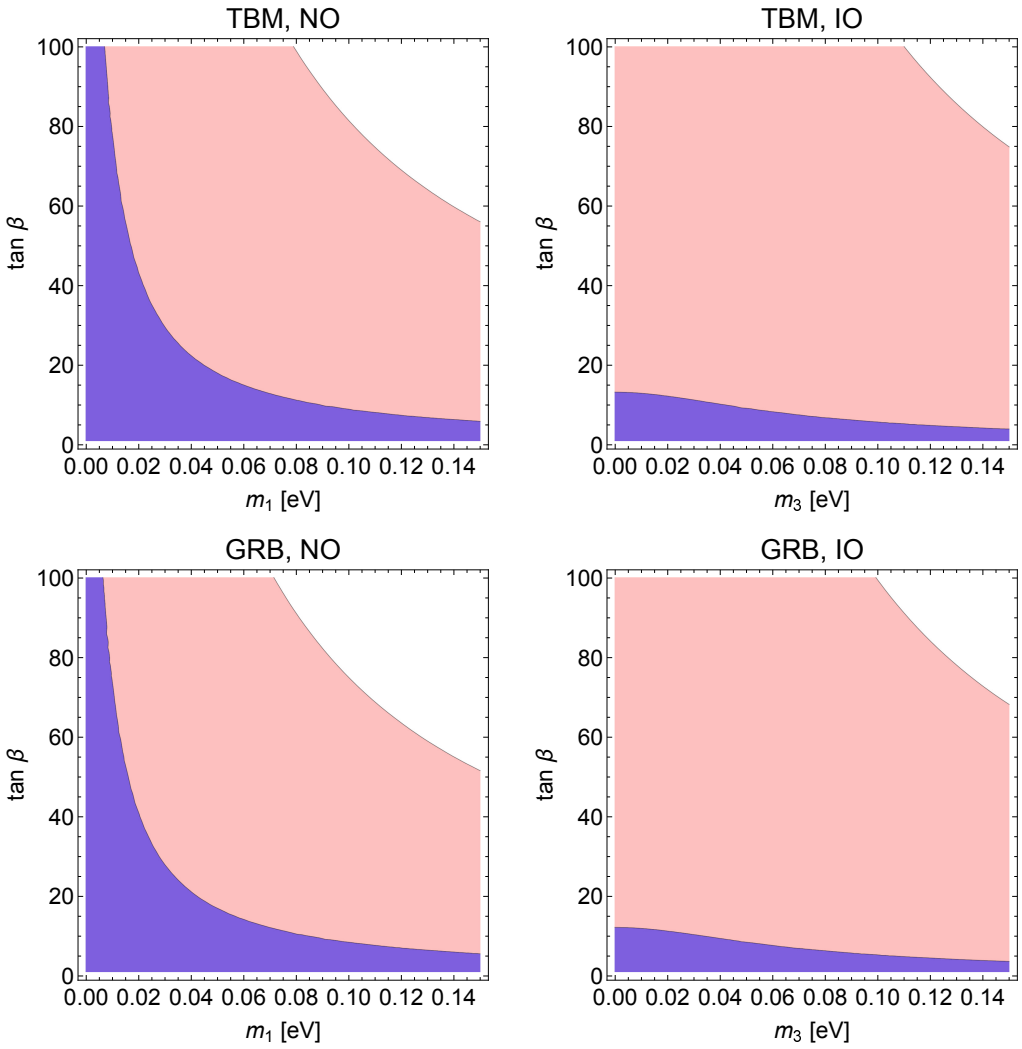

Figure 5.3. The same as in Fig. 5.2, but for the TBM and GRB mixing schemes.

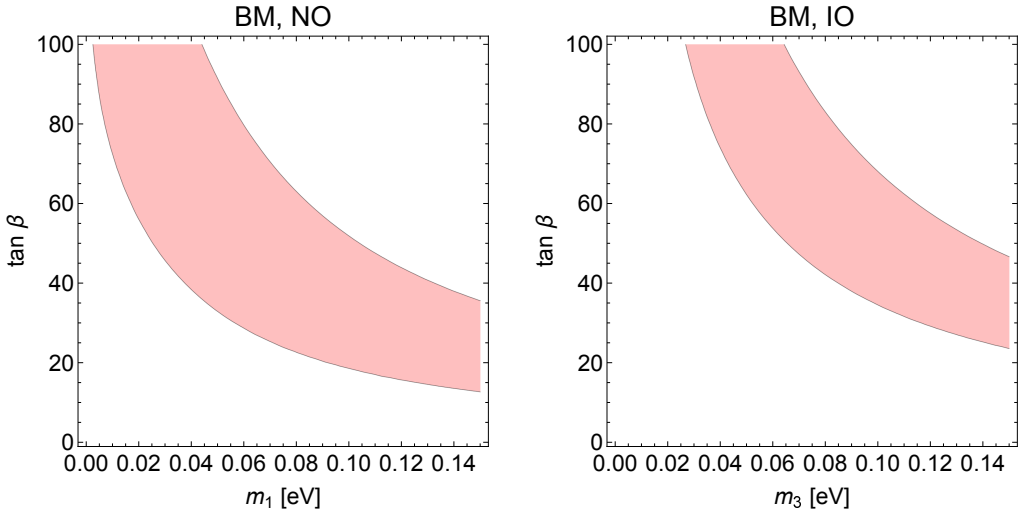

Figure 5.4. The same as in Fig. 5.2, but for the BM mixing scheme. For the minimal corrections there is no allowed parameter region which is compatible with $|\cos\delta| \leq 1$.

3σ allowed ranges of Δm^2_{23}, $\sin^2\theta_{13}$ (for the IO spectrum) and $\sin^2\theta_{12}$ given in eqs. (4.150), (4.3) and (4.1), respectively.

As can be understood from eq. (5.7), in the case of equal Majorana phases, the running of θ_{12} is maximal, while for $\alpha_2 - \alpha_1 = \pi$ it is maximally suppressed. Since for the TBM, GRA, GRB and HG symmetry forms the correction to the tree-level value of $\cos\delta$ is dominated by the running of θ_{12} (see subsection 5.3.2), we consider as an example the case of TBM and $\theta^e_{23} \neq 0$ with the values of $\alpha_2 - \alpha_1$ specified above. The results we obtain in the GRA, GRB and HG cases are very similar.

It is interesting to see, in particular, what is the quantitative relation between the corrections obtained in the set-up with relatively large $\tan\beta$, e.g., $\tan\beta = 30$, and suppression of θ_{12} running due to $\alpha_2 - \alpha_1 = \pi$, and the set-up with relatively small $\tan\beta$, e.g., $\tan\beta = 5$ or 10, but enhancement due to $\alpha_2 = \alpha_1$.

To answer this question, we employ a simplified one-step integration procedure (linearised running), in which the high-energy values of the mixing parameters entering the sum rule are obtained using one-step integration of the exact one-loop beta functions for the mixing parameters from [183]. We set θ_{13}, θ_{23}, Δm^2_{21}, $\Delta m^2_{31(23)}$ to their best fit values and impose (i) $\alpha_2 = \alpha_1$, and (ii) $\alpha_2 = \alpha_1 + \pi$. For each set of these low-energy values, we solve the high-energy sum rule for the low-energy value of θ_{12}.

In order to perform a statistical analysis of the low-energy data after RG corrections we construct the χ^2 function as

$$\chi^2(\vec{x}) = \sum_{i=1}^{6} \chi^2_i(x_i)\,, \tag{5.12}$$

where $\vec{x} = (\sin^2\theta_{12}, \sin^2\theta_{13}, \sin^2\theta_{23}, \delta, \Delta m^2_{21}, \Delta m^2_{31(23)})$ for the NO (IO) spectrum, and χ^2_i are one-dimensional projections taken from [162]. In order to obtain the one-dimensional projection $\chi^2(\delta)$ from the constructed $\chi^2(\vec{x})$ function we need to minimise the latter with respect to all other parameters ($\sin^2\theta_{ij}$, Δm^2_{21} and $\Delta m^2_{31(23)}$), i.e., we need to find a minimum of $\chi^2(\vec{x})$ for a fixed value of δ:

$$\chi^2(\delta) = \min\left[\chi^2(\vec{x})\big|_{\delta=\text{const}}\right]\,. \tag{5.13}$$

The likelihood function L, which represents the most probable values of δ in each of the considered cases, reads

$$L(\delta) = \exp\left(-\frac{\chi^2(\delta)}{2}\right)\,. \tag{5.14}$$

We will present the results in terms of the likelihood functions, considering three values for the absolute mass scale, $m_{\text{lightest}} = 0.005$, 0.01 and 0.05 eV, and four values of $\tan\beta = 5$, 10, 30 and 50.

It is worth noting here that, as shown in ref. [183] (see eq. (26) therein), for the running of the difference $\alpha_1 - \alpha_2$ we have up to $\mathcal{O}(\theta_{13})$ terms:

$$\frac{\mathrm{d}}{\mathrm{d}\,\ln(\mu/\mu_0)}(\alpha_1 - \alpha_2) \propto \sin(\alpha_1 - \alpha_2)\,. \tag{5.15}$$

This implies that if the phases are equal (different by π) at some scale to a good approximation, they remain equal (differ by π) at another scale. Thus, the relation imposed by us at the low scale holds also at the high scale (up to $\mathcal{O}(\theta_{13})$ corrections).

We present graphically the results obtained for the TBM symmetry form in Figs. 5.5 and 5.6 for the NO and IO neutrino mass spectra, respectively. The dotted black line

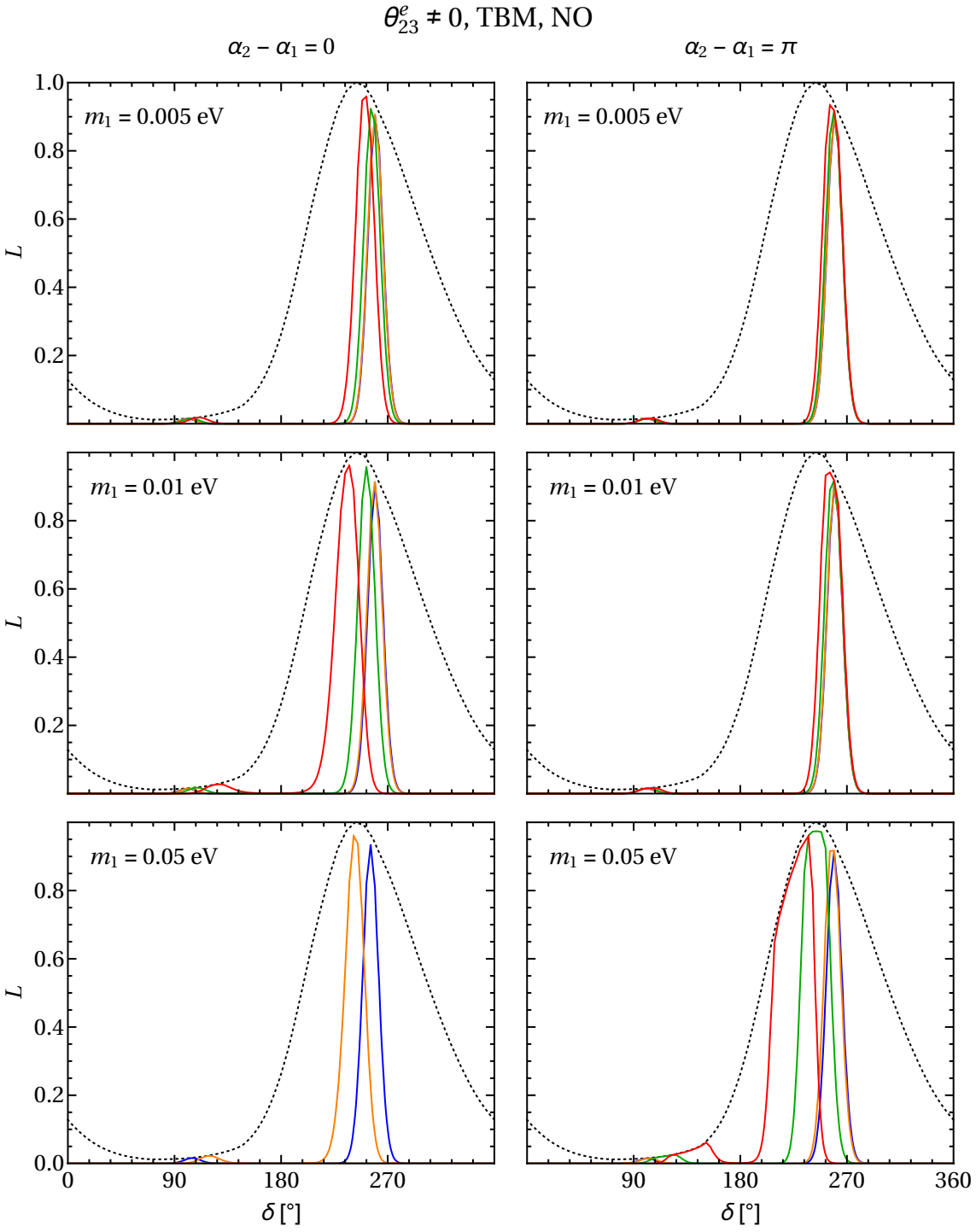

Figure 5.5. Likelihood function vs. δ in the case of non-zero θ_{23}^e for the TBM symmetry form of the matrix $\tilde{U}_\nu$ and the NO spectrum. The dotted black line stands for likelihood extracted from the global analysis in [162]. The blue, orange, green and red lines are for the running within MSSM with $\tan\beta = 5$, 10, 30 and 50, respectively. The left panels correspond to $\alpha_2 = \alpha_1$, while the right panels are for $\alpha_2 = \alpha_1 + \pi$.

stands for likelihood extracted from the global analysis [162]. The blue, orange, green and red lines are for $\tan\beta = 5$, 10, 30 and 50, respectively. The left panels in each of the two figures correspond to $\alpha_2 = \alpha_1$, while the right panels are for $\alpha_2 = \alpha_1 + \pi$.

Several comments are in order. As expected, the results for $\alpha_2 - \alpha_1 = \pi$ and small $\tan\beta$,

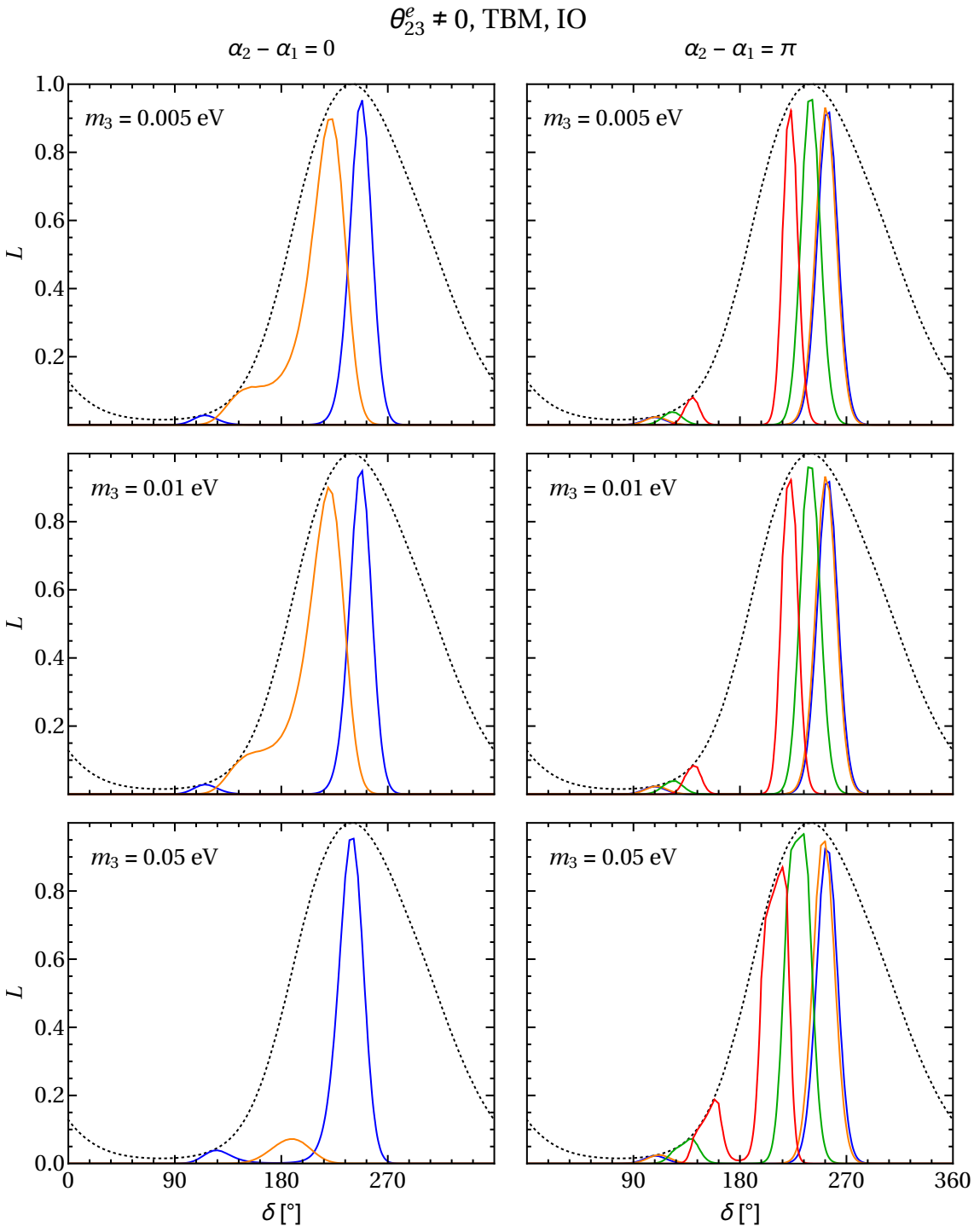

Figure 5.6. The same as in Fig. 5.5, but for the IO spectrum.

$\tan\beta = 5$ and 10 (blue and orange lines, respectively), are quantitatively very similar to the result without running (this is why we do not present the latter in the plots) for all three mass scales considered and both orderings due to the suppression of the running of θ_{12} discussed above. However, this is not the case for the large values of $\tan\beta = 30$ and 50 (green and red lines, respectively) and the NO spectrum with $m_1 = 0.05$ eV, and for all three values of m_3 considered in the case of IO spectrum. Clearly, the enhancement due to $\tan\beta$ prevails over the suppression due to the Majorana phases in these cases.

The next interesting point to note is that for the IO spectrum, the corrections in

the case of $\tan\beta = 5$ and $\alpha_2 = \alpha_1$ (blue line) are comparable with the corrections for $\tan\beta = 30$ and $\alpha_2 = \alpha_1 + \pi$ (green line) for all three mass scales considered. A similar observation holds also for the NO spectrum if $m_1 = 0.05$ eV: the corrections for $\tan\beta = 10$ and $\alpha_2 = \alpha_1$ (orange line) are similar in magnitude to those for $\tan\beta = 30$ and $\alpha_2 - \alpha_1 = \pi$ (green line).

Further, we note also that the absence of the green and red lines, corresponding to $\tan\beta = 30$ and 50 and equal Majorana phases, in all cases, except for NO with $m_1 = 0.005$ eV and $m_1 = 0.01$ eV, reflects the fact that the RG corrections lead, in particular, to a low-energy value of θ_{12}, which is outside of the current 3σ range. For the IO spectrum with $m_3 = 0.05$ eV and $\alpha_2 = \alpha_1$, even for $\tan\beta = 10$ (orange line) the RG corrections are quite large, such that only a small region of values of δ around π is allowed, with the likelihood of these values being suppressed.

For the BM symmetry form the results we obtain are quite different. In this case, we consider values of $m_{\text{lightest}} = 0.01$, 0.05 and 0.1 eV, and $\tan\beta = 5$, 10, 30 and 50. We find that the small values of $\tan\beta$ considered, $\tan\beta = 5$, 10, cannot provide the RG corrections which allow one to have $\cos\delta \in [-1, 1]$ and low-energy values of the mixing angles compatible with the current data (except for the small range of values of δ close to π allowed without running). For the large values of $\tan\beta$ and the NO spectrum, we get significant RG corrections compatible with all constraints, as can be seen from Fig. 5.7, (i) for $\alpha_2 - \alpha_1 = \pi$ (dashed lines), provided $m_1 \gtrsim 0.05$ eV, and (ii) for $\alpha_2 = \alpha_1$ (solid line) if $m_1 \approx 0.10$ eV and $\tan\beta = 50$. For the IO spectrum and $m_3 \gtrsim 0.05$ eV, the predictions are compatible with the data for $\alpha_2 = \alpha_1$ provided $\tan\beta = 50$. If $m_3 = 0.1$ eV, $\alpha_2 - \alpha_1 = \pi$ also contributes to the final likelihood profile for $\tan\beta = 50$, although this contribution is less favoured.

As has already been discussed above, the running of θ_{12} is suppressed if the difference of the Majorana phases is equal to π, otherwise the running of θ_{12} is always the dominant correction to $\cos\delta$. If the running of θ_{12} is minimal, the running of θ_{23} and θ_{13} is dominant (for a maximal running of θ_{13} we need additionally to have $\delta = \alpha_2$). Then $\delta\theta_{13}$ and $\delta\theta_{23}$ are roughly two orders of magnitude larger then $\delta\theta_{12}$. This implies that the correction to $\cos\delta$ in the HG, GRA, GRB and TBM mixing schemes is not longer determined by the running of θ_{12} but by the running of θ_{23} and θ_{13}. For BM mixing the contribution of $\delta\theta_{13}$ is still dominant. The sign and size of the correction to $\cos\delta$ depends on δ because the size of $\delta\theta_{13}$ depends on δ and the contributions to $\delta(\cos\delta)$ by the running of θ_{23} and θ_{13} are approximately equal.

Finally, we would like to note that the cases studied in the present subsection were analysed rather qualitatively in [111], considering only the running of θ_{12}. Our analysis goes beyond the discussion in [111], since we present explicitly in graphic form the impact of the RG effects on the likelihood functions (Figs. 5.5–5.7). In particular, as was discussed above, the results depend strongly on the symmetry form considered — the TBM, GRA, GRB and HG forms on the one hand and the BM form on the other hand — and this distinction was not discussed in [111]. Furthermore, in our quantitative results we find a region of parameter space where their conclusions are not fully correct. Although this region seems somewhat tuned, it is actually motivated, as we mentioned above, in set-ups with spontaneous CP violation. We find that, e.g., in the case of the TBM symmetry form, for $m_3 = 0.01$ eV (IO), $\tan\beta = 30$ and $\alpha_2 - \alpha_1 = \pi$ (green line in the corresponding panel of Fig. 5.6) the RG corrections are noticeable, in contrast to the conclusion in [111] that the RG corrections can be neglected for $\tan\beta \lesssim 35$ if the spectrum is not quasi-degenerate.

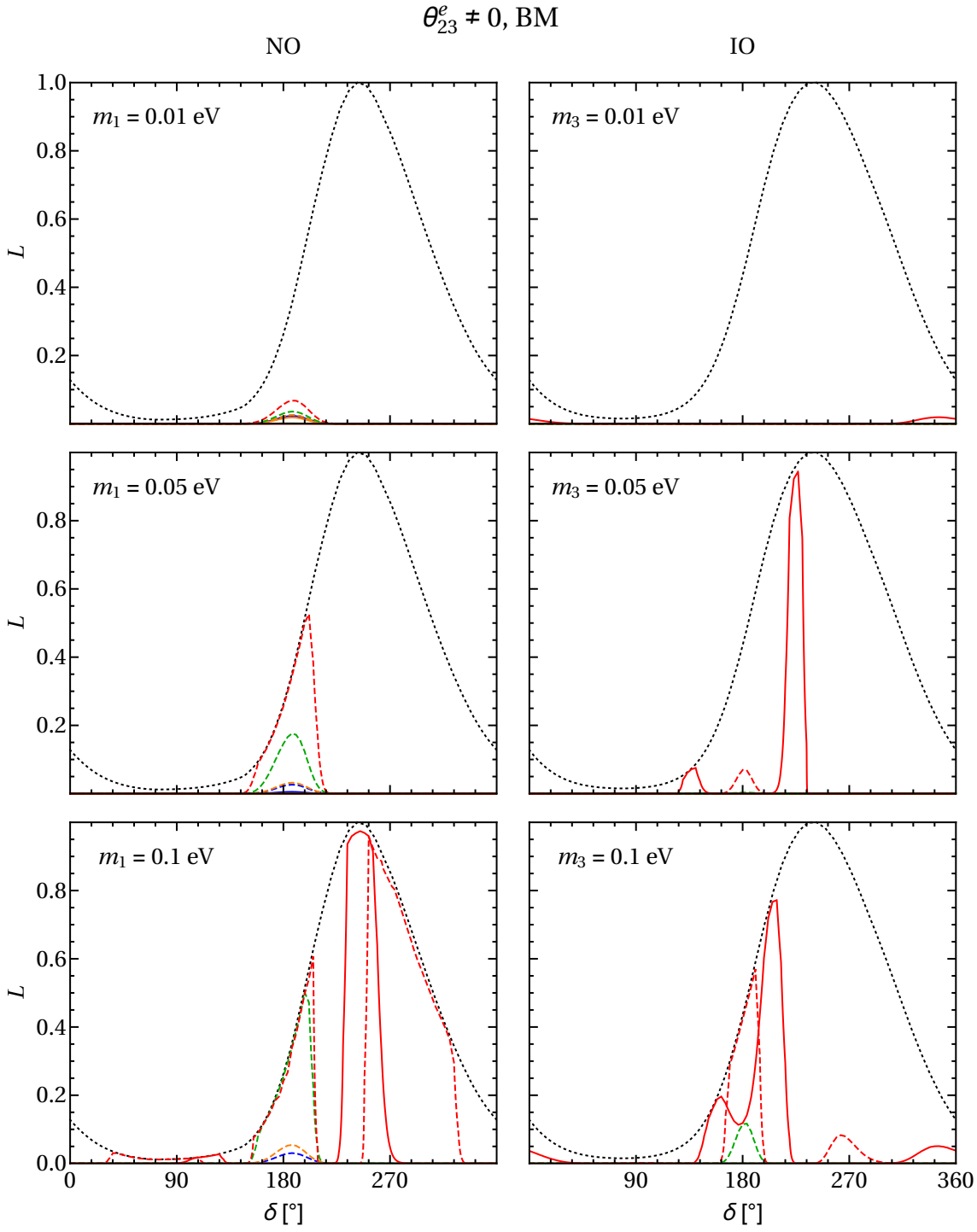

Figure 5.7. Likelihood function vs. δ in the case of non-zero θ^e_{23} for the BM symmetry form of the matrix $\tilde{U}_\nu$. The dotted black line stands for likelihood extracted from the global analysis in [162]. The blue, orange, green and red lines are for the running within MSSM with $\tan\beta = 5$, 10, 30 and 50, respectively. The solid lines correspond to $\alpha_2 = \alpha_1$. The dashed lines correspond to $\alpha_2 = \alpha_1 + \pi$. Note that the lines for $\tan\beta < 50$ are often barely visible.

5.3.4 Remarks on the case of zero θ^e_{23}

Before we turn to the numerical results we want to make a few more remarks on the case of $\theta^e_{23} = 0$, i.e., imposing also the sum rule from eq. (5.3) at the high scale. This will help to understand the numerical results in the next section. In eq. (5.6) we can replace

$\theta_{12}(M_S)$ by $\theta_{12}(M_Z)$ plus the small RG correction $\delta\theta_{12}$ in which we expand. Since θ_{13} and $\delta\theta_{13}$ are small we can neglect the latter ($\theta_{13}(M_S) \approx \theta_{13}(M_Z)$) and expand the correction in the first to end up with

$$\cos\delta(M_S) \approx \cos\delta(M_Z) + \frac{1 - \cos 2\theta_{12}\, \cos 2\theta_{12}^{\nu}}{\theta_{13}\, \sin^2 2\theta_{12}}\, \delta\theta_{12}\,. \tag{5.16}$$

In the case of BM mixing $\cos\delta(M_Z)$ is smaller than -1 for the best fit values of the angles and the correction is always negative since the running of θ_{12} has a fixed sign. Note, that the value of $\cos\delta(M_Z)$ could be adjusted by $\theta_{23}^e \neq 0$ to a value larger than -1, cf. eq. (5.5). So, from that estimate we expect the BM mixing scheme not to be valid in the case of $\theta_{23}^e = 0$. This is confirmed in our extensive numerical scan, where we employed the exact sum rules from eqs. (5.3) and (5.6) and the full one-loop β-functions for all parameters but did not find any physically acceptable points as well. Nevertheless, our estimate is a bit rough and a numerical scan cannot cover the whole parameter space such that a tiny, highly tuned region of the parameter space might still be allowed.

Let us now turn to the other mixing cases. There the absolute value of $\cos\delta(M_Z)$ in our estimate, eq. (5.16), is always smaller than one. For TBM and GRB it is still negative, and for TBM mixing, for instance, we get

$$\cos\delta(M_Z) \approx -0.21\,, \tag{5.17}$$

which allows for a sizeable correction of θ_{12} up to $-6.5°$, so that these two scenarios are not disfavoured by our estimate. For GRA and HG mixings the first term is even positive such that we can account for even more sizeable RG corrections in these cases.

5.4 Numerical results

In the present section, we will first describe our numerical approach before we show the results we obtain for the δ likelihood functions in the TBM, GRA, GRB, HG and BM mixing schemes in the cases of $\theta_{23}^e \neq 0$ and $\theta_{23}^e = 0$.

5.4.1 Numerical approach

To obtain the low-energy predictions for δ from the high-scale mixing sum rule, eq. (5.5) in the case of $\theta_{23}^e \neq 0$ (eq. (5.6) in the case of $\theta_{23}^e = 0$), we employ the running of the parameters using the `REAP` package [184]. For the running we set the low-energy scale to be M_Z and the high-energy scale to be equal to the seesaw scale $M_S \approx 10^{13}$ GeV. Since the dependence on the scales is only logarithmic a mild change of the high-energy or low-energy scale would not change our results significantly.

In our scans we present the results for the SM and MSSM extended minimally by the Weinberg operator. We have fixed the scale where we switch from the SM to MSSM RGEs to 1 TeV. Again the dependence on the scale is only logarithmic and hence weak. The exact SUSY particle spectrum plays only a minor role since we have neglected the SUSY threshold corrections [186–189].

In the MSSM we consider as benchmarks $\tan\beta = 30$ and $\tan\beta = 50$. In the SM the running is relatively small and hence the results are very similar to the results without running. In fact the SM results look like the results obtained in subsection 3.7.1 apart from relatively small changes due to the different global fit results [18] used therein. For a given

mass scale and a given model (SM or MSSM with a given $\tan\beta$), we employ the mixing sum rules at the high scale to determine δ (and θ_{23} for $\theta_{23}^e = 0$) at the low scale depending on the other parameters. For a given mass scale and a given model (SM or MSSM with a given $\tan\beta$), we determine the low-scale parameters (the angles, mass squared differences and the Majorana phases) such that the mixing sum rule in eq. (5.5) (eq. (5.6) for $\theta_{23}^e = 0$) at the high scale is fulfilled and their likelihood function is maximal. We choose a "small" neutrino mass scale, $m_{\text{lightest}} = 0.01$ eV, a "medium" mass scale, $m_{\text{lightest}} = 0.05$ eV, and a "large" mass scale, $m_{\text{lightest}} = 0.1$ eV. The "large" neutrino mass scale is still compatible with the cosmological bound on the sum of the neutrino masses [63]

$$\sum_j m_j < 0.49 \text{ eV}. \tag{5.18}$$

Note that for very small neutrino mass scales, $m_{\text{lightest}} \ll 0.01$ eV, and sufficiently small $\tan\beta$, the RG effects are negligibly small even in the MSSM. We present the results for the different cases considered in the present study in terms of the likelihood functions defined in eq. (5.14). For better comparison with results obtained in subsection 3.7.1 without taking the RG corrections into account, we present in Appendix H the corresponding likelihood functions for $\cos\delta$.

5.4.2 Results in the case of non-zero θ_{23}^e

We begin our discussion of the numerical results with the case of non-zero θ_{23}^e. In Figs. 5.8–5.11 we show the likelihood functions versus δ for the TBM, GRA, GRB and HG symmetry forms of the matrix $\tilde{U}_\nu$ in all set-ups. The blue line in these figures represents the SM running result, the green and red lines are for the MSSM running with $\tan\beta = 30$ and $\tan\beta = 50$, respectively. The SM line practically coincides with the line corresponding to the result without running, as expected. For this reason we do not show the latter in the plots. The dotted black line stands for the likelihood extracted from the global analysis [162] which corresponds to the likelihood for δ without imposing any sum rule. We note that the whole procedure is numerically very demanding and hence there are some tiny wiggles in the likelihoods which do not have any physical meaning. Note also that the mixing sum rule has two solutions but the solution $\delta \approx 90^\circ$ has a small likelihood and is therefore barely visible in the plots.

As we have already indicated, the SM results are very similar to the results obtained in subsection 3.7.1 without running. This implies that, as was concluded in Chapter 3, using the data on neutrino mixing angles and a sufficiently precise measurement of $\cos\delta$ it will be possible to distinguish between the three groups of schemes: the TBM and GRB group, the GRA and HG group, and the BM scheme. Distinguishing between the GRA and HG schemes is experimentally very demanding, but not impossible, while distinguishing between the TBM and GRB seems practically extremely difficult (if not impossible) to achieve (see subsection 3.7.1 for further details).

In the MSSM, the results depend on the value of the lightest neutrino mass, the type of spectrum — NO or IO — the neutrino masses obey, on the value of $\tan\beta$ as well as on the uncertainties in the measured values of the neutrino oscillation parameters. As expected, for increasing $\tan\beta$ and increasing absolute neutrino mass scale, the difference with the predictions without running increases. The allowed regions for δ start to broaden and, e.g., for the largest value of $\tan\beta = 50$ and $m_1 = 0.05$ eV and 0.10 eV ($m_3 = 0.01$ eV, 0.05 eV and 0.10 eV) in the case of NO (IO) spectrum, the likelihood profile in the

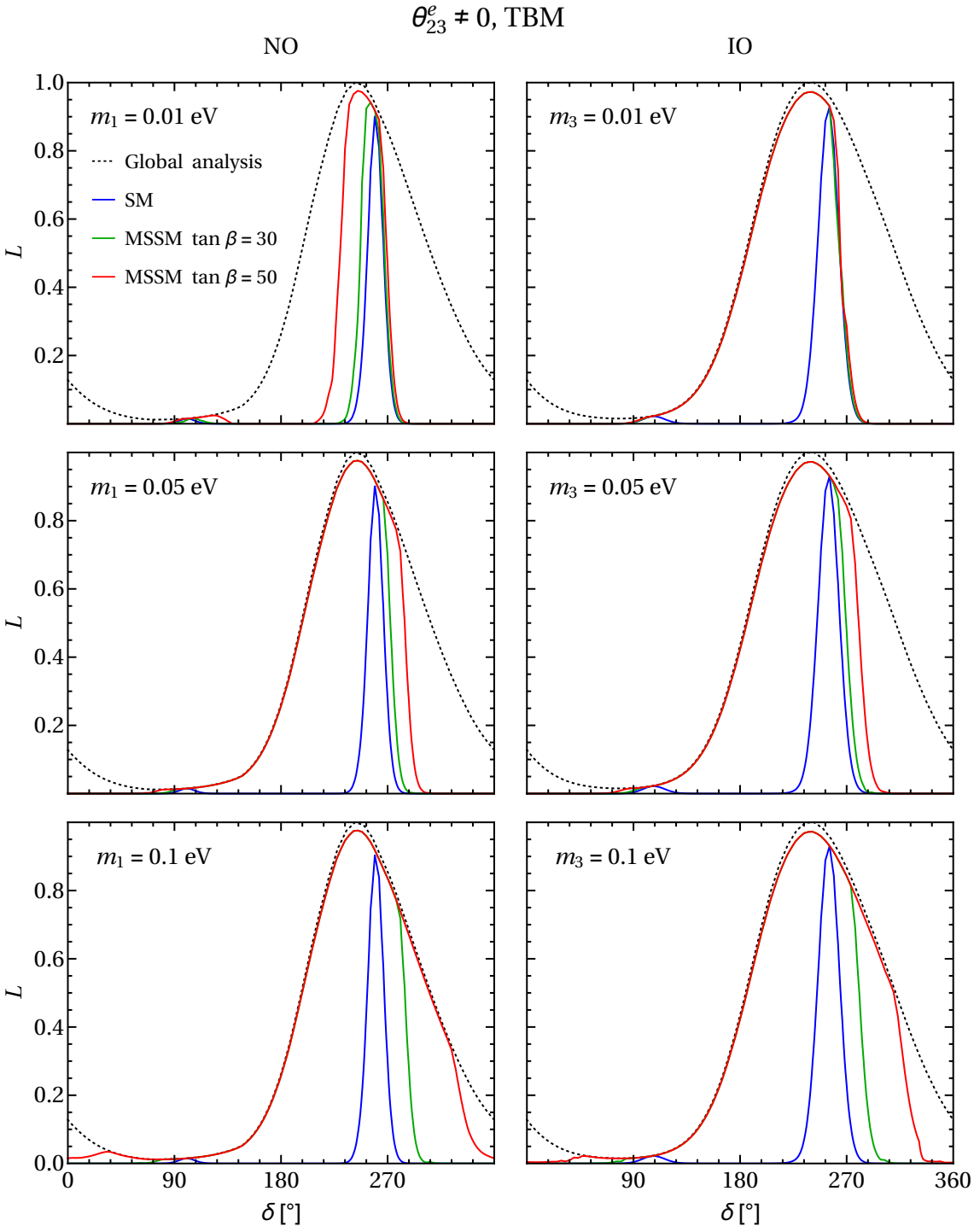

Figure 5.8. Likelihood function vs. δ in the case of non-zero θ_{23}^{e} for the TBM symmetry form of the matrix $\tilde{U}_{\nu}$ in all the set-ups considered. The dotted line stands for likelihood extracted from the global analysis in [162]. The blue line is for the SM running, while the green and red lines are for the running within MSSM with $\tan\beta = 30$ and $\tan\beta = 50$, respectively.

cases of the TBM, GRA, GRB and HG mixing schemes practically coincides with the likelihood for δ obtained without imposing the sum rule constraint, the difference between the two profiles being noticeable only for values of δ lying approximately in the interval $\delta \sim (270° - 360°)$. As already discussed in the previous section, the running of $\cos\delta$ in the TBM, GRA, GRB and HG mixing schemes is mainly influenced by the running of

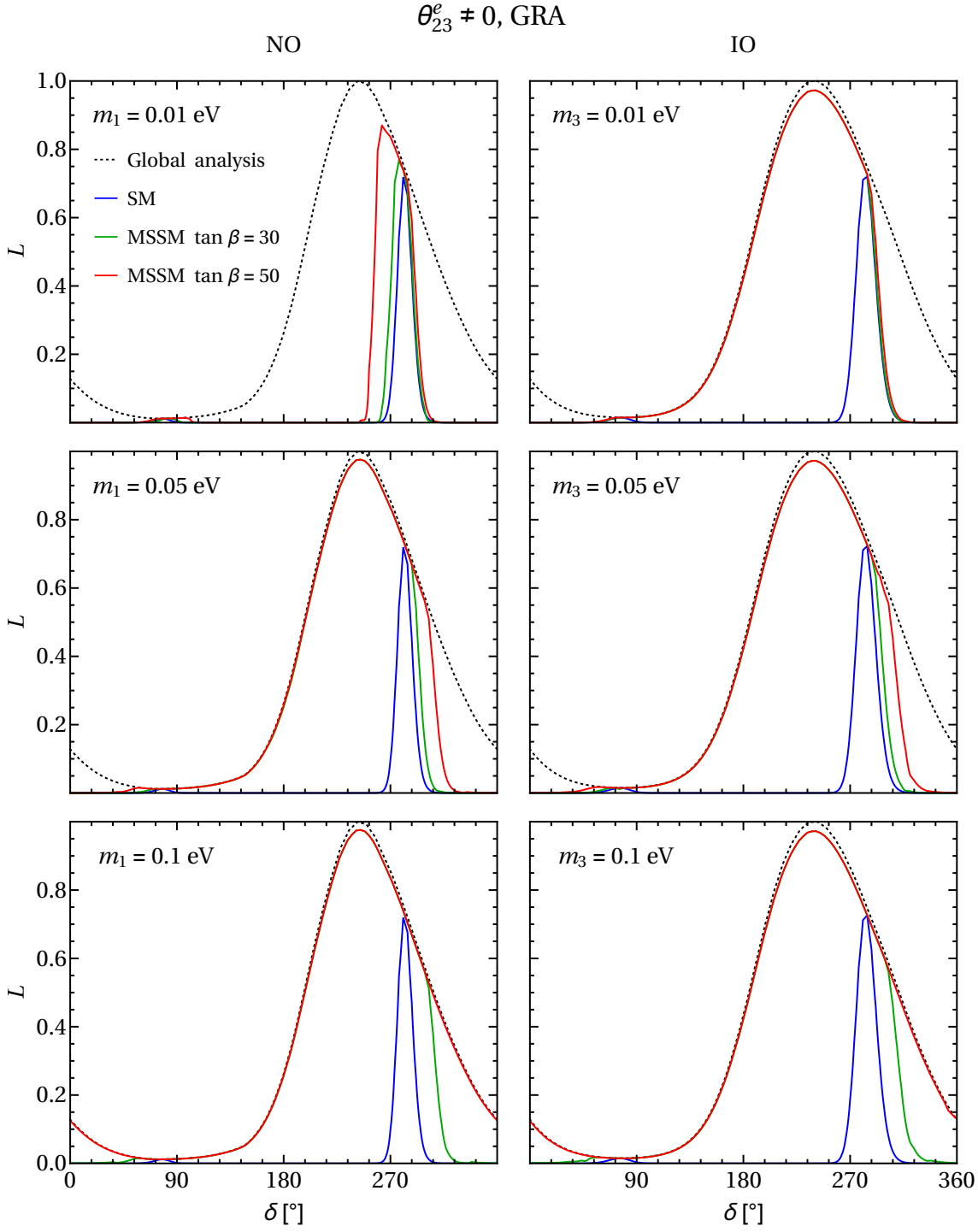

Figure 5.9. The same as in Fig. 5.8, but for the GRA symmetry form of the matrix $\tilde{U}_\nu$.

θ_{12} which has a fixed negative sign and hence has a tendency to shift δ to values smaller than 270°. For the NO spectrum, $m_1 \leq 0.01$ eV and $\tan\beta = 30$, a measured value of $\delta \lesssim 260°$ would favour the TBM and GRB schemes. For $m_1 = 0.05$ eV (or $m_1 = 0.01$ eV) and the same value of $\tan\beta = 30$, a measurement of $\delta \gtrsim 290°$ would make the GRA and HG schemes more probable. For $\tan\beta = 50$, $m_1 = 0.05$ eV (or $m_1 = 0.10$ eV), and given the current uncertainties in the measured values of the neutrino oscillation parameters, the TBM, GRA, GRB and HG schemes lead to very similar predictions for δ.

For the IO spectrum, the RG effects are larger and therefore the broadening happens

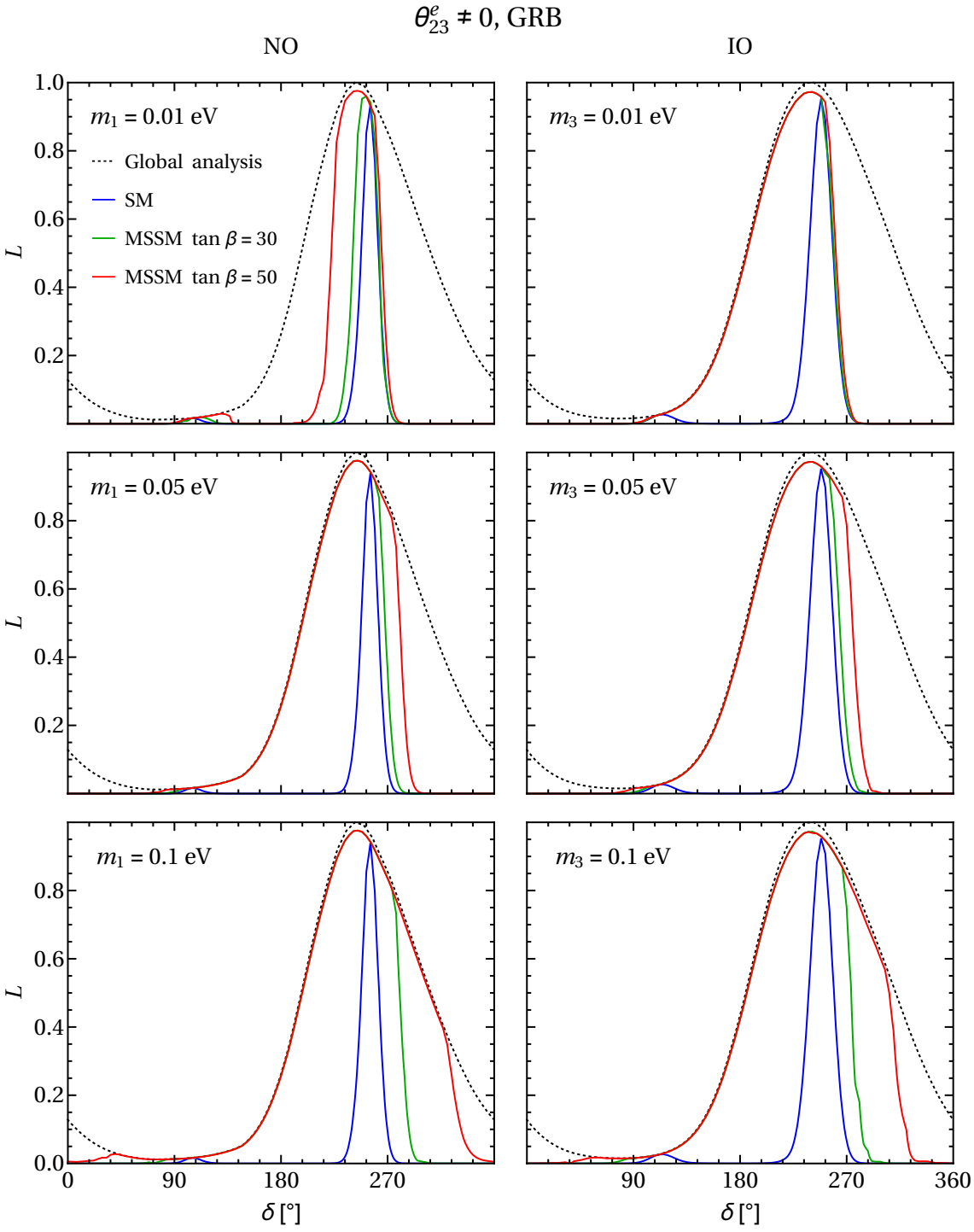

Figure 5.10. The same as in Fig. 5.8, but for the GRB symmetry form of the matrix $\tilde{U}_\nu$.

in the four schemes under discussion — TBM, GRA, GRB and HG — already for the "small" neutrino mass scale. Since the likelihood profiles are so broad and nearly identical even for the "small" and "medium" mass scales, except for certain differences in the interval $\delta \sim (270° - 360°)$, and given the current uncertainties in the measured values of the neutrino oscillation parameters, it will be difficult in the MSSM with $\tan\beta \gtrsim 30$ to distinguish between any of the four schemes considered using only a determination of δ.

For the BM mixing scheme the results are very different. This scheme is strongly disfavoured for the currently allowed ranges of the mixing parameters without considering

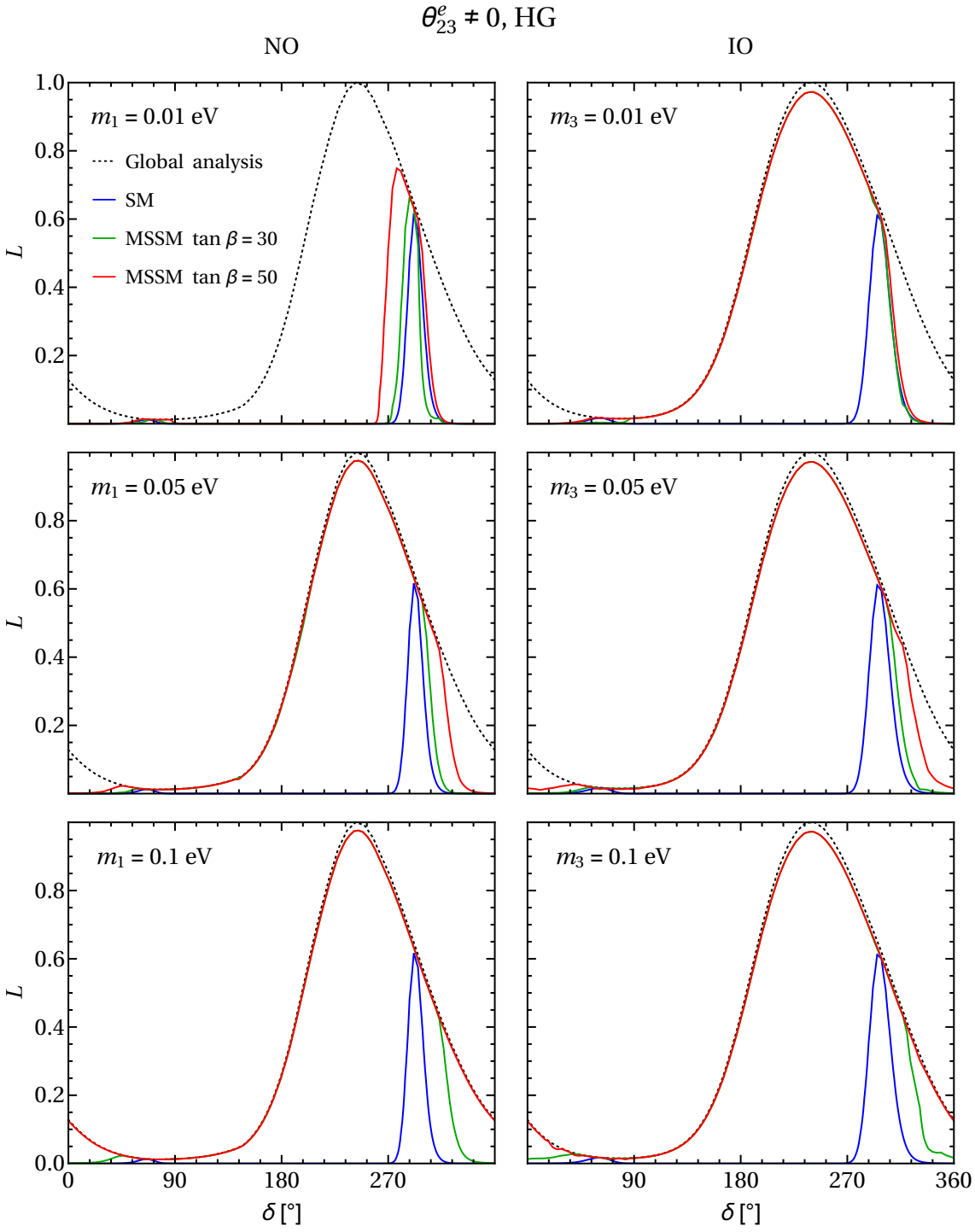

Figure 5.11. The same as in Fig. 5.8, but for the HG symmetry form of the matrix $\tilde{U}_\nu$.

RG effects. Therefore, the maximal value of the likelihood in the SM running case is relatively small. In the MSSM the running increases the value of $\cos\delta$ to physical values, as explained in the previous section. In addition both the maximal value of the likelihood function increases and the position of the likelihood maximum shifts from $\delta \approx 180°$ towards $\delta = 270°$ (see Fig. 5.12). Again the likelihood profile broadens with increasing of the absolute neutrino mass scale and $\tan\beta$ and at $\delta \lesssim 270°$ for the NO spectrum tends to approach the likelihood function for δ obtained without imposing the sum rule. In the case of IO spectrum, the BM scheme is strongly disfavoured for $m_3 \lesssim 0.05$ eV even for

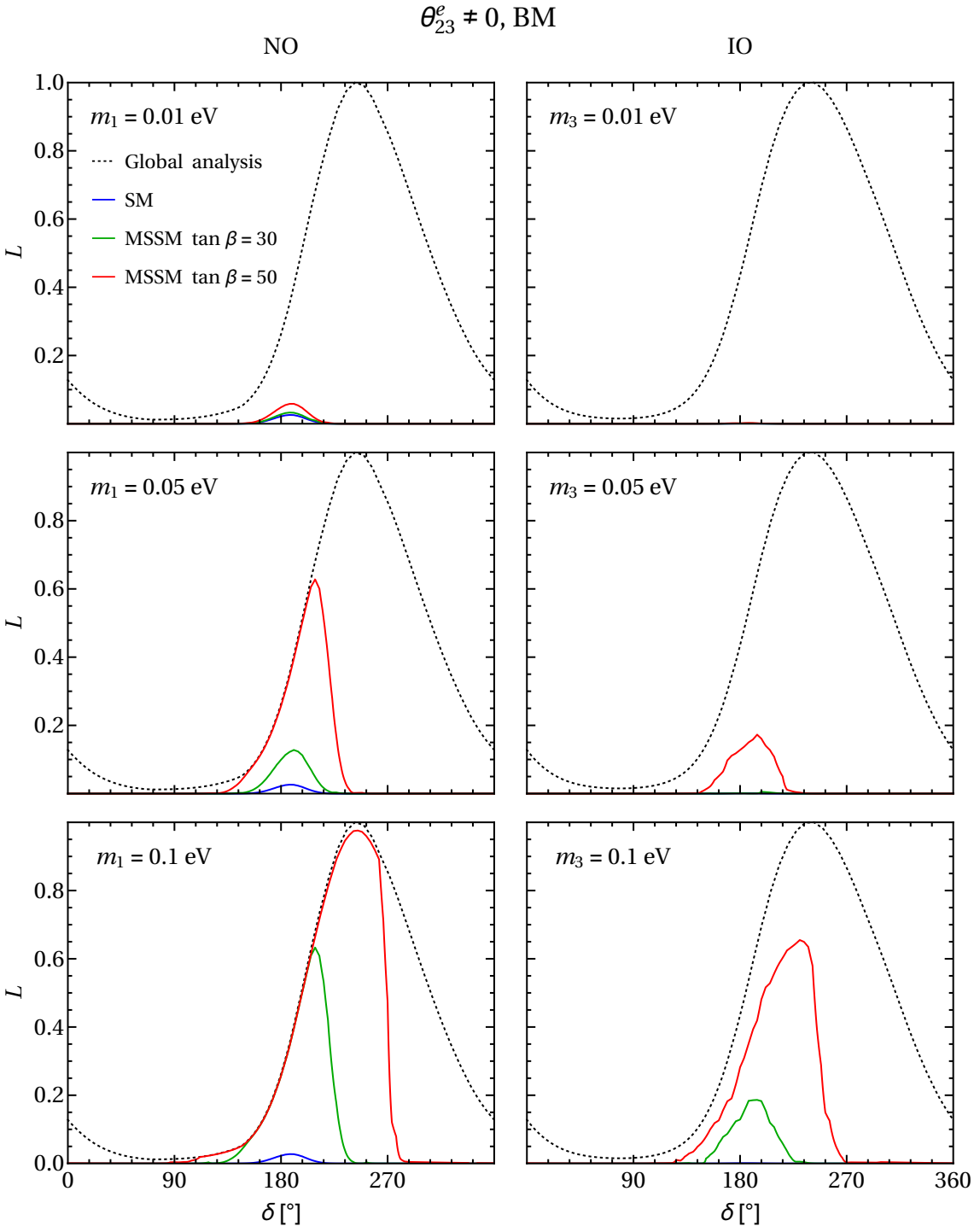

Figure 5.12. The same as in Fig. 5.8, but for the BM symmetry form of the matrix $\tilde{U}_\nu$.

$\tan\beta = 50$.

5.4.3 Results in the case of zero θ_{23}^e

In Figs. 5.13–5.16 we present the results in the case of $\theta_{23}^e = 0$. Again, the blue line in these figures represents the SM running result, the green and red lines are for the MSSM running with $\tan\beta = 30$ and $\tan\beta = 50$, respectively. The dotted black line stands for the likelihood extracted from the global analysis [162] which corresponds to the likelihood

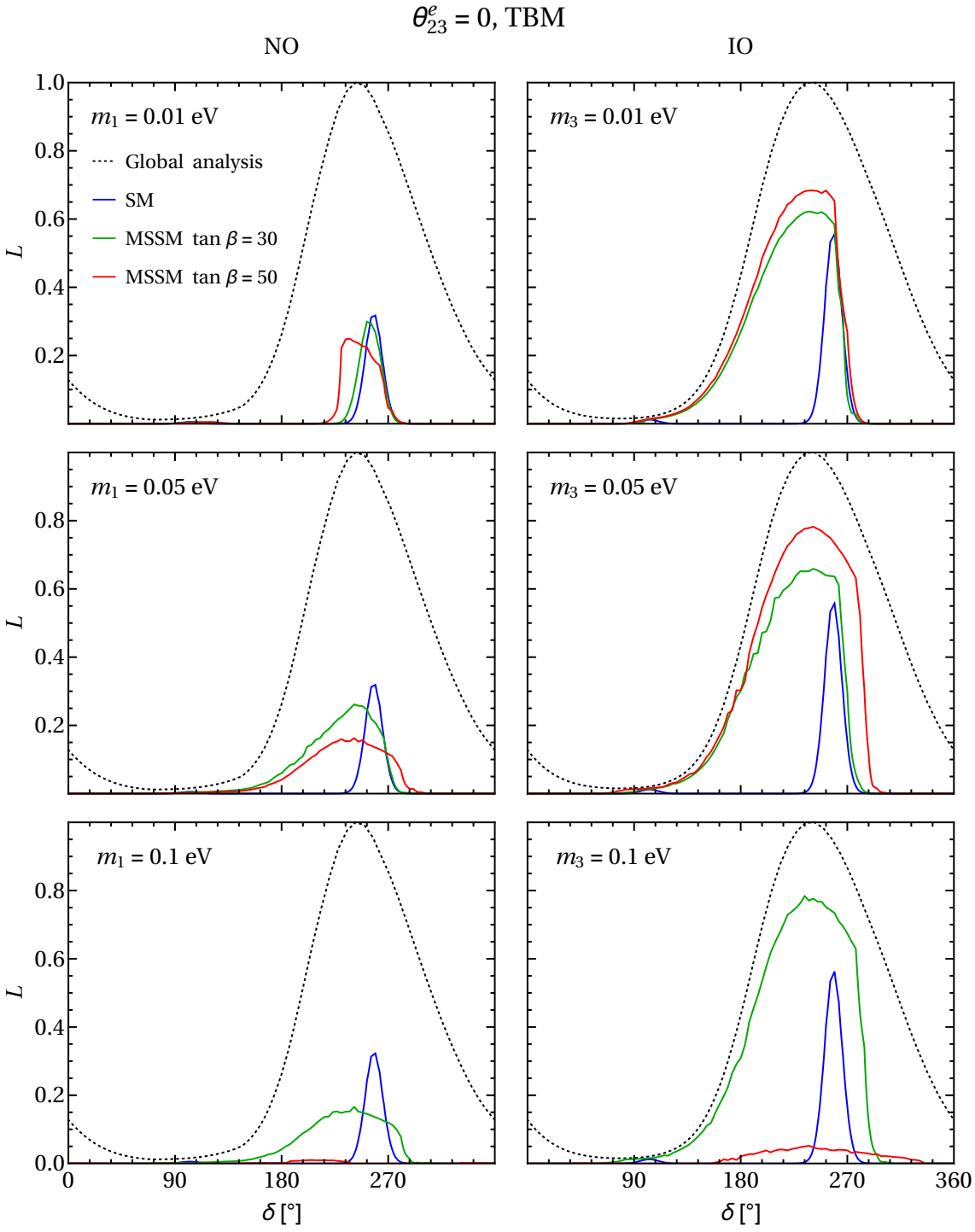

Figure 5.13. Likelihood function vs. δ in the case of zero θ^e_{23} for the TBM symmetry form of the matrix $\tilde{U}_\nu$ in all the set-ups considered. The dotted line stands for likelihood extracted from the global analysis in [162]. The blue line is for the SM running, while the green and red lines are for the running within MSSM with $\tan\beta = 30$ and $\tan\beta = 50$, respectively.

for δ without imposing any sum rule. Similar to the case of non-zero θ^e_{23}, the SM line practically coincides with the line corresponding to the result without running, as expected. Therefore, we do not show the latter in the plots. Note again that the small wiggles in the likelihoods are of numerical origin and not physical.

For the TBM, GRA, GRB and HG mixing schemes, we observe similar to the case of

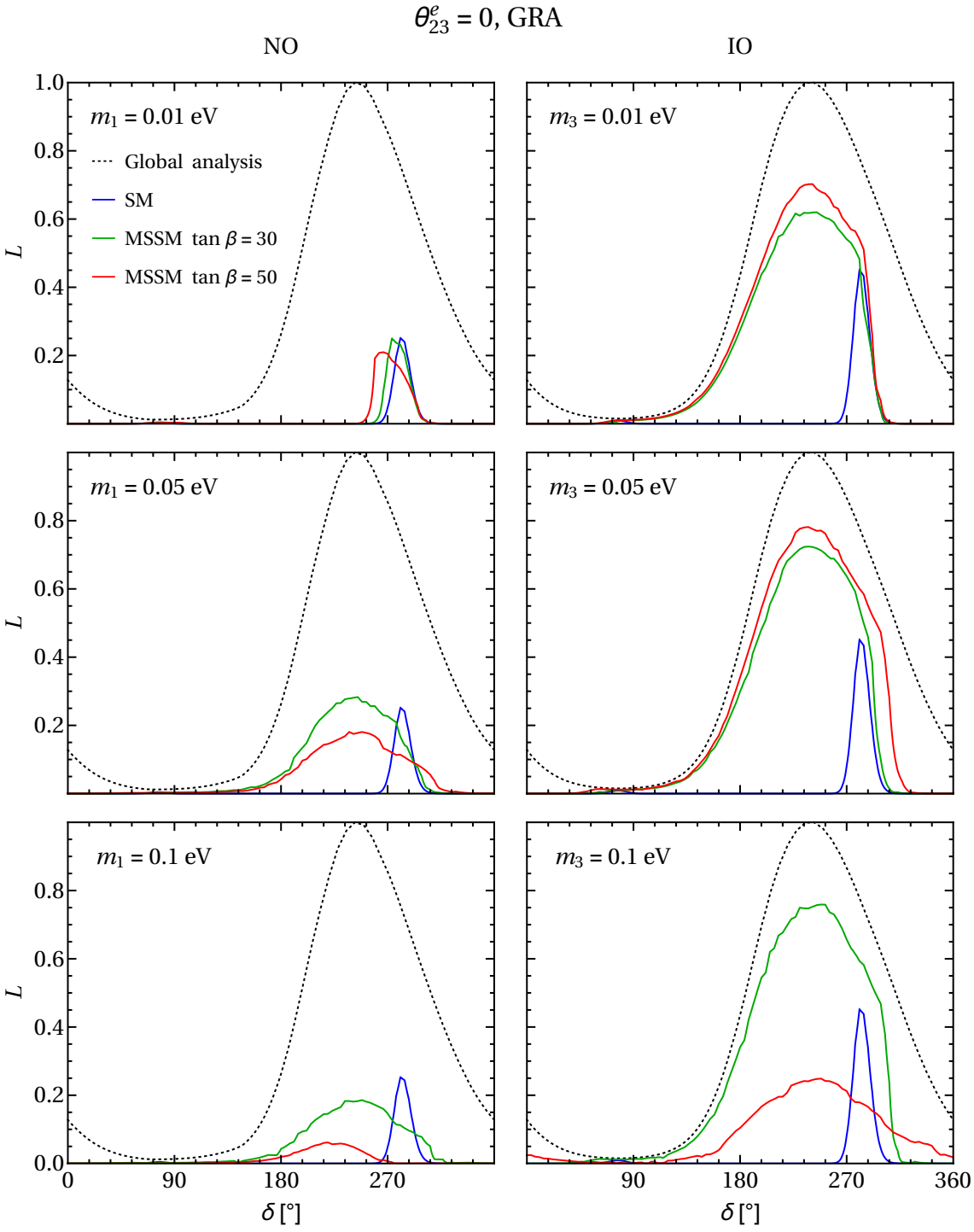

Figure 5.14. The same as in Fig. 5.13, but for the GRA symmetry form of the matrix $\tilde{U}_\nu$.

non-zero θ^e_{23} broadening of the likelihood with increasing $\tan\beta$ and increasing absolute neutrino mass scale. But in contrast to the case of $\theta^e_{23} \neq 0$, the likelihood does not reach the likelihood for δ without imposing the sum rule considered. The major difference with respect to the results obtained in the case of $\theta^e_{23} \neq 0$ is that due to the constraint on θ_{23} from eq. (5.3) at the high scale, the low-scale mixing parameters are more severely constrained and not necessarily close to their respective best fit values.

As Figs. 5.13–5.16 show, for the values of $\min(m_j)$ and $\tan\beta$ considered, the NO spectrum is less favoured (i.e., has a smaller likelihood for any given δ and smaller

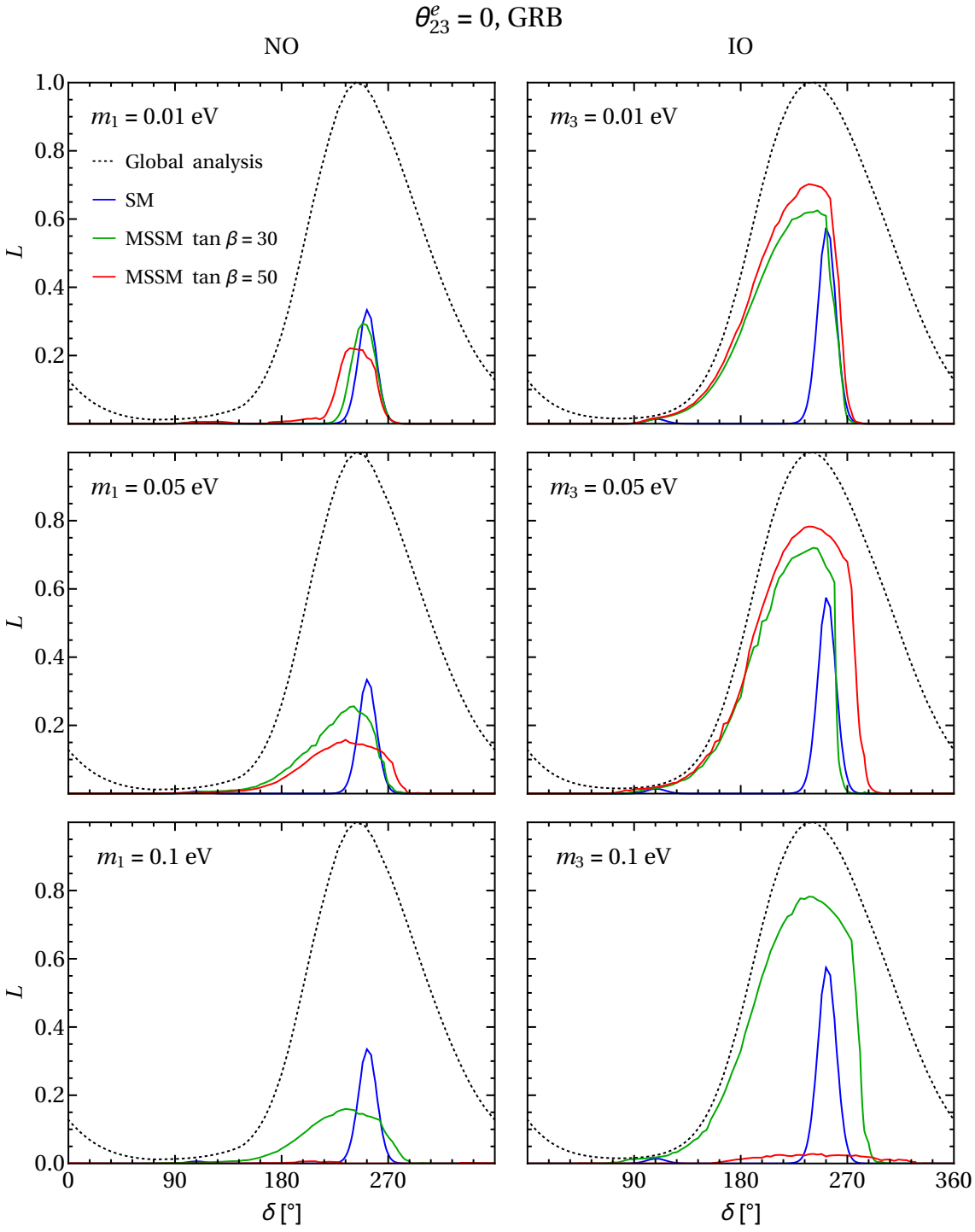

Figure 5.15. The same as in Fig. 5.13, but for the GRB symmetry form of the matrix $\tilde{U}_\nu$.

maximum likelihood) than the IO spectrum. The sum rule, eq. (5.3), restricts θ_{23} to be slightly smaller than 45° at the high scale. Since the running of this angle has a fixed negative sign for the NO spectrum, its low-scale value is larger than its high scale value and pushed outside of the NO 1σ region [162]. On the other hand, for the IO spectrum, the low-scale value of θ_{23} is always smaller than 45° due to the running and the sum rule. However, in this case there is a second 1σ region below maximal mixing besides the region around the best fit value which is larger than 45° [162].

In the case of TBM and GRB schemes, the case of $\min(m_j) = 0.10$ eV and $\tan\beta = 50$

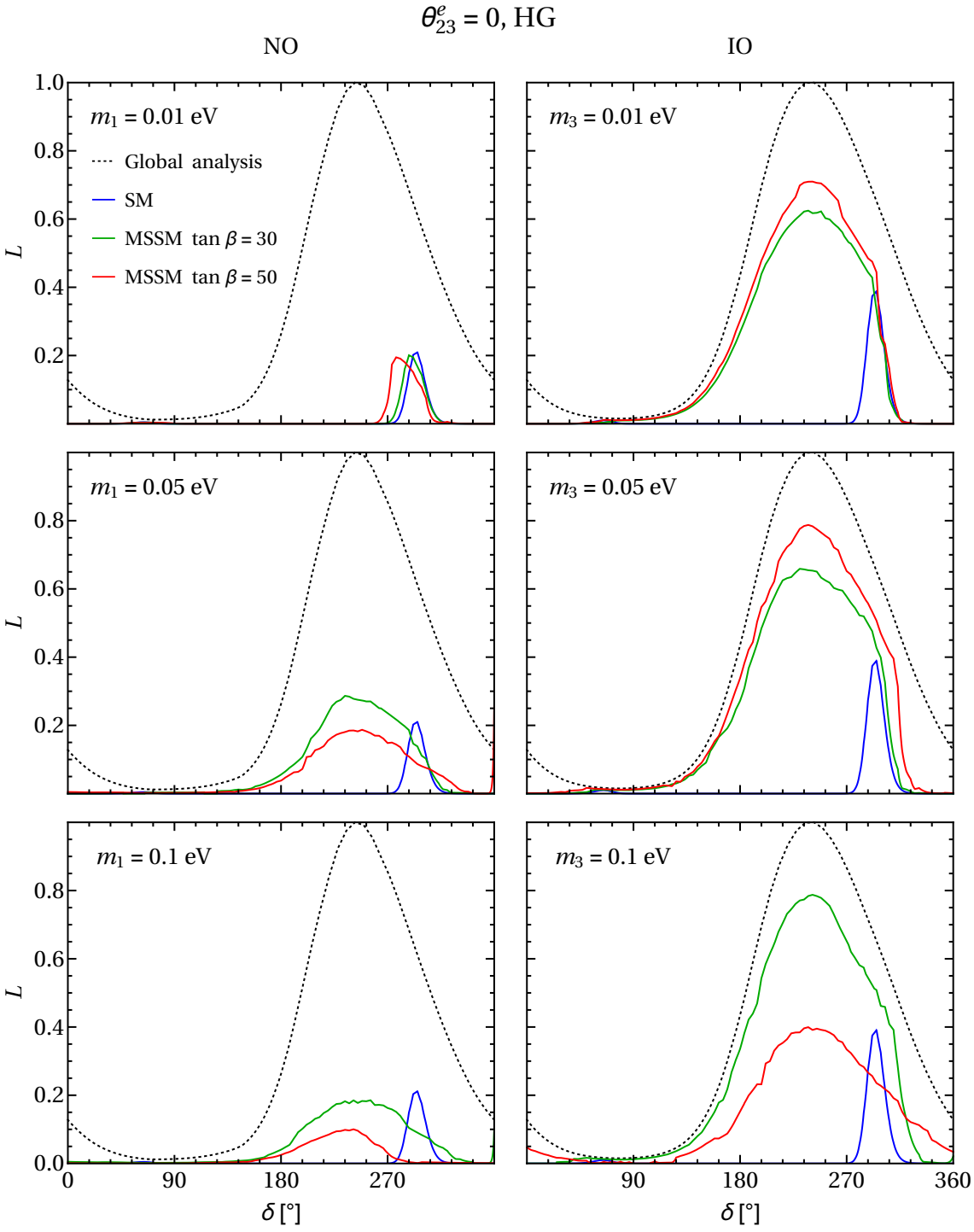

Figure 5.16. The same as in Fig. 5.13, but for the HG symmetry form of the matrix $\tilde{U}_\nu$.

is strongly disfavoured for both NO and IO spectra, while for the GRA and HG schemes it is less favoured than the $\min(m_j) = 0.10$ eV and $\tan\beta = 30$ case.

As explained in subsection 5.3.4, in order to satisfy the sum rule in eq. (5.6) for zero θ^e_{23}, θ_{12} is not allowed to run strongly. This leads to the relatively small likelihood for $\tan\beta = 50$ and $m_{\text{lightest}} = 0.1$ eV seen in Figs. 5.13–5.16. For TBM and GRB mixings, the constraint on the running of θ_{12} is even more severe than for GRA and HG mixings, and the likelihood in these schemes is hence even smaller for $\tan\beta = 50$ and $m_{\text{lightest}} = 0.1$ eV.

For BM mixing our analytical estimates have indicated that this scheme is not valid

due to the severe constraint on the running of θ_{12}. In our extensive numerical scans we did not find any valid, i.e., physically acceptable, parameter points as well.

5.5 Summary and conclusions

We presented a systematic study of the effects of RG corrections on sum rules for the Dirac CPV phase, eqs. (5.5) and (5.6). These corrections are present in every high-energy model, when running down to the low scale where experiments take place. We answered the question how stable the predictions from the sum rules are in the cases of charged lepton corrections characterised by (i) $\theta_{12}^e \neq 0,\ \theta_{23}^e \neq 0,\ \theta_{13}^e = 0$ and (ii) $\theta_{12}^e \neq 0,\ \theta_{23}^e = 0,\ \theta_{13}^e = 0$ to TBM, GRA, GRB, HG or BM mixing in the neutrino sector.

To this aim we first presented analytical estimates of the allowed parameter space if we take RG corrections into account. These estimates were subsequently verified numerically. To obtain the numerical results for the allowed ranges of δ we used as three benchmark cases the SM running (where the running effects are small) and the MSSM running with $\tan\beta = 30$ and $\tan\beta = 50$ (where the running effects become larger with increasing $\tan\beta$). Furthermore, we considered three mass scales: a "small" mass scale ($m_{\text{lightest}} = 0.01$ eV), a "medium" mass scale ($m_{\text{lightest}} = 0.05$ eV) and a "large" mass scale ($m_{\text{lightest}} = 0.1$ eV), where the RG effects increase with the mass scale. We presented the results in terms of the likelihood functions for each case (SM or MSSM with a given $\tan\beta$, and a given mass scale). Our numerical results are obtained using the current best fit values and uncertainties on the neutrino oscillation parameters derived in the global analysis of the neutrino oscillation data performed in [162].

Our results have shown that the RG effects can change significantly the allowed low-energy ranges for δ, especially when we employ the MSSM running with the "medium" and "large" mass scales. In the case of $\theta_{23}^e \neq 0$, the allowed regions for δ broaden and the likelihood profiles approach the likelihood for δ extracted from the global analysis (without imposing the sum rule considered). For the TBM, GRA, GRB and HG symmetry forms we found the allowed ranges of values of δ to be shifted from values close to (somewhat larger than) 270° to values somewhat smaller than (close to) 270°. For BM mixing, which is strongly disfavoured by the current data without taking into account the running of the neutrino parameters, we found that the RG corrections partially reconstitute compatibility of this symmetry form with the data. With the increasing of $\min(m_j)$ and $\tan\beta$, the values of δ in this case shift from $\delta \approx 180°$ towards 270°. In the case of $\theta_{23}^e = 0$ and for the TBM, GRA, GRB and HG mixing schemes, the likelihood profiles broaden with increasing $\tan\beta$ and increasing mass scale, similarly to the case of non-zero θ_{23}^e. The main difference is that now they do not reach the likelihood for δ obtained without imposing the sum rule. The reason for that is the constraint on θ_{23} from eq. (5.3) at the high scale, due to which the low-scale mixing parameters are more severely constrained and not necessarily close to their respective best fit values. Finally, we found that in this case the RG corrections are not sufficient to restore even partial compatibility of BM mixing with the current data.

In conclusion, our results show that the RG effects on the mixing sum rules in SUSY models with $\min(m_j) \gtrsim 0.01$ eV and $\tan\beta \gtrsim 30$ have to be taken into account to realistically probe the sum rule predictions in these models. In the case of the SM augmented with the Weinberg (dimension 5) operator, the RG corrections to the sum rule predictions are negligible.

Chapter 6

Conclusions and outlook

In the present PhD thesis, we have considered certain phenomenological aspects of the discrete symmetry approach to neutrino mixing and leptonic CP violation. This approach, based on the assumption of existence at some high-energy scale of a (lepton) flavour symmetry described by a non-Abelian finite group, leads to specific correlations between the neutrino mixing angles and the CPV phases present in the PMNS matrix. These correlations, usually referred to as neutrino mixing sum rules, can be tested in ongoing and future neutrino experiments. We have mainly focused on predictions for leptonic CP violation, the status of which is currently unknown.

In Chapters 2 and 3, we have obtained predictions for the Dirac CPV phase δ responsible for CP violation in neutrino oscillations. The currently running T2K [25,26] and NOνA [29] LBL neutrino oscillation experiments are already providing hints for CP violation in the lepton sector. The future planned T2HK [32] and DUNE [33–36] experiments, which are going to become operative by 2025–2026, will be able to establish the status of Dirac CP violation. With the experimental progress and accumulation of new data, the neutrino mixing angles and the Dirac phase will be measured with higher accuracy, which is crucial for testing the predictions obtained in the present PhD thesis. More specifically, the Daya Bay experiment [190, 191] will improve the precision in the determination of the reactor angle θ_{13}. The medium baseline JUNO experiment [157], which is expected to start data taking in 2021, will be able to provide a high precision measurement of the solar mixing angle θ_{12}. The above mentioned LBL neutrino oscillation experiments will perform better measurements of the atmospheric angle θ_{23}. The complex of these high precision measurements will rule out some of the cases considered by us in Chapters 2 and 3, and hopefully favour the others. The remaining viable cases, if any, will be considered as a strong indication of the existence of a new fundamental symmetry — a flavour symmetry — in the lepton sector.

In Chapter 4, we have demonstrated how the Majorana phases α_{21} and α_{31} can be constrained employing, in particular, a generalised CP symmetry. These phases are relevant, e.g., for $(\beta\beta)_{0\nu}$-decay. The experiments searching for $(\beta\beta)_{0\nu}$-decay are the only feasible experiments that can unveil possible Majorana nature of massive neutrinos. Constraining the Majorana phases allowed us to obtain predictions for the effective Majorana mass in $(\beta\beta)_{0\nu}$-decay. For the IH and QD types of neutrino mass spectrum, these predictions will be tested by the current (GERDA [192,193], KamLAND-Zen [194,195]) and future (CUORE [196], MAJORANA DEMONSTRATOR [197], nEXO [198], SNO+ [199], AMoRE [200], SuperNEMO [201]) $(\beta\beta)_{0\nu}$-decay experiments aiming to probe the region of values of $|\langle m \rangle|$ down to 0.01 eV.

Finally, in Chapter 5, we have studied the impact of the RG corrections on the sum rule predictions for the Dirac phase δ. We have shown that these corrections should be taken into account in SUSY models of flavour. If, however, the SM turns out to be valid

up to a very high-energy scale (say, a seesaw scale of approximately 10^{13} GeV), the RG corrections to the sum rule predictions will be negligible. This, in turn, will imply that the sum rules hold at a low-energy scale where experiments take place, and thus, can be tested directly at low energies.

In conclusion, the years ahead are undoubtedly very exciting for the field of neutrino physics. The wealth of experimental data to come will allow us to answer some of the long-standing questions and hopefully shed light on those which will remain. Our predictions, as well as the whole discrete symmetry approach to (lepton) flavour, will be critically tested, and we will gain an indication whether Nature follows the flavour symmetry path or not. We are looking very much forward to the years ahead.

Appendix A

Symmetry of a phenomenologically viable generalised CP transformation

If the neutrino sector respects a residual generalised CP symmetry $X_{\mathbf{3}\nu}$, the neutrino mass matrix satisfies eq. (1.50). The matrix $X_{\mathbf{3}\nu}$ must be unitary in order to preserve generalised CP invariance of the neutrino kinetic term. In what follows, we show that this matrix is additionally constrained to be symmetric in order for the neutrino masses to be different.

Expressing M_ν from eq. (1.18) and substituting it in eq. (1.50) yields

$$d_\nu \, \tilde{X}_{\mathbf{3}\nu} = \tilde{X}^*_{\mathbf{3}\nu} \, d_\nu \,, \tag{A.1}$$

where $d_\nu \equiv \mathrm{diag}(m_1, m_2, m_3)$, with m_j, $j = 1, 2, 3$, being the real neutrino masses, and

$$\tilde{X}_{\mathbf{3}\nu} \equiv U_\nu^\dagger \, X_{\mathbf{3}\nu} \, U_\nu^* \tag{A.2}$$

is unitary. Being 3×3 unitary, $\tilde{X}_{\mathbf{3}\nu}$ can be parametrised as the product of the three complex rotations U_{ij} defined as in eq. (2.3) and the three diagonal phase matrices Ψ_i defined in eq. (2.2) (see Appendix C):

$$\tilde{X}_{\mathbf{3}\nu} = \Psi_1 \, \Psi_2 \, \Psi_3 \, U_{23}(\vartheta_{23}, \delta_{23}) \, U_{13}(\vartheta_{13}, \delta_{13}) \, U_{12}(\vartheta_{12}, \delta_{12}) \,. \tag{A.3}$$

Equation (A.1) leads to the following relations:

$$e^{i(\psi_1 - \delta_{13})} \, m_1 \sin\vartheta_{13} = e^{-i(\psi_1 - \delta_{13})} \, m_3 \sin\vartheta_{13} \,, \tag{A.4}$$

$$e^{i(\psi_2 - \delta_{23})} \, m_2 \cos\vartheta_{13} \sin\vartheta_{23} = e^{-i(\psi_2 - \delta_{23})} \, m_3 \cos\vartheta_{13} \sin\vartheta_{23} \,, \tag{A.5}$$

$$e^{i(\psi_1 - \delta_{12})} \, m_1 \cos\vartheta_{13} \sin\vartheta_{12} = e^{-i(\psi_1 - \delta_{12})} \, m_2 \cos\vartheta_{13} \sin\vartheta_{12} \,. \tag{A.6}$$

From the non-degeneracy of the neutrino mass spectrum it follows that $\sin\vartheta_{13} = \sin\vartheta_{23} = \sin\vartheta_{12} = 0$. Thus, $\tilde{X}_{\mathbf{3}\nu}$ is constrained to be diagonal and hence symmetric, $\tilde{X}^T_{\mathbf{3}\nu} = \tilde{X}_{\mathbf{3}\nu}$. This finally implies that also $X^T_{\mathbf{3}\nu} = X_{\mathbf{3}\nu}$, i.e., a phenomenologically relevant generalised CP transformation $X_{\mathbf{3}\nu}$ must be symmetric.

It also follows from eq. (A.1) that the phases $\psi_i = 0$ or π, and thus, the matrix $\tilde{X}_{\mathbf{3}\nu}$ reads (cf. eq. (1.53))

$$\tilde{X}_{\mathbf{3}\nu} = \mathrm{diag}(\pm 1, \pm 1, \pm 1) \,. \tag{A.7}$$

Appendix B

The groups A_4, T', S_4 and A_5

A_4 is the symmetry group of even permutations of four objects (see, e.g., [81]). It is isomorphic to the tetrahedral symmetry group, i.e., the group of rotational symmetries of a regular tetrahedron. As such it can be defined in terms of two generators S and T, satisfying $S^2 = T^3 = (ST)^3 = 1$. In Chapter 2, we choose to work in the Altarelli-Feruglio basis [85] for the 3-dimensional representation of the S and T generators, see Table B.1.

The group T' is the double covering group of A_4 (see, e.g., [81]), which can be defined in terms of two generators S and T through the algebraic relations $R^2 = T^3 = (ST)^3 = 1$, $RT = TR$, where $R = S^2$. We use the basis for the 3-dimensional representation of the generators S and T from [143], summarised in Table B.1. Since we restrict ourselves to the triplet representation for the LH charged lepton and neutrino fields, there is no way to distinguish T' from A_4 [143].[42] Note that matrices representing S and T in Table B.1 for A_4, are related with those for T' by the following redefinition $S \to TST^2$, $T \to T^2$, where S and T before (after) the arrows are the matrices presented in Table B.1 for A_4 (T').

S_4 is the group of permutations of four objects, i.e., the rotational symmetry group of a cube (see, e.g., [81]). It can be defined in terms of three generators S, T and U, satisfying [83] $S^2 = T^3 = U^2 = (ST)^3 = (SU)^2 = (TU)^2 = (STU)^4 = 1$. We employ for the 3-dimensional representation of the S, T and U generators the basis given in [125] and summarised in Table B.1. As it was also shown in [125], this basis is equivalent to the basis widely used in the literature [176].

A_5 is the group of even permutations of five objects (see, e.g., [81]), i.e., the rotational symmetry group of an icosahedron, which can be defined in terms of two generators S and T, satisfying $S^2 = T^5 = (ST)^3 = 1$. We employ the basis defined in [144], which for the 3-dimensional representation of the generators S and T is summarised in Table B.1.

We conclude this appendix by noting that lists of the Abelian subgroups of A_4, T', S_4 and A_5 can be found in [121], [122], [125] and [144], respectively.

[42] It is worth noting that A_4 is not a subgroup of T'.

Table B.1. The 3-dimensional representation matrices $\rho_{\mathbf{3}}(g)$ for the generators $g = S$, T (and U) of A_4, T', (S_4) and A_5. We have defined $\omega = e^{2\pi i/3}$, $r = (1+\sqrt{5})/2$ and $\rho = e^{2\pi i/5}$.

Group	$\rho_{\mathbf{3}}(S)$	$\rho_{\mathbf{3}}(T)$	$\rho_{\mathbf{3}}(U)$
A_4	$\frac{1}{3}\begin{pmatrix} -1 & 2 & 2 \\ 2 & -1 & 2 \\ 2 & 2 & -1 \end{pmatrix}$	$\begin{pmatrix} 1 & 0 & 0 \\ 0 & \omega^2 & 0 \\ 0 & 0 & \omega \end{pmatrix}$	
T'	$\frac{1}{3}\begin{pmatrix} -1 & 2\omega & 2\omega^2 \\ 2\omega^2 & -1 & 2\omega \\ 2\omega & 2\omega^2 & -1 \end{pmatrix}$	$\begin{pmatrix} 1 & 0 & 0 \\ 0 & \omega & 0 \\ 0 & 0 & \omega^2 \end{pmatrix}$	
S_4	$\begin{pmatrix} -1 & 0 & 0 \\ 0 & 1 & 0 \\ 0 & 0 & -1 \end{pmatrix}$	$\frac{1}{2}\begin{pmatrix} i & -\sqrt{2}i & -i \\ \sqrt{2} & 0 & \sqrt{2} \\ i & \sqrt{2}i & -i \end{pmatrix}$	$\begin{pmatrix} 0 & 0 & i \\ 0 & -1 & 0 \\ -i & 0 & 0 \end{pmatrix}$
A_5	$\frac{1}{\sqrt{5}}\begin{pmatrix} 1 & -\sqrt{2} & -\sqrt{2} \\ -\sqrt{2} & -r & 1/r \\ -\sqrt{2} & 1/r & -r \end{pmatrix}$	$\begin{pmatrix} 1 & 0 & 0 \\ 0 & \rho & 0 \\ 0 & 0 & \rho^4 \end{pmatrix}$	

Appendix C

Parametrisations of a 3×3 unitary matrix

Parametrisations of a 3×3 unitary matrix W (see, e.g., [202–204]) can be obtained, e.g., from one of the six permutations of a product of three complex rotations and diagonal phase matrices, e.g., as follows:

$$W = \Psi_1 \, \Psi_2 \, \Psi_3 \, \overline{W} = \Psi_1 \, \Psi_2 \, \Psi_3 \, U_{ij} \, U_{kl} \, U_{rs} \, , \tag{C.1}$$

where we have assumed $ij \neq kl \neq rs$. It is worth noticing that sometimes it is convenient to use the parametrisations of $\overline{W}$ of the following form:

$$\overline{W} = U_{ij} \, U_{kl} \, \tilde{U}_{ij} \, . \tag{C.2}$$

As shown in [202], the number of distinctive parametrisations of a CKM-like matrix is nine. We have defined the phase matrices Ψ_i in eq. (2.2) and the complex rotation matrix in the i-j plane $U_{ij} \equiv U_{ij}(\theta_{ij}, \delta_{ij})$ in eq. (2.3). The latter can be always parametrised as a product of diagonal phase matrices and the rotation matrix $R_{ij} \equiv R_{ij}(\theta_{ij}) = U_{ij}(\theta_{ij}, 0)$, i.e.,

$$U_{ij} = P_i(\delta)^* \, R_{ij} \, P_i(\delta) = P_j(-\delta)^* \, R_{ij} \, P_j(-\delta) \, , \tag{C.3}$$

where $P_i(\delta)$ are diagonal matrices defined as follows:

$$P_1(\delta) = \mathrm{diag}(e^{i\delta}, 1, 1) \, , \quad P_2(\delta) = \mathrm{diag}(1, e^{i\delta}, 1) \, , \quad P_3(\delta) = \mathrm{diag}(1, 1, e^{i\delta}) \, . \tag{C.4}$$

Defining $P_{ij}(\alpha, \beta)$ as a product $P_{ij}(\alpha, \beta) \equiv P_i(\alpha) P_j(\beta)$, the following relation holds:

$$U_{ij}(\theta_{ij}, \delta_{ij}) \, P_{ij}(\alpha, \beta) = P_{ij}(\alpha, \beta) U_{ij}(\theta_{ij}, \delta'_{ij}) \, , \tag{C.5}$$

with $\delta'_{ij} = \delta_{ij} + \alpha - \beta$.

Starting from the general parametrisation of W in eq. (C.1) and the relation in eq. (C.5), we find convenient parametrisations for $\overline{W}$. They are summarised in Table C.1. The parametrisations of the matrix $U^\circ(\theta^\circ_{12}, \theta^\circ_{13}, \theta^\circ_{23}, \{\delta^\circ_{kl}\})$ defined in Section 2.1 have been obtained from Table C.1 after a redefinition of the phases $\{\delta^\circ_{kl}\}$. For example, in the first case when $U^\circ(\theta^\circ_{12}, \theta^\circ_{13}, \theta^\circ_{23}, \{\delta^\circ_{kl}\})$ is represented by the product

$$U_{12}(\theta^\circ_{12}, \delta^\circ_{12}) \, U_{23}(\theta^\circ_{23}, \delta^\circ_{23}) \, U_{13}(\theta^\circ_{13}, \delta^\circ_{13})$$

the following redefinition is used: $\delta^\circ_{12} - \delta^\circ_{13} + \delta^\circ_{23} \to \delta^\circ_{12}$.

The product of two complex rotations in the i-j plane can always be written as

$$U_{ij}(\theta^a_{ij}, \delta^a_{ij}) \, U_{ij}(\theta^b_{ij}, \delta^b_{ij}) = P_{ij}(\beta, -\alpha) \, R_{ij}(\hat{\theta}_{ij}) \, P_i(\alpha - \beta)$$

Table C.1. Equivalent parametrisations of $\overline{W}$ obtained using the result in eq. (C.5), which allows us to find the convenient form of the matrix $U^\circ(\theta^\circ_{12}, \theta^\circ_{13}, \theta^\circ_{23}, \{\delta^\circ_{kl}\})$ defined in Section 2.1.

Case	Initial form of $\overline{W}$	Final parametrisation of $\overline{W}$
A1	$U_{12}\,U_{23}\,U_{13}$	$P^*_{12}(\delta_{13},\delta_{23})\,U_{12}(\theta_{12},\delta_{12}-\delta_{13}+\delta_{23})\,R_{23}\,R_{13}\,P_{12}(\delta_{13},\delta_{23})$
A2	$U_{13}\,U_{23}\,U_{12}$	$P^*_{13}(\delta_{12},-\delta_{23})\,U_{13}(\theta_{13},\delta_{13}-\delta_{12}-\delta_{23})\,R_{23}\,R_{12}\,P_{13}(\delta_{12},-\delta_{23})$
A3	$U_{23}\,U_{13}\,U_{12}$	$P_{23}(\delta_{12},\delta_{13})\,U_{23}(\theta_{23},\delta_{23}+\delta_{12}-\delta_{13})\,R_{13}\,R_{12}\,P^*_{23}(\delta_{12},\delta_{13})$
B1	$U_{23}\,U_{12}\,U_{13}$	$P^*_{13}(\delta_{12},-\delta_{23})\,R_{23}\,R_{12}\,U_{13}(\theta_{13},\delta_{13}-\delta_{12}-\delta_{23})\,P_{13}(\delta_{12},-\delta_{23})$
B2	$U_{13}\,U_{12}\,U_{23}$	$P_{23}(\delta_{12},\delta_{13})\,R_{13}\,R_{12}\,U_{23}(\theta_{23},\delta_{23}+\delta_{12}-\delta_{13})\,P^*_{23}(\delta_{12},\delta_{13})$
B3	$U_{23}\,U_{13}\,U_{12}$	$P^*_{12}(\delta_{13},\delta_{23})\,R_{23}\,R_{13}\,U_{12}(\theta_{12},\delta_{12}-\delta_{13}+\delta_{23})\,P_{12}(\delta_{13},\delta_{23})$
C1	$U_{12}\,U_{23}\,U_{13}$	$P_3(\delta_{23})\,U_{12}(\theta_{12},\delta_{12})\,R_{23}\,U_{13}(\theta_{13},\delta_{13}-\delta_{23})\,P^*_3(\delta_{23})$
C2	$U_{13}\,U_{23}\,U_{12}$	$P_3(\delta_{23})\,U_{13}(\theta_{13},\delta_{13}-\delta_{23})\,R_{23}\,U_{12}(\theta_{12},\delta_{12})\,P^*_3(\delta_{23})$
C3	$U_{12}\,U_{13}\,U_{23}$	$P_3(\delta_{13})\,U_{12}(\theta_{12},\delta_{12})\,R_{13}\,U_{23}(\theta_{23},\delta_{23}-\delta_{13})\,P^*_3(\delta_{13})$
C4	$U_{13}\,U_{12}\,U_{23}$	$P_2(\delta_{12})\,U_{13}(\theta_{13},\delta_{13})\,R_{12}\,U_{23}(\theta_{23},\delta_{23}+\delta_{12})\,P^*_2(\delta_{12})$
C5	$U_{23}\,U_{12}\,U_{13}$	$P_2(\delta_{12})\,U_{23}(\theta_{23},\delta_{23}+\delta_{12})\,R_{12}\,U_{13}(\theta_{13},\delta_{13})\,P^*_2(\delta_{12})$
C6	$U_{23}\,U_{13}\,U_{12}$	$P_3(\delta_{13})\,U_{23}(\theta_{23},\delta_{23}-\delta_{13})\,R_{13}\,U_{12}(\theta_{12},\delta_{12})\,P^*_3(\delta_{13})$
C7	$U_{12}\,U_{23}\,\tilde{U}_{12}$	$P_3(\delta_{23})\,U_{12}(\theta_{12},\delta_{12})\,R_{23}\,U_{12}(\tilde{\theta}_{12},\tilde{\delta}_{12})\,P^*_3(\delta_{23})$
C8	$U_{13}\,U_{23}\,\tilde{U}_{13}$	$P^*_2(\delta_{23})\,U_{13}(\theta_{13},\delta_{13})\,R_{23}\,U_{13}(\tilde{\theta}_{13},\tilde{\delta}_{13})\,P_2(\delta_{23})$
C9	$U_{23}\,U_{12}\,\tilde{U}_{23}$	$P^*_1(\delta_{12})\,U_{23}(\theta_{23},\delta_{23})\,R_{12}\,U_{23}(\tilde{\theta}_{23},\tilde{\delta}_{23})\,P_1(\delta_{12})$

$$
\begin{aligned}
&= P_j(-\alpha-\beta)\,R_{ij}(\hat{\theta}_{ij})\,P_{ij}(\alpha,\beta)\\
&= P_{ij}(\alpha,-\beta)\,R_{ij}(\hat{\theta}_{ij})\,P_j(\beta-\alpha)\\
&= P_i(\alpha+\beta)\,R_{ij}(\hat{\theta}_{ij})\,P_{ij}(-\beta,-\alpha)\,,
\end{aligned}
\tag{C.6}
$$

where we have defined the angle $\hat{\theta}_{ij}$ as

$$
\sin\hat{\theta}_{ij} = \left| s^a_{ij}\,c^b_{ij}\,e^{-i\delta^a_{ij}} + c^a_{ij}\,s^b_{ij}\,e^{-i\delta^b_{ij}} \right| , \tag{C.7}
$$

and the phases α, β as

$$
\alpha = \arg\left[c^a_{ij}\,c^b_{ij} - s^a_{ij}\,s^b_{ij}\,e^{i(\delta^b_{ij}-\delta^a_{ij})} \right] , \quad \beta = \arg\left[s^a_{ij}\,c^b_{ij}\,e^{-i\delta^a_{ij}} + c^a_{ij}\,s^b_{ij}\,e^{-i\delta^b_{ij}} \right] , \tag{C.8}
$$

with $s^{a(b)}_{ij} \equiv \sin\theta^{a(b)}_{ij}$ and $c^{a(b)}_{ij} \equiv \cos\theta^{a(b)}_{ij}$.

Appendix D

Parametrisations of the PMNS matrix for fully broken G_e or G_ν

In the case when the group G_e is fully broken and $G_\nu = Z_n$, $n > 2$ or $Z_n \times Z_m$, $n, m \geq 2$, there are cases in which one can express $\cos\delta$ as a function of θ_{12}, θ_{13}, θ_{23} and θ°_{12}, θ°_{13}, θ°_{23}. In the cases

(i) $U_e^\dagger = U_{23(13)}(\theta^e_{23(13)}, \delta^e_{23(13)})\, U_{12}(\theta^e_{12}, \delta^e_{12})\,,$

(ii) $U_e^\dagger = U_{12(13)}(\theta^e_{12(13)}, \delta^e_{12(13)})\, U_{23}(\theta^e_{23}, \delta^e_{23})\,,$

(iii) $U_e^\dagger = U_{23(12)}(\theta^e_{23(12)}, \delta^e_{23(12)})\, U_{13}(\theta^e_{13}, \delta^e_{13})\,,$

which correspond, respectively, to cases D1 (D2), D3 (D4) and D5 (D6) of Section 2.6, we choose for convenience:

(i) $U^\circ(\theta^\circ_{12}, \theta^\circ_{13}, \theta^\circ_{23}, \delta^\circ_{12}) = U_{12}(\theta^\circ_{12}, \delta^\circ_{12})\, R_{23}(\theta^\circ_{23})\, R_{13}(\theta^\circ_{13})\,,$

(ii) $U^\circ(\theta^\circ_{12}, \theta^\circ_{13}, \theta^\circ_{23}, \delta^\circ_{23}) = U_{23}(\theta^\circ_{23}, \delta^\circ_{23})\, R_{13}(\theta^\circ_{13})\, R_{12}(\theta^\circ_{12})\,,$

(iii) $U^\circ(\theta^\circ_{12}, \theta^\circ_{13}, \theta^\circ_{23}, \delta^\circ_{13}) = U_{13}(\theta^\circ_{13}, \delta^\circ_{13})\, R_{23}(\theta^\circ_{23})\, R_{12}(\theta^\circ_{12})\,.$

The possible parametrisations of U presented in Table D.1 can be obtained from (i), (ii) and (iii) using eqs. (C.6)–(C.8). The angles θ^e_{ij}, $\hat{\theta}_{ij}$ and the phases δ^e_{ij}, $\hat{\delta}$ are free parameters. It can be seen from Table D.1 that if one of the fixed angles turns out to be zero, the number of free parameters reduces from four to three. The same situation happens if one of the two free phases is fixed. Thus, in some of these cases a sum rule for $\cos\delta$ can be derived.

In the case when the group $G_e = Z_n$, $n > 2$ or $Z_n \times Z_m$, $n, m \geq 2$ and G_ν is fully broken, we consider the following forms of the matrix U_ν,

(iv) $U_\nu = U_{12}(\theta^\nu_{12}, \delta^\nu_{12})\, U_{13(23)}(\theta^\nu_{13(23)}, \delta^\nu_{13(23)})\, Q_0\,,$

(v) $U_\nu = U_{23}(\theta^\nu_{23}, \delta^\nu_{23})\, U_{12(13)}(\theta^\nu_{12(13)}, \delta^\nu_{12(13)})\, Q_0\,,$

(vi) $U_\nu = U_{13}(\theta^\nu_{13}, \delta^\nu_{13})\, U_{12(23)}(\theta^\nu_{12(23)}, \delta^\nu_{12(23)})\, Q_0\,,$

which correspond, respectively, to cases E1 (E2), E3 (E4) and E5 (E6) of Section 2.7. For these forms, we choose for convenience:

(iv) $U^\circ(\theta^\circ_{12}, \theta^\circ_{13}, \theta^\circ_{23}, \delta^\circ_{12}) = R_{23}(\theta^\circ_{23})\, R_{13}(\theta^\circ_{13})\, U_{12}(\theta^\circ_{12}, \delta^\circ_{12})\,,$

(v) $U^\circ(\theta^\circ_{12}, \theta^\circ_{13}, \theta^\circ_{23}, \delta^\circ_{23}) = R_{13}(\theta^\circ_{13})\, R_{12}(\theta^\circ_{12})\, U_{23}(\theta^\circ_{23}, \delta^\circ_{23})\,,$

Table D.1. Parametrisations of the PMNS matrix U in the case of fully broken G_e (G_ν) and $G_\nu = Z_n$, $n > 2$ or $Z_n \times Z_m$, $n, m \geq 2$ ($G_e = Z_n$, $n > 2$ or $Z_n \times Z_m$, $n, m \geq 2$), when the matrix U_e (U_ν) has particular forms.

Case	Parametrisation of the PMNS matrix U
D1 (D2)	$U_{23(13)}(\theta^e_{23(13)}, \delta^e_{23(13)})\, R_{12}(\hat{\theta}_{12})\, P_1(\hat{\delta})\, R_{23}(\theta^\circ_{23})\, R_{13}(\theta^\circ_{13})\, Q_0$
D3 (D4)	$U_{12(13)}(\theta^e_{12(13)}, \delta^e_{12(13)})\, R_{23}(\hat{\theta}_{23})\, P_2(\hat{\delta})\, R_{13}(\theta^\circ_{13})\, R_{12}(\theta^\circ_{12})\, Q_0$
D5 (D6)	$U_{23(12)}(\theta^e_{23(12)}, \delta^e_{23(12)})\, R_{13}(\hat{\theta}_{13})\, P_1(\hat{\delta})\, R_{23}(\theta^\circ_{23})\, R_{12}(\theta^\circ_{12})\, Q_0$
E1 (E2)	$R_{23}(\theta^\circ_{23})\, R_{13}(\theta^\circ_{13})\, P_1(\hat{\delta})\, R_{12}(\hat{\theta}_{12})\, U_{13(23)}(\theta^\nu_{13(23)}, \delta^\nu_{13(23)})\, Q_0$
E3 (E4)	$R_{13}(\theta^\circ_{13})\, R_{12}(\theta^\circ_{12})\, P_2(\hat{\delta})\, R_{23}(\hat{\theta}_{23})\, U_{12(13)}(\theta^\nu_{12(13)}, \delta^\nu_{12(13)})\, Q_0$
E5 (E6)	$R_{23}(\theta^\circ_{23})\, R_{12}(\theta^\circ_{12})\, P_1(\hat{\delta})\, R_{13}(\hat{\theta}_{13})\, U_{12(23)}(\theta^\nu_{12(23)}, \delta^\nu_{12(23)})\, Q_0$

(vi) $U^\circ(\theta^\circ_{12}, \theta^\circ_{13}, \theta^\circ_{23}, \delta^\circ_{13}) = R_{23}(\theta^\circ_{23})\, R_{12}(\theta^\circ_{12})\, U_{13}(\theta^\circ_{13}, \delta^\circ_{13})\,.$

The parametrisations of U in (iv), (v) and (vi) presented in Table D.1 have been obtained making use of eqs. (C.6)–(C.8). The angles θ^ν_{ij}, $\hat{\theta}_{ij}$ and the phases δ^ν_{ij}, $\hat{\delta}$ are free parameters. It can be seen from Table D.1 that if one of the fixed angles turns out to be zero, the number of free parameters reduces from four to three. The same situation happens if one of the two free phases is fixed. Thus, in some of these cases a sum rule for $\cos\delta$ can be derived.

Appendix E

Results for $G_f = A_5$ and generalised CP symmetry

Models with A_5 and generalised CP symmetry have been recently developed by several authors [128–130]. We show that our results for the symmetry group A_5 under the same assumptions of [130] and the same breaking patterns reduce to the one derived in [130]. The results in eqs. (10), (11), (12) and (14) in [130] lead to the following phenomenologically viable cases:

(I) $U = \mathrm{diag}(1, i, -i)\, R_{23}(\theta^\circ_{23})\, R_{12}(\theta^\circ_{12})\ \mathrm{diag}(1, -i, i)\, R_{13}(\theta^\nu_{13})$ for $(G_e, G_\nu) = (Z_3, Z_2)$,

(II) $U = \mathrm{diag}(1, i, -i)\, R_{23}(\theta^\circ_{23})\, R_{12}(\theta^\circ_{12})\ \mathrm{diag}(1, -i, i)\, R_{13}(\theta^\nu_{13})$ for $(G_e, G_\nu) = (Z_5, Z_2)$,

(III) $U = \mathrm{diag}(1, 1, -1)\, R_{23}(\theta^\circ_{23})\, R_{12}(\theta^\circ_{12})\ \mathrm{diag}(1, 1, -1)\, R_{13}(\theta^\nu_{13})$ for $(G_e, G_\nu) = (Z_5, Z_2)$,

(IV) $U = R_{13}(\theta^\circ_{13})\, R_{12}(\theta^\circ_{12})\, R_{23}(\theta^\circ_{23})\ \mathrm{diag}(1, 1, -1)\, R_{23}(\theta^\nu_{23})$ for $(G_e, G_\nu) = (Z_2 \times Z_2, Z_2)$,

where we have in

(I) $\theta^\circ_{12} = \sin^{-1}(1/\sqrt{3})$ and $\theta^\circ_{23} = -\pi/4$,

(II) $\theta^\circ_{12} = \sin^{-1}(1/\sqrt{2+r})$ and $\theta^\circ_{23} = -\pi/4$,

(III) $\theta^\circ_{12} = \sin^{-1}(1/\sqrt{2+r})$ and $\theta^\circ_{23} = -\pi/4$,

(IV) $\theta^\circ_{12} = \sin^{-1}(1/(2r))$, $\theta^\circ_{13} = \sin^{-1}(1/\sqrt{2+r})$ and $\theta^\circ_{23} = \sin^{-1}(r/\sqrt{2+r})$.

Using $(\sin^2\theta^\circ_{12}, \sin^2\theta^\circ_{13}, \sin^2\theta^\circ_{23}) = (1/3, 0, 1/2)$ in case I, the results in eqs. (2.41)–(2.43), after defining $\hat{\theta}_{13} = \theta^\nu_{13} = \theta$ and setting $\hat{\delta}_{13} = \delta^\nu_{13} = \pi/2$, reduce to

$$\sin^2\theta_{13} = \frac{2}{3}\sin^2\theta\,, \quad \sin^2\theta_{12} = \frac{1}{3 - 2\sin^2\theta}\,, \quad \sin^2\theta_{23} = \frac{1}{2} \quad \text{and} \quad \cos\delta = 0\,.$$

Denoting $\hat{\theta}_{13} = \theta^\nu_{13} = \theta$ and setting $\hat{\delta}_{13} = \delta^\nu_{13} = \pi/2$ in case II, the results in eqs. (2.41)–(2.43) reduce to

$$\sin^2\theta_{13} = \frac{\sin^2\theta}{1 + (1-r)^2}\,, \quad \sin^2\theta_{12} = \frac{1}{1 + r^2\cos^2\theta}\,, \quad \sin^2\theta_{23} = \frac{1}{2} \quad \text{and} \quad \cos\delta = 0\,.$$

The difference between case III and case II consists only in the phase $\hat{\delta}_{13}$ which now is equal to π, $\hat{\delta}_{13} = \delta^\nu_{13} = \pi$. Therefore, while $\sin^2\theta_{13}$ and $\sin^2\theta_{12}$ remain unchanged, we find

$$\sin^2\theta_{23} = \frac{1}{2}\frac{(\sin\theta - \sqrt{1+r^2}\cos\theta)^2}{1 + r^2\cos^2\theta} \quad \text{and} \quad |\cos\delta| = 1\,.$$

Finally, in case IV, from eqs. (2.49)–(2.51), defining $\hat{\theta}_{23} = \theta^{\circ}_{23} - \theta^{\nu}_{23} = \theta^{\circ}_{23} - \theta$ and $\hat{\delta}_{23} = 0$, we get:

$$\sin^2\theta_{13} = \frac{1+(1-r)f(\theta)}{4}\,, \quad \sin^2\theta_{23} = \frac{1+r(\cos^2\theta - \sin 2\theta)}{3-(1-r)f(\theta)}\,,$$
$$\sin^2\theta_{12} = \frac{1+(1-r)(\cos^2\theta + \sin 2\theta)}{3-(1-r)f(\theta)} \quad \text{and} \quad |\cos\delta| = 1\,,$$

where $f(\theta) = (\sin^2\theta - \sin 2\theta)$. Therefore, the general results derived in subsections 2.3.1 and 2.3.2 with the choices as in (I), (II), (III) and (IV) and the additional restriction of the parameters due to the presence of a generalised CP symmetry allow one to find the formulae derived in [130].

Appendix F

Statistical details

In order to perform a statistical analysis of the considered cases, we construct the χ^2 function in the following way:

$$\chi^2(\sin^2\theta_{12}, \sin^2\theta_{13}, \sin^2\theta_{23}, \delta) = \chi^2_1(\sin^2\theta_{12}) + \chi^2_2(\sin^2\theta_{13}) + \chi^2_3(\sin^2\theta_{23}) + \chi^2_4(\delta)\,, \quad \text{(F.1)}$$

in which we have neglected the correlations among the oscillation parameters, since the functions χ^2_i are the one-dimensional projections taken from [18]. In order to quantify the accuracy of our approximation, we show in Fig. F.1 the confidence regions at 1σ, 2σ and 3σ for one degree of freedom in the planes $(\sin^2\theta_{23}, \delta)$, $(\sin^2\theta_{13}, \delta)$ and $(\sin^2\theta_{23}, \sin^2\theta_{13})$ in blue (dashed lines), purple (solid lines) and light-purple (dash-dotted lines) for the NO (IO) neutrino mass spectrum, respectively, obtained using eq. (F.1). The parameters not shown in the plot have been marginalised. It should be noted that what is also used in the literature is the Gaussian approximation, in which χ^2 can be simplified using the best fit values and the 1σ uncertainties as follows:

$$\chi^2_{\rm G} = \sum_{i=1}^{4} \frac{(x_i - \overline{x}_i)^2}{\sigma^2_{x_i}}\,. \quad \text{(F.2)}$$

Here $\vec{x} = (\sin^2\theta_{12}, \sin^2\theta_{13}, \sin^2\theta_{23}, \delta)$, $\overline{x}_i$ and σ_{x_i} being the best fit values and the 1σ uncertainties[43] taken from [18]. We present in Fig. F.2 the results of a similar two-dimensional analysis for the C.L. regions in the planes shown in Fig. F.1, but using the approximation for χ^2 given in eq. (F.2). It follows from these figures that the Gaussian approximation does not allow to reproduce the confidence regions given in ref. [18] with sufficiently good accuracy. For this reason in our analysis we use the more accurate procedure defined through eq. (F.1). In both figures the best fit points are indicated with a cross and an asterisk for the NO and IO spectra, respectively.

Each symmetry form considered in our analysis, which we label with an index m, depends on a set of parameters y^m_j, which are related to the standard oscillation parameters through expressions of the form $x_i = x^m_i(y^m_j)$. In order to produce the one-dimensional figures we minimise

$$\chi^2\left(\{x^m_i(y^m_j)\}\right) = \sum_{i=1}^{4} \chi^2_i\left(x^m_i(y^m_j)\right) \quad \text{(F.3)}$$

for a fixed value of the corresponding observable α, i.e.,

$$\chi^2(\alpha) = \min\left[\chi^2\left(\{x^m_i(y^m_j)\}\right)\big|_{\alpha=\text{const}}\right]\,, \quad \text{(F.4)}$$

with $\alpha = \{\delta, J_{\rm CP}, \sin^2\theta_{23}\}$.

[43] In the case of asymmetric errors we take the mean value of the two errors.

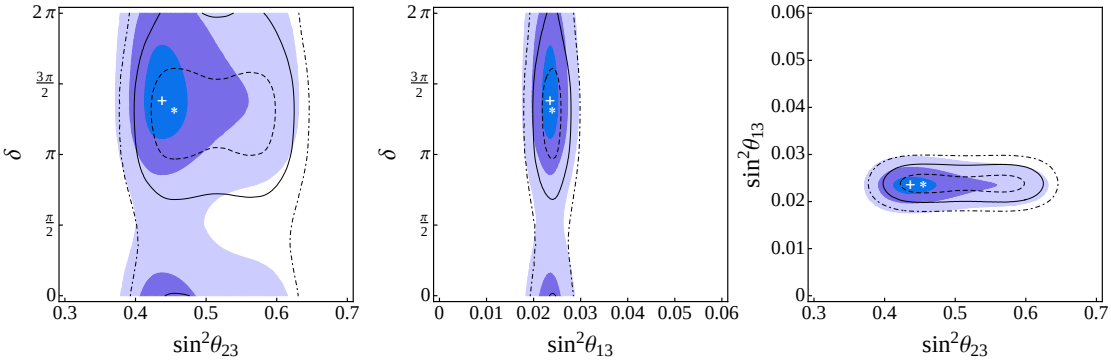

Figure F.1. Confidence regions at 1σ, 2σ and 3σ for one degree of freedom in the planes $(\sin^2\theta_{23}, \delta)$, $(\sin^2\theta_{13}, \delta)$ and $(\sin^2\theta_{23}, \sin^2\theta_{13})$ in blue (dashed lines), purple (solid lines) and light-purple (dash-dotted lines) for the NO (IO) neutrino mass spectrum, respectively, obtained using eq. (F.1). The best fit points are indicated with a cross and an asterisk for the NO and IO spectra, respectively.

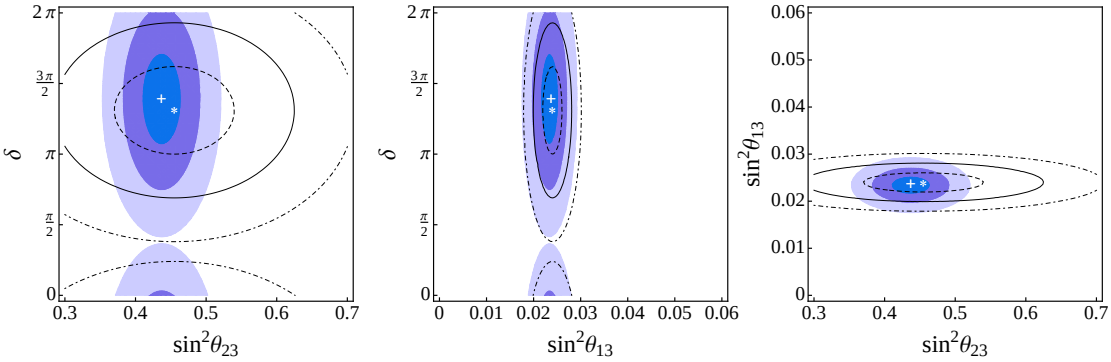

Figure F.2. The same as in Fig. F.1, but using the Gaussian approximation given in eq. (F.2).

The likelihood function for $\cos\delta$ is computed as follows:

$$L(\cos\delta) = \exp\left(-\frac{\chi^2(\cos\delta)}{2}\right) . \tag{F.5}$$

We use this procedure to produce the likelihood functions for the different symmetry forms in the case of the analysis based on the current knowledge of the neutrino mixing parameters.

In the case of the analysis with the prospective uncertainties in the determination of the neutrino mixing angles, we make use of the Gaussian approximation. Namely, in this case, we construct the χ^2 function as

$$\chi^2_{\rm G,future} = \sum_{i=1}^{3} \frac{(z_i - \overline{z}_i)^2}{\sigma^2_{z_i}} , \tag{F.6}$$

where $\vec{z} = (\sin^2\theta_{12}, \sin^2\theta_{13}, \sin^2\theta_{23})$, $\overline{z}_i$ are the potential best fit values of the indicated mixing parameters and σ_{z_i} are the prospective 1σ uncertainties in the determination of these mixing parameters. We use the following prospective relative 1σ uncertainties: (i) 0.7% on $\sin^2\theta_{12}$ from the JUNO experiment [156, 157]), (ii) 3% on $\sin^2\theta_{13}$ derived

from an expected error on $\sin^2 2\theta_{13}$ of 3% from the Daya Bay experiment [158–160]) and (iii) 5% on $\sin^2 \theta_{23}$ expected to be reached in the NOνA and T2K experiments [158]. The corresponding likelihood function is constructed as in eq. (F.5), where instead of $\chi^2(\cos\delta)$ the $\chi^2_{\mathrm{G,future}}$ function minimised for a given value of $\cos\delta$ is used.

Appendix G

Results for the atmospheric angle

For completeness, in Figs. G.1 and G.2 we give $N_\sigma \equiv \sqrt{\chi^2}$ as a function of $\sin^2\theta_{23}$ in cases B1 and B2 of Chapter 3. We recall that these cases are characterised by the following parametrisations of the PMNS natrix U:

(B1) $U = R_{12}(\theta^e_{12})\, R_{23}(\theta^e_{23})\, \Psi\, R_{23}(\theta^\nu_{23})\, R_{12}(\theta^\nu_{12})\, Q_0\,,$

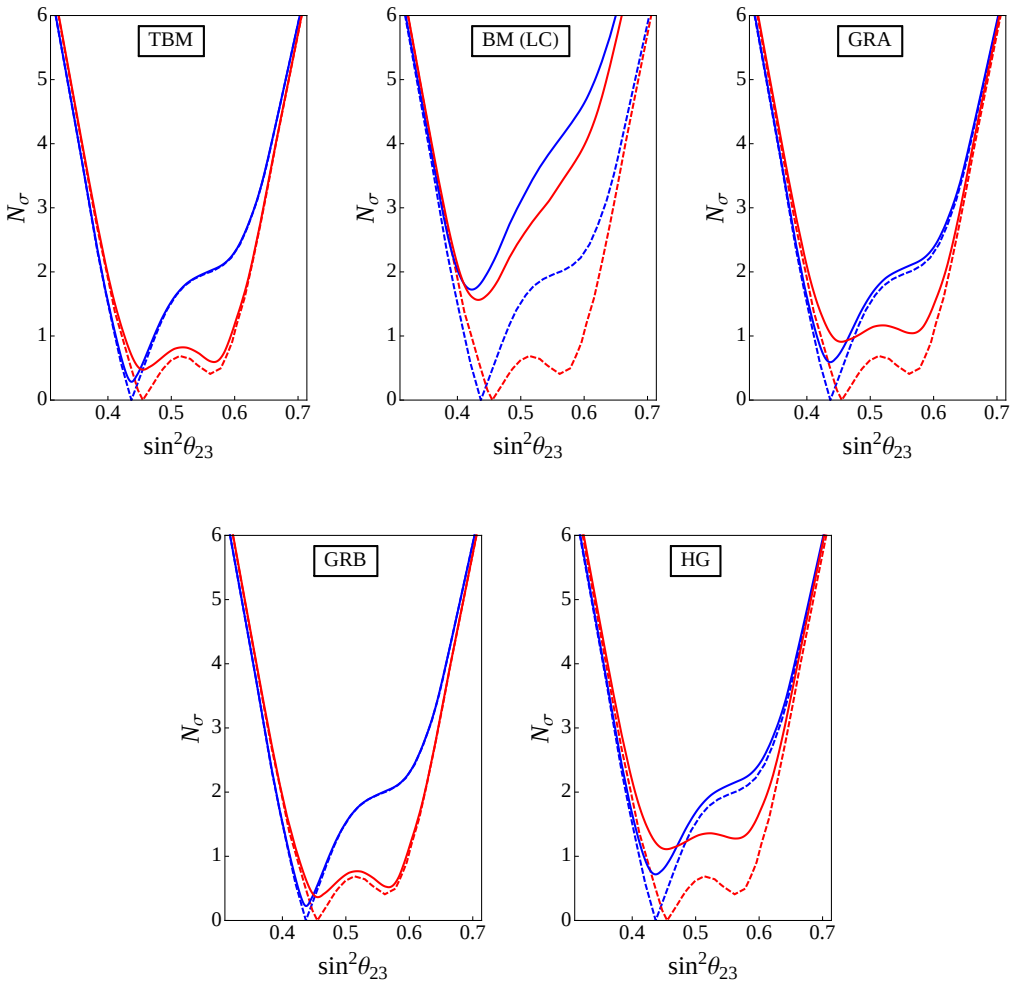

Figure G.1. $N_\sigma \equiv \sqrt{\chi^2}$ as a function of $\sin^2\theta_{23}$. The dashed lines represent the results of the global fit [18], while the solid lines represent the results we obtain for the TBM, BM (LC), GRA, GRB and HG symmetry forms of the matrix $\tilde{U}_\nu$ in case B1. The blue (red) lines are for the NO (IO) neutrino mass spectrum.

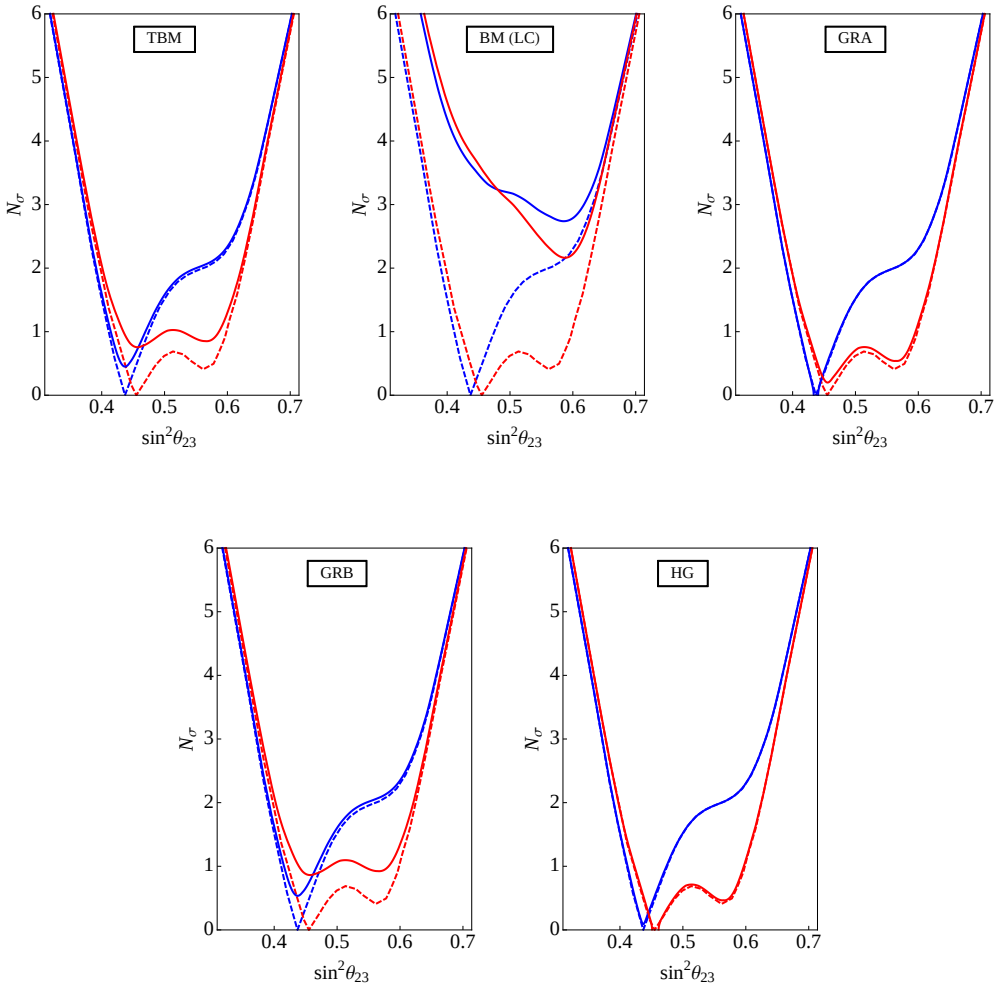

Figure G.2. The same as in Fig. G.1, but for case B2.

(B2) $U = R_{13}(\theta^e_{13})\, R_{23}(\theta^e_{23})\, \Psi\, R_{23}(\theta^\nu_{23})\, R_{12}(\theta^\nu_{12})\, Q_0\,.$

For a given symmetry form of the matrix $\tilde{U}_\nu = R_{23}(\theta^\nu_{23})\, R_{12}(\theta^\nu_{12})$, i.e., the TBM, BM (LC), GRA, GRB or HG form, we minimise the χ^2 function for a fixed value of $\sin^2\theta_{23}$ as explained in Appendix F.

Appendix H

Likelihood functions for $\cos\delta$

In subsection 3.7.1, results for the TBM, GRA, GRB, HG and BM mixing schemes were presented without taking the RG corrections into account. However, therein the likelihood functions for $\cos\delta$ and not for δ have been presented (see Fig. 3.1). For better comparison with these results we include in the present appendix Figs. H.1–H.5 (Figs. H.6–H.9) with the likelihood functions for $\cos\delta$ in the case of non-zero (zero) θ^e_{23}.

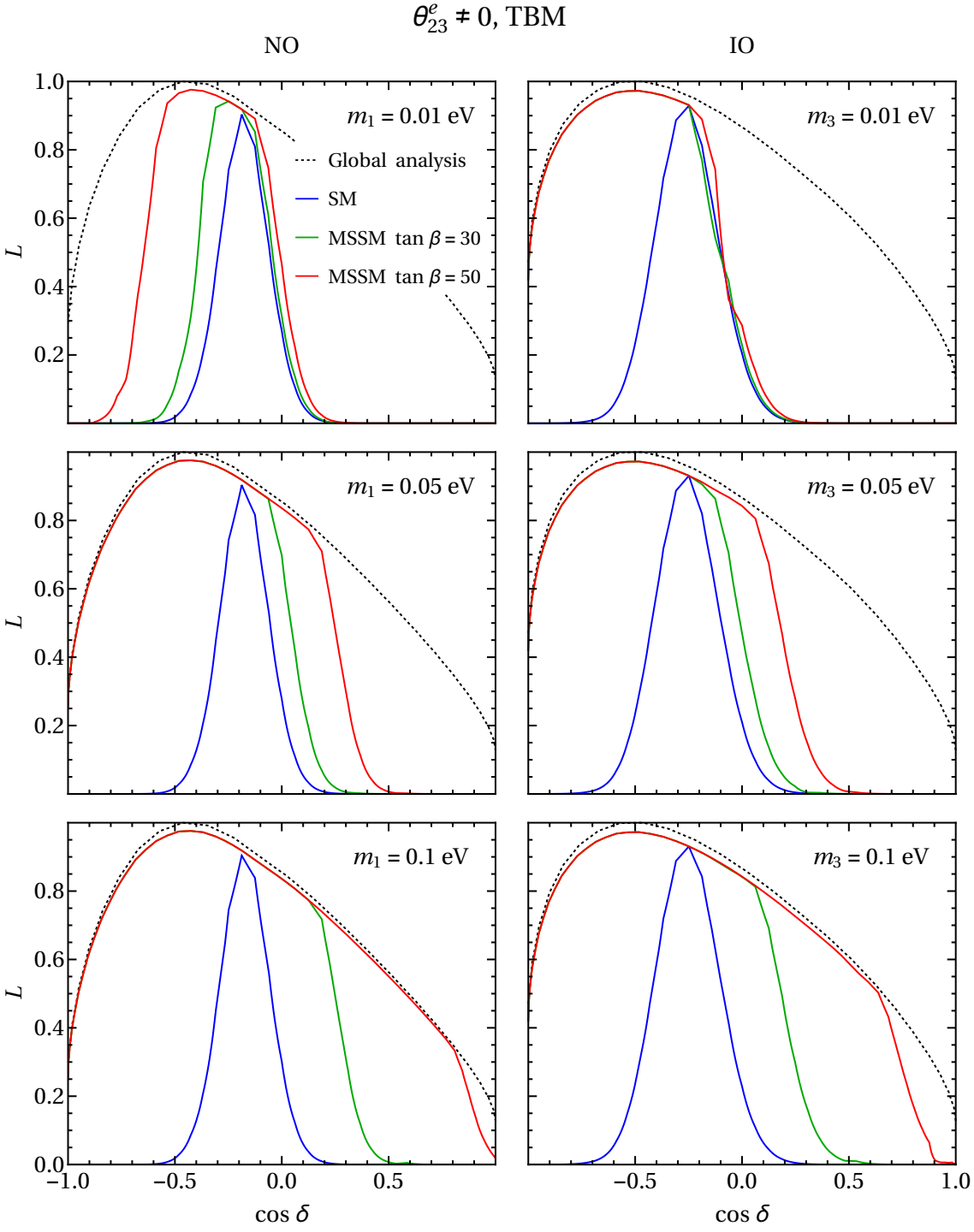

Figure H.1. Likelihood function vs. $\cos\delta$ in the case of non-zero θ_{23}^e for the TBM symmetry form of the matrix $\tilde{U}_\nu$ in all the set-ups considered. The dotted line stands for likelihood extracted from the global analysis in [162]. The blue line is for the SM running, while the green and red lines are for the running within MSSM with $\tan\beta = 30$ and $\tan\beta = 50$, respectively.

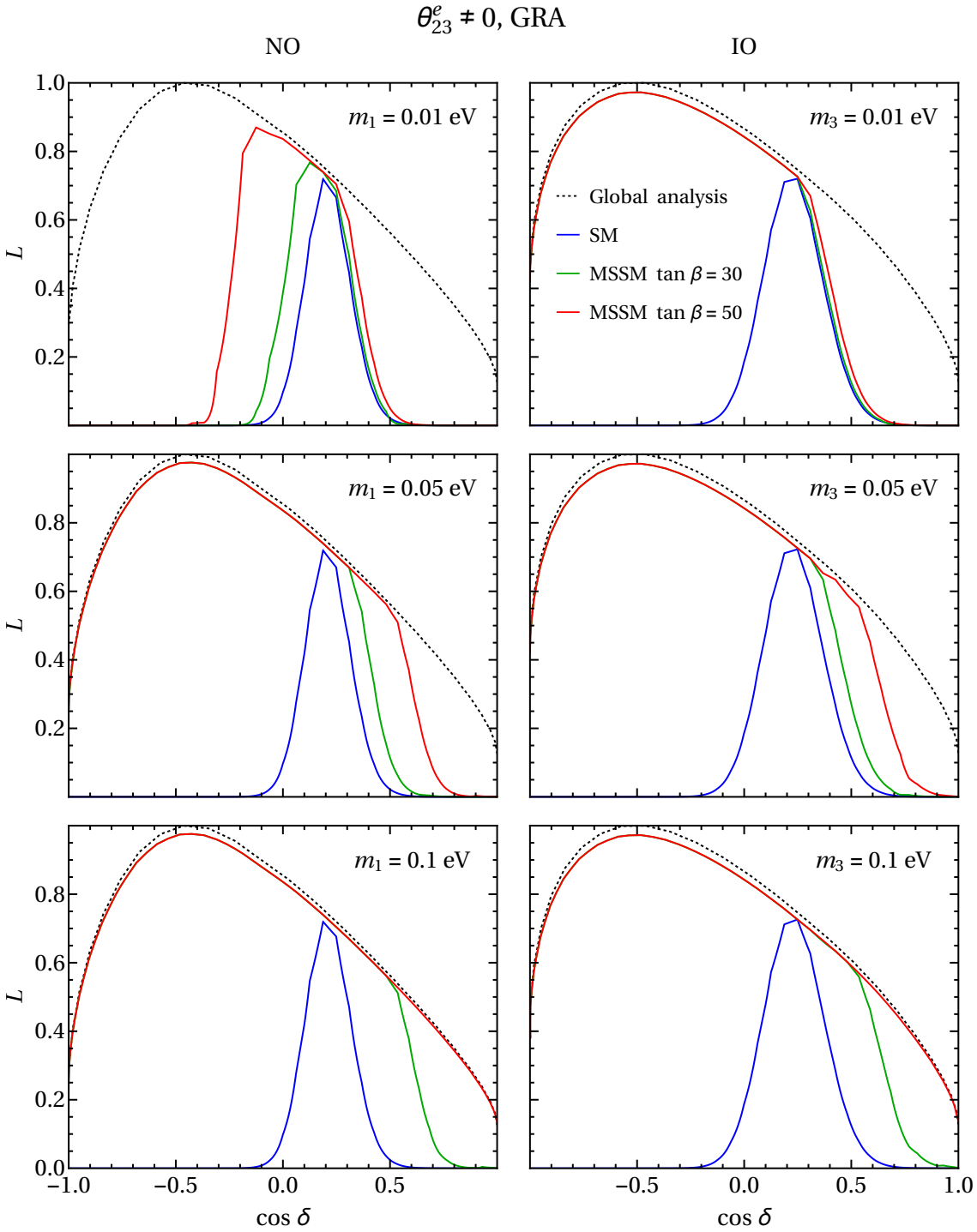

Figure H.2. The same as in Fig. H.1, but for the GRA symmetry form of the matrix $\tilde{U}_\nu$.

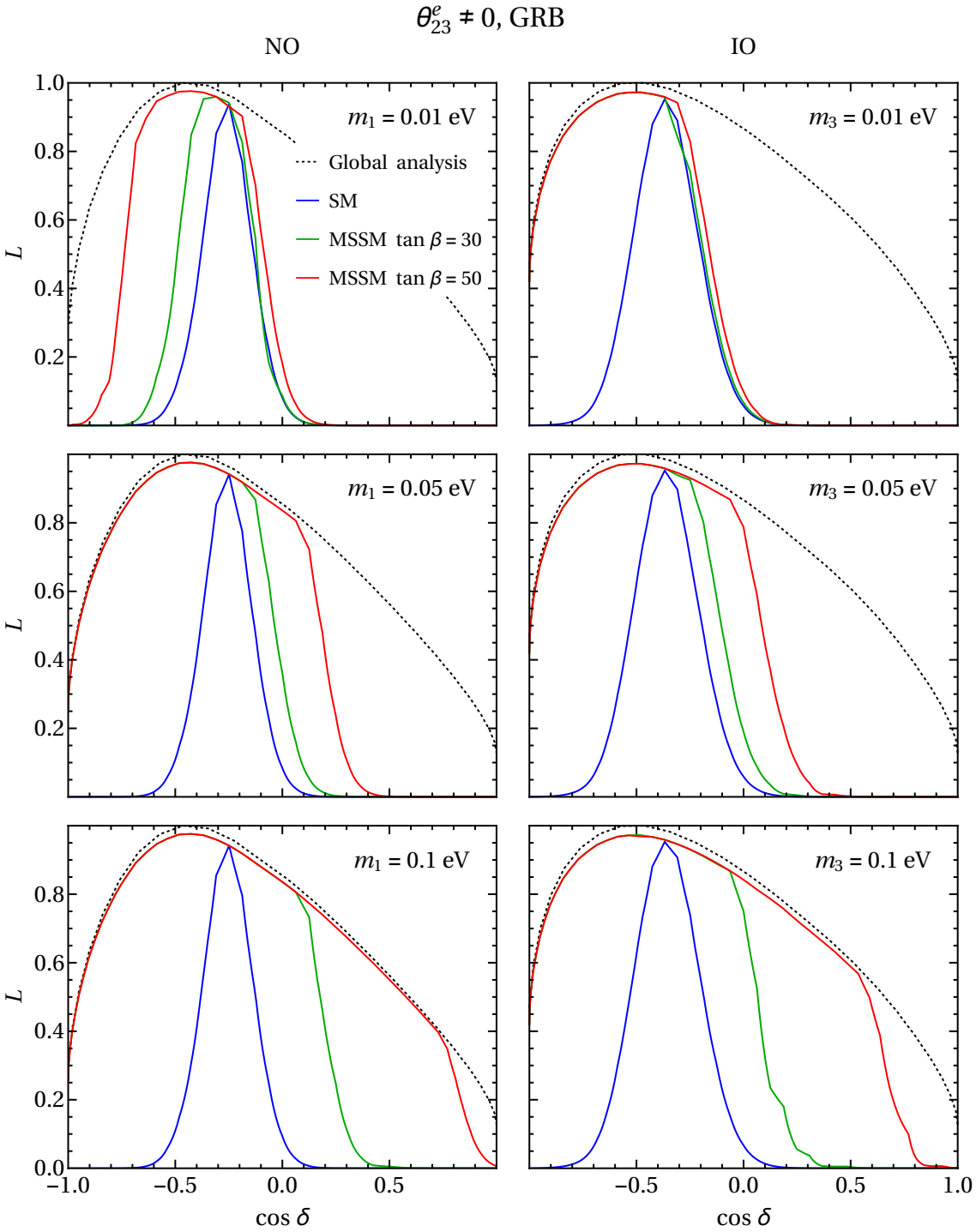

Figure H.3. The same as in Fig. H.1, but for the GRB symmetry form of the matrix $\tilde{U}_\nu$.

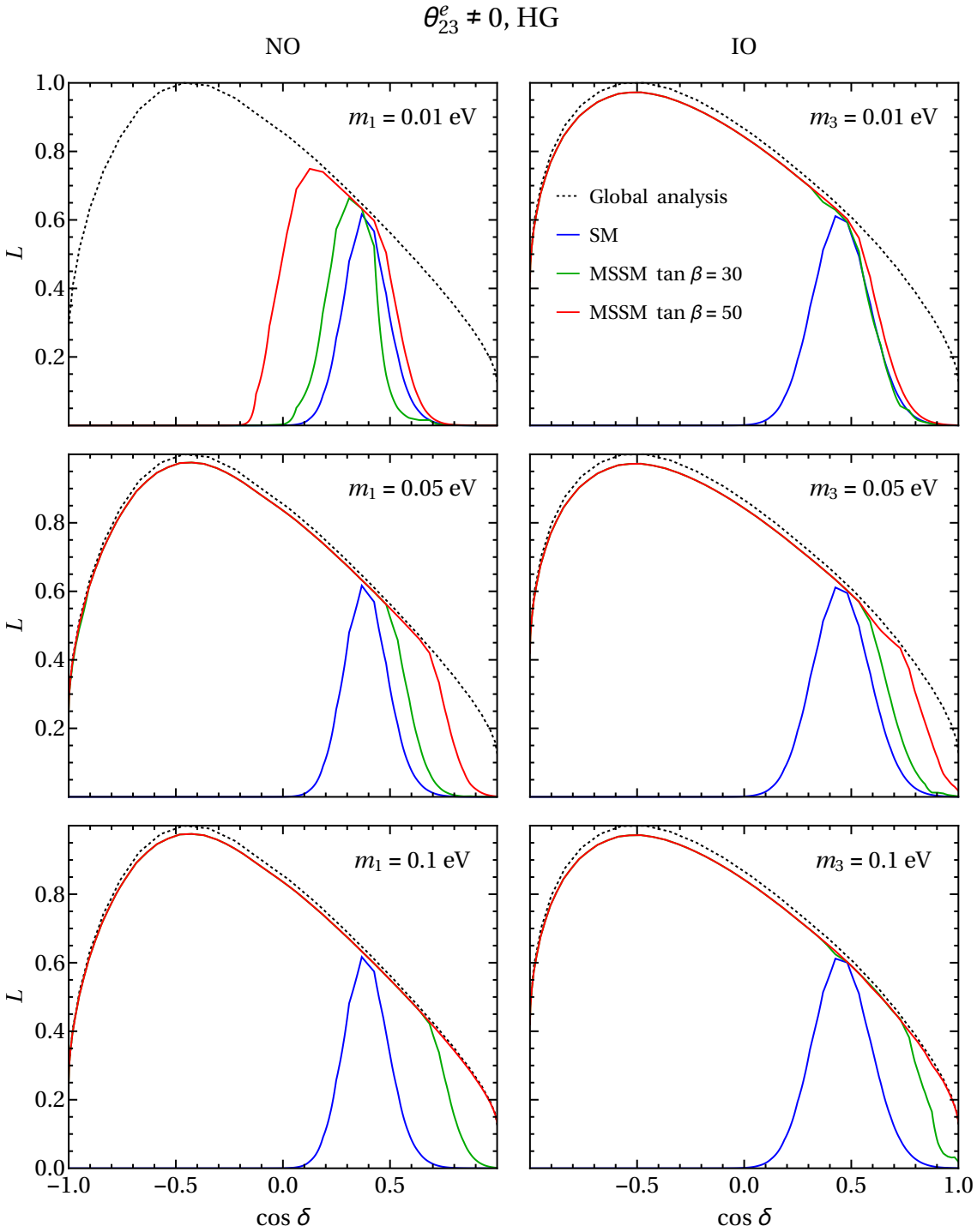

Figure H.4. The same as in Fig. H.1, but for the HG symmetry form of the matrix $\tilde{U}_\nu$.

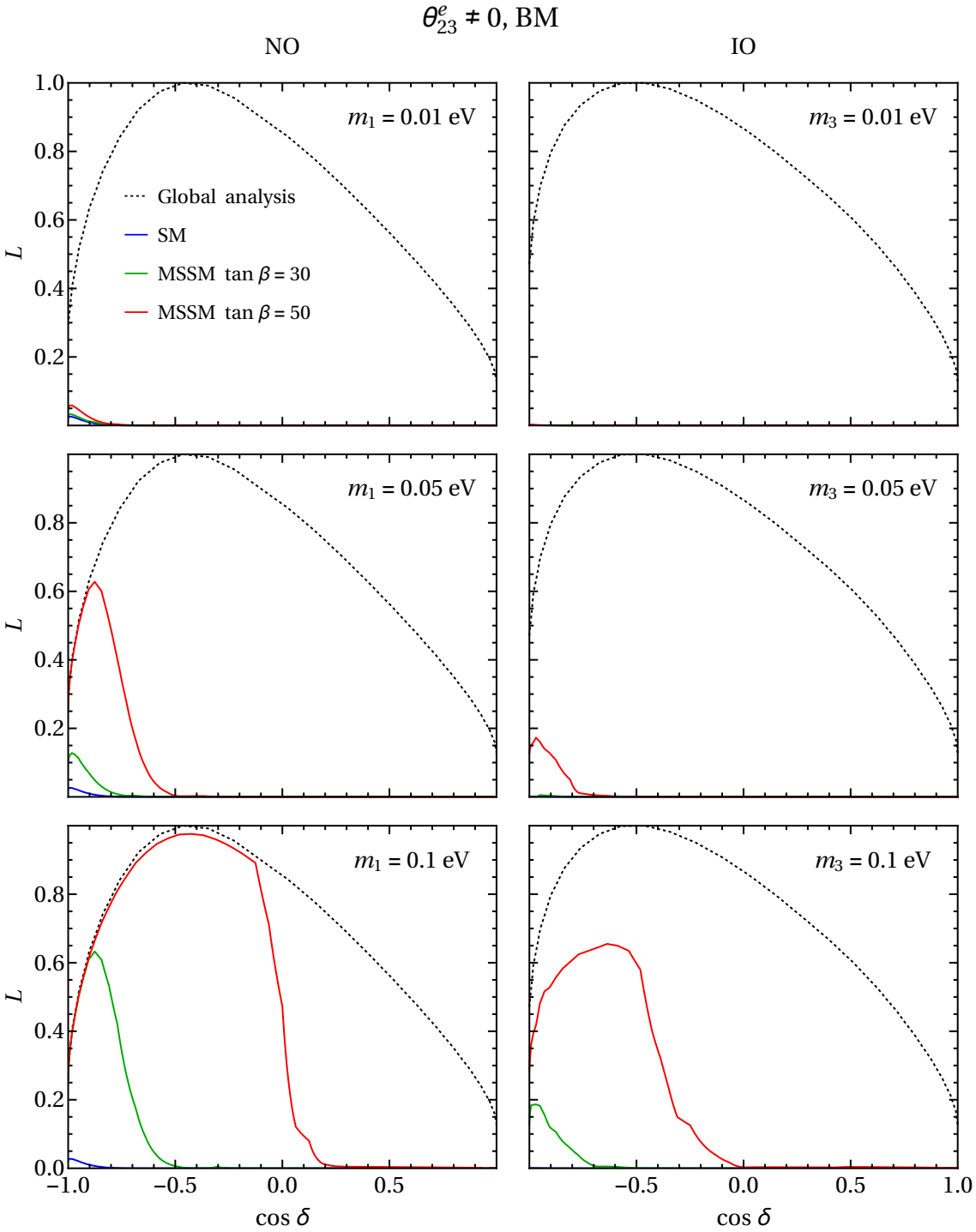

Figure H.5. The same as in Fig. H.1, but for the BM symmetry form of the matrix $\tilde{U}_\nu$.

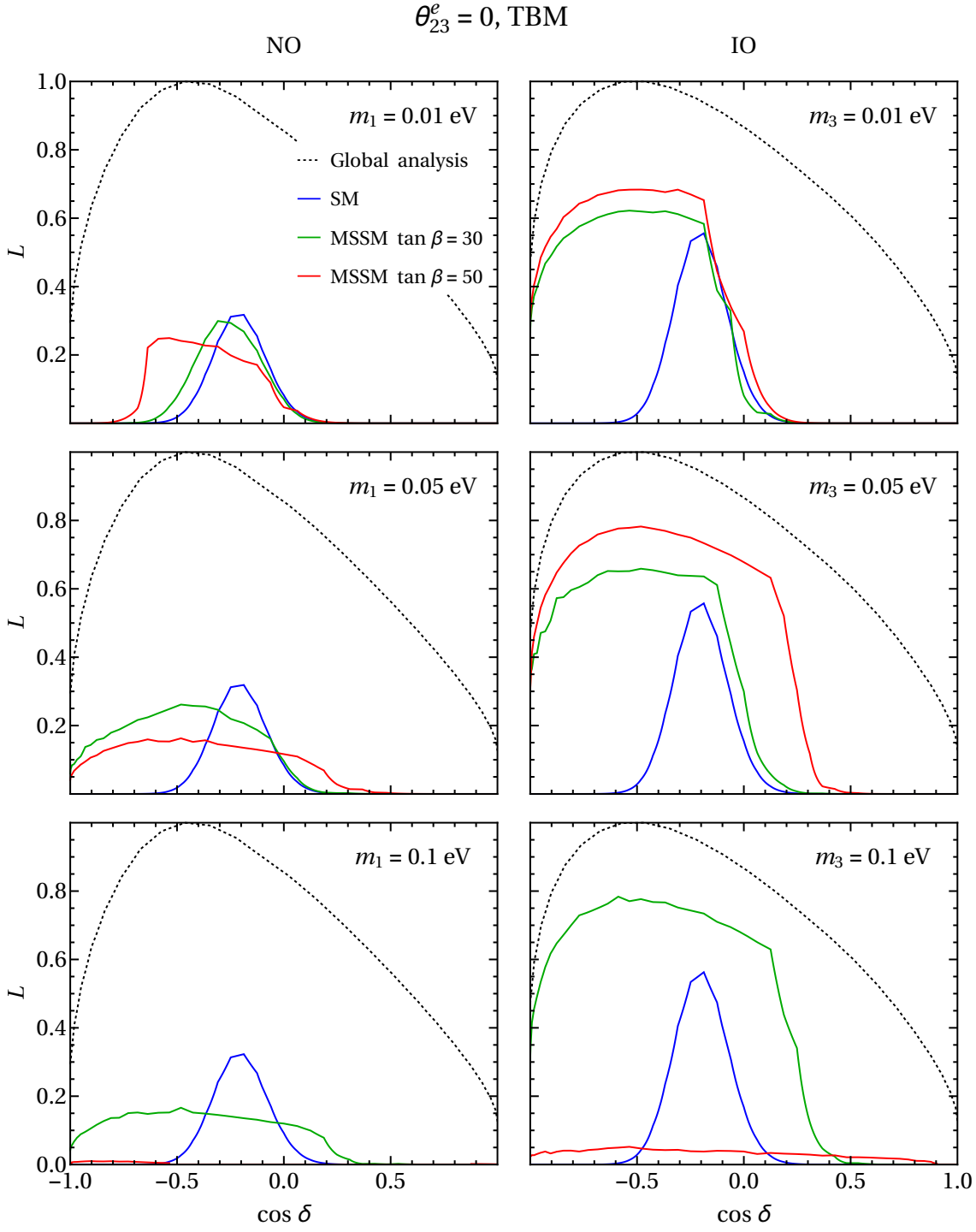

Figure H.6. Likelihood function vs. $\cos\delta$ in the case of zero θ^e_{23} for the TBM symmetry form of the matrix $\tilde{U}_\nu$ in all the set-ups considered. The dotted line stands for likelihood extracted from the global analysis in [162]. The blue line is for the SM running, while the green and red lines are for the running within MSSM with $\tan\beta = 30$ and $\tan\beta = 50$, respectively.

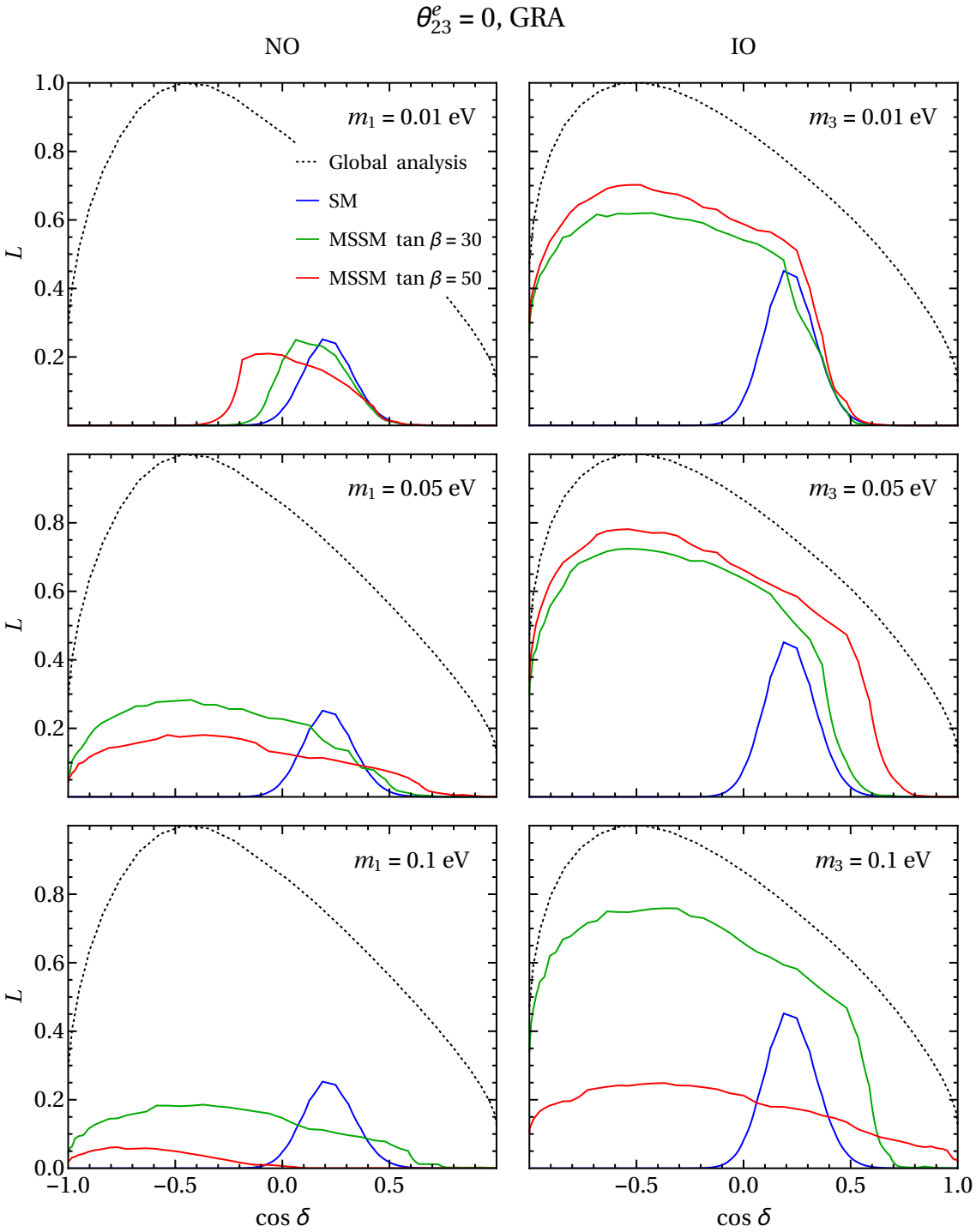

Figure H.7. The same as in Fig. H.6, but for the GRA symmetry form of the matrix $\tilde{U}_\nu$.

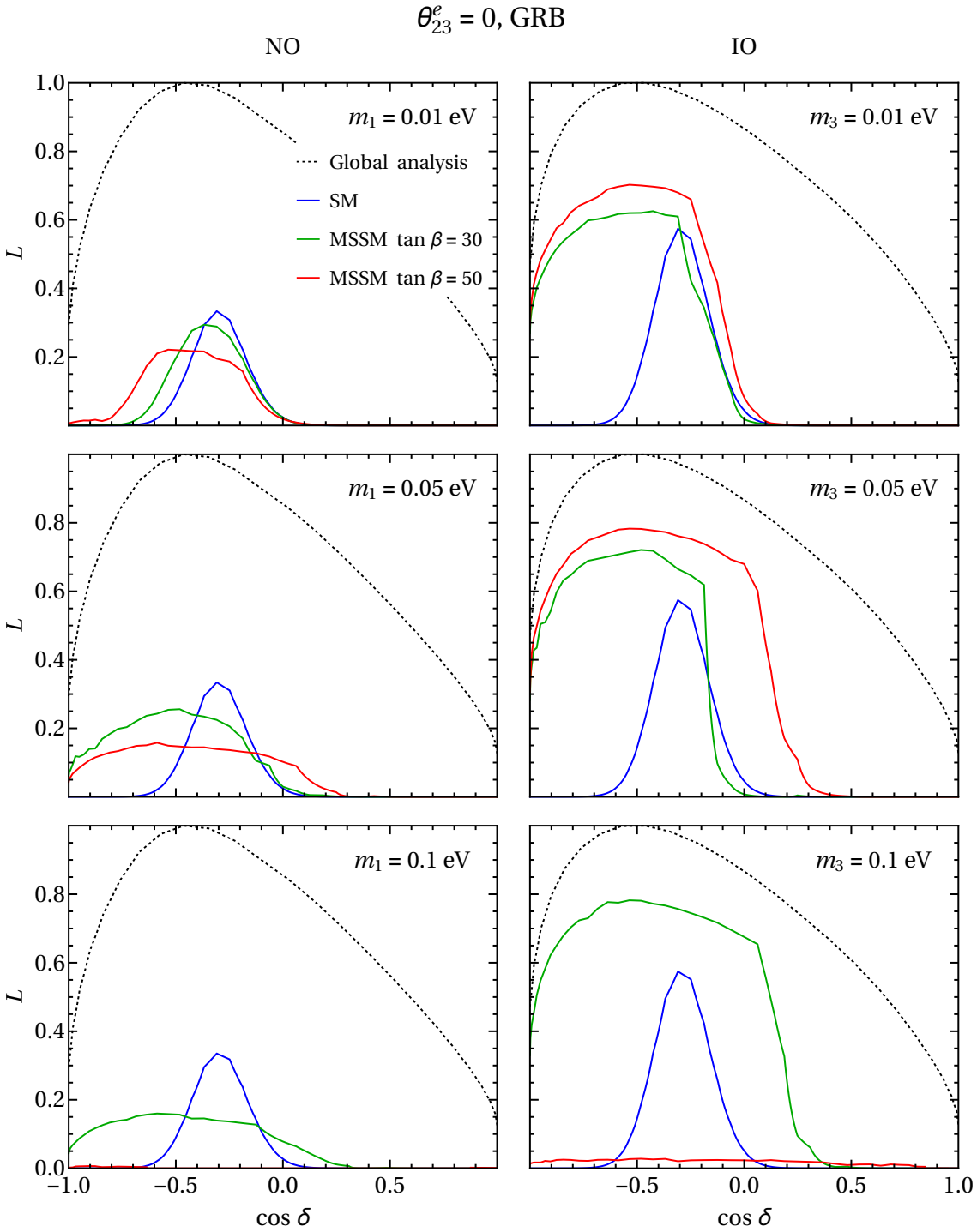

Figure H.8. The same as in Fig. H.6, but for the GRB symmetry form of the matrix $\tilde{U}_\nu$.

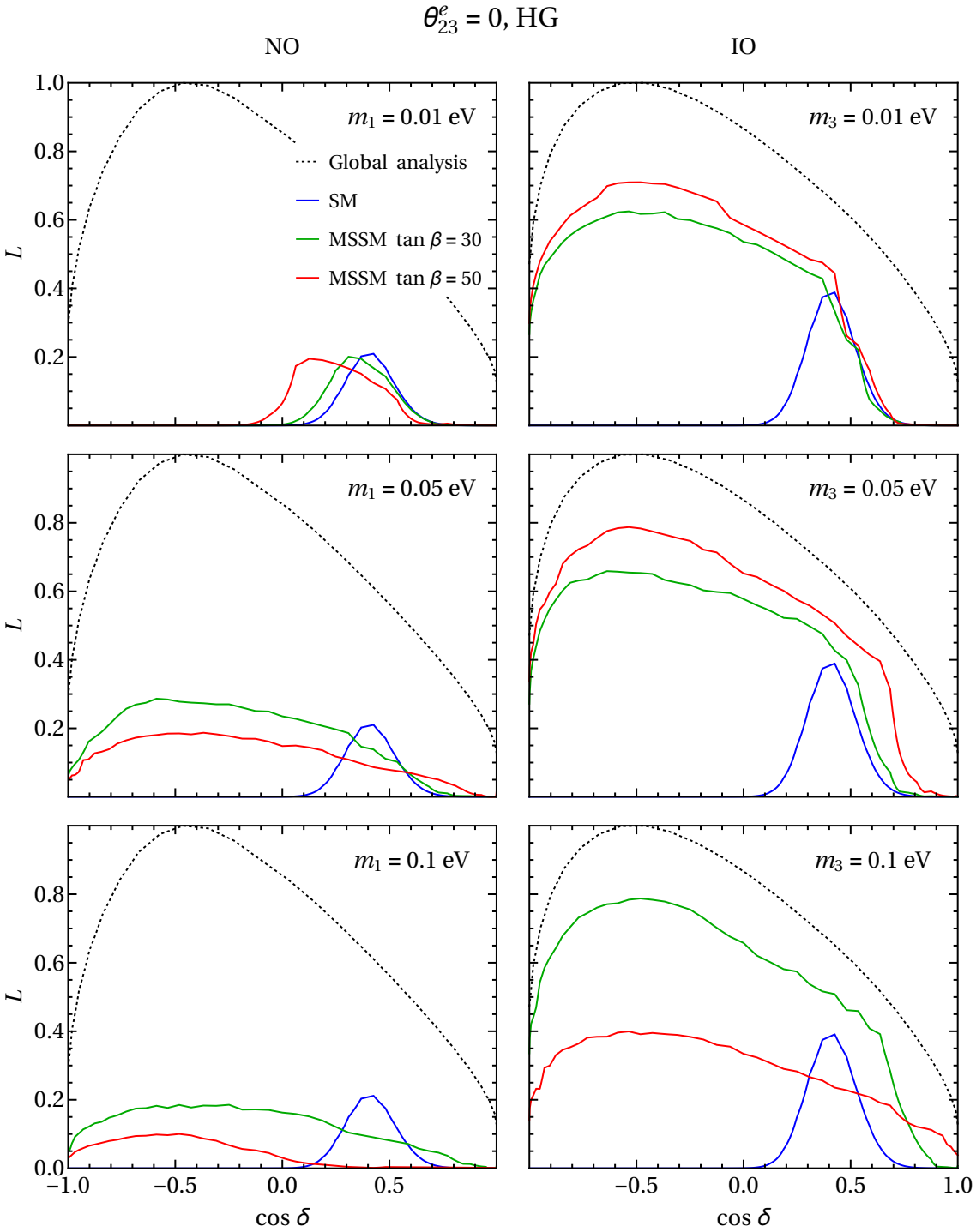

Figure H.9. The same as in Fig. H.6, but for the HG symmetry form of the matrix $\tilde{U}_\nu$.

Bibliography

[1] S. L. Glashow, *Partial Symmetries of Weak Interactions*, *Nucl. Phys.* **22** (1961) 579–588.

[2] S. Weinberg, *A Model of Leptons*, *Phys. Rev. Lett.* **19** (1967) 1264–1266.

[3] A. Salam, *Weak and Electromagnetic Interactions*, in *8th Nobel Symposium Lerum, Sweden, May 19–25, 1968*, pp. 367–377, 1968.

[4] B. Pontecorvo, *Mesonium and Anti-Mesonium*, *Sov. Phys. JETP* **6** (1957) 429.

[5] B. Pontecorvo, *Inverse Beta Processes and Nonconservation of Lepton Charge*, *Sov. Phys. JETP* **7** (1958) 172–173.

[6] Super-Kamiokande Collaboration, Y. Fukuda et al., *Evidence for Oscillation of Atmospheric Neutrinos*, *Phys. Rev. Lett.* **81** (1998) 1562–1567 [arXiv:hep-ex/9807003].

[7] SNO Collaboration, Q. R. Ahmad et al., *Measurement of the Rate of $\nu_e + d \to p + p + e^-$ Interactions Produced by ^8B Solar Neutrinos at the Sudbury Neutrino Observatory*, *Phys. Rev. Lett.* **87** (2001) 071301 [arXiv:nucl-ex/0106015].

[8] K. Nakamura and S. T. Petcov, *Neutrino Mass, Mixing, and Oscillations*, in Particle Data Group Collaboration, C. Patrignani et al., *Review of Particle Physics*, *Chin. Phys.* **C 40** (2016) 100001.

[9] Z. Maki, M. Nakagawa and S. Sakata, *Remarks on the Unified Model of Elementary Particles*, *Prog. Theor. Phys.* **28** (1962) 870–880.

[10] N. Cabibbo, *Unitary Symmetry and Leptonic Decays*, *Phys. Rev. Lett.* **10** (1963) 531–533.

[11] M. Kobayashi and T. Maskawa, *CP Violation in the Renormalizable Theory of Weak Interaction*, *Prog. Theor. Phys.* **49** (1973) 652–657.

[12] L.-L. Chau and W.-Y. Keung, *Comments on the Parametrization of the Kobayashi-Maskawa Matrix*, *Phys. Rev. Lett.* **53** (1984) 1802.

[13] S. M. Bilenky, J. Hošek and S. T. Petcov, *On the Oscillations of Neutrinos with Dirac and Majorana Masses*, *Phys. Lett.* **B 94** (1980) 495–498.

[14] F. Capozzi, E. Di Valentino, E. Lisi, A. Marrone, A. Melchiorri and A. Palazzo, *Global Constraints on Absolute Neutrino Masses and Their Ordering*, *Phys. Rev.* **D 95** (2017) 096014 [arXiv:1703.04471].

[15] I. Esteban, M. C. Gonzalez-Garcia, M. Maltoni, I. Martinez-Soler and T. Schwetz, *Updated Fit to Three Neutrino Mixing: Exploring the Accelerator-Reactor Complementarity*, *JHEP* **01** (2017) 087 [arXiv:1611.01514].

[16] D. V. Forero, M. Tortola and J. W. F. Valle, *Neutrino Oscillations Refitted*, *Phys. Rev.* **D 90** (2014) 093006 [arXiv:1405.7540].

[17] UTfit Collaboration, C. Alpigiani et al., *Standard Model Fit Results: Summer 2016*, http://www.utfit.org/UTfit/ResultsSummer2016SM.

[18] F. Capozzi, G. L. Fogli, E. Lisi, A. Marrone, D. Montanino and A. Palazzo, *Status of Three-Neutrino Oscillation Parameters, Circa 2013*, *Phys. Rev.* **D 89** (2014) 093018 [arXiv:1312.2878].

[19] M. C. Gonzalez-Garcia, M. Maltoni and T. Schwetz, *Updated Fit to Three Neutrino Mixing: Status of Leptonic CP Violation*, *JHEP* **11** (2014) 052 [arXiv:1409.5439].

[20] N. Cabibbo, *Time Reversal Violation in Neutrino Oscillation*, *Phys. Lett.* **72B** (1978) 333–335.

[21] V. Barger, K. Whisnant and R. J. N. Phillips, *CP Nonconservation in Three-Neutrino Oscillations*, *Phys. Rev. Lett.* **45** (1980) 2084.

[22] P. I. Krastev and S. T. Petcov, *Resonance Amplification and T Violation Effects in Three-Neutrino Oscillations in the Earth*, *Phys. Lett.* **B 205** (1988) 84–92.

[23] C. Jarlskog, *Commutator of the Quark Mass Matrices in the Standard Electroweak Model and a Measure of Maximal CP Nonconservation*, *Phys. Rev. Lett.* **55** (1985) 1039.

[24] C. Jarlskog, *A Basis Independent Formulation of the Connection Between Quark Mass Matrices, CP Violation and Experiment*, *Z. Phys.* **C 29** (1985) 491–497.

[25] T2K Collaboration, Y. Itow et al., *The JHF-Kamioka Neutrino Project*, in *Neutrino Oscillations and Their Origin. Proceedings, 3rd International Workshop, NOON 2001, Kashiwa, Tokyo, Japan, December 5–8, 2001*, pp. 239–248, 2001 [arXiv:hep-ex/0106019].

[26] T2K Collaboration, K. Abe et al., *The T2K Experiment*, *Nucl. Instrum. Meth.* **A 659** (2011) 106–135 [arXiv:1106.1238].

[27] T2K Collaboration, K. Abe et al., *Indication of Electron Neutrino Appearance from an Accelerator-Produced Off-Axis Muon Neutrino Beam*, *Phys. Rev. Lett.* **107** (2011) 041801 [arXiv:1106.2822].

[28] T2K Collaboration, K. Abe et al., *First Muon-Neutrino Disappearance Study with an Off-Axis Beam*, *Phys. Rev.* **D 85** (2012) 031103 [arXiv:1201.1386].

[29] NOνA Collaboration, D. S. Ayres et al., *NOνA: Proposal to Build a 30 Kiloton Off-Axis Detector to Study $\nu_\mu \to \nu_e$ Oscillations in the NuMI Beamline*, arXiv:hep-ex/0503053.

[30] NOνA Collaboration, P. Adamson et al., *First Measurement of Electron Neutrino Appearance in NOνA*, *Phys. Rev. Lett.* **116** (2016) 151806 [arXiv:1601.05022].

[31] NOνA Collaboration, P. Adamson et al., *First Measurement of Muon Neutrino Disappearance in NOνA*, *Phys. Rev.* **D 93** (2016) 051104 [arXiv:1601.05037].

[32] Hyper-Kamiokande Proto Collaboration, K. Abe et al., *Physics Potential of a Long-Baseline Neutrino Oscillation Experiment Using a J-PARC Neutrino Beam and Hyper-Kamiokande*, *PTEP* **2015** (2015) 053C02 [arXiv:1502.05199].

[33] DUNE Collaboration, R. Acciarri et al., *Long-Baseline Neutrino Facility (LBNF) and Deep Underground Neutrino Experiment (DUNE): Volume 1*, arXiv:1601.05471.

[34] DUNE Collaboration, R. Acciarri et al., *Long-Baseline Neutrino Facility (LBNF) and Deep Underground Neutrino Experiment (DUNE): Volume 2*, arXiv:1512.06148.

[35] DUNE Collaboration, J. Strait et al., *Long-Baseline Neutrino Facility (LBNF) and Deep Underground Neutrino Experiment (DUNE): Volume 3*, arXiv:1601.05823.

[36] DUNE Collaboration, R. Acciarri et al., *Long-Baseline Neutrino Facility (LBNF) and Deep Underground Neutrino Experiment (DUNE): Volume 4*, arXiv:1601.02984.

[37] P. Langacker, S. T. Petcov, G. Steigman and S. Toshev, *Implications of the Mikheev-Smirnov-Wolfenstein (MSW) Mechanism of Amplification of Neutrino Oscillations in Matter*, *Nucl. Phys.* **B 282** (1987) 589–609.

[38] S. M. Bilenky and S. T. Petcov, *Massive Neutrinos and Neutrino Oscillations*, *Rev. Mod. Phys.* **59** (1987) 671–754 [Errata: *ibid.* **60** (1988) 575, *ibid.* **61** (1989) 169].

[39] S. T. Petcov, *The Nature of Massive Neutrinos*, *Adv. High Energy Phys.* **2013** (2013) 852987 [arXiv:1303.5819].

[40] S. M. Bilenky, S. Pascoli and S. T. Petcov, *Majorana Neutrinos, Neutrino Mass Spectrum, CP Violation and Neutrinoless Double β Decay: The Three-Neutrino Mixing Case*, *Phys. Rev.* **D 64** (2001) 053010 [arXiv:hep-ph/0102265].

[41] W. Rodejohann, *Neutrinoless Double Beta Decay and Particle Physics*, *Int. J. Mod. Phys.* **E 20** (2011) 1833–1930 [arXiv:1106.1334].

[42] J. D. Vergados, H. Ejiri and F. Šimkovic, *Theory of Neutrinoless Double Beta Decay*, *Rept. Prog. Phys.* **75** (2012) 106301 [arXiv:1205.0649].

[43] S. Dell'Oro, S. Marcocci, M. Viel and F. Vissani, *Neutrinoless Double Beta Decay: 2015 Review*, *Adv. High Energy Phys.* **2016** (2016) 2162659 [arXiv:1601.07512].

[44] J. D. Vergados, H. Ejiri and F. Šimkovic, *Neutrinoless Double Beta Decay and Neutrino Mass*, *Int. J. Mod. Phys.* **E 25** (2016) 1630007 [arXiv:1612.02924].

[45] S. Pascoli, S. T. Petcov and C. E. Yaguna, *Quasi-Degenerate Neutrino Mass Spectrum, $\mu \to e + \gamma$ Decay and Leptogenesis*, *Phys. Lett.* **B 564** (2003) 241–254 [arXiv:hep-ph/0301095].

[46] S. T. Petcov, T. Shindou and Y. Takanishi, *Majorana CP-Violating Phases, RG Running of Neutrino Mixing Parameters and Charged Lepton Flavour Violating Decays*, *Nucl. Phys.* **B 738** (2006) 219–242 [arXiv:hep-ph/0508243].

[47] D. N. Dinh, A. Ibarra, E. Molinaro and S. T. Petcov, *The $\mu - e$ Conversion in Nuclei, $\mu \to e\gamma, \mu \to 3e$ Decays and TeV Scale See-Saw Scenarios of Neutrino Mass Generation*, *JHEP* **08** (2012) 125 [Erratum: *ibid.* **09** (2013) 023] [arXiv:1205.4671].

[48] S. Pascoli, S. T. Petcov and A. Riotto, *Connecting Low Energy Leptonic CP Violation to Leptogenesis*, *Phys. Rev.* **D 75** (2007) 083511 [arXiv:hep-ph/0609125].

[49] S. Pascoli, S. T. Petcov and A. Riotto, *Leptogenesis and Low Energy CP Violation in Neutrino Physics*, *Nucl. Phys.* **B 774** (2007) 1–52 [arXiv:hep-ph/0611338].

[50] M. Fukugita and T. Yanagida, *Baryogenesis without Grand Unification*, *Phys. Lett.* **B 174** (1986) 45–47.

[51] V. A. Kuzmin, V. A. Rubakov and M. E. Shaposhnikov, *On Anomalous Electroweak Baryon Number Non-conservation in the Early Universe*, *Phys. Lett.* **B 155** (1985) 36.

[52] P. Minkowski, $\mu \to e\gamma$ *at a Rate of One Out of* 10^9 *Muon Decays?*, *Phys. Lett.* **B 67** (1977) 421–428.

[53] T. Yanagida, *Horizontal Symmetry and Masses of Neutrinos*, in *Proceedings of Workshop on the Unified Theories and the Baryon Number in the Universe, Tsukuba, Japan, February 13–14, 1979*, pp. 95–99, 1979.

[54] M. Gell-Mann, P. Ramond and R. Slansky, *Complex Spinors and Unified Theories*, in *Proceedings of Supergravity Workshop, Stony Brook, New York, September 27–28, 1979*, pp. 315–321, 1979 [arXiv:1306.4669].

[55] R. N. Mohapatra and G. Senjanovic, *Neutrino Mass and Spontaneous Parity Non-conservation*, *Phys. Rev. Lett.* **44** (1980) 912.

[56] F. Perrin, *Possibilité d'émission de particules neutres de masse intrinsèque nulle dans les radioactivités* β, *Comptes Rendus* **197** (1933) 1625–1627.

[57] E. Fermi, *Tentativo di una teoria dei raggi* β, *Nuovo Cim.* **11** (1934) 1–19.

[58] C. Giunti and C. W. Kim, *Fundamentals of Neutrino Physics and Astrophysics*, Oxford University Press, 2007, DOI:10.1093/acprof:oso/9780198508717.001.0001.

[59] V. N. Aseev et al., *An Upper Limit on Electron Antineutrino Mass from the Troitsk Experiment*, *Phys. Rev.* **D 84** (2011) 112003 [arXiv:1108.5034].

[60] C. Kraus et al., *Final Results from Phase II of the Mainz Neutrino Mass Search in Tritium* β *Decay*, *Eur. Phys. J.* **C 40** (2005) 447–468 [arXiv:hep-ex/0412056].

[61] K. Eitel, *Direct Neutrino Mass Experiments*, *Nucl. Phys. Proc. Suppl.* **143** (2005) 197–204.

[62] G. Drexlin, V. Hannen, S. Mertens and C. Weinheimer, *Current Direct Neutrino Mass Experiments*, *Adv. High Energy Phys.* **2013** (2013) 293986 [arXiv:1307.0101].

[63] Planck Collaboration, P. A. R. Ade et al., *Planck 2015 Results. XIII. Cosmological Parameters*, *Astron. Astrophys.* **594** (2016) A13 [arXiv:1502.01589].

[64] Euclid Theory Working Group Collaboration, L. Amendola et al., *Cosmology and Fundamental Physics with the Euclid Satellite*, *Living Rev. Rel.* **16** (2013) 6 [arXiv:1206.1225].

[65] S. T. Petcov, *Theory Prospective on Leptonic CP Violation*, *Nucl. Phys.* **B 908** (2016) 279–301.

[66] H. Georgi and S. L. Glashow, *Unity of All Elementary Particle Forces*, *Phys. Rev. Lett.* **32** (1974) 438–441.

[67] J. C. Pati and A. Salam, *Lepton Number as the Fourth "Color"*, *Phys. Rev.* **D 10** (1974) 275–289 [Erratum: *ibid.* **D 11** (1975) 703].

[68] C. D. Froggatt and H. B. Nielsen, *Hierarchy of Quark Masses, Cabibbo Angles and CP Violation*, *Nucl. Phys.* **B 147** (1979) 277–298.

[69] Double Chooz Collaboration, Y. Abe et al., *Indication of Reactor $\bar{\nu}_e$ Disappearance in the Double Chooz Experiment*, *Phys. Rev. Lett.* **108** (2012) 131801 [arXiv:1112.6353].

[70] Daya Bay Collaboration, F. P. An et al., *Observation of Electron-Antineutrino Disappearance at Daya Bay*, *Phys. Rev. Lett.* **108** (2012) 171803 [arXiv:1203.1669].

[71] RENO Collaboration, J. K. Ahn et al., *Observation of Reactor Electron Antineutrino Disappearance in the RENO Experiment*, *Phys. Rev. Lett.* **108** (2012) 191802 [arXiv:1204.0626].

[72] P. F. Harrison, D. H. Perkins and W. G. Scott, *Tri-Bimaximal Mixing and the Neutrino Oscillation Data*, *Phys. Lett.* **B 530** (2002) 167 [arXiv:hep-ph/0202074].

[73] P. F. Harrison and W. G. Scott, *Symmetries and Generalizations of Tri-Bimaximal Neutrino Mixing*, *Phys. Lett.* **B 535** (2002) 163–169 [arXiv:hep-ph/0203209].

[74] Z.-z. Xing, *Nearly Tri-Bimaximal Neutrino Mixing and CP Violation*, *Phys. Lett.* **B 533** (2002) 85–93 [arXiv:hep-ph/0204049].

[75] X.-G. He and A. Zee, *Some Simple Mixing and Mass Matrices for Neutrinos*, *Phys. Lett.* **B 560** (2003) 87–90 [arXiv:hep-ph/0301092].

[76] L. Wolfenstein, *Oscillations Among Three Neutrino Types and CP Violation*, *Phys. Rev.* **D 18** (1978) 958–960.

[77] E. Ma and G. Rajasekaran, *Softly Broken A_4 Symmetry for Nearly Degenerate Neutrino Masses*, *Phys. Rev.* **D 64** (2001) 113012 [arXiv:hep-ph/0106291].

[78] K. S. Babu, E. Ma and J. W. F. Valle, *Underlying A_4 Symmetry for the Neutrino Mass Matrix and the Quark Mixing Matrix*, *Phys. Lett.* **B 552** (2003) 207–213 [arXiv:hep-ph/0206292].

[79] G. Altarelli and F. Feruglio, *Tri-Bimaximal Neutrino Mixing from Discrete Symmetry in Extra Dimensions*, *Nucl. Phys.* **B 720** (2005) 64–88 [arXiv:hep-ph/0504165].

[80] G. Altarelli and F. Feruglio, *Discrete Flavor Symmetries and Models of Neutrino Mixing*, *Rev. Mod. Phys.* **82** (2010) 2701–2729 [arXiv:1002.0211].

[81] H. Ishimori, T. Kobayashi, H. Ohki, Y. Shimizu, H. Okada and M. Tanimoto, *Non-Abelian Discrete Symmetries in Particle Physics*, *Prog. Theor. Phys. Suppl.* **183** (2010) 1–163 [arXiv:1003.3552].

[82] S. F. King and C. Luhn, *Neutrino Mass and Mixing with Discrete Symmetry*, *Rept. Prog. Phys.* **76** (2013) 056201 [arXiv:1301.1340].

[83] C. Hagedorn, S. F. King and C. Luhn, *A SUSY GUT of Flavour with $S_4 \times SU(5)$ to NLO*, *JHEP* **06** (2010) 048 [arXiv:1003.4249].

[84] S. F. King and C. Luhn, *A New Family Symmetry for $SO(10)$ GUTs*, *Nucl. Phys.* **B 820** (2009) 269–289 [arXiv:0905.1686].

[85] G. Altarelli and F. Feruglio, *Tri-Bimaximal Neutrino Mixing, A_4 and the Modular Symmetry*, *Nucl. Phys.* **B 741** (2006) 215–235 [arXiv:hep-ph/0512103].

[86] S. F. King, T. Neder and A. J. Stuart, *Lepton Mixing Predictions from $\Delta(6n^2)$ Family Symmetry*, *Phys. Lett.* **B 726** (2013) 312–315 [arXiv:1305.3200].

[87] C. Hagedorn, A. Meroni and L. Vitale, *Mixing Patterns from the Groups $\Sigma(n\phi)$*, *J. Phys.* **A 47** (2014) 055201 [arXiv:1307.5308].

[88] F. Vissani, *A Study of the Scenario with Nearly Degenerate Majorana Neutrinos*, arXiv:hep-ph/9708483.

[89] V. Barger, S. Pakvasa, T. J. Weiler and K. Whisnant, *Bimaximal Mixing of Three Neutrinos*, *Phys. Lett.* **B 437** (1998) 107–116 [arXiv:hep-ph/9806387].

[90] A. J. Baltz, A. S. Goldhaber and M. Goldhaber, *The Solar Neutrino Puzzle: An Oscillation Solution with Maximal Neutrino Mixing*, *Phys. Rev. Lett.* **81** (1998) 5730–5733 [arXiv:hep-ph/9806540].

[91] S. T. Petcov, *On Pseudo-Dirac Neutrinos, Neutrino Oscillations and Neutrinoless Double β-Decay*, *Phys. Lett.* **B 110** (1982) 245–249.

[92] A. Datta, F.-S. Ling and P. Ramond, *Correlated Hierarchy, Dirac Masses and Large Mixing Angles*, *Nucl. Phys.* **B 671** (2003) 383–400 [arXiv:hep-ph/0306002].

[93] Y. Kajiyama, M. Raidal and A. Strumia, *Golden Ratio Prediction for Solar Neutrino Mixing*, *Phys. Rev.* **D 76** (2007) 117301 [arXiv:0705.4559].

[94] L. L. Everett and A. J. Stuart, *Icosahedral (A_5) Family Symmetry and the Golden Ratio Prediction for Solar Neutrino Mixing*, *Phys. Rev.* **D 79** (2009) 085005 [arXiv:0812.1057].

[95] W. Rodejohann, *Unified Parametrization for Quark and Lepton Mixing Angles*, *Phys. Lett.* **B 671** (2009) 267–271 [arXiv:0810.5239].

[96] A. Adulpravitchai, A. Blum and W. Rodejohann, *Golden Ratio Prediction for Solar Neutrino Mixing*, *New J. Phys.* **11** (2009) 063026 [arXiv:0903.0531].

[97] C. H. Albright, A. Dueck and W. Rodejohann, *Possible Alternatives to Tri-Bimaximal Mixing*, *Eur. Phys. J.* **C 70** (2010) 1099–1110 [arXiv:1004.2798].

[98] J. E. Kim and M.-S. Seo, *Quark and Lepton Mixing Angles with a Dodeca-Symmetry*, *JHEP* **02** (2011) 097 [arXiv:1005.4684].

[99] S. T. Petcov, *Predicting the Values of the Leptonic CP Violation Phases in Theories with Discrete Flavour Symmetries*, *Nucl. Phys.* **B 892** (2015) 400–428 [arXiv:1405.6006].

[100] I. Girardi, S. T. Petcov and A. V. Titov, *Predictions for the Leptonic Dirac CP Violation Phase: A Systematic Phenomenological Analysis*, *Eur. Phys. J.* **C 75** (2015) 345 [arXiv:1504.00658].

[101] I. Girardi, S. T. Petcov, A. J. Stuart and A. V. Titov, *Leptonic Dirac CP Violation Predictions from Residual Discrete Symmetries*, *Nucl. Phys.* **B 902** (2016) 1–57 [arXiv:1509.02502].

[102] D. Marzocca, S. T. Petcov, A. Romanino and M. C. Sevilla, *Nonzero $|U_{e3}|$ from Charged Lepton Corrections and the Atmospheric Neutrino Mixing Angle*, *JHEP* **05** (2013) 073 [arXiv:1302.0423].

[103] M. Tanimoto, *Neutrinos and Flavor Symmetries*, *AIP Conf. Proc.* **1666** (2015) 120002.

[104] P. Ballett, S. F. King, C. Luhn, S. Pascoli and M. A. Schmidt, *Testing Atmospheric Mixing Sum Rules at Precision Neutrino Facilities*, *Phys. Rev.* **D 89** (2014) 016016 [arXiv:1308.4314].

[105] S.-F. Ge, D. A. Dicus and W. W. Repko, *Residual Symmetries for Neutrino Mixing with a Large θ_{13} and Nearly Maximal δ_D*, *Phys. Rev. Lett.* **108** (2012) 041801 [arXiv:1108.0964].

[106] A. D. Hanlon, S.-F. Ge and W. W. Repko, *Phenomenological Consequences of Residual $\mathbb{Z}_2^s$ and $\overline{\mathbb{Z}}_2^s$ Symmetries*, *Phys. Lett.* **B 729** (2014) 185–191 [arXiv:1308.6522].

[107] S. Antusch, S. F. King, C. Luhn and M. Spinrath, *Trimaximal Mixing with Predicted θ_{13} from a New Type of Constrained Sequential Dominance*, *Nucl. Phys.* **B 856** (2012) 328–341 [arXiv:1108.4278].

[108] S. F. King, A. Merle, S. Morisi, Y. Shimizu and M. Tanimoto, *Neutrino Mass and Mixing: from Theory to Experiment*, *New J. Phys.* **16** (2014) 045018 [arXiv:1402.4271].

[109] I. Girardi, S. T. Petcov and A. V. Titov, *Determining the Dirac CP Violation Phase in the Neutrino Mixing Matrix from Sum Rules*, *Nucl. Phys.* **B 894** (2015) 733–768 [arXiv:1410.8056].

[110] I. Girardi, S. T. Petcov and A. V. Titov, *Predictions for the Dirac CP Violation Phase in the Neutrino Mixing Matrix*, *Int. J. Mod. Phys.* **A 30** (2015) 1530035 [arXiv:1504.02402].

[111] P. Ballett, S. F. King, C. Luhn, S. Pascoli and M. A. Schmidt, *Testing Solar Lepton Mixing Sum Rules in Neutrino Oscillation Experiments*, *JHEP* **12** (2014) 122 [arXiv:1410.7573].

[112] L. J. Hall, H. Murayama and N. Weiner, *Neutrino Mass Anarchy*, *Phys. Rev. Lett.* **84** (2000) 2572–2575 [arXiv:hep-ph/9911341].

[113] N. Haba and H. Murayama, *Anarchy and Hierarchy*, *Phys. Rev.* **D 63** (2001) 053010 [arXiv:hep-ph/0009174].

[114] A. de Gouvêa and H. Murayama, *Statistical Test of Anarchy*, *Phys. Lett.* **B 573** (2003) 94–100 [arXiv:hep-ph/0301050].

[115] A. de Gouvêa and H. Murayama, *Neutrino Mixing Anarchy: Alive and Kicking*, *Phys. Lett.* **B 747** (2015) 479–483 [arXiv:1204.1249].

[116] F. Feruglio, *Are Neutrino Masses Modular Forms?*, arXiv:1706.08749.

[117] F. Feruglio, C. Hagedorn and R. Ziegler, *Lepton Mixing Parameters from Discrete and CP Symmetries*, *JHEP* **07** (2013) 027 [arXiv:1211.5560].

[118] M. Holthausen, M. Lindner and M. A. Schmidt, *CP and Discrete Flavour Symmetries*, *JHEP* **04** (2013) 122 [arXiv:1211.6953].

[119] G. C. Branco, L. Lavoura and M. N. Rebelo, *Majorana Neutrinos and CP Violation in the Leptonic Sector*, *Phys. Lett.* **B 180** (1986) 264–268.

[120] G.-J. Ding, S. F. King, C. Luhn and A. J. Stuart, *Spontaneous CP Violation from Vacuum Alignment in S_4 Models of Leptons*, *JHEP* **05** (2013) 084 [arXiv:1303.6180].

[121] G.-J. Ding, S. F. King and A. J. Stuart, *Generalised CP and A_4 Family Symmetry*, *JHEP* **12** (2013) 006 [arXiv:1307.4212].

[122] I. Girardi, A. Meroni, S. T. Petcov and M. Spinrath, *Generalised Geometrical CP Violation in a T' Lepton Flavour Model*, *JHEP* **02** (2014) 050 [arXiv:1312.1966].

[123] F. Feruglio, C. Hagedorn and R. Ziegler, *A Realistic Pattern of Lepton Mixing and Masses from S_4 and CP*, *Eur. Phys. J.* **C 74** (2014) 2753 [arXiv:1303.7178].

[124] C.-C. Li and G.-J. Ding, *Generalised CP and Trimaximal TM_1 Lepton Mixing in S_4 Family Symmetry*, *Nucl. Phys.* **B 881** (2014) 206–232 [arXiv:1312.4401].

[125] C.-C. Li and G.-J. Ding, *Deviation from Bimaximal Mixing and Leptonic CP Phases in S_4 Family Symmetry and Generalized CP*, *JHEP* **08** (2015) 017 [arXiv:1408.0785].

[126] J.-N. Lu and G.-J. Ding, *Alternative Schemes of Predicting Lepton Mixing Parameters from Discrete Flavor and CP Symmetry*, *Phys. Rev.* **D 95** (2017) 015012 [arXiv:1610.05682].

[127] J. T. Penedo, S. T. Petcov and A. V. Titov, *Neutrino Mixing and Leptonic CP Violation from S_4 Flavour and Generalised CP Symmetries*, arXiv:1705.00309.

[128] C.-C. Li and G.-J. Ding, *Lepton Mixing in A_5 Family Symmetry and Generalized CP*, *JHEP* **05** (2015) 100 [arXiv:1503.03711].

[129] A. Di Iura, C. Hagedorn and D. Meloni, *Lepton Mixing from the Interplay of the Alternating Group A_5 and CP*, *JHEP* **08** (2015) 037 [arXiv:1503.04140].

[130] P. Ballett, S. Pascoli and J. Turner, *Mixing Angle and Phase Correlations from A_5 with Generalized CP and Their Prospects for Discovery*, *Phys. Rev.* **D 92** (2015) 093008 [arXiv:1503.07543].

[131] J. Turner, *Predictions for Leptonic Mixing Angle Correlations and Nontrivial Dirac CP Violation from A_5 with Generalized CP Symmetry*, *Phys. Rev.* **D 92** (2015) 116007 [arXiv:1507.06224].

[132] C. C. Nishi, *Generalized CP Symmetries in $\Delta(27)$ Flavor Models*, *Phys. Rev.* **D 88** (2013) 033010 [arXiv:1306.0877].

[133] G.-J. Ding and Y.-L. Zhou, *Predicting Lepton Flavor Mixing from $\Delta(48)$ and Generalized CP Symmetries*, *Chin. Phys.* **C 39** (2015) 021001 [arXiv:1312.5222].

[134] G.-J. Ding and Y.-L. Zhou, *Lepton Mixing Parameters from $\Delta(48)$ Family Symmetry and Generalised CP*, *JHEP* **06** (2014) 023 [arXiv:1404.0592].

[135] G.-J. Ding and S. F. King, *Generalized CP and $\Delta(96)$ Family Symmetry*, *Phys. Rev.* **D 89** (2014) 093020 [arXiv:1403.5846].

[136] G.-J. Ding and S. F. King, *Generalized CP and $\Delta(3n^2)$ Family Symmetry for Semi-Direct Predictions of the PMNS Matrix*, *Phys. Rev.* **D 93** (2016) 025013 [arXiv:1510.03188].

[137] C. Hagedorn, A. Meroni and E. Molinaro, *Lepton Mixing from $\Delta(3n^2)$ and $\Delta(6n^2)$ and CP*, *Nucl. Phys.* **B 891** (2015) 499–557 [arXiv:1408.7118].

[138] S. F. King and T. Neder, *Lepton Mixing Predictions Including Majorana Phases from $\Delta(6n^2)$ Flavour Symmetry and Generalised CP*, *Phys. Lett.* **B 736** (2014) 308–316 [arXiv:1403.1758].

[139] G.-J. Ding, S. F. King and T. Neder, *Generalised CP and $\Delta(6n^2)$ Family Symmetry in Semi-Direct Models of Leptons*, *JHEP* **12** (2014) 007 [arXiv:1409.8005].

[140] I. Girardi, S. T. Petcov and A. V. Titov, *Predictions for the Majorana CP Violation Phases in the Neutrino Mixing Matrix and Neutrinoless Double Beta Decay*, *Nucl. Phys.* **B 911** (2016) 754–804 [arXiv:1605.04172].

[141] S. Weinberg, *Baryon- and Lepton-Nonconserving Processes*, *Phys. Rev. Lett.* **43** (1979) 1566–1570.

[142] J. Gehrlein, S. T. Petcov, M. Spinrath and A. V. Titov, *Renormalisation Group Corrections to Neutrino Mixing Sum Rules*, *JHEP* **11** (2016) 146 [arXiv:1608.08409].

[143] F. Feruglio, C. Hagedorn, Y. Lin and L. Merlo, *Tri-Bimaximal Neutrino Mixing and Quark Masses from a Discrete Flavour Symmetry*, *Nucl. Phys.* **B 775** (2007) 120–142 [Erratum: *ibid.* **B 836** (2010) 127–128] [arXiv:hep-ph/0702194].

[144] G.-J. Ding, L. L. Everett and A. J. Stuart, *Golden Ratio Neutrino Mixing and A_5 Flavor Symmetry*, *Nucl. Phys.* **B 857** (2012) 219–253 [arXiv:1110.1688].

[145] J. Gehrlein, J. P. Oppermann, D. Schäfer and M. Spinrath, *An $SU(5) \times A_5$ Golden Ratio Flavour Model*, *Nucl. Phys.* **B 890** (2014) 539–568 [arXiv:1410.2057].

[146] A. Meroni, S. T. Petcov and M. Spinrath, *A SUSY $SU(5) \times T'$ Unified Model of Flavour with Large θ_{13}*, *Phys. Rev.* **D 86** (2012) 113003 [arXiv:1205.5241].

[147] D. Marzocca, S. T. Petcov, A. Romanino and M. Spinrath, *Sizeable θ_{13} from the Charged Lepton Sector in SU(5), (Tri-)Bimaximal Neutrino Mixing and Dirac CP Violation*, *JHEP* **11** (2011) 009 [arXiv:1108.0614].

[148] S. Antusch, C. Gross, V. Maurer and C. Sluka, *$\theta_{13}^{PMNS} = \theta_C/\sqrt{2}$ from GUTs*, *Nucl. Phys.* **B 866** (2013) 255–269 [arXiv:1205.1051].

[149] M.-C. Chen and K. T. Mahanthappa, *Group Theoretical Origin of CP Violation*, *Phys. Lett.* **B 681** (2009) 444–447 [arXiv:0904.1721].

[150] Y. Shimizu, M. Tanimoto and K. Yamamoto, *Predicting CP Violation in Deviation from Tri-Bimaximal Mixing of Neutrinos*, *Mod. Phys. Lett.* **A 30** (2015) 1550002 [arXiv:1405.1521].

[151] P. H. Frampton, S. T. Petcov and W. Rodejohann, *On Deviations from Bimaximal Neutrino Mixing*, *Nucl. Phys.* **B 687** (2004) 31–54 [arXiv:hep-ph/0401206].

[152] R. de Adelhart Toorop, F. Feruglio and C. Hagedorn, *Discrete Flavour Symmetries in Light of T2K*, *Phys. Lett.* **B 703** (2011) 447–451 [arXiv:1107.3486].

[153] F. Bazzocchi, *Tri-Permuting Mixing Matrix and Predictions for θ_{13}*, arXiv:1108.2497.

[154] S. F. King, C. Luhn and A. J. Stuart, *A Grand $\Delta(96) \times SU(5)$ Flavour Model*, *Nucl. Phys.* **B 867** (2013) 203–235 [arXiv:1207.5741].

[155] W. Rodejohann and H. Zhang, *Reducing θ_{13} to 9°*, *Phys. Lett.* **B 732** (2014) 174–181 [arXiv:1402.2226].

[156] Y. Wang, *JUNO: A Multi-Purpose LS-based Experiment*, *PoS* **Neutel2013** (2013) 030.

[157] JUNO Collaboration, F. An et al., *Neutrino Physics with JUNO*, *J. Phys.* **G 43** (2016) 030401 [arXiv:1507.05613].

[158] Intensity Frontier Neutrino Working Group Collaboration, A. de Gouvêa et al., *Working Group Report: Neutrinos*, in *Proceedings, 2013 Community Summer Study on the Future of U.S. Particle Physics: Snowmass on the Mississippi (CSS2013): Minneapolis, MN, USA, July 29 – August 6, 2013*, 2013 [arXiv:1310.4340].

[159] Daya Bay Collaboration, C. Zhang, *Recent Results from the Daya Bay Experiment*, *AIP Conf. Proc.* **1666** (2015) 080003 [arXiv:1501.04991].

[160] Daya Bay Collaboration, J. Ling, *Precision Measurement of $\sin^2(2\theta_{13})$ and $|\Delta m^2_{ee}|$ from Daya Bay*, *PoS* **ICHEP2016** (2016) 467.

[161] P. Coloma, H. Minakata and S. J. Parke, *Interplay Between Appearance and Disappearance Channels for Precision Measurements of θ_{23} and δ*, *Phys. Rev.* **D 90** (2014) 093003 [arXiv:1406.2551].

[162] F. Capozzi, E. Lisi, A. Marrone, D. Montanino and A. Palazzo, *Neutrino Masses and Mixings: Status of Known and Unknown 3ν Parameters*, *Nucl. Phys.* **B 908** (2016) 218–234 [arXiv:1601.07777].

[163] J. F. Nieves and P. B. Pal, *Minimal Rephasing-Invariant CP-Violating Parameters with Dirac and Majorana Fermions*, *Phys. Rev.* **D 36** (1987) 315.

[164] J. A. Aguilar-Saavedra and G. C. Branco, *Unitarity Triangles and Geometrical Description of CP Violation with Majorana Neutrinos*, *Phys. Rev.* **D 62** (2000) 096009 [arXiv:hep-ph/0007025].

[165] J. F. Nieves and P. B. Pal, *Rephasing-Invariant CP-Violating Parameters with Majorana Neutrinos*, *Phys. Rev.* **D 64** (2001) 076005 [arXiv:hep-ph/0105305].

[166] S. Pascoli and S. T. Petcov, *The SNO Solar Neutrino Data, Neutrinoless Double Beta Decay and Neutrino Mass Spectrum*, *Phys. Lett.* **B 544** (2002) 239–250 [arXiv:hep-ph/0205022].

[167] S. Pascoli and S. T. Petcov, *The SNO Solar Neutrino Data, Neutrinoless Double Beta Decay and Neutrino Mass Spectrum: Addendum*, *Phys. Lett.* **B 580** (2004) 280–289 [arXiv:hep-ph/0310003].

[168] W. Rodejohann, *Cancellations in Neutrinoless Double Beta Decay and the Neutrino Mass Matrix*, *Nucl. Phys.* **B 597** (2001) 110–126 [arXiv:hep-ph/0008044].

[169] S. Pascoli, S. T. Petcov and L. Wolfenstein, *Searching for the CP Violation Associated with Majorana Neutrinos*, *Phys. Lett.* **B 524** (2002) 319–331 [arXiv:hep-ph/0110287].

[170] S. Pascoli, S. T. Petcov and W. Rodejohann, *On the CP Violation Associated with Majorana Neutrinos and Neutrinoless Double Beta Decay*, *Phys. Lett.* **B 549** (2002) 177–193 [arXiv:hep-ph/0209059].

[171] S. Pascoli, S. T. Petcov and T. Schwetz, *The Absolute Neutrino Mass Scale, Neutrino Mass Spectrum, Majorana CP Violation and Neutrinoless Double Beta Decay*, *Nucl. Phys.* **B 734** (2006) 24–49 [arXiv:hep-ph/0505226].

[172] GERDA Collaboration, M. Agostini et al., *Results on Neutrinoless Double-β Decay of ^{76}Ge from Phase I of the GERDA Experiment*, *Phys. Rev. Lett.* **111** (2013) 122503 [arXiv:1307.4720].

[173] C. N. Leung and S. T. Petcov, *A Comment on the Coexistence of Dirac and Majorana Massive Neutrinos*, *Phys. Lett.* **B 125** (1983) 461–466.

[174] S. T. Petcov and S. T. Toshev, *Conservation of Lepton Charges, Massive Majorana and Massless Neutrinos*, *Phys. Lett.* **B 143** (1984) 175–178.

[175] L. L. Everett, T. Garon and A. J. Stuart, *A Bottom-Up Approach to Lepton Flavor and CP Symmetries*, *JHEP* **04** (2015) 069 [arXiv:1501.04336].

[176] G. Altarelli, F. Feruglio and L. Merlo, *Revisiting Bimaximal Neutrino Mixing in a Model with S_4 Discrete Symmetry*, *JHEP* **05** (2009) 020 [arXiv:0903.1940].

[177] M. A. Schmidt and A. Yu. Smirnov, *Quark Lepton Complementarity and Renormalization Group Effects*, *Phys. Rev.* **D 74** (2006) 113003 [arXiv:hep-ph/0607232].

[178] S. Boudjemaa and S. F. King, *Deviations from Tri-Bimaximal Mixing: Charged Lepton Corrections and Renormalization Group Running*, *Phys. Rev.* **D 79** (2009) 033001 [arXiv:0808.2782].

[179] S. Antusch, S. F. King and M. Malinsky, *Perturbative Estimates of Lepton Mixing Angles in Unified Models*, *Nucl. Phys.* **B 820** (2009) 32–46 [arXiv:0810.3863].

[180] J. Zhang and S. Zhou, *Radiative Corrections to the Solar Lepton Mixing Sum Rule*, *JHEP* **08** (2016) 024 [arXiv:1604.03039].

[181] S. Antusch, S. F. King and M. Spinrath, *Spontaneous CP Violation in $A_4 \times SU(5)$ with Constrained Sequential Dominance 2*, *Phys. Rev.* **D 87** (2013) 096018 [arXiv:1301.6764].

[182] S. Antusch, S. F. King and M. Spinrath, *Measurable Neutrino Mass Scale in $A_4 \times SU(5)$*, *Phys. Rev.* **D 83** (2011) 013005 [arXiv:1005.0708].

[183] S. Antusch, J. Kersten, M. Lindner and M. Ratz, *Running Neutrino Masses, Mixings and CP Phases: Analytical Results and Phenomenological Consequences*, *Nucl. Phys.* **B 674** (2003) 401–433 [arXiv:hep-ph/0305273].

[184] S. Antusch, J. Kersten, M. Lindner, M. Ratz and M. A. Schmidt, *Running Neutrino Mass Parameters in See-Saw Scenarios*, *JHEP* **03** (2005) 024 [arXiv:hep-ph/0501272].

[185] S. Antusch, S. F. King, C. Luhn and M. Spinrath, *Right Unitarity Triangles and Tri-Bimaximal Mixing from Discrete Symmetries and Unification*, *Nucl. Phys.* **B 850** (2011) 477–504 [arXiv:1103.5930].

[186] L. J. Hall, R. Rattazzi and U. Sarid, *The Top Quark Mass in Supersymmetric $SO(10)$ Unification*, *Phys. Rev.* **D 50** (1994) 7048–7065 [arXiv:hep-ph/9306309].

[187] R. Hempfling, *Yukawa Coupling Unification with Supersymmetric Threshold Corrections*, *Phys. Rev.* **D 49** (1994) 6168–6172.

[188] M. Carena, M. Olechowski, S. Pokorski and C. E. M. Wagner, *Electroweak Symmetry Breaking and Bottom-Top Yukawa Unification*, *Nucl. Phys.* **B 426** (1994) 269–300 [arXiv:hep-ph/9402253].

[189] T. Blažek, S. Raby and S. Pokorski, *Finite Supersymmetric Threshold Corrections to CKM Matrix Elements in the Large $\tan\beta$ Regime*, *Phys. Rev.* **D 52** (1995) 4151–4158 [arXiv:hep-ph/9504364].

[190] Daya Bay Collaboration, X. Guo et al., *A Precision Measurement of the Neutrino Mixing Angle θ_{13} Using Reactor Antineutrinos at Daya-Bay*, arXiv:hep-ex/0701029.

[191] Daya Bay Collaboration, F. P. An et al., *A Side-by-Side Comparison of Daya Bay Antineutrino Detectors*, *Nucl. Instrum. Meth.* **A 685** (2012) 78–97 [arXiv:1202.6181].

[192] GERDA Collaboration, K. H. Ackermann et al., *The GERDA Experiment for the Search of $0\nu\beta\beta$ Decay in ^{76}Ge*, *Eur. Phys. J.* **C 73** (2013) 2330 [arXiv:1212.4067].

[193] GERDA Collaboration, M. Agostini et al., *Background-Free Search for Neutrinoless Double-β Decay of ^{76}Ge with GERDA*, *Nature* **544** (2017) 47–52 [arXiv:1703.00570].

[194] KamLAND-Zen Collaboration, A. Gando et al., *Measurement of the Double-β Decay Half-Life of ^{136}Xe with the KamLAND-Zen Experiment*, *Phys. Rev.* **C 85** (2012) 045504 [arXiv:1201.4664].

[195] KamLAND-Zen Collaboration, A. Gando et al., *Search for Majorana Neutrinos near the Inverted Mass Hierarchy Region with KamLAND-Zen*, *Phys. Rev. Lett.* **117** (2016) 082503 [Erratum: *ibid.* **117** (2016) 109903] [arXiv:1605.02889].

[196] CUORE Collaboration, D. R. Artusa et al., *Searching for Neutrinoless Double Beta Decay of ^{130}Te with CUORE*, *Adv. High Energy Phys.* **2015** (2015) 879871 [arXiv:1402.6072].

[197] Majorana Collaboration, N. Abgrall et al., *The MAJORANA DEMONSTRATOR Neutrinoless Double Beta Decay Experiment*, *Adv. High Energy Phys.* **2014** (2014) 365432 [arXiv:1308.1633].

[198] nEXO Collaboration, B. Mong, *nEXO — Neutrinoless Double Beta Decay Experiment*, *PoS* **HQL2016** (2017) 074.

[199] SNO+ Collaboration, S. Andringa et al., *Current Status and Future Prospects of the SNO+ Experiment*, *Adv. High Energy Phys.* **2016** (2016) 6194250 [arXiv:1508.05759].

[200] AMoRE Collaboration, V. Alenkov et al., *Technical Design Report for the AMoRE $0\nu\beta\beta$ Decay Search Experiment*, arXiv:1512.05957.

[201] SuperNEMO Collaboration, R. Arnold et al., *Probing New Physics Models of Neutrinoless Double Beta Decay with SuperNEMO*, *Eur. Phys. J.* **C 70** (2010) 927–943 [arXiv:1005.1241].

[202] H. Fritzsch and Z.-z. Xing, *Parametrization of Flavor Mixing in the Standard Model*, *Phys. Rev.* **D 57** (1998) 594–597 [arXiv:hep-ph/9708366].

[203] A. Rasin, *Diagonalization of Quark Mass Matrices and the Cabibbo-Kobayashi-Maskawa Matrix*, arXiv:hep-ph/9708216.

[204] W. Rodejohann, H. Zhang and S. Zhou, *Systematic Search for Successful Lepton Mixing Patterns with Nonzero θ_{13}*, *Nucl. Phys.* **B 855** (2012) 592–607 [arXiv:1107.3970].

Acknowledgements

First of all, I am very grateful to my supervisor Professor Serguey T. Petcov for having triggered my interest in neutrino physics. His guidance, support and constant availability were of invaluable help during all my PhD studies and made the present thesis possible. I am truly fortunate having had so many interesting discussions with him, not only scientific ones, but also about history of science, art and, in general, about life. I also thank him for the opportunity to travel and present the results of our research at several international conferences and workshops.

Next, I am very thankful to my friend and collaborator Ivan, without whom the studies presented in this thesis would not be possible. I have learned a lot from him. Working together was a pleasure and big luck for me. Moreover, I was very lucky to find a true friend. Thank you for all our crazy laughs and thank you for being around when I needed help.

Further, I would like to acknowledge my collaborators Alex, Julia, Martin and João, with whom I had the opportunity to work on different projects. I am indebted to Alex and Martin for their support. I would also like to thank Sanjib and Sabya for the collaboration we started recently.

I would like to express my deep gratitude to Riccardo, Federica and Luisella from the SISSA Students' Secretariat for their great organisational support and availability.

I thank all members of the Theoretical Particle Physics and Astroparticle Physics Groups. Especially, I would like to thank my classmates Emtinan, Pietro, Himanshu and Denis, with whom I started the PhD adventure, for the moments we shared together and various interesting discussions we had. I am very thankful to my office mates Ivan and Cristiano for all the chats, laughs, lunches, dinners and drinks we had together. It was really nice to share office with you.

My very special thanks go to my friend Pietro. Thank you for all the conversations, lunches and walks, for all the enjoyable time we shared in Trieste and Treviso. I would also like to thank Silvia and Francesco for all the facetious chats. I am deeply grateful to Francesco for his kindness and help, and, of course, for his concerts with music from the 1960s.

Music was another lovely part of my life in Trieste. In this regard, I am very thankful to Antonio for having created the piano evenings and organised them so many times in Caffè San Marco and Caffè degli Specchi. I am grateful to Ina and Francesca with whom I had a pleasure to play piano four hands. Thank you for all the rehearsals and performances we had. Francesca, thank you for your regard. I would also like to thank Lucia, Sophie, Song and Alexey for their company and music. My big thanks go to Stefano for a very good time we spent during his visits to Trieste and for his music.

I am thankful to Aurora for her kindness and help. I thank Alberto and Vizhe, Vladimir and Tatyana, Marco and Fiamma. Many thanks go to Džejla, Maja and Mariam for the nice chats we had during these years. There are so many people at SISSA with whom I had interesting conversations and shared remarkable moments. I thank them all. I apologise for not listing each of them individually.

I would also like to express my gratitude to Francesca, Matteo and Eleonora for their amazing classes of Italian I was following during my first two years in Trieste. I am also grateful to all my Italian (and not only Italian) friends who gave me the opportunity to communicate in Italian and improve my knowledge of this beautiful language. I am thankful also to my landlord Luca for his availability and help.

I acknowledge the Institute for Particle Physics Phenomenology in Durham, UK, where the work on the present thesis has been completed, for a nice working atmosphere. Especially, I am grateful to Professor Silvia Pascoli for her support. My special thanks go to Jessica and Holger for their kindness. Jessica, I value our long-standing friendship.

I am very grateful to Alessandra, Giulia, Mauro and their parents for their hospitality and support. I would also like to thank Marco for his nice company.

This thesis would not be possible without my parents and my brothers Jenya and Alesha. Thank you for your care and invaluable help all along my life. Thank you for always having been on the other end of Skype to share my worries and successes. I would also like to thank my sisters-in-law Natasha and Anya, and, of course, my niece Maja. Each (not so often) occasion when we meet is so nice and important.

The most special thanks go to Alessandra. Having you by my side (even if sometimes at the distance of hundreds or thousands of kilometres) has done the last years so special for me. Thank you very much for your continuous dedication, patience and understanding. Thank you very much for supporting me in my choices. Thank you very much for your invaluable help and support, in particular, while finishing the work on the present thesis.